



NBS BUILDING SCIENCE SERIES 143

# Investigation of the Kansas City Hyatt Regency Walkways Collapse

U.S. DEPARTMENT OF COMMERCE • NATIONAL BUREAU OF STANDARDS



## NATIONAL BUREAU OF STANDARDS

The National Bureau of Standards<sup>1</sup> was established by an act of Congress on March 3, 1901. The Bureau's overall goal is to strengthen and advance the Nation's science and technology and facilitate their effective application for public benefit. To this end, the Bureau conducts research and provides: (1) a basis for the Nation's physical measurement system, (2) scientific and technological services for industry and government, (3) a technical basis for equity in trade, and (4) technical services to promote public safety. The Bureau's technical work is performed by the National Measurement Laboratory, the National Engineering Laboratory, and the Institute for Computer Sciences and Technology.

**THE NATIONAL MEASUREMENT LABORATORY** provides the national system of physical and chemical and materials measurement; coordinates the system with measurement systems of other nations and furnishes essential services leading to accurate and uniform physical and chemical measurement throughout the Nation's scientific community, industry, and commerce; conducts materials research leading to improved methods of measurement, standards, and data on the properties of materials needed by industry, commerce, educational institutions, and Government; provides advisory and research services to other Government agencies; develops, produces, and distributes Standard Reference Materials; and provides calibration services. The Laboratory consists of the following centers:

Absolute Physical Quantities<sup>2</sup> — Radiation Research — Chemical Physics — Analytical Chemistry — Materials Science<sup>2</sup>

**THE NATIONAL ENGINEERING LABORATORY** provides technology and technical services to the public and private sectors to address national needs and to solve national problems; conducts research in engineering and applied science in support of these efforts; builds and maintains competence in the necessary disciplines required to carry out this research and technical service; develops engineering data and measurement capabilities; provides engineering measurement traceability services; develops test methods and proposes engineering standards and code changes; develops and proposes new engineering practices; and develops and improves mechanisms to transfer results of its research to the ultimate user. The Laboratory consists of the following centers:

Applied Mathematics — Electronics and Electrical Engineering<sup>2</sup> — Manufacturing Engineering — Building Technology — Fire Research — Chemical Engineering<sup>2</sup>

**THE INSTITUTE FOR COMPUTER SCIENCES AND TECHNOLOGY** conducts research and provides scientific and technical services to aid Federal agencies in the selection, acquisition, application, and use of computer technology to improve effectiveness and economy in Government operations in accordance with Public Law 89-306 (40 U.S.C. 759), relevant Executive Orders, and other directives; carries out this mission by managing the Federal Information Processing Standards Program, developing Federal ADP standards guidelines, and managing Federal participation in ADP voluntary standardization activities; provides scientific and technological advisory services and assistance to Federal agencies; and provides the technical foundation for computer-related policies of the Federal Government. The Institute consists of the following centers:

Programming Science and Technology — Computer Systems Engineering.

<sup>1</sup>Headquarters and Laboratories at Gaithersburg, MD, unless otherwise noted; mailing address Washington, DC 20234.

<sup>2</sup>Some divisions within the center are located at Boulder, CO 80303.

NBS BUILDING SCIENCE SERIES 143

# Investigation of the Kansas City Hyatt Regency Walkways Collapse

R. D. Marshall  
E. O. Pfrang  
E. V. Leyendecker  
K. A. Woodward

Center for Building Technology  
National Engineering Laboratory

R. P. Reed  
M. B. Kasen  
T. R. Shives

Center for Materials Science  
National Measurement Laboratory

National Bureau of Standards  
Washington, DC 20234



---

U.S. DEPARTMENT OF COMMERCE, Malcolm Baldrige, Secretary  
NATIONAL BUREAU OF STANDARDS, Ernest Ambler, Director

Issued May 1982

Library of Congress Catalog Card Number: 81-600538

**National Bureau of Standards Building Science Series 143**

Nat. Bur. Stand. (U.S.), Bldg. Sci. Ser.143, 360 pages (May 1982)

CODEN: BSSNBV

U.S. GOVERNMENT PRINTING OFFICE  
WASHINGTON: 1982

---

For sale by the Superintendent of Documents, U.S. Government Printing Office, Washington, DC 20402  
Price

(Add 25 percent for other than U.S. mailing)

ERRATA SHEET

NBS Building Science Series 143  
Investigation of the Kansas City Hyatt Regency  
Walkways Collapse

R. D. Marshall, E. O. Pfrang, E. V. Leyendecker, K. A. Woodward

- page iii Delete last paragraph of Abstract.
- Page ix Section 1.2 begins on page 2.  
Section 2.3 begins on page 6.
- Page 6 Second paragraph, replace E sign with ●  
in front of each code and standard listed.
- Page 10 Fourth paragraph and tenth line, delete  
comma after Kansas City.
- Page 25 Figure 3.8 (at top of page), replace 1 5/8"  
with 2 1/8" for dimension of distance from  
left end of stringer to center line of holes  
in clip angle.
- Page 35 First paragraph of Section 4.3, replace E  
sign with ● in front of each eyewitness  
account.
- Page 46 Fourth line of Section 5.2.1, replace El. 45.00  
with Elev. 45.00.
- Page 227 First paragraph of Section 9.3.3, the equation  
should read:
- $$0.7854 \left( D - \frac{0.9743}{n} \right)^2$$
- Page A-98 Delete last paragraph of Abstract.



## ABSTRACT

An investigation into the collapse of two suspended walkways within the atrium area of the Hyatt Regency Hotel in Kansas City, Mo., is presented in this report. The investigation included on-site inspections, laboratory tests and analytical studies.

Three suspended walkways spanned the atrium at the second, third, and fourth floor levels. The second floor walkway was suspended from the fourth floor walkway which was directly above it. In turn, this fourth floor walkway was suspended from the atrium roof framing by a set of six hanger rods. The third floor walkway was offset from the other two and was independently suspended from the roof framing by another set of hanger rods. In the collapse, the second and fourth floor walkways fell to the atrium floor, with the fourth floor walkway coming to rest on top of the lower walkway.

Based on the results of this investigation, it is concluded that the most probable cause of failure was insufficient load capacity of the box beam-hanger rod connections. Observed distortions of structural components strongly suggest that the failure of the walkway system initiated in the box beam-hanger rod connection on the east end of the fourth floor walkway's middle box beam.

Two factors contributed to the collapse: inadequacy of the original design for the box beam-hanger rod connection, which was identical for all three walkways, and a change in hanger rod arrangement during construction that essentially doubled the load on the box beam-hanger rod connections at the fourth floor walkway. As originally approved for construction, the contract drawings called for a set of continuous hanger rods which would attach to the roof framing and pass through the fourth floor box beams and on through the second floor box beams. As actually constructed, two sets of hanger rods were used, one set extending from the fourth floor box beams to the roof framing and another set from the second floor box beams to the fourth floor box beams.

Based on measured weights of damaged walkway spans and on a videotape showing occupancy of the second floor walkway just before the collapse, it is concluded that the maximum load on a fourth floor box beam-hanger rod connection at the time of collapse was only 31 percent of the ultimate capacity expected of a connection designed under the Kansas City Building Code. It is also concluded that had the original hanger rod arrangement not been changed, the ultimate capacity would have been approximately 60 percent of that expected under the Kansas City Building Code. With this change in hanger rod arrangement, the ultimate capacity of the walkways was so significantly reduced that, from the day of construction, they had only minimal capacity to resist their own weight and had virtually no capacity to resist additional loads imposed by people.

Supplementary material is contained in an appendix to this report and published as NBSIR 82-2465A.

Key Words: building; collapse; connection; construction; failure; steel; walkway.



## EXECUTIVE SUMMARY

On July 17, 1981, two suspended walkways within the atrium area of the Hyatt Regency Hotel in Kansas City, Mo., collapsed, leaving 113 people dead and 186 injured. In terms of loss of life and injuries, this was the most devastating structural collapse ever to take place in the United States.

On July 20, 1981, Senator Thomas F. Eagleton's office contacted the National Bureau of Standards and requested that technical assistance be provided to Kansas City. Shortly thereafter Kansas City Mayor Richard L. Berkley asked NBS to determine the most probable cause of the walkways' collapse. Senators Thomas F. Eagleton and John C. Danforth and Congressman Richard Bolling endorsed the Mayor's request for the NBS to conduct an independent investigation. NBS researchers first arrived in Kansas City on July 21, 1981. During the course of the investigation, the NBS team of engineers and scientists inspected the Hyatt Regency atrium area and the warehouse where the walkway debris was stored.

In the early phases of the investigation, NBS involvement was limited by court order to visual and photographic observations and measurements. NBS requested permission to weigh selected walkway spans and to remove for additional study and destructive examination certain portions of the walkway box beams, hanger rods, concrete decks, and nuts and washers. The Bureau's requests were eventually granted under court orders after agreement was reached with litigants involved in various legal actions stemming from the collapse of the walkways.

Documents such as drawings, specifications, inspection reports, test reports, and construction logs, as well as photographs and videotapes became available to NBS from a number of sources. These were useful in gaining information about the walkways as originally approved for construction and as modified during the construction process.

NBS conducted extensive laboratory tests on Bureau-fabricated mockups of parts of the walkways. Tests were also conducted by NBS on portions of the debris. Analytical models were developed to predict the response of the walkways to various loading conditions. Also, tests were conducted to determine material properties and weld and fracture characteristics.

The Hyatt Regency consists of three main sections: a high-rise section, a "function block," and a connecting atrium area. As built, three suspended walkways spanned the atrium at the second, third, and fourth floor levels and connected the high-rise and function sections. The second floor walkway was suspended from the fourth floor walkway which was directly above it. In turn, this fourth floor walkway was suspended from the atrium roof framing by a set of six hanger rods. The third floor walkway was offset from the other two and was independently suspended from the roof framing by another set of hanger rods.

In the collapse, the second and fourth floor walkways fell to the atrium floor, with the fourth floor walkway coming to rest on top of the lower walkway. Most of those killed or injured were either on the first floor level of the atrium or on the second floor walkway. The third floor walkway was not involved in the collapse.

As originally approved for construction by the Kansas City Codes Administration Office, the plans for the walkways called for a single set of hanger rods (attached to the roof framing) which would pass through the fourth floor box beams and on through the second floor box beams. The box beams--made up of a pair of 8-inch steel channels with the flanges welded toe to toe--were to rest on hanger-rod washers and nuts below each set of beams. Under this arrangement each box beam would separately transfer its load directly into the hanger rods.

However, during construction, shop drawings were prepared by the steel fabricator which called for the use of two sets of hanger rods rather than a single set. One set of hanger rods extended from the fourth floor box beams to the roof framing and another set extended from the second floor box beams to the fourth floor box beams. Under this arrangement all of the second floor walkway load was first transferred to the fourth floor box beams, where both that load and the fourth floor walkway load were transmitted through the box beam-hanger rod connections to the ceiling hanger rods. As indicated by their stamps, these shop drawings were reviewed by the contractor, structural engineer, and architect.

Efforts were made to establish as accurately as possible the loads on the walkways at the time of the collapse. Weighing of selected walkway debris along with measurements taken on concrete cores removed from the walkway decks permitted NBS to determine that the actual walkway dead load (self-weight) was approximately 8 percent higher than the nominal dead load. (The nominal dead load is an estimate based solely on the project's contract drawings.) Estimates of the loads due to people present on the walkways at the time of collapse (live load) were much more difficult to make. Witnesses made a number of conflicting statements regarding the numbers and activities of people on the walkways just prior to the collapse. However, a television crew had videotaped parts of the walkway minutes before the collapse. By studying this videotape, NBS concluded that 63 people represented a credible estimate of combined second and fourth floor walkway occupancy at the time of collapse.

Based on field, laboratory, and analytical investigations, NBS concluded that:

1. *Collapse of the walkways occurred under the action of loads that were substantially less than the design loads specified by the Kansas City Building Code.*
2. *The ultimate capacity of box beam-hanger rod connections can be predicted on the basis of laboratory test results.*
3. *Under the action of the loads estimated to have been present on the walkways at the time of collapse, all fourth floor box beam-hanger rod connections were candidates for initiation of walkway collapse.*
4. *Observed distortions of structural components strongly suggest that failure of the walkway system initiated in the box beam-hanger rod connection at location 9UE (east end of middle box beam in fourth floor walkway).*

5. *As constructed, the box beam-hanger rod connections, the fourth floor to ceiling hanger rods, and the third floor walkway hanger rods did not satisfy the design provisions of the Kansas City Building Code.*
6. *The change in hanger rod arrangement from a continuous rod to interrupted rods essentially doubled the load to be transferred by the fourth floor box beam-hanger rod connections.*
7. *The box beam-hanger rod connection would not have satisfied the Kansas City Building Code under the original hanger rod detail (continuous rod).*
8. *Under the original hanger rod arrangement (continuous rod) the box beam-hanger rod connections as shown on the contract drawings would have had the capacity to resist the loads estimated to have been acting at the time of collapse.*
9. *Neither the quality of workmanship nor the materials used in the walkway system played a significant role in initiating the collapse.*



## TABLE OF CONTENTS

	<u>Page</u>
ABSTRACT .....	iii
EXECUTIVE SUMMARY .....	v
1. INTRODUCTION .....	1
1.1 Background .....	1
1.2 Objective and Scope of the Investigation .....	1
1.3 Organization of the Report .....	2
2. DOCUMENTS REVIEWED BY THE NBS INVESTIGATIVE TEAM .....	5
2.1 Introduction .....	5
2.2 Access to Documents .....	5
2.3 Project Specifications and Relevant Code Provisions .....	5
2.4 Architectural and Structural Drawings .....	6
2.5 Shop Drawings .....	7
2.6 Daily Logs and Inspection Reports .....	8
2.7 Other Documents and Materials Reviewed .....	9
2.8 Summary .....	10
3. DESCRIPTION OF THE WALKWAY SYSTEM PRIOR TO COLLAPSE .....	13
3.1 Introduction .....	13
3.2 General Layout of the Hyatt Regency Atrium .....	13
3.3 Structural and Architectural Features of the Walkways .....	14
3.4 Probable Sequence of Erection .....	16
3.5 Designation of Walkway Components .....	16
3.6 Summary .....	17
4. DESCRIPTION OF THE WALKWAY COLLAPSE .....	33
4.1 Introduction .....	33
4.2 Summary of Events Preceding and Following the Collapse .....	33
4.3 Eyewitness Accounts of Collapse .....	35
4.4 Estimate of Walkway Occupancy at Time of Collapse .....	36
4.5 Removal and Storage of Walkway Debris .....	37
4.6 Summary .....	38
5. SITE INVESTIGATION .....	45
5.1 Introduction .....	45
5.2 Survey of the Hyatt Regency Atrium .....	45
5.2.1 Embedded Plates and Bearing Seats .....	46
5.2.2 Fourth Floor to Ceiling Hanger Rods .....	46
5.2.3 Impact Points on Atrium Floor .....	47

## TABLE OF CONTENTS (Continued)

	<u>Page</u>
5.2.4 Alignment of Walkways Prior to Collapse .....	47
5.2.5 Other Observations Relevant to the Investigation .....	48
5.3 Observations of Walkway Debris .....	49
5.3.1 General .....	49
5.3.2 Hanger Rod Pull-through .....	49
5.3.3 Box Beam Longitudinal Welds .....	50
5.3.4 Box Beam to Clip Angle Fillet Welds .....	52
5.3.5 Other Observations Relevant to the Investigation .....	52
5.3.6 Determination of Span Weights .....	53
5.4 Removal of Specimens .....	54
5.4.1 Criteria for Specimen Selection .....	54
5.4.2 Specimen Removal .....	54
5.4.3 Specimen Cataloging and Preparation for Shipment .....	55
5.4.4 Specimen Storage and Handling .....	56
5.5 Replication of Walkway Weld Fracture Surfaces .....	56
5.6 Summary .....	57
6. NBS STRUCTURAL TESTING PROGRAM .....	97
6.1 Introduction .....	97
6.2 Background .....	97
6.3 Overview .....	98
6.4 Test Specimen Description .....	98
6.4.1 Full Length Box Beam .....	98
6.4.2 Short Box Beam .....	98
6.4.3 Fabrication .....	99
6.5 Test Setup .....	100
6.6 Loading Equipment .....	101
6.7 Instrumentation .....	102
6.8 Data Acquisition and Reduction .....	103
6.9 Loading Sequence .....	104
6.10 NBS Short Box Beam Tests .....	105
6.10.1 Parameters .....	105
6.10.2 Short Box Beam Specimens .....	106
6.10.3 Welding Process .....	107
6.10.4 Weld Area .....	109
6.10.5 Other Observations .....	110
6.10.6 Summary .....	113

## TABLE OF CONTENTS (Continued)

	<u>Page</u>
6.11 NBS Full-Length Box Beam Tests .....	113
6.12 Tests on Walkway Box Beam .....	113
6.12.1 Full-Length Box Beam Test .....	113
6.12.2 Short Box Beam Tests .....	114
6.13 Box Beam-Hanger Rod Connection Capacity .....	116
6.14 Conclusions .....	117
7. NBS MATERIALS EVALUATION PROGRAM .....	157
7.1 Introduction .....	157
7.2 Initial Inspection .....	158
7.2.1 Visual .....	158
7.2.2 Radiography .....	158
7.3 Mechanical Properties of Structural Steel and Weldments .....	159
7.3.1 NBS Channel Specimens .....	159
7.3.2 Walkway Box Beams .....	160
7.3.3 Walkway Hanger Rods .....	161
7.3.4 Walkway Box Beam Longitudinal Welds .....	161
7.4 Metallography and Hardness Measurements .....	162
7.4.1 Box Beam Weldments .....	162
7.4.2 Walkway Hanger Rods .....	163
7.4.3 Washers .....	163
7.5 Chemical Analysis .....	164
7.6 Properties of Concrete .....	164
7.7 Conclusions .....	166
8. FRACTOGRAPHIC ANALYSIS .....	195
8.1 Introduction .....	195
8.2 Specimen Preparation and NBS Fracture Results .....	195
8.3 Walkway Fracture Replicas .....	196

## TABLE OF CONTENTS (Continued)

	<u>Page</u>
8.3.1 General Observations .....	196
8.3.2 Box Beam Longitudinal Welds .....	197
8.3.3 Washer/Nut Contact Area .....	197
8.3.4 Washers .....	198
8.3.5 Clip Angle Fillet Welds .....	198
8.4 Direct Analysis of Walkway Box Beam Fractures .....	199
8.4.1 Procedures .....	199
8.4.2 Results .....	199
8.5 Summary .....	200
9. STRUCTURAL ANALYSIS .....	223
9.1 Introduction .....	223
9.2 Loads .....	223
9.2.1 Dead Load .....	223
9.2.2 Live Loads .....	225
9.3 Analysis of Walkway Structural Components .....	226
9.3.1 General .....	226
9.3.2 Box Beam-Hanger Rod Connections .....	226
9.3.3 Hanger Rods .....	227
9.3.4 Summary of Analysis .....	227
9.4 Forces Acting on the Hanger Rods at Time of Collapse .....	228
9.5 Walkway Deflections .....	229
9.6 Effects of Dynamic Excitation .....	229
9.6.1 Dynamic Characteristics of the Walkways .....	229
9.6.2 Sources of Dynamic Excitation .....	231
9.7 Summary .....	232
10. INTERPRETATION OF TESTS, ANALYSES AND OBSERVATIONS .....	243
10.1 Introduction .....	243
10.2 Comparison of Loads and Box Beam-Hanger Rod Connection Capacities .....	243
10.3 Ultimate Capacity Based on Code Requirements .....	244
10.4 Probable Sequence of Collapse .....	245
10.5 Effect of Change in Hanger Rod Arrangement .....	246

TABLE OF CONTENTS (Continued)

	<u>Page</u>
10.6 Quality of Materials and Workmanship .....	246
10.7 Summary .....	248
11. SUMMARY AND CONCLUSIONS .....	253
12. REFERENCES .....	257
APPENDIX .....	A-1
A6.10 - A6.11 .....	A-2
A7.2 - A7.5 .....	A-19
A7.6 .....	A-83
A9.2 .....	A-92



## 1. INTRODUCTION

### 1.1 BACKGROUND

On July 17, 1981, at approximately 7:05 p.m., two suspended walkways within the atrium area of the Hyatt Regency Hotel in Kansas City, Mo., collapsed, killing 111 people and injuring 188. Two of the injured subsequently died. In terms of loss of life and injuries, this was the most devastating structural collapse ever to take place in the United States.

At the time of the collapse, the hotel had been in service for approximately 1 year. The Hyatt Regency consists of three main sections; a 40-story tower section, a function block, and a connecting atrium area. The atrium is a large open area approximately 117 ft (36 m) by 145 ft (44 m) in plan and 50 ft (15 m) high. Three suspended walkways spanned the atrium at the second, third, and fourth floor levels. These walkways connected the tower section and the function block. The third floor walkway was independently suspended from the atrium roof trusses while the second floor walkway was suspended from the fourth floor walkway, which in turn was suspended from the roof framing.

In the collapse, the second and fourth floor walkways fell to the atrium first floor, with the fourth floor walkway coming to rest on top of the second. Most of those killed or injured were either on the atrium first floor level or on the second floor walkway.

On July 20, 1981, Senator Thomas F. Eagleton's office contacted the National Bureau of Standards (NBS) and requested that technical assistance be provided to the city of Kansas City. This was followed later that day by a request to NBS from Mayor Richard L. Berkley for technical advice regarding the tragedy and its cause. Accordingly, two NBS structural research engineers arrived in Kansas City on July 21 and met with the Mayor and other city officials. On July 22, Mayor Berkley formally requested that the NBS independently ascertain the most probable cause of the collapse of the Hyatt Regency walkways. On July 24 in a letter to Mayor Berkley, Senators Eagleton and Danforth and Congressman Bolling endorsed the Mayor's request for NBS to conduct an impartial investigation.

## 1.2 OBJECTIVE AND SCOPE OF THE INVESTIGATION

The objective of this investigation was to determine the most probable cause of the collapse. As part of this investigation, it was necessary to reconstruct the events that preceded the collapse and the condition of the walkways at the time of the collapse. To carry out its study, the NBS investigative team used data obtained from on-site inspections; drawings, specifications and other records maintained by the city of Kansas City; documents and other information from parties involved in the construction and operation of the Hyatt Regency Hotel; information from those who participated in the rescue operation and from eyewitnesses; and photographs, videotapes, and other records available from the media. NBS also conducted inspections and took measurements in the atrium area and on the debris from the collapse. NBS conducted extensive laboratory studies on materials and mockups representative of materials and assemblies used in the walkway construction. Extensive laboratory studies were also conducted on specimens obtained from the walkway debris. NBS acquired these specimens under the terms of several court orders. These studies were in turn supported by analytical studies aimed at predicting the structural performance of the walkways.

## 1.3 ORGANIZATION OF THE REPORT

This report is organized in 12 chapters:

Chapter 2 describes the various documents reviewed during the course of this investigation and the procedures followed by the NBS investigative team in gaining access to them. Documents described include project specifications, relevant codes and standards, contract and shop drawings, daily logs, and inspection reports.

Chapter 3 describes the general layout of the Hyatt Regency atrium, the structural and architectural details of the walkways, their probable sequence of erection, and the system established to designate walkway components.

Chapter 4 summarizes events preceding and following the collapse and eyewitness accounts of the collapse. This chapter also discusses the walkway occupancy prior to the collapse and presents what is believed to be a credible estimate of walkway occupancy at the time of collapse. The chapter closes with a description of the removal and storage of walkway debris.

Chapter 5 addresses the site investigation which included detailed observations of the walkway debris and a survey of that part of the atrium occupied by the walkways. The damage observed is related to probable mode of failure. Also described are the procedures followed in weighing selected walkway spans, removing specimens from the debris, and obtaining replicas of the weld fracture surfaces.

Chapter 6 describes the NBS structural testing program which involved the testing of box beams fabricated at the NBS and a box beam removed from the walkway debris. Test specimens, instrumentation, loading systems, and loading sequence are described. Various parameters studied and their effects on box

beam-hanger rod connection capacity are discussed in detail. The chapter concludes with an assessment of the capacities of the box beam-hanger rod connections in the fourth floor walkway.

Chapter 7 describes the NBS materials testing program and the results of tests carried out on materials used to fabricate NBS test specimens and on materials removed from the walkway debris. Included in this chapter are results of a radiographic analysis of longitudinal welds on a walkway box beam, mechanical properties of structural steel and weldments, metallographic examinations, hardness measurements, chemical analyses of structural steel and weld material, and mechanical properties of concrete used in the walkway decks.

Chapter 8 addresses the fractographic analysis of weld fracture surfaces in selected NBS box beams and in the walkway box beams. Results obtained from direct optical and scanning electron microscopy using replicas and actual fracture surfaces are discussed. Also addressed are washer fractures and washer/nut contact areas.

Chapter 9 addresses structural analysis. Included are dead and live loads, forces acting on the hanger rods, walkway deflections, analysis of the walkway structural components and their compliance with codes and standards, and the significance of dynamic excitation.

Chapter 10 interprets the results of structural tests and analyses and discusses the probable sequence of the walkway collapse. Also discussed is the significance of replacing the continuous hanger rod arrangement as shown on the contract drawings with interrupted rods in the second and fourth floor walkway system. The chapter closes with an assessment of the quality of materials and workmanship.

Chapter 11 summarizes the findings of the investigation and presents conclusions reached by the NBS investigative team.

Chapter 12 lists the references cited in the text.



## 2. DOCUMENTS REVIEWED BY THE NBS INVESTIGATIVE TEAM

### 2.1 INTRODUCTION

Section 2.2 of this chapter describes the procedure followed in obtaining access to documents.

Sections 2.3, 2.4 and 2.5 discuss documents prepared during the design stage, prior to actual construction of the walkways. Section 2.6 deals with daily logs and inspection reports filed during the construction phase, while section 2.7 in large part addresses documents relating to the collapse and the rescue operation. Section 2.8 provides a summary of the findings reported in this chapter.

### 2.2 ACCESS TO DOCUMENTS

This chapter describes the various documents reviewed and the procedures followed in gaining access to them. In arranging for access to documents, the Bureau submitted its requests to the Office of the Mayor which in turn contacted the appropriate firms and agencies, requesting their cooperation and assistance. Access by NBS to the requested documents was therefore voluntary. Firms contacted by the Office of the Mayor and their roles in the design, construction, and operation of the Hyatt Regency Hotel were as follows:

- Crown Center Redevelopment Corporation - Owner
- Hyatt Hotels Corporation - Operator
- Patty Berkebile Nelson Duncan Monroe Lefebvre (PBNMML),  
Architects Planners, Incorporated - Architect
- Gillum-Colaco, Consulting Structural Engineers - Structural engineer
- Concordia Project Management Limited - Construction manager
- Eldridge & Son Construction Company - General contractor
- Havens Steel Company - Steel fabricator

### 2.3 PROJECT SPECIFICATIONS AND RELEVANT CODE PROVISIONS

Shortly after the collapse, the Kansas City Public Works Department assembled documents in its possession related to the design, construction, and inspection of the Hyatt Regency Hotel. The Office of the City Attorney made these documents available for public review beginning July 21, 1981.

Included in these documents was a set of project specifications for the Hyatt Regency Hotel. They had been prepared by Patty Berkebile Nelson Duncan Monroe Lefebvre Architects Planners, Inc. (PBDML), the project architects, and were dated August 28, 1978 [2.1]. Section 0510 of the project specifications covers structural steel and, among other things, refers to applicable standards, quality assurance, fabrication, erection, and field quality control. Codes and standards referenced in the project specifications include, but are not limited to, the following:

- ‡ AISC\* "Code of Standard Practice for Steel Buildings and Bridges"  
(No date)
- ‡ AISC "Specification for the Design, Fabrication and Erection of  
Structural Steel for Buildings" (No date)
- ‡ AWS\*\*D1.1 "Structural Welding Code" (No date).

Also included in the documents provided by the Office of the City Attorney was a copy of the Kansas City Building Code [2.2] in effect at the time the Hyatt Regency project specifications and design drawings were reviewed by the Public Works Department. This issue of the Kansas City Building Code is, with minor exceptions, an adoption of the Uniform Building Code, 1976 Edition [2.3]. The AISC Specification for the Design, Fabrication and Erection of Structural Steel for Buildings [2.4] forms the basis for the steel design provisions of the Uniform Building Code and the Kansas City Building Code. Certain provisions of the Kansas City Building Code and the codes referenced in the project specifications are referred to later in this report.

### 2.4 ARCHITECTURAL AND STRUCTURAL DRAWINGS

In addition to the project specifications just described, the Office of the City Attorney also made available sets of architectural and structural drawings. The drawings listed below were "issued for revision" or "issued for construction" during the period August 1-28, 1978, and were referred to during the course of this investigation.

---

\* American Institute of Steel Construction

\*\* American Welding Society

## Architectural

A302 Floor Plan, Level 106 North  
A303 Floor Plan, Level 121 North  
A304 Floor Plan, Level 136 North  
A305 Floor Plan, Level 151 North  
A412 Building Section  
A508 Details, Expansion Joints, Bridge

## Structural

## Date prepared

S302	Framing Plan, Level 106 North	March 30, 1978
S303	Framing Plan, Level 121 North	March 30, 1978
S304	Framing Plan, Level 136 North	March 30, 1978
S305	Framing Plan, Level 151 North	March 30, 1978
S306	Framing Plan, Level 166 North	March 30, 1978
S405.1	Steel Details	May 12, 1978
S601	General Notes	March 10, 1978

Simplified versions of the framing plans at levels 106 to 166\* and a sectional elevation of the atrium were developed by NBS as part of this investigation and are included in sections 3.2 and 3.3 of this report. The General Notes (Dwg. S601) set out the design criteria, including a design live load of 100 psf (4.8 kPa) for hotel corridors and lobby areas. These are interpreted by NBS to include the walkways in the atrium.

### 2.5 SHOP DRAWINGS

Shop drawings detailing the walkway structural system were made available to the NBS investigative team by the Crown Center Redevelopment Corporation, the hotel's owner. Initially, review of the drawings was by appointment at the Crown Center corporate offices with visits for such purpose occurring on August 7 and 10, 1981. Arrangements were subsequently made for NBS to take custody of the drawings until issuance of its report. The following shop drawings, prepared by the steel fabricator, Havens Steel Company, dated between January 7, 1979, and February 9, 1979, and reviewed, as indicated by their stamps on the drawings, by the contractor, structural engineer and architect, were received from the Crown Center Redevelopment Corporation on September 2, 1981:

---

\* The contract and shop drawings used during the construction of the Hyatt Regency Hotel use this notation to designate the various floors within the atrium. For convenience this same system is adopted for use in this report. The second floor walkway was level 121, the third floor walkway was level 136, and the fourth floor walkway was level 151.

Shop Drawing NumberSubject

E3	Framing plan at Elev. 121'-0" and elevation at column lines 8, 9, and 10
E4	Framing plan at Elev. 136'-0"
E5	Framing plan at Elev. 151'-0" and expansion bearing detail
30	Box beams, cross beams, and hanger rods
31	Stringers, slide bearing plates, and bearing seats
23	Beams at Elev. 167'-1" and hanger rod brackets
E2	Framing plan at Elev. 167'-1"
E1	Truss elevation
8	Truss T3
12	Truss T3
8A	Truss T3 member layout
12A	Truss parts (T3)

The first five of the above listed drawings were referred to extensively during the course of this investigation. Field observations and measurements show that, in general, the structural details, member sizes, and dimensions of the as-built structure faithfully reflected that which was called for on the drawings. No attempt was made to check or confirm the details of the structural work above the upper hanger rod brackets at Elev. 165'-7", this being deemed to be beyond the scope of the investigation.

## 2.6 DAILY LOGS AND INSPECTION REPORTS

Portions of the daily logs maintained by the architect during construction of the Hyatt Regency Hotel were made accessible to NBS and were reviewed at the offices of Duncan Associates, Inc.\* on two occasions--September 4 and 25, 1981. These portions contained limited reference to construction of the walkways. In a number of logs, reference is made to construction work in the atrium along column lines 7 and 11 and at levels 136 and 151. However, there is very little specific information on the walkways. Those logs that did refer to the walkways can be summarized as follows:

#312 September 14, 1979

Notes that Havens Steel Company completed rewelding of composite deck studs at the walkways.

#320 September 26, 1979

Mentions placement of concrete for bridges 151, 136, and 121 from column lines 7 to 11.

---

\* A member firm of PBNMML.

#344 October 30, 1979

Mentions report "... that fitters were refusing to work on the 151 bridge because of a comment made by the inspection team now looking at the atrium connections."

#372 December 7, 1979

Notes problem on 151 bridge where piping and granite hangers were in conflict.

On September 4, 1981, a visit was made to the offices of the owner's inspection agency, General Testing Laboratories, Inc., where an inspection report was reviewed which mentioned the inspection of bolted connections on August 17 and 20, 1979. The report noted that the hanging walkways were inaccessible due to metal decking or "difficulty of position" and that the connections were not checked by calibrated torque wrench. Representatives of General Testing Laboratories indicated that unless the specific dates of walkway construction were known, it would be very difficult for them to retrieve reports of interest to the NBS team.

Also on September 4, 1981, copies of inspection reports related to construction in the atrium area were reviewed in the offices of Blackwell, Sanders, Matheny, Weary, and Lombardi, legal counsel to Concordia Project Management Ltd. These reports, filed by General Testing Laboratories, did not provide any additional information on the walkways. In response to an earlier request, NBS investigators were shown a handwritten note indicating the following schedule for walkway construction:

August 8-15, 1979	Erect bridges.
September 7-12, 1979	Pour bridge concrete on fourth level.
September 10-14, 1979	Pour bridge concrete on third level.
January 31-Feb. 7, 1980	Pour bridge concrete on second level.

It appears that only the erection of structural steel sometime before August 17, 1979, is consistent with dates mentioned in the various daily logs and inspection reports reviewed by the NBS team. Given the limited quantity of concrete in the walkway decks, the single-day placement indicated in the architect's daily logs seems more credible.

## 2.7 OTHER DOCUMENTS AND MATERIALS REVIEWED

In addition to the specifications, drawings, logs and reports described above, the NBS investigative team also reviewed several hundred photographs taken immediately after the collapse, during the rescue operation and on the day following the collapse. The following agencies and establishments allowed members of the NBS team to inspect and, in some cases, retain copies of their photographs:

Kansas City Fire Department  
Kansas City Police Department  
Crown Center Redevelopment Corporation  
The Kansas City Star  
The Kansas City Times.

Videotapes from various news services were also reviewed. Of particular importance was a videotape obtained from KMBC TV, Kansas City, Mo., which contained footage taken immediately before and after the collapse. Analysis of information contained on this tape is described in chapter 4.

The NBS team also reviewed photographs and documents related to an investigation conducted by the U.S. Occupational Safety and Health Administration (OSHA) following a fatal construction accident at the Hyatt Regency Hotel in October 1979. As the OSHA investigation was not concerned with or related to the walkway construction, only limited portions of the walkways could be identified in the photographs.

With regard to construction materials, the firm of Miller and Glynn, legal counsel for Havens Steel Company, allowed the NBS team to review mill reports related to the walkway hanger rods and the MC8 x 8.5 shapes used to fabricate the walkway box beams. Information was also provided on welding procedures and electrodes believed by the steel fabricator to have been used in fabricating structural components of the walkways.

Of particular interest to the NBS investigative team were the original structural design calculations and any change orders involving the walkway structural system. However, efforts by the Office of the Mayor to obtain these documents were not successful. With regard to review and modification of the walkway design, the Office of the City Attorney provided copies of two documents that are relevant to this investigation. The first document, dated March 10 and March 16, 1978, contains six pages of handwritten notes addressing the issue of fire endurance of the walkway structural steel. It was prepared in the course of a routine design review by the Codes Administration Office, Kansas City, Public Works Department. The second document, dated April 4, 1978, is a two-page summary of a meeting between representatives of the Codes Administration Office and the architects, PBDML. These documents, which resulted in an agreement to encase the walkway structural steel with gypsum board, are referred to in section 9.2 of this report.

One other document of considerable value to this investigation is a report describing dynamic response measurements carried out on the third floor walkway just prior to its removal during the night of July 22-23, 1981 [2.5]. These measurements made it possible to validate the dynamic modeling of the walkways as described in section 9.6 of this report. Access to this material was arranged by the Crown Center Redevelopment Corporation.

## 2.8 SUMMARY

The following summarizes the results of efforts by NBS to obtain and review documents and other materials that are relevant to the design and construction

of the Hyatt Regency walkways and that provide information on events immediately preceding and following the collapse:

1. Codes and specifications applicable to the design, fabrication, and erection of the walkway structural system were referenced in the project specifications.
2. The AISC Specification for the Design, Fabrication and Erection of Structural Steel for Buildings forms the basis for the steel design provisions of the Kansas City Building Code.
3. Drawings obtained for review and reference included architectural and structural drawings and the fabricator's shop drawings.
4. The project design criteria specify a design live load of 100 psf (4.8 kPa) for hotel corridors and lobby areas. This is interpreted by NBS to include the walkways.
5. Efforts to obtain copies of the structural design calculations were unsuccessful.
6. Gypsum board encasement of the walkway structural steel was added during the design review stage to meet code requirements for fire endurance.
7. A videotape containing footage of activities in the atrium immediately before and after the walkway collapse was reviewed by the NBS investigative team.
8. Results of vibration testing of the third floor walkway were provided to NBS and were subsequently used to check analytical models of the walkway dynamic response.



### 3. DESCRIPTION OF THE WALKWAY SYSTEM PRIOR TO COLLAPSE

#### 3.1 INTRODUCTION

This chapter describes the structural features of the walkway system and the probable sequence of construction with emphasis on those structural aspects that are believed to be of significance to the investigation of the collapse. Extensive use is made of the contract and shop drawings referred to in chapter 2. In the remainder of this report all drawings other than shop drawings will be referred to collectively as "contract drawings." Only where a specific drawing is referred to will the terms "architectural" and "structural" be used.

Section 3.2 describes the Hyatt Regency atrium and location of the walkways. Also described are the areas served by the walkways and means of access from the atrium main floor, the tower section, and the hotel function block.

Section 3.3 describes the structural and architectural features of the walkways, again with major emphasis on those features that are believed to be of importance in identifying the most probable cause of collapse.

Section 3.4 discusses the probable sequence of construction. Where possible, this is related to documents referred to in chapter 2. However, very little of the construction sequence could actually be documented, and this section is by necessity based on what is considered to be a logical progression of construction. Section 3.5 describes a unified system used in this report for designating walkway components. Findings reported in this chapter are summarized in section 3.6.

#### 3.2 GENERAL LAYOUT OF THE HYATT REGENCY ATRIUM

The atrium is centrally located between the 40-story tower section to the north and the function block directly to the south (figure 3.1). Plan dimensions of the atrium are approximately 117 ft (36 m) north-south by 145 ft (44 m) east-west. Clear ceiling height is approximately 50 ft (15 m). The west portion of the atrium between column lines F and I and part of the tower section to the north of column line 11 are shown in plan view on figure 3.2. As can be seen

from figure 3.2, the main entrance is located on column line I, between column lines 10 and 11. The registration and cashier desks are located to the east of column line F, directly under a second floor terrace which extends over the entire east side of the atrium. Direct access to the terrace and to the shops and restaurants on the second floor of the adjoining function block (level 121) is by stairway or escalator located in the southeast corner of the atrium. An adjacent escalator provides access to the ballroom area on the third floor of the function block (level 136). A focal point of the atrium was a sunken lounge area on the main floor between column lines 8 and 10 (shown cross-hatched in figure 3.2).

Spanning the atrium in the north-south direction were three walkways as shown in figure 3.3. NOTE THAT THIS FIGURE IS BASED UPON AN ARCHITECTURAL DRAWING (DWG. A412) ISSUED FOR CONSTRUCTION ON AUGUST 28, 1978, AND DOES NOT ACCURATELY REFLECT THE SECOND AND FOURTH FLOOR HANGER ROD DETAIL ACTUALLY USED IN THE CONSTRUCTION OF THE WALKWAYS. The hanger rod detail actually used will be explained in the discussion of figures 3.9-3.11.

In addition to providing a direct traffic way between the tower section and the function block, the walkways were a dominant feature of the atrium and afforded a view of the atrium and terrace. Of the three walkways, the second floor walkway was most easily accessible from the atrium floor--by stairway or elevator (between column lines G and H) in the tower section and by stairway or escalator in the atrium. The third floor walkway, which served the ballroom area, evidently was intended to carry larger volumes of traffic since it was slightly wider than the other two walkways. The fourth floor walkway (level 151) served a health club and sports area in the upper portion of the function block and was accessible only by elevator or stairway in the tower section. Of the three walkways, the fourth floor walkway quite likely carried the least traffic. A schematic view of the walkways from the north end of the atrium is shown in figure 3.4.

### 3.3 STRUCTURAL AND ARCHITECTURAL FEATURES OF THE WALKWAYS

Structural framing plans for the three walkways are shown in figures 3.5 to 3.7. Unless noted otherwise, all structural steel is ASTM\* A36. Aside from the fact that the third floor walkway is 1'-3 5/8" (0.397 m) wider than the second and fourth floor walkways, structural details are identical. Each walkway consisted of four spans made up of W16 x 26 stringers placed 7'-6 3/8" (2.295 m) center to center (third floor = 8'-10" (2.692 m)) with W8 x 10 cross beams on 7'-3 3/4" (2.229 m) centers. Details of the stringers, including a 1/4 x 6 in (6 x 152 mm) bent plate used to form up the edge of the 3 1/4 in (83 mm) light-weight concrete deck are shown in figure 3.8. As shown in figure 3.9, the concrete deck was placed on a 20 ga (1 mm) formed steel deck with 6 in (152 mm) pitch and 1 1/2 in (38 mm) rib height. The walkway spans apparently were designed to act as composite beams and were constructed without shores (i.e., it is assumed that the concrete deck does not participate in resisting forces

---

\* American Society for Testing and Materials.

and moments due to self-weight of the concrete and structural steel). Shear studs are 3/4 in (19 mm) diameter x 3 1/2 in (89 mm) long. Reinforcement is W2.1 x W2.1 welded wire fabric with 6 in (152 mm) spacing each way.

The W16 x 26 stringers were bolted to clip angles welded to box beams located on column lines 8, 9 and 10. High strength 3/4 in (19 mm) bolts (ASTM A325) were used to fasten the stringer to clip angle connections. Details of the box beams and box beam to stringer clip angles are shown in figure 3.10.

The box beams were fabricated from MC8 x 8.5 shapes joined toe to toe by continuous longitudinal welds. The associated welding symbols included in figure 3.10 are as shown on the shop drawing (Havens Steel Company Dwg. 30). In the absence of a backing strip and with complete joint penetration indicated, this welding symbol is interpreted to mean a prequalified partial joint penetration groove weld as defined in section 2.10 of AWS D1.1-79, Structural Welding Code-Steel [3.1]. This welding symbol and its applicability to the box beam longitudinal welds are discussed further in chapters 5 and 10 of this report.

The walkway hangers were 1 1/4 in (32 mm) diameter rods threaded top and bottom to receive a nut and washer. Layout of the holes for the box beam-hanger rod connections is shown in figure 3.10. Layout of the box beams and hanger rods for the three walkways is shown in figure 3.11. Note that two hanger rods with a 4 in (102 mm) offset at the fourth floor walkway were substituted for the single continuous hanger rod arrangement shown in figure 3.3 and detailed on contract drawings A508 and S405.1. The significance of this change is discussed in chapter 10 of this report. The second and fourth floor walkways were suspended from the W18 x 40 beams shown on the atrium ceiling framing plan in figure 3.12 while the third floor walkway was suspended from the bottom chord of truss T1, also shown in figure 3.12. A detail of the hanger rod to beam connection at Elev. 165'-7" is shown in figure 3.11. A similar detail was used to connect the third floor walkway hanger rods to truss T1.

The south end (column line 7) of each walkway was supported by field welding the clip angles to 1/2 in (13 mm) plates embedded in the perimeter floor beams of the function block. The north end (column line 11) was supported by expansion bearings as detailed in figure 3.13.

The walkway handrail assembly consisted of 40 x 57 1/2 in (1.016 x 1.460 m) panels of 1/2 in (13 mm) tempered plate glass set in extruded aluminum grips supported by 4 x 3 x 5/16 angles running along each edge of the concrete deck as indicated in figure 3.9. Adjustment of the supporting angle was achieved by shim packs field welded to the concrete deck edging plate described previously. An extruded brass section capped the top edge of the plate glass panels and a continuous wood handhold completed the handrail assembly.

Documents on file with the Kansas City Public Works Department indicate that to satisfy requirements for fire endurance as specified in the Kansas City Building Code, the sides and bottom of each walkway were encased with two layers of 5/8 in (16 mm) gypsum board, supported by 22 ga (0.8 mm) metal studs and nailing strips attached to the structural steel by power driven fasteners.

A simplified detail of the structural system, handrail, and gypsum board encasement is shown in figure 3.14. Not shown is a lighting strip along the base of the handrail assembly and a system of 20 ga (1 mm) aluminum slats suspended from the bottom face of the walkways. The 1 1/4 in (32 mm) diameter hanger rods were also encased with insulating material, resulting in an overall diameter of 3 1/2 in (89 mm). A sprinkler system was suspended from the W8 x 10 cross beams of each walkway.

### 3.4 PROBABLE SEQUENCE OF ERECTION

Although a number of documents relating to construction of the walkways were reviewed during the course of this investigation, the actual construction sequence could not be clearly established. With regard to the second and fourth floor walkways, it is likely that all structural steel was erected and bolted prior to placement of metal decking. The next step would likely have been the arc spot welding (puddle welding) of the formed steel deck and placement of shear studs on the W8 x 10 cross beams, followed by placement of concrete by pumping. The daily construction log described in section 2.6 indicates that placement of concrete on all three walkways was carried out on September 26, 1979.

Since the concrete deck was unshored during construction and the W16 x 26 stringers were supplied without camber, the fraction of dead load due to the structural steel, formed steel deck, and the concrete produced midspan deflections of the order of 1/2 in (13 mm). To correct for this, a sand/cement topping course was added later. This is discussed further in chapter 5. The above procedure meets the provisions contained in the general notes of Dwg. S601.

Upon completion of the deck, the next logical step in the construction sequence would have been the installation of the handrail system. The midspan deflections described in the previous paragraph are apparent when the vertical alignment of the handrail supporting angle is compared relative to the top flange of the W16 x 26 stringers. All increments of dead load added during this and subsequent phases of construction were resisted by composite action of the stringer/deck system. Completion of the walkways involved the installation of the nailing strips and gypsum board, sprinkler system, aluminum slats, footlights, and walkway carpeting with underlying pad.

### 3.5 DESIGNATION OF WALKWAY COMPONENTS

Various components of the three walkways will be referred to rather extensively in the remainder of this report. So that these components can be clearly and concisely identified in the text, a unified system for designating walkway components will be adopted. In this system column lines 7 through 11 will be used to designate walkway components located on or between those lines while the letters U, M, and L (for upper, middle, and lower) will be used to designate the fourth, third, and second floor walkways, respectively. The letters E and W will be used to differentiate between the east and west sides of the walkways. For example, the designation "span U8-9" refers to the second span from the south end of the fourth floor walkway while "clip angle 10LW" refers to a clip

angle on the west end of the box beam in the second floor walkway at column line 10. Where it is clear that a particular level is intended, the U, M, or L designations are not included as, for example, in discussing the fourth floor to ceiling hanger rod at location 8E (column line 8, east side). This unified system applied to the fourth floor walkway is illustrated in figure 3.15.

### 3.6 SUMMARY

The following summarizes information available to the NBS investigative team regarding the layout of the Hyatt Regency atrium, location of the walkways and their accessibility, structural and architectural features of the walkways, and the probable sequence of their erection.

1. As its name implies, the atrium is central to hotel activities. The walkways were the dominant feature of the atrium.
2. Of the three walkways, the second floor walkway was most easily accessible from the atrium main floor. The third floor walkway served the hotel ballroom and, because of its greater width, was evidently intended to carry larger volumes of traffic than the second or fourth floor walkways. The fourth floor walkway was the least accessible and is likely to have carried less traffic than the other two walkways.
3. The walkway spans were apparently designed to act as composite beams and were constructed without shores (i.e., it is assumed that the concrete deck does not participate in resisting forces and moments due to self-weight of the concrete and structural steel).
4. In preparing the shop drawings, two hanger rods with a 4 in (102 mm) offset at the fourth floor walkway were substituted for the single continuous hanger rod arrangement detailed on the contract drawings.

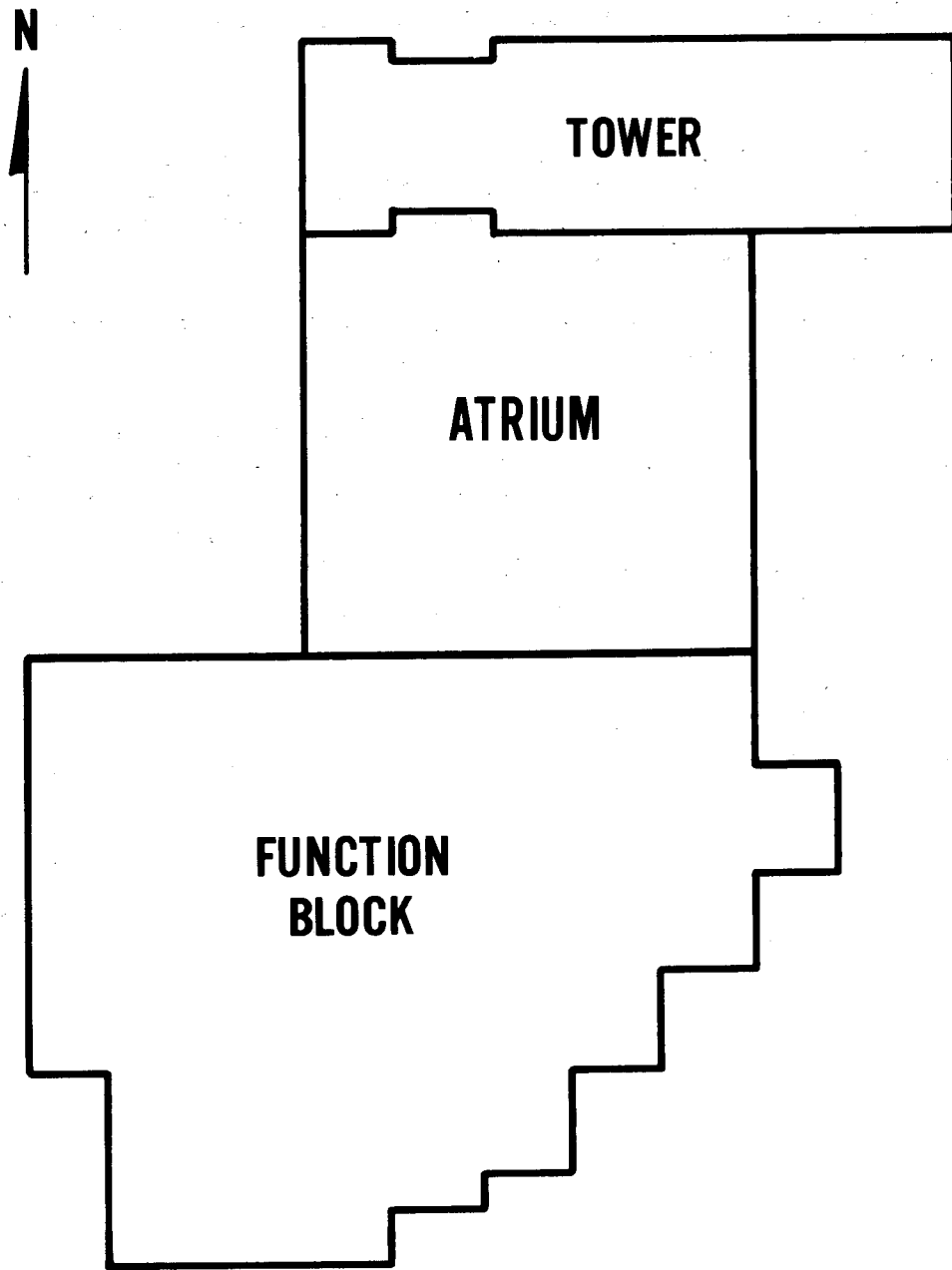


Figure 3.1 Plan showing outline of tower section, atrium, and function block.

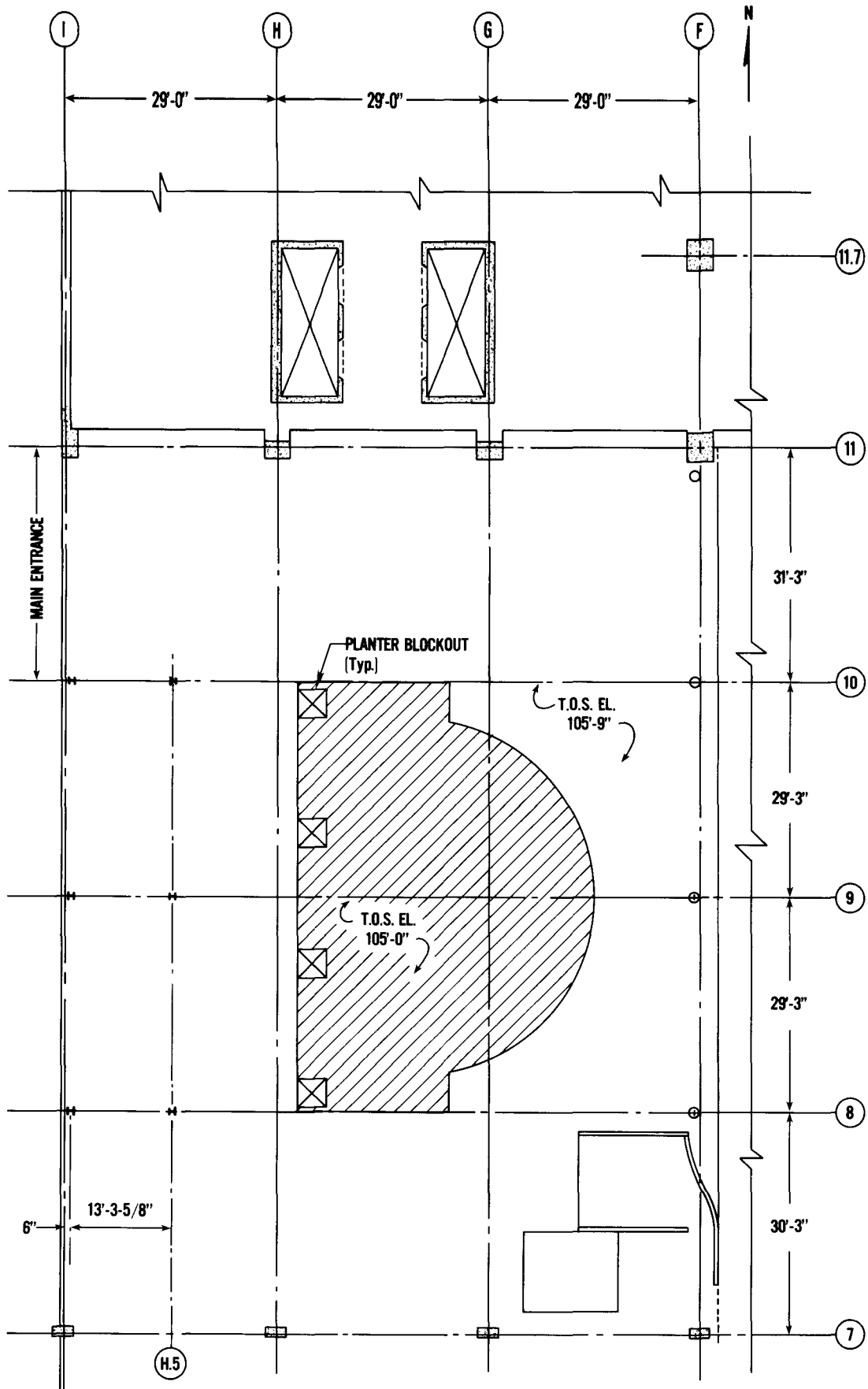


Figure 3.2 Plan view of atrium main floor (first floor) at level 106.

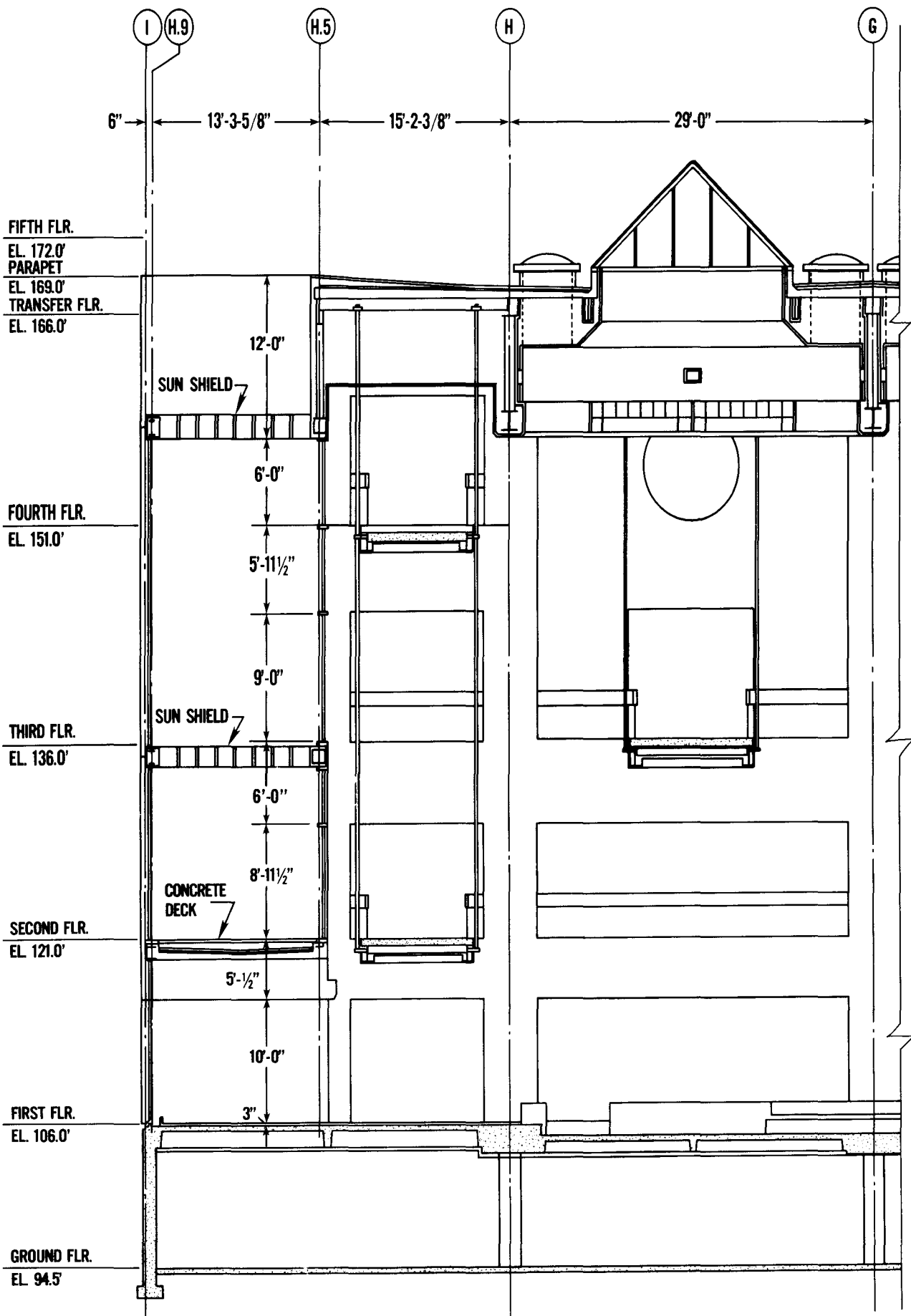


Figure 3.3 Elevation of atrium between column lines 8 and 9, looking north.

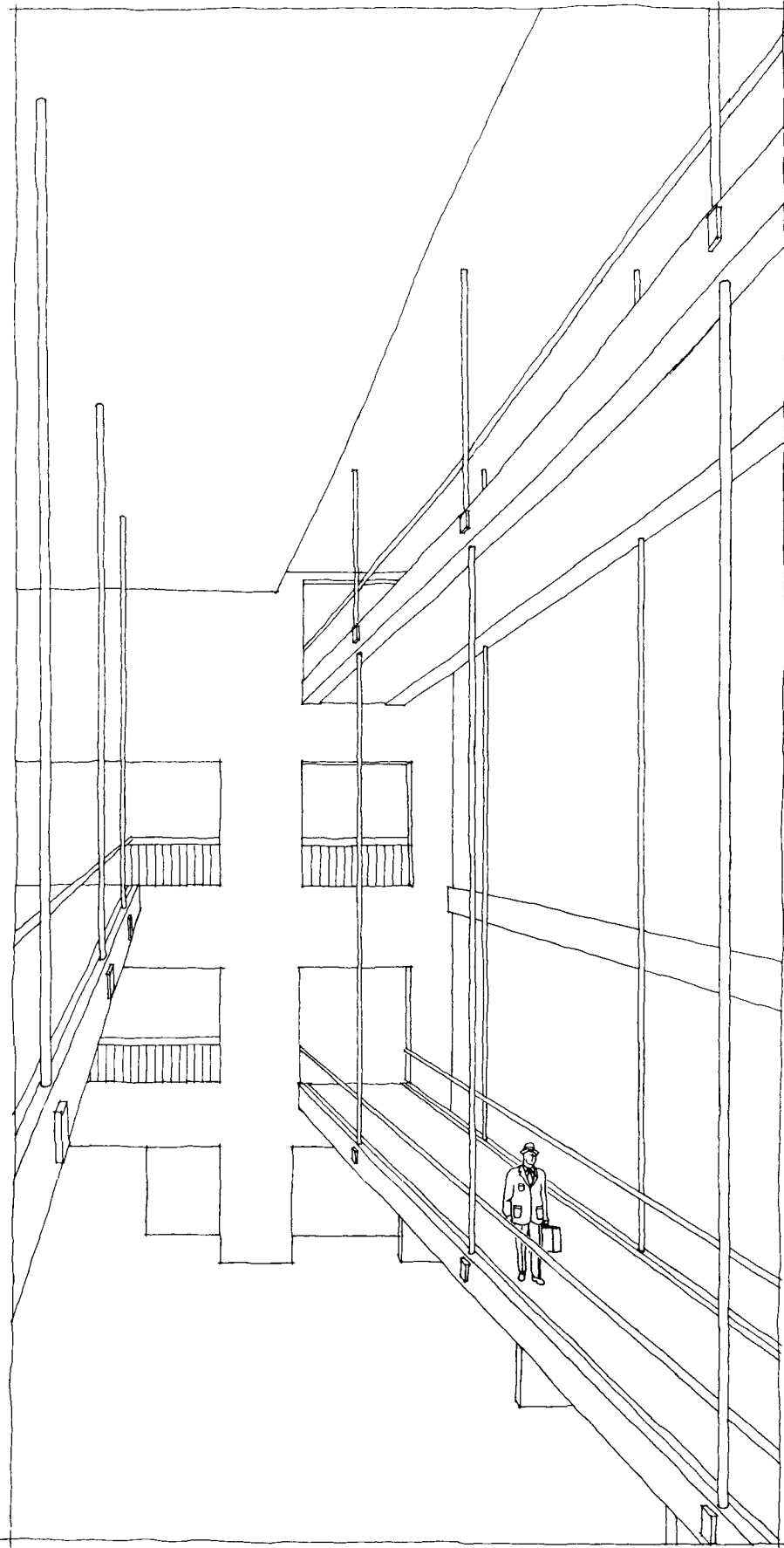


Figure 3.4 Schematic of walkways as viewed from north wall of atrium.

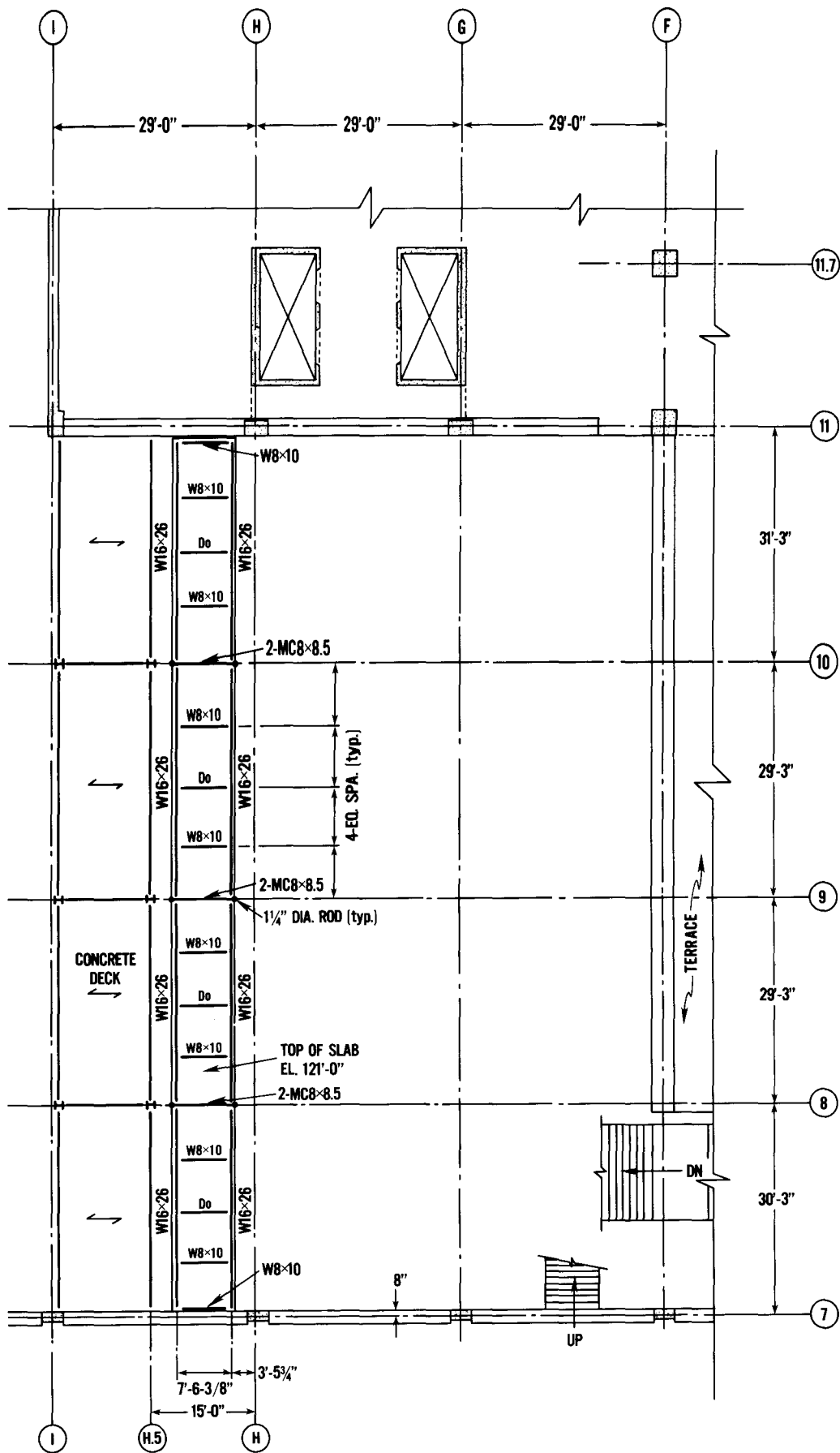


Figure 3.5 Second floor walkway framing plan - level 121.

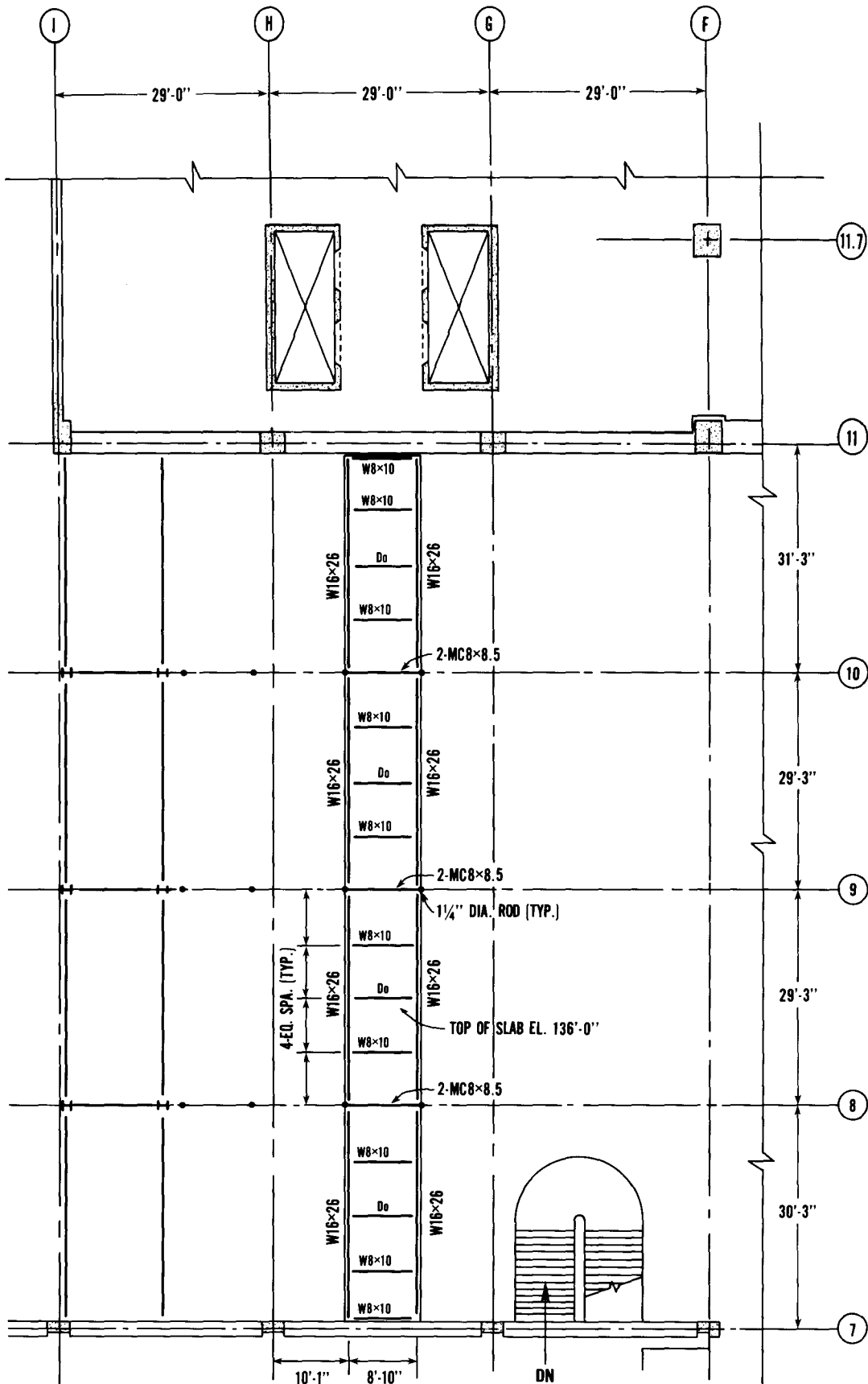


Figure 3.6 Third floor walkway framing plan - level 136.

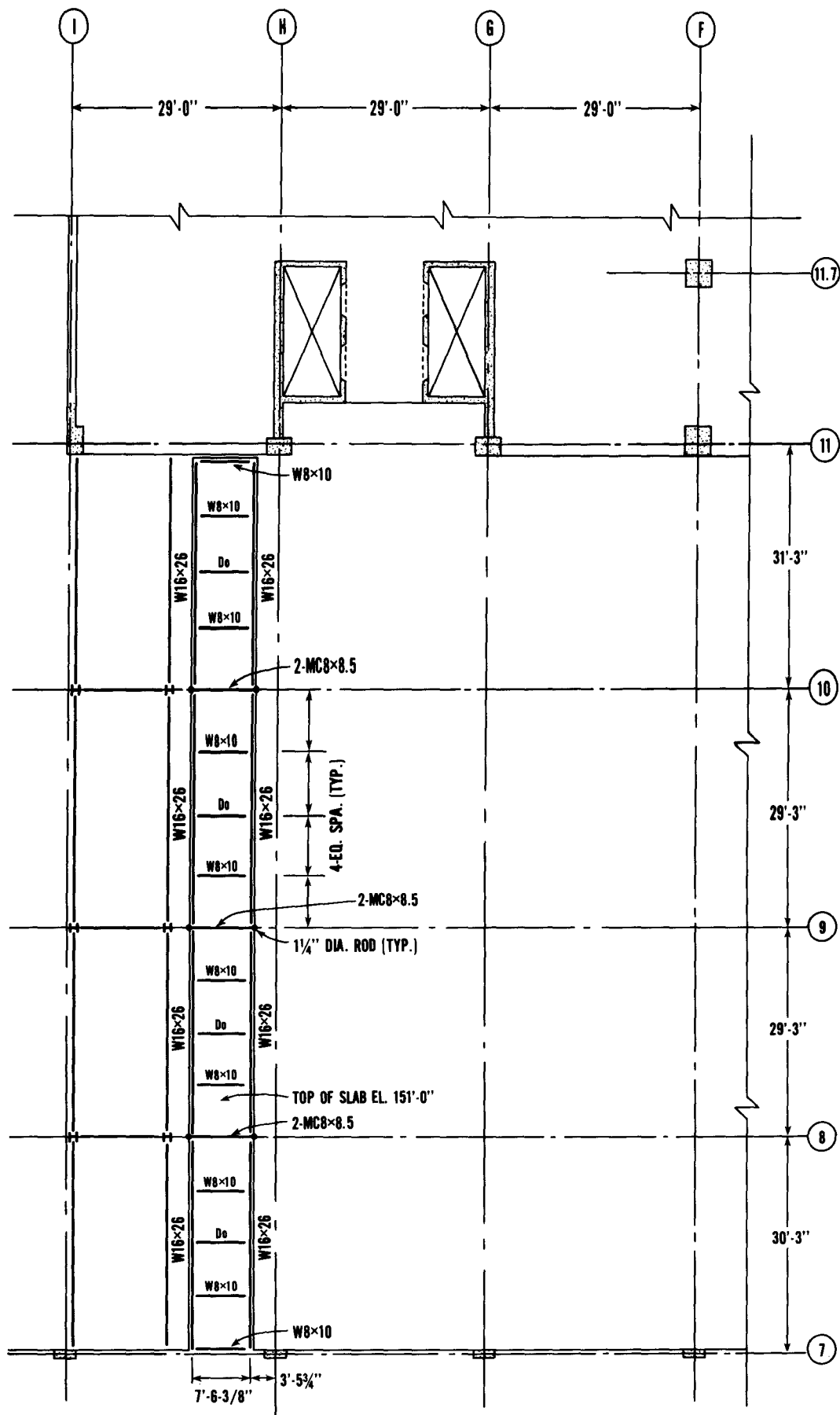


Figure 3.7 Fourth floor walkway framing plan - level 151.

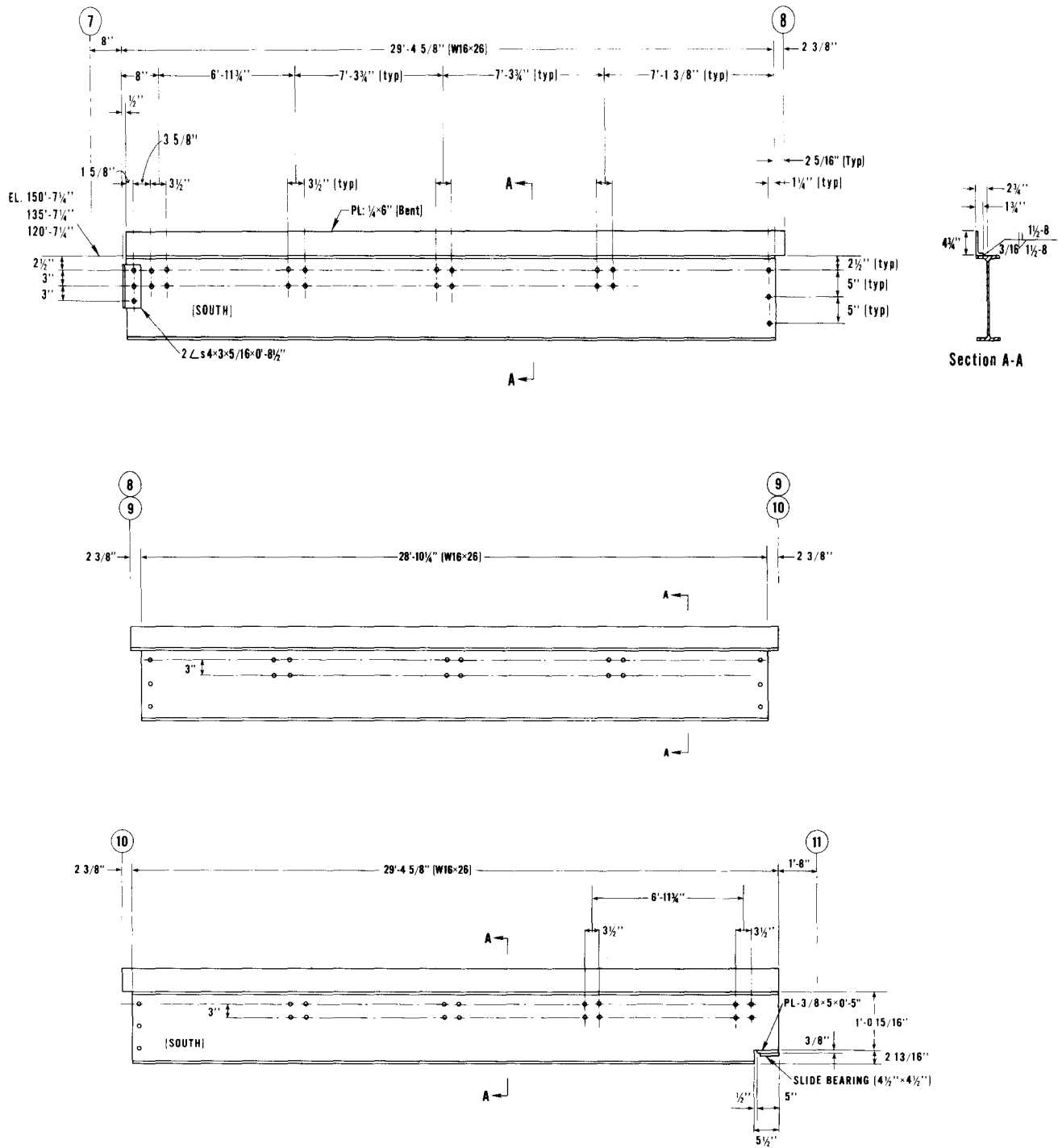


Figure 3.8 Details of walkway stringers.

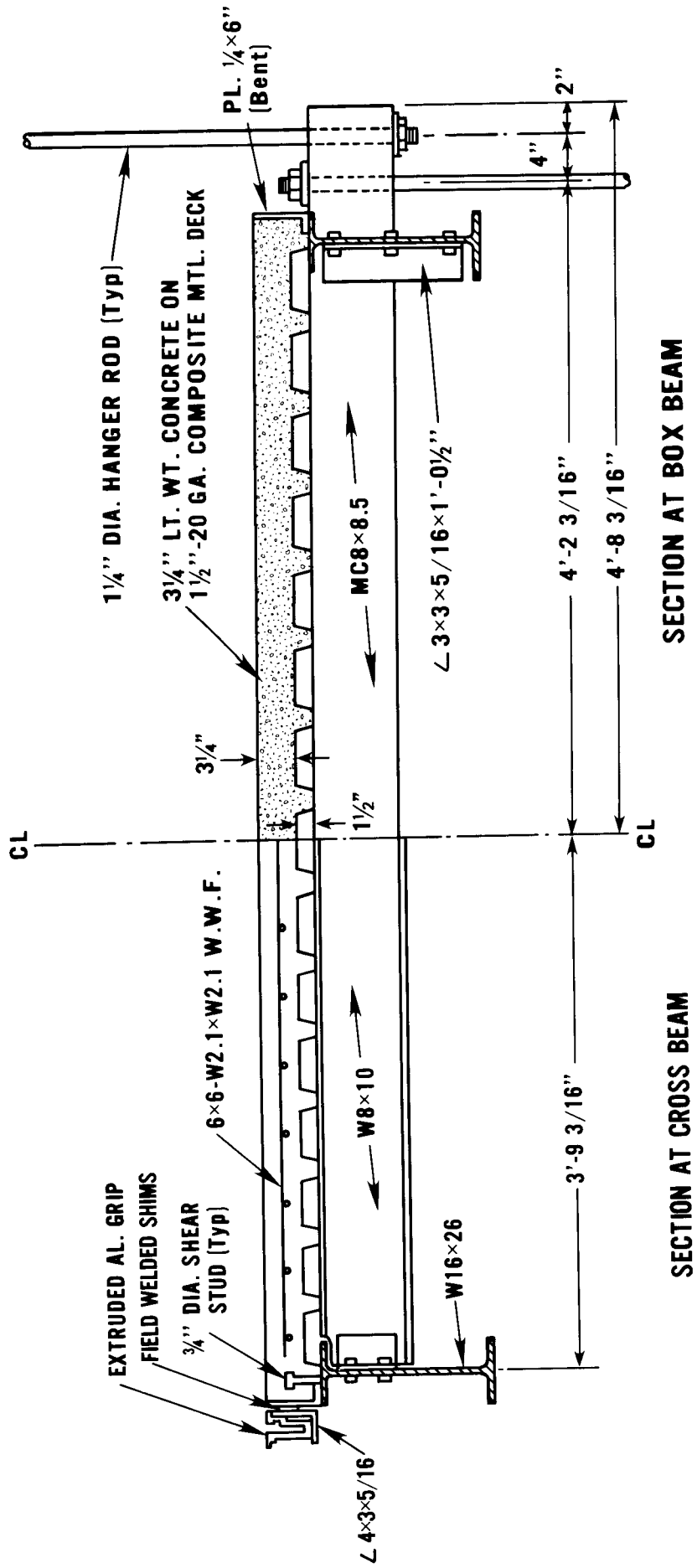


Figure 3.9 Typical transverse section of walkway deck.

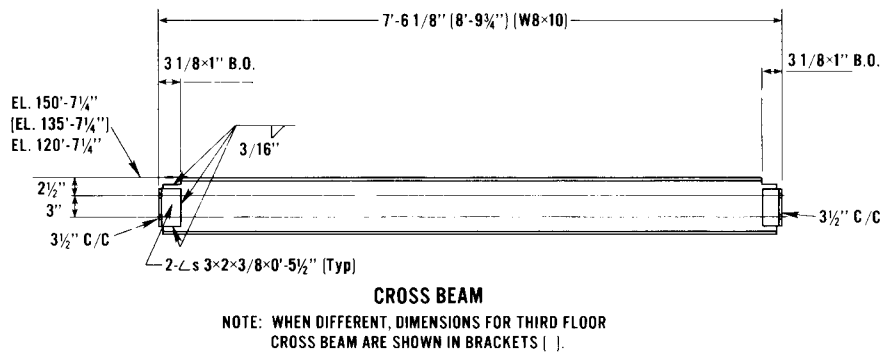
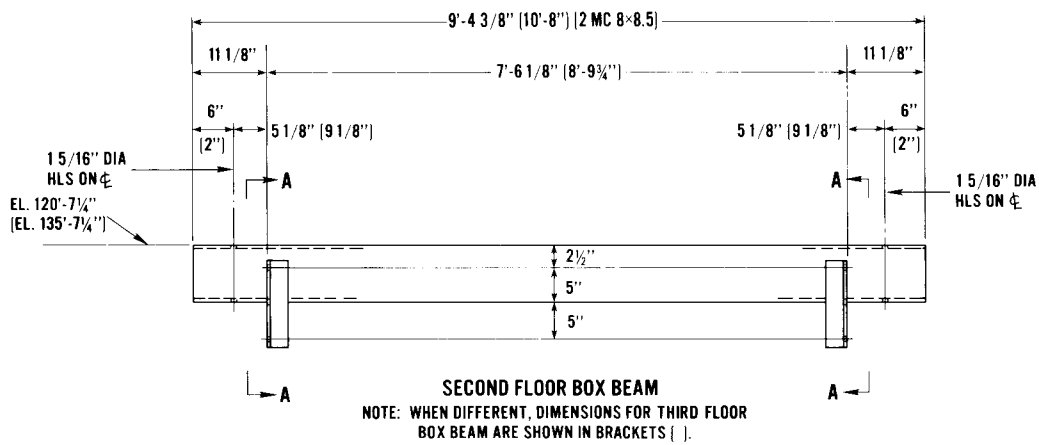
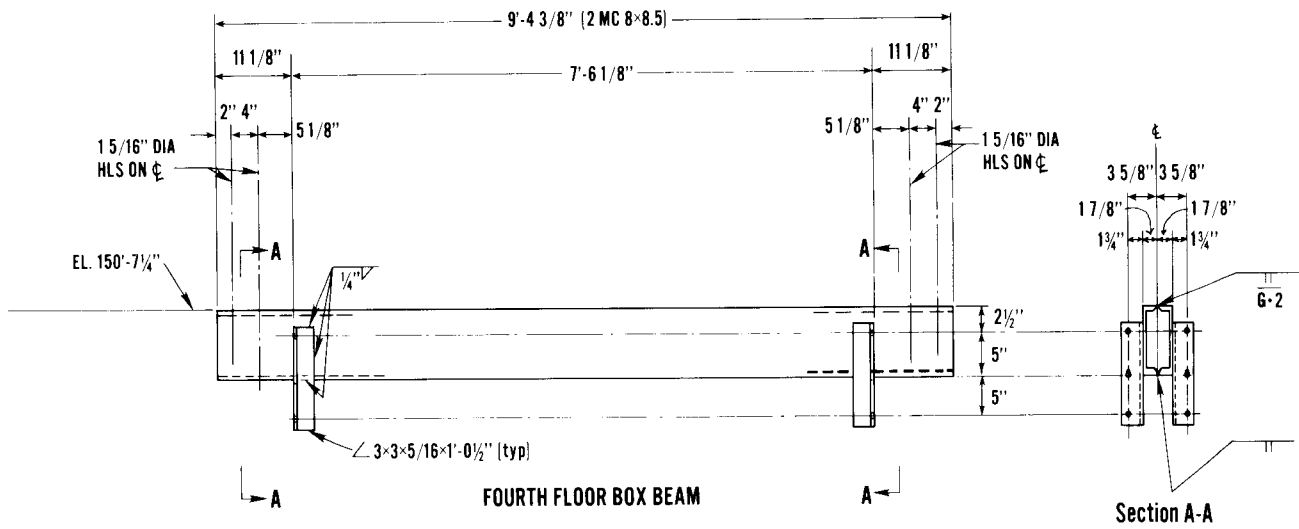


Figure 3.10 Details of walkway box beams and cross beams.

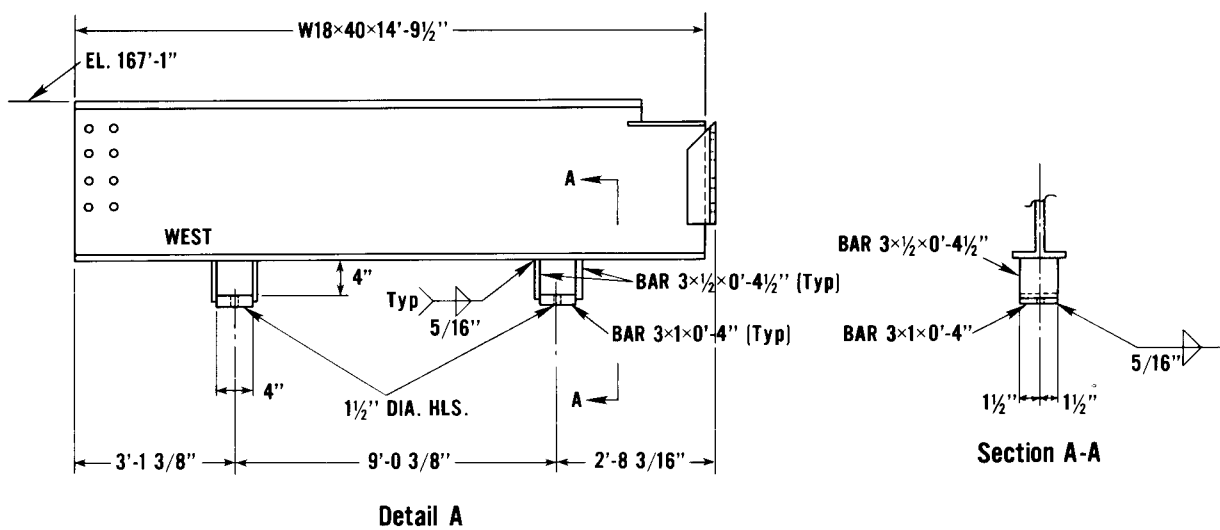
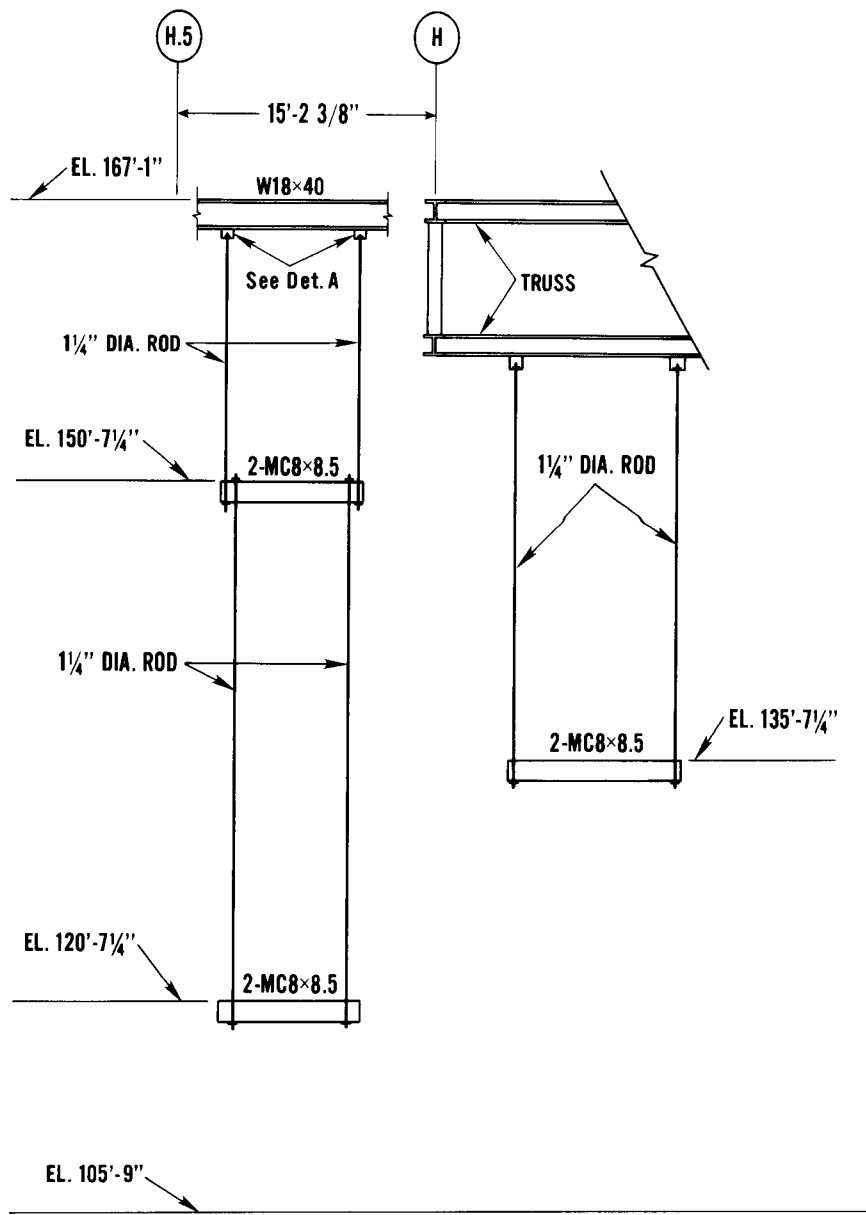


Figure 3.11 Elevation of typical box beam-hanger rod assembly.

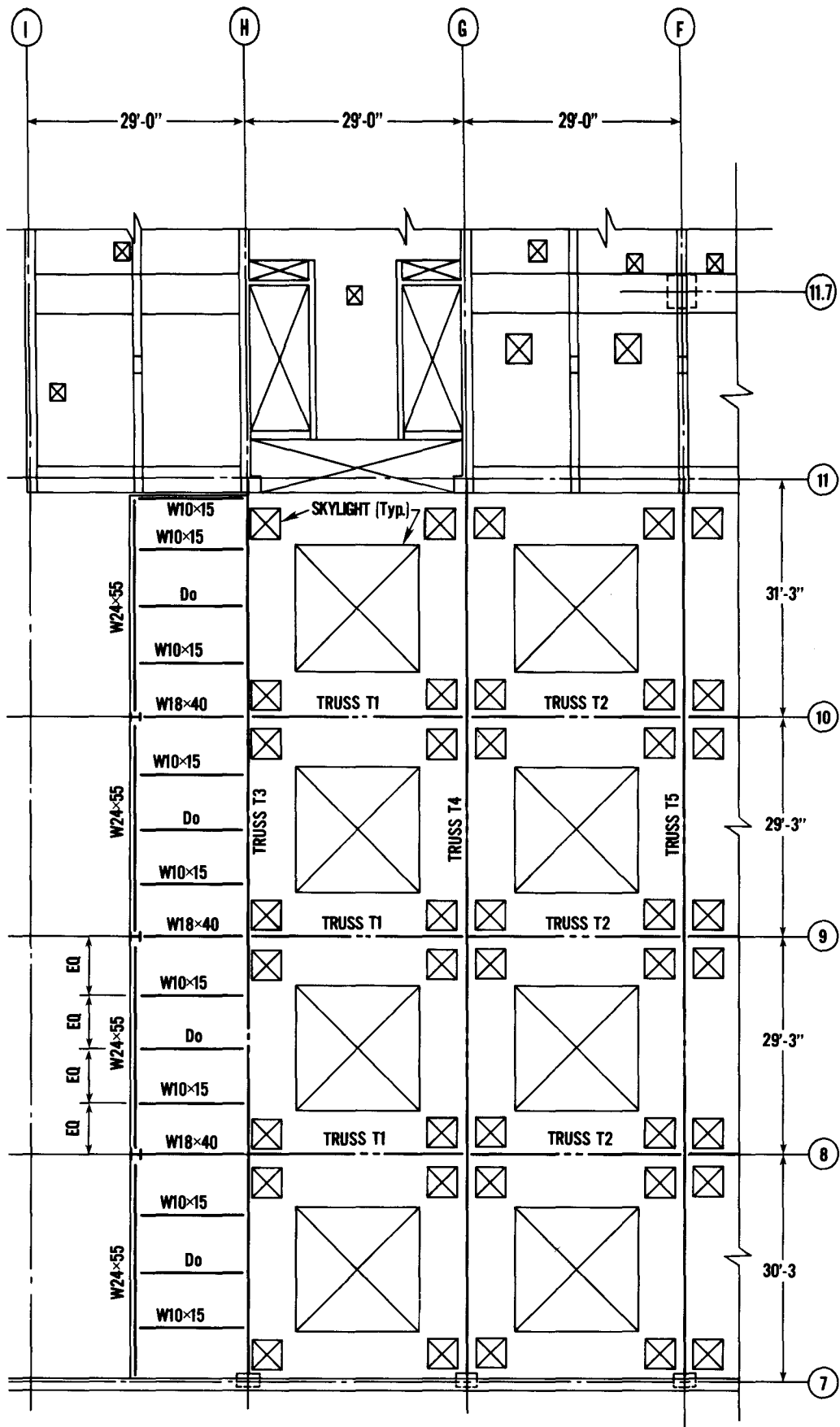


Figure 3.12 Framing plan for atrium roof.

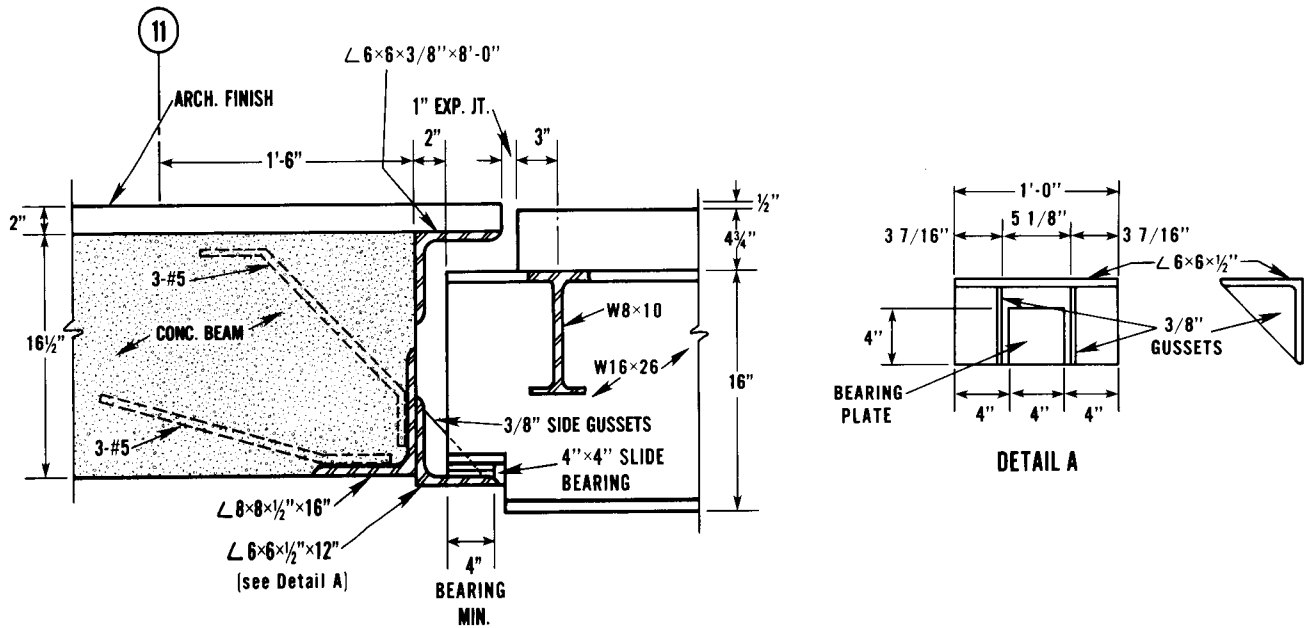


Figure 3.13 Detail of walkway expansion bearing at column line 11.

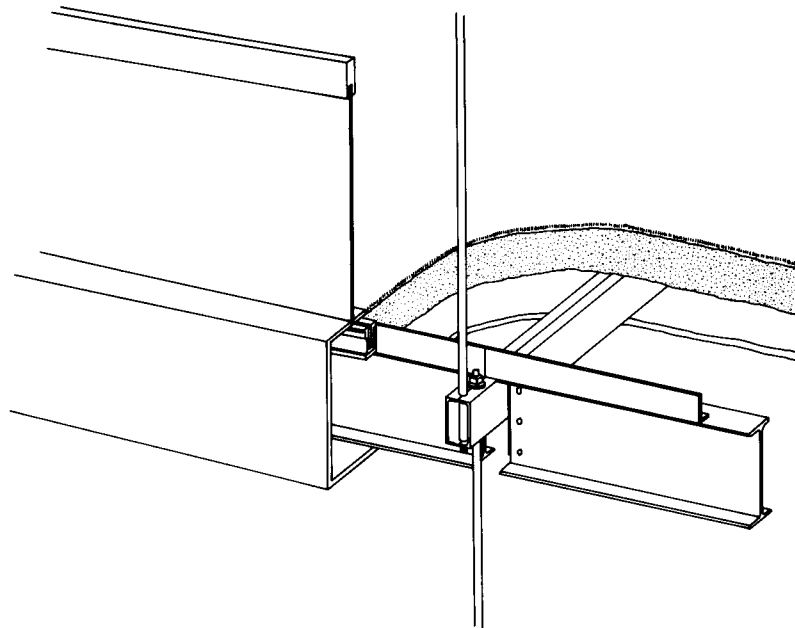


Figure 3.14 Simplified detail of walkway structural system and architectural treatment.

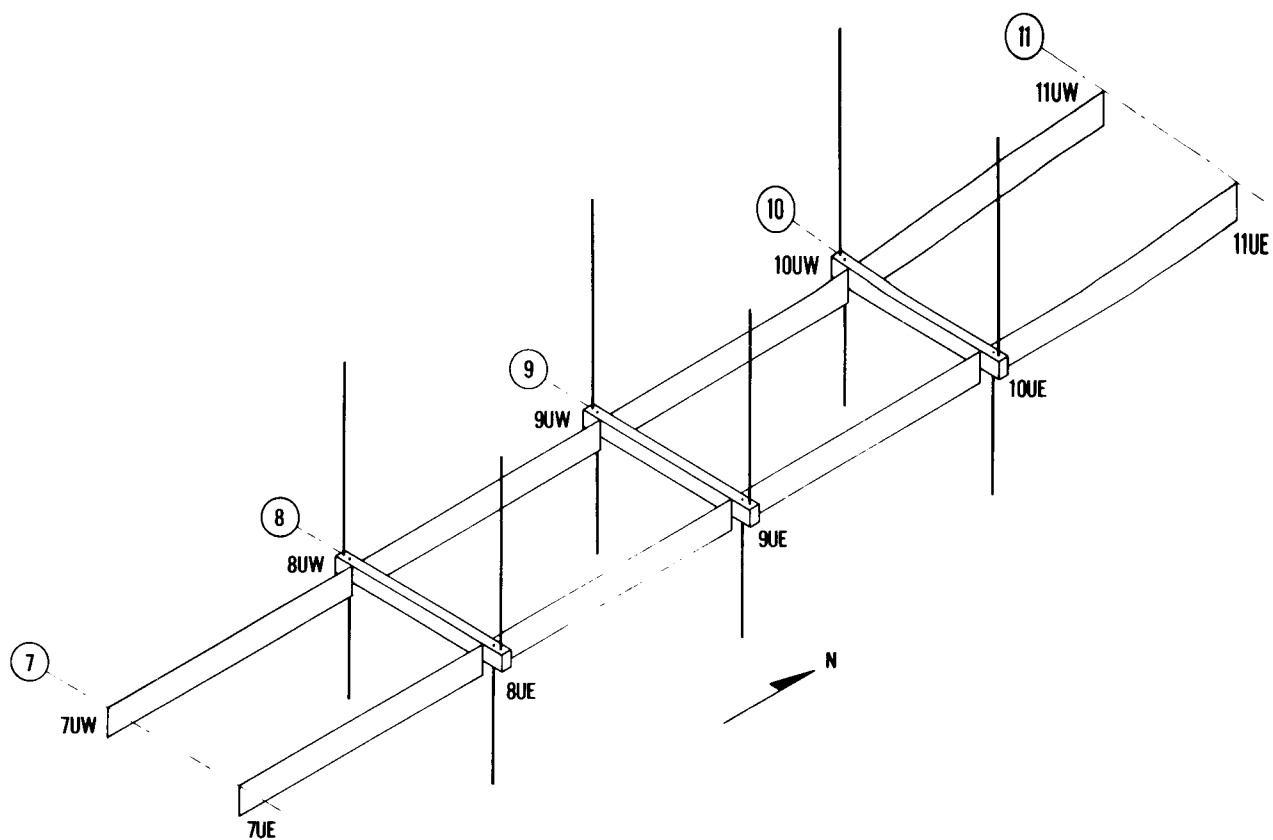


Figure 3.15 Unified designation of walkway components (fourth floor walkway shown).



## 4. DESCRIPTION OF THE WALKWAY COLLAPSE

### 4.1 INTRODUCTION

This chapter addresses the major events related to the collapse of the walkways, the rescue operation, and the removal and storage of the debris. Walkway occupancy at the time of collapse is also discussed.

Section 4.2 gives a chronology of events during the night of July 17-18, and presents photographs showing the walkway spans immediately after the collapse and after completion of the rescue operation. Section 4.3 summarizes eyewitness accounts of the collapse as reported in local newspapers.

Section 4.4 describes the analysis of videotape footage taken just prior to the collapse and presents an estimate, based in large part on this analysis, of walkway occupancy at the time of collapse.

Section 4.5 describes the removal and storage of the walkway debris, inspection of the atrium by NBS engineers, and removal of the third floor walkway. Findings reported in this chapter are summarized in section 4.6.

### 4.2 SUMMARY OF EVENTS PRECEDING AND FOLLOWING THE COLLAPSE

The following is a summary of events related to the walkway collapse and to the rescue operation as reported in The Kansas City Times, Metropolitan Edition, Saturday, July 18, 1981, and in The Kansas City Star, Extra, Sunday, July 19, 1981.

#### Friday, July 17

3:00 PM - People begin to arrive for dance event.

4:30 PM - Seating on first floor of atrium is fully occupied; people begin to occupy seating on atrium terrace and to assemble on walkways.

7:00 PM - Crowd in atrium area is estimated at 1500 to 2000.

- 7:04 PM - Band returns from break and begins to play for dance contest.
- 7:05 PM - Second and fourth floor walkways collapse.
- 7:08 PM - Kansas City Fire Department (KCFD) dispatcher receives first call for help.
- 7:09 PM - Kansas City Police Department (KCPD) dispatcher called.
- 7:12 PM - KCFD rescue squad at scene calls for additional help.
- 7:18 PM - Seven city ambulances at scene.
- 7:19 PM - Call goes out for cutting tools.
- 7:23 PM - Call goes out for forklift.
- 7:52 PM - More than 100 firefighters and emergency workers involved in rescue operation.
- 8:30 PM - Heavy crane arrives.
- 10:30 PM - Cranes moved into position near west wall of atrium.

Saturday, July 18

- 3:15 AM - First walkway section (span U8-9) lifted by cranes.
- 4:30 AM - Last survivor removed from debris.
- 6:00 AM - Span U7-8 lifted and set aside.
- 7:45 AM - Last span (presumably L7-8) is lifted and 31 bodies are removed.

As of Sunday, July 19, the reported death toll was 111. The number of injured was reported to be 188. (Two of the injured subsequently died.)

Figures 4.1 and 4.2 show the walkways shortly after the collapse, just as the rescue operation was getting under way. The photograph in figure 4.1 appears to have been taken from the stairway landing at the south side of the atrium between the second and third floors. The view is to the west-northwest and shows part of span U7-8 which lodged in the second-floor portal originally occupied by span L7-8. Spans U8-9 and U9-10 can be seen behind the trees in the middle of the picture. The photograph in figure 4.2 was taken from the third floor with the view directly to the north along the axis of the walkways. Span U7-8 is in the foreground and the third floor walkway can be seen to the upper right. Span U10-11 is visible at the far (north) side of the atrium. The north end of this span appears to have experienced an appreciable displacement to the west during the collapse. Water is coming from walkway sprinkler pipes severed when the north walkway spans were pulled off of their bearing seats.

A general view of the walkway debris after all victims had been removed is shown in figure 4.3. The view is to the south and shows span L9-10 resting on span U9-10 in the foreground. Directly to the south is span U8-9 (left) and span L8-9 (right). At the upper left is the south end of span U7-8. Span L7-8 is at the top of the picture, directly below its original position in the second floor walkway. Much of the debris is timber cribbing used to support the spans during the rescue operation. Span L10-11 is out of view in the left foreground and span U10-11 has been moved through the main entrance (to the right) and into the hotel driveway.

#### 4.3 EYEWITNESS ACCOUNTS OF COLLAPSE

In the same newspapers cited in section 4.2, eyewitness accounts of the collapse are reported as well as estimates of the number of people on the walkways and on the atrium floor directly below. These accounts can be summarized as follows:

- £ Individual standing at end of walkway (level unknown) saw upper walkway collapse at center first and then fall onto second floor walkway. Estimated about 50 people standing on fourth floor walkway, 100 people on second floor walkway and 200 people on atrium floor beneath the walkways.
- £ Individual (vantage point unknown) observed at least 40 persons on fourth floor walkway dancing or looking at scene below. Fourth floor began to buckle and collapsed. Area under walkway in vicinity of bar was jammed. Glass exploded, hitting people 100 to 150 ft away with shards.
- £ Individual on bandstand observed second floor walkway split in middle and begin to fall.
- £ Individual was "... sitting on steps in front part of lobby after walking across the catwalk moments before." Saw top walkway come straight down and hit second walkway which then fell. Estimated about a dozen people on fourth floor walkway, 75 to 100 on the second floor walkway, and 100 to 150 people below the walkways.

In view of the conflicting nature of eyewitness accounts and the availability of videotape showing parts of the walkways a few minutes before the collapse, this investigation did not include any organized effort to interview the injured or to solicit eyewitness accounts of the collapse. Attempts to obtain information from rescue workers regarding the numbers of dead and injured removed from the various sections of the walkways were largely unsuccessful, not because of any unwillingness to cooperate, but primarily because of great difficulty in recalling and discussing the event.

As will be discussed in chapters 5 and 10, it is possible to partially reconstruct the mode of collapse based on physical evidence contained in the walkway debris. However, the number of people and their location on the walkways at the time of collapse can only be estimated and will never be known

with certainty. Efforts to establish such an estimate are described in the following section.

#### 4.4 ESTIMATE OF WALKWAY OCCUPANCY AT TIME OF COLLAPSE

The most significant and helpful information regarding walkway occupancy is contained on a videotape shot by KMBC TV, channel 9, Kansas City, Mo. The news team was in the Hyatt Regency Hotel to film activities at the dance and was in the process of changing batteries when the collapse occurred. The tape contains scenes showing portions of the second and third floor walkways a few minutes before the collapse and scenes immediately following the collapse.

Three segments of the tape provided by KMBC TV were suitable for analysis. The scene in figure 4.4 is from the third floor balcony on the north side of the atrium with the view to the southwest. All of span L7-8 and most of span L8-9 of the second floor walkway are visible. A portion of the third floor walkway is visible at the upper right. The time bracket is believed to be 6:50 to 7:00 PM, based on the scheduled break of the band and their absence from the bandstand which is located directly below the banner on the south wall of the atrium. There appear to be 11 people on span L7-8 and 16 people on span L8-9. Of the 11 people on span L7-8, 10 appear to be standing at the handrail. Of the 16 people on span L8-9, 12 appear to be standing at the handrail.

The scene in figure 4.5, believed to have been taken a few minutes after the frame shown in figure 4.4, appears to be from the landing of the main stairway in the southeast corner of the atrium, looking northwest. Part of span L8-9 and all of spans L9-10 and L10-11 of the second floor walkway are visible. Eight or nine people are occupying the south portion of span L9-10 along the handrail and span L10-11 is not occupied.

The scene in figure 4.6, taken a few frames later, appears to be from the same location as that in figure 4.5, but shows more of span L8-9. Judging from their relative heights, the people on span L9-10 have not moved from their positions shown in figure 4.5. It appears that the count on span L9-10 is now 11, but blurring makes an accurate count difficult.

Figure 4.7 is a close-up of the southernmost span (span M7-8) in the third floor walkway. The view is from the same location as figure 4.4. Again, it is difficult to make an accurate count, but at least 11 persons can be observed.

Based on information obtained from the KMBC TV videotape, it is likely that the second floor walkway was occupied by approximately 40 people shortly before the collapse. The loading is taking place from south to north which is consistent with the location of the stairway and escalator in the southeast corner of the atrium. It is also consistent with the location of the bandstand and the dance contest in progress at the time of collapse.

In view of the relative inaccessibility of the fourth floor walkway, as described in section 3.2 of this report and the number of persons observed on the more accessible second and third floor walkways, the eyewitness accounts of

from 40 to 50 people on the fourth floor walkway would appear to be an exaggeration.

Based on information obtained from the KMBC TV videotape, an occupancy of the order of 16 to 20 people with 10 to 12 of them standing along the handrail is believed to be a reasonable upper bound for a second floor walkway span. It is also believed that three to four people per span, substantially less than the number observed on the second or third floor spans, is a reasonable upper bound for a fourth floor walkway span. Given these bounds and the fact that the bandstand and dance contest could best be observed from the south spans of the walkways, the distribution indicated in table 4.1 is considered to be a credible upper-bound estimate of walkway occupancy at the time of the collapse. The combined occupancy of the second and fourth floor walkways as indicated in this table is 63. However, it must be emphasized that the actual number of walkway occupants and their distribution never will be known with certainty.

#### 4.5 REMOVAL AND STORAGE OF WALKWAY DEBRIS

The initial removal of debris from the atrium area involved materials such as broken glass, gypsum board and aluminum slats that could not be identified with a specific walkway span. After marking each span with a code to identify its origin, the second and fourth floor walkway spans, along with segments of handrail and hanger rods, were moved by the Crown Center Redevelopment Corporation to a warehouse located at 28th and Warwick Streets, Kansas City, on the night of July 21-22.

On July 22, two NBS engineers were given access to the Hyatt Regency atrium and were allowed to take photographs. This visit was limited to making very general observations. The condition of the fourth floor to ceiling hanger rods was noted, including the absence of washers at locations 8E and 9E. The third floor walkway was still in place and small pieces of walkway debris remained on the atrium floor.

On the night of July 22-23, the third floor walkway was removed by the Crown Center Redevelopment Corporation and transported to the warehouse for storage with the spans of the other two walkways. Just prior to its removal, vibration measurements were obtained by the Crown Center Redevelopment Corporation. These measurements are referred to later in this report.

Based on subsequent inspections of the third floor walkway spans in the warehouse, the spans apparently were removed by the use of lifting slings placed around the W8 x 10 crossbeams at the quarter points of each span. This necessitated four cuts through the deck of each span to expose the ends of the cross beams. Span M9-10 appears to have been removed first since the stringers had been cut just short of the stringer to box beam connection on each end of the span. Removal then progressed each way from span M9-10 with each span retaining one box beam and remnants of the hanger rods which were cut just above the level of the handrail.

On August 13, the walkway hanger rods between the third floor and ceiling and between the fourth floor and ceiling, embedded plates at column line 7, and

the bearing seats at column line 11 also were removed from the atrium and sent to the warehouse for storage.

#### 4.6 SUMMARY

The following summarizes information and findings presented in this chapter:

1. The collapse of the second and fourth floor walkways is believed to have occurred at approximately 7:05 PM, Friday, July 17, 1981.
2. Analysis of the KMBC TV videotape indicates approximately 40 people on the second floor walkway shortly before the collapse.
3. A reasonable upper bound for single-span occupancy is believed to be 16 to 20 people.
4. It is concluded that a total of 63 people represents a credible upper-bound combined occupancy of the second and fourth floor walkways at the time of collapse.

Table 4.1 Estimated Upper Bound on Walkway Occupancy at Time of Collapse

<u>Span Number</u>	<u>No. of Persons Standing at East Handrail</u>	<u>No. of Persons Standing Near Walkway Center Line</u>
<u>Fourth Floor Walkway</u>		
U7-8	3	0
U8-9	2	0
U9-10	1	0
U10-11	1	0
<u>Second Floor Walkway</u>		
L7-8	12	8
L8-9	12	6
L9-10	10	4
L10-11	4	0



Figure 4.1 Walkways shortly after the collapse. View is to the west-northwest with span U7-8 sloping down and to the right. Spans U8-9 and U9-10 are visible behind the trees. Photo by Greg Smith, reprinted by permission of The Kansas City Times, © 1981, The Kansas City Star Company.



Figure 4.2 Walkways shortly after the collapse. View is directly to the north along the axis of the walkways. Span U7-8 is in foreground and third floor walkway is at upper right. Water is coming from broken sprinkler pipes. Photo by Greg Smith, reprinted by permission of The Kansas City Times, © 1981, The Kansas City Star Company.

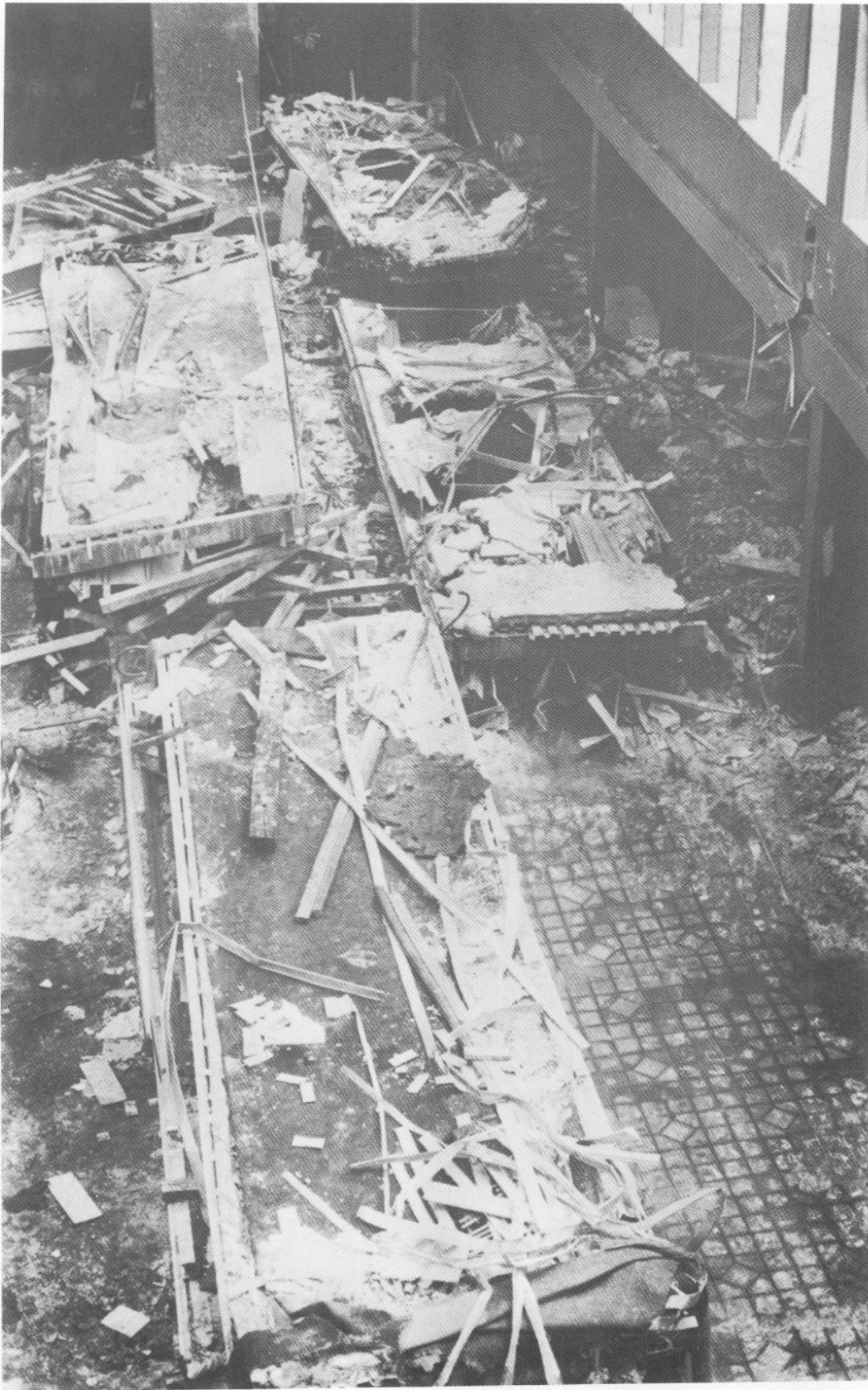


Figure 4.3 Aftermath. View is to the south with span L9-10 resting on span U9-10 in foreground. Next are spans U8-9 (left) and L8-9 (right). Span U7-8 is at upper left and span L7-8 is at upper right. Photo courtesy of Kansas City Police Department.



Figure 4.4 Scene from third floor balcony on north side of atrium. View to the southwest showing spans L7-8 and L8-9 of second floor walkway. Videotape courtesy of KMBC TV.

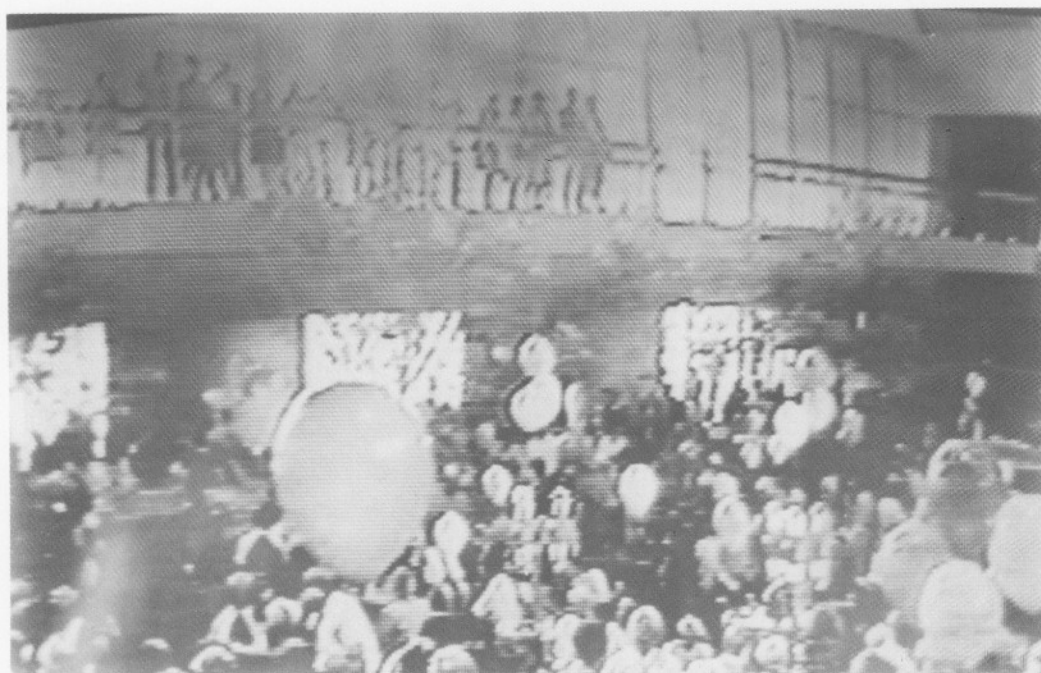


Figure 4.5 Scene from landing of main stairway in southeast corner of atrium. View to northwest shows part of span L8-9 and all of spans L9-10 and L10-11 of second floor walkway. Videotape courtesy of KMBC TV.



Figure 4.6 Same view as figure 4.5, but a few frames later. Videotape courtesy of KMBC TV.



Figure 4.7 View from third floor balcony on north side of atrium. View to southwest showing southernmost span (span M7-8) of third floor walkway. Videotape courtesy of KMBC TV.

## 5. SITE INVESTIGATION

### 5.1 INTRODUCTION

This chapter deals exclusively with measurements and observations made in the course of several visits to the Hyatt Regency atrium and to the warehouse during the period July 28 to December 17, 1981.

Section 5.2 describes the survey of the Hyatt Regency atrium and the probable alignment of the walkways prior to collapse. Initial movement of the walkway spans and their general drift during the collapse are related to observations of hanger rod distortion and points of impact on the atrium floor.

Section 5.3 describes the layout of the walkway spans in the warehouse and their general condition. Emphasis is on the box beams of the fourth floor walkway. Distortions of the box beams due to hanger rod pull-through and fractures along the longitudinal box beam welds are described in detail. Also described in this section is the procedure used to estimate the original weights of the walkway spans.

Section 5.4 describes the criteria used for selection of physical specimens, procedures followed in marking and removing the specimens, and their cataloging and handling after arrival at NBS. Section 5.5 describes the procedure used in obtaining replicas of fracture surfaces and the subsequent removal of selected fracture surfaces for scanning electron microscopy. Section 5.6 summarizes the conclusions drawn in this chapter.

### 5.2 SURVEY OF THE HYATT REGENCY ATRIUM

To establish the actual alignment of the second and fourth floor walkways prior to collapse, NBS commissioned a survey of the west portion of the Hyatt Regency atrium [5.1]. This survey was carried out on August 5, 1981, after removal of the third floor walkway but prior to removal of the fourth floor to ceiling hanger rods and the embedded plates and bearing seats at column lines 7 and 11, respectively. No measurements were made with respect to the third floor walkway.

For convenience, a benchmark was established on the atrium floor at a point 0.15 ft (45 mm) west and 0.10 ft (30 mm) south of the southwest corner of the column located at the intersection of column lines 11 and H. For the purposes of this survey, the benchmark elevation was assumed to be 0.00. To establish relative horizontal position, three transit lines (T.L.) were located on the atrium floor; (1) T.L. 1 parallel to column line 11 on the north side of the atrium. (2) T.L. 2 on a north-south line centered with the first-floor passageways directly under the walkway at column lines 7 and 11. (3) T.L. 3 parallel to column line 7 on the south side of the atrium (see figure 5.1). Positions of hanger rods, bearing seats, and points of impact on the atrium floor are subsequently described as north-south and east-west departures from the intersection of T.L. 1 and T.L. 2. All distances and elevations were determined to the nearest 0.01 ft (3 mm).

#### 5.2.1 Embedded Plates and Bearing Seats

Locations of the embedded plates and wall openings at column line 7 (south) and the expansion bearing seats and wall openings at column line 11 (north) are shown in figure 5.1. It is apparent from figure 5.1 that the embedded plates at column line 7 on the fourth floor level (El.45.00 with respect to the datum of this survey) are approximately 0.15 ft (45 mm) south of the corresponding plates on the second floor level. As will be discussed subsequently, this misalignment required a retrofit of the bearing pads on the stringers of the north span of the fourth floor walkway (span U10-11). North-south alignment of the bearing seats at column line 11 is far better, the fourth floor bearing seats being 0.02 ft (5 mm) north of those at the second floor level.

Each embedded plate at column line 7 is made up of two 1/2 x 6 x 14 in (13 x 152 x 356 mm) plates placed as shown in figure 5.2. Also shown in figure 5.2 are the locations of the fillet welds which made up the shear connection with the walkway stringers. Based on these dimensions, the east-west alignment of the walkways with respect to T.L. 2 at column line 7 was as follows:

Fourth floor walkway = 0.01 ft (3 mm) E  
Second floor walkway = 0.04 ft (10 mm) E

The expansion bearing seats at column line 11 have already been described in section 3.3 (see figure 3.13). The gusset plates, in addition to increasing the stiffness of the bearing seats, also served as lateral guides for the stringer bearing pads. Assuming these pads were centered between the gusset plates, the east-west alignment of the walkways with respect to T.L. 2 at column line 11 was as follows:

Fourth floor walkway = 0.05 ft (15 mm) E  
Second floor walkway = 0.05 ft (15 mm) E

#### 5.2.2 Fourth Floor to Ceiling Hanger Rods

In table 5.1 are listed the north-south and east-west coordinates of the fourth floor to ceiling hanger rods which remained in place during the collapse. As previously noted, these coordinates are referenced to the point of intersection

of T.L. 1 and T.L. 2. Two sets of coordinates are presented in table 5.1--one set for the hanger rod positions at a point approximately 18 in (460 mm) below the plane of the ceiling and one set for the lower end of the hanger rods. Ideally, the coordinates of the hanger rods at the upper hanger fixture should have been established, but this was not possible with the ceiling panels in place. The upper coordinates are based on the assumption that the hanger rods are centered in the 3 1/2 in (89 mm) diameter fire resisting encasement.

The elevations of the lower rod tips and the elevations of the points at which the hanger rods pass through the ceiling are presented in table 5.2. Again, these elevations are referenced to Elev. 0.00 (assumed datum) at the first floor level. The overall length of the fourth floor to ceiling hanger rods was subsequently determined to be 15'-11 1/8" (4.85 m).

### 5.2.3 Impact Points on Atrium Floor

When the second floor walkway impacted the atrium floor, the second to fourth floor hanger rods and the second floor walkway stringers punched through or otherwise damaged the floor tiles at column lines 8, 9 and 10. At column lines 9 and 10 these hanger rod impact points were clearly identifiable. The corresponding impact points at column line 8 are believed to have been caused by the stringers in the south span of the second-floor walkway (L7-8). At column line 10 there are two sets of hanger rod impact points (see figure 5.3), indicating rebound of the walkway and possibly the effect of the fourth floor walkway impacting. Coordinates of major impact points are listed in table 5.3.

### 5.2.4 Alignment of Walkways Prior to Collapse

With the survey data just presented and with measurements obtained from the walkway debris (see section 5.3.5), it is possible to establish the general alignment of the walkways prior to collapse. In doing this it is convenient to use the second floor walkway as a base line because of its apparent good fit with the embedded plates and bearing seats and because it is directly related to the observed impact points on the atrium floor. It is assumed here that both walkways had no horizontal curvature and that the hanger rod holes were located in the box beams according to the dimensions indicated in figure 3.10.

Alignment of the upper hanger rods at their intersection with the ceiling and the alignment of the fourth floor walkway, all relative to the second floor walkway, are presented in table 5.4. Other than the problem with the embedded plates on the fourth floor at column line 7 as previously described, the horizontal misalignment of the walkway system was less than 0.10 ft (30 mm). It should be noted that the upper ends of the fourth floor to ceiling hanger rods were more closely aligned with the fourth floor walkway than with the second.

The survey data and measurements from the walkway debris (table 5.8) also make it possible to check the positioning of the walkway stringers on the beam seats at column line 11 prior to collapse. Typically, the 4 in x 4 in (102 x 102 mm) slide bearing plates are positioned 3/8 in (10 mm) from the south edge of the bearing seats. Based on measurements of actual member lengths as described in section 5.3.5 and accounting for the fact that retrofit of the fourth floor

bearing pads extended the stringers by 2 1/4 in (57 mm), the calculated overlap of the slide bearing plates is 4.2 in (107 mm) and 3.7 in (94 mm) at the second and fourth levels, respectively. Scratch marks observed on the slide bearing plates indicate that the actual overlap was very close to 4 in (102 mm) for both walkways.

With regard to vertical alignment of the fourth floor walkway, measurements taken on the embedded plates and bearing seats in the atrium and on the debris subsequent to its removal and storage indicate the top flanges of the W16 x 26 stringers were positioned 0.44 to 0.48 ft (135 to 145 mm) below the level of the finished floor (Elev. 45.00). Assuming the structural steel was properly leveled during erection, the minimum protrusion of the fourth floor to ceiling hanger rods through the bottom face of the box beams would have been 0.14 ft (45 mm) at hanger rod 10E. Subsequent measurements indicated a maximum combined thickness of nut and washer equal to 0.115 ft (35 mm). Therefore, with the fourth floor properly leveled, there would have been adequate clearance to install a nut and washer on each fourth floor to ceiling hanger rod.

#### 5.2.5 Other Observations Relevant to the Investigation

In table 5.5 the locations of the impact points are listed in terms of departures from the lower hanger rod positions at the second floor walkway prior to collapse. All four spans in the second floor walkway experienced a consistent drift to the west and south during the collapse. The westward drift suggests initial loss of support along the east side of the walkway system while the fixity at column line 7 would be expected to promote a southward drift of both walkways. There was no visible sign of the walkway spans contacting the north wall of the atrium, suggesting that they continued to move to the south after the stringer bearing pads cleared the bearing seats. The locations of the impact points in the vicinity of column line 8 strongly suggest that span L7-8 rotated vertically around its supports at column line 7 and that the north end of the span drifted to the west before the bottom flanges of the stringers impacted the atrium floor.

There was extensive damage to the granite paneling on the south wall of the atrium at the second floor level. It is likely that most of this damage resulted from impact of the south span of the fourth floor walkway which came to rest with its stringers positioned on the second floor edge beam and slightly west of the original alignment.

As has been noted in section 4.5, washers were missing from the lower ends of the fourth floor to ceiling hanger rods at locations 8UE and 9UE. It was also observed during the course of the atrium survey that the washer at location 9UW had fractured along two radial lines, resulting in the loss of a short segment. This will be discussed further in section 5.3.2.

One final observation of importance is the pronounced bend to the west at the bottom end of hanger rod 10UW and a lesser bend at the bottom of hanger rod 8UW as can be seen in figure 5.4. Not apparent in figure 5.4 is a slight bend at the bottom of hanger rod 9UW which was detected after the hanger rods had been removed to the warehouse. The absence of appreciable distortions in hanger

rods 8UE, 9UE, and 10UE strongly suggests that failure initiated along the east line of hanger rods.

### 5.3 OBSERVATIONS OF WALKWAY DEBRIS

On July 29, 1981, the NBS investigative team was allowed its first access to the walkway debris. Under the terms of a court order dated July 24, 1981, issued by the Circuit Court of Jackson County, Mo., and covering protective custody of the debris, the taking of impressions, marking, or otherwise disturbing any of the debris was expressly forbidden. Until permission was eventually obtained to weigh the walkway spans and to remove certain physical specimens, on-site activities of the investigative team were limited to visual observations, taking of photographs, and dimensional measurements.

The layout, orientation and identification of the walkway spans in the warehouse at 28th and Warwick Streets in Kansas City are indicated on figure 5.5. Also indicated in this figure are the locations of the box beams which remained attached to one or the other adjacent spans during the collapse. A general view of the fourth floor walkway spans is shown in figure 5.6.

#### 5.3.1 General

It was evident that the moving and storage of the debris had been carried out with considerable planning and great care. The NBS team found no reason to believe that any of the spans suffered additional damage or were otherwise altered during the move from the hotel. The NBS team also found all spans to be reasonably accessible and properly identified.

In general, the rescue operation at the hotel caused only superficial damage to the spans as can be seen from photographs taken immediately after the collapse. This included loss of some glass panels in the handrail assembly which was necessary for positioning of the lifting slings, penetration of the concrete deck by jackhammering, and various cuts in the second to fourth floor hanger rods. The one exception was span L8-9 where extensive portions of the deck had been removed and the stringers had been flame cut near the north end of the span. It also appeared that the bolts in the clip angle to stringer connections at the south end of span U7-8 had been removed and reinstalled.

#### 5.3.2 Hanger Rod Pull-Through

The fourth floor to ceiling hanger rods had pulled through both the bottom and top flanges of each box beam in the fourth floor walkway (figure 5.7). The mode of failure involved the upward rotation of the bottom flanges of the MC8 x 8.5 shapes and extensive localized yielding in each web directly above the fillet line (figure 5.8). This was accompanied by fracture of the lower longitudinal weld back to the inner hanger rod hole and, in some cases, well beyond the inner hole. Pull-through in the upper flange generally resulted in less distortion of the flanges and the localized yielding in the webs much closer to the fillet line. Similar plastic deformation of the box beam ends was also observed at several locations in the third floor walkway (figure 5.9).

Hanger rod pull-through was marked by substantial scraping and gouging damage to the flange surfaces adjacent to the bottom outer hanger rod holes in the fourth floor box beams. Steps in the abraded region indicated that slippage of the washer/nut combination was periodically arrested during the failure process. Figure 5.10 illustrates this "slip-stick" type of failure at location 9UE. The absence of impact marks on the inner flange surfaces around the upper hole at location 8UW indicates the upper longitudinal weld seam was widely separated at the time of pull-through. The mangled condition of the box beam at location 10UW is believed to have been caused by the 1/4 x 6 in (6 x 152 mm) edging plate on span U10-11 running past the box beam on impact (figures 5.11 and 5.12). A similar effect was observed at location 8UW.

Washers were missing from the lower ends of the fourth floor to ceiling hanger rods at locations 8UE and 9UE. However, part of the washer at location 9UW was also missing (figure 5.13), suggesting that the missing washers fractured and were lost during the collapse. Figure 5.10 provides clear evidence that a washer was originally installed at location 9UE. There was also visual evidence which indicated that a washer was present at location 8UE. This was later confirmed by detailed examination of the washer/nut contact area as described in chapter 8.

There is a symmetry to the deformation and distortion of the box beam ends in the fourth floor walkway. As illustrated by figure 5.14, there is no evidence of rotation in the north-south direction of box beam 9U during the collapse. Conversely, the beam ends at 8UE and 10UE display rotational distortions having a mirror symmetry around 9UE. Damage to the beam ends at locations 8UW and 10UW was much more severe as has been pointed out. It is possible that rotation of the fourth floor walkway about the west line of hanger rods, as evidenced by the previously described hanger rod distortions and impact points, contributed to this damage. Again, the distortions clearly indicate a symmetry about box beam 9U. These combined rotations strongly suggest an initial failure at box beam-hanger rod connection 9UE.

### 5.3.3 Box Beam Longitudinal Welds

Box beam longitudinal welds had been made in a single pass from the exterior by either a manual or semi-automatic process as evidenced by the rough contour of the weld reinforcement (weld cap). The reinforcements had been removed from the top surface of all box beams as called for on the shop drawings. Reinforcement had also been removed from the bottom surface of all box beams for a distance of approximately 19 in (480 mm) from the beam ends except for box beam 8M in the third floor walkway where the weld reinforcement had been entirely removed. Presumably the reinforcement was removed to provide a flat surface for arc spot welding of the formed steel deck on the top surface of the box beam and for hanger rod washer contact on the bottom surface.

In addition to the exterior welds just described, interior tack welds were observed along the longitudinal seam in the region between the outermost hanger rod hole and the end of the beam. At most locations these welds were placed along the seam in both the top and bottom flange. As these welds are not called out on the fabricator's drawings, it is assumed that their purpose was to facilitate alignment of the MC8 x 8.5 shapes preparatory to placing the exterior

longitudinal welds. As will be shown in chapter 6, these interior tack welds have a significant effect on resistance to hanger rod pull-through. A summary of the length and position of these welds is presented in table 5.6. Because of gross distortions of the flange material caused by hanger rod pull-through, true longitudinal dimensions can be expected to differ from the listed values by as much as  $\pm 0.1$  in (2.5 mm). In the case of location 8MW, saw marks are visible at the outer ends of the welds, indicating the box beam was trimmed to final length after placement of the welds. In other instances it was evident that no final trimming was performed.

In the case of the fourth floor box beams where the longitudinal welds had been fractured during hanger rod pull-through, it was possible to make a visual assessment of weld quantity and quality. There was no evidence of joint preparation and no evidence to indicate that any root opening (separation of members at root of joint) had been provided. The faying surfaces were observed to be continuously curved over the entire depth of the flange toes. In general, joint penetration did not exceed the distance from the outside face of the flange to the point of tangency of the faying surfaces. The resulting weld could, in most cases, best be described as a flare-V-groove weld as defined in reference 5.2. However, as noted in section 3.3, the welding symbol shown on the shop drawings called for a prequalified partial joint penetration groove weld. This is further discussed in section 10.6.

In general, observed variability in penetration along a given weld (figure 5.15) was not considered excessive for a manual or semi-automatic weld, given the geometry of the flange toes of the MC8 x 8.5 shapes. More variability in depth of penetration was noted from weld to weld. For example, penetration at the top longitudinal weld between the hanger rod holes at location 9UW appeared to be about 1.5 mm as compared to a depth of penetration of about 2.8 mm for the bottom longitudinal weld at that same location. The longitudinal welds appeared to contain a substantial amount of porosity in the shape of elongated pores oriented in the through-wall direction and of dimensions approximating that of the weld penetration (figure 5.16). Results of field measurements of top and bottom longitudinal and interior tack weld penetration at the ends of the fourth floor box beams are presented in table 5.7. More detailed descriptions of the box beam longitudinal welds are presented in chapters 7 and 8 of this report.

Weld fractures occurred predominantly along the center line of the welds as indicated in figure 5.16. In several cases a shear lip caused by fracture transition from the weld center line to the fusion line was observed near the inner hanger rod hole. A marked exception to this failure mode was noted at the upper longitudinal welds between the hanger rod holes at locations 8UE and 9UE. Here the weld failure appeared to have occurred predominantly at the fusion line (figure 5.17). In some cases the flange tips were curled up at the weld line, suggesting plastic weld behavior. In other cases the flanges were perfectly straight, suggesting less ductile behavior of the longitudinal welds.

What appeared to be a crack was noted in the lower interior tack weld at location 8MW (figure 5.18). Similarly, an apparent small crack was noted at the lower extremity of 8ME (figure 5.18), apparently having developed in a

region of metal flashing left over from the beam cutting operation. There was no interior tack weld at this location.

#### 5.3.4 Box Beam to Clip Angle Fillet Welds

The clip angles, which served as shear connections between the W16 x 26 stringers and the box beams, were welded to the box beams in accordance with the detail shown in figure 3.10. Clip angles had separated from one side or the other of each box beam by fracture through the weld metal or through the heat-affected zone. In some cases (8UE, 9UE, 10UW and 9LE) cracks were observed in the bottom fillet welds of the clip angles that remained attached (see figure 5.19). Evidence of a pull-out or tensile type failure was observed at the top fillet weld on 11 out of the 13 box beam to clip angle weld failures in the second and fourth floor walkways. This suggests that the fractures were, in most cases, initiated by positive bending moment at the ends of the spans causing shearing failure of the bottom fillet weld, followed by a tension failure (or mixed shear-tension failure) progressing upward and across the top fillet weld. Figures 5.20 and 5.21 illustrate this failure mode for location 9UE. Exceptions were noted at locations 9UW and 9LW where failure of the fillet welds on the box beam web appeared to be entirely of the shear type (figure 5.22). No cracks were in evidence in the bottom fillet welds of the clip angles that remained attached at those locations.

Figure 5.23 clearly shows a tear in the upper end of the north clip angle at location 8UE, suggesting that the connection experienced a negative bending moment at some time during the collapse. However, the south clip angle at this same location appears to have separated from the box beam under the action of positive bending as is evidenced by the shape of the tear in the box beam web shown in figure 5.24. Based on these observations, it is likely that the upper spans at column line 8 first experienced severe negative bending, followed by positive bending prior to final separation of the clip angles from the south web of the box beam. It is also likely that the concrete deck developed a pronounced transverse tension crack, accompanied by failure of the wire reinforcement, during the negative moment phase. With moment reversal, the crack then closed and span rotation was centered about a point near mid-depth of the deck.

There is no evidence of moment reversal in the fourth floor walkway at column line 9, the connection apparently failing under continuously increasing positive moment. The situation at column line 10 is similar to that at column line 8, but the indicators of moment reversal are not as pronounced in the clip angle distortions and fillet weld failures.

Visual examination of the intact box beam to clip angle fillet welds and the fracture surfaces of separated welds indicated welds of good quality. Leg lengths of the fillet welds were typically 5-8 mm.

#### 5.3.5 Other Observations Relevant to the Investigation

Other welds having structural significance and not previously described include the clip angle to embedded plate welds at the south ends of spans U7-8 and

L7-8, and the stringer bearing pad welds at the north ends of spans U10-11 and L10-11. Attachment of the clip angles to the embedded plates at column line 7 was by field welding. Inspection of the embedded plates after their removal from the atrium showed lack of penetration into the clip angles at the bottom of connection 7UE and at the top of 7UW as can be seen from figures 5.25 and 5.26. However, distortion of the clip angles, which remained attached to the W16 x 26 stringers during the collapse, clearly indicates large vertical rotations of the stringers before failure of the clip angle fillet welds. Leg lengths of these fillet welds were typically 5-7 mm except for location 8UE where leg lengths of 6-9 mm were noted.

As indicated in section 5.2.1, misalignment of the embedded plates at column line 7, fourth floor level, required a retrofit of the stringer bearing pads at the north end of the fourth floor walkway. This was accomplished by cutting out the original bearing pad and welding on a pair of 6 x 3 1/2 x 3/8 angles with the short legs machined down to clear the gusset plates in the slide bearing seats. This effectively extended the fourth floor stringers by 2 1/4 in (57 mm). The modification at location 11UW is shown in figure 5.27.

Certain dimensional checks were made to confirm the sizes of structural shapes shown on the fabricator's shop drawings. In addition, length measurements of the stringers and stringer gaps at the box beams were made to check the longitudinal alignment of the walkways prior to collapse as discussed in section 5.2.4. These measurements are summarized in table 5.8.

A final observation is that the stringer to clip angle bolted connections performed very well. The only cases where bolt slip was evident occurred when the connection was badly distorted by direct impact.

#### 5.3.6 Determination of Span Weights

Preliminary estimates of span weights prior to collapse indicated that the weight of the concrete deck could account for as much as 50 percent of the total weight, thus making such estimates particularly sensitive to measurements of deck thickness. The variability in thickness of concrete and topping material, which in some cases could only be measured at the ends of the spans, was considered too high to place any confidence in this approach, and permission was therefore requested of Crown Center Redevelopment Corporation by NBS to weigh selected walkway spans. This operation was carried out on September 3, 1981.

The weighing procedure consisted of temporarily supporting an individual span on four electronic load cells whose output signals are proportional to applied force. Transfer of support was accomplished by raising the span from its supporting timber cribs with hydraulic jacks and inserting the load cells between the bottom flange of the W16 x 26 stringers and the floor. Typically, the spans were raised 1/8 to 1/4 in (3 to 6 mm) during this operation. To prevent damage to the stringer flanges, the jacks and load cells were topped with jacking pads consisting of a 1/2 x 5 1/2 x 5 1/2 in (13 x 140 x 140 mm) steel plate faced with a 1/4 in (6 mm) neoprene sheet. Since some stringers were severely distorted, hardwood wedges were used as required to ensure the level positioning of the jacking pads.

Unless otherwise indicated, the load cells were positioned directly under the center of the bolt groups for those cross beams located a nominal distance of 7'-3 3/4" (2.229 m) north and south of the midspan cross beam (see definition sketch, table 5.9). Tolerances on the horizontal positioning of the load cells were  $\pm 1/4$  in (6 mm) in the north-south direction and  $\pm 1/8$  in (3 mm) in the east-west direction. Prior to recording load cell outputs, the timber cribs were checked for freedom of movement to ensure complete load transfer.

Results of the load cell measurements are summarized in table 5.9. Regression analysis of the load cell calibration data indicates a standard error of estimate of 20 lbs (89 N) for individual load cell readouts over the range of weights encountered.

#### 5.4 REMOVAL OF SPECIMENS

Shortly after the start of the investigation, comprehensive structural and materials testing programs were undertaken as described in chapters 6 and 7 of this report. Tests were carried out on structural assemblies and materials believed to be faithful representations of those assemblies and materials used in the actual walkway construction. To confirm this, a formal request for permission to remove and test certain specimens from the walkway debris was submitted by NBS to the Crown Center Redevelopment Corporation on September 18, 1981. This was followed by a request to the Liaison Committee of Plaintiffs' Counsel and the Liaison Committee of Defendants' Counsel on October 27, 1981. Criteria for specimen selection and details of the request are described in the following section.

##### 5.4.1 Criteria for Specimen Selection

Criteria for choice of specimens to be removed from the walkway debris were as follows:

1. No truly unique specimens to be removed from the debris.
2. Specimen location and method of removal to be chosen so as to minimize disturbance of the walkway debris.
3. Amount of material to be removed from a given component or assembly to be limited so that, if necessary, similar specimens can be obtained and independently tested by others.
4. Specimens to be representative of materials and fabrication techniques used in the construction of the walkways.

Based on these criteria, a detailed list of specimens was developed, including the type of test or examination and purpose, as shown in table 5.10.

##### 5.4.2 Specimen Removal

Permission to remove specimens from the walkway debris was granted in the form of a modified order issued by both the Jackson County Circuit Court and the

United States District Court for the Western District of Missouri on October 28, 1981. Actual removal of specimens was carried out over the period November 3-5, 1981. The first step in removing structural steel specimens was to mark the specimens in place with cut lines and specimen identification numbers. After photographing, the specimens were then removed and engraved by representatives of NBS and the Crown Center Redevelopment Corporation. The specimens were again photographed to show the specimen numbers and engraving. Although flame cutting would have been faster and more convenient, an abrasive saw was used to minimize heat effects near the cut lines. With the exception of the box beam at location 9M, all structural steel specimens were easily accessible.

To remove box beam 9M, the remnants of the third floor to ceiling hanger rods were first removed, followed by the bolts in each of the four clip angle to stringer connections. Concrete around the shear studs at each end of the box beams was then removed by impact hammer, followed by separation of the arc spot welds attaching the formed steel deck to the top flange of the box beam. Hanger rod nuts and washers were retained with the box beam for subsequent use in structural tests. Photographs of specimens 1, 2 and 3 before and after removal are shown in figures 5.28 - 5.30. Specimens 5A and 5B are shown in figure 5.31.

Cores were removed from the concrete decks of 6 of the 12 walkway spans using a 2 in (51 mm) I.D. diamond coring bit as shown in figure 5.32. To obtain homogeneous cores with flat ends for subsequent density and compression tests, it was necessary to center the bit over the flat portion of the formed steel deck and, at the same time, avoid the welded wire reinforcement. Where possible, cores were removed at a point directly over a cross beam and at the quarter- and mid-points in the cross beam spacing to obtain some measure of the variation in slab thickness. Considerable difficulty was encountered in obtaining complete cores from the second and fourth floor walkways because of fractures in the concrete decks. A total of 24 cores were removed, but only 19 of these were considered to be of sufficient quality for testing. Each core was assigned a specimen number on removal and the same specimen number was marked on the deck adjacent to the core hole. Table 5.11 lists the cores and their locations. The cores selected for testing and actually removed from the warehouse are shown in figure 5.33.

At the same time the concrete cores were removed, measurements of topping thickness for each span in the second and fourth floor walkway were obtained. For those spans having most of the carpeting and footlights in place, measurements were extremely limited. Topping removed with the cores was included in the measurements to obtain the average thicknesses listed in table 5.12.

#### 5.4.3 Specimen Cataloging and Preparation for Shipment

Upon removal from the debris, each specimen was measured and all identifying marks were noted. All specimens were then wrapped in clear plastic sheet to await final inspection by designated representatives of the Liaison Committee of the Plaintiffs' Counsel and the Liaison Committee of the Defendants' Counsel. Prior to this inspection a listing of all specimens, complete with descriptions

of origin and physical features, was jointly prepared by representatives of NBS and the Crown Center Redevelopment Corporation.

On November 5, 1981, after representatives of the Liaison Committees had inspected and certified the specimens, custody was transferred to NBS and all specimens were then wrapped for shipment and wax seals were affixed. NBS personnel transported the specimens by van to the NBS laboratories at Gaithersburg, Maryland, arriving on November 6.

Because of problems encountered with the replication of fracture surfaces (see section 5.5), four fracture surfaces from the bottom flanges of the fourth floor box beams were removed on December 16-17, 1981. Five additional hanger rod nuts and washers were also removed at this time for the purpose of obtaining hardness measurements. A description of all specimens removed from the walkway debris and their corresponding NBS identification numbers are presented in table 5.13.

#### 5.4.4 Specimen Storage and Handling

Upon arrival at NBS, the specimens were stored in a secure area to await inspection of the seals by NBS personnel and photographic documentation. After this was completed on November 9, 1981, a detailed physical description of each specimen was prepared.

Because of the many tests and operations which had to be carried out simultaneously, a chain of possession was maintained for each specimen. In the case of box beam 9M (specimen No. 3), physical descriptions were prepared and chains of possession were maintained for the five subspecimens cut from the beam for use in structural tests.

The procedure followed in subdividing a specimen was to mark clearly the cut lines and the subspecimen identification numbers on the specimen. The specimen was then photographed and the subspecimens were removed and machined to final shape. Each subspecimen identification number was unique and was coded to provide information on both the origin and orientation of the subspecimen. For example, the number "2-LN1" designates a tensile coupon removed from specimen no. 2. It is oriented in the longitudinal direction on the north face of the beam and is the first in a series of such specimens.

#### 5.5 REPLICATION OF WALKWAY WELD FRACTURE SURFACES

In addition to specimens of construction materials, the request of October 27, 1981, also addressed the field replication of certain fracture and washer contact surfaces for the purpose of fractographic analysis. This work was carried out over the period November 2-4, 1981.

The replication procedure involved the application of cellulose acetate (C.A.) tape to the fracture surface. A 1 in (25.4 mm) piece of tape with a thickness of 0.001 in (0.03 mm) was softened by applying several drops of acetone to one surface. One to two drops of acetone were applied to the fracture surface and the tape was then worked into place with light finger pressure. Entrapped air bubbles were worked out by smoothing pressure, allowing the softened tape to

conform with the fracture surface. After drying for approximately 1 hour, the replica was removed by carefully lifting the edges until free.

The first replica removed from each fracture surface usually contained most of the surface corrosion products and dust. In each case this replica was retained as the archival sample. Additional replicas were stripped until no significant amount of rust was observed. Each successive replica was edge-notched to indicate the side oriented with the outside surface of the box beam.

In some cases a plastic tape (butyrate) with 0.010 in (0.25 mm) thickness and a longer drying time was applied. The details of the fracture topography replicated with butyrate and C.A. were essentially identical. After the final replication, each fracture and washer contact surface replicated was given two spray coats of protective acrylic (Krylon).\* Table 5.14 lists the locations of fracture and washer contact surfaces and the number of replications of each surface.

Subsequent examination of these replicas by scanning electron microscope (SEM) revealed that attempts to replicate the lower fracture surfaces at the ends of the fourth floor box beams were only partially successful. This prompted an additional request to the Liaison Committees by NBS on November 30, 1981, for permission to remove portions of certain fracture surfaces for direct scanning electron microscopy.

On December 16-17, 1981, four fracture surfaces from the bottom flanges of the fourth floor box beams were removed and transported to NBS for SEM examination. The fracture surfaces, which are listed in table 5.13, were removed by cutting longitudinally along the fillet-web tangent line and then directly across the flange to a point midway between the two hanger rod holes. Details of these specimens are described in chapter 8. Transfer of custody involved the same inspection and certification procedures described in section 5.4.3.

## 5.6 SUMMARY

Based on measurements and observations made during the site investigation, the following conclusions were drawn:

1. The walkways were properly aligned on their bearing seats prior to the collapse.
2. There was sufficient room to install a nut and washer on the lower end of each fourth floor to ceiling hanger rod with the fourth floor walkway properly leveled.

---

\* Certain commercial equipment, instruments or materials are identified in this report in order to adequately specify the experimental procedure. Such identification does not imply recommendation or endorsement by the National Bureau of Standards, nor does it imply that the materials or equipment identified are necessarily the best available for the purpose.

3. Observed distortions in the west line of fourth floor to ceiling hanger rods and the absence of similar distortions in the east line of fourth floor to ceiling hanger rods suggest that the collapse initiated along the east line of hanger rods.
4. Impact points on the atrium floor indicate a general drift of the walkway spans to the south and west during the collapse. This drift was approximately 1.0 ft (300 mm) south and 0.9 ft (270 mm) west.
5. With one exception, damage done to the walkway spans during the rescue operation was superficial.
6. All of the fourth floor to ceiling hanger rods pulled through both the lower and upper flanges of the fourth floor box beams.
7. Evidence indicates that all hanger rod washers were installed.
8. There is a mirror symmetry to the deformation and distortion of the box beam ends with respect to box beam 9U in the fourth floor walkway.
9. Observed distortions strongly suggest an initial failure at box beam-hanger rod connection 9UE.
10. The actual box beam longitudinal welds can best be described as flare-V-groove welds.
11. Variability in penetration for a given box beam longitudinal weld was not excessive, but penetration varied considerably from weld to weld.
12. Interior tack welds were highly variable in length, location, and penetration. In some cases there was no interior tack weld.
13. In general, the clip angle to box beam fillet welds were of good quality.
14. Observed clip angle failure modes strongly suggest moment reversal at column line 8 and possibly column line 10. No signs of moment reversal at column line 9 were observed.
15. The shear connections at column line 7 experienced large rotational distortion prior to failure of the fillet welds.

Table 5.1 Coordinates of Fourth Floor to Ceiling Hanger Rods

<u>Hanger Rod</u>	<u>Upper End*</u>	<u>Lower End</u>
8E	4.65' E 83.90' S	4.62' E 83.81' S
8W	4.40' W 83.84' S	4.48' W 83.81' S
9E	4.64' E 54.64' S	4.68' E 54.68' S
9W	4.42' W 54.60' S	4.47' W 54.63' S
10E	4.64' E 25.39' S	4.73' E 25.38' S
10W	4.42' W 25.37' S	4.46' W 25.37' S

\* Approximately 18 in (460 mm) below the plane of the ceiling.

1 in = 25.4 mm

Table 5.2 Elevations of Fourth Floor to Ceiling Hanger Rods  
(Referenced to Elev. 0.00 assumed datum at first floor level)

<u>Hanger Rod</u>	<u>Intersection with Ceiling</u>	<u>Lower End</u>
8E	52.48	43.59
8W	52.47	43.55
9E	52.44	43.70
9W	52.45	43.55
10E	52.44	43.71
10W	52.43	43.53

Table 5.3 Coordinates of Major Impact Points on Atrium Floor

<u>Hanger Rod Impact Point</u>	<u>Coordinates</u>
8E*	3.36' E 86.76' S
8W*	5.10' W 86.84' S
9E	3.36' E 55.32' S
9W	5.01' W 55.60' S
10E (primary impact)	3.41' E 26.29' S
(secondary impact)	3.17' E 26.30' S
10W	5.01' W 26.24' S

\* Observed tile damage in vicinity of column line 8 was probably due to impact of north end of W16 x 26 stringers in span L7-8.

1 in = 25.4 mm

Table 5.4 Alignment of Upper Hanger Rods and Fourth Floor Walkway Relative to Second Floor Walkway

<u>Upper Hanger Rods at Ceiling</u>		<u>Fourth Floor Walkway</u>	
8E	0.09' E 0.15' S	ℰ at South end of Walkway (Col. Line 7)	0.03' W 0.15' S
8W	0.07' E 0.09' S	ℰ at Col. Line 8	0.02' W 0.16' S
9E	0.08' E 0.14' S	ℰ at Col. Line 9	0.02' W 0.17' S
9W	0.05' E 0.10' S	ℰ at Col. Line 10	0.01' W 0.19' S
10E	0.08' E 0.14' S	ℰ at North end of Stringers (Col. Line 11)	0.00' 0.21' S
10W	0.01' E 0.13' S		

1 in = 25.4 mm

Table 5.5 Locations of Impact Points on Atrium Floor Relative to Original Hanger Rod Positions at Second Floor Walkway

<u>Hanger Rod Impact Point</u>	<u>Relative Location</u>
8E*	0.87' W 3.01' S
8W*	0.96' W 3.09' S
9E	0.87' W 0.82' S
9W	0.87' W 1.10' S
10E (Primary impact)	0.82' W 1.05' S
(Secondary impact)	1.06' W 1.06' S
10W	0.87' W 1.00' S

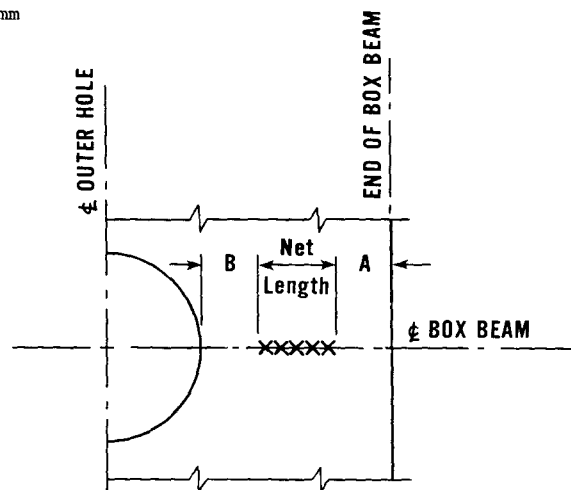
\* Observed tile damage in vicinity of column line 8 was probably due to impact of north end of W16 x 26 stringers in span L7-8.

1 in = 25.4 mm

Table 5.6 Length and Position of Box Beam Interior Tack Welds

Connection Number	Bottom Flange			Top Flange		
	Net Length (inches)	Dimension A (inches)	Dimension B (inches)	Net Length (inches)	Dimension A (inches)	Dimension B (inches)
8UE	1.42	0	0	No weld		
8UW	1.38	0	0	No weld		
9UE	0.98	0	0.47	0.71	0.28	0.31
9UW	1.06	0.20	0	1.18	0	0
10UE	1.18	0.20	0	0.87	0.28	0.24
10UW	1.30	0	0	1.30	0	0
8LE	No weld			1.97	0	--
8LW	1.73	0	3.43	2.24	0	2.90
9LE	1.77	0	--	1.57	0	--
9LW	2.56	0.20	--	1.50	0.08	--
10LE	1.54	0.08	--	1.73	0	--
10LW	1.69	0.12	--	1.57	0.12	--
8ME	No weld			1.10	0.35	--
8MW	0.39	0	--	0.75	0.12	--
9ME	1.26	0	0	No weld		
9MW	0.75	0	0.67	No weld		
10ME	1.06	0.08	--	No weld		
10MW	1.14	0.08	--	No weld		

1 in = 25.4 mm



PLAN VIEW  
(Definition Sketch)

Table 5.7 Field Measurements of Weld Penetration at Ends of Fourth Floor Walkway Box Beams

Connection Number	Weld Penetration (mm)			
	Bottom Flange		Top Flange	
	Exterior	Interior	Exterior	Interior
8UE	1.0 - 1.5	0 - 2.0	1.0 - 1.5	no weld
8UW	Complete Penetration <sup>(a)</sup>		2.0	no weld
9UE	1.5 - 2.0	2.5	1.5	2.0
9UW	1.5 - 2.0 <sup>(b)</sup>	1.5 - 2.5 <sup>(b)</sup>	1.0 - 2.0	1.0 - 2.0
10UE	2.0	2.0 - 2.5	1.5 - 2.0	2.0 - 3.0
10UW	1.5	2.0 - 3.0	Complete Penetration <sup>(a)</sup>	

Note: (a) Exterior and the interior welds merged, leading to complete penetration.

(b) Edge of hole badly damaged by nut and washer.

1 in = 25.4 mm

Table 5.8 Measured Lengths of Stringers and Stringer Connections

Connection Number	Span Number	Distance From End of Stringer to End of Adjoining Stringer (inches)		Length of Stringer (feet)	
		East	West	East	West
U7	U7-8	0.43	0.35	*	29.38
U8	U8-9	4.65	4.61	28.85	28.85
U9	U9-10	4.72	4.65	28.84	28.84
U10	U10-11	*	4.57	29.39	29.38
U11**		2.25	2.25		
L7	L7-8	0.51	0.51	*	29.33
L8	L8-9	4.65	4.76	*	*
L9	L9-10	4.84	4.76	28.88	28.85
L10	L10-11	4.72	4.69	29.40	29.38

Notes:

\* Could not be accurately measured due to severe damage. Nominal values used in calculations.

\*\* Represents extension of stringer bearing pad.

1 in = 25.4 mm

Table 5.9 Measured Weights of Damaged Spans

Span No.	Weight in lbs at Indicated Load Cell				Total (lbs)
	No. 1	No. 2	No. 3	No. 4	
U7-8(1)	4,450	3,410	3,690	4,210	15,760
U8-9	4,610	3,250	4,030	4,060	15,950
U9-10	4,030	3,370	4,160	3,040	14,600
U10-11	3,570	3,610	4,230	2,590	14,000
L7-8	4,760	3,030	4,060	3,280	15,130
L8-9(2)					
L9-10	3,320	3,790	3,500	3,550	14,160
L10-11	3,420	3,230	3,610	2,910	13,170
M8-9(3)	5,020	4,190	5,890	3,720	18,820

Notes:

- (1) Load cells 2 and 3 were positioned 12 in (305 mm) north of normal positions due to inaccessibility.
- (2) Span L8-9 not weighed because of excessive damage.
- (3) Load cells 1 and 4 were positioned 5'-6" (1.68 m) south and load cells 2 and 3 were positioned 7'-0 1/8" (2.14 m) north of normal positions due to inaccessibility.

1 lb = 0.4536 kg

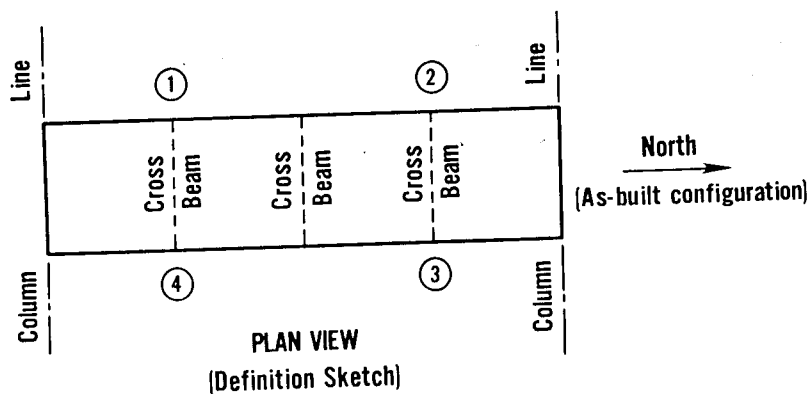


Table 5.10 Request for Physical Specimens from Hyatt Regency Walkway Debris

MATERIALS TESTING

<u>Specimen Description</u>	<u>Type of Examination</u>	<u>Purpose</u>
<p>1. Segment of box beam 9U. A 24 in longitudinal segment beginning at a point 30 in from the west end of 9U and extending inward.</p> <p>2. Segment of box beam 8L. A 36 in longitudinal segment beginning at the west end of 8L.</p>	<p>Tensile tests per ASTM E8.</p> <p>a) Transverse weld tensile tests.</p> <p>b) Metallography and hardness of weld, heat-affected zone, parent metal.</p> <p>c) Chemical analysis, weld metal, and parent metal.</p>	<p>Conformance to mechanical property specifications.</p> <p>Weldment mechanical property variability.</p> <p>Assessment of microstructure phases contributing to low weldment toughness.</p> <p>Conformance to composition specification.</p>
<p>3. Box beam 9M. The full box beam will be obtained by removing the bolts connecting the stringer to the clip angles and removal of limited concrete to allow separation of the box beam from the deck.</p>	<p>Destructive structural load tests.</p>	<p>Determine resistance of box beam to hanger rod pull-through load.</p>
<p>4. 3 in diameter cores of concrete deck. Up to 30 cores taken at random locations on walkway decks.</p>	<p>Length of core and unit weight determination.</p>	<p>Establish average weight of concrete deck per unit of area.</p>
<p>5. 36 in lengths of 1 1/4 in <math>\phi</math> hanger rod. One specimen to be removed from straight segment of 4th floor to 2nd floor hanger rod, and one specimen to be removed from ceiling to 4th floor hanger rod.</p>	<p>Tensile tests to determine yield strength, tensile strength, elongation, and reduction of area in accordance with ASTM E8.</p>	<p>To clearly establish grade and yield strength of steel used in hanger rod assemblies.</p>
<u>FRAC TOGRAPHY</u>		
<p>1. Access for field replication of:</p> <p>a) lower fracture surfaces of box beams 8U, 9U, and 10U</p> <p>b) fracture surface of clip angle at box beam 9UE</p> <p>c) tack welds at level M.</p>	<p>Scanning and transmission electron microscopy.</p>	<p>Assessment of weld failure mode.</p>
<p>2. A 2 in section of the upper fracture at connection 8UW (north surface) centered at a point 9 in from the west end. Depth of cut to extend 1/2 in from fracture surface.</p>	<p>Replication and direct scanning electron microscopy.</p>	<p>Validation of replication technique for fractographic analysis.</p>

1 in = 25.4 mm

Table 5.11 Locations of Concrete Cores

<u>Core Number</u>	<u>Span Number</u>	<u>E-W Coordinate (feet)</u> (Dist. from toe of east handrail support angle)	<u>N-S Coordinate (feet)</u> (Dist. from north end of east stringer)
4-01	U10-11	2.85	10.3
02	"	2.95	10.3
03	"	2.85	16.8
04	"	1.85	17.1
4-05	U9-10	5.85	9.3
06	"	2.80	9.0
07	"	2.20	14.5
4-08	L10-11	2.90	11.5
09	"	2.35	13.0
10	"	2.90	15.2
		(Dist. from toe of west handrail support angle)	(Dist. from north end of west stringer)
4-11	L9-10	2.35	14.4
12	"	2.30	16.5
13	"	2.85	18.0
		(Dist. from inside face of west handrail glass panel)	(Dist. from north end of west stringer)
4-14	M8-9	2.60	14.0
15	"	2.60	10.9
16	"	2.60	8.9
		(Dist. from inside face of east handrail glass panel)	(Dist. from centerline of 1st crossbeam from south end)
4-17	M9-10	3.00	3.5
18	"	2.55	3.5
19	"	2.00	6.9

1 in = 25.4 mm

Table 5.12 Thickness of Topping Material

Span Number	Thickness of Topping (inches)			Number of Observations
	Average	Maximum	Minimum	
U7-8	0.16	0.47	0	6
U8-9	0.20	0.39	0	7
U9-10	0.38	0.68	0	13
U10-11	0.47	0.75	0	13
L7-8	0.17	0.47	0	9
L8-9	0.44	0.67	0.08	10
L9-10	0.20	0.43	0	15
L10-11	0.04	0.39	0	14

1 in = 25.4 mm

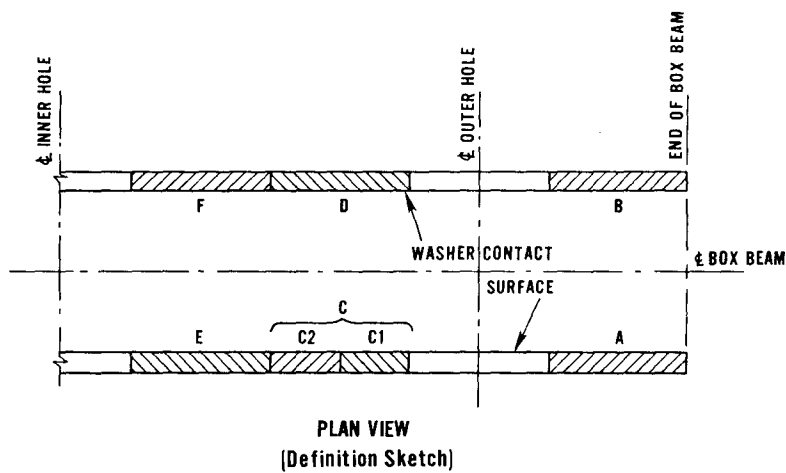
Table 5.13 Specimens Removed From Walkway Debris

NBS Specimen Number	Specimen Description and Origin
Specimens Removed November 3-5, 1981	
1	A 23.2 in longitudinal segment of box beam 9U beginning at a point 30 in from west end of 9U and extending inward.
2	A 35.7 in longitudinal segment from west end of box beam 8L. Includes bent segment of hanger rod, complete with nut and washer.
3	Box beam 9M, complete with hanger rod nuts and washers.
4-01 to 4-19	Concrete cores located as shown in table 5.11. Nominal diameter = 2 in.
5A	A 35.7 in segment from upper end of fourth floor to ceiling hanger rod at location 8UE, complete with nut and washer.
5B	A 35.8 in segment from second floor to fourth floor hanger rod. Installed location unknown.
6	A 2 in section of upper longitudinal weld fracture at location 8UW (north surface) centered 9 in from west end of box beam.
Specimens Removed December 16-17, 1981	
7	Fracture surface, location 8UE, bottom flange, north surface.
8	Fracture surface, location 9UE, bottom flange, south surface.
9	Fracture surface, location 9UW, bottom flange, north surface.
10	Fracture surface, location 10UE, bottom flange, south surface.
11A	Nut from upper end of fourth floor to ceiling hanger rod at location 9UE.
11B	Washer from upper end of fourth floor to ceiling hanger rod at location 9UE.
12A	Nut from upper end of fourth floor to ceiling hanger rod at location 10UW.
12B	Washer from upper end of fourth floor to ceiling hanger rod at location 10UW.
13A	Nut from upper end of third floor to ceiling hanger rod at location 8MW.
13B	Washer from upper end of third floor to ceiling hanger rod at location 8MW.
14A	Nut from upper end of third floor to ceiling hanger rod at location 9ME.
14B	Washer from upper end of third floor to ceiling hanger rod at location 9ME.
15A	Nut from upper end of third floor to ceiling hanger rod at location 10MW.
15B	Washer from upper end of third floor to ceiling hanger rod at location 10MW.

1 in = 25.4 mm

Table 5.14 Replicas of Fracture and Washer Contact Surfaces

<u>Location</u>	<u>Number of Replications</u>
8UE - B	4
- C1	3
- Washer contact surface (south)	3
- Washer contact surface (north)	3
9UE - A	5
- B	5
- D	6
- E	5
- Washer contact surface (south)	3
- Washer contact surface (north)	3
9UW - A	5
- C	4
- F	4
- Washer contact surface (south)	3
- Washer contact surface (north)	1
10UE - A	4
- C2	3
- Washer contact surface (south)	2
9UE - North clip angle weld fracture (top)	2
- North clip angle weld fracture (middle)	2
- North clip angle weld fracture (bottom)	2
8MW - Interior tack weld (bottom)	3



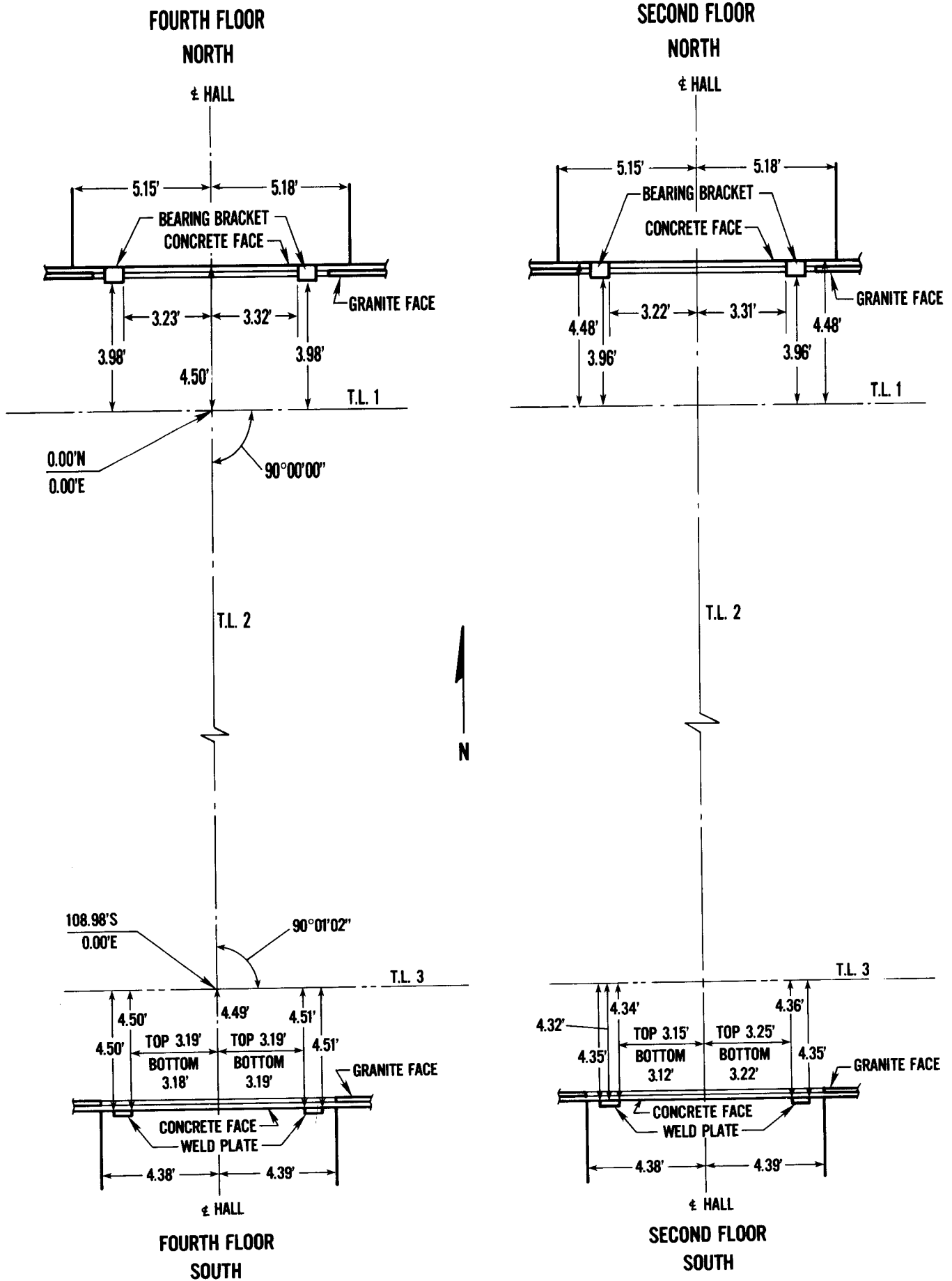


Figure 5.1 Locations of embedded plates and bearing seats.

## DETAILS OF EMBEDDED PLATES - COL. LINE 7

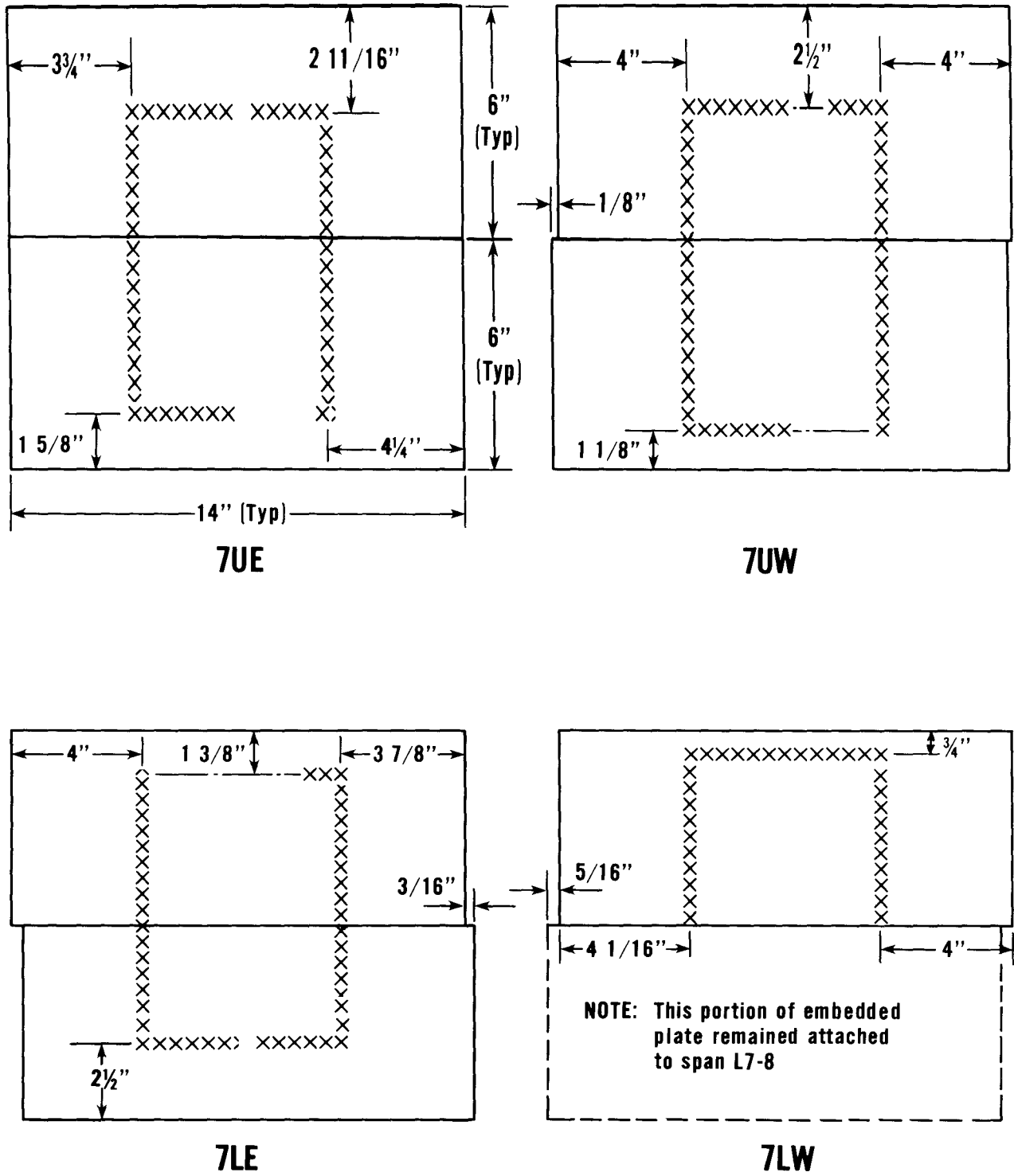


Figure 5.2 Details of embedded plates and fillet welds at column line 7.

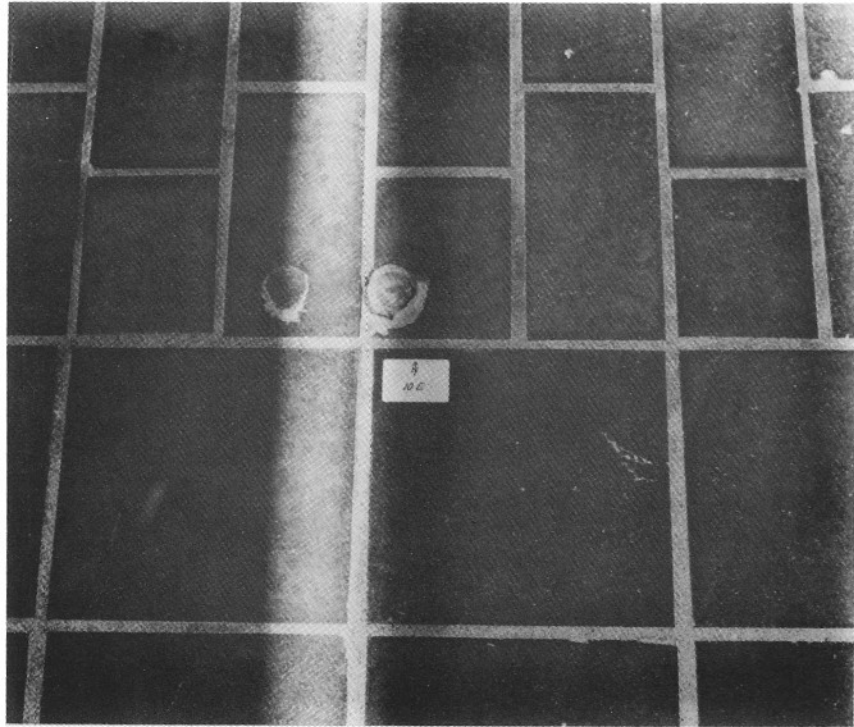


Figure 5.3 Tile damage caused by second floor hanger rod 10E.



Figure 5.4 Fourth floor to ceiling hanger rods. View from fourth floor looking south.

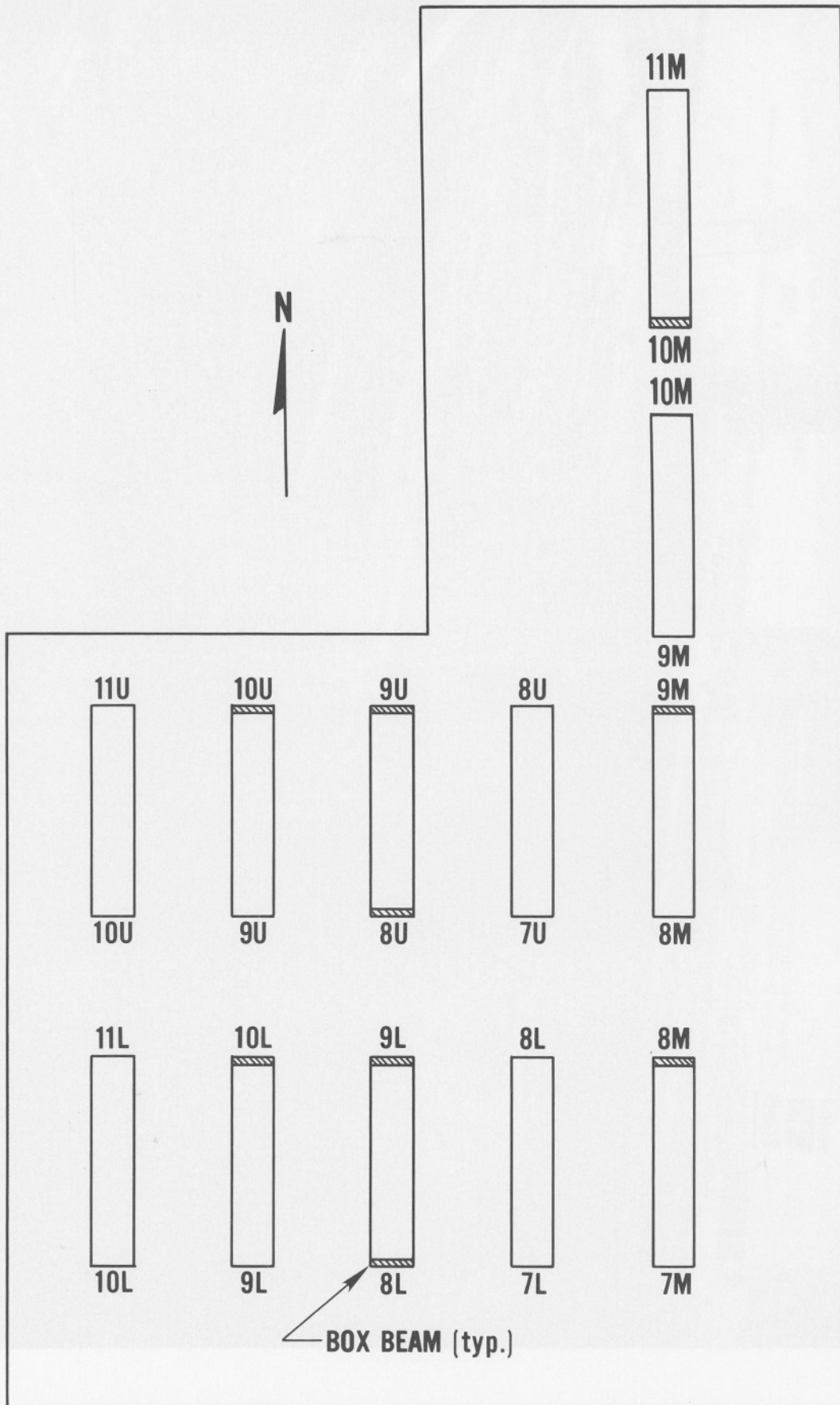


Figure 5.5 Layout of walkway spans in warehouse.

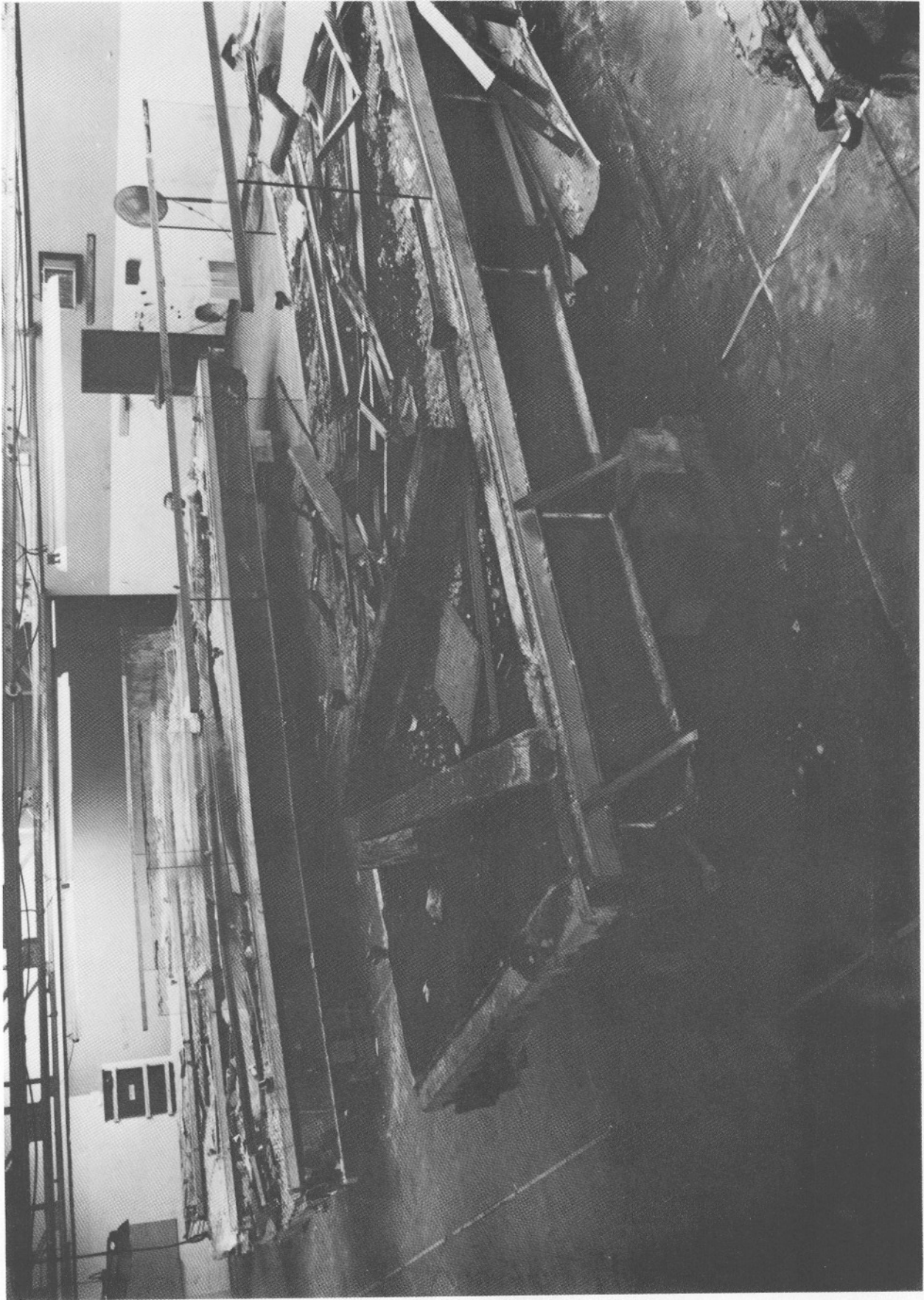


Figure 5.6 General view showing spans of fourth floor walkway.

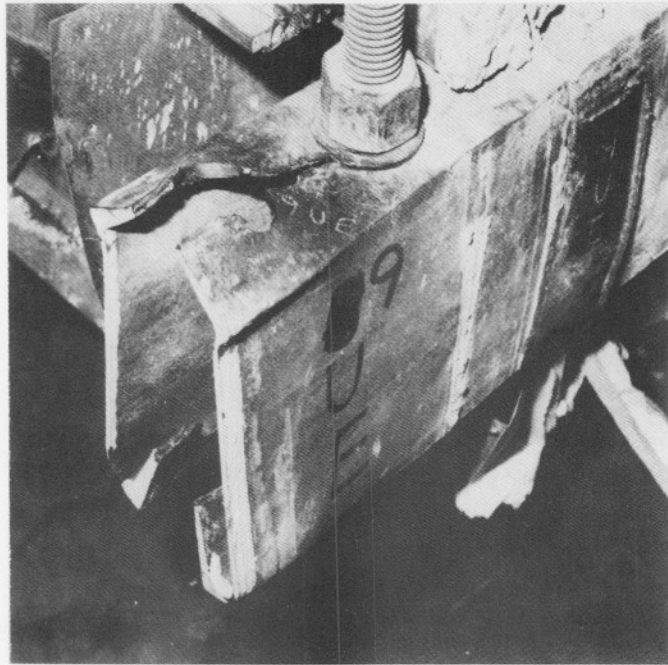


Figure 5.7 Hanger rod pull-through at location 9UE.

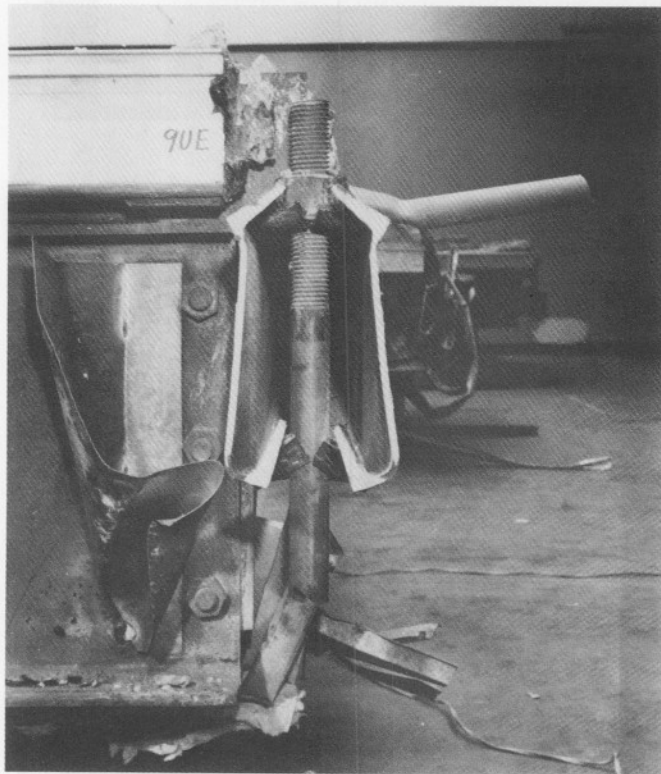
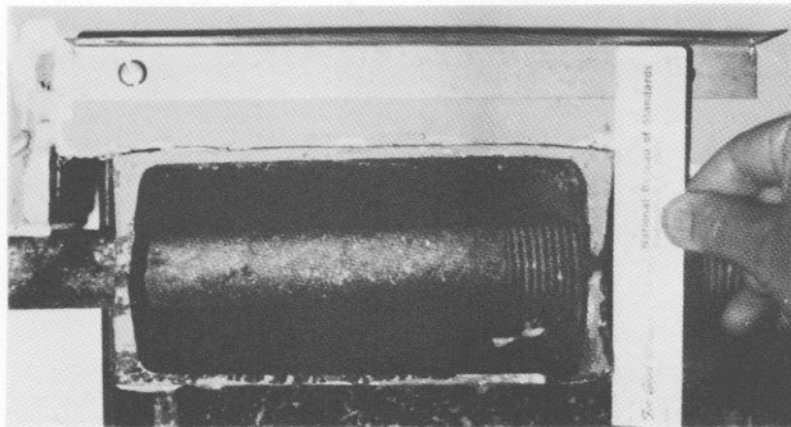
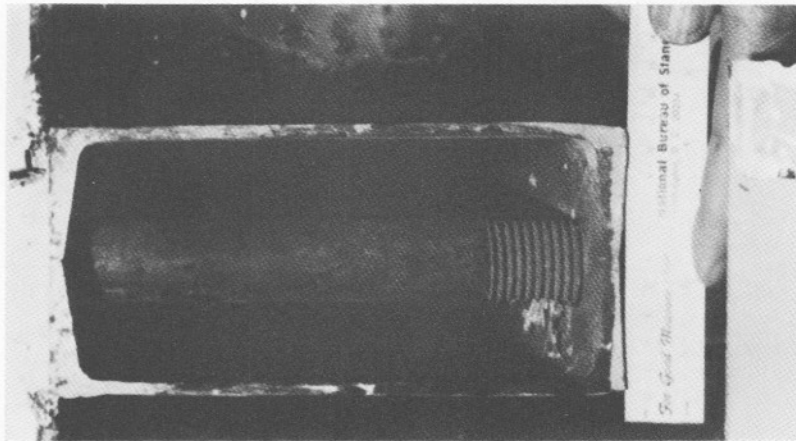


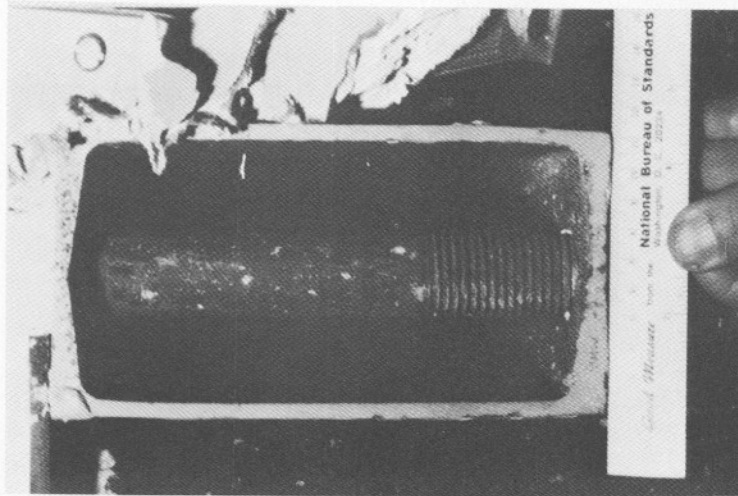
Figure 5.8 End view of box beam at location 9UE.



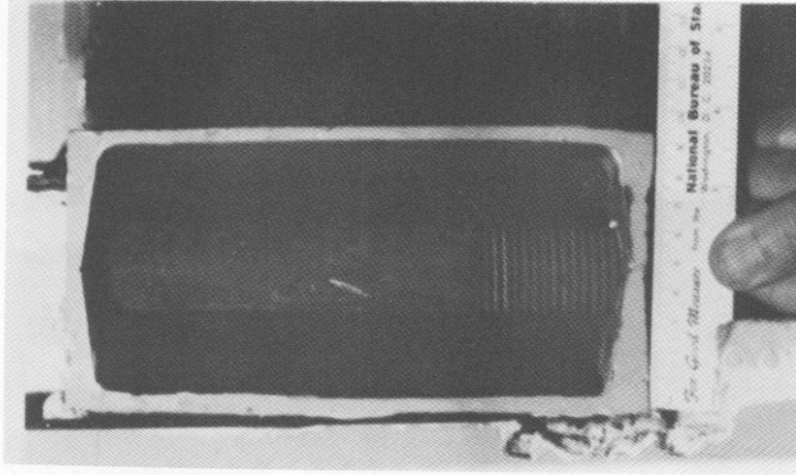
a) Location 8MW.



b) Location 8ME.



c) Location 9MW.



d) Location 10MW.

Figure 5.9 Evidence of permanent distortion in box beam ends of third floor walkway.

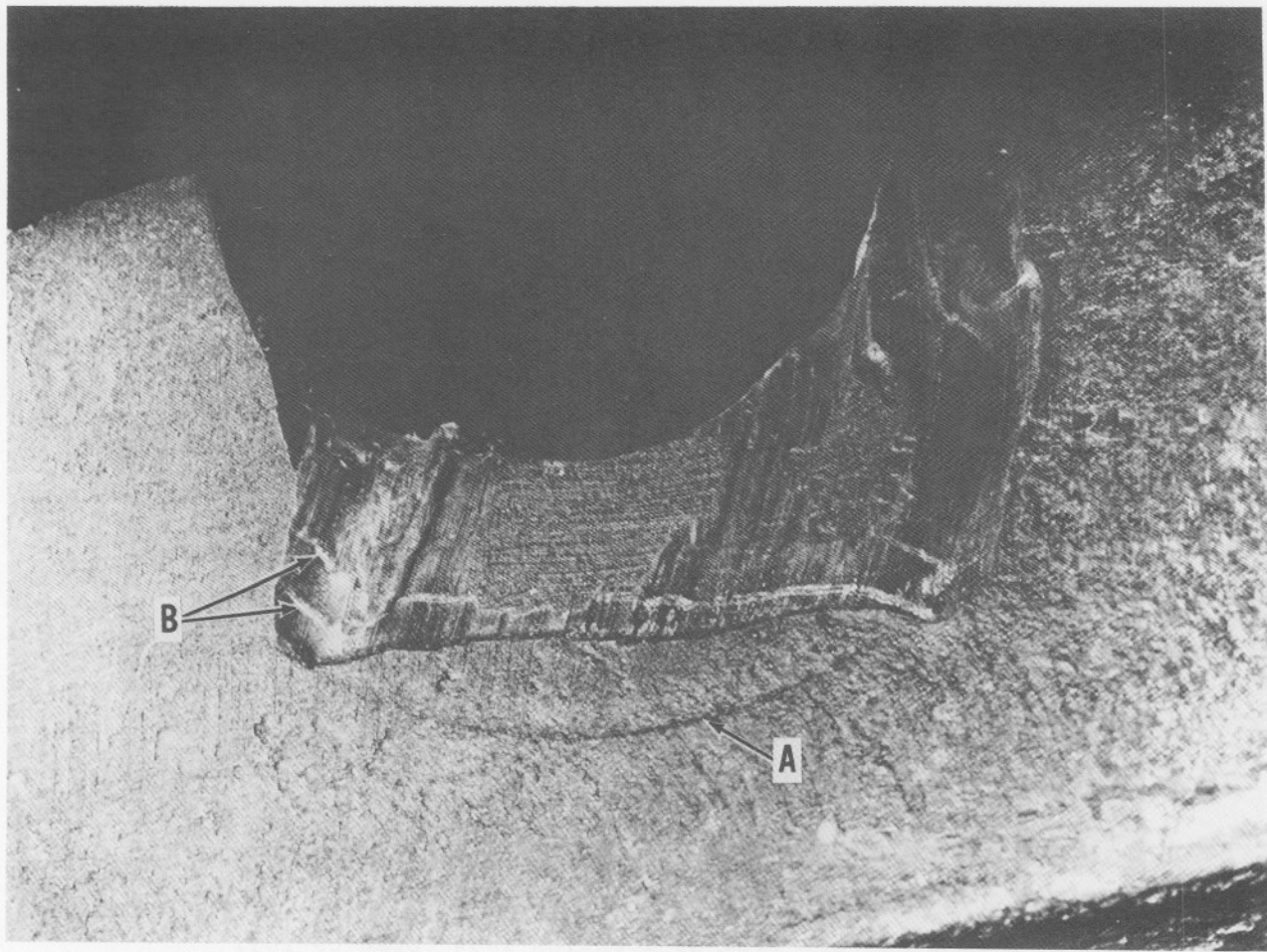


Figure 5.10 Deformation at underside, outer hole, location 9UE due to pull-through of washer/nut assembly. Note imprint of washer (A) and evidence of slip-stick progressive failure (B).

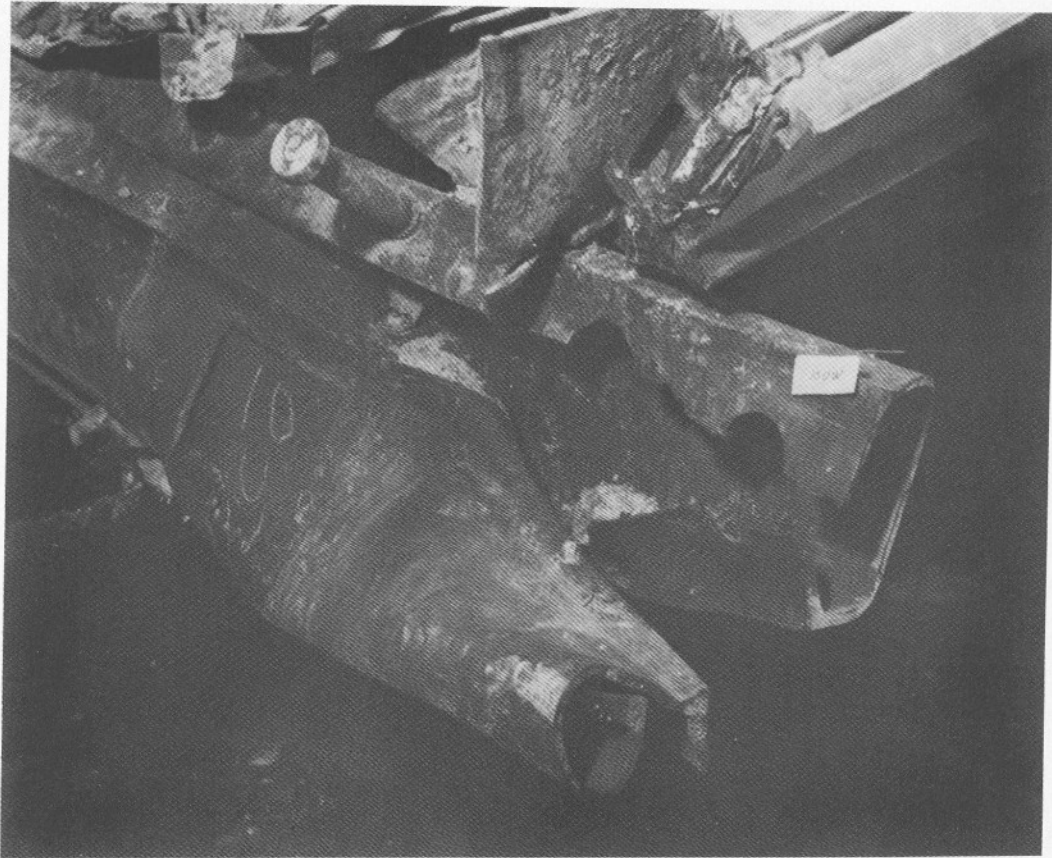


Figure 5.11 Box beam at location 10UW (Span U9-10).

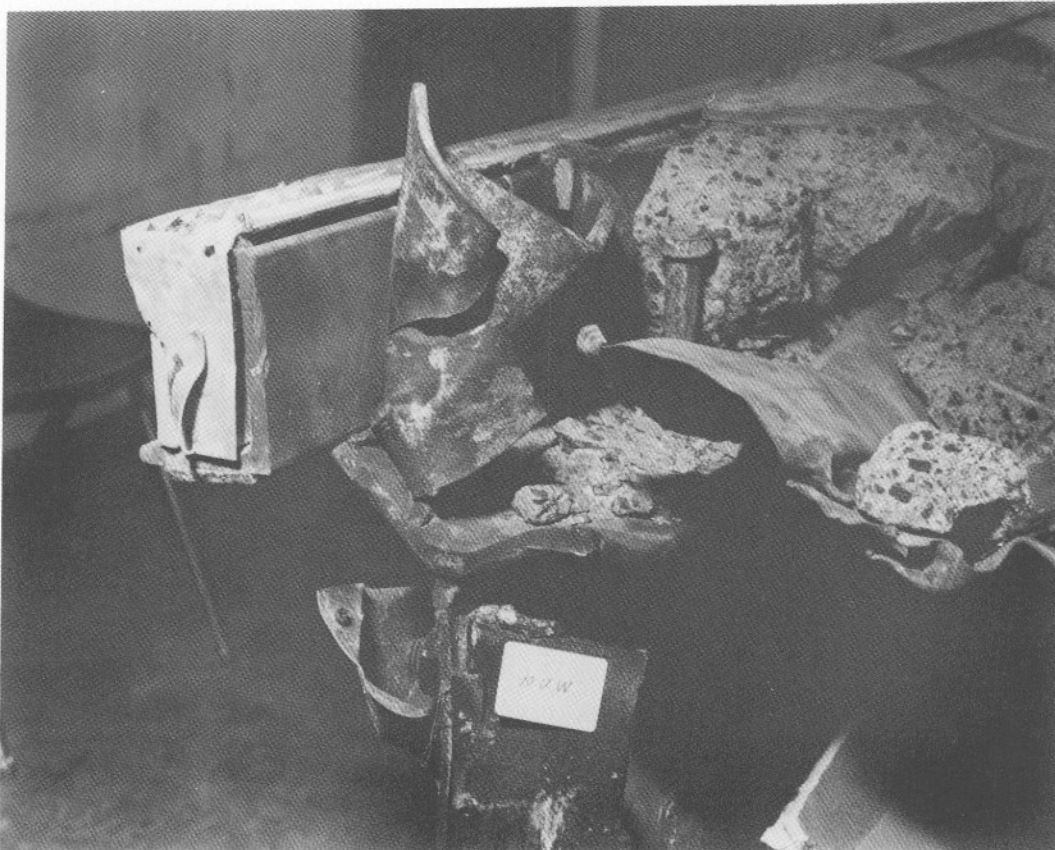


Figure 5.12 End view of 1/4" x 6" edging plate at location 10UW (Span U10-11).

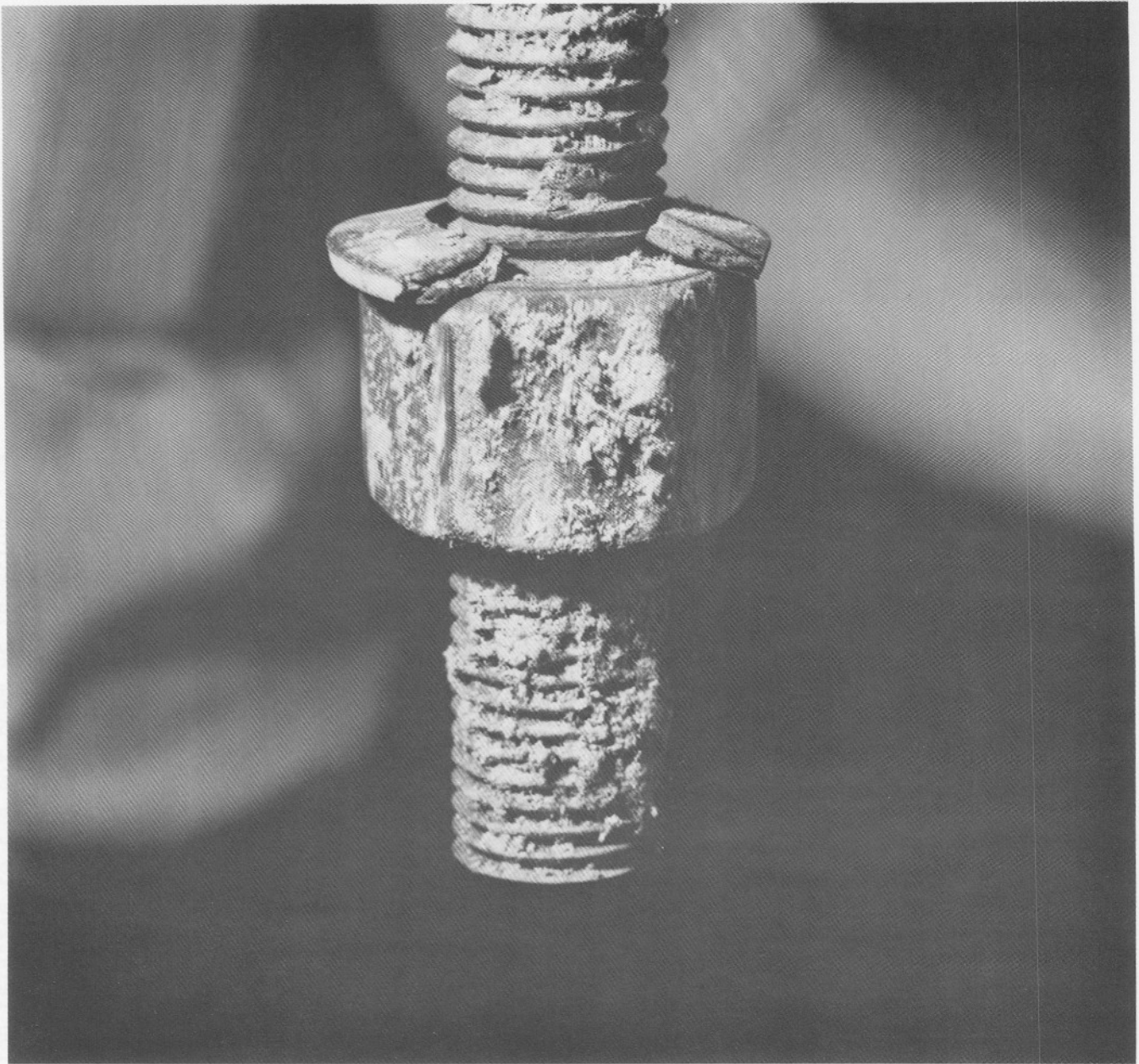
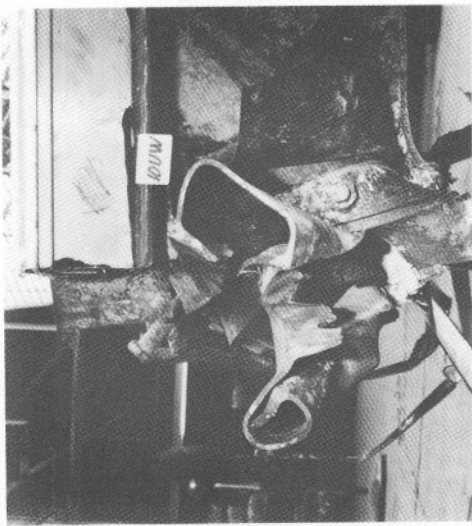
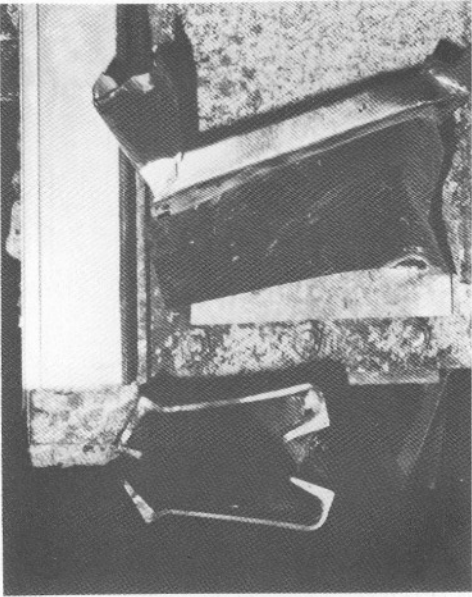


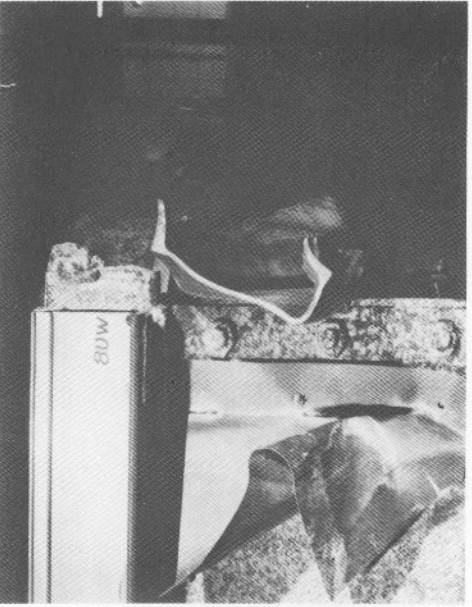
Figure 5.13 Washer at bottom end of fourth floor to ceiling hanger rod 9UW.



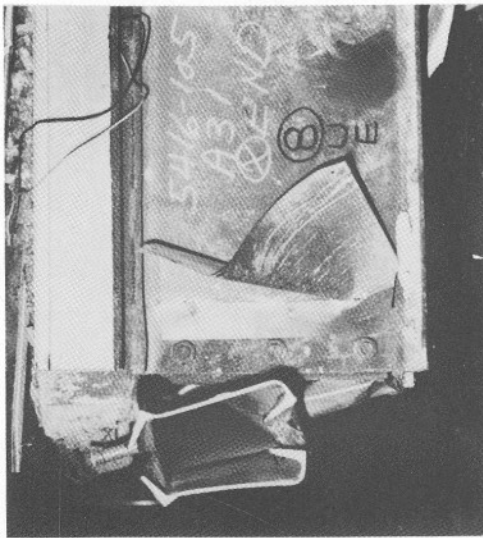
a) Location 10UW.



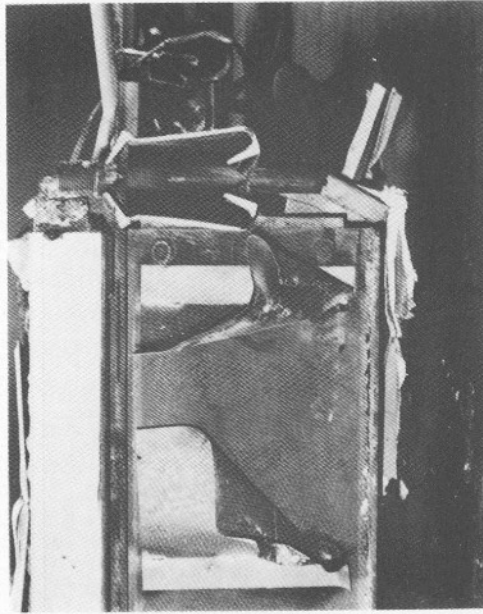
b) Location 9UW.



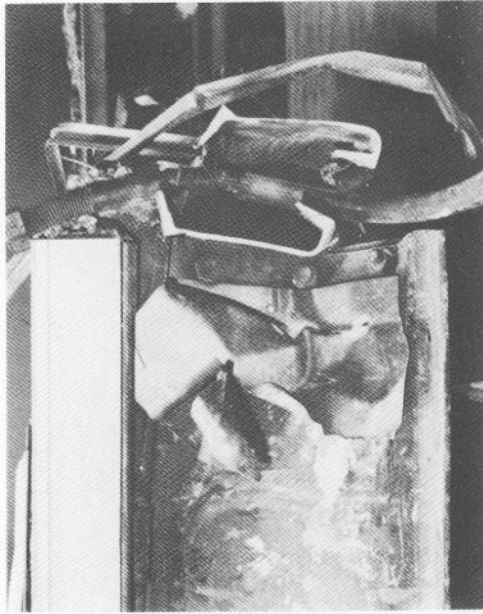
c) Location 8UW.



d) Location 8UE.



e) Location 9UE.



f) Location 10UE.

Figure 5.14 Observed symmetry of distortion of box beams at locations 8U and 10U relative to the box beam at location 9U.



Figure 5.15 Weld penetration at location 8UW, upper flange.

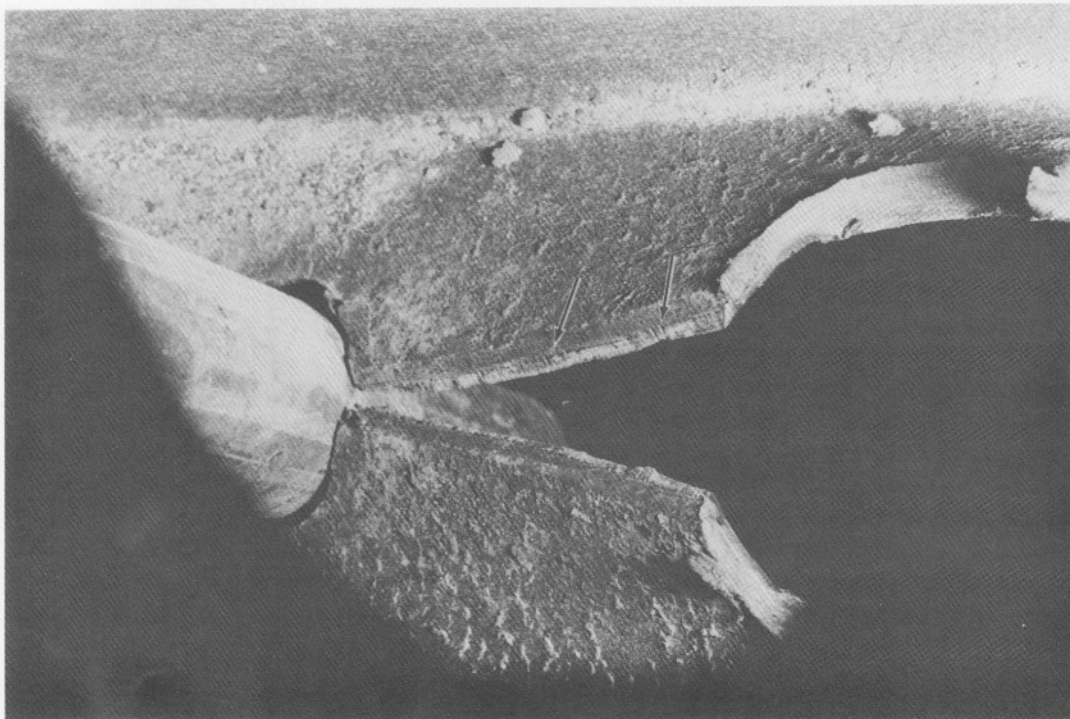
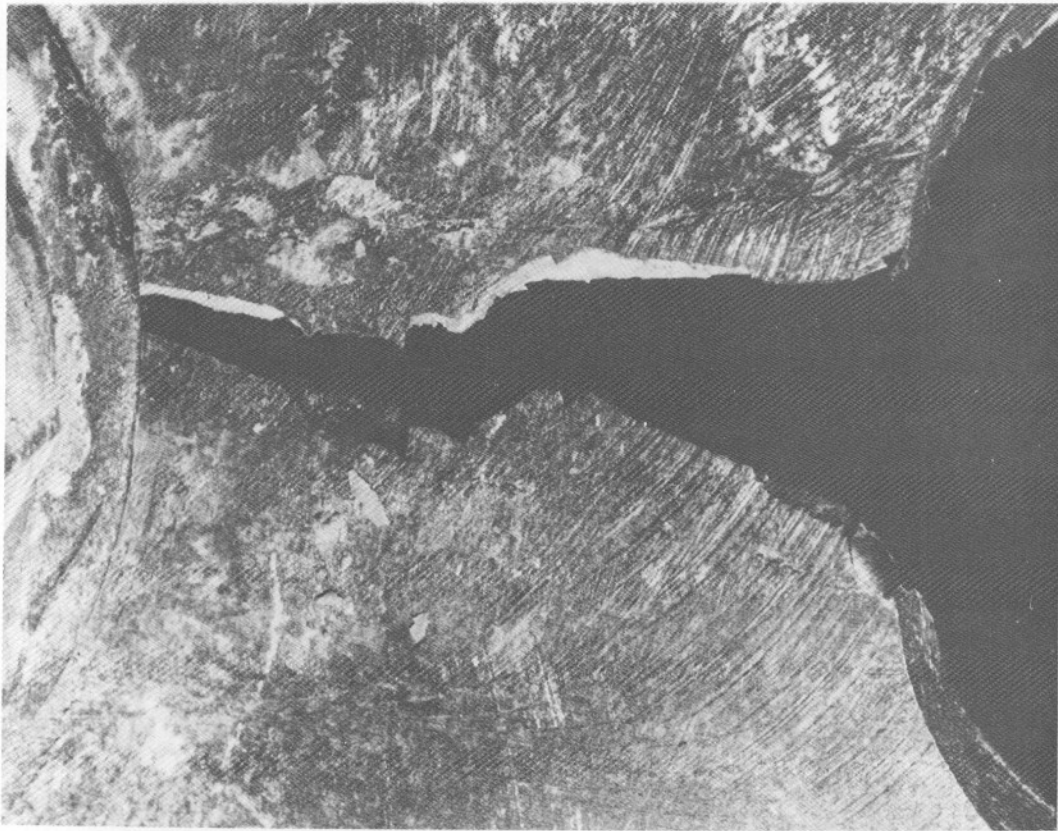
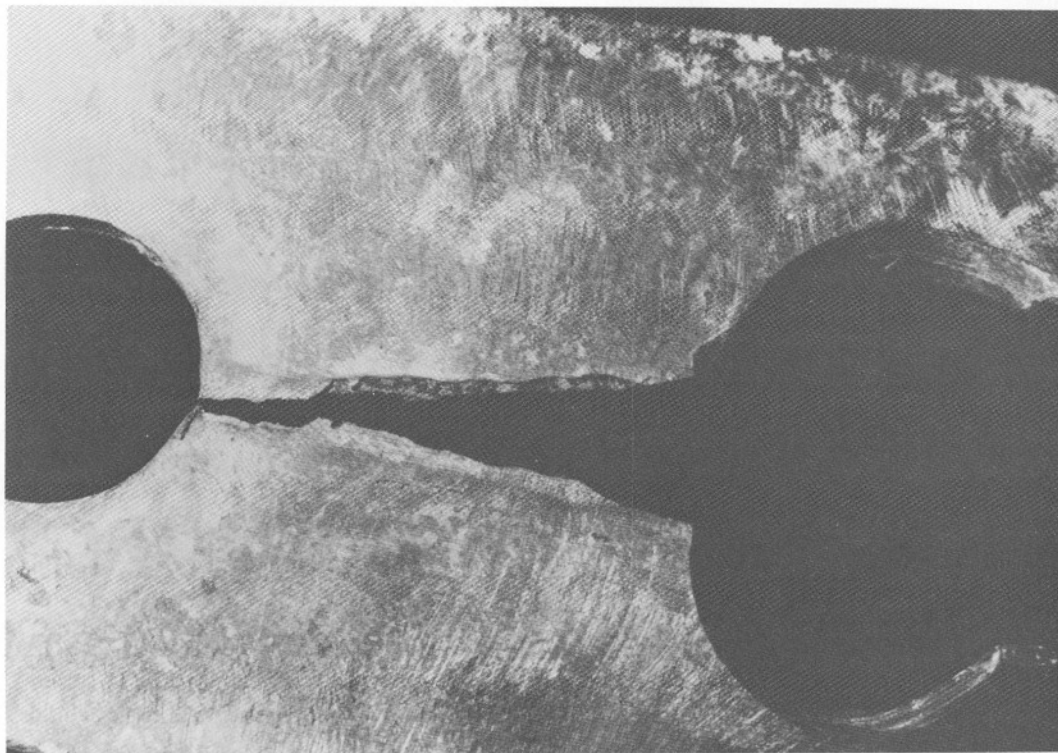


Figure 5.16 Fracture through the weld at location 9UE, lower flange. Weld porosity denoted by arrows.

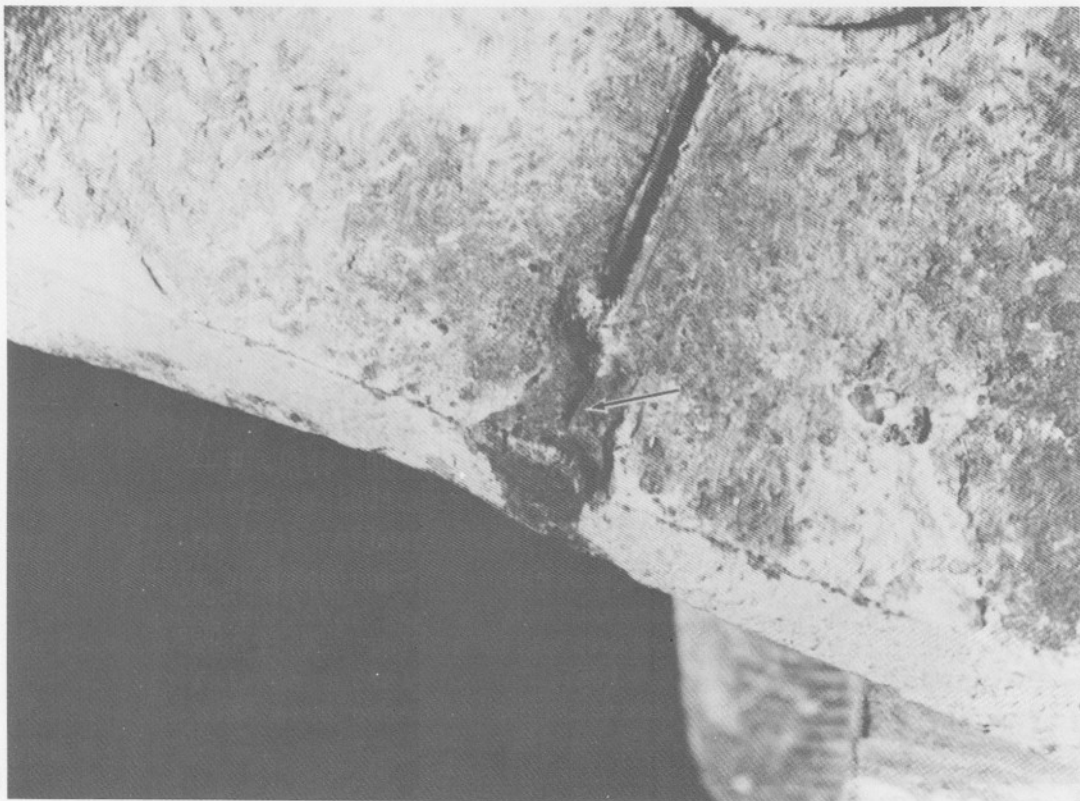


(a)

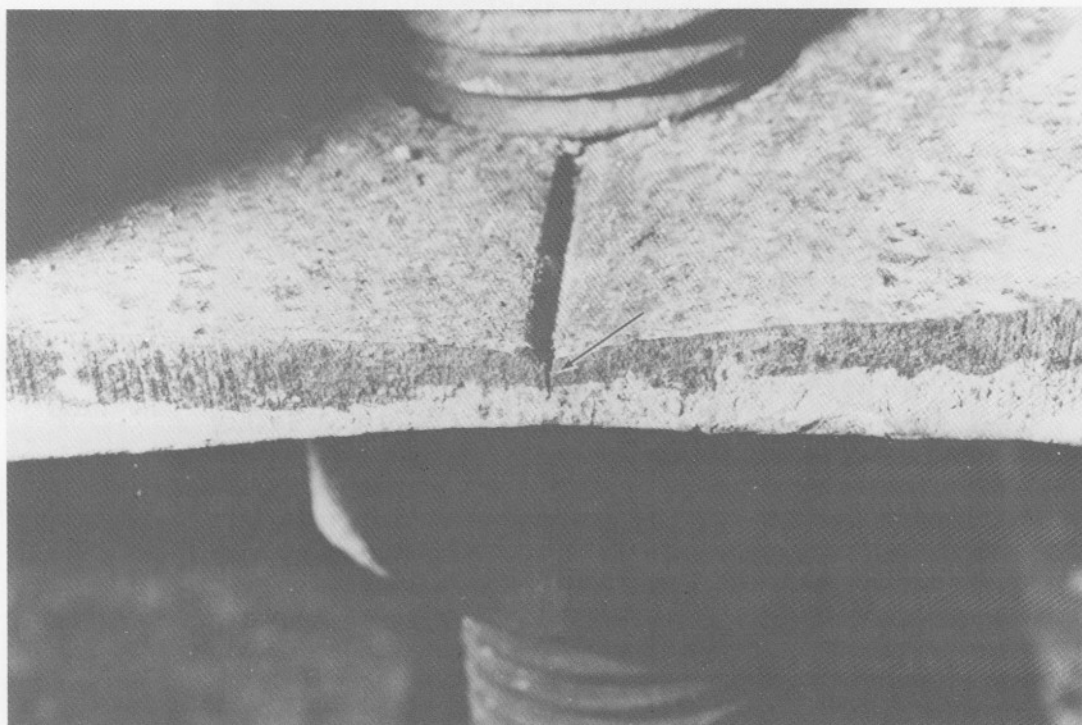


(b)

Figure 5.17 Fusion line weld fractures between hanger rod holes, upper flange weld, locations 9UE(a) and 8UE(b).



a) Location 8MW. Tack weld crack.



b) Location 8ME. End crack.

Figure 5.18 Apparent cracks (arrows) in lower welds of box beams in third floor walkway.

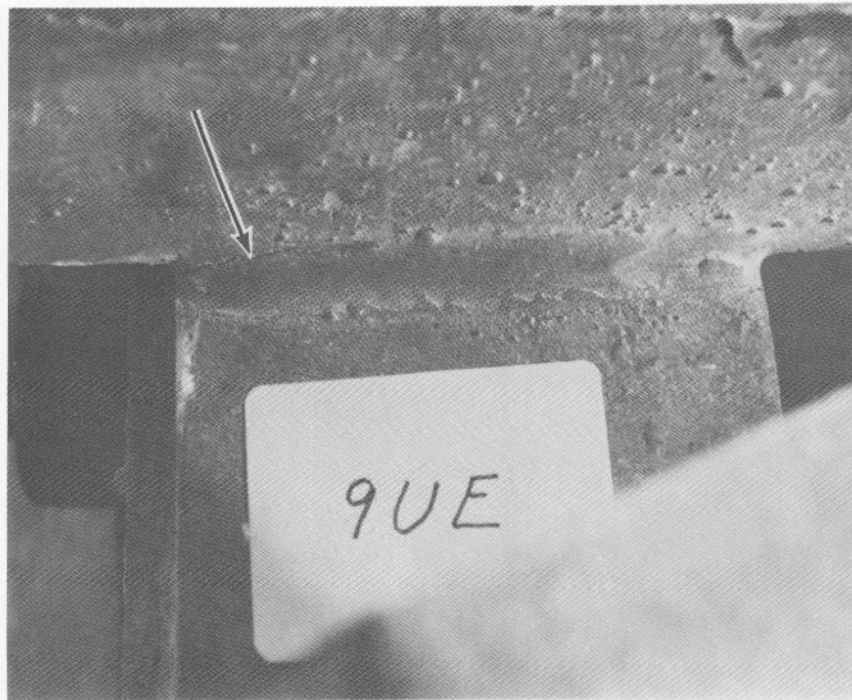


Figure 5.19 Incipient shear failure, bottom fillet weld of intact clip angle, location 9UE, south side.

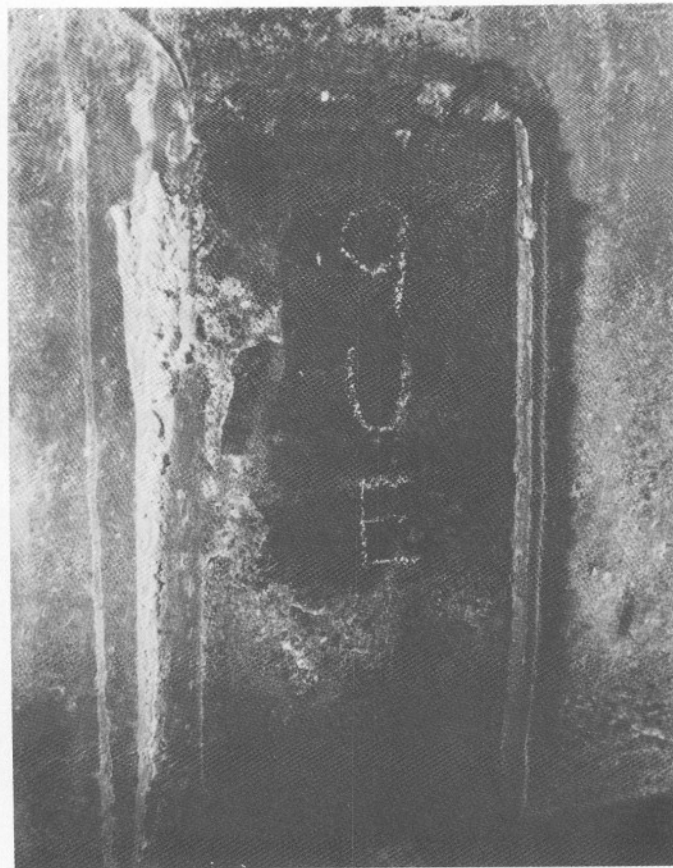


Figure 5.20 Shear failure at bottom and pull-out failure at top of clip angle, location 9UE, north side.

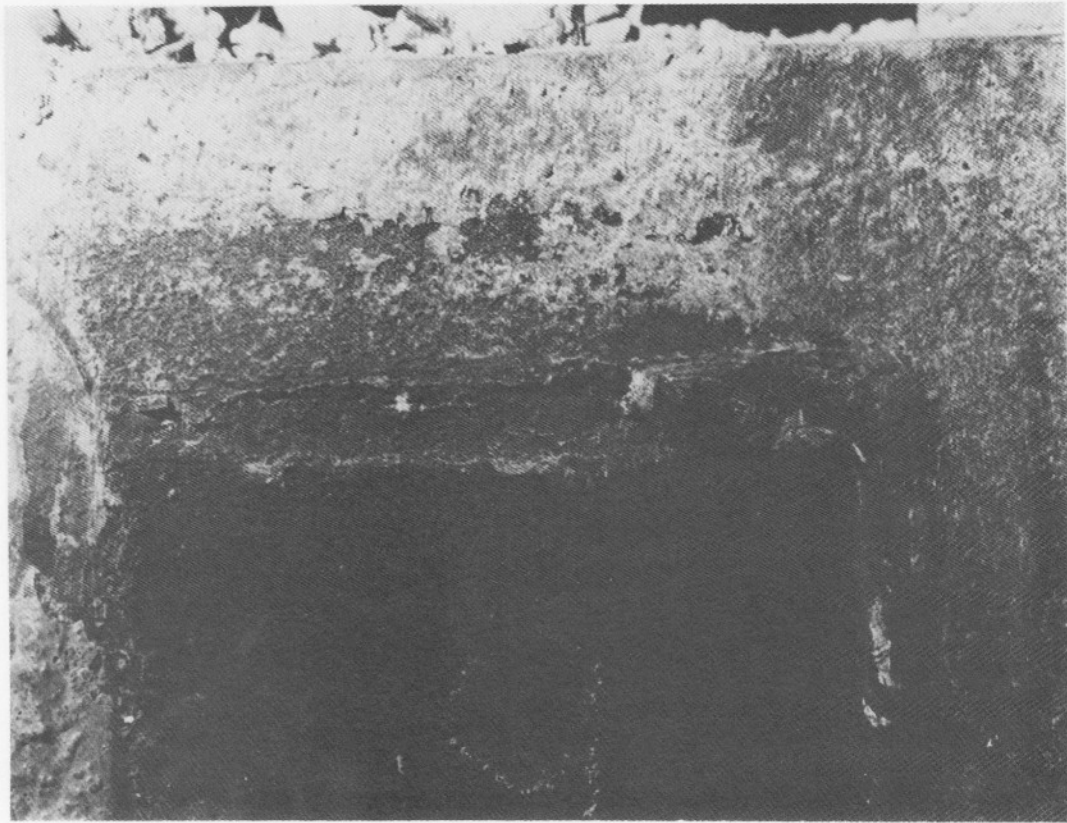


Figure 5.21 Pull-out failure of top fillet weld on box beam web, location 9UE, north side.



Figure 5.22 Shear failure in clip angle fillet weld at location 9UW, north side. This weld and the corresponding weld at location 9LW did not show evidence of a pull-out (tensile) failure at the top fillet weld.



Figure 5.23 Tearing of top end of north clip angle at location 8UE.



Figure 5.24 Tear in box beam web at location 8UE.



Figure 5.25 Embedded plate at connection 7UE.

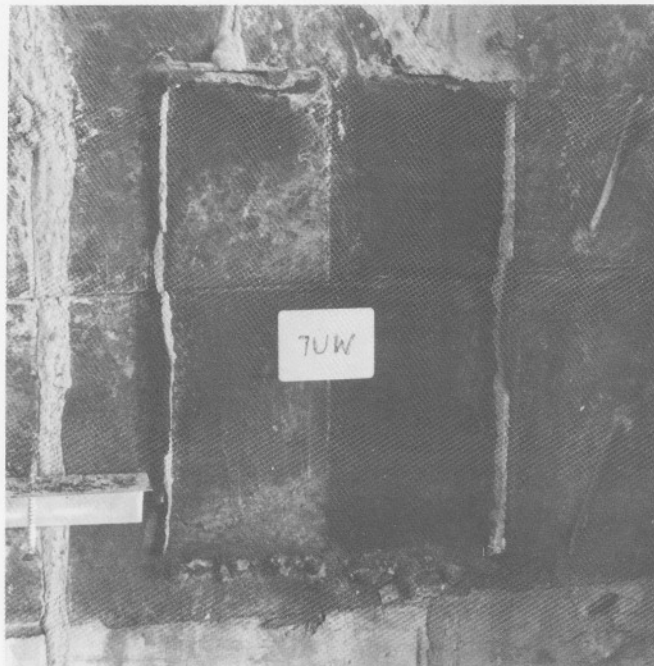


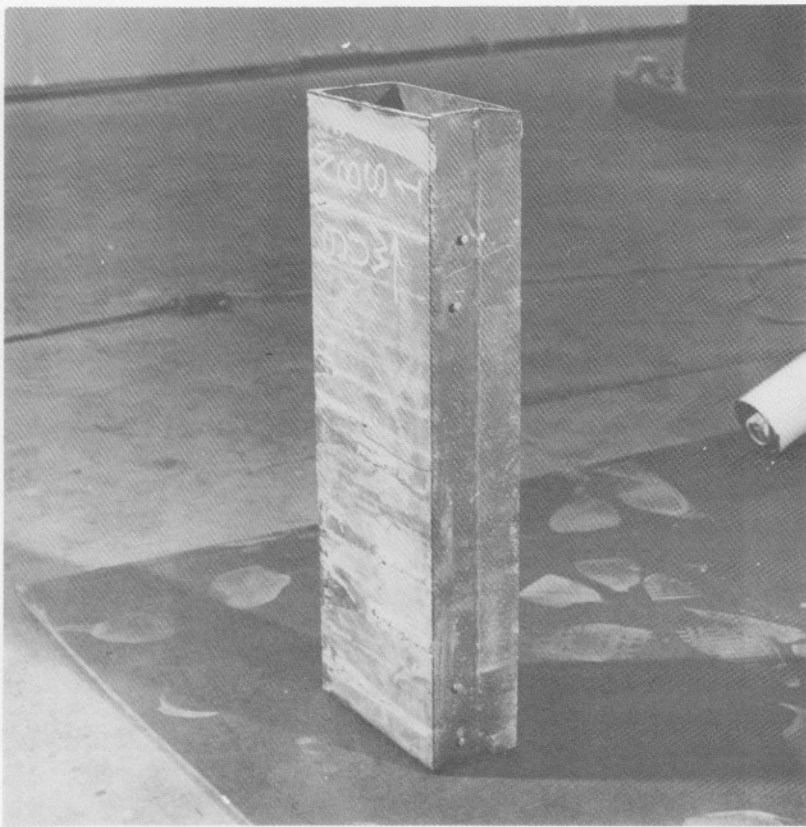
Figure 5.26 Embedded plate at connection 7UW.



Figure 5.27 Modified bearing pad at location 11UW.



a) Before removal.

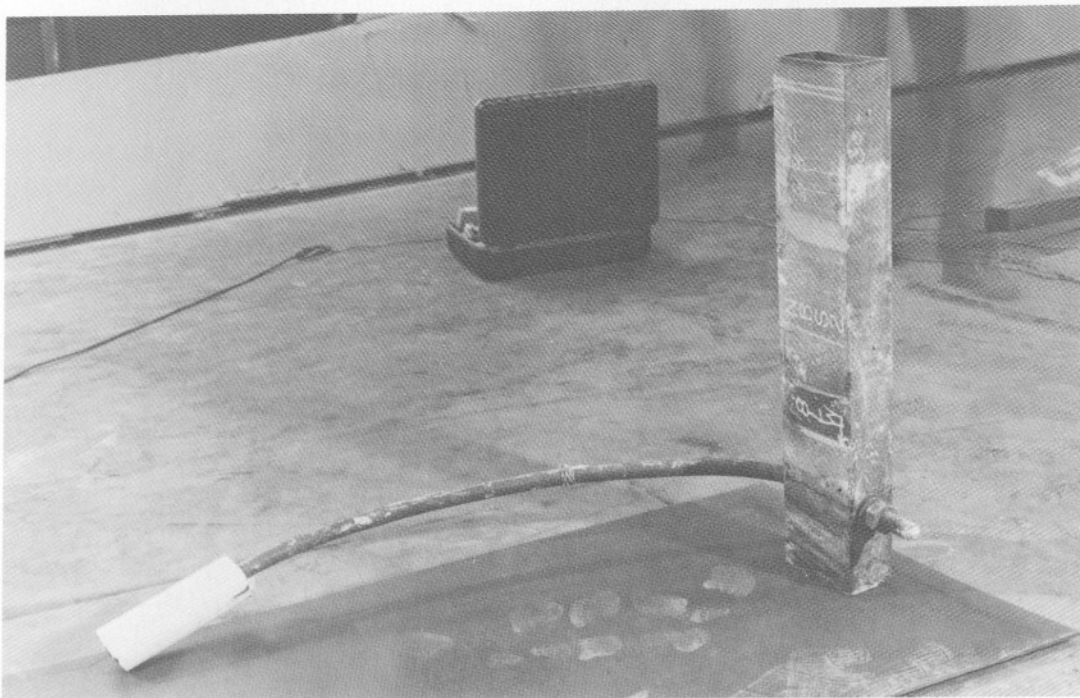


b) After removal.

Figure 5.28 Specimen no. 1 before and after removal.

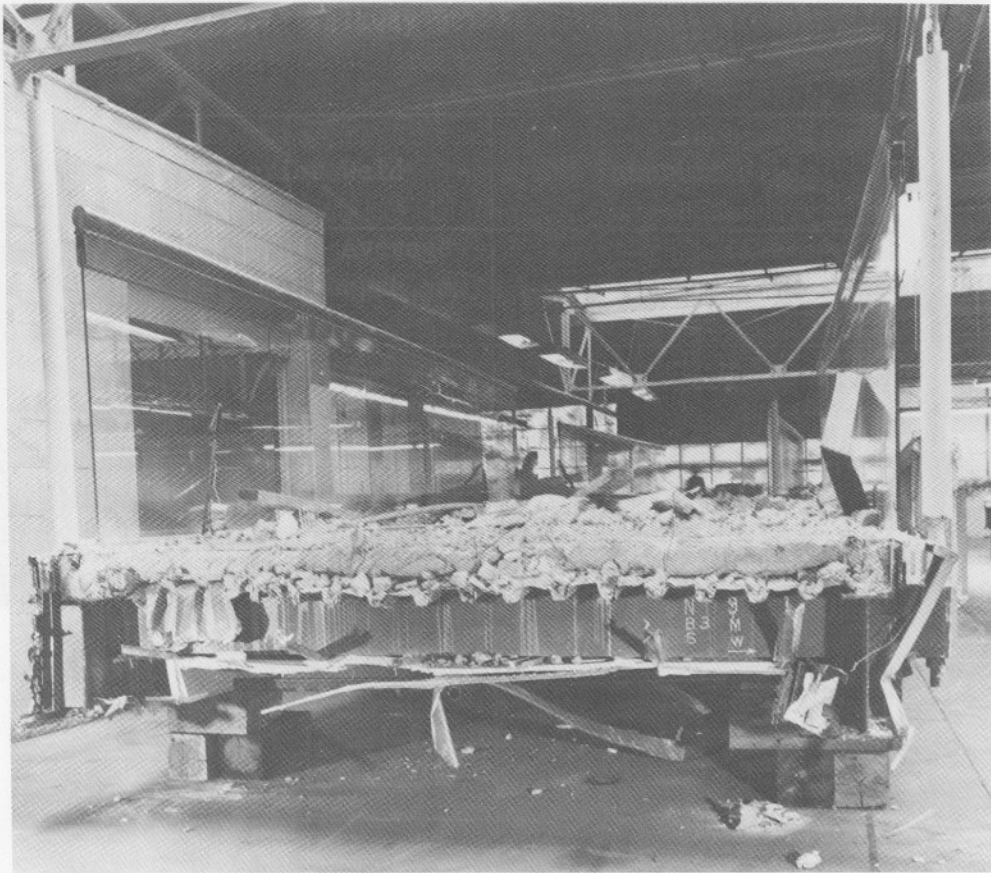


a) Before removal.

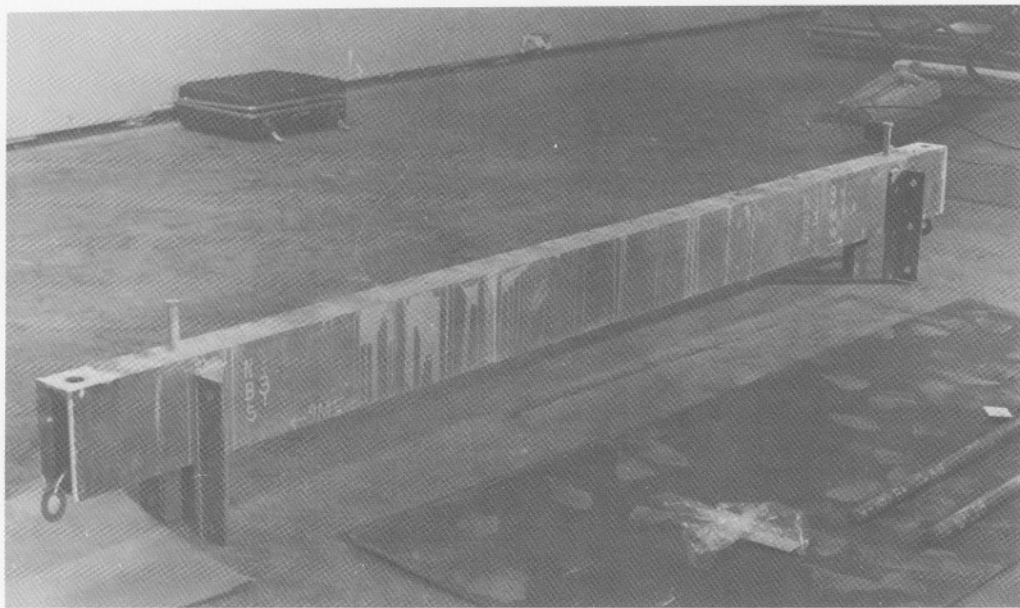


b) After removal.

Figure 5.29 Specimen no. 2 before and after removal.



a) Before removal.



b) After removal.

Figure 5.30 Specimen no. 3 before and after removal.

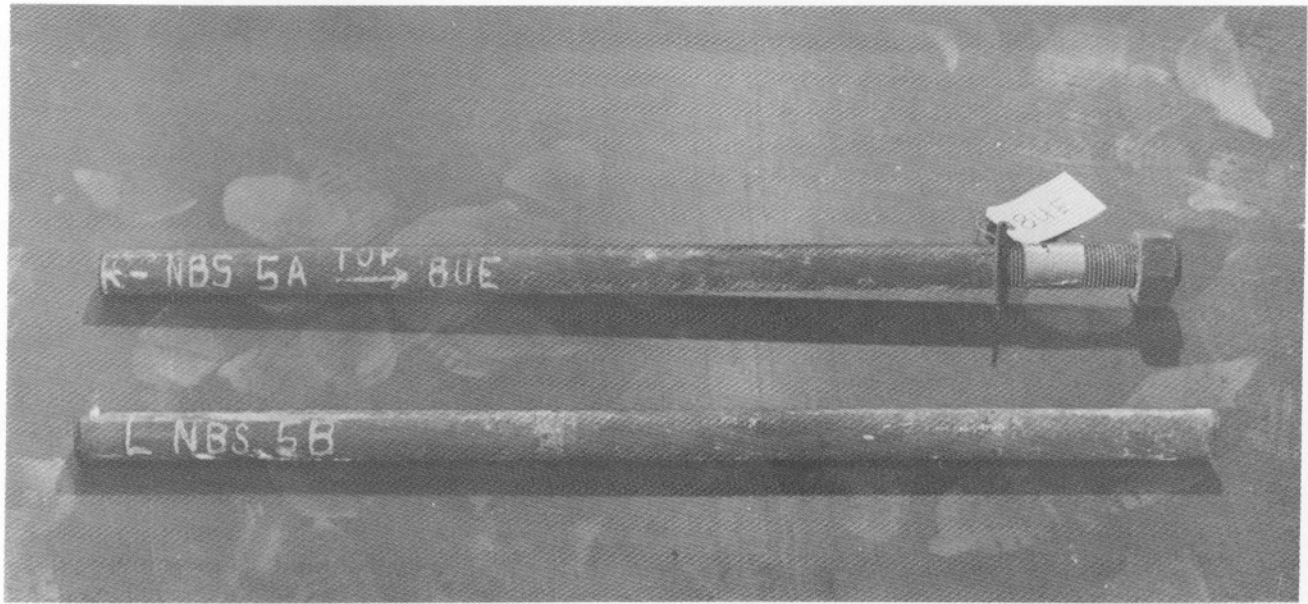


Figure 5.31 Specimen no. 5A and 5B after removal.

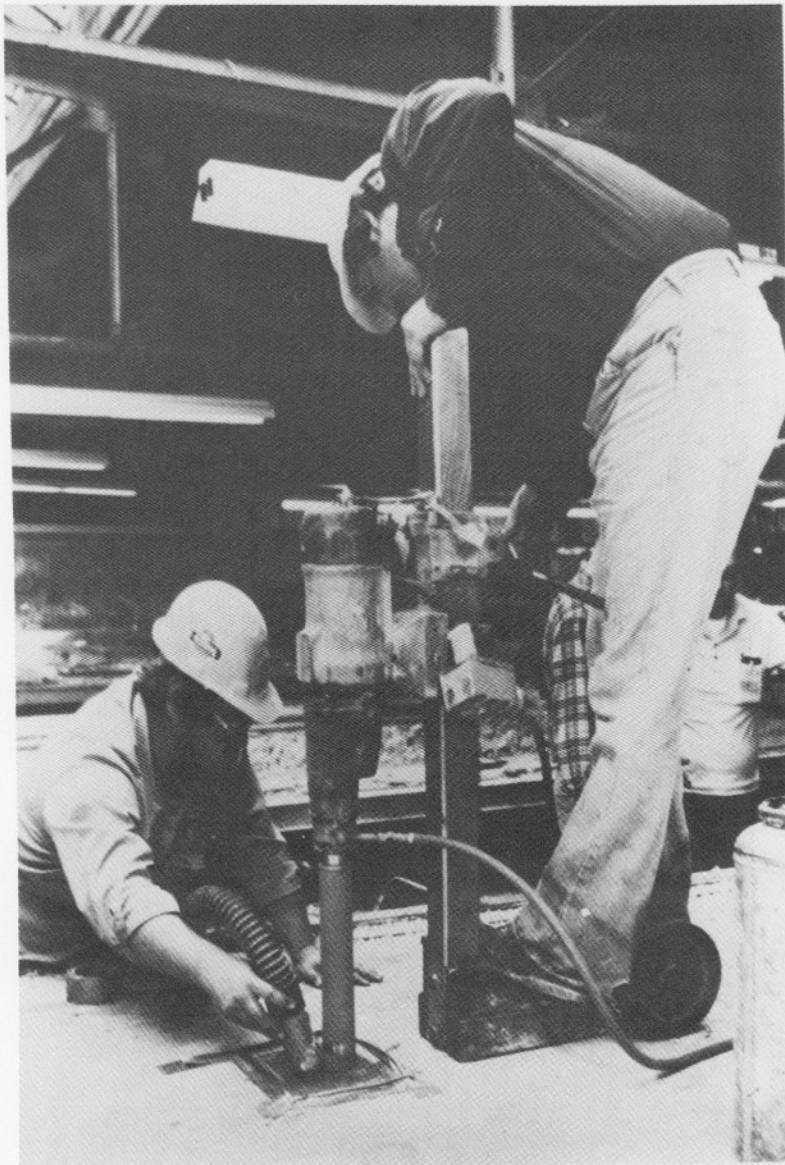


Figure 5.32 Concrete core drilling.



Figure 5.33 Concrete cores.



## 6. NBS STRUCTURAL TESTING PROGRAM

### 6.1 INTRODUCTION

This chapter describes the NBS structural testing program relating to the walkway collapse, presents the test results, and discusses observations made based on the test results. In addition, the estimated load capacity for each of the upper walkway box beam-hanger rod connections is presented with a discussion of how the capacities were determined.

Section 6.2 presents a background to the test program and section 6.3 presents an overview of the test program. Section 6.4 describes the geometry of the test specimens and fabrication methods. Section 6.5 presents a detailed description of the physical setup for testing the specimens, while section 6.6 describes the equipment used to load the specimens. Section 6.7 describes the instrumentation used in monitoring specimen performance while section 6.8 presents the method of acquiring, storing, and processing data. Section 6.9 discusses the sequence of applying loads to the specimens. Section 6.10 presents a detailed description of the NBS-fabricated short box beam specimens and presents the pertinent test results. Section 6.11 similarly presents the NBS-fabricated full-length box beam tests. Section 6.12 discusses the structural tests (both full-length and short specimens) performed on walkway box beam 9M. Section 6.13 presents estimates of the upper walkway box beam-hanger rod connection load capacities. Section 6.14 presents the significant conclusions reached in this chapter.

### 6.2 BACKGROUND

The purpose of the test program was to estimate the walkway box beam-hanger rod connection load capacities. The load capacities could be defined adequately only by examining the influence of a number of parameters. The limitations imposed by the unavailability of as-built drawings, actual materials (in the initial stages of the investigation), and design calculations made it necessary to vary the parameters to take into account the range of variations that were likely for the actual walkway construction. The parameters were varied to examine their influence on load capacity and in this way identify and emphasize the parameters most affecting capacity.

### 6.3 OVERVIEW

The structural test program to examine the box beam-hanger rod connection capacity used two types of test specimens: 1) short box beam and 2) full-length box beam. The specimen types are described in more detail in section 6.4. Two sources of material were used for the test specimens. A supply of steel channel, all from a common heat, was purchased for the box beams fabricated by NBS. Welding, using several different processes, was done in the NBS shops. Additional tests, both full-length and short box beam types, were conducted on material obtained from the actual walkway structure. The short box beam specimen was developed as a simple and cost-effective alternative to the full-length box beam and was used as the main test specimen to permit the examination of a number of variables. The full-length box beam tests were used to validate the short box beam tests.

### 6.4 TEST SPECIMEN DESCRIPTION

Two types of specimens were tested in the investigation of box beam-hanger rod connection capacity. The full-length box beam specimens were dimensionally similar to a typical fourth floor walkway box beam (figure 3.10). The short box beams were essentially the end 22 in (560 mm) of a full-length box beam. Sixty short box beams and seven full-length box beams were fabricated by NBS and tested. Four short box beam specimens and one full-length box beam specimen were prepared from an actual walkway box beam and tested.

#### 6.4.1 Full-Length Box Beam

The full-length box beams were fabricated using the dimensions shown on the walkway box beam shop drawing (figure 3.10). All material was nominally as specified on the shop drawing. A detailed description of the actual properties of these materials is presented in chapter 7.

#### 6.4.2 Short Box Beam

Examination of the walkway debris indicated that the zone of distress in the box beam-hanger rod connection was generally limited to the portion of the box beam between the end of the box beam and the stringer connection with the box beam. The distress zone was primarily near the hanger rod locations. Based on the visual examination, the short box beam could have been made by cutting the full-length box beam at the stringer connection. However, a slightly longer test specimen was used to conform to the physical constraints of the laboratory test facility. The comparability of full-length and short box beam behavior is discussed in section 6.11.

The actual test specimen, figure 6.1, was approximately 22 in (560 mm) long. The specimen was mounted to a test rig through two angles welded parallel to the webs at one end of the specimen. The hole size and locations in the test specimens were as specified on the shop drawings for the walkway box beams. The first tests on specimens without stringer-box beam clip angles, using a whitewash coating on the specimen as a brittle coating, indicated that the

zone of distress did not extend to the clip angle position. It was thus concluded that the effect of the clip angles was minimal and for simplicity they were omitted in all but four tests. The validity of this assumption was confirmed by four tests that are described in section 6.10.5.

### 6.4.3 Fabrication

All test specimens were fabricated by the same experienced welder who used different techniques until he could consistently produce a weld that was visually similar to the observed walkway box beam welds specified as part of the testing program. A supply of channel the same size as that used in the walkway was obtained in 20 ft (6.1 m) lengths from a single source and was specified as being from a single heat. Each box beam, identified in tables 6.1, 6.2, 6.3, and 6.4, was made from channel pieces taken from a single 20 ft (6.1 m) length of channel.

The walkway box beams had been fabricated by laying a weld bead along the channel flange tips from the outside of the box beam over the entire length of the beam. For purposes of describing the structural tests, such a weld is termed an exterior weld in this chapter. The depth of exterior weld penetration (figure 6.2) estimated from visual examination of the damaged walkway box beams was used as a guide in the fabrication of the short box beams. The welder fabricating the short box beams was able to produce welds having a fairly uniform penetration along the beam. However, to examine the significance of exterior weld penetration, specimens having penetration less than and greater than the estimated penetration were fabricated. The majority of short box beams were fabricated with a weld penetrating partially into the flange thickness and were termed "shallow penetration" welds. Several specimens were fabricated in which the welder was told to "fully penetrate" the flange thickness without using a backing strip. These welds were termed "deep penetration." Two specimens were fabricated with no weld bead laid along the outer 8 in (203 mm) of the short box beam except for a small tack weld at the free end of the specimen (figure 6.3). These two specimens were termed "no weld" specimens and were tested to determine a lower bound strength of the box beam-hanger rod connection.

The walkway box beams had weld beads of varying lengths on the interior of the flange joint outboard of the exterior hole (figure 6.4). These weld beads are termed interior welds in this chapter. Short box beams were fabricated having several variations of the interior weld length. Insofar as possible, the penetration of the interior weld was kept constant. The penetration was such that the interior weld and the exterior weld roots were separated by a small gap (figure 6.4). The lengths of interior weld were nominally equal to zero, 1/2 in (13 mm), 1 in (25 mm), and 1 3/8 in (35 mm). In the NBS beams the interior weld was laid prior to boring the rod holes. The 1 3/8 in (35 mm) length resulted from welding to the centerline of the exterior rod hole (2 in or 51 mm) and removing the weld in the hole location during the hole boring operation to obtain the actual length of 1 3/8 in (35 mm). In the NBS beams the interior welds were laid after the exterior weld and were done by the same process as that used for the exterior weld.

All short box beams in series A through R, excluding I3 (listed in table 6.5) were cut to length prior to welding. The remaining short box beams (except for the S series described below) were cut 1 in (25 mm) longer than their final length and then welded. This was done in an effort to control possible variation in welding due to startup of the welding process at the beam end. After all welding was completed the extra length was removed at the ends and the hanger rod holes bored. Full-length box beams (table 6.4) L1 and L2 were cut to length, while L3 through L7 were cut 2 in (51 mm) longer than their final length. After welding, 1 in (25 mm) was cut off from each end of the beam.

The S-series short box beam with stringer-box beam clip angles were fabricated by removing the unfailed ends of four full-length box beams as is discussed further in section 6.10.5. Specimens L5, L4, L6 and L3 were used to fabricate S1 through S4 respectively.

The sequence of fabrication for both NBS short and full-length box beams was as follows:

- Tack weld the interior of the ends of the box beam, top and bottom
- Weld along the exterior of the box beam seam, top and bottom
- Weld along the interior of the box beam seam (if specified), top and bottom
- Weld on the attachment clip angles used to fasten the specimen to a reaction buttress described in section 6.5
- Grind off the exterior weld bead flush with the surface completely along the top and at least 12 in (305 mm) from the end(s) on the bottom
- Bore a pilot hole for each hanger rod hole. Finish the hole using a numerically controlled milling machine. Each hole was made in a separate operation.

## 6.5 TEST SETUP

Full-Length Box Beam. A photograph of the test setup simulating a fourth floor box beam is shown in figure 6.5. A drawing with the various parts of the test setup labeled is shown in figure 6.6. The full-length box beam test setup was contained within a self-reacting structural steel test frame. The test frame was bolted to a structural tie-down floor. The frame columns were 12 in (305 mm) deep wide flange shapes and each reaction beam was made of two 36 in (915 mm) deep wide flange sections placed side by side with a 1 1/2 in (38 mm) gap between the flanges to permit the loading rods to pass through. The two load transducers for the upper loading rods rested on a 1 in (25 mm) thick steel plate which spanned the gap between the beam flanges. A hardened steel washer and heavy hex nut terminated the upper loading rods and rested against the top surface of the load transducer.

Each hydraulic cylinder was held in place against the lower surface of the lower reaction beam by a frame bolted to the reaction frame. The load transducers were separated from the hydraulic cylinder piston by a 1/2 in (13 mm) thick steel plate. The lower end of the loading rod was terminated by a hardened washer and a heavy hex nut.

The upper walkway loading system applied the simulated fourth floor dead load to the box beam through the stringer-box beam clip angles (figure 6.7). The system used a spreader beam with three pinned attachment points which enabled the spreader beam to rotate while keeping the applied load acting vertically. A plate was bolted between and below the clip angles to permit attachment of the clevis to the box beam (figure 6.8). The middle pin was the connection point for the loading rod. The attachment of the spreader beam to the clip angle was through a pin and clevis arrangement as shown in figure 6.9.

Short Box Beam. The test setup, figures 6.10 and 6.11, used an existing structural tie-down floor and reaction buttress plus two specially made vertical reaction supports. The vertical reaction supports provided the reaction for the hydraulic cylinders applying load to the upper (fourth floor) and lower (second floor) hanger rods. The reaction supports were bolted to the tie down floor to resist both shear and overturning forces. The test specimen was bolted to the reaction buttress. Prior to each test the bolts holding the test specimens were pretensioned using an impact wrench.

The assembled test specimen was rotated 90 degrees from its normal orientation. The webs of the box beam were parallel to the floor. The hanger rods (loading rods) were also parallel to the floor. Each loading rod passed through the specimen, reaction support, center-hole hydraulic cylinder, and center-hole load transducer and was terminated with a hardened washer and heavy hex nut.

## 6.6 LOADING EQUIPMENT

Full-Length Box Beam. The loading equipment included three 100 ton (890 kN), 10 in (254 mm) travel, double acting hydraulic cylinders; an electric hydraulic pump; and a ten channel hydraulic pressure maintainer. The hydraulic pump had a discharge rate of 0.26 gallons per minute ( $16.4 \times 10^{-6} \text{ m}^3/\text{s}$ ).

The hydraulic cylinders were of the center hole type to permit the loading rod to pass through the cylinder. The loading rod was centered in the cylinder by a wooden sleeve. The lower walkway hydraulic cylinders were connected by manifolds to common pressure and return lines. Thus, while there were three hydraulic cylinders, there were only two pressure channels, one for the upper walkway hydraulic cylinder and one for the two lower walkway hydraulic cylinders. The hydraulic cylinders were supplied with oil by means of the hydraulic pressure maintainer and the hydraulic pump. The hydraulic pump supplied oil to the maintainer at a nominal pressure of 5000 psi (35 MPa). The maintainer controlled the hydraulic pressure actually applied to each cylinder. The operator adjusted the pressure in each pressure channel independent of the other.

Short Box Beam. The loading equipment consisted of two 60 ton (534 kN), 3 in (76 mm) travel, single acting, spring return hydraulic cylinders; an electric hydraulic pump; and a ten-channel hydraulic pressure maintainer. The hydraulic pump and pressure maintainer were the same as used for the full-length box beam tests.

The hydraulic cylinders were of the center hole type to permit the loading rod to pass through the cylinder. The loading rod was centered in the cylinder by two teflon sleeves. The hydraulic cylinders rested on a wooden cradle fabricated so that the cylinder centerline was in line with the box beam-hanger rod hole centerline.

## 6.7 INSTRUMENTATION

Full-Length Box Beams. The instrumentation included five load transducers, one for each loading rod, two pressure transducers, four linear potentiometers (LPs), two rotary potentiometers (RPs), and four linear variable differential transformers (LVDTs). All devices were connected to a common DC power supply. The load transducers were of a full bridge resistance strain gage type. The load transducers were center holed with machined steel bearing surfaces fabricated to center the transducer on the loading rod.

The displacement measuring devices were placed as shown in figure 6.12. The instrumentation was identical on each end of the beam so only one end is described. Two mounting beams were bolted to each test frame column, one above and one below the box beam. These beams served as attachment points for the displacement measuring LPs and RPs. The linear potentiometers had 10 in (254 mm) travel. One LP was attached to the box beam about 1 in (25 mm) from the end and to the upper mounting beam such that it was vertical. Similarly the other LP was attached to the lower loading rod nut and the upper mounting beam. The rotary potentiometer measured linear displacement through a cable and spring mechanism. The RP had a total travel of over 20 in (508 mm). The mechanism was attached to the lower mounting beam and the cable ran vertically to the upper loading rod. The cable was attached to the rod by a hook screwed into a hole tapped in the end of the rod. Two LVDTs measured the transverse (out-of-plane) distortion of the box beam webs. The LVDTs were mounted on one web of the box beam and spanned to plates mounted on the other web. One LVDT was mounted near the middle of the box beam depth and the other LVDT was mounted near the bottom of the box beam.

One pressure transducer was placed in the common pressure line for the two lower loading rod hydraulic cylinders and the other pressure transducer was placed in the pressure line for the upper walkway loading rod.

Short Box Beam. The instrumentation consisted of two load transducers, one for each loading rod, and up to six linear variable differential transformers (LVDTs) for measuring displacements. All devices were connected to a common DC power supply.

The load transducers were placed between the hydraulic cylinders and terminating nut (figure 6.11) with a 1 in (25 mm) thick plate between the transducer and the

cylinder and a hardened washer placed between the transducer and the nut. The load transducers were of a full bridge resistance strain gage type. The transducers were also center holed with machined steel bearing surfaces fabricated to center the transducer on the loading rod.

The LVDTs were ordinarily placed as shown in figure 6.13. Three LVDTs measured the out-of-plane or transverse distortion of the box beam webs and three LVDTs measured the in-plane displacement of the loading rods and box beam free end. All tests used the in-plane LVDTs. However, when photographs or videotapes were taken of the tests in progress the specimen had either no transverse LVDTs or only the middle transverse LVDT. The transverse LVDTs were mounted on one web of the box beam and spanned to plates mounted on the other web. The in-plane LVDTs were mounted on stands resting on the tie-down floor and spanned to either the specimen end of the rods or the upper flange of the box beam near its free end.

## 6.8 DATA ACQUISITION AND REDUCTION

Both data acquisition and reduction were computer based operations. The hardware components of the system consisted of a minicomputer with a variety of peripherals and a high speed amplifier/multiplexer analog-to-digital converter. The software component was a test executive which interfaced the operator and the hardware. The software performed the data conversion and reduction as well as controlled the acquisition of the data.

The analog-to-digital converter had a sample rate of 50 kHz. The time required to sample all data channels (maximum of 9) once (a scan) was about 180 microseconds. In most of the tests a scan was acquired every three seconds except during breaks in loading when no scans were required. All data signals were amplified by the analog-to-digital converter such that the maximum expected analog signal was at least half of the converter's full scale (10 volts) range. The analog-to-digital converter transferred binary representations of the input analog signal to the minicomputer through direct memory access. Software then stored the data on disk and manipulated the data to produce converted and reduced data.

The binary representation of the analog signal is converted to a decimal number knowing the amplifier gains and the full scale range of the converter. The decimal voltages are reduced by using a selected scan as a zero reference and adjusting all subsequent values to reflect the zero reference value. The zero reference scan is a data scan acquired prior to activating the hydraulics. The reduced values for the load transducers are corrected for excitation voltage changes. The voltages are supplied by a regulated power source and do not vary during a test. However, the load transducers are calibrated at a 6.00 volt excitation level, but the test excitation level is generally slightly different (e.g., 6.08 volt). The reduced values also include a multiplicative coefficient which expresses the voltage in terms of any desired unit (e.g., kips).

## 6.9 LOADING SEQUENCE

The stress state in the box beam-hanger rod connection region is dictated by the loads from both the lower and upper walkway hanger rods. The exact distribution of load between the two rods is influenced by a number of factors, but it can be approximated by the assumption that all of the load from the lower walkway hanger rod is transferred to the adjoining upper walkway hanger rod in addition to the contribution due to upper walkway loads. The general loading sequence used in most of the box beam tests is based on applying only dead load to the upper walkway and dead load plus all live load to the lower walkway. This loading is not an exact simulation of the actual situation but, as discussed in section 4.4, is reasonably consistent with the small number of people believed to have been present on the fourth floor walkway at the time of collapse. The test results also indicate that the load capacity is not significantly affected by small variations in loading sequence, as pointed out in section 6.10.5.

The hydraulic loading system used in the tests applies load as long as there is resistance to the stroke of the hydraulic cylinder. As failure begins to occur, the applied load decreases until the movement of the cylinder can "catch up" with the movement of the structural member. The actual walkway loading was a gravity-type loading. That is, the loads remained in place regardless of the deformation of the structure. Thus, as the structure begins to fail the gravity load remains constant although the resistance of the structure is decreasing with deformation. These two methods of loading, that is, hydraulic vs. gravity, will produce little difference in structural response until deformations become large. At that point, the gravity-type loading causes a more rapid failure of the structure than the hydraulic loading. The ultimate capacity which would be obtained by either method of loading would be expected to be the same. The load-deformation curves would also be expected to be the same up until the maximum load is reached.

Full-Length Box Beam. The upper walkway dead load was applied to the box beam through the upper walkway loading system. The lower loading rods were kept unloaded. After the upper walkway dead load was reached the hydraulic pressure maintainer kept the load constant. The load in the lower rods was then gradually increased until failure occurred. Using this loading procedure the load carried by the upper rod was equal to dead load from the fourth floor and dead load plus live load from the second floor. In most tests the loading was terminated after lower flange failure at the location of an upper walkway hanger rod while in other tests loading was continued until failure also occurred in the upper flange. The upper flange failure load was always smaller than the lower flange failure load and the large deformations involved following lower flange failure made additional distortion measurements of questionable value.

Short Box Beam. The loading sequence used in nearly all short box beam tests was as follows:

1. Load the upper rod to a value representing the nominal fourth floor dead load contribution keeping the lower rod unloaded.

2. Once the nominal dead load value was reached in the upper rod, load was added equally to both rods until the test was terminated when full piston stroke for the upper rod was reached. The load carried by the upper rod was then equal to dead load from the fourth floor and dead load plus live load from the second floor. The maximum load capacity was achieved in all but one test prior to reaching the stroke limit.

## 6.10 NBS SHORT BOX BEAM TESTS

### 6.10.1 Parameters

A range of parameters was studied in order to define adequately the load carrying capacity of the box beam-hanger rod connection. A number of parameters were required for reasons such as:

- variability of details among the walkway box beams (e.g., interior weld length)
- uncertainty of conditions at the onset of failure (e.g., nut orientation, washer presence), and
- unavailability of walkway box beam properties at early stages of the test program (e.g., welding process, washer hardness).

The parameters studied in the short box beam tests were:

- Welding Process
- Exterior Weld Penetration
- Interior Weld Length
- Interior Weld Position
- Washer Presence
- Washer Hardness
- Washer Thickness
- Nut Shape
- Nut Orientation
- Loading Configuration
- Initial Upper Rod Load
- Stringer-Box Beam Clip Angle Presence

These are discussed in detail in the following subsections along with the test results.

#### 6.10.2 Short Box Beam Specimens

The characteristics of each short box beam specimen along with the peak load resistance for each specimen determined by the load in the upper rod are listed in tables 6.1, 6.2, and 6.3. Data for specimens which used hardened washers beneath the fourth floor rod connecting nut are listed in table 6.1 while specimens which used unhardened washers are listed in table 6.2. Three specimens tested without washers are listed in table 6.3.

Three different failure types, assigned the identifiers I, II, and III, were observed and are shown in figure 6.14. The bottom flanges of specimen K2, and others exhibiting type I behavior, fold back about a plastic hinge in the web and do not show any discernible bending. The flanges in type III behavior, illustrated by J1, fold back about the plastic hinge in the web but also show pronounced bending in the flange. Type II behavior exhibits slight bending in the flange tips as illustrated by specimen M1. None of the washers fractured in these tests.

Three typical in-plane load-deflection curves for the short box beam specimens are shown in figure 6.15. (A complete set of load-deflection curves is presented in appendix A.6.10.) Each curve is a plot of the load measured by the upper rod load transducer versus the displacement of the rod measured by the LVDT at the box beam terminus of the upper loading rod (LVDT no. 2 in figure 6.13). The peak load achieved by each of the specimens is shown on their respective curves. The asterisk on each curve indicates the end of reliable measurement by the displacement device and does not necessarily denote final rod pull-through.

The in-plane load-deflection curves in figure 6.15 illustrate specimen behavior usually associated with failure types I, II, III and are again illustrated by specimen C3, specimen T3, and specimen F2, respectively.

Type I behavior is characterized by a load-deflection curve which shows a relatively sharp peak at maximum load. In addition to general observations which were made on the behavior of all specimens, several specimens were subjected to detailed observations during their entire loading sequence. Observation of the inside of the box beam, which was whitewashed, indicates that the exterior weld between the two rod holes begins to crack at an upper rod load of between 5 to 7.5 kips (22 to 33 kN). The interior weld (or exterior weld if no interior weld was present) between the outer hanger rod hole and the beam end begins to crack adjacent to the outer hanger rod hole at an upper rod load of from 8 to 10 kips (36 to 44 kN). Web deformation became visible at 10 to 12 kips (44 to 53 kN). The achievement of maximum load is accompanied by fracture of the interior weld (or exterior weld if no interior weld is present) between the exterior hole and the beam end. After the exterior weld breaks the bottom flanges fold back about a plastic hinge in the web. The bottom flanges exhibit no discernible bending.

Type III behavior is usually characterized by a load-deflection curve which has a relatively rounded shape (as compared to type I) at maximum load. Visual observation of a few specimens indicates that the exterior weld between the lower flange hanger rod holes also cracks between 6 to 8 kips (27 to 36 kN) of upper rod load. Cracking of the interior weld begins adjacent to the outer hanger rod hole at between 10 to 12 kips (44 to 53 kN) and progresses to the end of the beam by about 15 kips (67 kN). Shortly after this stage of cracking the deformations become visible. At the maximum load the interior weld has not yet fractured between the exterior hole and the beam end. The resistance to load decreases with increased deflection, but at a constant rate. The rate is quite similar to the load loss rate following the peak load in the type I behavior. The gradual loss in resistance to load continues with progressive cracking until the interior weld between the outer hole and the beam end fractures, at which point there is a sharp drop in load resistance. The bottom flanges exhibit pronounced bending as illustrated by specimen J1 in figure 6.14.

Type II behavior is between the two extremes (figure 6.15). Initially it exhibits the characteristics of type III behavior. However, the interior weld between the exterior hanger rod hole and beam end fractures at or just after the peak load, unlike the type III beams. The bottom flanges appear more like type I but show a small amount of bending as for specimen T3 in figure 6.14.

The out-of-plane load-deflection curves show the same trends as exhibited by the in-plane load-deflection curves. The out-of-plane load-deflection curves for the above described specimens are shown in figure 6.16. Each curve is a plot of the same load described for figure 6.15 versus the displacement measured by the middle transverse LVDT (figure 6.13). These data show that the web is beginning to deform outward shortly after the application of dead load from the second floor is started.

A complete discussion of the effects each parameter has on the ultimate capacity is presented in the following subsections.

### 6.10.3 Welding Process

Since there was uncertainty regarding the welding process actually used in the box beam fabrication, the influence of welding process was examined by using several different procedures to fabricate the short box beams. The selection was made by visually comparing the results of welds made using several types of electrodes used in shielded metal arc welding (SMAW) [6.1] with the visual observations of the walkway box beam welds. Specimens were fabricated with AWS class E7014 and E7018 stick electrodes to give an indication of the effect electrodes had on load carrying capacity. Both the E7014 and E7018 electrodes were 5/32 in (3.97 mm) in diameter.

After a number of specimens had been fabricated and tested, information was received from legal counsel (section 2.7) to the steel fabricator indicating either SMAW, or "MIG welding" was used in the walkway fabrication. Legal counsel further stated that if "MIG welding" were used, the electrode was flux cored. "MIG welding" was taken to include flux cored arc welding (FCAW) or gas metal-arc welding (GMAW). Visually, the GMAW process with a mild steel

electrode most closely resembled the walkway welds. Therefore, a mild steel electrode was used in fabricating the bulk of the remaining short box beams. However, four short box beams were also fabricated using a flux cored electrode. These four specimens provided additional indications as to the effect of different electrodes. The mild steel electrode, AWS class E70S-3, was manufactured by Racco and was 0.045 in (1.14 mm) in diameter. The flux cored electrode, AWS class E70T-1, was a Hobart Fabco 81 electrode also 0.045 in (1.14 mm) in diameter.

The four processes are summarized below:

#### Process 1

GMAW - Gas metal arc welding process using a 0.045 in (1 mm) diameter mild steel electrode.

In all cases the gas was carbon dioxide delivered at 20 cfm (0.009 m<sup>3</sup>/sec).

In all cases the voltage was 26 volts and the current was 150 amps.

#### Process 2

FCAW - Flux cored arc welding process using a 0.045 in (1 mm) diameter flux cored electrode.

In all cases the gas was carbon dioxide delivered at 20 cfm (0.009 m<sup>3</sup>/sec).

In all cases the voltage was 26 volts and the current was 150 amps.

#### Process 3

S14 - An E7014 stick electrode was used without preheat

In all cases the rod diameter was 5/32 in (4 mm)

In all cases DC straight polarity was used

In the C, F, and G series the current was 150 amps

In the A and E series the current was 185 amps

In the D series the current was 180 amps

#### Process 4

S18 - An E7018 stick electrode was used without preheat

In all cases the rod diameter was 5/32 in (4 mm)

In all cases DC reverse polarity was used

In all cases the current was 140 amps

Comparisons between specimens in which the only intentional difference is the welding process appear in figure 6.17. Six sets of data, each consisting of comparable specimens, are shown enclosed in the figure. Hardened washer data are used where possible since it was found (section 6.10.5) that hardened washers were used in the actual walkway construction. The specimens compared for a particular process were fabricated at the same time. This selection of data was done to maintain as much similarity as possible since there was variation in the amount of weld material deposited and, as discussed in

section 6.10.4, the peak upper rod load was later found to vary in proportion to weld area.

Data for deep penetration welds (no interior weld) are used to compare process 3 and 4 (specimens A1, A2, and B1, table 6.1). There is no difference between the average for process 4 data and the process 3 test specimen.

Two further data sets with no interior weld are compared. For specimens with hardened washers (specimens C1, C3, I1, and I2, table 6.1) the average peak upper rod load for process 1 is only 500 lb (2.2 kN) more than process 3. For unhardened washers (specimens LS1, LS2, P1, and P2, table 6.2) the maximum difference in the average is 700 lb (3.1 kN) comparing processes 1 and 2. Even this difference is only about five percent of the peak upper rod load.

The 1/2 in (13 mm) interior weld data set (specimens K1, K2, G1, and G2, table 6.1) comparing process 1 and 3 differs by only an average of 300 lb (1.3 kN). The two data sets for a 1 3/8 in (35 mm) interior weld are for hardened (specimens J1, J2, F1, and F2, table 6.1) and unhardened washers (specimens M2, N1, and N2, table 6.2). The average difference is zero for the comparison of process 1 and 3 with hardened washers. The comparison of process 1 and 2 for unhardened washers differs in the average by only 400 lb (1.8 kN).

Because of these small differences it is concluded that the welding process itself, within the range of variation considered by NBS, does not have a significant effect on the peak upper rod load for the short box beams. Based on this result data comparisons are not differentiated by weld process.

#### 6.10.4 Weld Area

Exterior Weld Penetration. The exterior weld penetration depth for specimens without an interior weld has a significant effect on the peak upper rod load of the short box beams, as shown in figure 6.18. The average peak loads for specimens E1 and E2 having no weld (no penetration), C1 and C3 having a shallow penetration weld, and A1 and A2 having a deep penetration weld are shown in the figure to illustrate that there is significant difference in load resistance between the case of shallow penetration and deep penetration. The difference is about 2.5 kips (11.1 kN).

Interior Weld Length. The length of interior weld has a significant effect on load resistance of the short box beams. A limited comparison of test results is shown in figure 6.19 to illustrate this point. Data shown include shallow penetration weld specimens shown in table 6.1 except for variations due to weld position, washer thickness, nut shape, nut orientation, clip angle presence, initial rod load, and number of rods. Although a regression analysis was not done it is apparent that increasing the interior weld length increases the load resistance. The increase in load resistance is roughly linearly proportional to the increase in interior weld length. However length of interior weld alone is insufficient to account for load variation since it does not consider penetration of either the interior or exterior welds.

Weld Area. The effect of weld length and depth of penetration of the exterior and interior weld was examined by determining the interior and exterior weld areas between the beam end and the hole for the fourth floor rod. Fracture surfaces between the exterior hole and beam end were examined under magnification for all short box beam specimens. Lengths and depths were measured. Depths were measured at five locations and averaged. These average measurements are summarized in tables 6.1, 6.2, and 6.3, and 6.4 for the NBS tests. Weld area was determined as the sum of the products of the average depth and length for the exterior and interior welds. The peak upper rod load is plotted in figure 6.20 against the weld area. Weld area is used as a measure or index for effectiveness of the weld material to resist load although it is realized that this is a simplification. The trend of the data is as expected; an increase in capacity occurs with the addition of weld metal.

The data shown in figure 6.20 include all tests on short box beams with hardened washers as listed in table 6.1 except for round nut bevel, initial rod load, single rod and clip angle presence. These latter parameters are discussed in section 6.10.5.

The correlation coefficient,  $r$ , is 0.90 for the equation for the mean peak upper rod load [6.2]. An  $r$  value of 1.0 indicates perfect correlation. The  $r^2$  value is 0.80, indicating that 80 percent of the total variation in the peak upper rod load is accounted for by the regression line. The other 20 percent is unaccounted for by the weld area alone. Thus the equation for the mean based on the weld area is a reasonable representation of the load resistance within the range of the test data. A 95 percent confidence band for the data is also shown in figure 6.20. Ninety five percent of the test results for individual specimens are expected to be within the limits of the band.

#### 6.10.5 Other Observations

Stringer-Box Beam Clip Angle Presence. Four short box beam tests were conducted to examine the influence of stringer-box beam clip angles on load resistance. These specimens were obtained by cutting off the outside 22 in (560 mm) of full-length beams L3 through L6 that did not fail during the full-length box beam tests described in section 6.11. Except for the presence of clip angles and the fact that the specimens had been loaded during full-length box beam tests, tests were conducted in the same manner as used for typical short box beam specimens.

The presence of clip angles does not significantly affect the peak upper rod load capacities of the short box beams as is apparent from the data for specimens S1-S4 shown in figure 6.21 compared to the mean peak upper rod load and the 95 percent confidence band. This observation was expected based on the zone of distress observed on the white-washed box beams since the zone of distress did not extend to the location of the stringer-box beam clip angle.

Initial Upper Rod Load. The short box beam tests began prior to the weighing of the walkway spans. The nominal upper walkway dead load was calculated on the basis of the contract drawings and thus for this part of the laboratory test program the dead load contribution to the upper hanger rod was

set at 7500 pounds (33 kN) in all but three of the short box beam tests. The two remaining specimens were tested using an initial upper rod load of 9000 pounds (40 kN) to examine the effect of the initial rod load on the load resistance of the box beam-hanger rod connection. As evidenced by a comparison of these two tests (figure 6.22) with the regression analysis from figure 6.20, the influence of initial upper rod load on peak load capacity is insignificant for the range of 7500 pounds (33 kN) to 9000 pounds (40 kN).

Loading Configuration. The bulk of the short box beam tests used a two rod loading configuration as discussed in section 6.5. The two-rod configuration best modelled the actual upper walkway box beam loading. However, the original design of the second and fourth floor walkways called for a continuous hanger rod and the third floor walkway connections had a single-rod configuration. For purposes of comparison, four short box beams were loaded using only a single hanger rod. All loads were applied through the upper loading rod. The lower floor loading rod was omitted for the single rod tests although the hole was bored.

A comparison of the single rod data for B2, H1, X1 and X2 listed in table 6.1 is presented in figure 6.23. These data are consistently about 2.0 kips (9 kN) higher than the mean for double rods for a given weld area. Thus the single rod tests are considered to be outside the range of the regression analysis and were not used as part of the data base in estimating load resistance of connections loaded by two hanger rods.

Nut Shape. Based on the observed dimensions of the walkway hanger rod nuts it was determined that they were 1 1/4 in (32 mm) heavy hex nuts. Such nuts were procured locally and their dimensions were similar to the walkway hanger rod nuts. However, the amount of bevel at the intersection of corners and bearing surface was greater on the actual walkway hanger rod nuts (figure 6.24). The effect of nut shape was explored by testing two specimens with nuts which were altered to a geometry similar to the walkway hanger rod nuts. This is referred to as a "round" nut bevel while the nut used on most tests has a "square" bevel.

The comparison of data for specimens V1 and V2 is presented in figure 6.25 for the hardened washer tests. The comparison indicates that nut shape may have an effect on peak upper rod load, with the rounded nuts reducing the load resistance. Although the reduction is within the data scatter the two specimens are considered to be outside the range of the regression analysis and were not used as part of the data base in estimating load resistance.

Washer Presence. Early in the investigation it was uncertain whether or not washers were present on all of the upper walkway box beam-hanger rod connections since two were missing from the debris.

The majority of the short box beams were tested with washers, but three specimens were tested without a washer between the upper rod nut and the box beam. Washers were always used between the second floor loading rod nut and box beam. The absence of a washer on the upper floor rod reduces the peak upper rod load by about 2.5 kips (11 kN) for a given weld area as shown in figure 6.26. As noted in section 8.3.3 of this report, there is strong evidence

that washers were present prior to the collapse. Thus these data are not used as part of the data base in estimating capacity.

Washer Hardness. Prior to obtaining material from the walkway debris it was not possible to determine whether the washers were hardened or unhardened. Initially, the short box beam specimens were tested using hardened steel washers. These were followed by a series of short box beams tests using unhardened washers.

Based on the data shown in figure 6.27 it is estimated that an unhardened washer reduces the load resistance by approximately 2.0 kips (9 kN) below that of the hardened washer. Since all of the tests on debris indicated hardened washers were used, these data were not used in estimating load resistance.

Seven unhardened washer data points are identified separately in figure 6.27. This was done for convenience in discussing subsequent parameters.

Interior Weld Position. In all but two short box beams with interior welds, the weld began at the box beam free end and extended inwards (termed the edge position). The two remaining specimens (R1 and R2) with unhardened washers had the interior weld extending from the exterior hole edge outwards (termed the hole position). The weld position was varied to explore the importance of weld material at the hole position as compared to weld material near the free end.

The lengths of interior weld beginning at the edge of the hole are 1/4 in (6 mm) and 5/16 in (8 mm). Comparison of these data with other unhardened washer data in figure 6.27 indicates that the location of the interior weld within the length between the edge of the exterior hole and the beam end is not a significant parameter within the range of variation studied.

Washer Thickness. All but one short box beam was tested with washers having a thickness of about 0.15 in (3.8 mm). Specimen N6 (table 6.2) was tested using an unhardened washer having a thickness of about 0.18 in (4.6 mm).

The data in figure 6.27 shows that the test result for N6 is within the overall scatter of the data. Although a thicker washer should improve the load resistance, the small variation tested appears to make no difference.

Nut Orientation. The orientation of the nuts on the walkway hanger rods at the time of failure could not accurately be ascertained. For purposes of the investigation a uniform orientation was used for most tests, but three specimens (N3, N4, and N5) with unhardened washers were tested using a different orientation. The normal nut orientation was with two nut faces parallel to the short box beam longitudinal axis. The alternate orientation had two nut faces perpendicular to the short box beam longitudinal axis (figure 6.28).

The data points for nut orientation are shown in figure 6.27. Based on these data nut orientation is not considered a significant parameter.

### 6.10.6 Summary

The short box beam data base was discussed in sections 6.10.4 and 6.10.5. After review of the parameters it is concluded that additional data may be used as part of the data base used to develop figure 6.20. Specifically, all of the data for hardened washers should be used except that for single rod tests (B2, H1, X1, and X2) and nut shape tests (V1 and V2). All of the data in tables 6.2 and 6.3 for tests using unhardened washers and no washers are also excluded.

A regression line is shown in figure 6.29 based on these 28 tests. This regression line for the mean peak upper rod load is shown with a 95 percent confidence band for the data and has a correlation coefficient,  $r$ , of 0.91 and an  $r^2$  of 0.84. This line of best fit characterizes the NBS short box beam test results.

### 6.11 NBS FULL-LENGTH BOX BEAM TESTS

Seven full-length box beams fabricated by NBS were tested with the parameters shown in table 6.4. All seven were dimensionally identical. All full-length box beams were fabricated using the GMAW process and the same mild steel electrode used in the short box beam tests. The first two full-length box beams (L1 and L2) had a 1/2 in (13 mm) interior weld extending from each end of the top and bottom flanges while the remaining five full-length box beams (L3-L7) were constructed similarly except that the interior weld extended 1 3/8 in (35 mm). Load-deflection curves are presented in appendix A6.11.

The full-length box beam data are compared to the regression analysis results for the short box beam tests (from figure 6.29) in figure 6.30. Based on the comparisons between the full-length and short box beam tests, it was concluded that there is good agreement between the results obtained using either type of test specimen. Therefore, a regression analysis was performed using the short box beam data shown in figure 6.29 along with the full-length box beam data points shown in figure 6.30. The results of this analysis, which incorporates all of the applicable results of the NBS test program as indicated (35 tests), are shown in figure 6.31. The correlation coefficient,  $r$ , is 0.87 and the  $r^2$  value is 0.76.

### 6.12 TESTS ON WALKWAY BOX BEAM

One full-length box beam was obtained from column line 9 of the third floor walkway (figure 6.7). One full-length box beam test and four short box beam tests were conducted on this beam. Specimen characteristics are shown in table 6.5.

#### 6.12.1 Full-Length Box Beam Test

The third floor walkway box beam, designated KCL, was longer than the second and fourth floor walkway box beams and only had holes for a single hanger rod at each end (figure 3.10). The holes for the lower loading rods were made at NBS in the same way as holes in the NBS box beams were made. The nuts and

washers used on the exterior (upper) loading rods at the box beam were those taken by NBS from the walkway box beam during removal. The interior (lower) loading rods were fitted with NBS rounded nuts and hardened washers.

The extra beam length was located between the clip angles and was accommodated in the test setup by repositioning the loading rods and hydraulic cylinders. A longer spreader beam was used to span between the clip angles. The instrumentation was identical to that used in the NBS full-length box beam tests except that for purposes of videotaping the transverse LVDTs were omitted.

The first failure occurred at the west lower flange exterior hole. The interior weld on this flange did not extend to the exterior hole while the interior weld on the east lower flange did extend fully to the exterior hole. The rod load (upper west rod) at first failure was approximately 19.4 kips (86 kN). The second failure occurred at the west upper flange exterior hole. No interior weld was observed on this flange. The rod load at failure was approximately 16.2 kips (72 kN). The upper rod loads versus channel tip displacements are shown in figure 6.32.

Specimen KCL was recorded on videotape, which included a record of load on the videotape image. Thus, the load-deflection behavior in figure 6.32 may be described by correlation with the videotape. Due to the test setup it was not possible to observe directly the weld surfaces on the interior of the box beam. However, based on observations of other NBS tests, cracking probably occurred in the exterior welds between the two rod holes on the lower flange by a load of 7.5 kips (33 kN) representing the dead load from the fourth floor walkway. By approximately 11 kips (49 kN) cracking probably started in the interior weld near the outer hanger rod hole and progressed towards the end of the box beam. Observation of the videotape showed that at about 16 kips (71 kN) the web bending was pronounced. At about that load level the load-displacement curve is beginning to show increasing nonlinearity.

The videotape which included an audio track indicated, based on noise emitted, that considerable weld fracturing occurred between 18.1 and 15.5 kips (81 and 69 kN) on the descending portion of the load-displacement curve with complete fracture (visible on the video portion of the tape) occurring at about 15.5 kips (69 kN) with the load dropping rapidly to 12.8 kips (57 kN). At about 8 kips (36 kN) on the descending portion of the curve the washer fractured with the load dropping almost immediately to 5.9 kips (26 kN).

#### 6.12.2 Short Box Beam Tests

After the full-length box beam test, the box beam was sawn into four lengths which were made into short box beams. The first short box beam included the unfailed east end of the full-length box beam. The other three short box beams were taken in succession along the length of the box beam. The longitudinal welds were not modified. The first short box beam included the stringer connection clip angles. A fifth short box beam was included in this series and was fabricated using the NBS channel sections.

The first short box beam (KCl) was a continuation of the test of the full-length box beam's east end. The next three short box beams were similar except for the nut and washer used on the upper loading rod. The fifth box beam was an NBS box beam (I3), but the nut and washer on the upper loading rod was from the walkway debris.

The in-plane load deflection curves for the short box beam tests are shown in figure 6.33. Each curve is a plot of the upper rod load transducer versus the displacement of the rod measured by the LVDT at the box beam terminus of the upper loading rod. The peak load achieved by each of the specimens is shown on their respective curves. The asterisks on each curve indicate the end of reliable measurement by the LVDT.

Specimen KCl exhibited a double peak load deflection curve as shown in figure 6.34. This is a continuation of the data shown in figure 6.33. The unloading shown in figure 6.34 at about 1.8 in (46 mm) of displacement was necessary since the stroke of the piston in the hydraulic ram had been reached. After repositioning the piston, load was reapplied. After exhibiting typical behavior through about the first 1.8 in (46 mm) of displacement, another resistance mechanism took effect which enabled the load to increase again. As larger deformations occurred the web buckling progressed further into the length of the box beam. Apparently the progression was stopped by the clip angles which stiffened the web. The load increased again to a second peak of 23.6 kips (105 kN). The weld between the outer rod hole and the beam end cracked but never completely fractured. Pull-through was achieved only after full separation of the flanges between the rod holes occurred. An end view of the KCl deformed shape is shown in figure 6.35.

It is emphasized that the fourth floor walkway box beams that failed on July 17 did not exhibit the same behavior mechanism described for KCl. Their behavior, as shown by the end views in figure 6.36 was much more typical of the NBS specimens (figure 6.14) as were the other specimens sawn from specimen KCL.

Specimens KCl, KC2, and I3 also used washers obtained from the walkway debris. The washers fractured in all three instances but only after the peak upper rod load had been reached (figure 6.33). The KCl washer fractured at a load of about 15 kips (67 kN) while the washers for KC2 and I3 fractured at about 7 kips (31 kN) and 6 kips (26 kN) respectively. In I3 only a sector of the washer fractured as compared to complete fractures for KCl and KC2. Washers did not fracture in the KC3 and KC4 tests which used NBS hardened and unhardened washers respectively.

Specimen KC4, which consisted of a walkway short box beam tested with an NBS unhardened washer, is shown plotted in figure 6.27. When compared with the results of NBS box beams tested with unhardened washers, KC4 appears to give consistent results.

The remainder of the box beam test results involving walkway materials are shown in figure 6.37. Since the weld of specimen KCl never fully fractured the weld area recorded for this specimen is an estimate based on the area of

the weld at the center line of the longitudinal seam rather than the weld area actually measured on the fracture surface. Since the regression analysis was based on weld fracture area, direct comparison of the KCl test with other data is difficult. Specimen I3, which consisted of an NBS short box beam tested with a walkway washer, shows a load resistance which is consistent with the other NBS box beam test data.

Specimen KC3, which consisted of a walkway short beam tested with an NBS hardened washer, similarly shows a load resistance which is consistent with the NBS box beam data. Specimens KCL, KCl, and KC2, which were the only tests conducted on specimens with the box beam, nut, and washers of walkway origin, fall within or near the 95 percent confidence band for the NBS test data. However, two of the three specimens are either at or just outside the upper boundary of the 95 percent confidence band.

The size of the data base for NBS box beams with NBS hardened washers is of reasonable size (35 specimens shown in fig. 6.31), and thus, can be used with reasonable confidence as a tool for predicting ultimate strength of box beam hanger rod connections having similar characteristics. While the walkway test results generally fall within the 95 percent confidence band for the NBS data base, it must be recognized that the walkway data base is extremely limited (three specimens with walkway box beams, nuts and washers) and does show a tendency toward the upper boundary of the 95 percent confidence band of the NBS data base.

As noted earlier, and as shown in table 6.6, the walkway box beams had a somewhat heavier cross-section which might be expected to slightly increase load resistance. Recognizing this limitation, the NBS data base is used as the basis for estimating the ultimate strengths of the fourth floor walkway box beam-hanger rod connections. The validity of the ultimate strengths thus derived is further discussed in chapter 10.

### 6.13 BOX BEAM-HANGER ROD CONNECTION CAPACITY

The regression equation shown in figure 6.38, along with the 95 percent confidence band for single values of pullout load, is used to estimate ultimate strengths for the fourth floor box beam-hanger rod connections. The figure is the same as the one shown in figure 6.31, but with the data points omitted. It was developed based on the short box beam data described in section 6.10.6 and the full-length box beam data described in section 6.11. Furthermore, the regression analysis was validated by the use of actual walkway test specimens.

The meaning of figure 6.38 is amplified by discussing box beam-hanger rod connection 9UE as an example. Simply described, if many specimens like 9UE were tested, their average should fall close to the regression line. However, for a single test one can be 95 percent confident that the test result would fall within the 95 percent confidence band. Thus each connection should be thought of in terms of the range of ultimate strength as well as the average.

Weld areas were determined by examination of the actual fracture surfaces for 8UE, 9UE, 9UW, and 10UE. The weld lengths and depths were measured, the

depths being measured at 5 locations along the weld length. Computed areas are shown in table 6.7. Weld areas for fracture surfaces 8UW and 10UW are based on field measurements since the actual fracture surfaces were not obtained. These weld areas are also shown in table 6.7.

These ultimate capacities are summarized in figure 6.39 on a layout of the six box beam-hanger rod connections. A bar diagram is shown adjacent to each hanger rod. Location 8UE is described to denote the meaning. The range from 16.3 to 20.2 kips (73 to 90 kN) is the 95 percent confidence interval estimate for this particular box beam-hanger rod connection. The mean ultimate capacity of 18.2 kips (81 kN) is also shown. The mean capacity for all connections is 18.6 kips (83 kN).

Although these comparisons indicate that the regression analysis based on the data shown in figure 6.31 reflects the trend of the walkway data, the walkway section is slightly heavier than the section used in the NBS tests, as shown in table 6.6. Thus, somewhat greater ultimate strength might be anticipated for the walkway cross-sections. This heavier cross-sectional area may explain why the test data fall essentially between the average and the upper portion of the confidence band with none below (recall that KC4 was tested with an unhardened washer).

The regression analyses were developed for the double or interrupted rod connection that was actually used in the walkway. Based on the results in section 6.10.5 the original continuous hanger rod arrangement would have been about 2.0 kips (9 kN) higher than the arrangement actually used. Thus the average ultimate capacity would have been about 20.5 kips (91 kN).

#### 6.14 CONCLUSIONS

The following conclusions are made subject to the limitations on the range of variables tested.

1. The welding process has little effect on ultimate capacity.
2. Three types of washers were used during the test series. Hardened and unhardened washers were used in the NBS test program. A third type of washer which exhibited a hardness similar to that of the NBS hardened washer was obtained from the walkway debris. However, this washer differed from the NBS washer in that it fractured during testing. However, the fracture occurred after the peak load had been reached and at a load smaller than the peak load. None of the washers tested by NBS other than those from the debris fractured.
3. Ultimate capacity of the double rod connection varies linearly with an index weld area consisting of the sum of the exterior and interior weld area in the region between the outer hanger rod hole and the beam end. The variation for hardened washers is  $P = 13.18 + 0.0391A$  with a correlation coefficient of 0.87.

4. Test results for box beam samples from the walkway debris were within or near the 95 percent confidence interval estimate based on the use of the linear equation developed using the NBS test data.
5. The ultimate capacity of box-beam hanger rod connections can be predicted on the basis of laboratory test results. Estimates for the mean box beam-hanger rod connection ultimate capacities and a 95 percent confidence interval estimate for the walkway box beam-hanger rod connections are listed below.

Connection	Mean Ultimate Capacity kips (kN)	95% Confidence Range kips (kN)
8UE	18.2 (81)	16.3 to 20.2 (73 to 90)
8UW	19.3 (86)	17.3 to 21.4 (77 to 95)
9UE	18.2 (81)	16.2 to 20.2 (72 to 90)
9UW	18.3 (81)	16.3 to 20.3 (73 to 90)
10UE	19.1 (85)	17.1 to 21.1 (76 to 94)
10UW	18.3 (81)	16.3 to 20.3 (73 to 90)

These capacities ranged from 18.2 kips (81 kN) to 19.3 kips (86 kN) with an average of 18.6 kips (83 kN).

6. Ultimate capacity for the single rod connection is about 2.0 kips (9 kN) higher than for a double rod connection or an average value of about 20.5 kips (91 kN).

Table 6.1 NBS Short Box Beam Series Test Data, Hardened Washers

SPECIMEN	Weld Process	Exterior Penetration		Nominal Interior Weld Length	Interior Weld Position	Washer Thickness	Nut Bevel Shape	Nut Orientation	Initial Rod Load, kips	No. of Rods	Clip Angle Presence	Average Dimensions and Area				Peak Load, kips	Failure Mode		
		No Weld	Shallow									Deep	Length, mm	depth, mm	Length, mm		depth, mm	Area, mm <sup>2</sup>	I
A1	1			0	N.A.	Thin	Square	Parallel	7.5	2 Rods	Present	36	3.6	---	---	129.6	18.9	•	
A2	2				N.A.							34	3.8	---	---	129.2	17.2	•	
B1	3				N.A.							35	3.1	---	---	108.5	18.1	•	
B2	4				N.A.				N.A.	1 Rod		35	5.0	---	---	175.0	23.6	•	
C1	3				N.A.							30	1.8	---	---	54.0	16.0	•	
C3	3				N.A.							36	1.8	---	---	64.8	15.4	•	
D1	3				N.A.							35	1.8	---	---	63.0	16.4	•	
E1	N.A.				N.A.							0	0	---	---	0	13.7	•	
E2	N.A.				N.A.							0	0	---	---	0	13.0	•	
F1	3											32	1.7	---	1.9	115.2	19.4	•	•
F2	3											---	---	---	---	---	19.8	•	•
G1	3											33	1.9	---	1.9	89.3	16.8	•	
G2	3											35	2.0	---	1.5	92.5	17.1	•	
H1	4				N.A.				N.A.	1 Rod		34	3.0	---	---	102.0	18.8	•	
I1	1				N.A.							35	1.8	---	---	63.0	15.5	•	
I2	1				N.A.							36	2.6	---	---	93.6	16.9	•	
J1	1				N.A.							33	2.0	---	2.4	145.2	20.0	•	•
J2	1											---	---	---	---	---	19.1	•	•
K1	1											34	2.4	---	1.5	101.1	16.3	•	
K2	1											33	2.4	---	1.8	100.8	17.1	•	
S1	1											34	2.0	---	2.5	153.0	18.7	•	•
S2	1											35	2.1	---	2.5	161.0	19.7	•	•
S3	1											35	1.8	---	2.2	140.0	19.0	•	•
S4	1											35	2.1	---	2.3	154.0	18.9	•	•
T1	1											35	2.0	---	0.75	77.5	15.4	•	•
T2	1											35	2.5	---	2.1	127.4	16.3	•	
T3	1											35	2.0	---	2.2	131.6	17.8	•	
U1	1											35	2.0	---	2.2	131.6	17.8	•	•
U2	1											35	2.0	---	3.1	178.5	19.0	•	•
V1	1											35	1.9	---	2.0	136.5	18.4	•	•
V2	1											35	2.1	---	2.7	168.0	18.4	•	•
W1	1											35	2.0	---	2.7	164.5	18.4	•	•
W2	1											35	2.1	---	2.3	154.0	19.2	•	•
W3	1											35	2.1	---	3	73.5	15.6	•	•
X1	1								N.A.	1 Rod		35	1.6	---	2.6	147.0	18.8	•	•
X2	1								N.A.	2 Rods		35	1.8	---	2.2	140.0	20.1	•	•
X2	1								N.A.	2 Rods		35	1.8	---	2.2	140.0	20.9	•	•

- Notes: 1. Process 1 - Gas Metal Arc Welding  
 Process 2 - Flux Cored Arc Welding  
 Process 3 - Shielded Metal Arc Welding, E7014 Electrode  
 Process 4 - Shielded Metal Arc Welding, E7018 Electrode
2. Weld between hole and box beam end did not fracture. Weld areas not available.
3. Interior weld not counted due to apparent lack of fusion to base metal.

Table 6.2 NBS Short Box Beam Series Test Data, Unhardened Washers

SPECIMEN	Weld Process <sup>1</sup>	Exterior Penetration		Nominal Interior Weld Length		Interior Weld Position	Washer Thickness	Nut Bevel Shape	Nut Orientation	Initial Rod Load, kips		No. of Rods	Clip Angle Presence	Average Weld Dimensions and Area				Peak Load, kips	Failure Mode	SPECIMEN												
		No Weld	Shallow	Deep	0					1/2"	1"			1 3/8"	Edge	Hole	Parallel				Perpendicular	7.5	9.0	1 Rod	2 Rods	Present	Absent	Length, mm	depth, mm	Length, mm	depth, mm	Area, mm <sup>2</sup>
K3	1						Thin	Square	Parallel		7.5	2 Rods	Present	34	2.6	3	35	2.2	3	88.4		14.9	I	K3								
K4	1						Thin	Square	Parallel		7.5	2 Rods	Present	35	2.2	3	34	2.5	3	77.0		15.4	I	K4								
K5	1						Thin	Square	Parallel		7.5	2 Rods	Present	34	2.5	25	35	1.7	25	110.0		16.1	I	K5								
K6	1						Thin	Square	Parallel		7.5	2 Rods	Present	35	1.7	25	34	2.2	25	84.5		15.5	I	K6								
LS1	2						Thin	Square	Parallel		7.5	2 Rods	Present	34	2.0	32	32	2.0	35	74.8		13.5	I	LS1								
LS2	2						Thin	Square	Parallel		7.5	2 Rods	Present	32	2.0	35	35	1.5	35	64.0		13.5	I	LS2								
M1	2						Thin	Square	Parallel		7.5	2 Rods	Present	35	1.6	32	32	1.6	29	108.5		18.0	I	M1								
M2	2						Thin	Square	Parallel		7.5	2 Rods	Present	33	2.2	33	33	2.2	33	83.1		16.4	I	M2								
N1	2						Thin	Square	Parallel		7.5	2 Rods	Present	35	2.2	35	35	2.2	35	135.3		16.7	I	N1								
N2	2						Thin	Square	Parallel		7.5	2 Rods	Present	35	2.0	33	33	2.0	10	122.5		15.6	I	N2								
N3	2						Thin	Square	Parallel		7.5	2 Rods	Present	33	2.0	33	33	2.0	10	88.0		14.1	I	N3								
N4	2						Thin	Square	Parallel		7.5	2 Rods	Present	34	2.0	34	34	2.0	34	146.2		17.0	I	N4								
N5	2						Thin	Square	Parallel		7.5	2 Rods	Present	31	2.0	31	31	2.0	31	124.0		18.5	I	N5								
N6	2						Thin	Square	Parallel		7.5	2 Rods	Present	33	1.9	33	33	1.9	33	145.2		16.5	I	N6								
O1	2						Thin	Square	Parallel		7.5	2 Rods	Present	---	---	---	---	---	---	---	---	---	18.4	I	O1							
O2	2						Thin	Square	Parallel		7.5	2 Rods	Present	---	---	---	---	---	---	---	---	---	16.8	I	O2							
P1	3						Thin	Square	Parallel		7.5	2 Rods	Present	34	1.5	34	34	1.5	34	51.0		14.3	I	P1								
P2	3						Thin	Square	Parallel		7.5	2 Rods	Present	35	1.7	35	35	1.7	35	59.5		14.0	I	P2								
R1	3						Thin	Square	Parallel		7.5	2 Rods	Present	35	1.9	35	35	1.9	35	66.5		14.9	I	R1								
R2	3						Thin	Square	Parallel		7.5	2 Rods	Present	35	2.2	8	35	2.2	8	85.0		13.4	I	R2								

- Notes: 1. Process 1 - Gas Metal Arc Welding  
 Process 2 - Flux Cored Welding  
 Process 3 - Shielded Metal Arc Welding, E7014 Electrode  
 Process 4 - Shielded Metal Arc Welding, E7018 Electrode
2. Weld between hole and box beam end did not fracture, fracture in base metal. Weld areas not available.
3. Interior weld not counted due to apparent lack of fusion to base metal.





Table 6.4 NBS Full-length Box Beam Series Test Data

SPECIMEN	Weld Process	Exterior Penetration		Nominal Interior Weld Length	Interior Weld Position	Washer Thickness	Nut Bevel Shape	Nut Orientation	Initial Rod Load, kips	No. of Rods	Clip Angle Presence	Average Weld Dimensions and Area				Peak Load, kips	Failure Mode		SPECIMEN
		No Weld	Shallow									Deep	Length, in	depth, in	Area, in <sup>2</sup>		Length, in	depth, in	
L1	1			0	Edge	Thin	Square	Parallel	7.5	1 Rod	Present	34	1.7	--2	57.8	13.7			L1
L2	2			1/2"	•	•	•	•	•	•	•	25	3.0	--2	75.0	14.2	•		L2
L3	3			1"	•	•	•	•	•	•	•	35	1.6	35	126.0	19.4			L3
L4	4			1 3/8"	•	•	•	•	•	•	•	35	1.5	35	122.5	20.0			L4
L5	1			0	•	•	•	•	•	•	•	35	2.0	--2	70.0	15.5	•		L5
L6	2			0	•	•	•	•	•	•	•	34	2.3	12	104.6	17.5	•		L6
L7	3			0	•	•	•	•	•	•	•	35	1.9	--2	66.5	17.4	•		L7

- Notes: 1. Process 1 - Gas Metal Arc Welding  
 Process 2 - Flux Cored Welding  
 Process 3 - Shielded Metal Arc Welding, E7014 Electrode  
 Process 4 - Shielded Metal Arc Welding, E7018 Electrode
2. Interior weld not counted due to apparent lack of fusion to base metal.

Table 6.5 Walkway Box Beam Test Series Data

SPECIMEN <sup>a</sup>	Weld Process <sup>1</sup>	Exterior Penetration	Nominal Interior Weld Length	Interior Weld Position	Washer Thickness	Nut Bevel Shape	Nut Orientation	Initial Rod Load, kips	No. of Rods	Clip Angle Presence	Average Dimensions and Area				Peak Load, kips	Failure Mode	SPECIMEN <sup>b</sup>	
											Exterior Weld Length, in.	Exterior Weld depth, in.	Interior Weld Length, in.	Interior Weld depth, in.				Area, in. <sup>2</sup>
KCL	1	No Weld	0	Edge	Thick	Square	Parallel	7.5	1 Rod	Present	35	1.9	1.7	1.8	97.1	19.4	I	KCL
KC1	2	Shallow	1/2"	•	3	Round	•	•	•	•	35	1.3	35	2.3	126.0	20.0/23.6	II	KC1
KC2	3	Deep	1 3/8"	N.A.	3	•	•	•	•	•	34	2.6	---	---	88.4	17.0	•	KC2
KC3	4	No Weld	•	N.A.	3	•	•	•	•	•	36	2.6	---	---	93.6	16.3	•	KC3
KC4	5	Shallow	•	N.A.	5	7	•	•	•	•	35	2.3	---	---	80.5	14.7	•	KC4
I3	6	•	•	N.A.	6	7	•	•	•	•	35	1.9	---	---	66.5	15.2	•	I3

Notes: 1. Process 1 - Gas Metal Arc Welding  
 Process 2 - Flux Cored Welding  
 Process 3 - Shielded Metal Arc Welding, E7014 Electrode  
 Process 4 - Shielded Metal Arc Welding, E7018 Electrode

2. The weld was not modified on the walkway member.

3. Actual walkway washer.

4. Actual walkway nut.

5. NBS hardened washer.

6. NBS unhardened washer.

7. NBS squared bevel nut.

8. KCL was a full-length box beam, all others were short box beams.

Table 6.6 Cross-sectional Dimensions

Sec. Property	Weight lb/ft	d (in)	$b_f$ (in)	$t_w$ (in)	
				Max	Min
Nominal	8.5	8.00	1.874	0.179	
Walkway Specimens	8.84	8.050	1.860	0.194	0.185
NBS Section	8.43	7.975	1.833	0.186	0.182

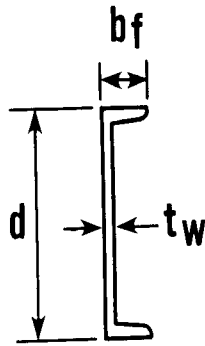


Table 6.7 Walkway Box Beam Weld Measurements

Box Beam-Hanger Rod Connection	Exterior Weld		Interior Weld		Total Area, mm <sup>2</sup>
	Length, mm	Average Depth, mm	Length, mm	Average Depth, mm	
8UE	36	1.8	36	1.8	129.6
8UW	35	4.5	---	---	157.5
9UE	38	1.8	25	2.4	128.4
9UW	32	1.7	16 11*	2.4 3.4	130.2
10UE	35	2.4	35	1.9	150.5
10UW	33	1.5	33	2.5	132.0

\* A portion of 9UW was deeply penetrated.

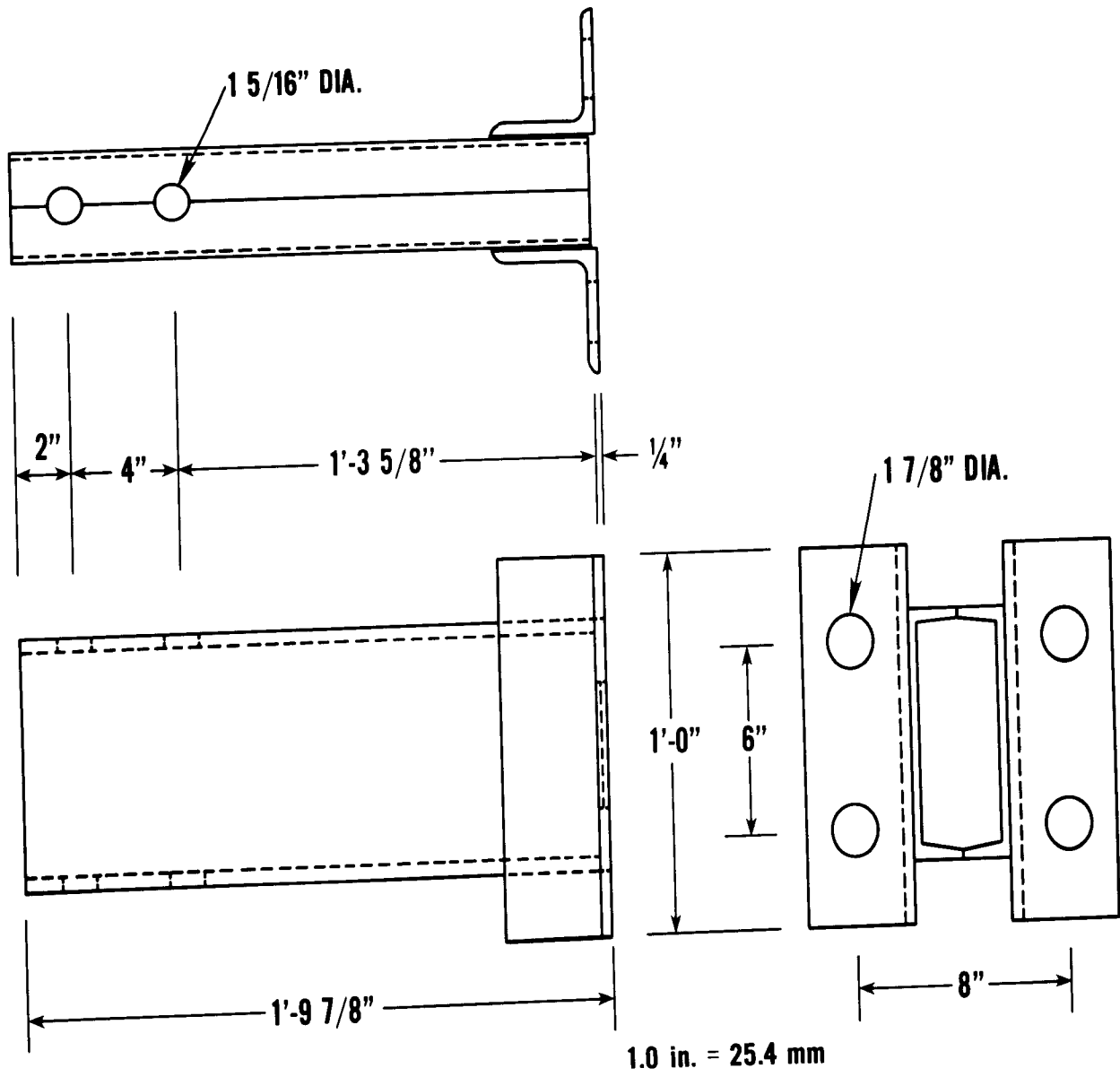


Figure 6.1 Short box beam test specimen.

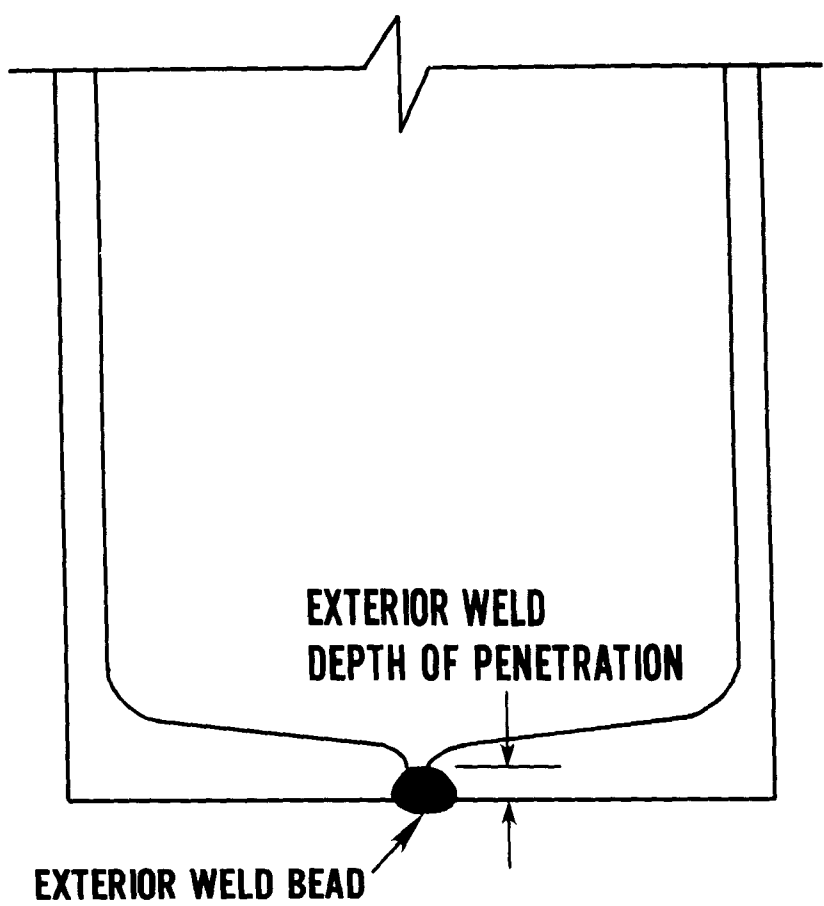


Figure 6.2 Exterior weld penetration.

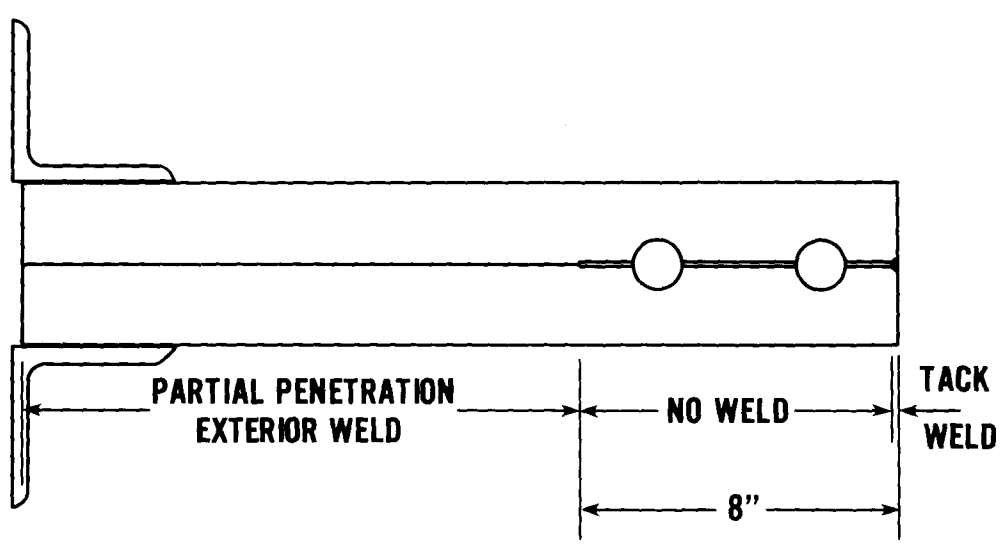


Figure 6.3 No weld specimen.

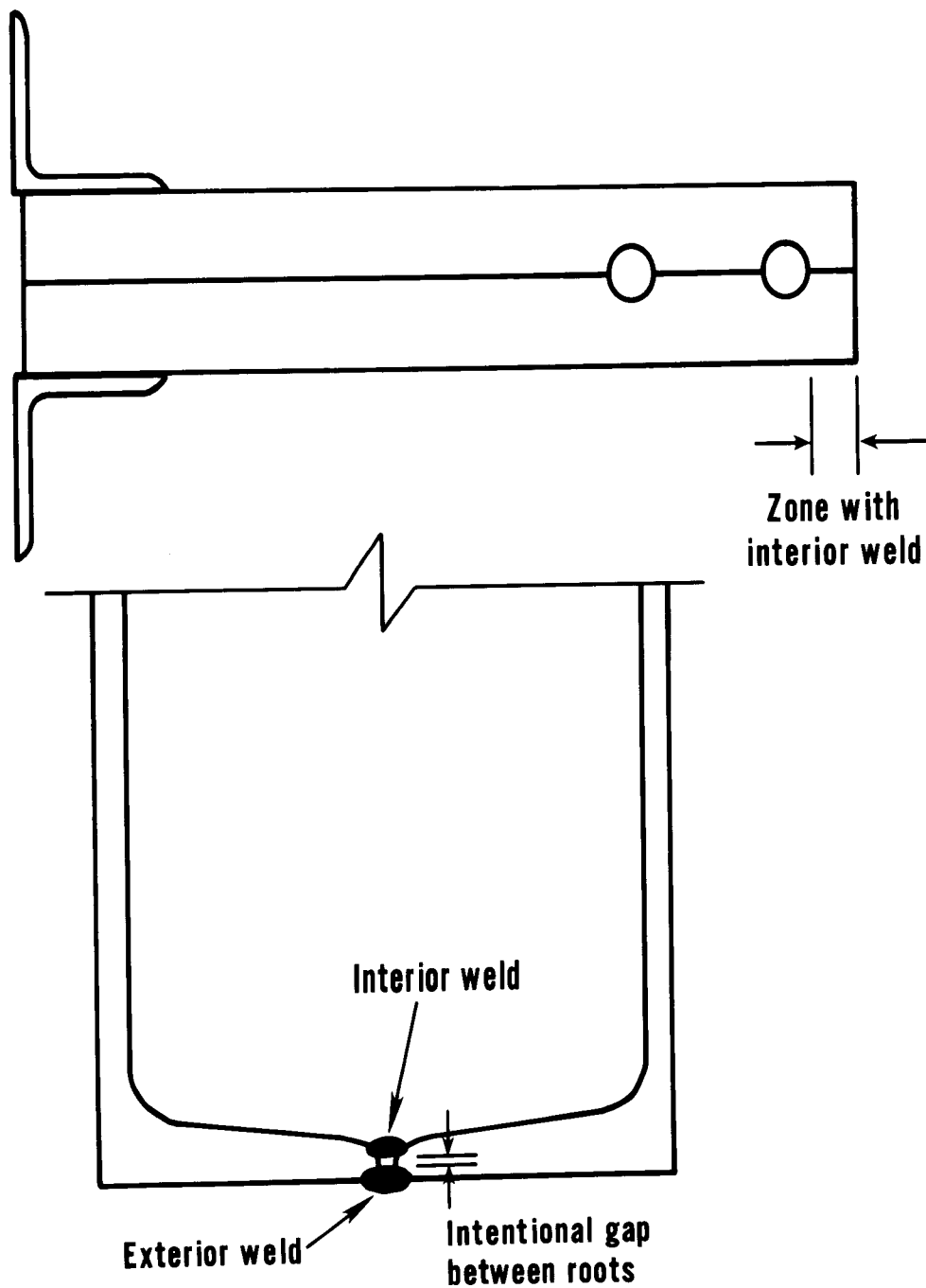


Figure 6.4 Interior weld location.

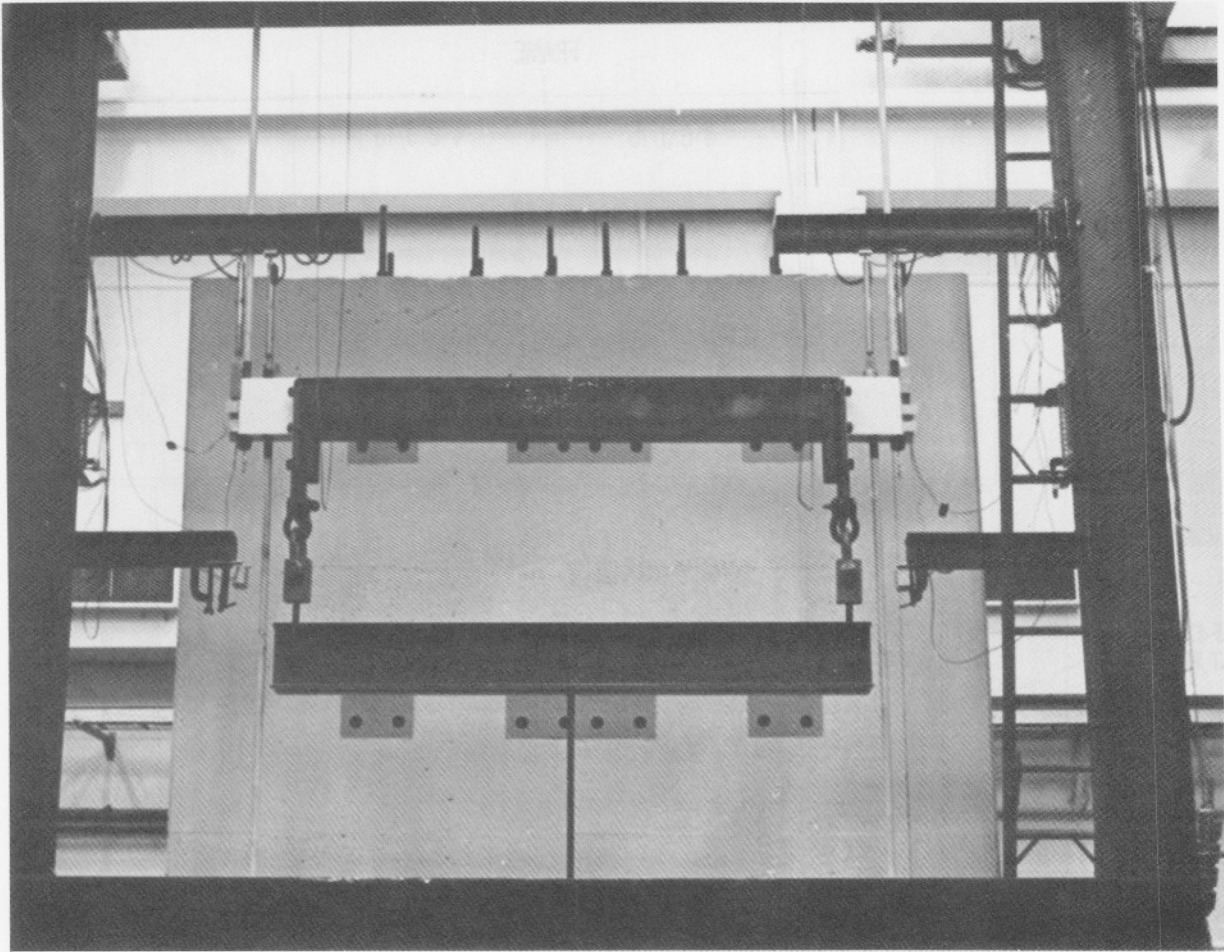


Figure 6.5 Full length box beam test in progress.

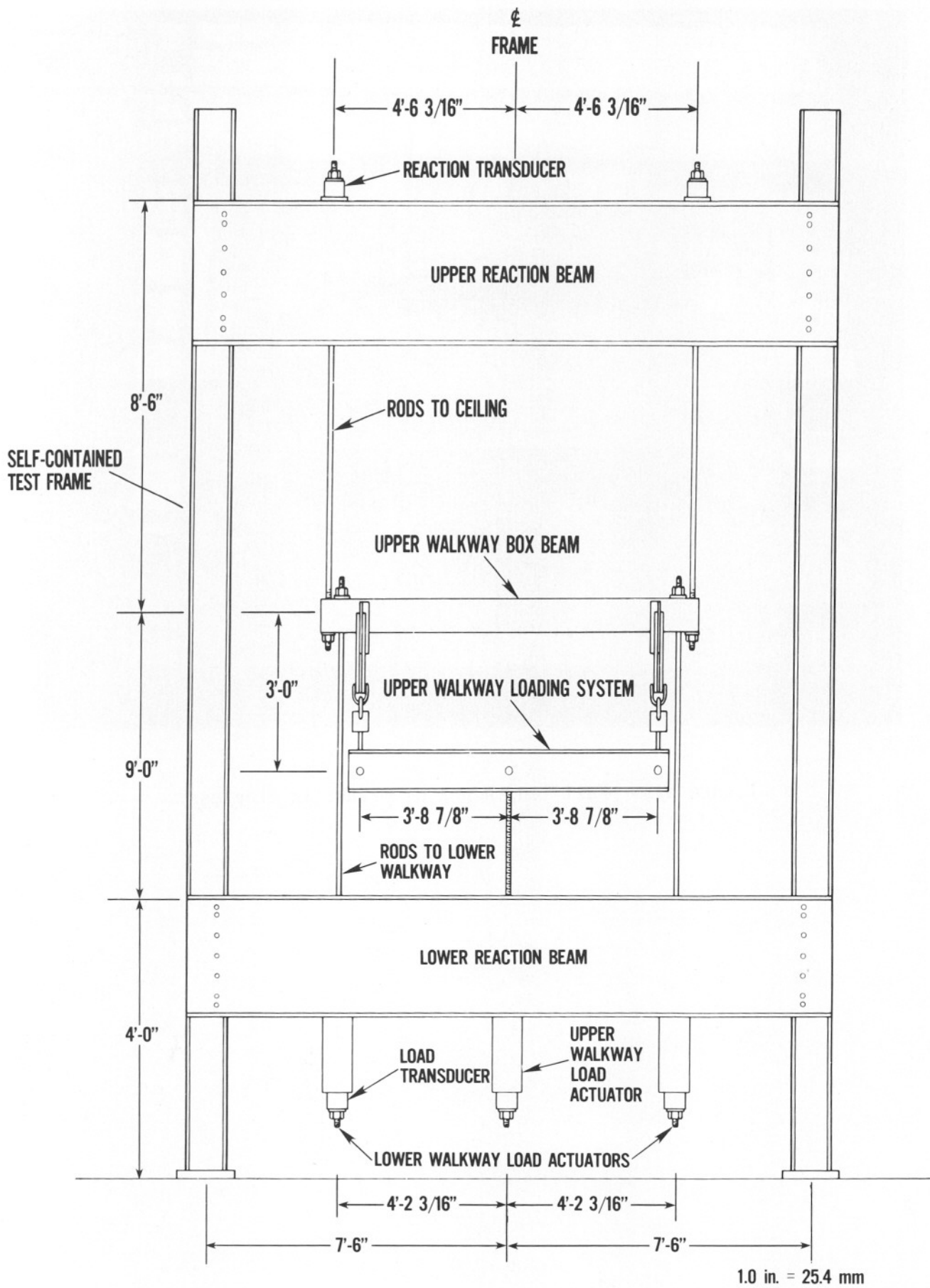


Figure 6.6 Detail of full length box beam test setup drawing.

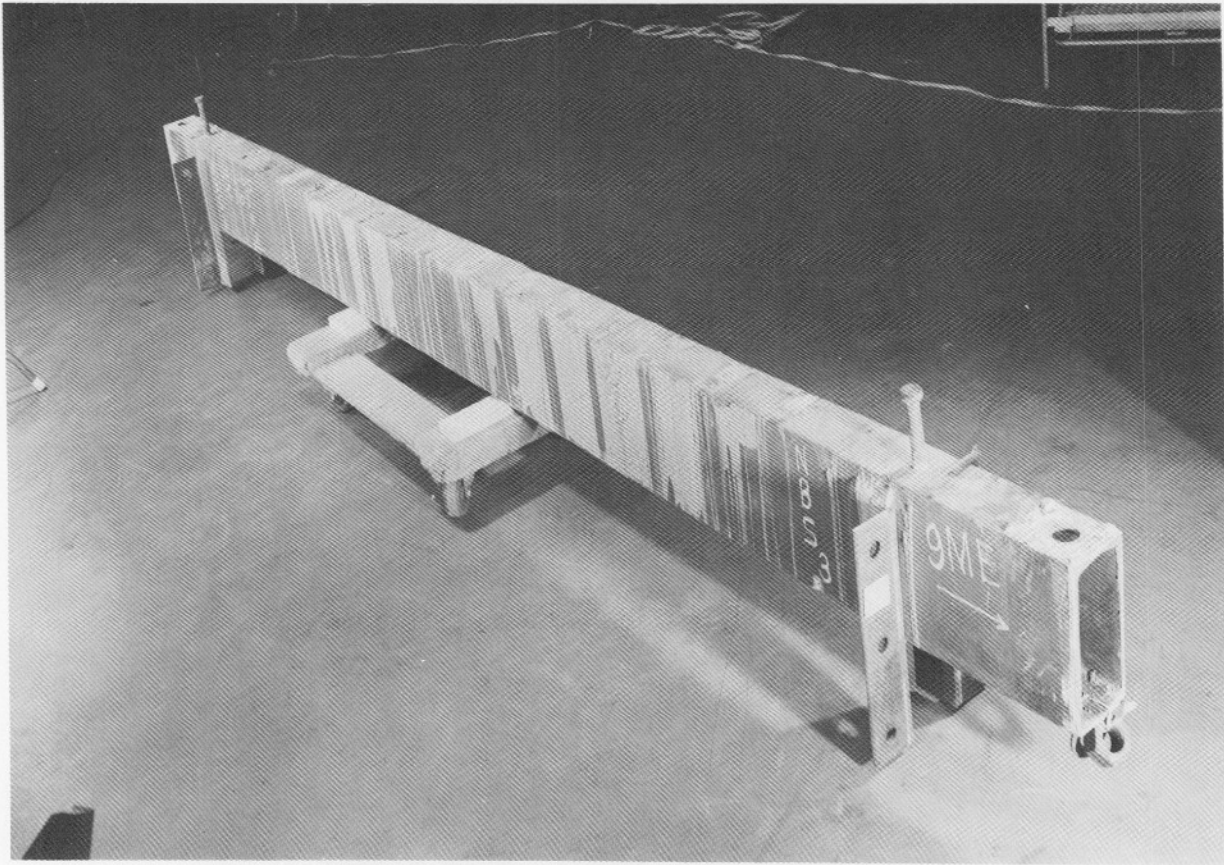


Figure 6.7 Full length box beam showing stringer-box beam clip angles.

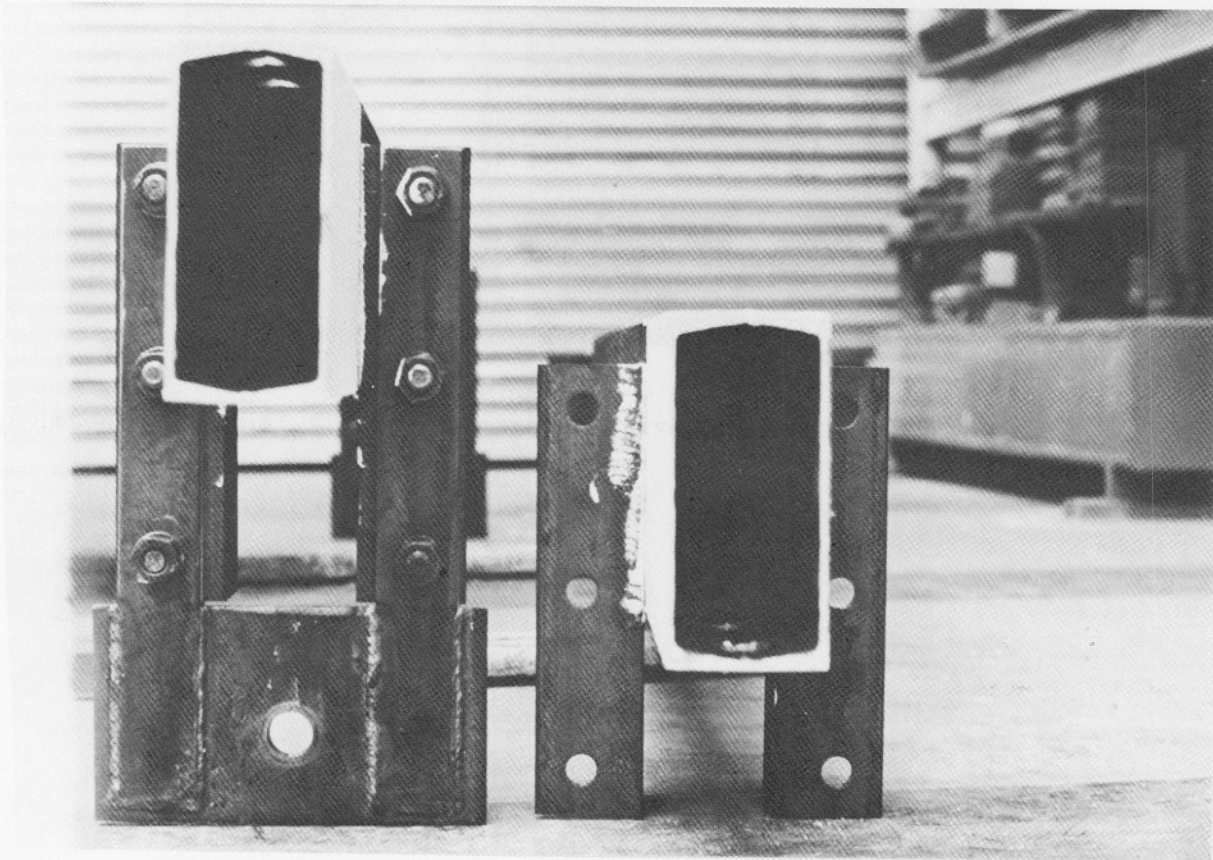


Figure 6.8 Clip angle strap on full length box beam.

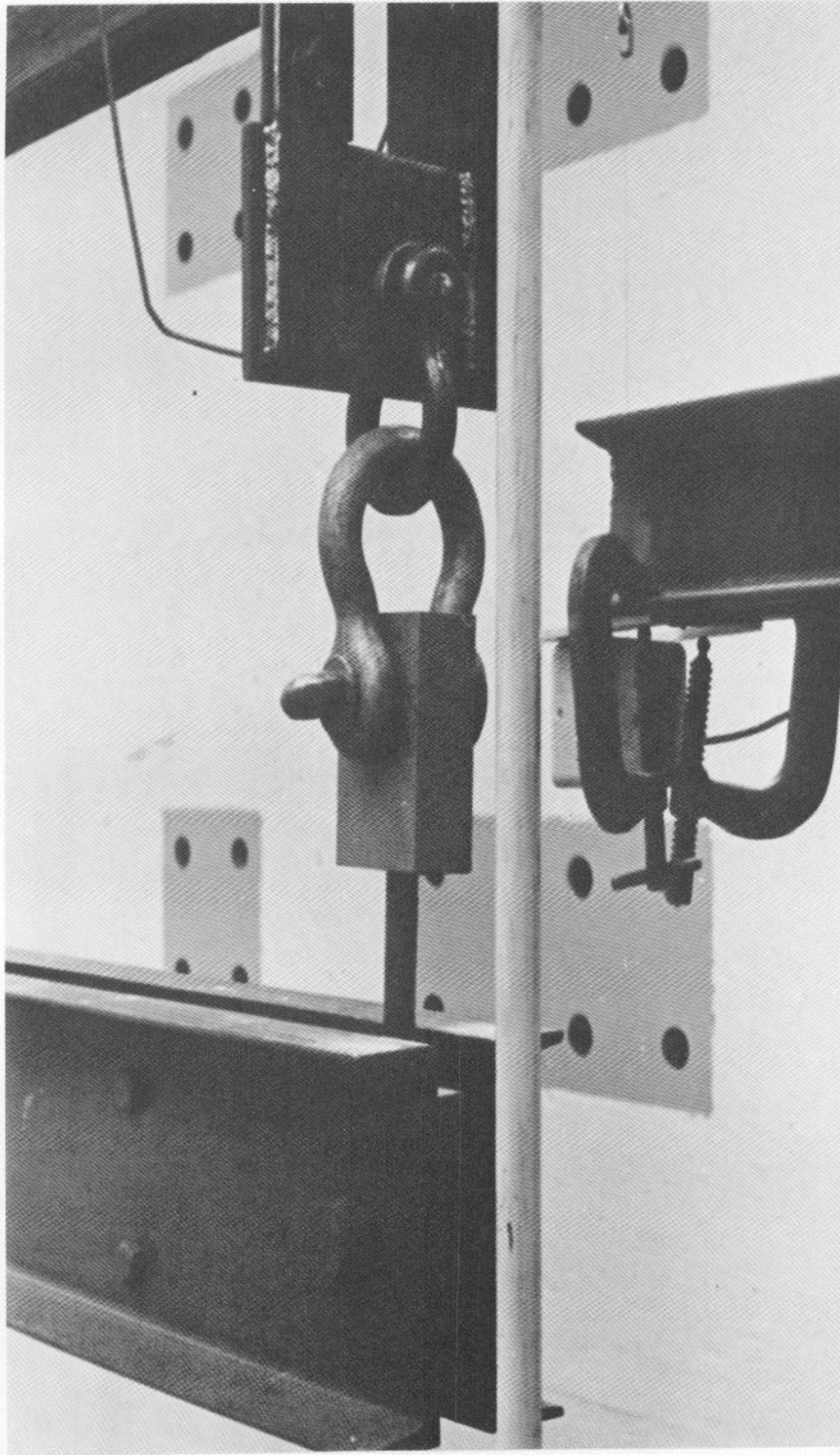


Figure 6.9 Pin and clevis arrangement on full length box beam.

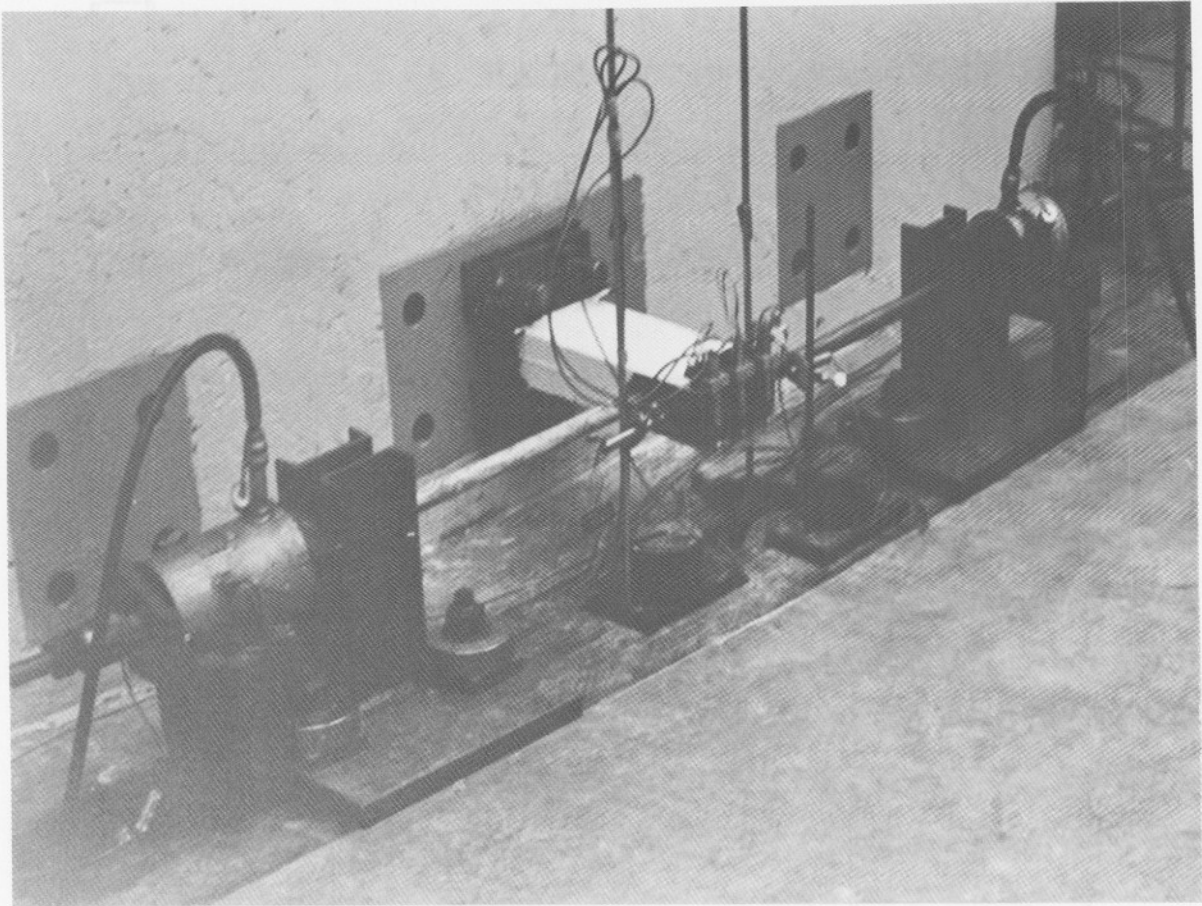


Figure 6.10 Short box beam test.

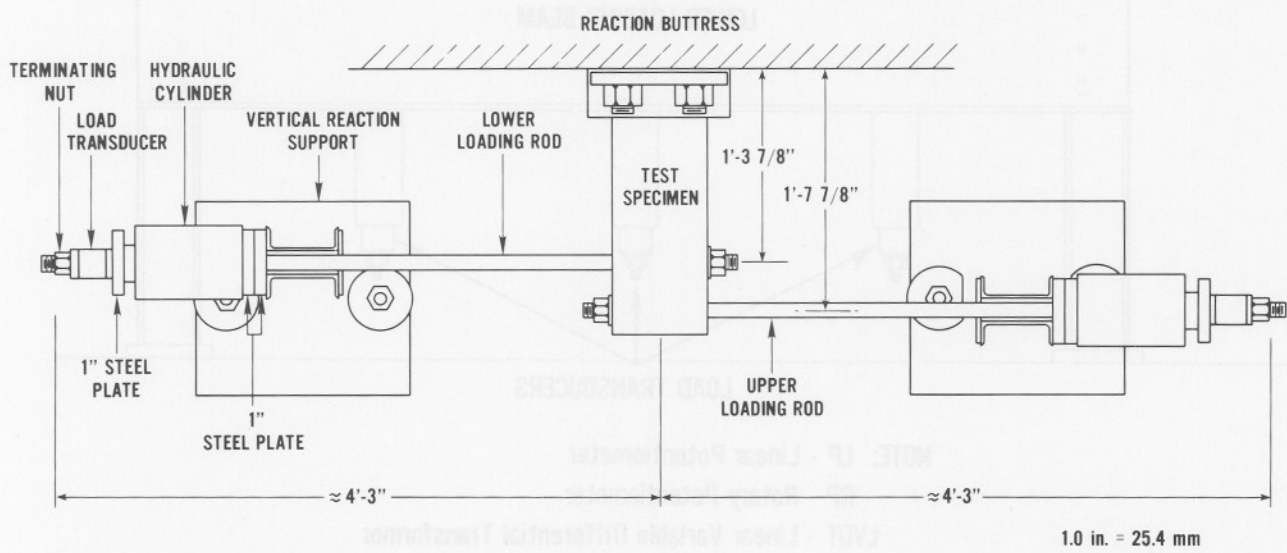
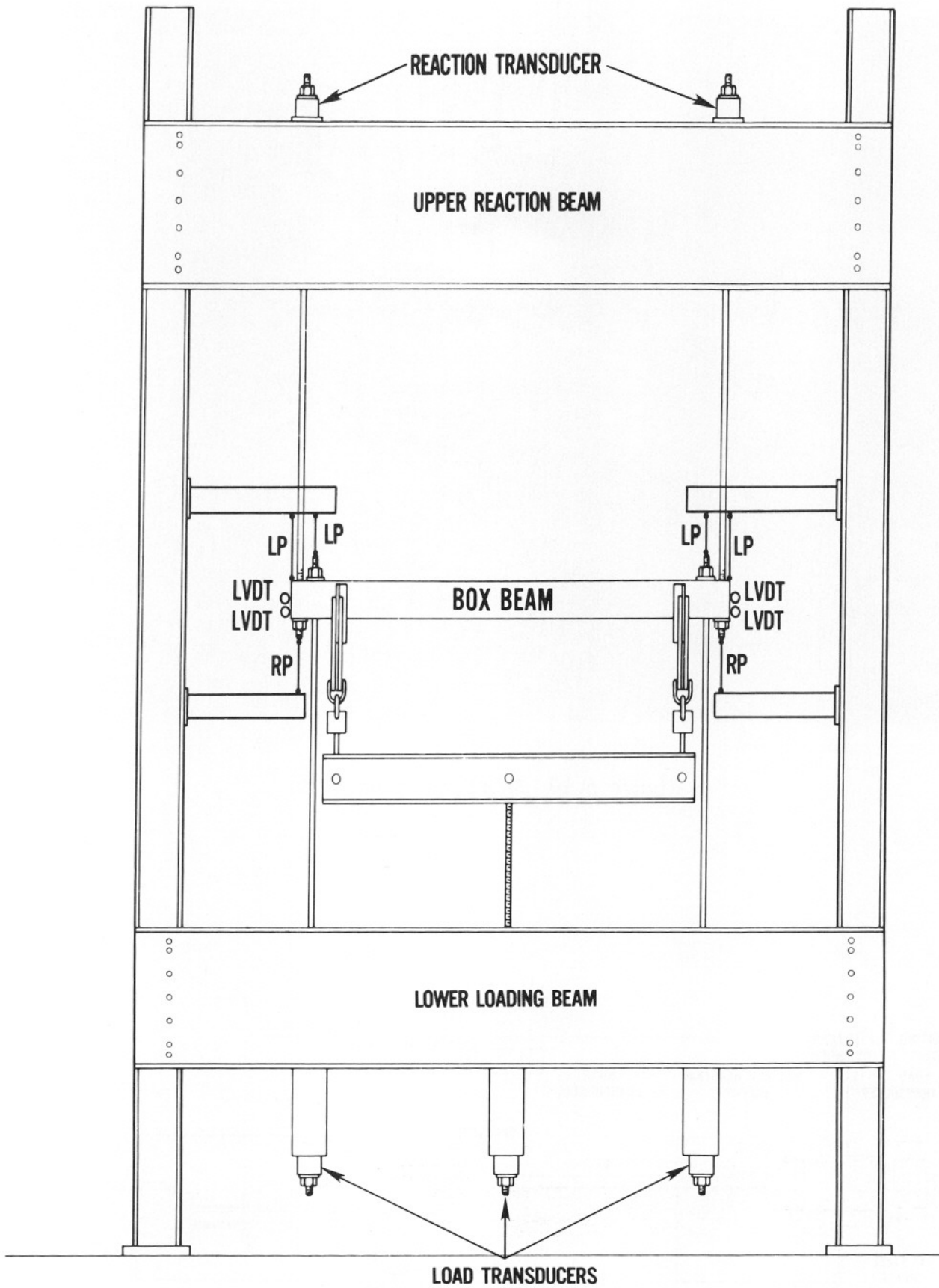


Figure 6.11 Short box beam test setup.



NOTE: LP - Linear Potentiometer  
 RP - Rotary Potentiometer  
 LVDT - Linear Variable Differential Transformer

Figure 6.12 Full length box beam instrumentation.

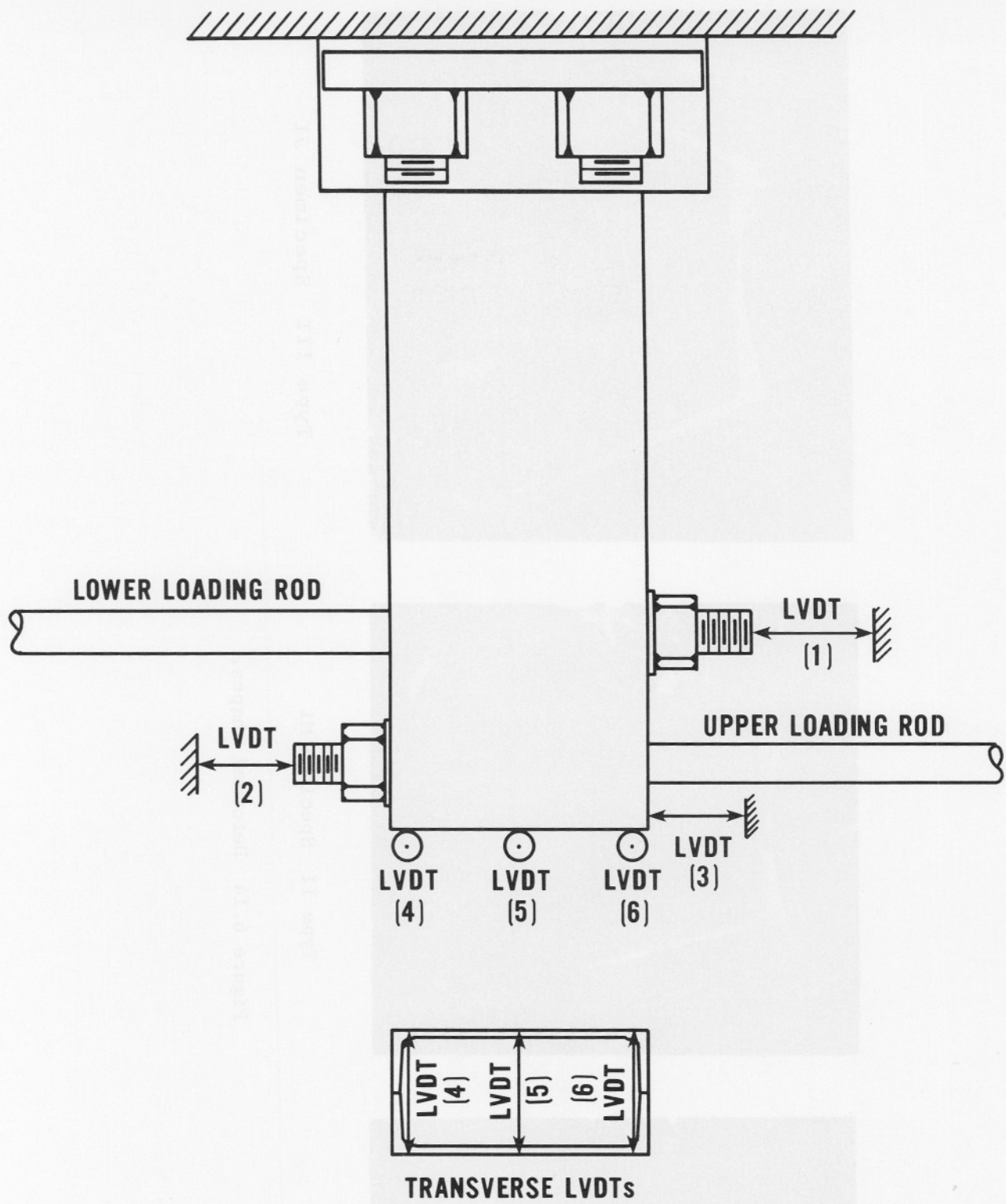
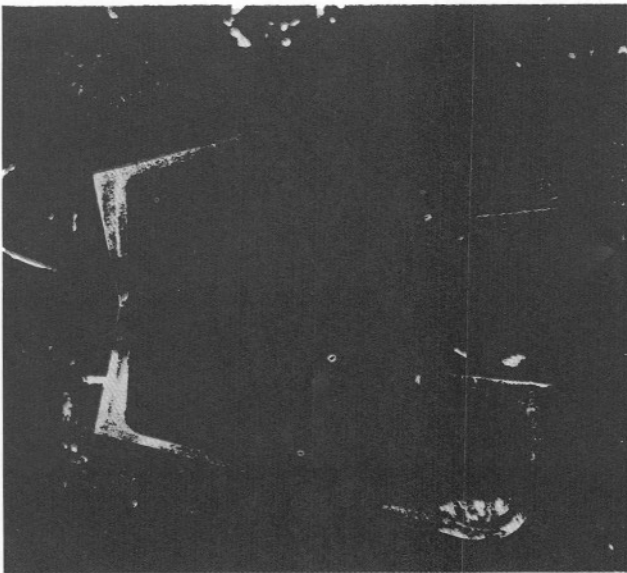
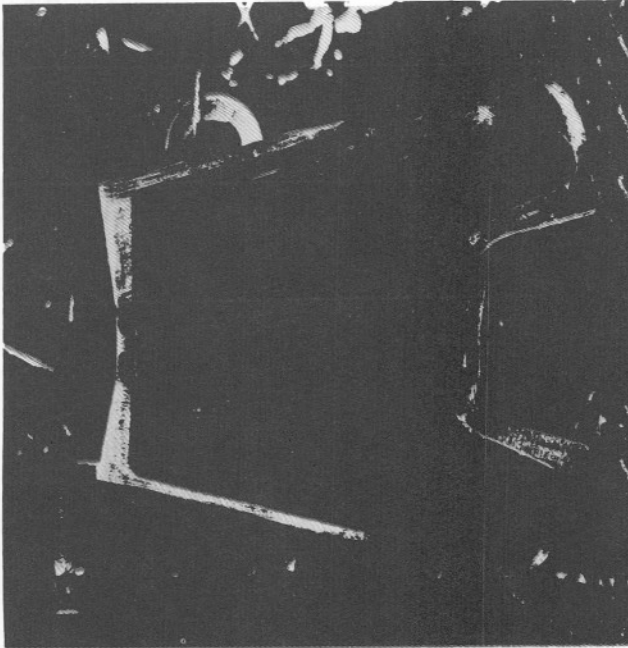


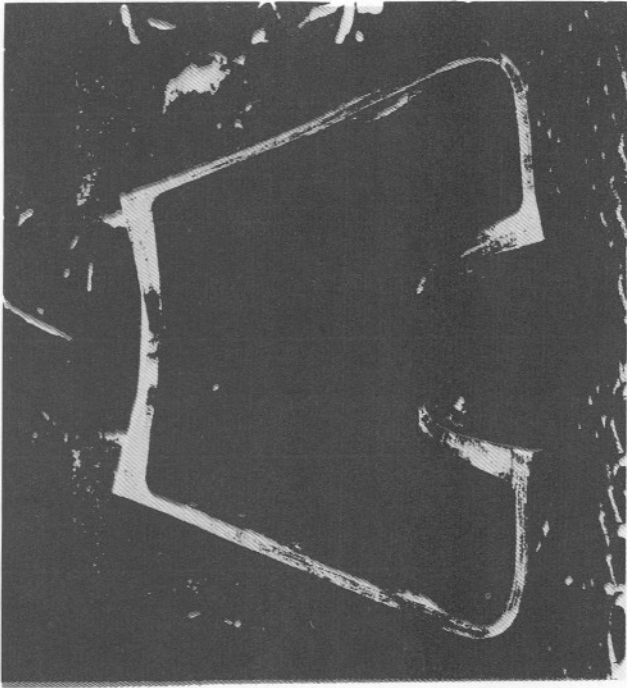
Figure 6.13 Short box beam instrumentation.



Type I Specimen K2



Type II Specimen M1



Type III Specimen J1

Figure 6.14 Deformed shapes.

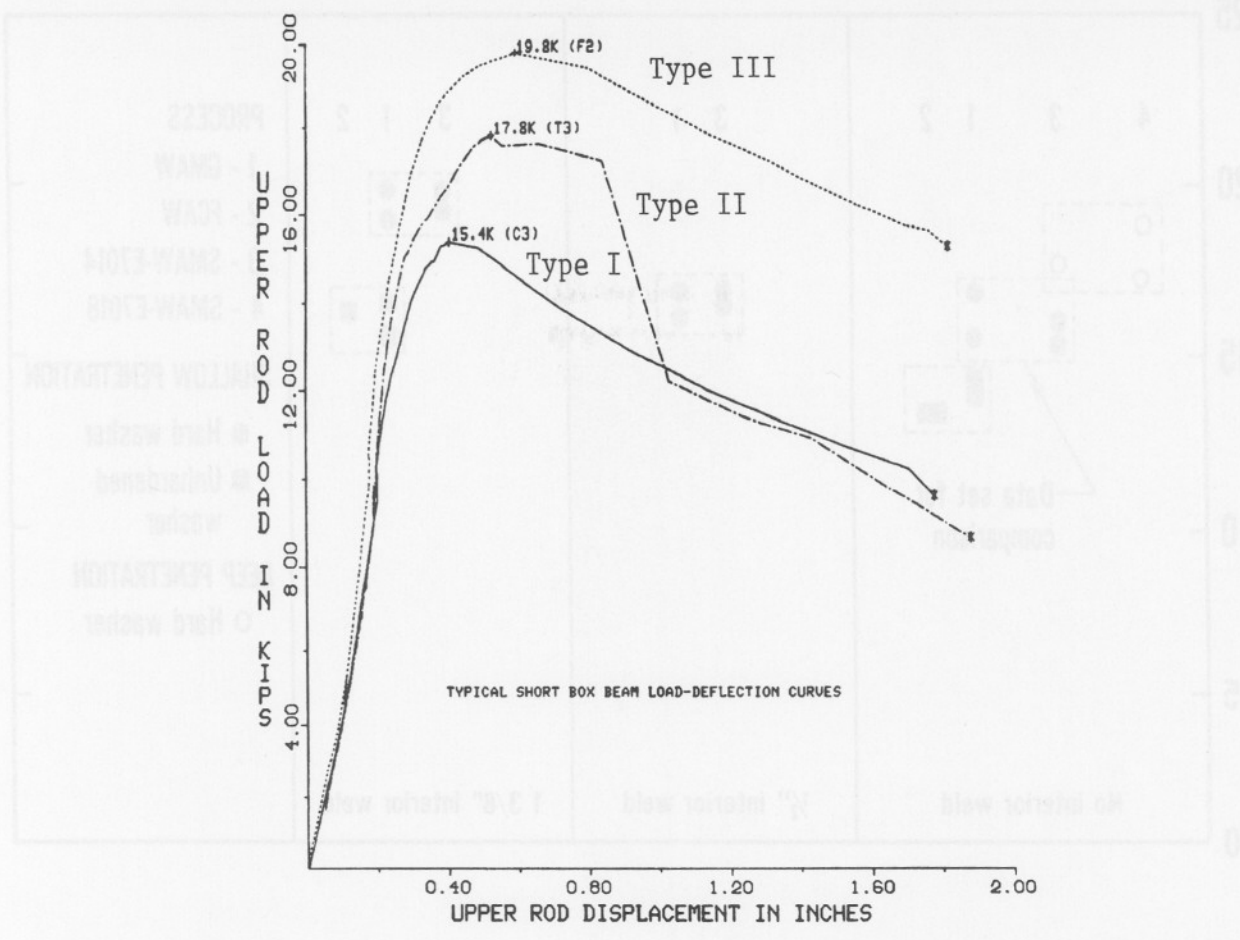


Figure 6.15 In-plane load deflection curves for specimens C-3, F-2, and T-3.

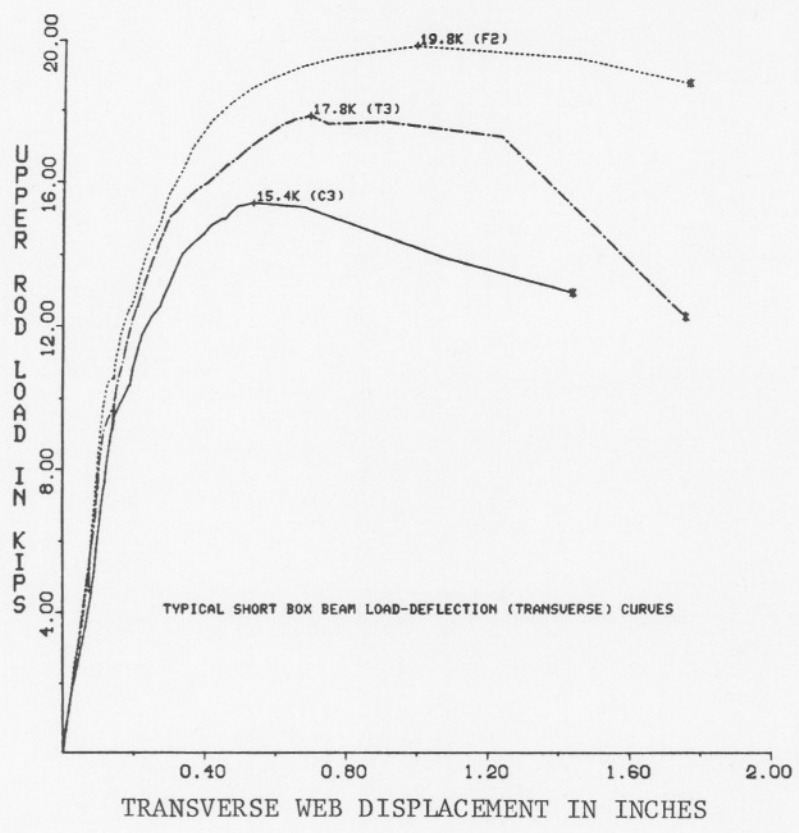


Figure 6.16 Out-of-plane web load displacement curves for specimens C-3, F-2, and T-3.

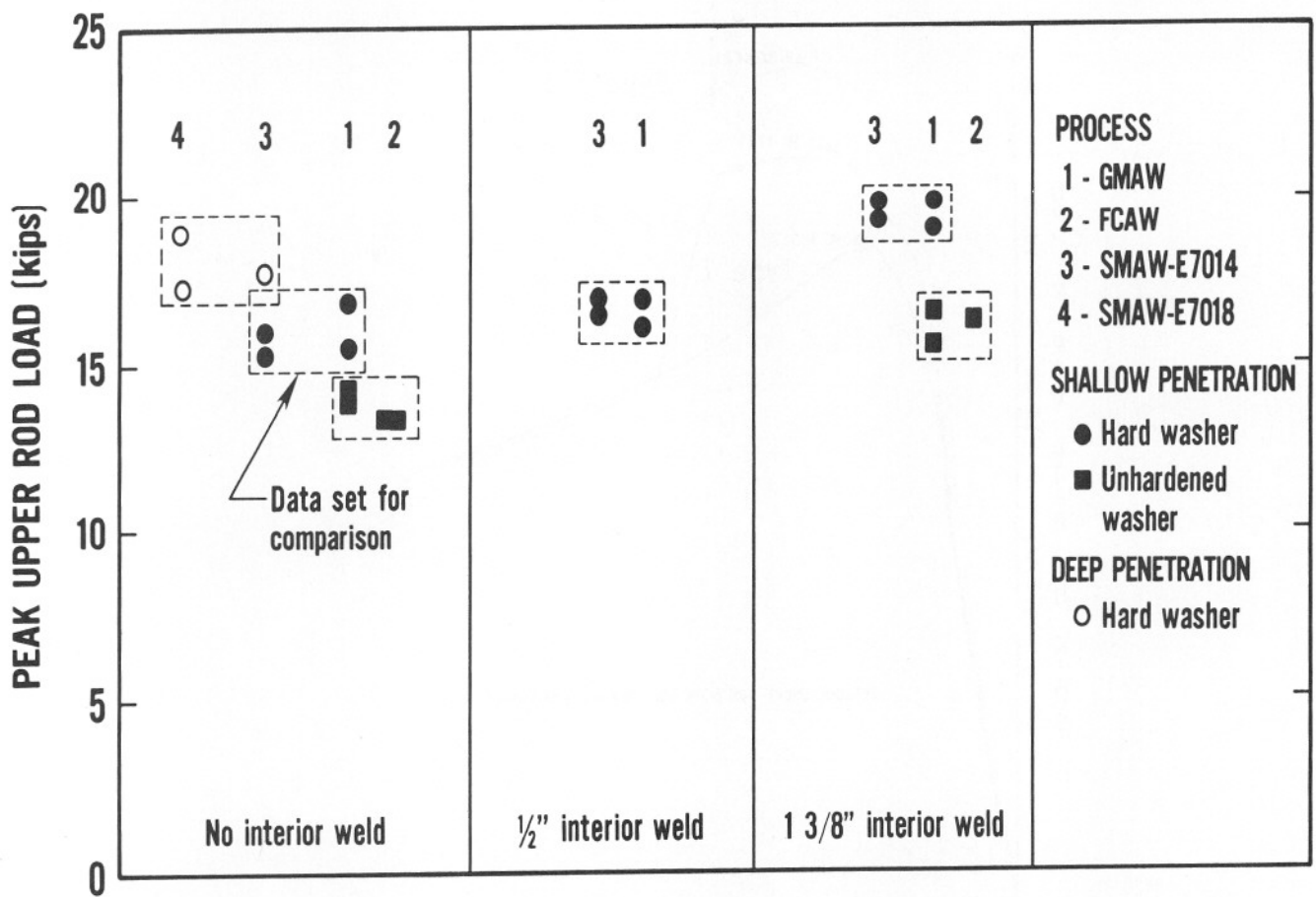


Figure 6.17 Effect of weld process.

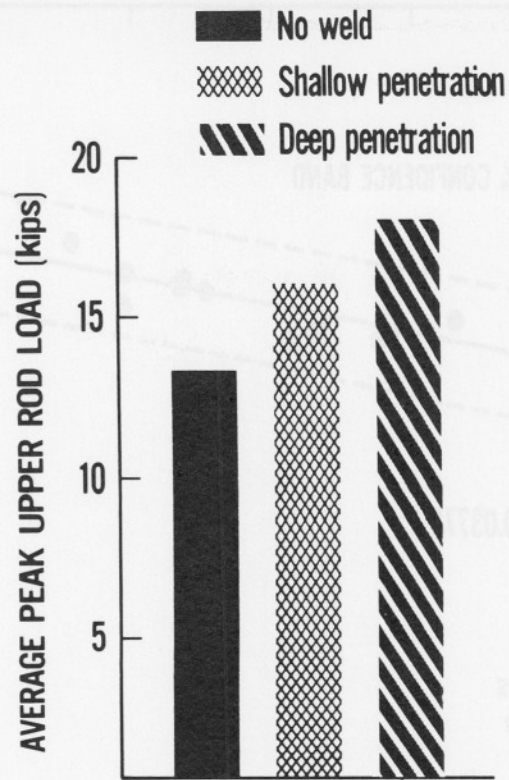


Figure 6.18 Effect of exterior weld penetration.

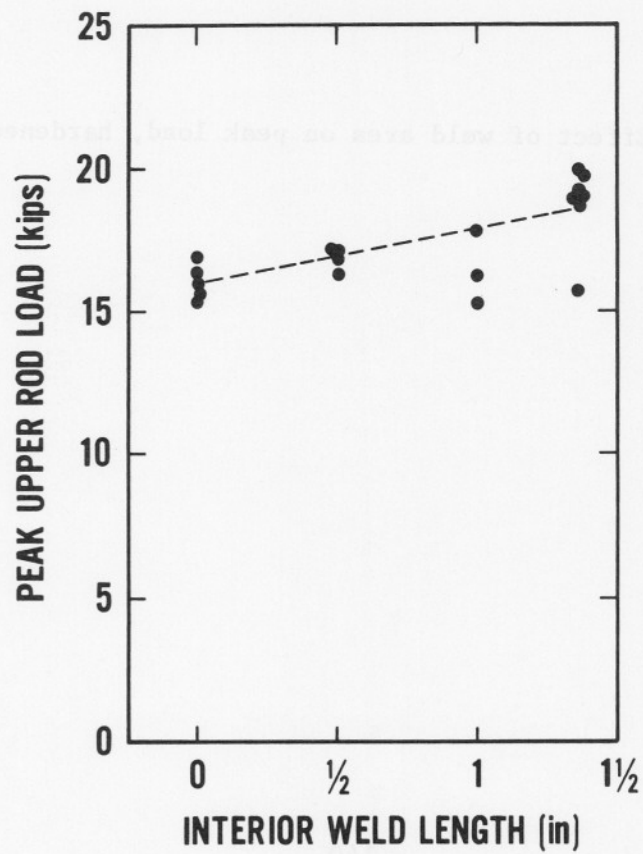


Figure 6.19 Effect of interior weld length on peak load.

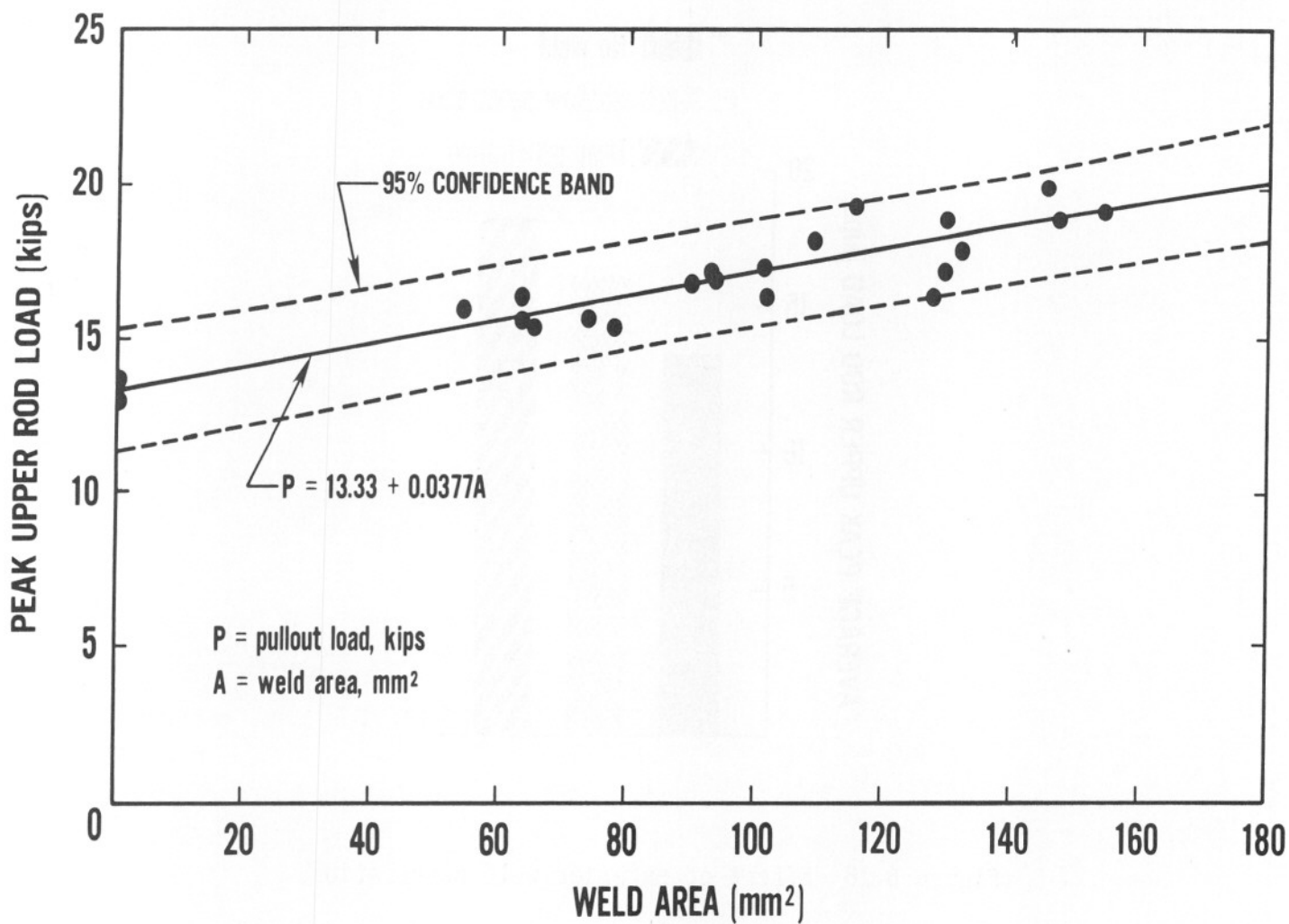


Figure 6.20 Effect of weld area on peak load, hardened washers.

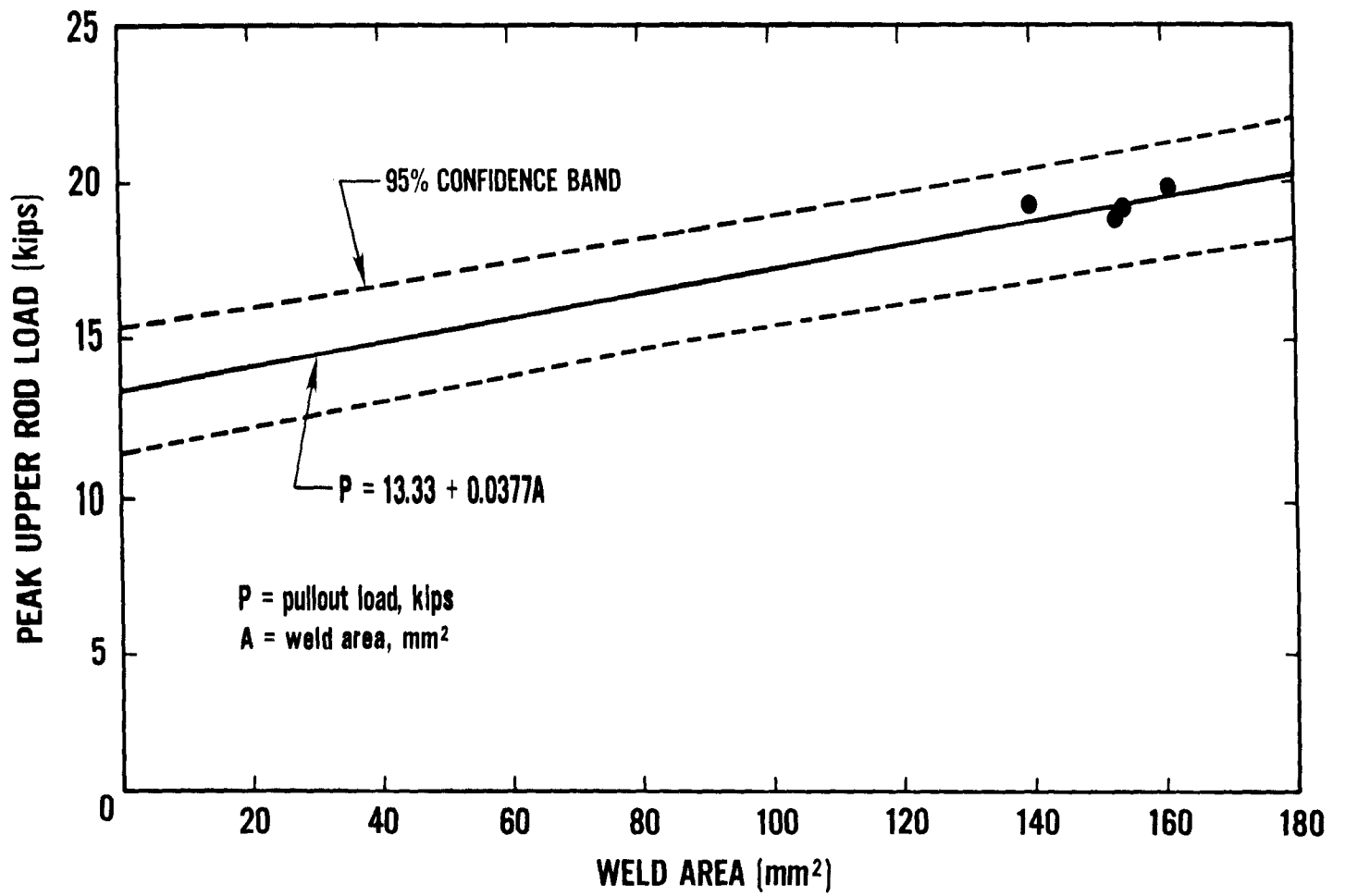


Figure 6.21 Effect of clip angles.

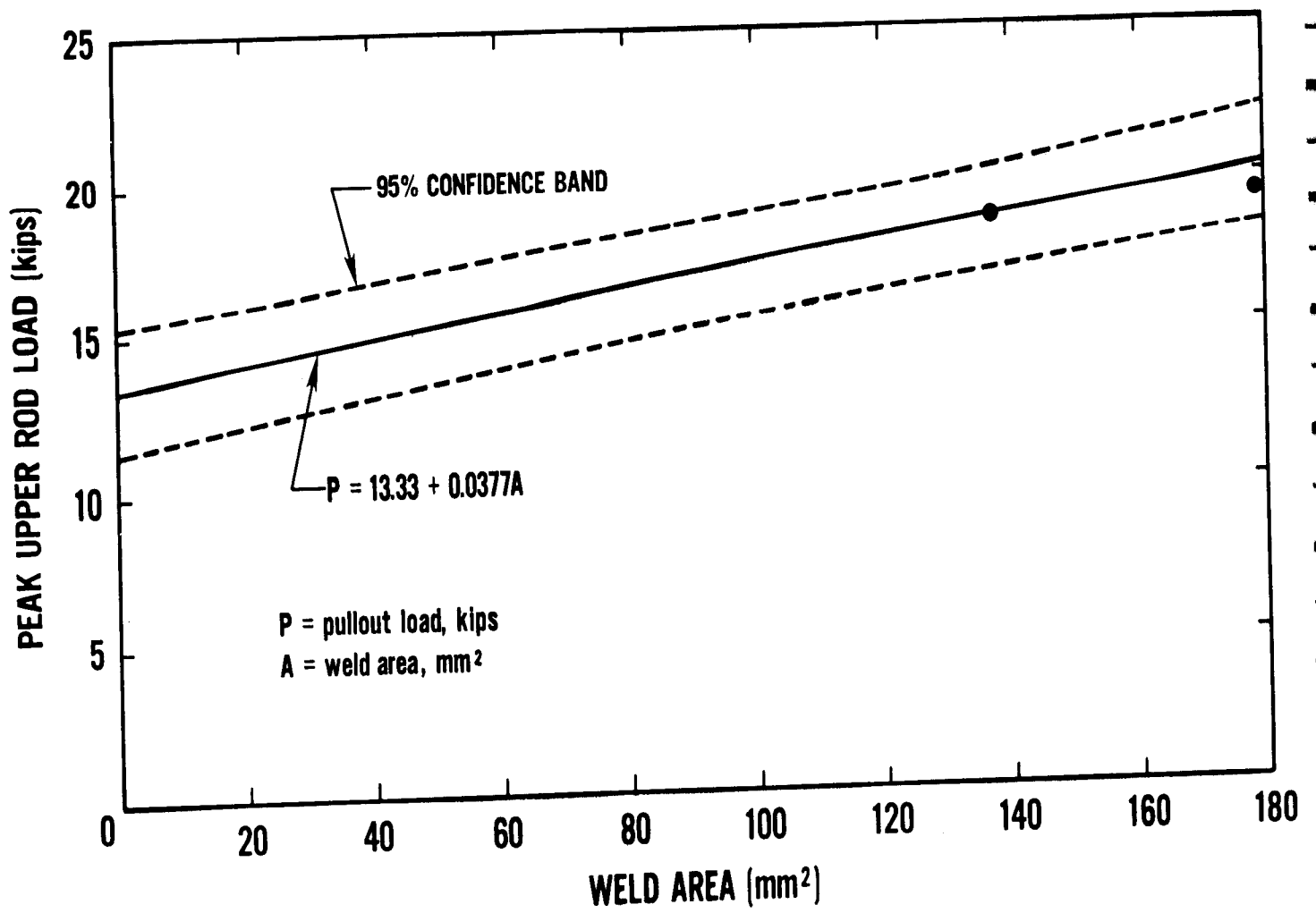


Figure 6.22 Effect of initial upper rod load.

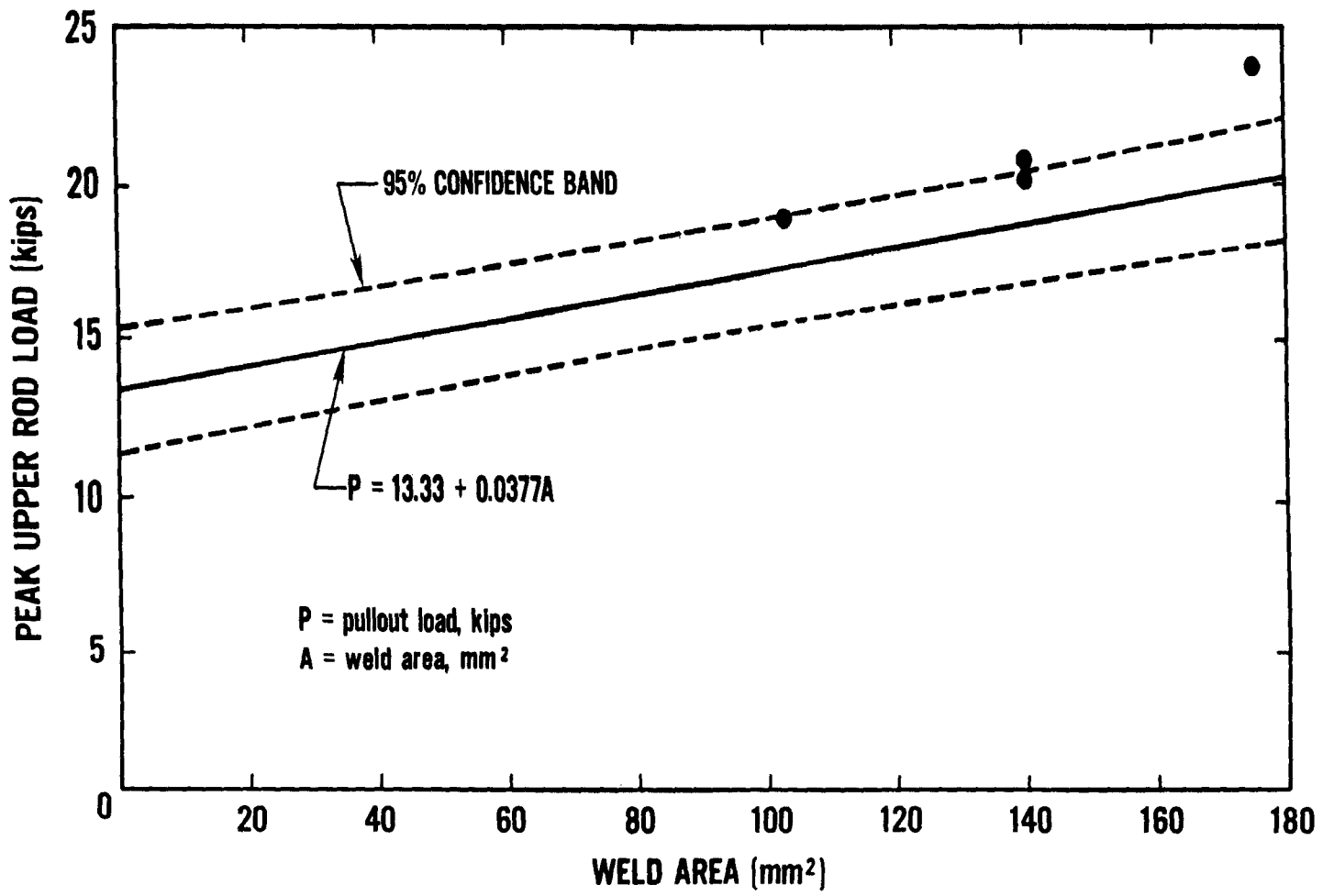


Figure 6.23 Effect of loading configuration.

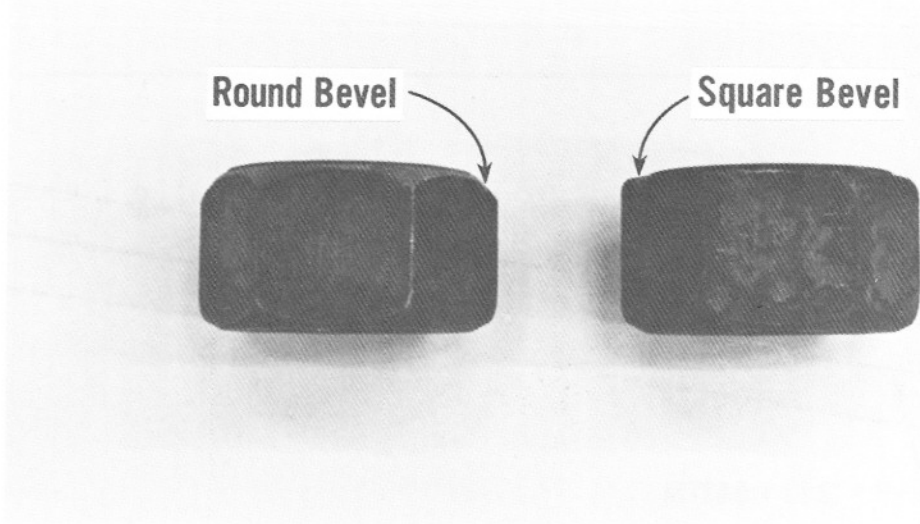


Figure 6.24 Nut shape.

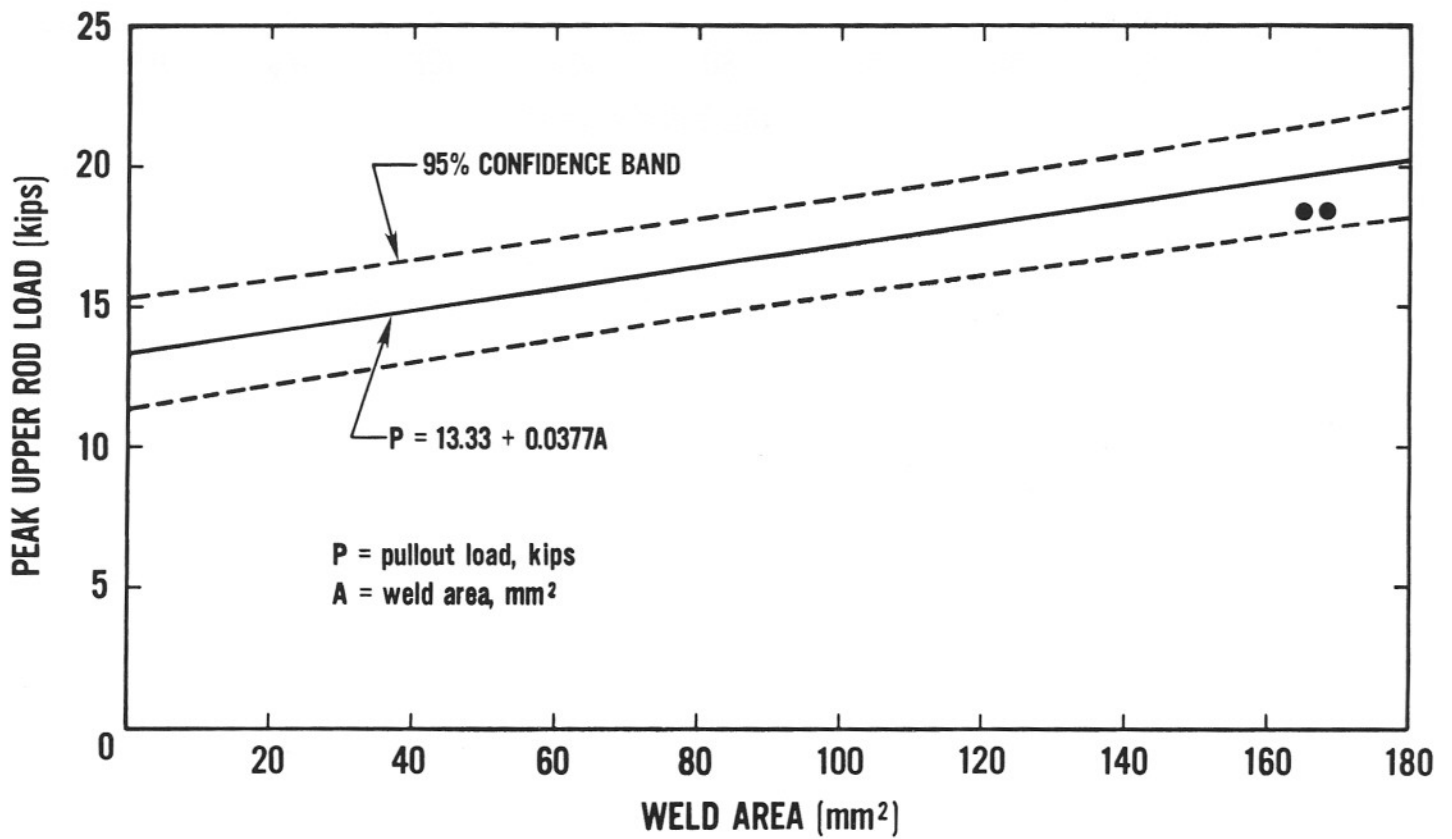


Figure 6.25 Effect of nut shape.

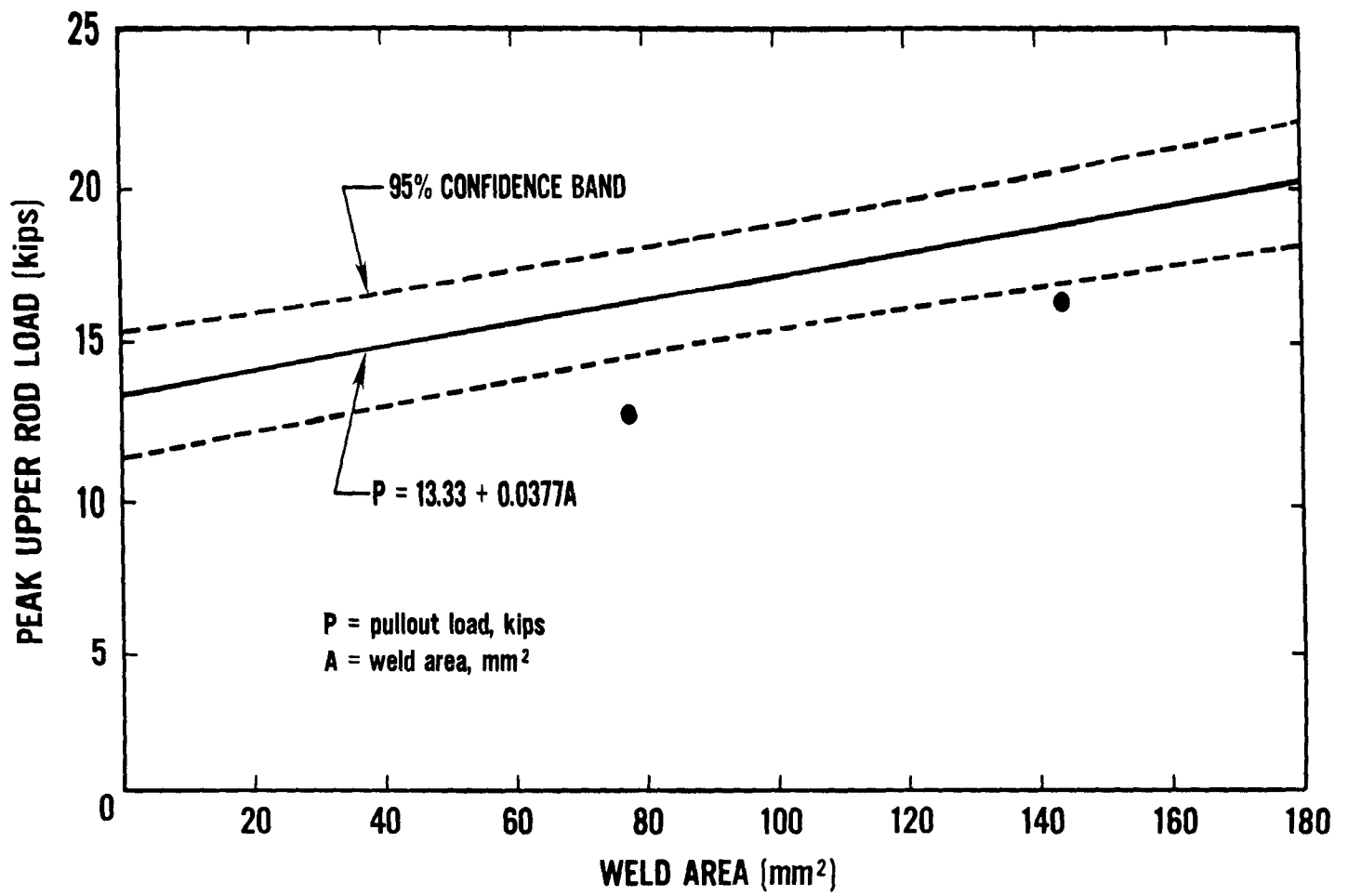


Figure 6.26 Effect of washer presence.

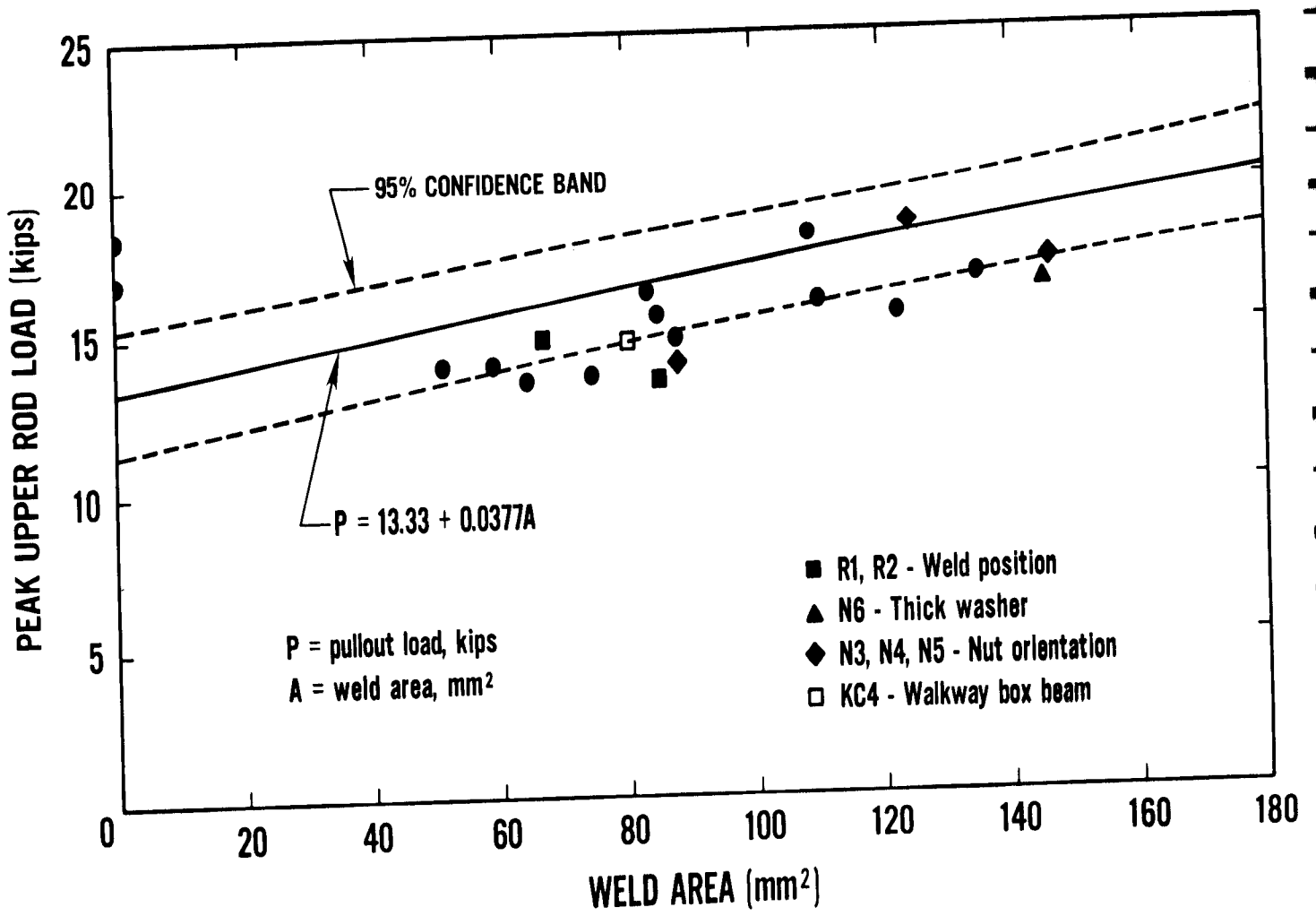
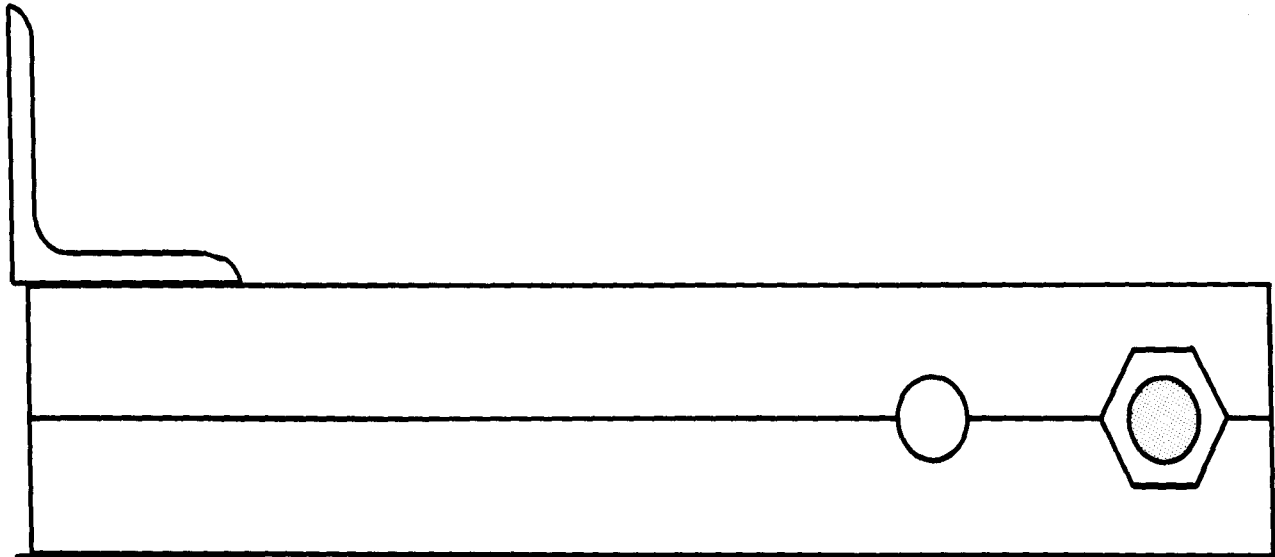
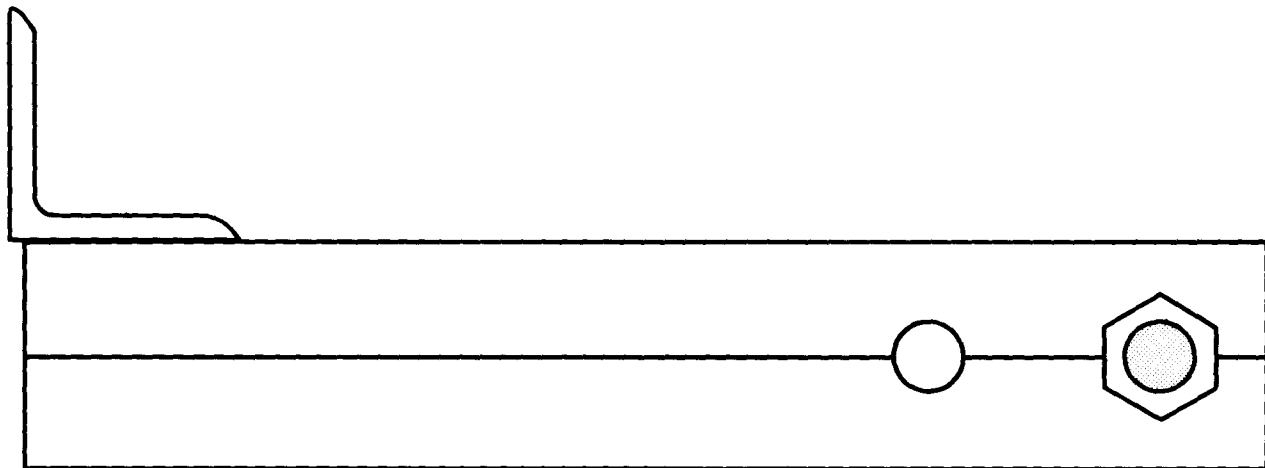


Figure 6.27 Effect of unhardened washers.



**NUT FACE PARALLEL TO BEAM  
LONGITUDINAL AXIS**



**NUT FACE PERPENDICULAR TO BEAM  
LONGITUDINAL AXIS**

Figure 6.28 Nut orientation.

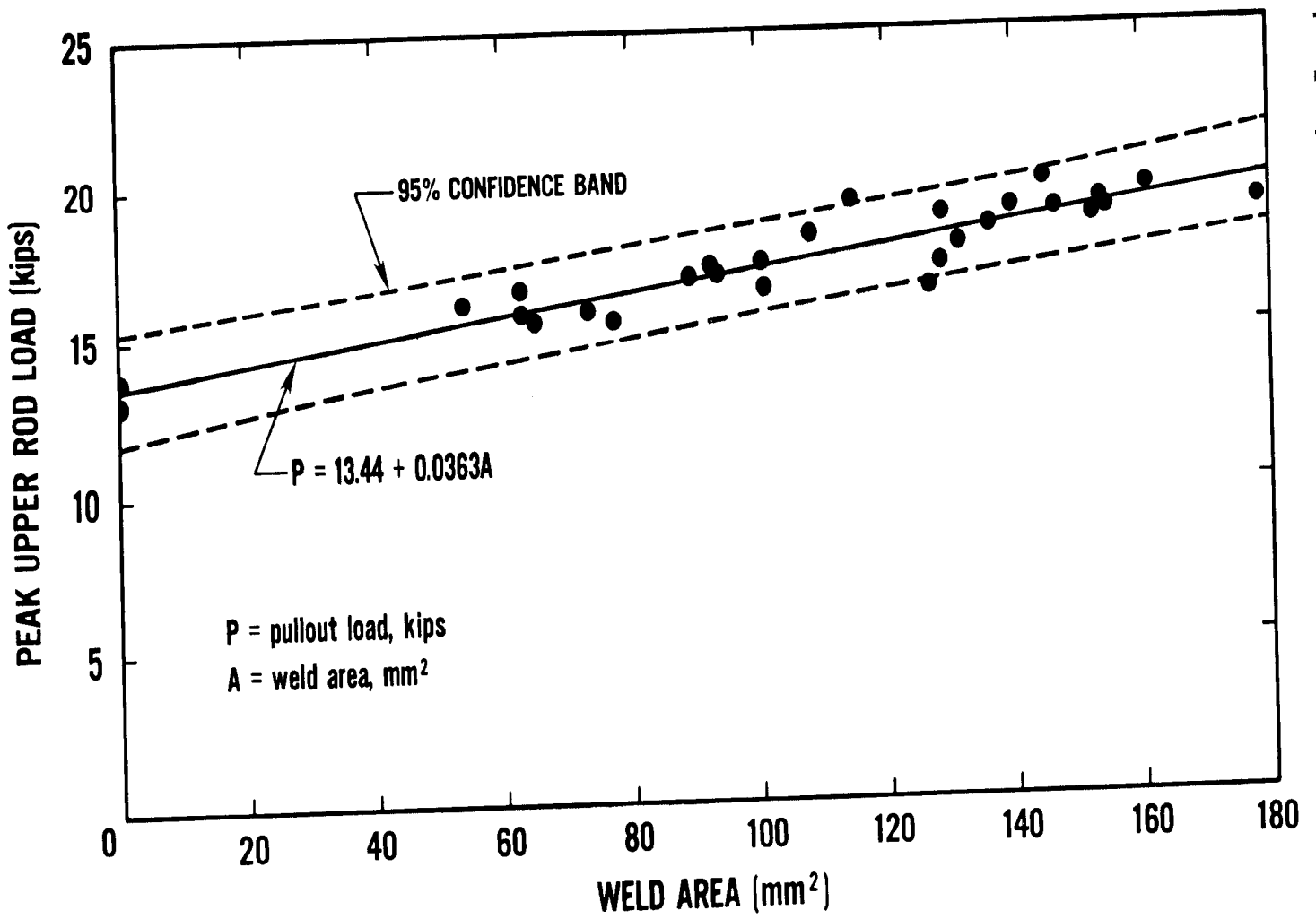


Figure 6.29 Effect of weld area on pullout load for short box beams.

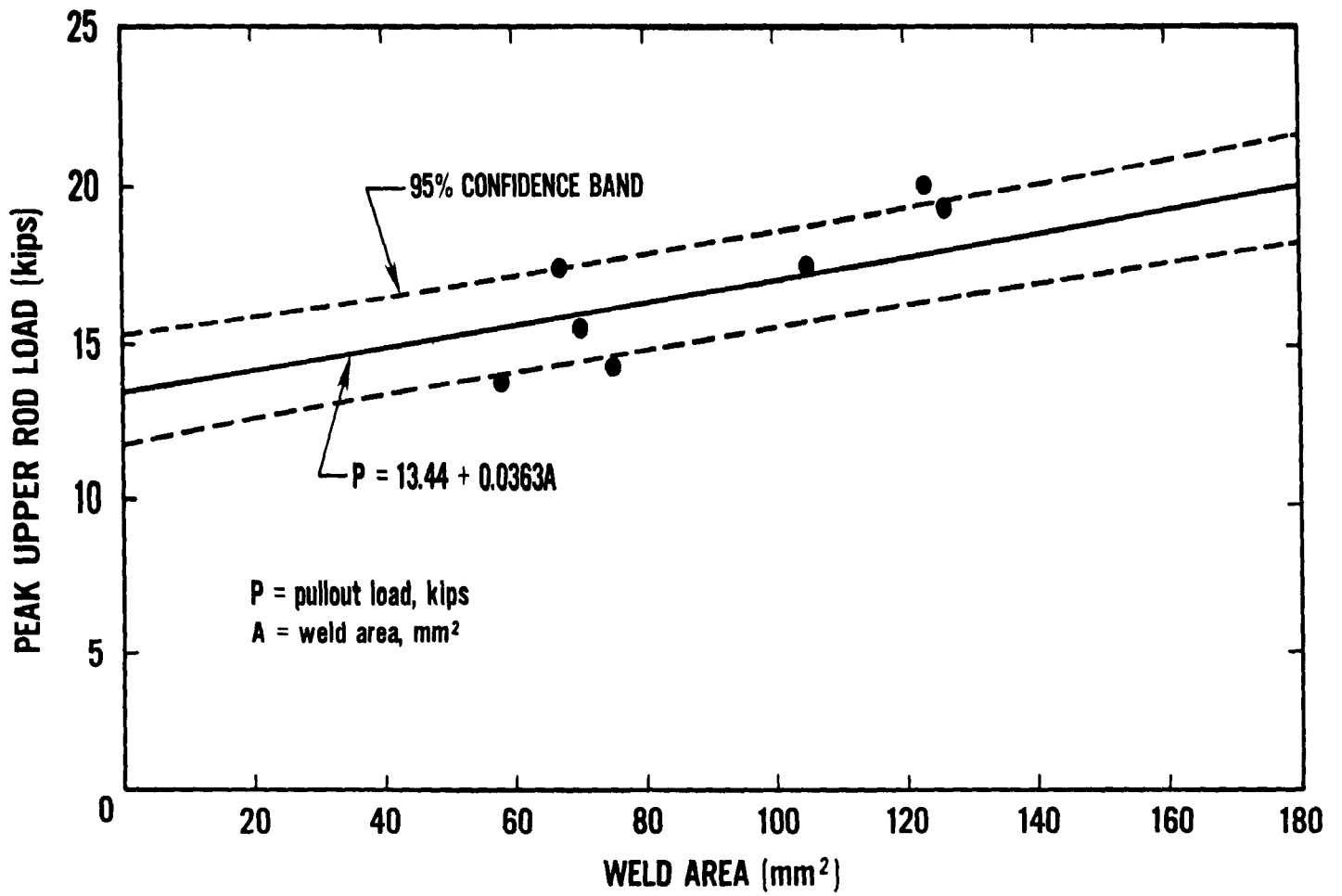


Figure 6.30 Comparison of full-length box beams with short box beam results.

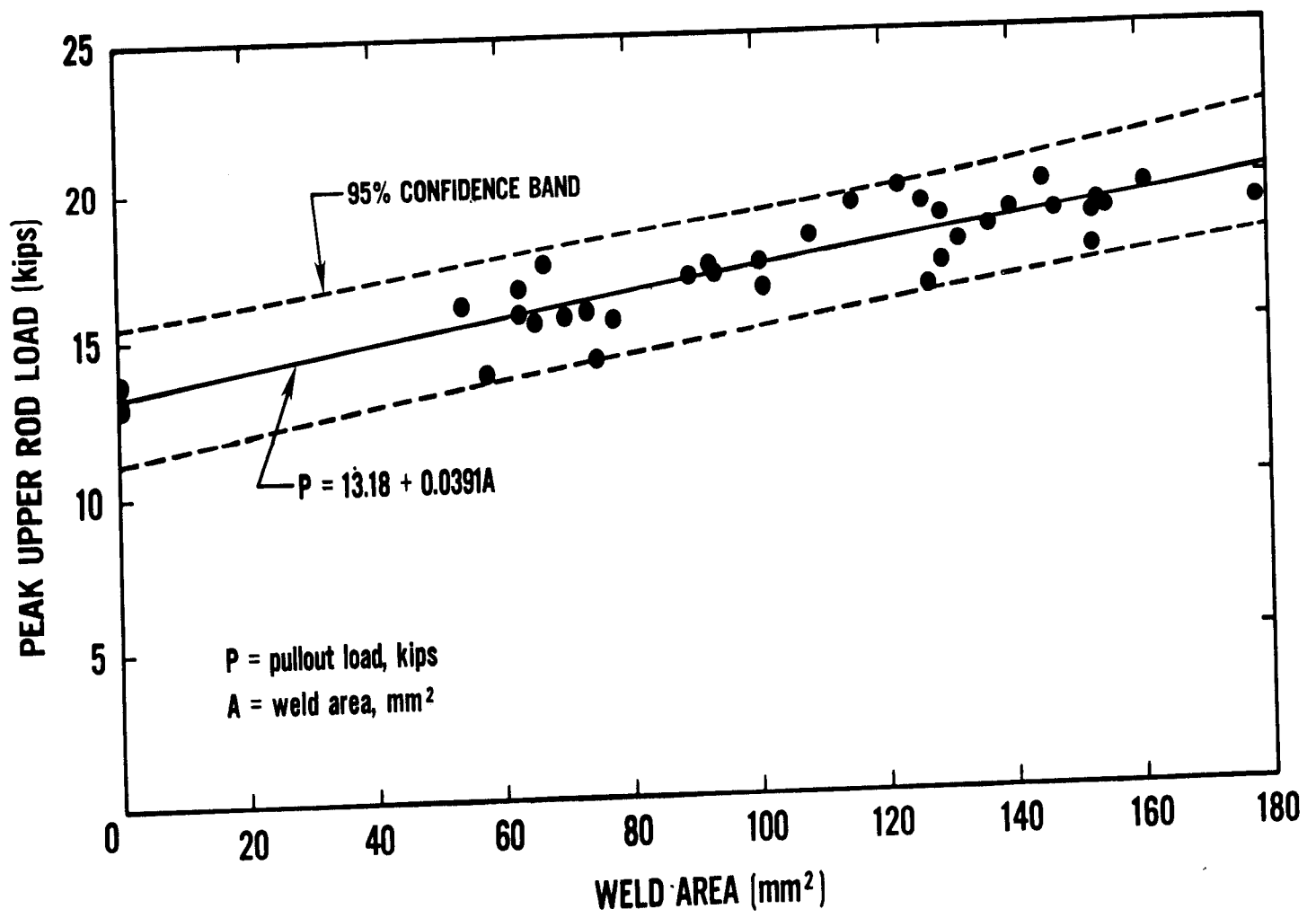


Figure 6.31 Effect of weld area on pullout load for NBS tests.

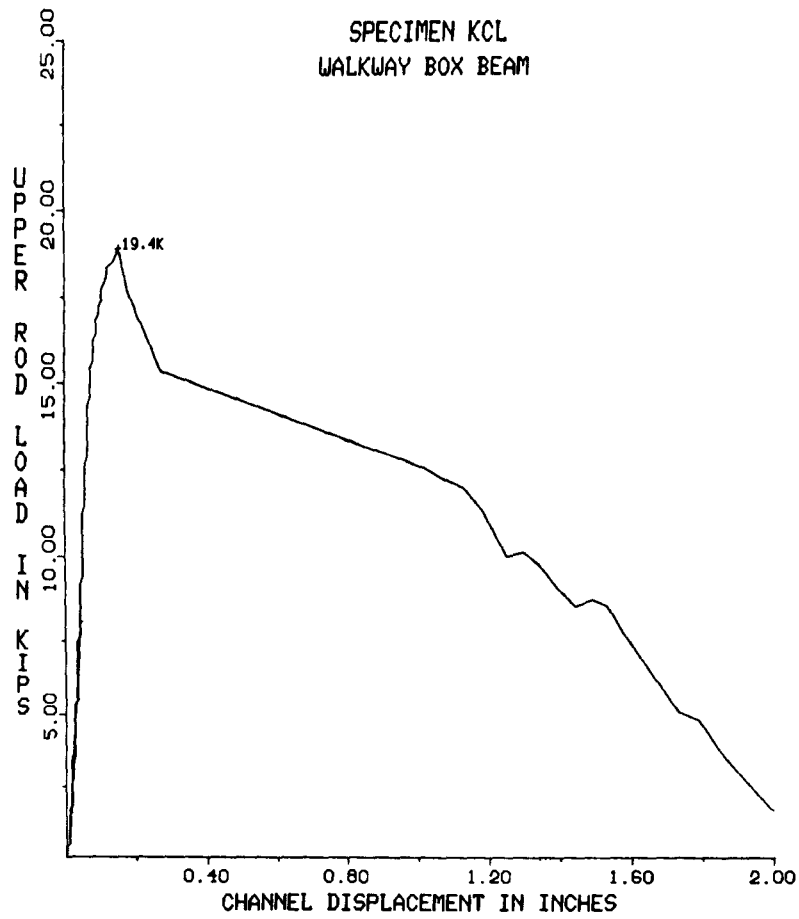


Figure 6.32 In-plane load vs deflection curve for full length box beam specimen taken from third floor walkway.

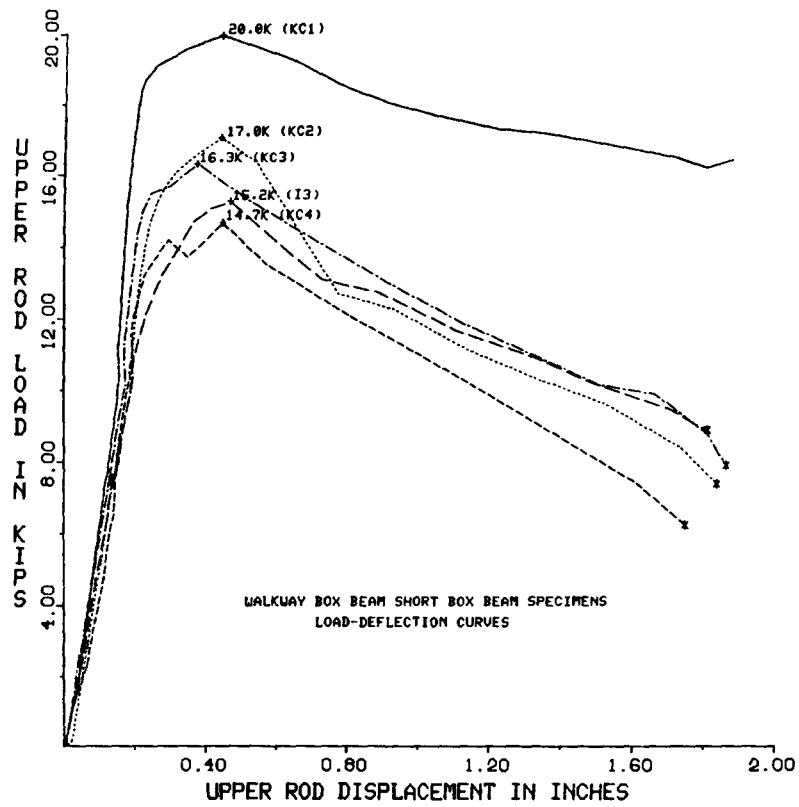


Figure 6.33 In-plane load vs displacement curves for specimens KC1-KC4 and I3.

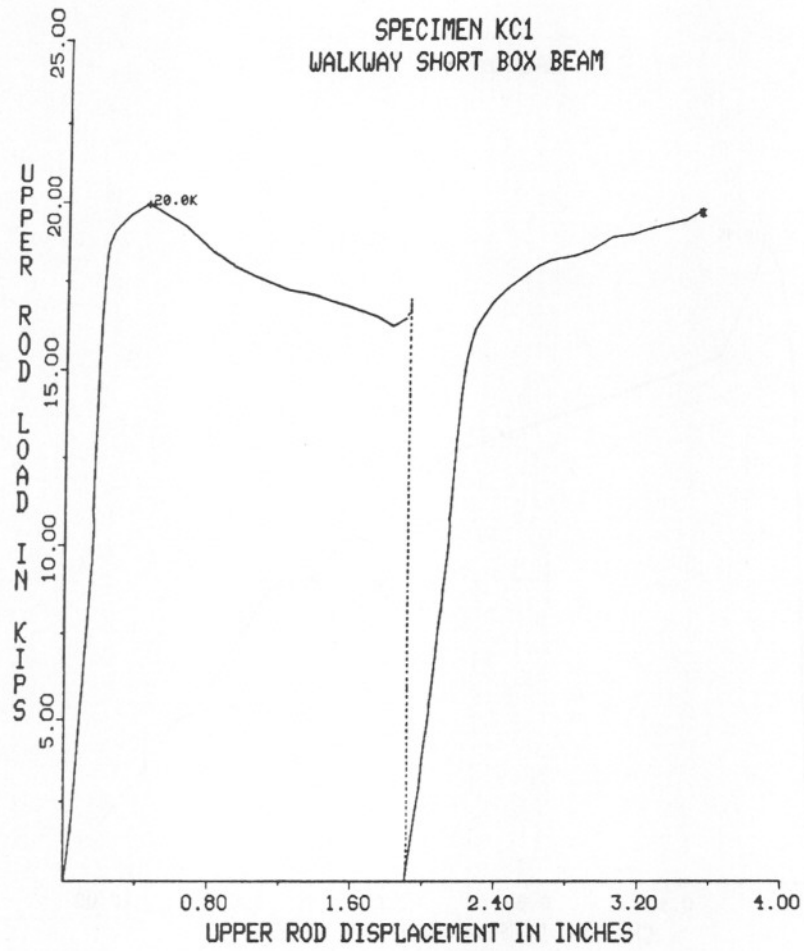


Figure 6.34 In-plane load vs deflection curve for specimen KC1.

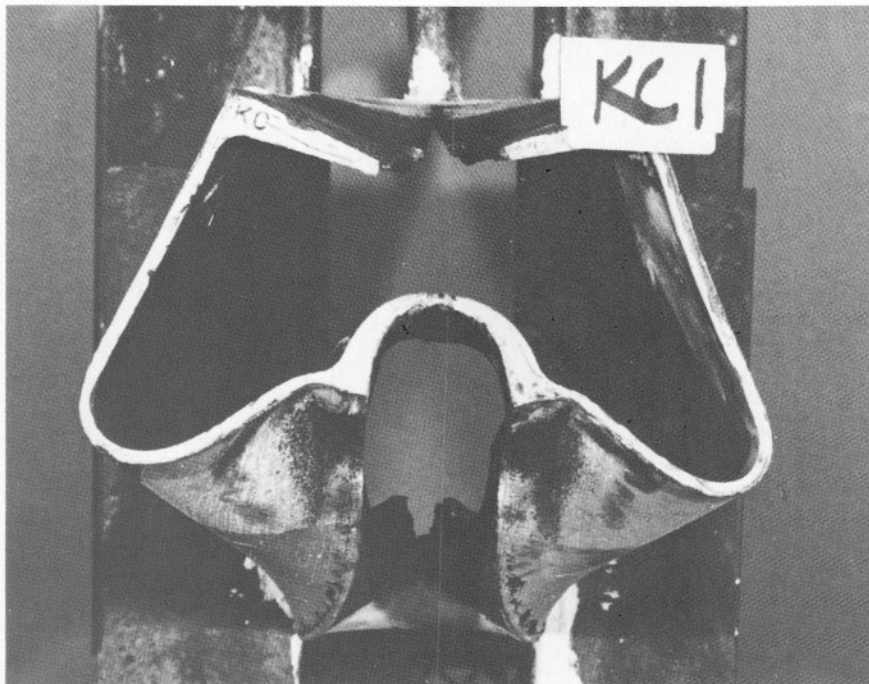
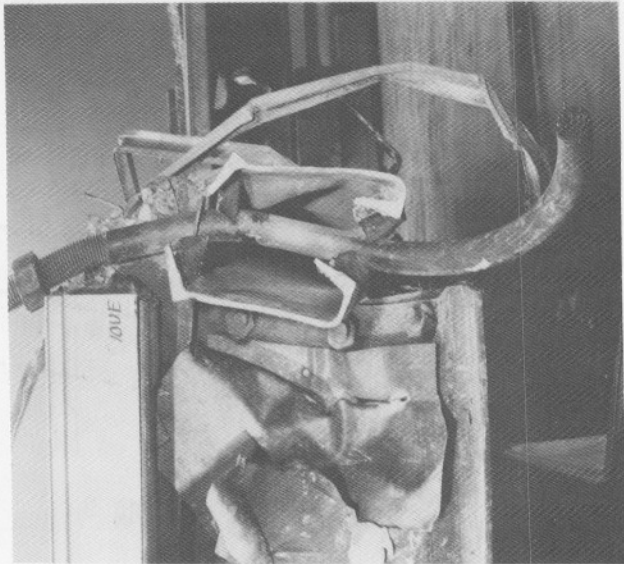
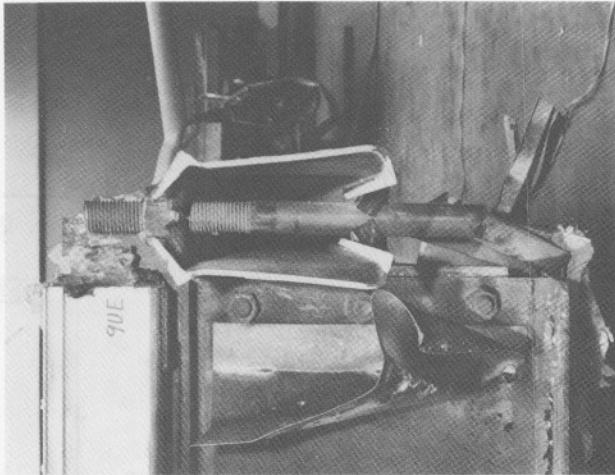
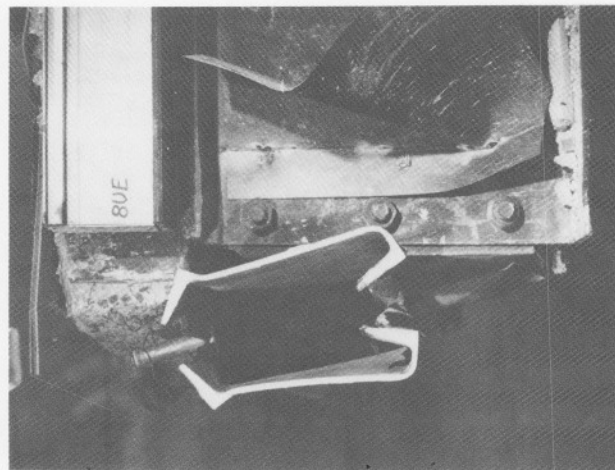
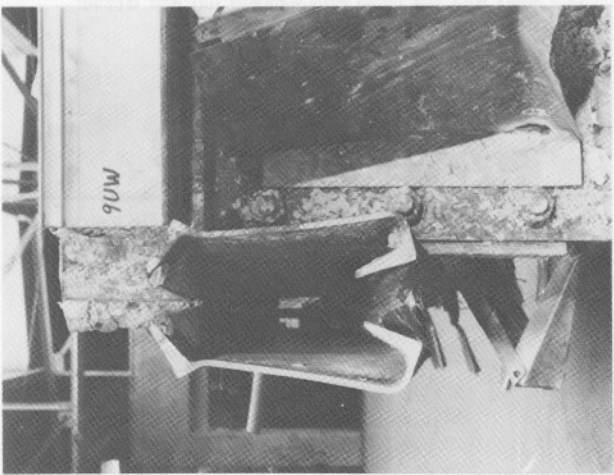


Figure 6.35 Deformed shape of walkway specimen KC1.



80VW 90VW 80VE 90VE 80E 90E 80W 90W

Figure 6.36 Walkway deformed shapes.

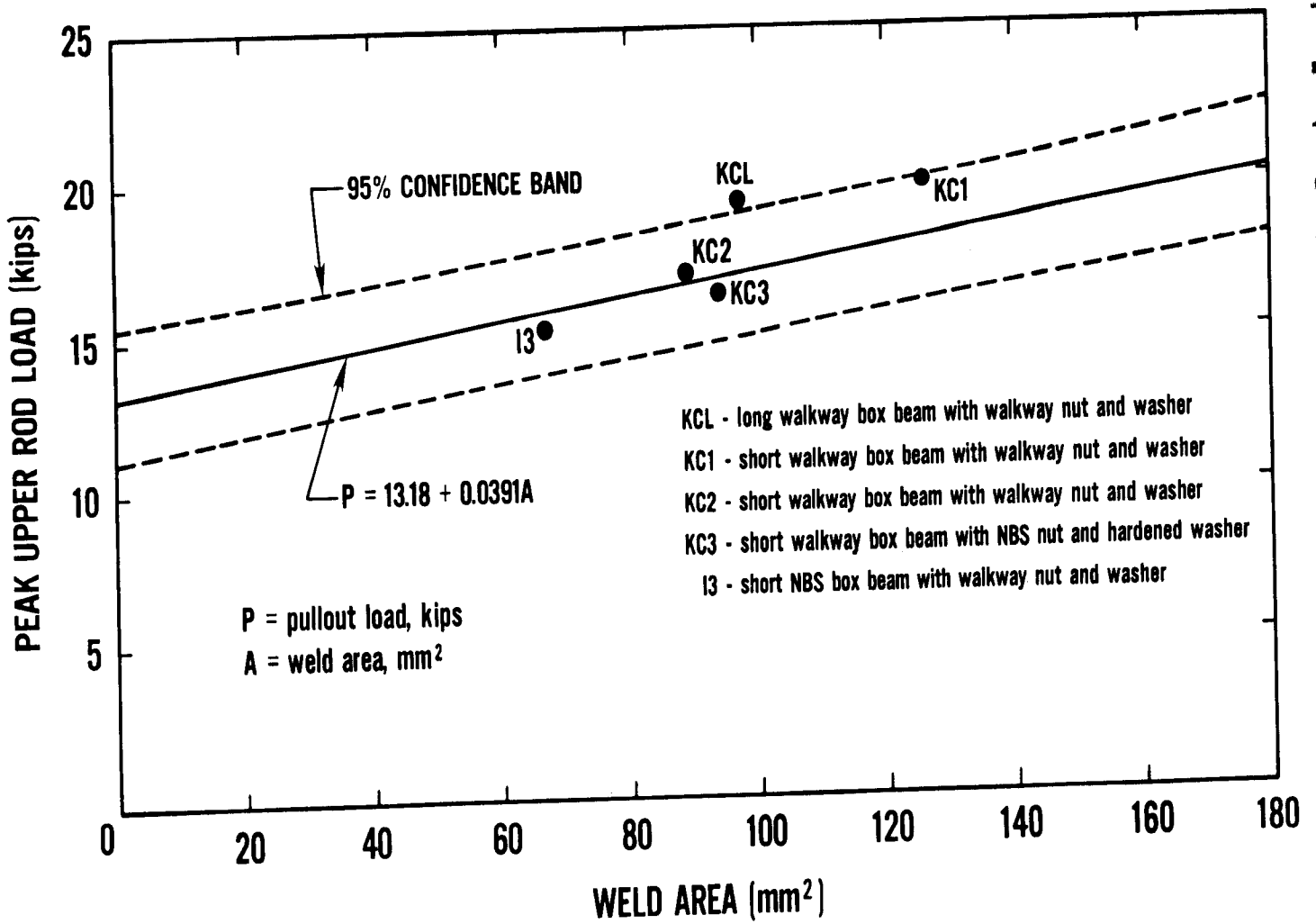


Figure 6.37 Comparison of walkway test series with NBS test results.

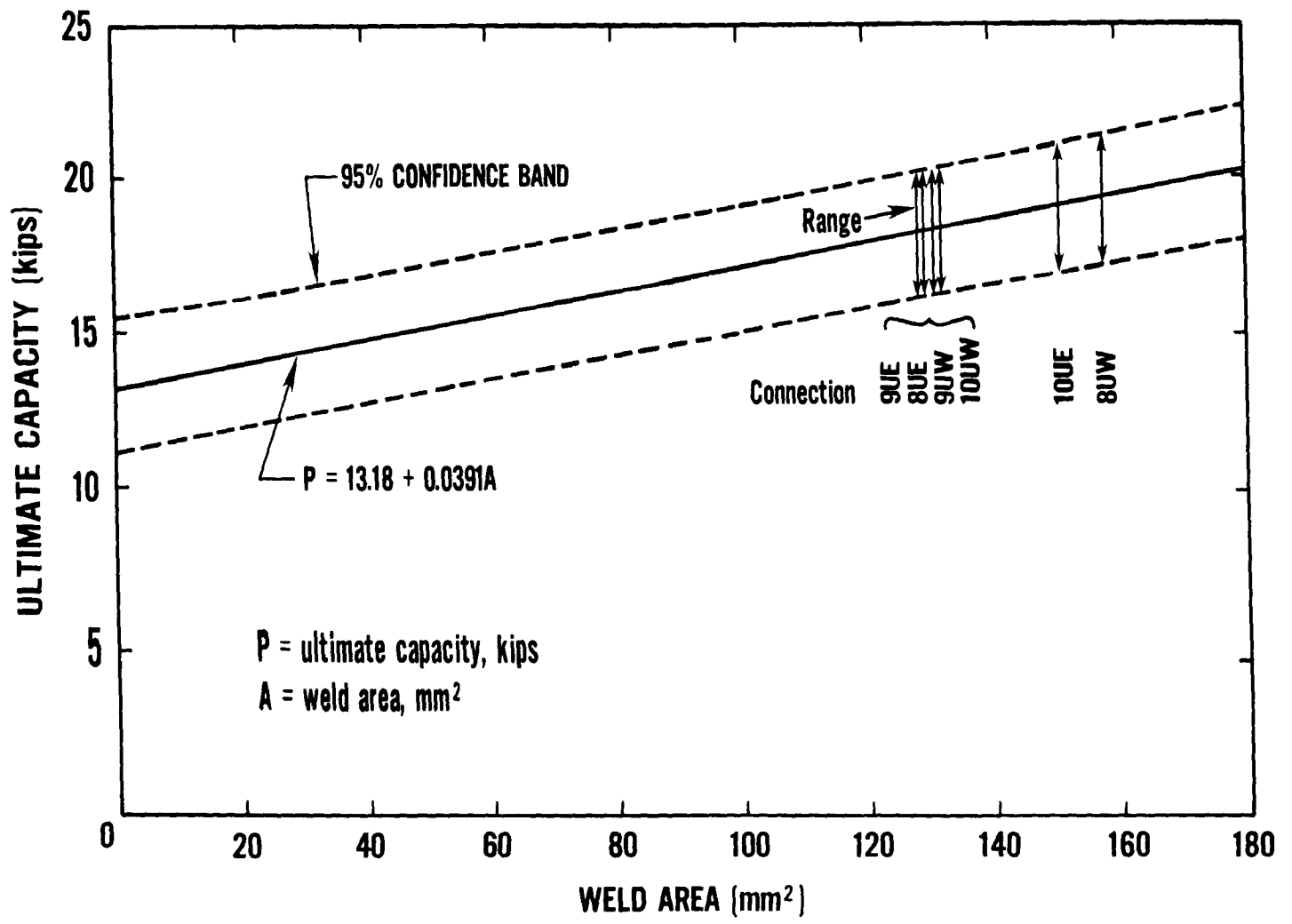


Figure 6.38 Estimated ultimate capacity for walkway box beam-hanger rod connections.

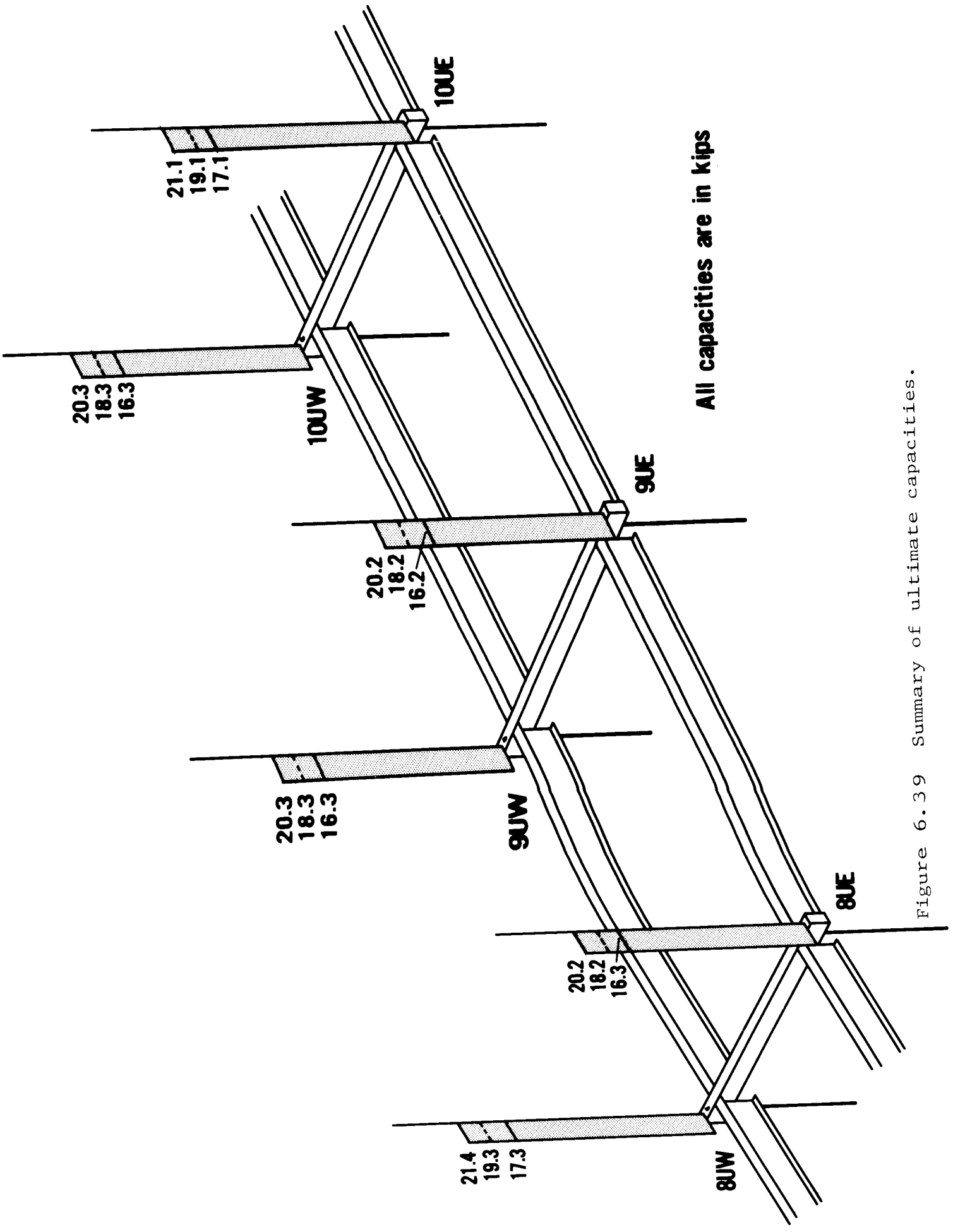


Figure 6.39 Summary of ultimate capacities.

## 7. NBS MATERIALS EVALUATION PROGRAM

### 7.1 INTRODUCTION

This chapter describes the procedures and results of various tests and evaluations of NBS test materials and of materials obtained from the walkway debris. The objective was to determine compliance with appropriate codes and standards and to characterize the construction materials and the weldments.

Section 7.2 describes visual inspection and the radiographic examination of the longitudinal welds in a box beam removed from the walkway debris and assesses conformance of weld quality to AWS D1.1-79, Structural Welding Code-Steel [3.1].

Section 7.3 describes the tests to determine the mechanical properties of the structural steel and weldments. These tests were performed to characterize the materials and to determine whether the materials conformed to the requirements of ASTM A36 (Standard Specification for Structural Steel) [7.1]. Properties determined by these tests include ultimate tensile strength, yield strength, elongation and reduction of area.

Section 7.4 describes the results of metallographic examinations and hardness measurements carried out on parent material and on weld material and heat affected zones associated with the box beam longitudinal welds. Also included in this section are metallographic and hardness data obtained from hanger rod specimens, from steel washers used in the walkway construction and from washers used in the NBS structural testing program described in chapter 6.

Section 7.5 presents the results of chemical analyses to determine conformance of the structural steel to the requirements of ASTM A36 and to determine, if possible, the type of electrode used to fabricate the walkway box beams.

The results of physical tests carried out on concrete cores removed from the walkway decks are described in section 7.6. Included here is the determination of bulk specific gravity, modulus of elasticity and compressive strength of the concrete. Also included is the bulk specific gravity of the topping material used to level the walkway decks.

Section 7.7 summarizes the conclusions drawn in this chapter.

## 7.2 INITIAL INSPECTION

### 7.2.1 Visual

Section 0510 (Parts 1.4b and 3.3d) of the project specifications [2.1] allows for the visual inspection and nondestructive spot testing of shop and field welds by the owner's inspection agency. As noted in section 2.6 of this report, inspection reports that were made available to the NBS investigative team contained very little information that was relevant to the construction of the walkways. Therefore, it is not known what, if any, nondestructive testing was carried out on the walkway box beam welds. In the absence of such information, the criterion used by NBS to determine weld quality was visual inspection as described in Par. 8.15.1 of AWS D1.1-79. No cracks or piping porosity were observed. Weld profiles were normal. The weld quality therefore conformed to the welding code requirements under visual inspection.

### 7.2.2 Radiography

A radiographic examination was made of the top and bottom longitudinal welds in box beam 9M (NBS 3). The top longitudinal weld had been ground flush for the entire length of the beam and the bottom weld had been ground flush for a short distance from each end as discussed in section 5.3.3.

The welds were marked off in 1 ft (300 mm) sections and numbered sequentially beginning with the bottom weld at location 9MW (No. 1), traversing to 9ME (No. 11), beginning again at the top weld at location 9MW (No. 12) and continuing along the beam to 9ME (No. 22). Two exposures were made at each section; one to achieve 2 percent radiographic sensitivity through the toe of the flange adjacent to the center of the weld and another to achieve a readable radiographic density at the center of the weld. Radiography was performed at 140 KVP using a 2 mm aluminum filter, a source-to-film distance of 1 meter with focal spot of 0.4 mm x 0.4 mm. Two sheets of Kodak type M film were used in flexible cassettes containing a 0.005 in (0.13 mm) thick front lead screen and a 0.010 in (0.25 mm) thick back lead screen. Exposure conditions varied from 8 to 36 milliampere-minutes, depending on results desired for a particular section. A reproduction of the radiographs of sections 1, 11, 12 and 22 encompassing the beam ends appears in figure A7.2.2-1 of the appendix.

The radiographs revealed porosity lying along the weld centerline in all sections. Study of the fracture surface of a small length of weld at section 11 confirmed the presence of porosity. More porosity was evident between the beam ends and the outer hanger rod holes than between the hanger rod holes. Portions of the welds were free of porosity, suggesting that its development coincided with the start of a weld run.

Linear indications on the radiographs apparently deviating from the weld centerline at locations 7 in (178 mm) and 10 in (254 mm) from the end of beam at section 1 had the appearance of cracks. These were not confirmed by metallographic sectioning and fracturing the welds at these locations.

### 7.3 MECHANICAL PROPERTIES OF STRUCTURAL STEEL AND WELDMENTS

As has been described in chapter 6, all NBS box beam replicas were fabricated from MC8 x 8.5 structural channel believed to have been produced from a single heat. Tensile tests were performed to establish consistency within the lot and to determine conformance to the requirements of ASTM A36. Components from which specimens were machined included two walkway box beam segments, the full-length walkway box beam, hanger rod segments, and NBS box beam channels. Tests were also carried out to determine the tensile properties of the walkway box beam longitudinal weldments.

#### 7.3.1 NBS Channel Specimens

Specimens were machined from two NBS channel segments coded B and Y. Three specimens transverse to the rolling direction and three longitudinal specimens were machined from the web region and one longitudinal specimen was prepared from each of the two flange regions of the B-coded channel. Two transverse and two longitudinal specimens were machined from the web region and one longitudinal specimen was prepared from each of the two flange regions of the Y-coded channel. All specimens conformed to ASTM E8-81 (Standard Methods of Tension Testing of Metallic Materials) [7.1]. A representative specimen is shown in figure 7.1, left side. These specimens were 8 in (200 mm) long,  $0.500 \pm 0.010$  in ( $12.70 \pm 0.25$  mm) wide at the reduced section and had a  $2.000 \pm 0.005$  in ( $50.80 \pm 0.13$  mm) gage length. The web specimens were tested full thickness (ranging from 0.180 to 0.183 in (4.57 to 4.65 mm)) whereas the flange specimens were machined to a uniform nominal thickness of 0.24 in (6.1 mm) to remove the taper.

Specimens were tested to failure in tension in one of three testing machines: (A) a 25,000 kgf (245 kN) capacity Satec Systems machine (NBS No. 184093), calibrated October 14, 1981, (B) a 50,000 lbf (222 kN) capacity Gilmore testing machine (NBS No. 172647), calibrated October 12, 1981, or (C) a 10,000 lbf (44.5 kN) capacity Gilmore testing machine (NBS No. 172648), calibrated October 15, 1981. Estimated load inaccuracy is  $\pm 1$  percent.

Strain data were recorded during the initial part of each test by an LVDT extensometer attached to the reduced section of the specimen. Estimated strain inaccuracy was  $\pm 3$  percent. The extensometer was removed from the specimen when the strain exceeded the yield point of the material. The testing machine crosshead speed was maintained at 0.02 in (0.5 mm) per minute until the extensometer was removed from the specimen. Subsequent crosshead speed was 0.05 in (1.3 mm) or 0.10 in (2.5 mm) per minute. Ultimate tensile strength, 0.2 percent offset yield strength, percent elongation in 2 in (50.8 mm), and reduction of area at the fracture were calculated. Individual test results are listed in table 7.1. Load-strain plots are given in section A7.3.1 of the appendix. Representative load-strain curves for a longitudinal web specimen, a transverse web specimen, and a longitudinal flange specimen are given in figures 7.2 - 7.4. Increasing load as a function of strain beyond 1.5 - 2 percent strain noted on these curves reflects the onset of work hardening.

There were no significant variations of tensile properties between channels nor were there significant differences between longitudinal and transverse tensile properties or between the web and flange region tensile properties. The average ultimate tensile strength for all specimens was 71,000 psi (490 MPa) with a range of 70,500 to 71,500 psi (486 to 493 MPa). The average yield strength for all specimens was 44,800 psi (309 MPa) with a range of 43,700 to 45,500 psi (302 to 314 MPa). Average elongation was 33.5 percent with a range of 30.4 to 36.8 percent. Variation in strength was minor.

ASTM Standard A36 for structural steel requires an ultimate tensile strength of 58,000 to 80,000 psi (400 to 552 MPa), a minimum yield strength of 36,000 psi (248 MPa), and a minimum elongation of 21 percent in 2 in (50.8 mm). All values for tensile strength, yield strength and elongation satisfy the requirements of ASTM A36.

### 7.3.2 Walkway Box Beams

Two longitudinal and two transverse specimens were machined from the web regions and one longitudinal specimen was machined from the flange region of each channel piece of each of the two box beam segments (9U, 8L) and the full-length box beam (9M) obtained from the walkway debris. The specific locations of the specimens in the box beams are shown in section A7.3.2 of the appendix. Specimen identification, specimen orientation, and the face of the box beam from which the specimen was machined are listed for each specimen in table 7.2.

Specimens were prepared in accordance with ASTM Standard E8-81 for rectangular tension specimens and have the same dimensions as the specimens prepared from the NBS channel. The web specimens were tested full thickness (0.147 to 0.189 in (3.73 to 4.80 mm)), whereas the flange specimens were machined to a uniform nominal thickness of 0.24 in (6.1 mm) to remove the taper. Operation of the LVDT extensometer and the machine crosshead speeds were as described in section 7.3.1.

The results are presented in table 7.3. Load-strain plots are presented in section A7.3.2 of the appendix. Representative load-strain curves are given in figures 7.5 - 7.7 for a longitudinal web specimen, a transverse web specimen, and a longitudinal flange specimen, respectively.

Neither the ultimate tensile strength nor the yield strength varied significantly between the beam segments. In addition, there was no discernable variation between longitudinal and transverse orientations in the web or between the web and flange regions. Ultimate tensile strength values ranged from 69,000 to 71,500 psi (476-493 MPa) with an average of 70,100 psi (484 MPa). Yield strength values ranged from 41,900 to 47,100 psi (289 to 325 MPa) with an average of 44,400 psi (306 MPa).

Average elongation for all tests was 32.3 percent, ranging from 27.6 to 38.0 percent. The average elongation for longitudinal specimens was about 10 percent greater than that for transverse specimens in the case of box beam 9U and about 18 percent greater in the case of box beam 8L. The difference in

average elongation between transverse and longitudinal specimens from beam 9M was less (about 4 percent).

The results from all tests fell well within the requirements of ASTM A36 as stated in section 7.3.1 of this report for tensile strength, yield strength and elongation. The results from these tests agree very well with the results from the NBS channel tests.

### 7.3.3 Walkway Hanger Rods

Two round test specimens were prepared from each of the two hanger rod segments obtained from the walkway debris. These specimens were machined in accordance with ASTM E8-81 for round tension specimens with a 5 in (127 mm) length,  $0.500 \pm 0.010$  in ( $12.70 \pm 0.25$  mm) reduced section diameter and a gage length of  $2.000 \pm 0.005$  in ( $50.80 \pm 0.13$  mm). The locations of the specimens from hanger rod segments NBS 5A and NBS 5B are shown in section A7.3.3 of the appendix. A representative specimen is shown in figure 7.1. The testing procedure was the same as that used for the NBS channel and the walkway box beam specimens. The results of these tests are given in table 7.4 and a representative load-strain plot for one of the specimens is shown in figure 7.8. Load-strain plots for all of the specimens are given in section A7.3.3 of the appendix.

The ultimate tensile strength ranged from 62,500 psi (431 MPa) to 69,000 psi (476 MPa), meeting the ASTM A36 requirement of strength specified as 58,000 psi (400 MPa) to 80,000 psi (552 MPa). The 0.2 percent offset tensile yield strength ranged from 35,900 psi (248 MPa) to 46,900 psi (324 MPa) with three of the four specimens giving values over the ASTM A36 specified minimum of 36,000 psi (248 MPa). The yield strength of the remaining specimen was within 100 psi (690 KPa) of the specified minimum and is considered to have met the criterion in view of the estimated  $\pm 360$  psi (2.48 MPa) measurement inaccuracy. Elongation values ranged from 36 to 42 percent, thereby conforming to the ASTM A36 specification of 21 percent minimum.

It is concluded that the tensile properties of the walkway hanger rod material satisfied the requirements of the ASTM A36 specification.

### 7.3.4 Walkway Box Beam Longitudinal Welds

Variation in the transverse strength of the walkway box beam longitudinal welds was determined by testing 1.0 in (25.4 mm) wide tensile coupons to failure. Weld caps were machined flush to simulate conditions near the beam ends. The results, summarized in table 7.5, show a substantial variation in breaking load among specimens taken from the same beam. The observed variability is not unusual for the type of weldment tested considering the small weldment area sampled by each specimen. Figure 7.9 shows the variability in the amount of weld metal from specimen to specimen at the fracture. This variability correlates reasonably well with the specimen breaking loads (table 7.5). Differences in the amount of porosity found on the fracture surfaces of the specimens also contribute to the ultimate strength variation.

## 7.4 METALLOGRAPHY AND HARDNESS MEASUREMENTS

This section summarizes the results of metallographic examination and hardness tests performed on box beam longitudinal welds, on walkway hanger rods and on washers used in the box beam-hanger rod connections. Details of these studies appear in section A7.4 of the appendix.

### 7.4.1 Box Beam Weldments

Metallographic and hardness studies were performed on cross sections taken from the longitudinal weld region of an NBS weldment and from walkway beams 9U, 8L and 9M. The regions examined included the channel flanges and portions of the channel web as well as the weld and heat-affected zone.

Figure 7.10 illustrates the appearance of an NBS weldment made by the GMAW process, while figures 7.11-7.13 illustrate the appearance of weld regions in box beams 9U, 8L and 9M, respectively. Basic walkway weldment hardnesses were normal. Maximum hardnesses were 92-95 Rockwell B (HRB) for the weld regions, 85-93 HRB for the heat-affected zones and 70-79 HRB for the unaffected parent metal. Small zones of increased hardness (28-33 HRC) were noted in the heat-affected zones of one section taken from location 9U and one section taken from location 8L. The structure of the hard zones appeared to be tempered martensite.

Walkway weldment microstructure was normal and comparable to the NBS weldment microstructure. The weld metal structure was primarily bainitic; the heat-affected zones contained ferrite primarily as a network in prior austenite grain boundaries plus bainite, partially spheroidized carbides and tempered martensite; while the base metal structure contained ferrite and pearlite in a normalized structure.

Figures 7.10 to 7.13 illustrate a substantial variability in the contour of the mating flange ends forming the faying surfaces for welding. The effect, coupled with differences in weld penetration, creates regions of varying notch acuity in the weld region. However, no cracks were observed to have initiated from such notches in any of the sections studied.

A series of optical and metallographic measurements of longitudinal weld penetration in the interiors of box beams 9U, 8L and 9M and at the ends of box beams at locations 8UE, 9UE, 9UW and 10UE are summarized in figure 7.14. The latter set was taken in the lower flange region between the beam end and the outer hanger rod hole following weldment fracture. From figure 7.14 the weld penetration data from the sectional specimens average about 2.2 mm. The data from the fracture surface at location 10UE average about 2.4 mm, while the average weld penetration at locations 8UE, 9UE, and 9UW is near 1.5 mm. All weld penetration data from fractures represent minimum values, considering that the surfaces examined represent final reductions in area at fracture.

It is known that the depth of weld penetration will be less at the beginning of a weld run than it is after steady welding conditions have been attained. Progressively increasing penetration from the beam ends toward the outer hanger

rod holes at locations 8UE, 9UE and 9UW (figure 7.14) suggests that a "run-on" tab was not used in walkway beam fabrication. Weld penetration at location 10UE suggests that this beam was cut to length after the welding operation. Evidence of such an operation was also noted at location 8UW during the site investigation (section 5.3.3).

Interior tack welds were present at the bottom flanges of all beam ends examined. The location of these welds relative to the beam ends and their approximate overall depth as measured from photographs of the fractures are shown in figure 7.15. Estimates were made of the total area of interior tack weld plus the longitudinal weld in the box beam length between the outer hanger rod hole and the box beam end. The data in table 7.6 were compiled by measuring the penetration depth of the longitudinal and tack welds along the fractures at 1 mm intervals on 10X photographic enlargements. Areas of both welds were calculated from the profiles. As illustrated by the sketch accompanying table 7.6, the total cross-sectional area ( $T \times B$ ) was taken as the projected area of the flange toes and the additional weld metal due to tack weld buildup beyond this area was not considered. Had this been considered, the percent weld area reported in table 7.6 would have been substantially increased.

In summary, typical box beam longitudinal weld penetration averages about 2.2 mm, approximately the depth from the flange surface to the point of tangency of the mating sides. At some beam ends, due probably to weld start-up, the depth of weld penetration is less than 2.2 mm. At these locations, however, there is always an interior tack weld present and the cross-sectional area produced by a combination of longitudinal plus interior tack weld areas exceeds the area achieved with only a longitudinal weld of penetration depth equal to 2.2 mm.

#### 7.4.2 Walkway Hanger Rods

Transverse and longitudinal sections removed from two walkway hanger rod segments (NBS 5A and 5B) were examined metallographically and were tested for hardness. The microstructure, consisting of ferrite and pearlite in a normalized condition, is considered typical of A36 structural steel. The microstructure in NBS 5B was slightly coarser (ASTM grain size 7.5-8) than in NBS 5A (ASTM grain size 9), but this variation is not significant. Hardness values were normal at 66-76 HRB.

#### 7.4.3 Washers

Metallographic and hardness studies on washers from the walkway and washers used in NBS tests proceeded in two stages. The initial effort was a general characterization of the walkway washers associated with the initial components of the debris removed for analysis. These were identified as the upper washer from the fourth floor to ceiling hanger rod at location 8UE, the lower washer from location 8LW, and the two lower washers from box beam 9M. Two washers from the NBS tests, one hardened and one unhardened, were included in this initial study. Additional hardness tests were conducted on (1) three walkway washers obtained as a result of a petition for access to additional debris material, (2) a walkway washer identified as 9MW that had been used in an NBS test on

box beam 9M and had fractured during the test, and (3) three additional NBS hardened washers. Results of the hardness tests, summarized in table 7.7, confirmed that hardened washers had been used in the walkway construction.

Core hardness (obtained after removal of the soft decarburized layer) was also measured on selected specimens and the data are included in table 7.7. The data in table 7.7 indicate that the walkway washers were, on the average, slightly harder than the NBS washers; walkway washer average was 41.6 HRC with a range of 34.5-45.0 HRC and NBS washer average was 39.1 HRC with a range of 36.0-41.9 HRC. Little difference was noted between surface and core hardness.

Photomicrographs of the fractured washer (9MW) and of the NBS hardened washer in figure 7.16 show a tempered martensite interior and a thin decarburized layer on the surface. This is typical for hardened washers.

## 7.5 CHEMICAL ANALYSIS

Chemical analysis was performed on the base metal and on longitudinal welds of box beams from the walkway and from box beams fabricated by NBS. An interior tack weld from the walkway and specimens removed from the walkway hanger rods were also analyzed. Details of the locations analyzed and of analytical procedures used are given in section A7.5 of the appendix.

Table 7.8 shows that the NBS and walkway structural channel and the walkway hanger rod compositions are within the specifications of ASTM A36 for structural steel.

Table 7.9 compares the chemical composition of weld metal in NBS box beam longitudinal welds made with various processes with the composition determined for the walkway box beam longitudinal welds from 9U, 8L and 9M and the interior tack weld from location 8LW. NBS welding procedures have been discussed in section 6.10.2.

Similarity in composition between the walkway longitudinal and interior tack welds suggests they were made by the same welding process. Similarity of composition between the walkway welds and the NBS weld made with the flux-cored electrode suggests this process was used in welding the walkway box beams. The evidence is not conclusive, however, because solid welding wire giving the same chemical composition is available. The lower manganese and silicon contents determined for weld metal deposited with the E7018 and E7014 stick electrodes as compared to that of the walkway welds indicate that these electrodes were not used in the fabrication of the walkway box beams.

## 7.6 PROPERTIES OF CONCRETE

Laboratory tests were carried out on the 19 cores removed from the concrete decks to determine modulus of elasticity, compressive strength and bulk specific gravity. The bulk specific gravity of the topping material recovered with the cores was also determined. Prior to conducting these tests, each core was photographed, weighed, and measured. In most cases the topping material had separated from the main body of the core during the coring operation. In those

few cases where it remained attached, the topping was removed and the weight and length measurements were repeated. After noting its general condition and subjectively classifying its quality based upon surface smoothness, distribution of aggregate, and flatness of ends, each core was closely examined for the presence of surface cracks or wire reinforcement. Results of this examination are summarized in table 7.10.

Bulk specific gravity of the concrete and of the topping material was determined for two conditions: (1) air dry as received from the warehouse and (2) after oven drying for 24 hours. Sample preparation and weighing were carried out in accordance with the provisions of ASTM C642-75 (Standard Test Method for Specific Gravity, Absorption, and Voids in Hardened Concrete) [7.1] except for the determination of saturated weight after boiling.

A total of nine cores was used to determine modulus of elasticity and compressive strength. Each core was instrumented with two resistance strain gages oriented in the lengthwise direction and positioned 180 degrees apart. Gage length was 2 in (51 mm) and the gages were operated in a full-bridge configuration. The cores were capped and tested in accordance with ASTM C617-76 (Standard Method for Capping Cylindrical Concrete Specimens), C469-79 (Standard Test Method for Static Modulus of Elasticity and Poisson's Ratio for Concrete in Compression) and C39-72 (Standard Test Method for Compressive Strength of Cylindrical Concrete Specimens) [7.1].

Table 7.11 lists the unit weights, the modulus of elasticity (E) and the compressive strength ( $f'_c$ ) for the various cores tested. The unit weights for the concrete in the air dry condition are very consistent with an average of 113.5 pcf (1,820 kg/m<sup>3</sup>) and a range of 109.0 to 118.4 pcf (1,750 to 1,900 kg/m<sup>3</sup>), based on results from 10 cores. For the oven dry condition the average was 108.1 pcf (1,730 kg/m<sup>3</sup>) and the range was 104.0 to 112.1 (1,670 to 1,800 kg/m<sup>3</sup>). The variation in unit weights obtained for the topping material is greater. For the air dry condition the average of eight specimens was 116.8 pcf (1,870 kg/m<sup>3</sup>) and the range was 101.5 to 135.2 pcf (1,630 to 2,170 kg/m<sup>3</sup>). For the oven dry conditions the average was 113.7 pcf (1,820 kg/m<sup>3</sup>) and the range was 99.1 to 133.9 pcf (1,590 to 2,150 kg/m<sup>3</sup>).

Based on nine cores tested, the modulus of elasticity (secant modulus at 40 percent of compressive strength) averaged  $1.86 \times 10^6$  psi ( $12.8 \times 10^3$  MPa) and ranged from  $1.75$  to  $2.08 \times 10^6$  psi ( $12.1$  to  $14.4 \times 10^3$  MPa). The average compressive strength based on these same nine cores and corrected for core aspect ratio was 5,030 psi (34.7 MPa) and ranged from 4,440 to 5,520 psi (30.6 to 38.1 MPa). Measurements upon which the values listed in table 7.11 are based can be found in section A7.6 of the appendix.

The average unit weight for concrete of 113.5 pcf (1,820 kg/m<sup>3</sup>) compares with a nominal value of 110 pcf (1,760 kg/m<sup>3</sup>) for lightweight concrete. The average compressive strength of 5,030 psi (34.7 MPa) is well above the 3000 psi (20.2 MPa) minimum for lightweight concrete fill on metal deck indicated in the General Notes (Dwg. S601). There are no specific requirements stated for modulus of elasticity.

## 7.7 CONCLUSIONS

The following conclusions are made subject to limitations of the materials evaluated and the test variables selected:

1. Quality of the box beam longitudinal welds conformed to the visual inspection requirements of AWS D1.1-79 Structural Welding Code-Steel.
2. There were no significant differences in tensile properties and chemical compositions between NBS and walkway box beam channel material.
3. Tensile properties and chemical compositions of NBS channels, walkway box beam channels and hanger rod materials satisfy the requirements of ASTM Standard A36 for structural steel.
4. Microstructure and hardness of the NBS channels, walkway box beam channels and hanger rod materials were normal. Differences were noted in grain size and in apparent pearlite-to-ferrite ratio in the two hanger rods examined; however, the differences are not considered to be significant.
5. Microstructure and hardness of longitudinal and interior walkway box beam welds were normal.
6. Longitudinal weld penetration in the box beam interior averaged about 2.2 mm, approximating the distance from the point of tangency of the mating flange surfaces to the outside face of the channel flanges. Some lesser penetration was noted near the beam ends in regions reinforced with interior tack welds; however, the presence of interior tack welds considerably increased the total weldment cross-sectional area at these locations.
7. Hardened washers had been installed in the walkway. The hardness of these washers was slightly higher than that of hardened washers used in the NBS test series.
8. Compressive strength of lightweight concrete used in the walkway decks exceeded the requirement of the project design criteria.

Table 7.1 Tensile Test Results - NBS Channel

<u>Specimen</u>	<u>Specimen Location</u>	<u>Specimen Orientation</u>	<u>Ultimate Tensile Strength, psi(a)</u>	<u>Yield Strength 0.2% Offset, psi(b)</u>	<u>Elongation, %(c)</u>	<u>Reduction of Area, %(d)</u>
A. Code B Channel						
BL1	web	long.	71,000	44,700	35.0	56
BL2	"	"	71,000	45,200	35.0	56
BL3	"	"	70,500	44,000	36.8	56
BT1	web	transverse	71,000	45,200	31.6	54
BT2	"	"	71,000	45,500	35.6	55
BT3	"	"	71,000	45,000	34.0	51
BF1	flange	long.	71,000	43,700	33.0	58
BF2	"	"	71,000	45,200	33.2	58
B. Code Y Channel						
YL1	web	long.	70,500	44,700	34.2	55
YL2	"	"	71,000	44,700	33.2	55
YT1	web	transverse	71,000	45,100	30.4	51
YT2	"	"	71,500	44,900	32.6	50
YF1	flange	long.	71,000	44,200	33.0	58
YF2	"	"	71,000	44,200	31.6	57

(a) Rounded to nearest 500 psi in accordance with ASTM Standard E8-81.

(b) Rounded to nearest 100 psi in accordance with ASTM Standard E8-81.

(c) Rounded to nearest 0.2 percent in accordance with ASTM Standard E8-81.

(d) Rounded to nearest 1.0 percent.

1000 psi = 6.9 MPa

Table 7.2 Walkway Box Beam Tensile Specimen Identification

<u>Specimen Code</u>	<u>Specimen Orientation</u>	<u>Location</u>	
A. Box Beam 9U (NBS 1)			
1-LS1	longitudinal	web	south face
1-LS2	"	"	south face
1-LN1	"	"	north face
1-LN2	"	"	north face
1-TS1	transverse	web	south face
1-TS2	"	"	south face
1-TN1	"	"	north face
1-TN2	"	"	north face
1-TFS	longitudinal	flange	top south
1-TFN	"	"	top north
B. Box Beam 8L (NBS 2)			
2-LS1	longitudinal	web	south face
2-LS2	"	"	south face
2-LN1	"	"	north face
2-LN2	"	"	north face
2-TS1	transverse	web	south face
2-TS2	"	"	south face
2-TN1	"	"	north face
2-TN2	"	"	north face
2-TFS	longitudinal	flange	top south
2-TFN	"	"	top north
C. Box Beam 9M (NBS 3)			
3-LS1	longitudinal	web	south face
3-LS2	"	"	south face
3-LN1	"	"	north face
3-LN2	"	"	north face
3-TS1	transverse	web	south face
3-TS2	"	"	south face
3-TN1	"	"	north face
3-TN2	"	"	north face
3-TFS	longitudinal	flange	top south
3-TFN	"	"	top north

Table 7.3 Tensile Test Results - Walkway Box Beam Channel

<u>Specimen</u>	<u>Ultimate Tensile Strength, psi<sup>(a)</sup></u>	<u>Yield Strength 0.2% Offset, psi<sup>(b)</sup></u>	<u>Elongation, %<sup>(c)</sup></u>	<u>Reduction of Area, %<sup>(d)</sup></u>
A. Box Beam 9U (NBS 1)				
1-LS1	69,000	44,200	36.0	56
1-LS2	70,000	43,700	32.6	55
1-LN1	70,000	44,400	32.4	54
1-LN2	71,000	45,300	33.4	54
1-TS1	69,000	44,600	31.0	47
1-TS2	69,500	45,800	30.4	48
1-TN1	71,000	47,100	29.6	48
1-TN2	71,000	44,700	33.8	47
1-TFS	69,500	43,400	36.6	57
1-TFN	70,000	43,200	35.2	61
B. Box Beam 8L (NBS 2)				
2-LS1	71,000	45,900	28.4	54
2-LS2	69,500	43,700	33.0	53
2-LN1	71,000	46,800	33.6	54
2-LN2	70,500	44,300	34.8	56
2-TS1	71,500	45,600	29.6	48
2-TS2	70,500	45,200	27.6	46
2-TN1	71,000	44,500	29.8	48
2-TN2	71,000	46,000	29.0	48
2-TFS	70,000	45,400	38.0	59
2-TFN	70,000	43,200	37.0	60
C. Box Beam 9M (NBS 3)				
3-LS1	70,000	43,200	31.4	54
3-LS2	70,000	44,400	31.4	54
3-LN1	69,500	43,000	30.8	54
3-LN2	69,500	44,600	33.0	54
3-TS1	70,000	44,300	31.6	51
3-TS2	70,000	44,100	30.2	51
3-TN1	69,000	43,500	31.6	50
3-TN2	69,000	41,900	30.6	51
3-TFS	70,500	42,400	33.8	58
3-TFN	69,500	43,500	33.4	61

(a) Rounded to nearest 500 psi in accordance with ASTM Standard E8-81.

(b) Rounded to nearest 100 psi in accordance with ASTM Standard E8-81.

(c) Rounded to nearest 0.2 percent in accordance with ASTM Standard E8-81.

(d) Rounded to nearest 1.0 percent.

1000 psi = 6.9 MPa

Table 7.4 Results of Tensile Tests on Walkway Hanger Rods

<u>Hanger Rod</u>	<u>Specimen</u>	<u>Ultimate Tensile (a) Strength, psi</u>	<u>Yield Strength (b) 0.2% Offset, psi</u>	<u>Elongation, %(c)</u>	<u>Reduction of (d) Area %</u>
NBS 5A	5AT1	69,000	44,700	36.6	62
	5AT2	65,500	46,900	36.4	63
NBS 5B	5BT1	62,500	35,900	40.8	67
	5BT2	68,500	42,900	41.6	67

- (a) Rounded to nearest 500 psi in accordance with ASTM Standard E8-81.
- (b) Rounded to nearest 100 psi in accordance with ASTM Standard E8-81.
- (c) Rounded to nearest 0.2% in accordance with ASTM Standard E8-81.
- (d) Rounded to nearest 1.0%.

1000 psi = 6.9 MPa

Table 7.5 Results of Tensile Tests on Walkway Box Beam Weldments

Box Beam	Specimen	Maximum Load (lbs)
9U	1BX3W2	6740
	1BX3W4	5890
8L	2BX3W2	4790
	2BX3W4	2200
9M	3BW1	3920
	3BW4	5100

1000 lbs = 4.448 kN

Table 7.6 Percent of Longitudinal Box Beam Weld Plus Interior Tack Weld Area as a Function of Total Cross Sectional Area for Walkway Beam Weldments

Beam End to Outer Hanger Rod Hole

<u>Location</u>	<u>Percent Weld Area</u>
8UE	63
9UE	55
9UW	58
10UE	92
Penetration to 2.2 mm	48

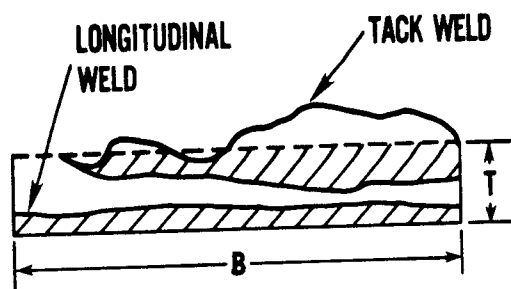


Table 7.7 Results of Washer Hardness Tests

<u>Washer Identification</u>	<u>Number of Measurements</u>	<u>Hardness</u>			
		<u>HRC (surface)</u>		<u>HRC (core)</u>	
		<u>Average</u>	<u>Range</u>	<u>Average</u>	<u>Range</u>
8UE Top	8	40.2	39.0-41.0		
8LW Top	8	43.0	40.0-45.0		
9ME Top	8	37.5	34.5-40.5		
9MW Top	8	44.0	42.5-45.0		
8MW	5/5*	40.0	39.0-41.0	40.3	39.7-40.7
9UE	5/5	43.6	42.5-45.0	43.3	40.7-44.2
10MW	5/5	40.2	39.0-41.5	42.7	42.7
NBS Hardened (1)	5	39.6	38.5-41.9		
NBS hardened (2)	4/5	39.0	38.5-39.5	39.8	37.7-40.7
NBS hardened (3)	5/5	37.5	36.0-38.5	39.2	37.7-39.7
NBS hardened (4)	4/5	40.5	40.0-41.0	41.9	41.7-42.2
NBS Regular Grade	5	[60.7]** [58.9-61.3]**			

\* surface/core

\*\* Rockwell Hardness B (HRB)

Microhardness Survey

<u>Washer Identification</u>	<u>Average HK500(HRC)</u>	<u>Range HK500(HRC)</u>
8MW	456 (44.3)	395-476 (39.5-45.5)
9UE	516 (48.4)	485-532 (46.5-49.5)
10MW	456 (44.5)	450-457 (44.0-44.5)
NBS hardened (1)	457 (44.5)	---
NBS hardened (2)	444 (43.5)	---
NBS hardened (3)	442 (43.1)	323-465 (32.0-45.0)

Table 7.8 Chemical Composition Range of Base Materials

Percent by Weight\*

<u>Element</u>	<u>NBS Box<sup>(a)</sup> Beam Channel</u>	<u>Walkway Box<sup>(b)</sup> Beam Channel</u>	<u>Walkway<sup>(c)</sup> Hanger Rod</u>	<u>ASTM A36 Specification</u>
Carbon	0.179 - 0.183	0.181 - 0.188	0.159 - 0.200	Max 0.26
Phosphorus	0.012 - 0.013	0.016 - 0.017	0.009 - 0.038	Max 0.04
Sulfur	0.022 - 0.023	0.016 - 0.017	0.033 - 0.046	Max 0.05

## Notes:

(a) Eight channels, two analyses per channel.

(b) Six channels, two or three analyses per channel.

(c) Two rods, one or two analyses per rod.

\* Encompasses specimens 1BX4, 2BX1, 3BX1 and 2TFX4 (cf, table A7.5-1).

Table 7.9 Chemical Composition Range of Weld Metal

Percent by Weight

Element	NBS(a)					Walkway(b) Longitudinal	Walkway(c) Interior Tack
	SMA (E7018)	SMA (E7014)	Mild Steel	Flux Core			
Carbon	0.093 - 0.097	0.117 - 0.119	0.123	0.123 - 0.124		0.117 - 0.140	0.091 - 0.095
Phosphorus	0.009 - 0.011	0.014	0.010 - 0.011	0.008		0.011 - 0.013	0.012 - 0.013
Sulfur	0.022	0.023	0.023	0.021		0.017 - 0.021	0.018
Manganese	0.588 - 0.615	0.786 - 0.810	0.590 - 0.647	1.109 - 1.178		0.946 - 1.143	1.086 - 1.096
Silicon	0.249 - 0.266	0.270 - 0.272	0.193 - 0.210	0.437 - 0.450		0.370 - 0.480	0.442 - 0.452

(a) One weld, two analyses.

(b) Four welds, two analyses per weld.

(c) One weld, two analyses.

Table 7.10 Condition of Concrete Cores Prior to Testing

Core Number	Span Number	General Condition				Poor or Damaged		Visible Cracks		Wire Reinforcement	
		Excellent	Good	Fair	Poor or Damaged	Yes	No	Yes	No		
4-01	U10-11	X									X
02	"				X			X			X
03	"		X								
04	"				X			X			
05	U9-10	X									X
06	"		X								
07	"	X									
08	L10-11										X
09	"					X					X
10	"										X
11	L9-10		X							X	X
12	"					X					
13	"		X								
14	M8-9		X								X
15	"		X								X
16	"		X								X
17	M9-10		X								X
18	"	X									X
19	"	X									X

Table 7.11 Properties of Concrete Cores

Core Number	Thickness (in)		Unit Weight (pcf)				E (a) (psi)	$f'_c$ (b) (psi)
			Concrete		Topping			
	Concrete	Topping	Air Dry	Oven Dry	Air Dry	Oven Dry		
4-01	3.55	0.35	---	---	---	--	$2.08 \times 10^6$	5,450
02	--	0.60	114.0	109.0	128.3	125.8	--	---
03	3.43	0.53	113.4	107.8	127.8	125.8	--	---
04	3.44	0.44	114.6	109.0	101.5	100.9	--	---
05	3.38	0.67	---	----	---	---	1.78	4,940
06	3.43	0.53	114.0	109.6	128.3	122.7	--	---
07	3.43	0.68	---	---	---	---	1.96	5,110
08	3.25	--	118.4	112.1	---	---	--	---
09	3.16	--	114.6	109.0	---	---	--	---
10	3.18	--	---	---	---	---	1.88	5,140
11	3.24	0.38	110.9	105.9	135.2	133.9	--	---
12	3.35	0.41	---	---	---	---	1.81	4,790
13	3.45	0.38	---	---	---	---	1.75	4,440
14	3.08	0.58	109.0	104.0	104.0	99.7	--	---
15	2.92	0.73	113.4	107.8	103.4	99.1	--	---
16	2.91	0.68	---	---	---	---	1.75	4,550
17	3.59	0.72	112.8	107.2	105.9	101.5	--	---
18	3.45	0.84	---	---	---	---	1.90	5,520
19	3.47	0.78	---	---	---	---	1.80	5,290

(a) Secant modulus at 40 percent of  $f'_c$

(b) Reduced to nearest 10 psi in accordance with ANSI/ASTM Standard C 42-74.

1 in = 25.4 mm

1 pcf = 16.02 kg/m<sup>3</sup>

1000 psi = 6.9 MPa

Date	Thickness (in)		Gage length (in)		Yield strength (ksi)	Tensile strength (ksi)
	Original	Final	Original	Final		
4-01	0.25	0.25	2.00	2.00	2.00	2.40
02	0.40	0.40	1.80	1.80	1.80	2.20
03	0.40	0.40	1.80	1.80	1.80	2.20
04	0.40	0.40	1.80	1.80	1.80	2.20
05	0.40	0.40	1.80	1.80	1.80	2.20
06	0.40	0.40	1.80	1.80	1.80	2.20
07	0.40	0.40	1.80	1.80	1.80	2.20
08	0.40	0.40	1.80	1.80	1.80	2.20
09	0.40	0.40	1.80	1.80	1.80	2.20
10	0.40	0.40	1.80	1.80	1.80	2.20
11	0.40	0.40	1.80	1.80	1.80	2.20
12	0.40	0.40	1.80	1.80	1.80	2.20
13	0.40	0.40	1.80	1.80	1.80	2.20
14	0.40	0.40	1.80	1.80	1.80	2.20
15	0.40	0.40	1.80	1.80	1.80	2.20
16	0.40	0.40	1.80	1.80	1.80	2.20
17	0.40	0.40	1.80	1.80	1.80	2.20
18	0.40	0.40	1.80	1.80	1.80	2.20
19	0.40	0.40	1.80	1.80	1.80	2.20
20	0.40	0.40	1.80	1.80	1.80	2.20

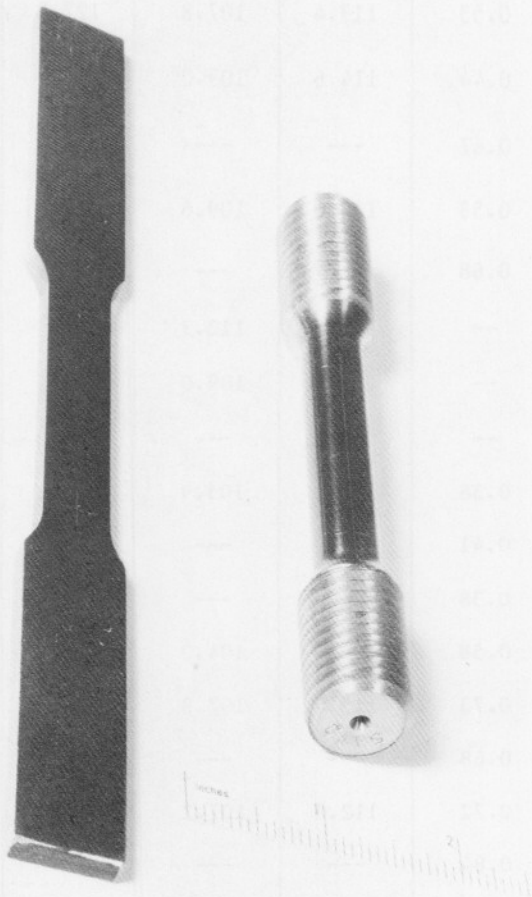


Figure 7.1 ASTM E8-81 tension test specimens. The rectangular specimen on the left was obtained from channel material and the round specimen on the right was obtained from hanger rod material.

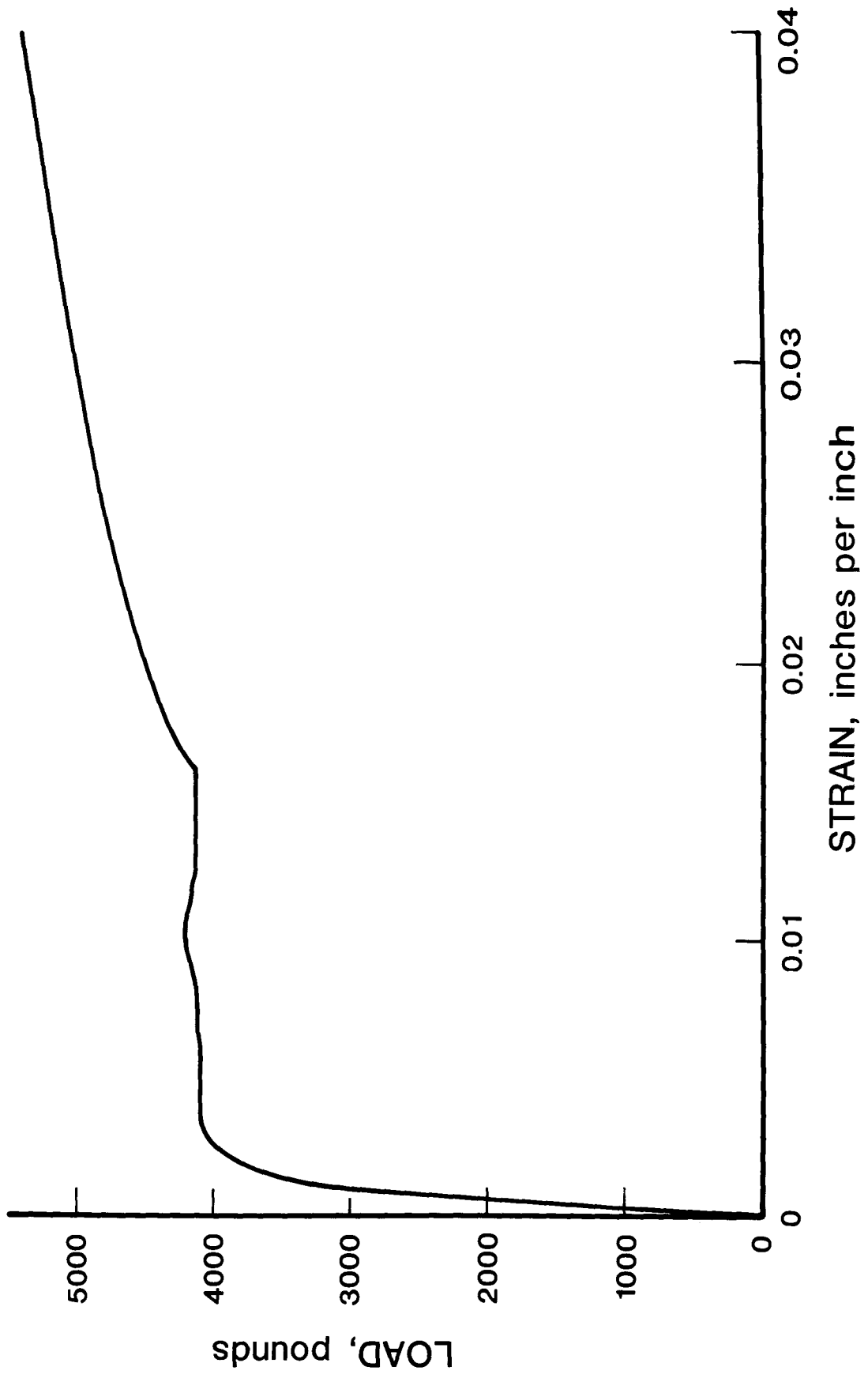


Figure 7.2 Representative load-strain plot for NBS channel. Longitudinal web specimen YL1.

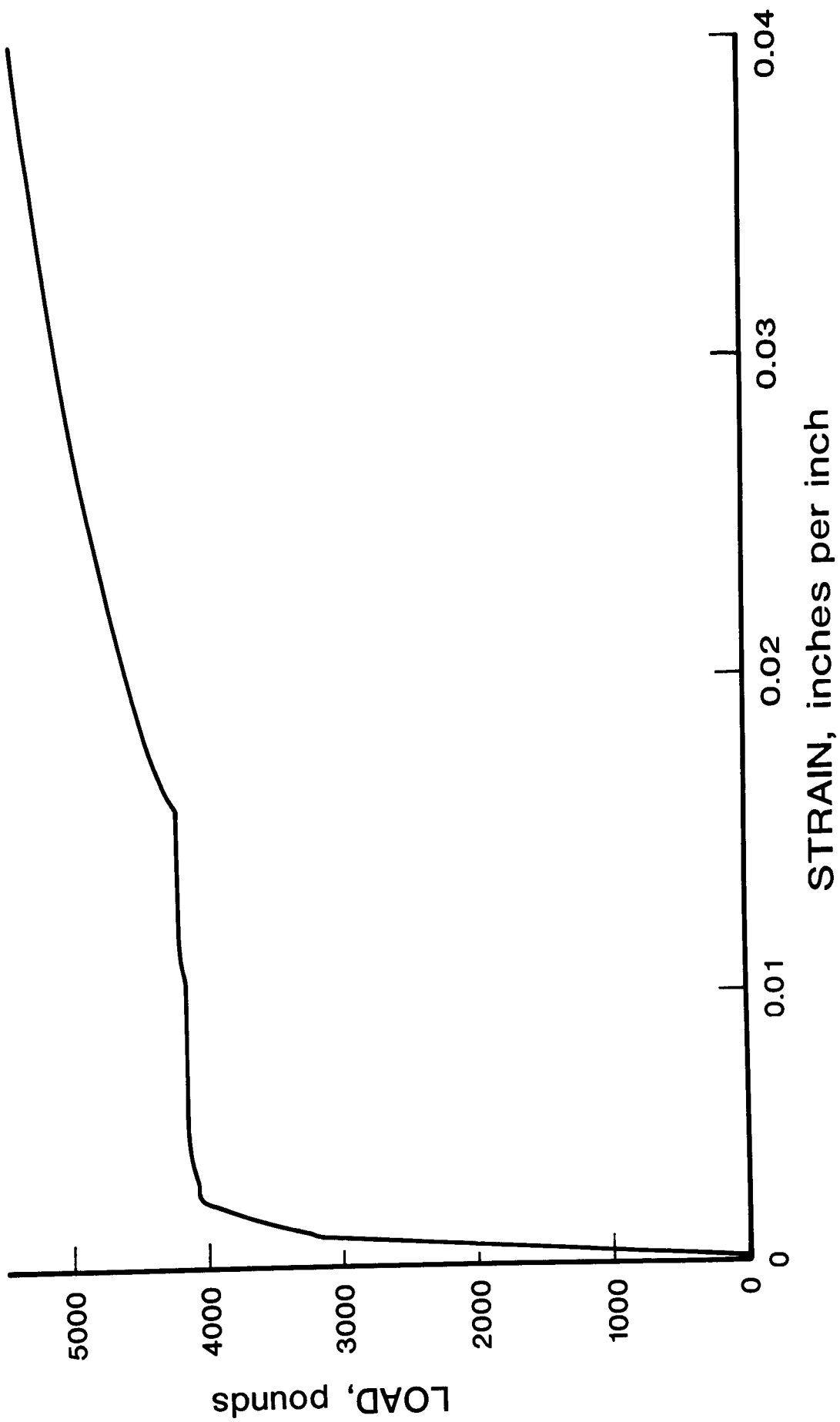


Figure 7.3 Representative load-strain plot for NBS channel. Transverse web specimen YT2.

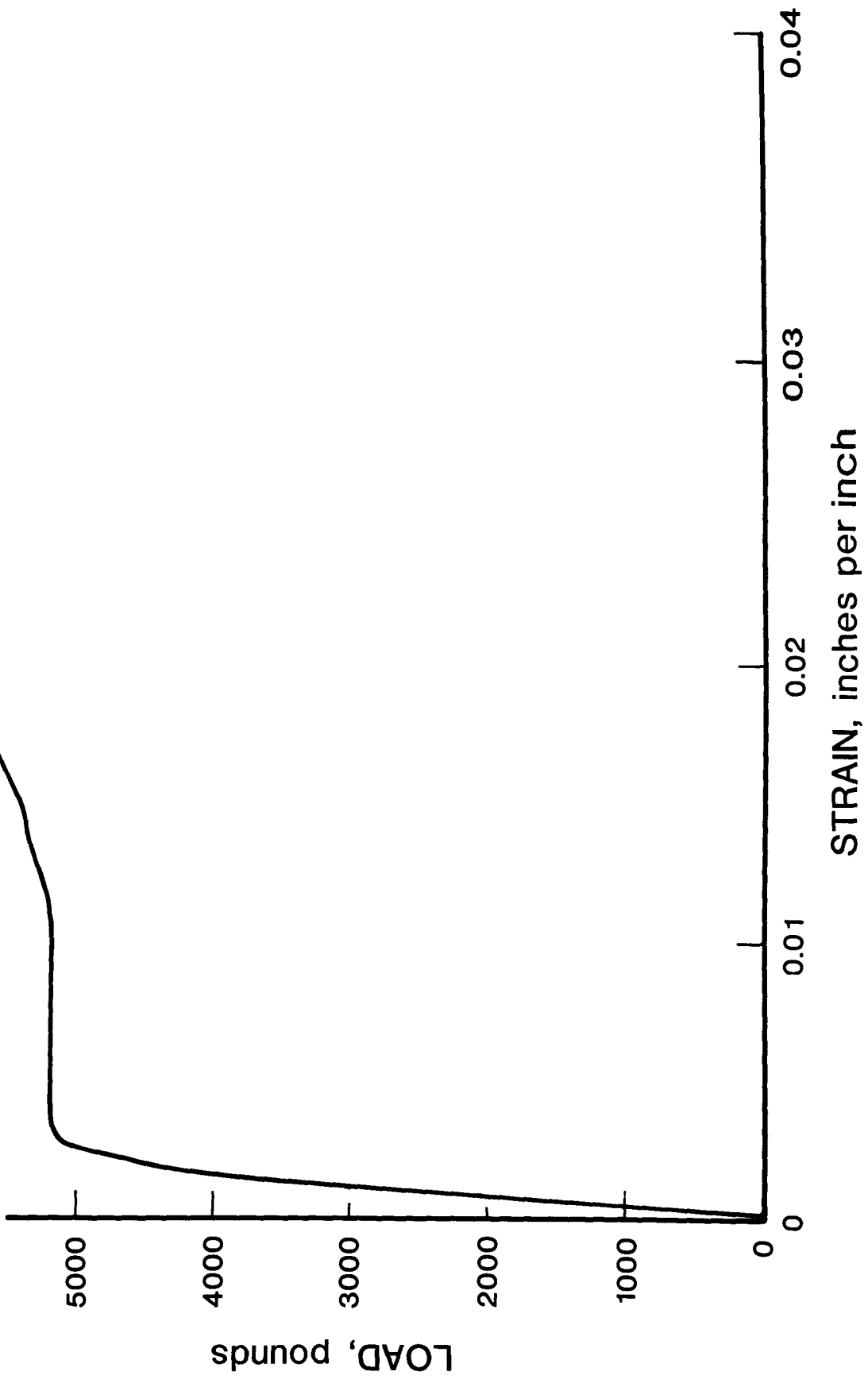


Figure 7.4 Representative load-strain plot for NBS channel. Longitudinal flange specimen BFl.

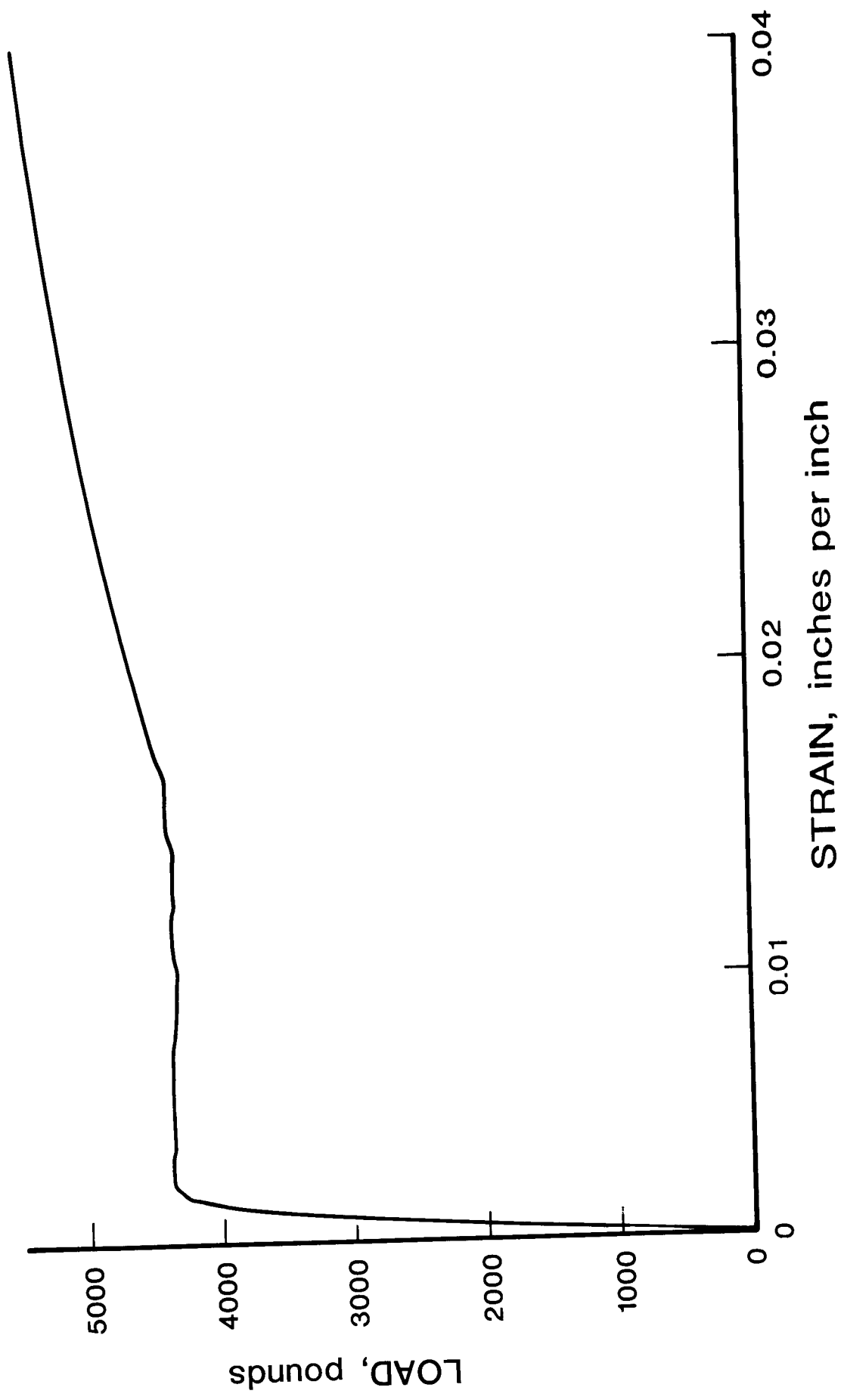


Figure 7.5 Representative load-strain plot for walkway box beam 8L.  
 Longitudinal web specimen 2-LN1.

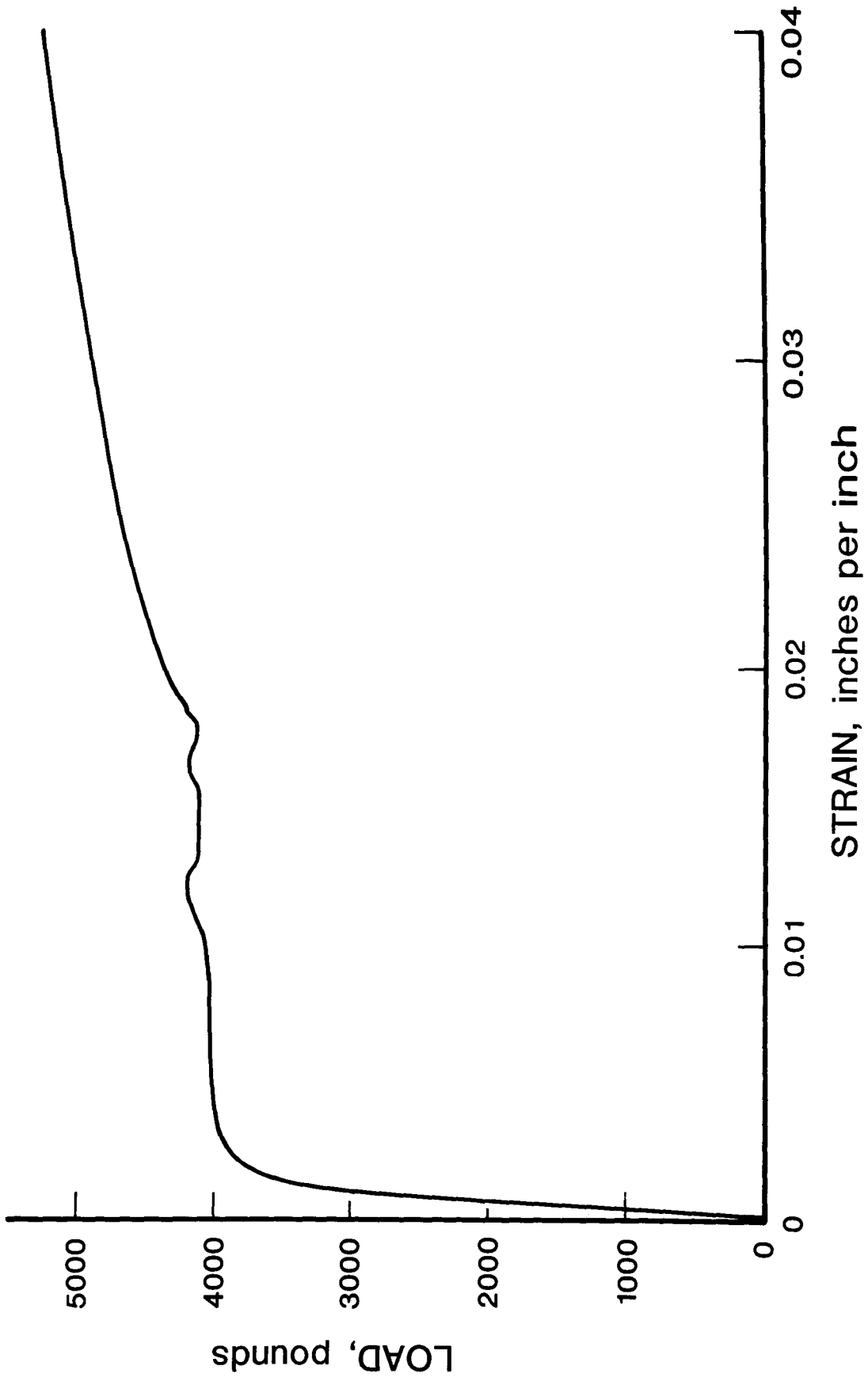
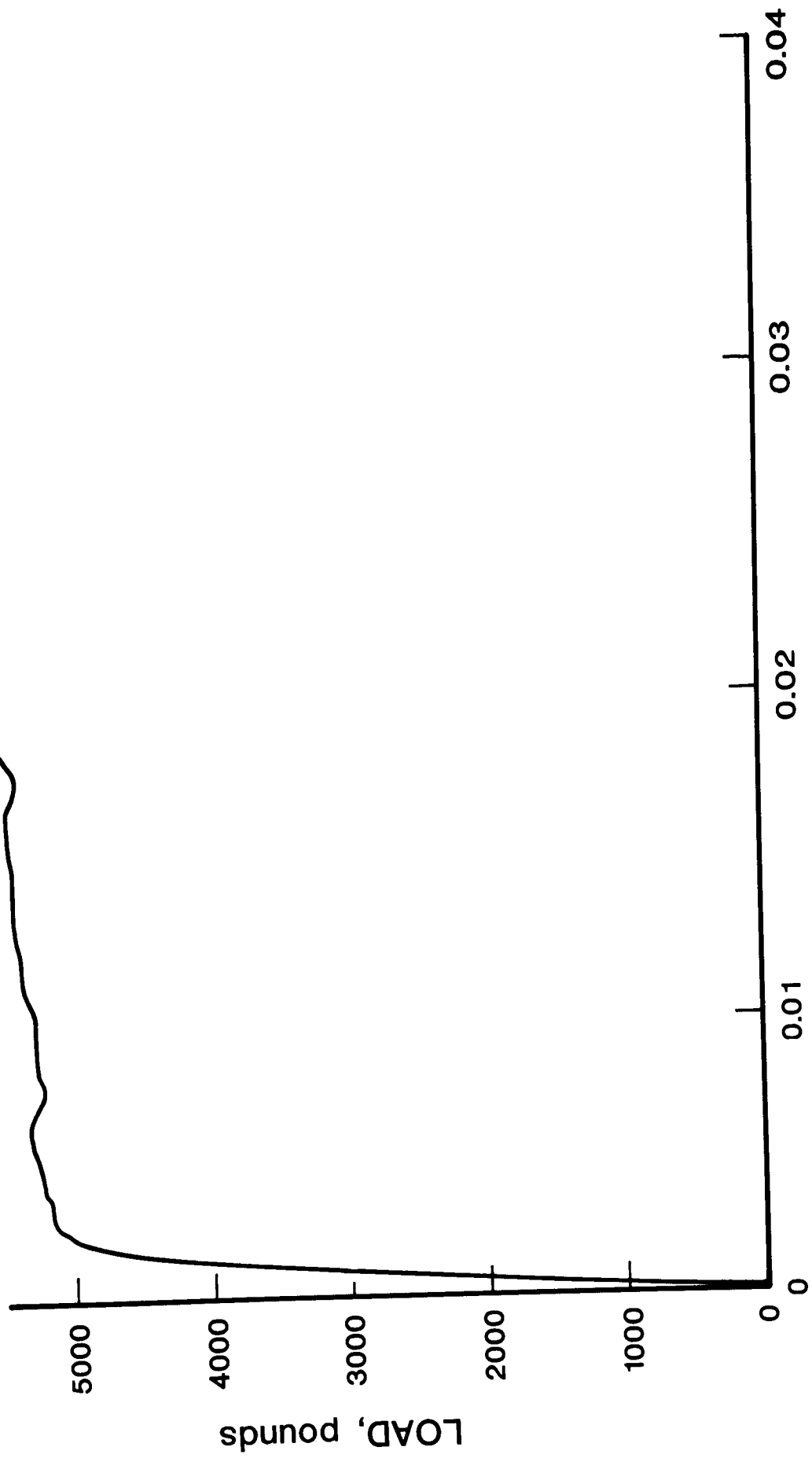


Figure 7.6 Representative load-strain plot for walkway box beam 9M.  
Transverse web specimen 3-TN1.



STRAIN, inches per inch

Figure 7.7 Representative load-strain plot for walkway box beam 9U.  
Longitudinal flange specimen 1-TFN.

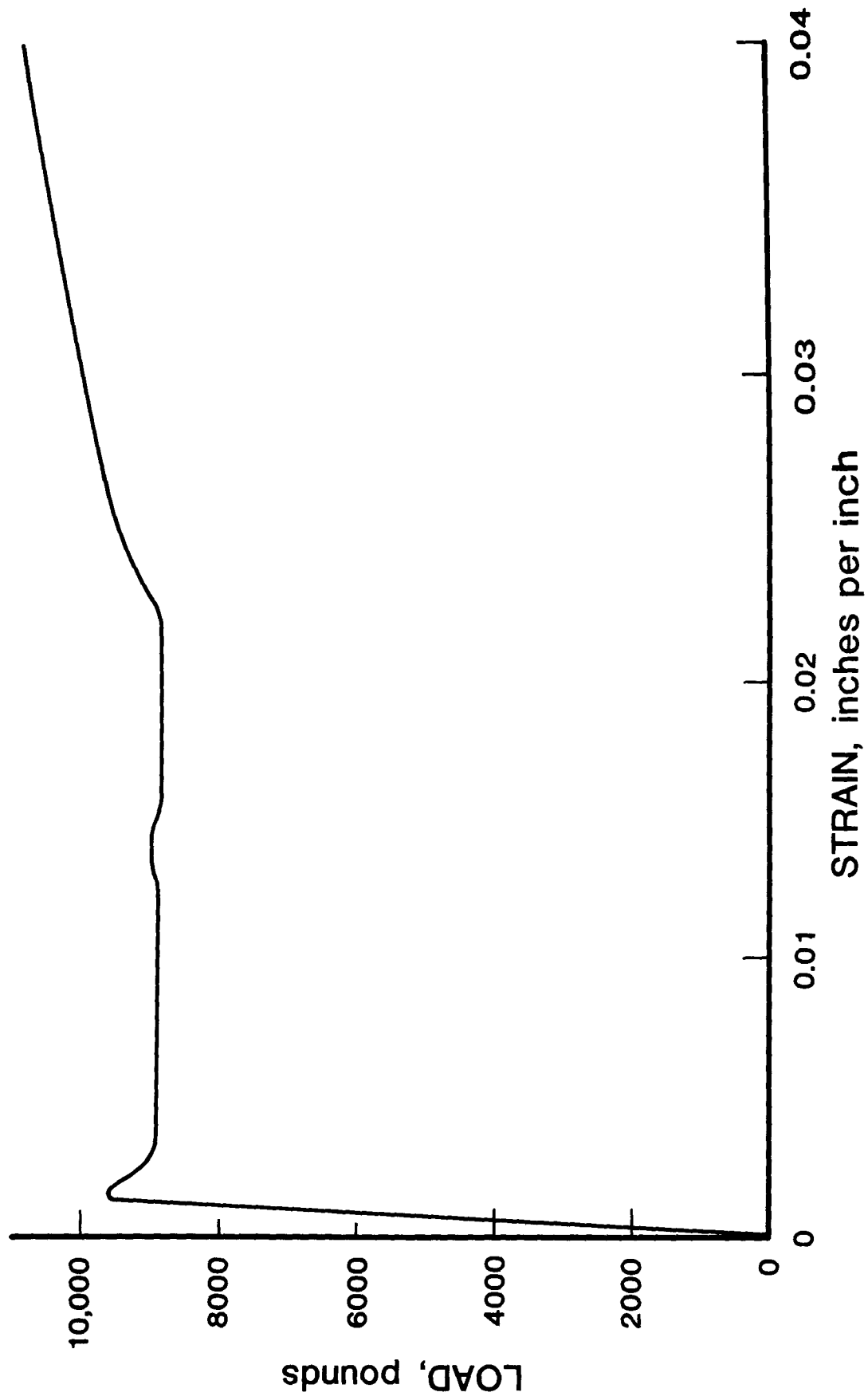


Figure 7.8 Representative load-strain plot for walkway hanger rod specimen 5AT1.

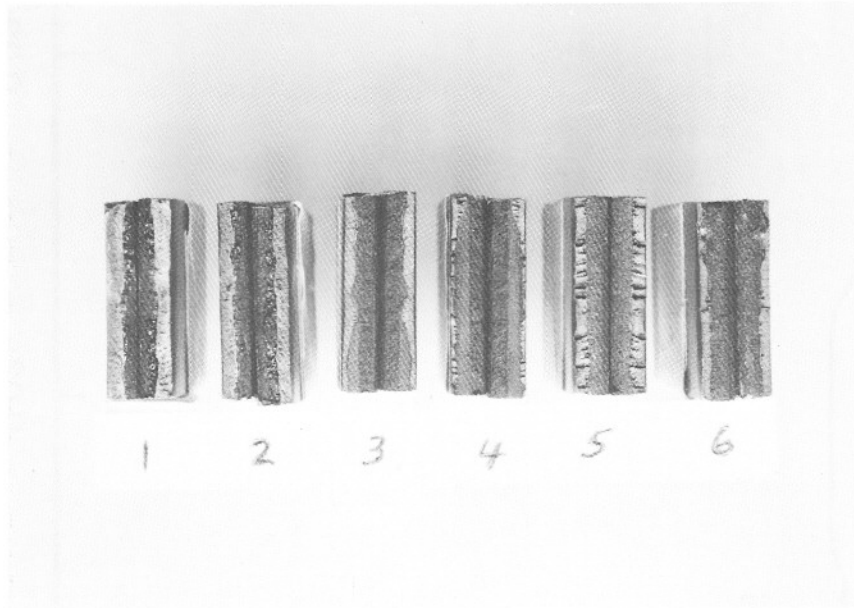
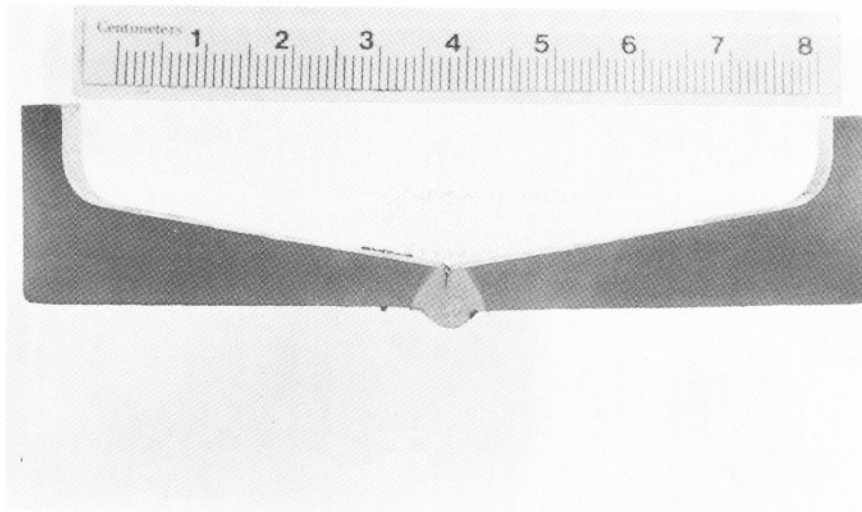
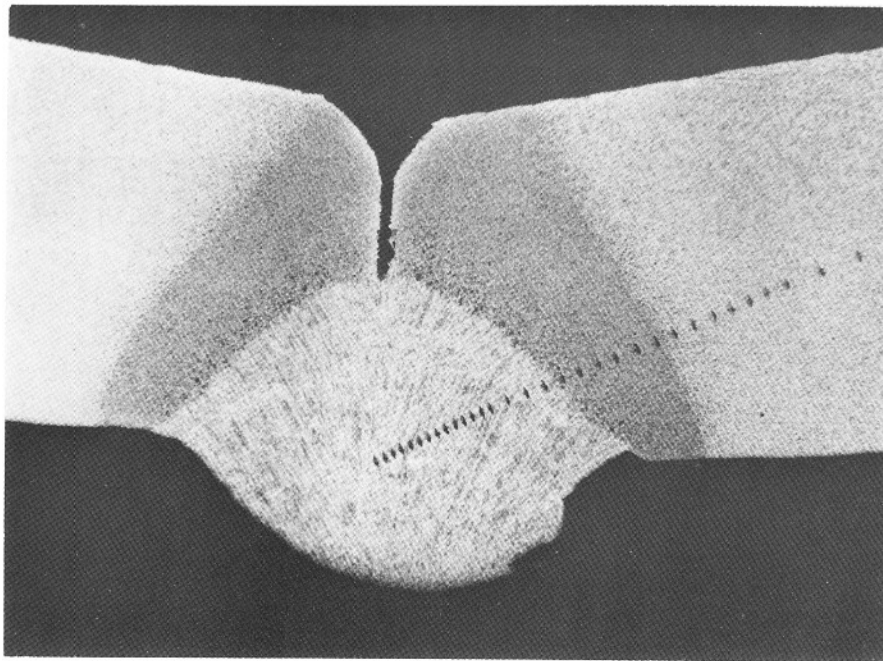


Figure 7.9 Fracture surfaces of walkway weldment tensile specimens. Both halves of each fracture are shown. The bright regions represent fracture and indicate the depth of weld penetration. Specimen key is as follows. X1

1. 1BX3W2
2. 1BX3W4
3. 2BX3W2
4. 2BX3W4
5. 3BW4
6. 3BW1



a



b

Figure 7.10 Transverse section through NBS weldment IC welded by the GMAW process. Dark regions separating weld metal from flange base metal are heat-affected portions of base metal. Aligned indentations are microhardness measurements. a, X1; b, X8 1/2

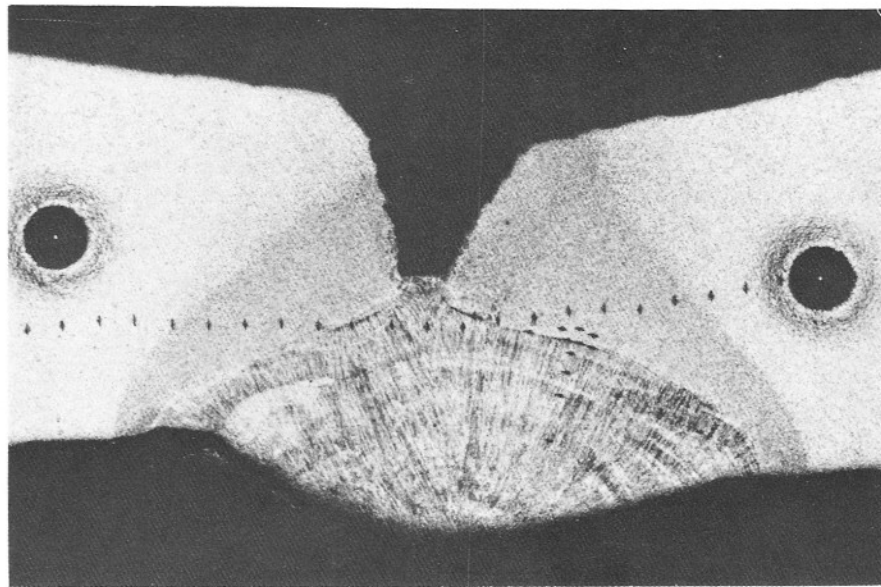
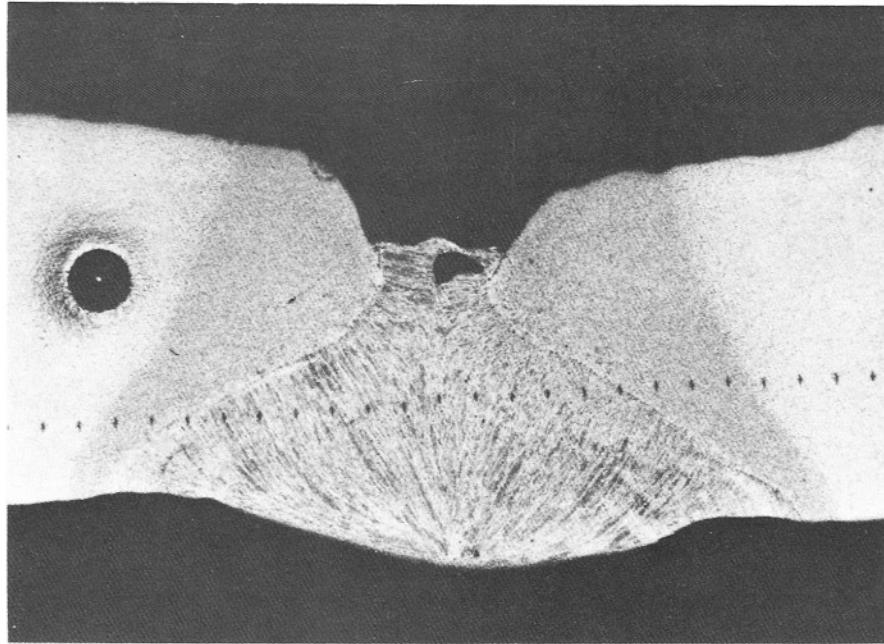


Figure 7.11 Cross sections through weld regions of box beam 9U (NBS 1). Sections were separated about 7 in (180 mm) along the beam length. Microhardness indentations traverse the surfaces. X 8 1/2

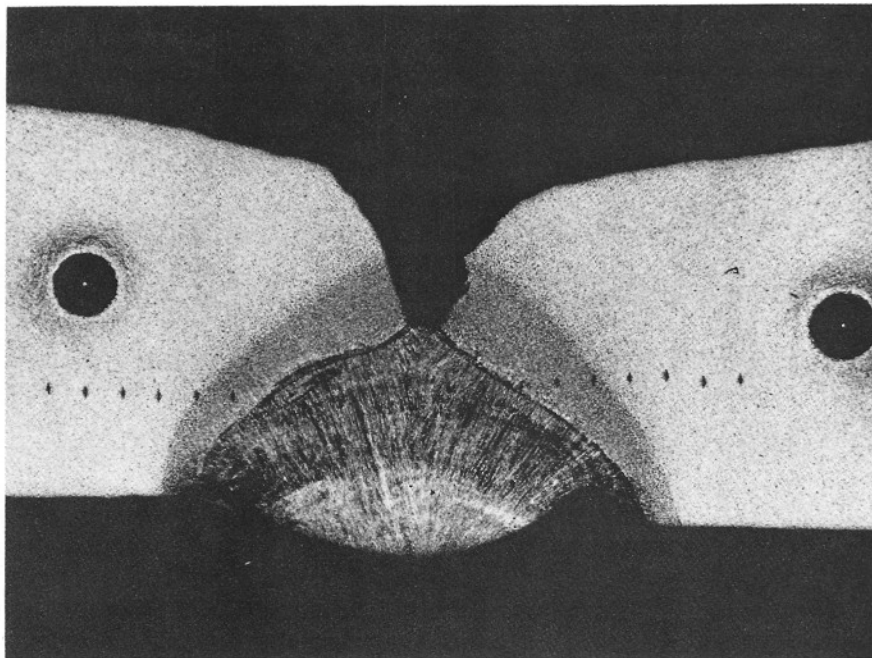
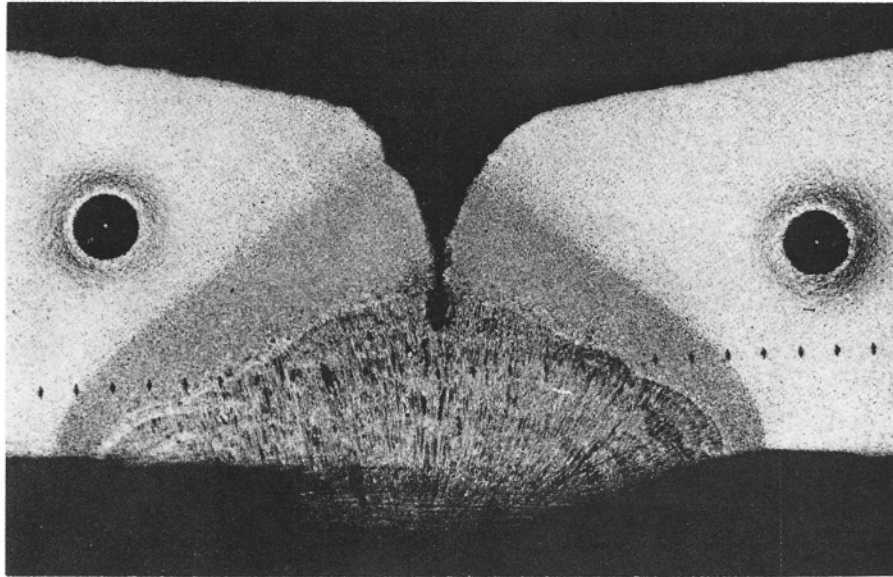


Figure 7.12 Cross sections through weld regions of box beam 8L. Sections were separated about 7.5 in (190 mm) along the beam length. Microhardness indentations traverse the surfaces. X8 1/2

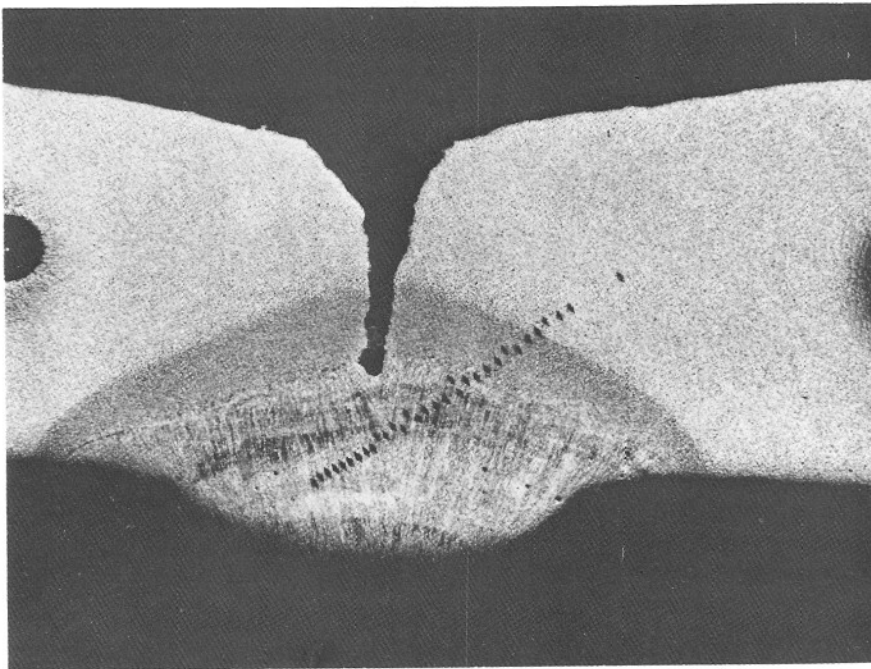
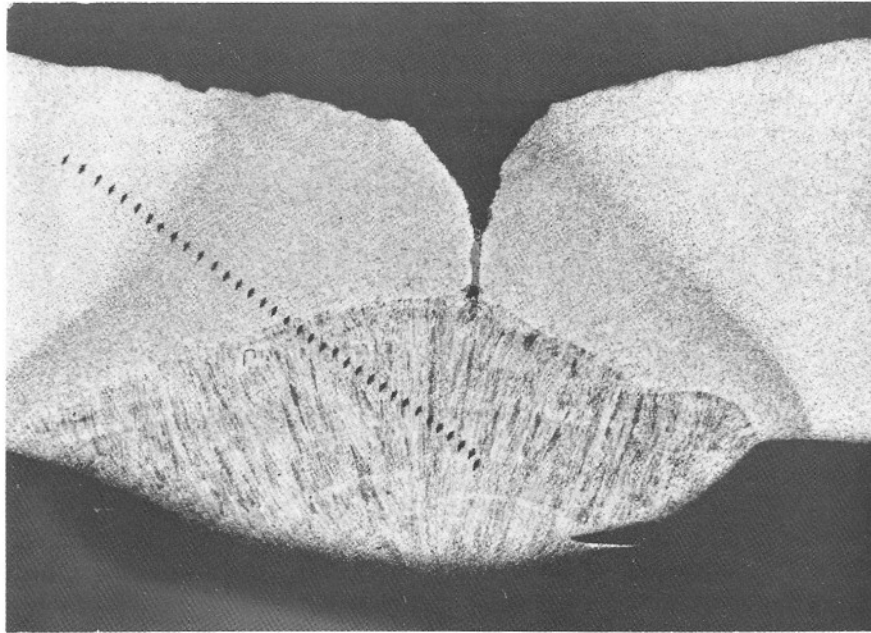


Figure 7.13 Cross sections through weld regions of box beam 9M. Sections were separated about 7.5 in (190 mm) along the beam length. Microhardness indentations traverse the surfaces. X8 1/2



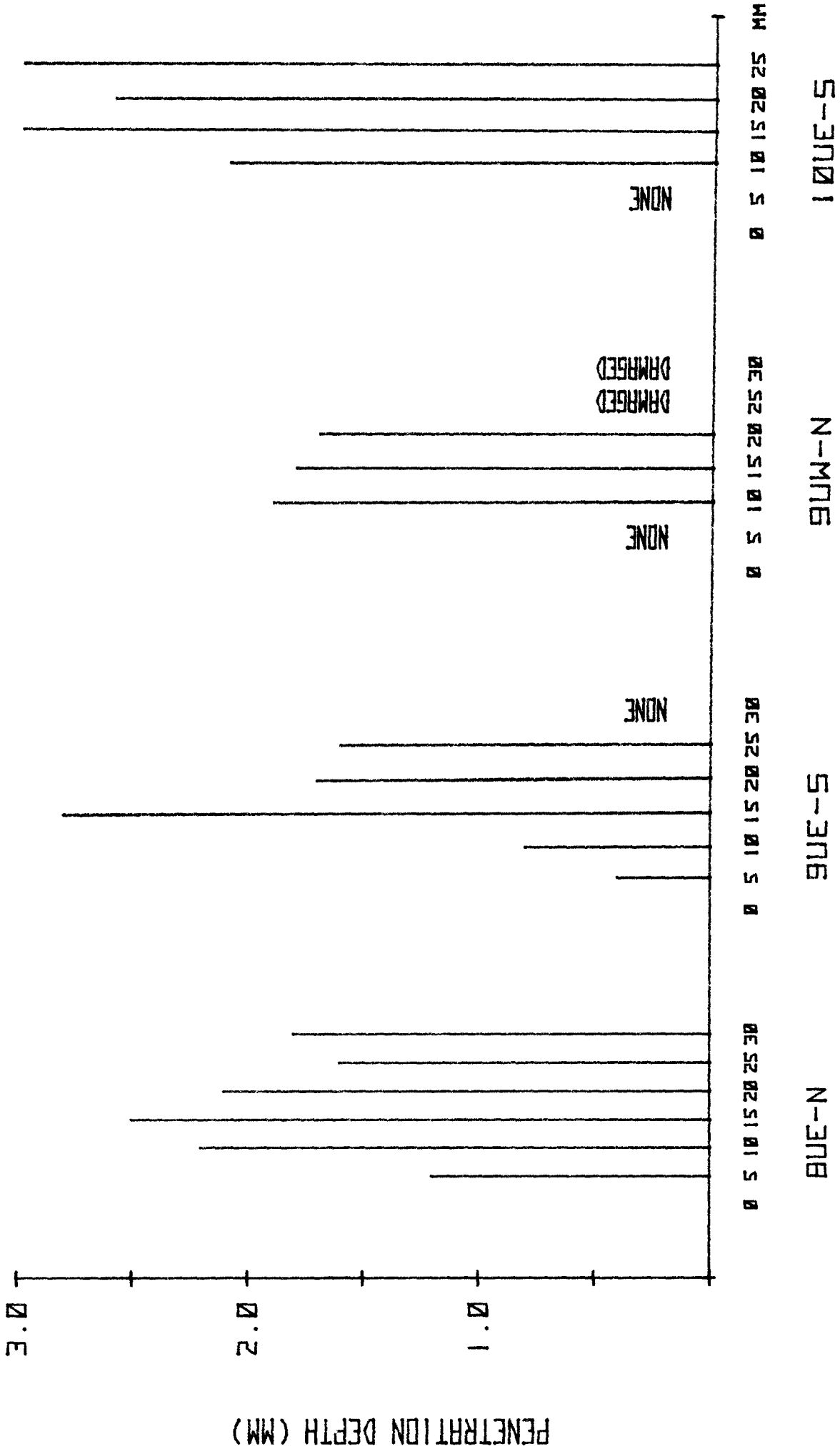


Figure 7.15 Overall depth of interior tack welds measured from fractures with data points reflecting equally spaced measurements from beam end (left) to hanger rod hole (right). NONE indicates no tack weld at that location.



a



b

Figure 7.16 Microstructures of washers from 9MW (NBS specimen 3), (a), and of hardened washer used in NBS tests, (b). Whiter layer near surface (top of illustrations) is decarburized layer. Interior structure is tempered martensite. Etchant: Picral. X200



## 8. FRACTOGRAPHIC ANALYSIS

### 8.1 INTRODUCTION

This chapter describes the specimen preparation and application of optical and scanning electron microscope (SEM) fractography to relate the microstructural features of fractured or deformed portions of the walkway structure to the mode of failure.

Section 8.2 reviews studies conducted on fractures of longitudinal welds produced during testing of box beams fabricated in the NBS shops. Replica and metal specimen preparation for fractography are discussed. Experience was gained in replicating fractures under conditions similar to those in the fields and data were obtained which allowed comparison of the macroscopic aspects of the fractures with those of the actual walkway structure.

Section 8.3 describes studies of fracture surface replicas from the walkway debris.

Section 8.4 reviews the results obtained from direct optical and scanning electron microscopy on selected fractures removed from the walkway box beams.

Section 8.5 summarizes fractographic analysis results.

### 8.2 SPECIMEN PREPARATION AND NBS FRACTURE RESULTS

Procedures used to replicate the fracture surfaces have been described in section 5.5. The replication technique is capable of reproducing details of the fracture surface with reasonable fidelity, provided that intimate contact is achieved between the replication media and the surface (figure 8.1). Failure to achieve contact produces artifacts in the replica that must be discounted in the analysis. The replica is a mirror image of the original surface and may have a different sense of image contrast--in one case the image contrast is due to both topography and composition variation (8.1a) and in the other the image contrast is due to topography alone (8.1b). Selection of a specific replica from each surface for study was based on visual evaluation of the

largest intact replica contact area and on the least amount of embedded rust and other debris. The replicas were trimmed of excess plastic and attached to a 1 in (25 mm) diameter SEM support stub by a small piece of doublesided adhesive tape. Three point contacts of either carbon or silver paint were then made between the SEM stub and the replica corners to increase their support and to provide electrical contact to the sputter coating later applied to the replicas. A replica identification was also inscribed on the stub at this time.

Replicas were sputter coated by placing three replica-mounted stubs on the pedestal of a DC sputter coating unit. The coater electrode was a circular planar magnetron triode having a pulse mode deposition capability which allowed a 5 second ON-OFF cycle. This maintained specimen temperature below 25°C. After reducing chamber pressure to 30 millitorr (40 kPa), argon gas was bled into the system to produce a stable pressure of 95 millitorr (127 kPa). A deposition time of 5 to 7 minutes with a 60 Au-40 Pd alloy at a target-to-specimen distance of 1 in (25 mm) and a plasma current of 15 mA was used. These conditions produced an electrically conductive and thermally protective film allowing examination and SEM photomicrography at magnifications ranging from 5 X to 2,000 X. Stereo pair views of the fracture surfaces and washer contact areas were made by tilting the replicas approximately 5 to 6 degrees between the first and second exposure from a nominal tilt angle of 0 degrees. These were used for the analysis of the spatial relationships of the topographic features.

Metal specimens for direct SEM examination were cleaned in an ultrasonic tank containing acetone or ethyl alcohol. The cleaning solution was changed as required to remove all water, oil, and loosely adhering debris. These specimens were then mounted on a spring-clip holder stub for SEM observation. All residual magnetization was removed by passing the mounted specimens through a demagnetizing coil several times in different directions.

Figure 8.2 illustrates that the gross features of the fracture in the lower longitudinal weld between the outer hanger rod hole and beam end of box beams tested to failure were similar, regardless of whether the beam had been fabricated at NBS or had been obtained from the walkway debris. Rounded and piping porosity are evident in both fractures. The sharply delineated weld region in these figures indicates the absence of rust on the freshly fractured surfaces.

### 8.3 WALKWAY FRACTURE REPLICAS

Replicas from the walkway fracture and washer contact surfaces have been described in section 5.5 and are listed in table 5.13.

#### 8.3.1 General Observations

Rounded gas porosity (both large and fine) and piping (elongated) porosity similar to that illustrated in figure 8.2 were evident in the fracture areas of the interior tack and exterior longitudinal welds at locations 8UE, 9UE, 9UW, and 10UE. Fractographic examination indicated that these flaws did not serve preferentially as crack initiation sites. It appears that, in the case of the lower exterior welds, cracks initiated at the root of the weld and propagated

through the porosity (figure 8.3). While many of the replicated sections provided reasonable resolution of the fractographic features, figure 8.4 illustrates that in some cases a very tight oxide layer had modified the original fracture surface.

### 8.3.2 Box Beam Longitudinal Welds

Different textures in the fracture topography provided evidence that cracks had existed in the weld roots in the regions between the hanger rod holes and in the regions between the outer hanger rod holes and beam ends prior to gross weld failure at the time of collapse. Figures 8.5 (a-c) illustrate the appearance of several such regions in the exterior longitudinal welds at locations 9UW, 9UE and 8UW.

As opposed to the lower exterior welds, fracture in the lower interior tack welds initiated at the weld surface and propagated towards the weld root. An example is shown for location 9UE in figure 8.6. Topographic features developed by momentary crack front arrest and changes in crack propagation direction are helpful in defining the crack path (figure 8.3), while interpretation of micro-dimple patterns in the ductile fracture are useful in defining the point of origin. These observations suggest that the crack observed in the tack weld at location 8MW during the site investigation (figure 5.18a) indicated an initial stage of weldment failure. Fractures in the lower exterior longitudinal welds were found to initiate at the root of the weld with the crack front propagating towards the outside surface of the box beam where the shear lip is observed. These observations are consistent with deflection of the flange regions upward during deformation prior to structural collapse.

No indications of fatigue failure were observed. The predominant failure mode in the weld metal was ductile rupture, although small areas of cleavage were observed in the vicinity of the weld center line at locations 9UW and 10UE (figure 8.7).

### 8.3.3 Washer/Nut Contact Area

Two regions of washer contact were typically observed on the lower surface of the box beam flanges. The outermost region contains imprints of the washer edge and shows relatively shallow striations reflecting slippage of the washer in the initial deformation phase. Transition to a more intensely abraded region was observed nearer the hanger rod hole (figure 8.8) for location 9UE.

Evidence for a slip-stick mode of failure in which the washer and/or nut combination was periodically arrested was observed in the deeply abraded region at all locations examined. One indication of this mode can be seen at location 9UE (figure 8.8), while multiple indications can be seen at location 10UE (figure 8.9). This indicates that pull-through of the washer/nut assembly proceeded in a slip-stick manner, with the hardened steel washer digging into the comparatively soft steel of the flange.

Washers at locations 9UE and 8UE were missing after the collapse. However, figures 8.8 and 8.10 provide clear evidence that washers had been installed at both locations.

#### 8.3.4 Washers

As noted in chapter 6, some washers obtained from the walkway debris fractured in the course of NBS beam tests while hardened washers purchased by NBS did not fracture under similar test conditions. Examination of the fracture surface of a walkway washer at location 9MW that failed during an NBS test conducted on walkway box beam 9M revealed that the washer had failed in a predominantly brittle manner. This is evidenced by the dominant intergranular and cleavage modes of failure illustrated in figure 8.11b. This is a magnified photomicrograph of the central region of the fracture surface shown in figure 8.11a. By contrast, figure 8.11c shows predominantly ductile failure at the surface decarburized layer of the washer.

Prominent elongated MnS inclusions can be observed on the fracture surfaces in figures 8.11a and 8.11c. Hardened washers bent around a direction parallel to such inclusions could be expected to display low ductility.

Other comparisons were made of the fracture characteristics of the walkway and NBS washers. Walkway washers included for study were identified as NBS 11B, 13B and 15B. Their original locations are described in table 5.13. Two randomly selected hardened washers purchased by NBS for in-house studies were also included. These are designated NBS 2 and 3. These washers were initially intact and were fractured by bending to provide surfaces for examination. In addition, a section of a walkway washer that fractured into two pieces during an NBS shortbeam test on walkway box beam 9M was also included. This latter washer was designated KCl to correspond to the designation of the test in which it fractured (chapter 6). Photomicrographs of the fractured surfaces of some of these washers are shown in figures 8.12 to 8.15. Macroscopic features are illustrated by low magnification views while the microscopic features at mid-thickness are detailed in higher magnification views.

These figures show that the fracture characteristics of the walkway and NBS washers were basically similar. Both contained elongated stringers of MnS (figures 8.12a and 8.14a). Fracture characteristics of the walkway and NBS washers varied from predominantly ductile (figures 8.12 and 8.14) to predominantly intergranular (figures 8.13 and 8.15). However, the walkway washers displayed a higher percentage of intergranular fracture.

#### 8.3.5 Clip Angle Fillet Welds

Replicas taken from the failed clip angle fillet weld surfaces at location 9UE indicated ductile failure and that: a) the bottom fillet weld failed primarily by shear normal to the box beam axis, b) the vertical side fillet weld failed by shear with the top weld acting as a hinge, and c) the top fillet weld failed primarily in tension. Figure 8.16 illustrates that failure of the top weld initiated at the lower edge (location A), propagated upward, and terminated at a shear lip at the upper edge (location C).

## 8.4 DIRECT ANALYSIS OF WALKWAY BOX BEAM FRACTURES

### 8.4.1 Procedures

As has been noted in chapter 5, one half of the lower fracture surfaces at the following box beam-hanger rod connections were removed from the debris for direct optical and SEM fractographic analysis:

8UE - north half  
9UE - south half  
9UW - north half  
10UE - south half

Each specimen consisted of a section of the bottom flange cross cut to the flange fracture surface, then cut 4 1/4 in (108 mm) inward from the beam end along the web toe of the fillet as indicated on figure 8.17. Two layers of duct tape were applied to the fracture surfaces for protection prior to cutting. Upon delivery to the NBS laboratories the duct tape was removed, the specimens were cleaned with paint thinner, rinsed in petroleum ether and photographed. A third cut (figure 8.17) was then made with a jeweller's saw. Sections containing the fracture surfaces from the beam end to the outer hanger rod hole were then prepared for fractographic analysis by ultrasonic cleaning under acetone.

### 8.4.2 Results

Figures 8.18 and 8.19 illustrate the overall appearance of the lower longitudinal weld fractures between the outer hanger rod hole and beam end at locations 9UE, 9UW, 8UE and 10UE, respectively. Figures 8.20 and 8.21 illustrate the weld fractures between the two hanger rod holes running from the outer hole to cut #2 (figure 8.17). The weld regions and other salient features are identified on these figures.

A much higher concentration of piping porosity is observed in the region from the beam end to the outer hanger rod hole than between the two holes. This was also noted in the radiographic examination of walkway box beam 9M (section 7.2.2) and suggests that the porosity is associated with the beginning of a weld run. There was no evidence of cracks preferentially initiating from this porosity.

Figure 8.18b suggests that the length of weld from the outer hanger rod hole to the beam end was less at location 9UW than at other locations. However, this was not the case because the outer hole region at 9UW had been severely damaged during pull-through of the hanger rod and some of the original metal at that location had been fractured away or distorted out of the plane of the weld. The fracture surface at 10UE (figure 8.19b) shows similar damage in the outer hole region.

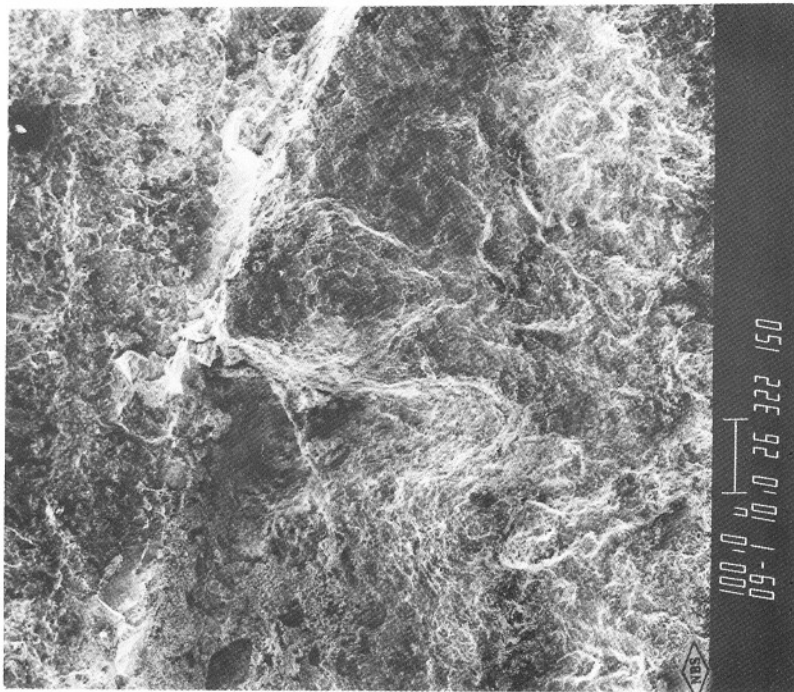
Evidence of cracks existing prior to final weld failure was observed at location 9UE in both the lower exterior longitudinal and lower interior tack weld regions between the outer hanger rod hole and beam end (figure 8.18a). A very small area of preexisting crack was identified at location 8UE in the

interior tack weld region (figure 8.19a). Areas of preexisting cracks were noted in the longitudinal weld regions between the hanger rod holes at locations 9UE, 8UE and 10UE (figures 8.20a and 8.21a,b). The difference in topography in the preexisting crack region and in the region through which the final crack propagated at location 9UE is illustrated on figure 8.22. The preexisting crack region was heavily oxidized while the final fracture surface was relatively clean and exhibits fine ductile fracture dimples. It is not certain whether these preexisting cracks were formed during fabrication of the beams, during construction of the walkways or after the walkways were put into service. However, their locations in regions of maximum stress support the premise that they were formed during construction or during service. While the final fracture generally initiated at the root of the lower exterior longitudinal weld and propagated toward the exterior beam surface, and in the upper surface of the interior tack weld and propagated toward its root, no specific evidence was noted that preexisting cracks at these locations initiated the final fracture preferentially.

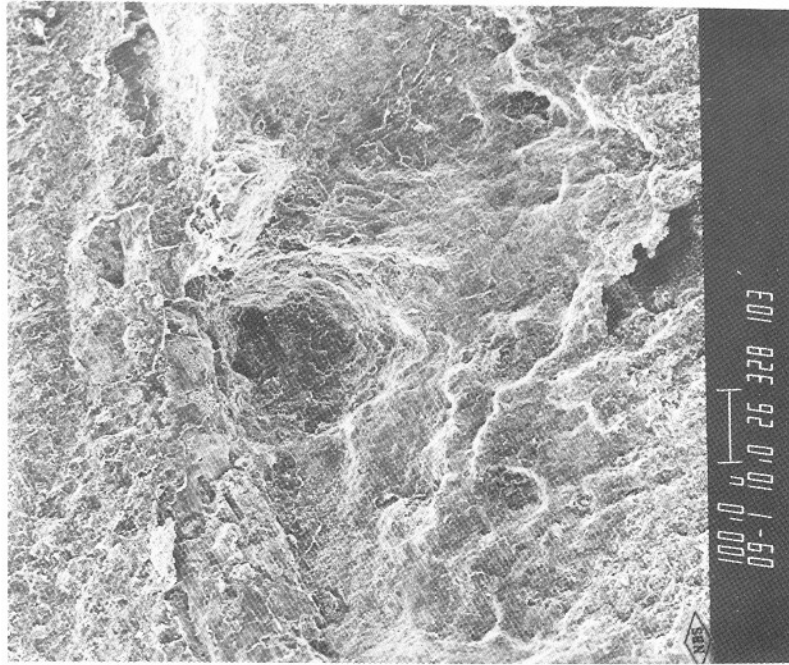
### 8.5 SUMMARY

1. Gross features of the fractures of the lower longitudinal exterior welds of both NBS fabricated box beams and walkway box beams were similar.
2. Rounded and piping porosity were observed in all lower longitudinal exterior welds in the fourth floor walkway box beams, but no evidence was noted of preferential crack initiation from such flaws.
3. The predominant failure mode in the lower longitudinal exterior welds was ductile rupture. Between the beam end and outer hole, crack initiation appeared to be at the top of the interior tack weld with propagation toward the weld root. Failure in the lower longitudinal exterior welds at these locations initiated at the root and propagated toward the exterior beam surface in a direction normal to the flange surface.
4. Evidence was obtained of cracks existing in the welds prior to final weld failure during collapse. Their location supports the premise that these cracks were formed during construction or during service. There is no specific evidence that these preexisting cracks were the preferential sites of final fracture initiation.
5. No evidence of a fatigue failure mode was observed.
6. Evidence indicates that washers at locations 8UE and 9UE, missing after the collapse, had been initially installed.
7. Two regions of washer imprints were observed on the bottom surfaces of the box beam flanges. The outermost region contains the imprint of the washer and shows shallow striations. Nearer the hanger rod hole, there was a transition to a more deeply abraded region. This region showed evidence that the failure proceeded in a slip-stick manner.

8. The fracture characteristics of the walkway and NBS washers varied from predominantly ductile to predominantly brittle. However, the walkway washers displayed a higher percentage of intergranular fracture.

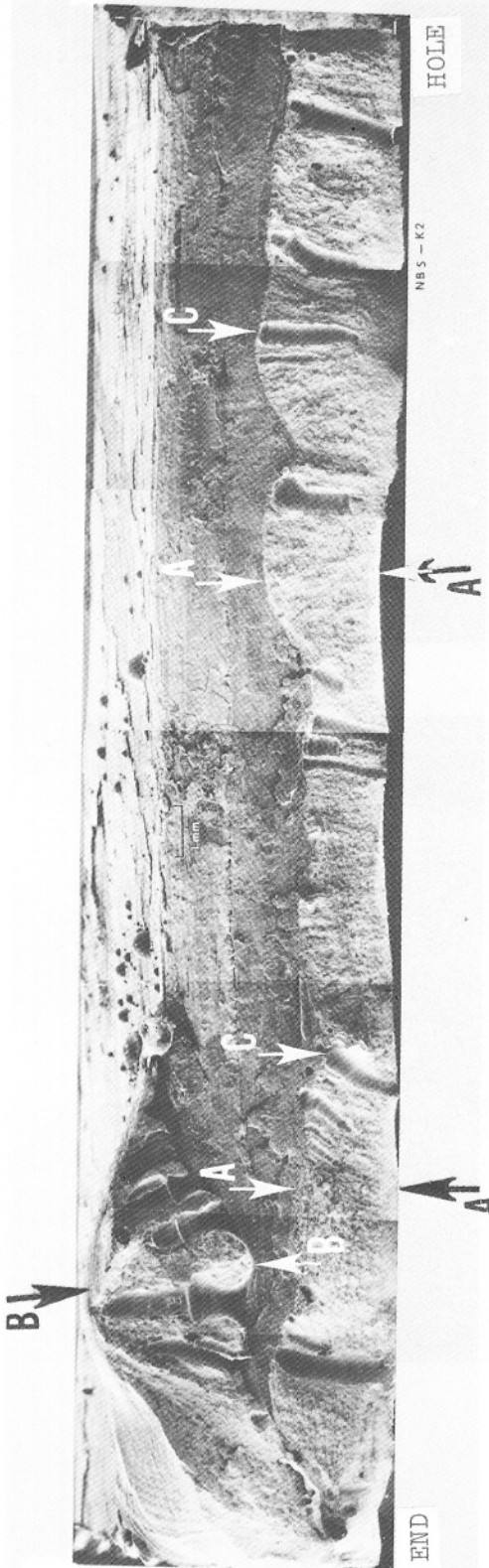


(a)

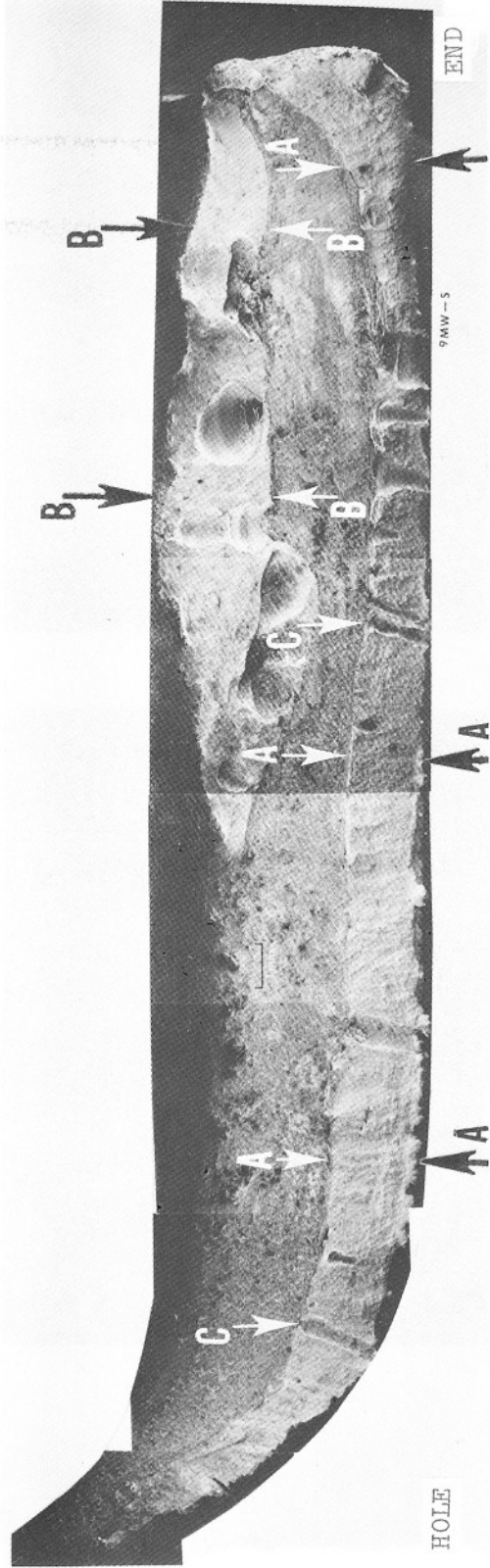


(b)

Figure 8.1 Comparison of quality of image by direct SEM (a) and by replication (b) where replica contact is ideal. Fracture surface is located at root of upper exterior longitudinal weld of walkway box beam at location 8UW (north). Magnification X100.

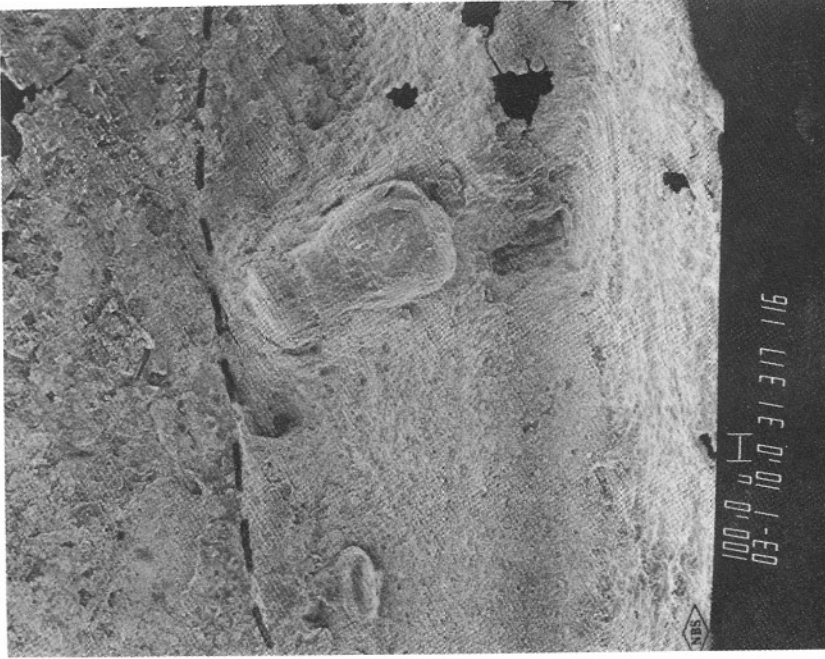


(a) NBS box beam K2.

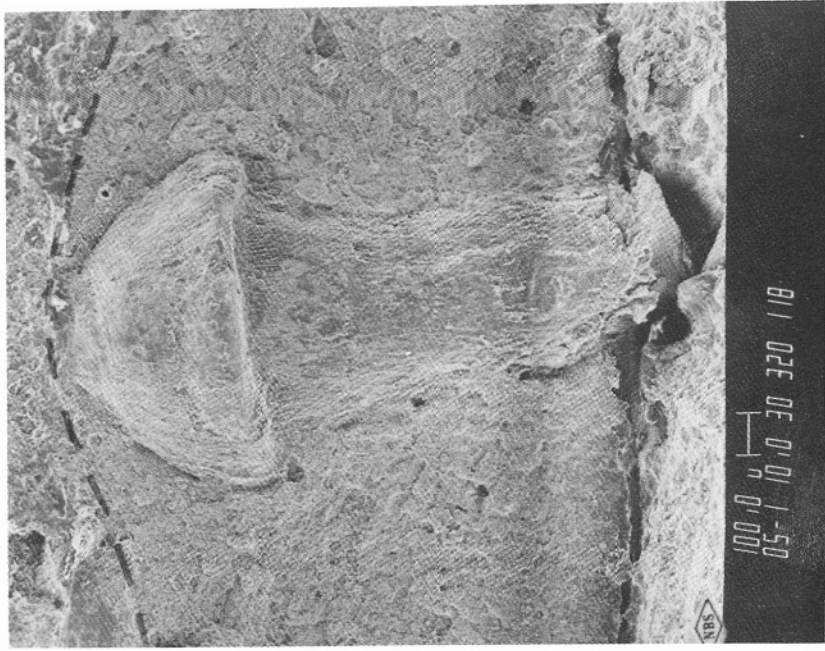


(b) Walkway box beam 9M, location 9MW (south).

Figure 8.2 One half of box beam fracture surface between beam end and outer hanger rod hole for NBS fabricated box beam K2 (a) and for walkway box beam 9M tested at NBS (b). Exterior longitudinal weld indicated by arrows A, interior tack weld indicated by arrows B, examples of piping porosity indicated by arrows C. Magnification X6.



(a)



(b)

Figure 8.3 Photomicrographs showing that the crack initiated at the root of the weld and propagated to the exterior of the box beam (location 9UE). Figure (a) is located 3 mm from the end of the beam. Crack is propagating downward and slightly to the right. Figure (b) is located 18 mm from end of beam. Magnification (a) X30 and (b) X60.

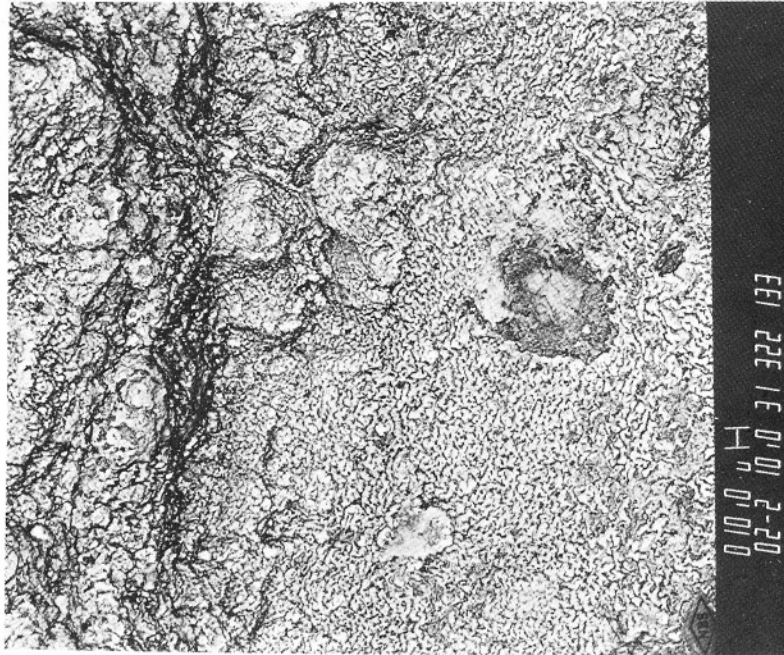
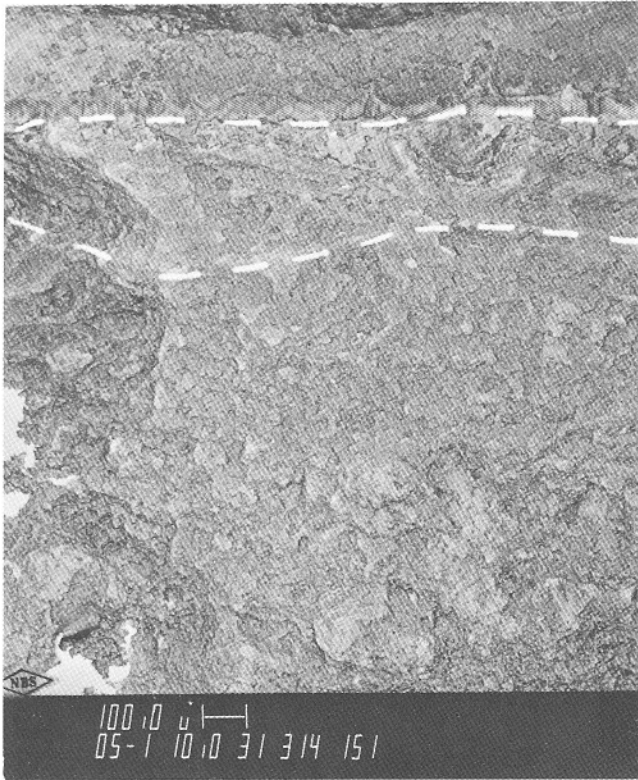
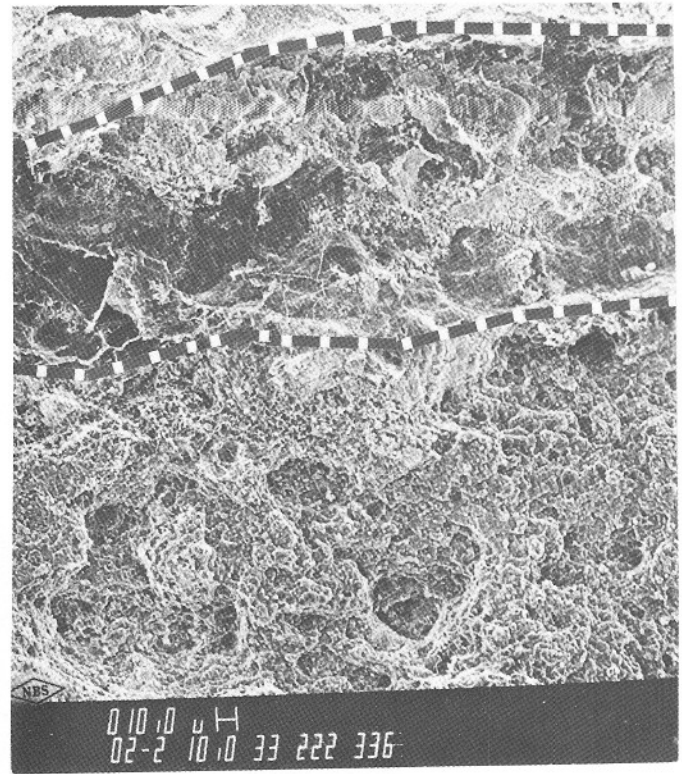


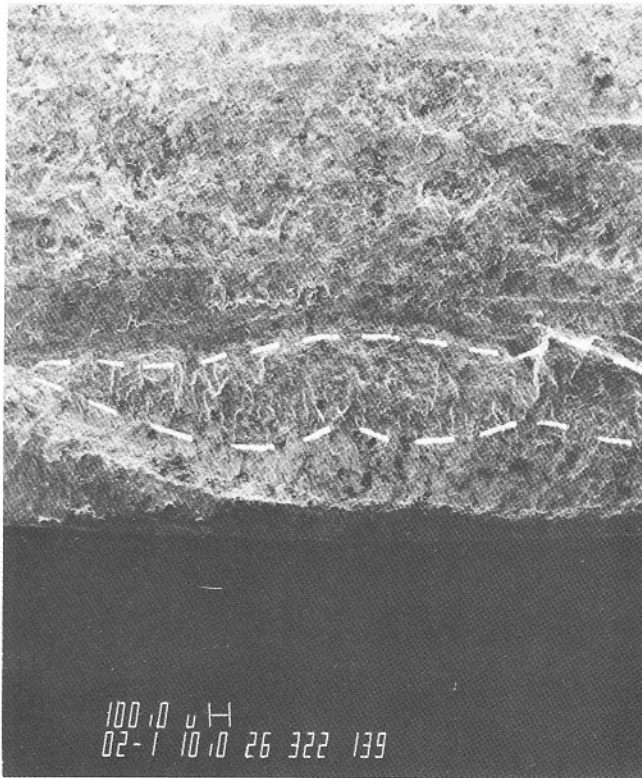
Figure 8.4 Photomicrograph of a replica from the shear lip region at location 8UE. The surface oxidation has removed the fine shear dimpled rupture features in this area. Magnification X250.



(a)



(b)



(c)

Figure 8.5 Fractographic evidence of pre-existing cracks in walkway box beam exterior longitudinal welds at locations (a) 9UW, (b) 9UE, (c) 8UW. Regions interpreted as cracks outlined by dashed lines. Magnifications X55, X250, and X25, respectively.

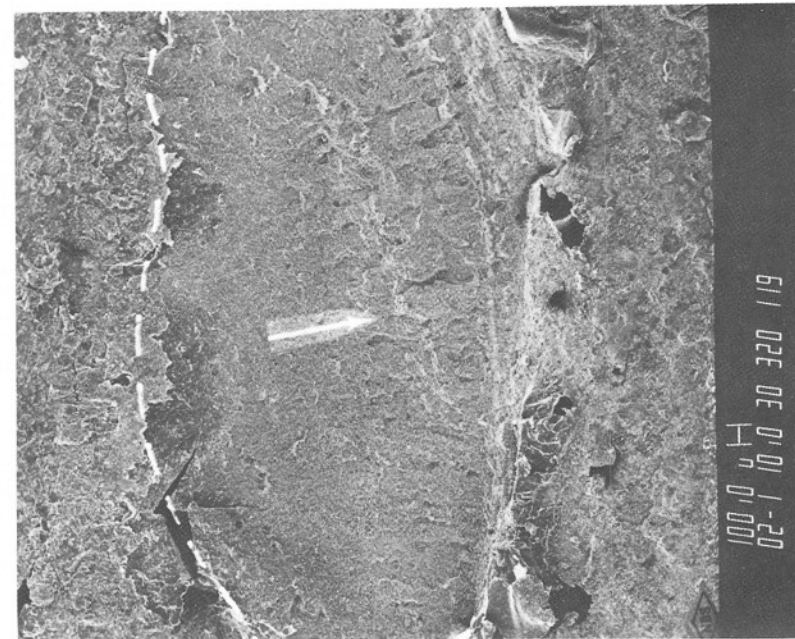


Figure 8.6 Evidence of fracture initiation from upper surface of interior tack weld (dashed line) at location 9UE. Direction of propagation is toward the weld root (arrow) normal to the welding direction. Magnification X25.

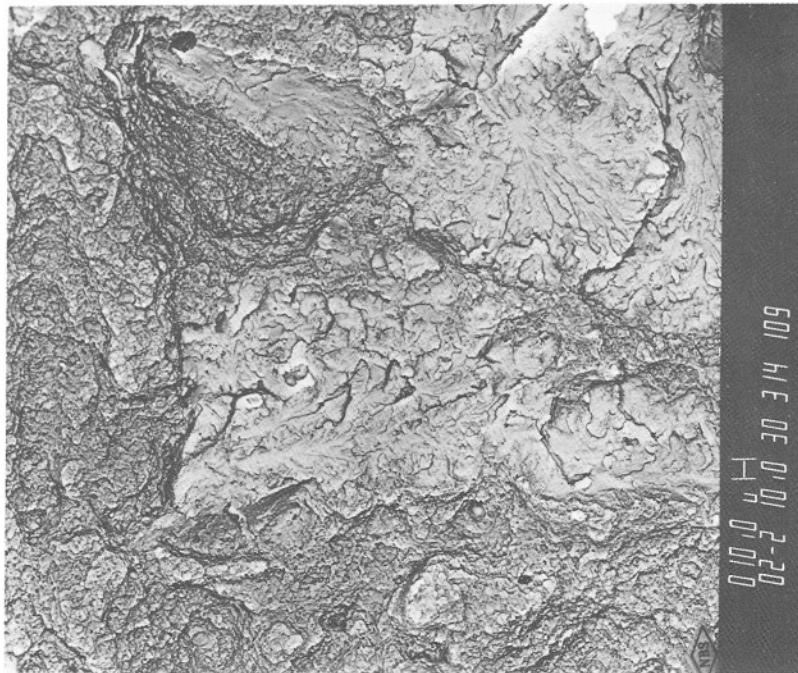


Figure 8.7 Cleavage facets observed at center line of lower exterior longitudinal weld at location 9UW (bright areas). Magnification X250.



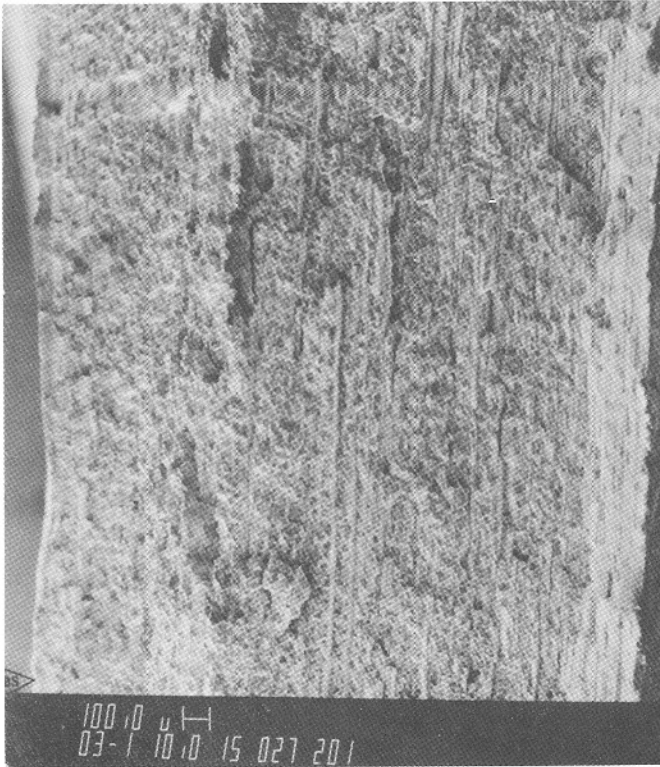
Figure 8.8 Abrasion pattern on bottom flange at location 9UE (north). Arrow denotes initial washer imprint. (A) denotes change in abrasion mechanism. (B) denotes a slip-stick region in progressive failure. Magnification X15.



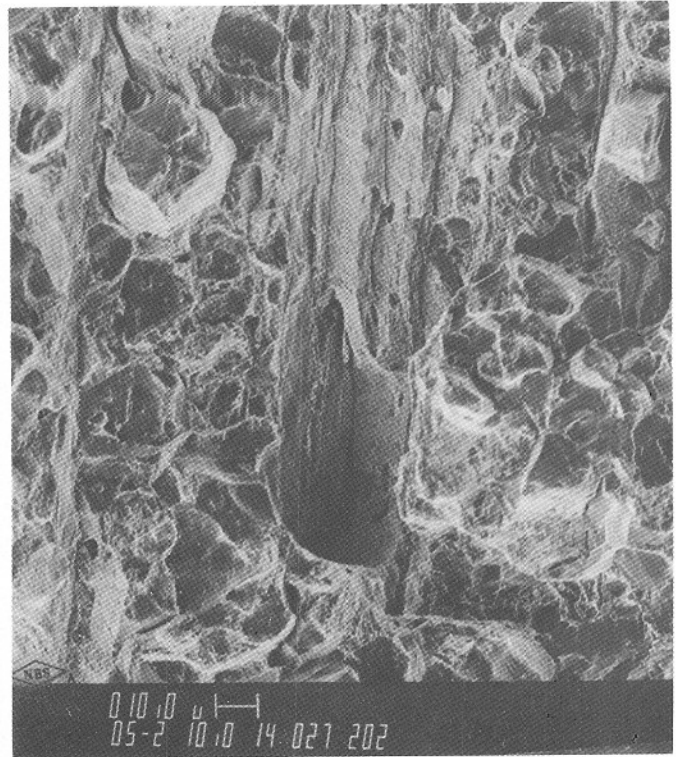
Figure 8.9 Abrasion pattern on bottom flange at location 10UE (south) showing multiple slip-stick regions. Arrow denotes initial washer contact. Magnification X15.



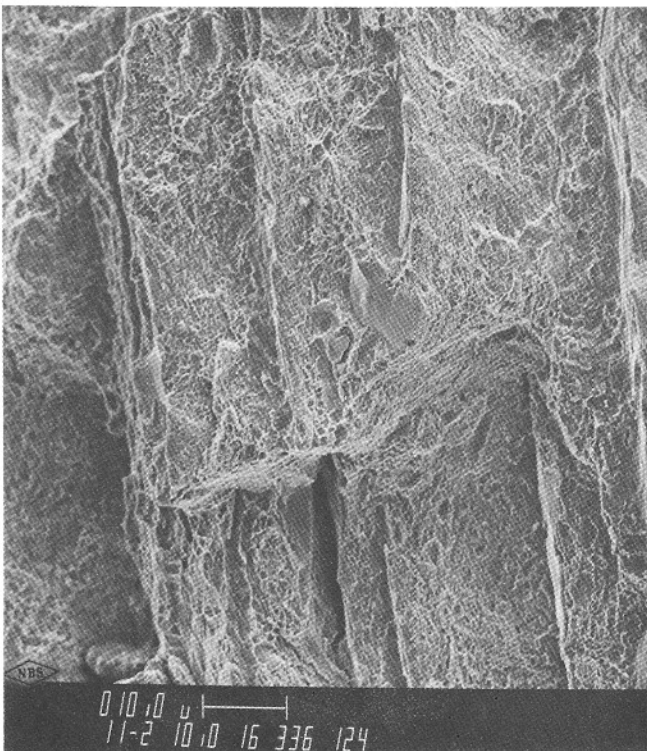
Figure 8.10 Washer contact region on bottom flange at location 8UE (north).  
Arrow denotes initial washer position. Magnification X1.5.



(a)

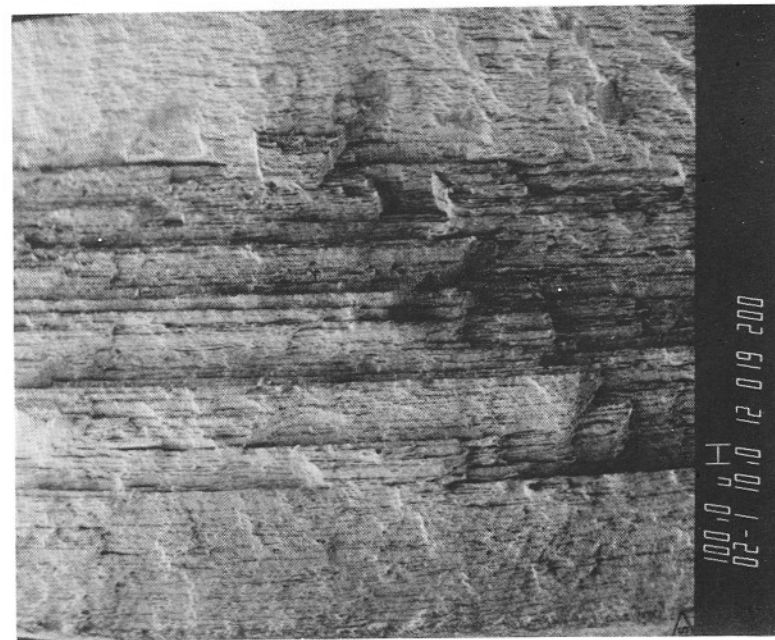


(b)

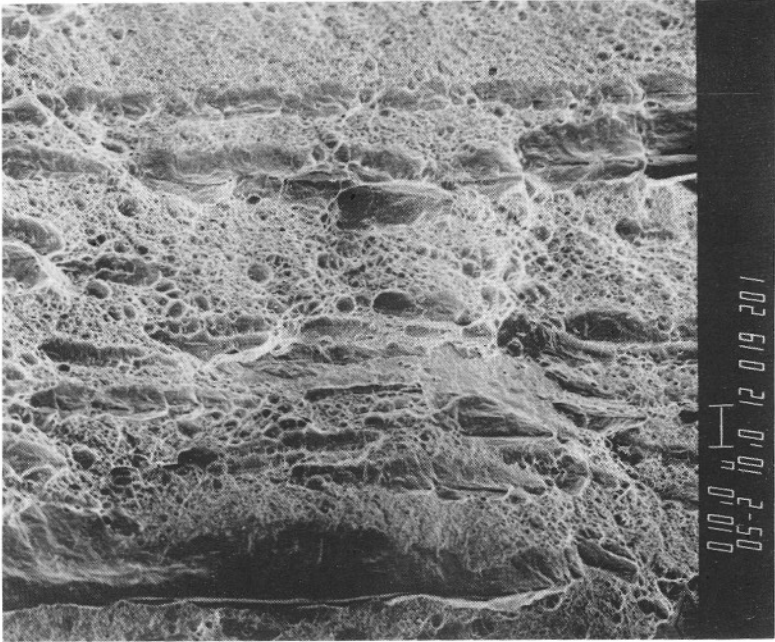


(c)

Figure 8.11 Fractographic appearance of hardened washer fractured in NBS test of walkway box beam 9M, washer installed at location 9MW (a). Center portion, area (b), reveals a mixture of brittle (intergranular and cleavage) and ductile fracture. Area (c) reveals ductile rupture through a decarburized surface layer. Elongated features are indicative of MnS stringers. Magnifications (a) X35, (b) X550, (c) X1050.

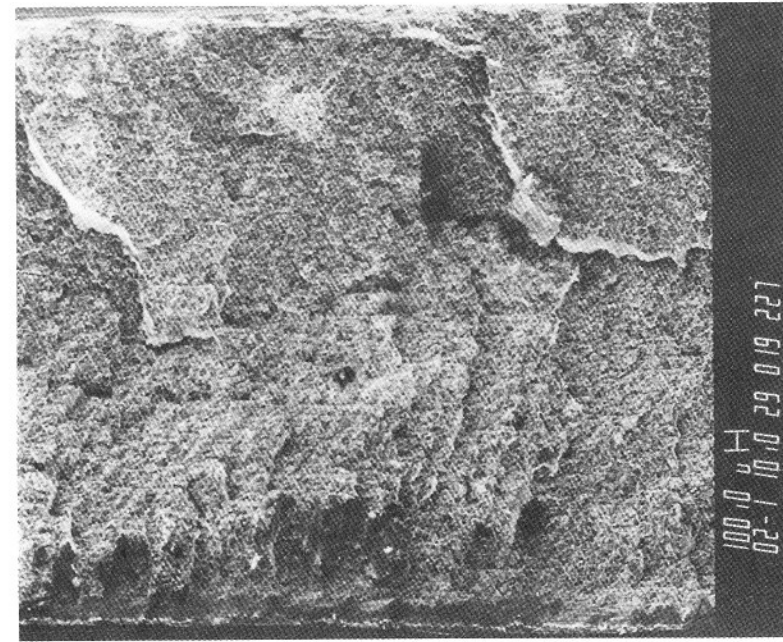


(a)

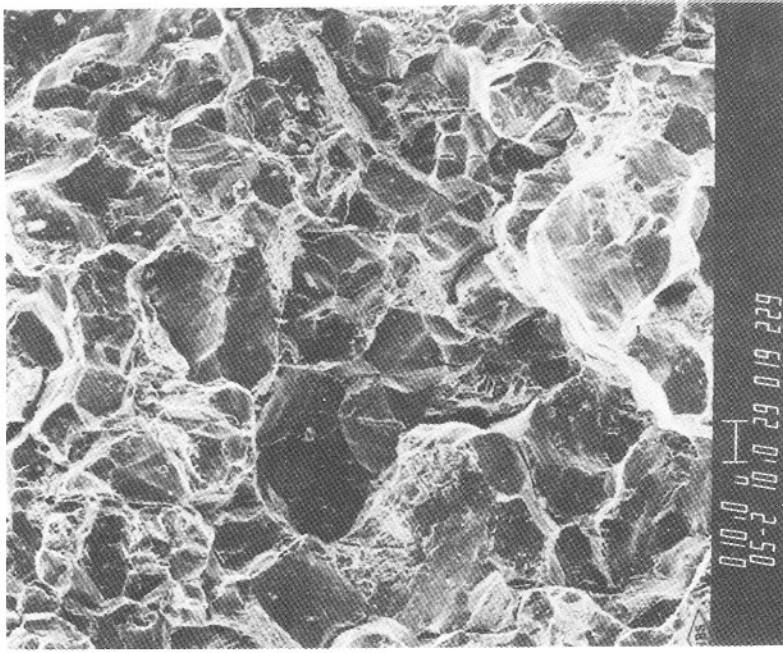


(b)

Figure 8.12 Fractographic appearance of walkway washer fractured in NBS test of box beam 9M (specimen KCl). Lower magnification view (a) shows high density of MnS stringers oriented parallel to the bend axis. Higher magnification view of center portion (b) shows mostly ductile rupture. Magnification (a) X25, (b) X550.

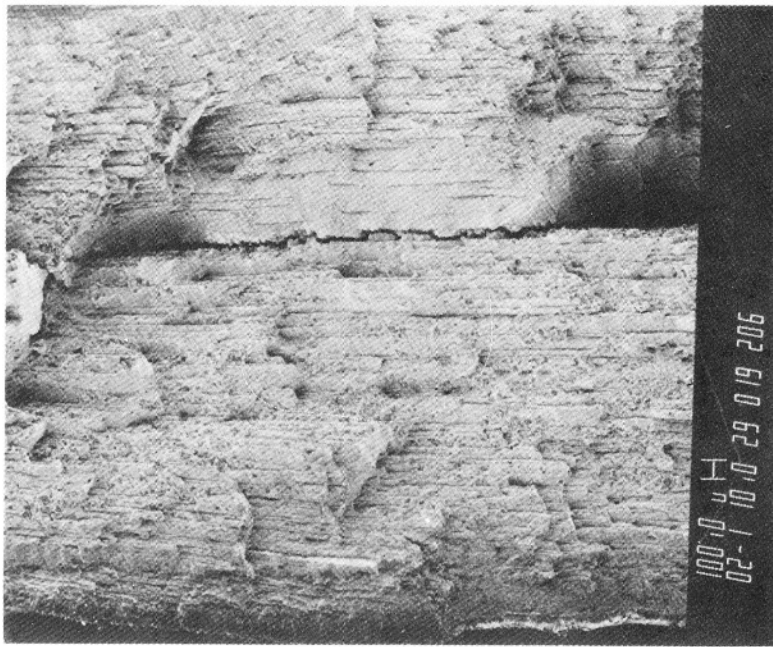


(a)

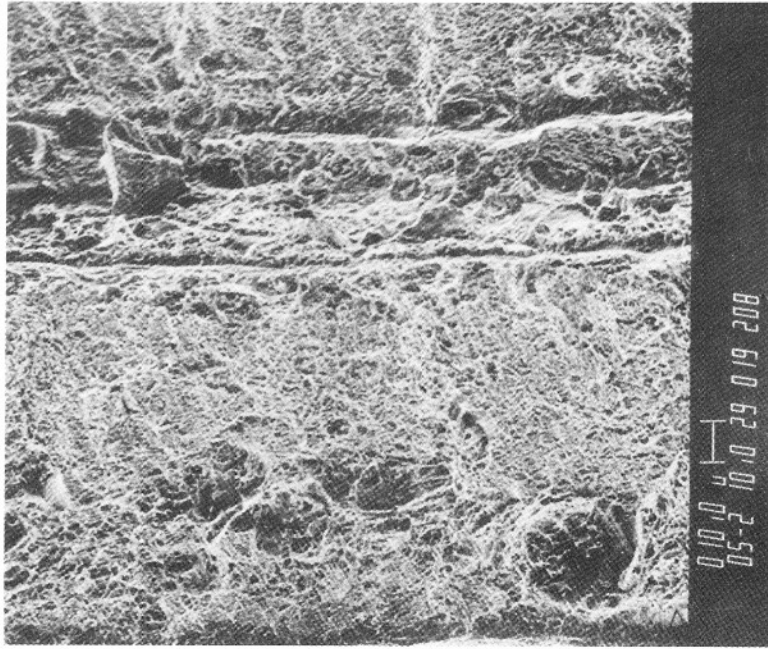


(b)

Figure 8.13 Fractographic appearance of walkway washer from upper end of hanger rod at location 9UE (NBS 11B) broken at NBS. Lower magnification view (a) shows no prominent MnS inclusions. Higher magnification view of center portion (b) shows essentially brittle intergranular fracture with a small amount of ductile rupture. Magnification (a) X25, (b) X550.

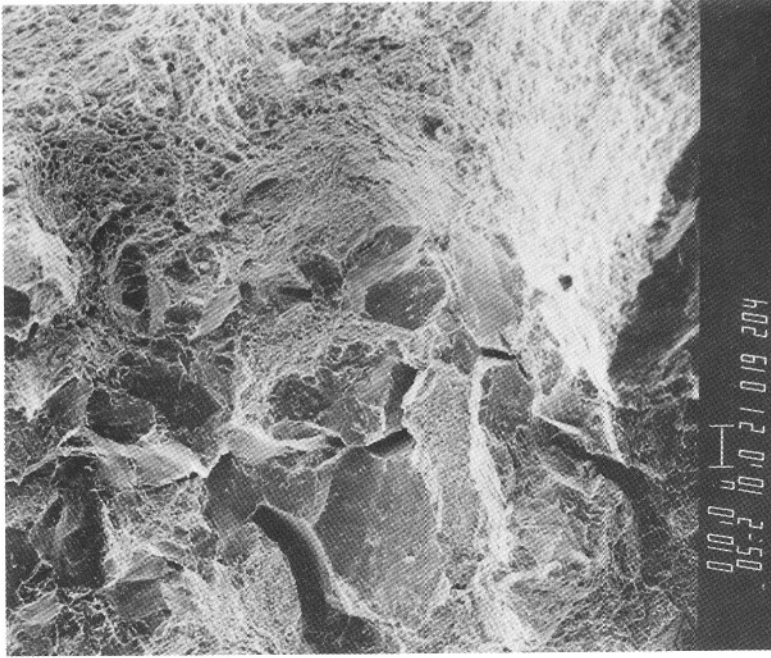


(a)



(b)

Figure 8.14 Fractographic appearance of NBS washer No. 3 broken at NBS. Low magnification view (a) shows elongated MnS inclusions. Higher magnification view of center portion (b) shows essentially ductile rupture. Magnification (a) X25, (b) X550.



(a)



(b)

Figure 8.15 Fractographic appearance of NBS washer No. 2 broken at NBS. Low magnification view (a) shows no prominent MnS inclusions. Higher magnification view of center portion (b) shows 15-20 percent brittle intergranular fracture along with ductile rupture. Magnification (a) X35, (b) X550.

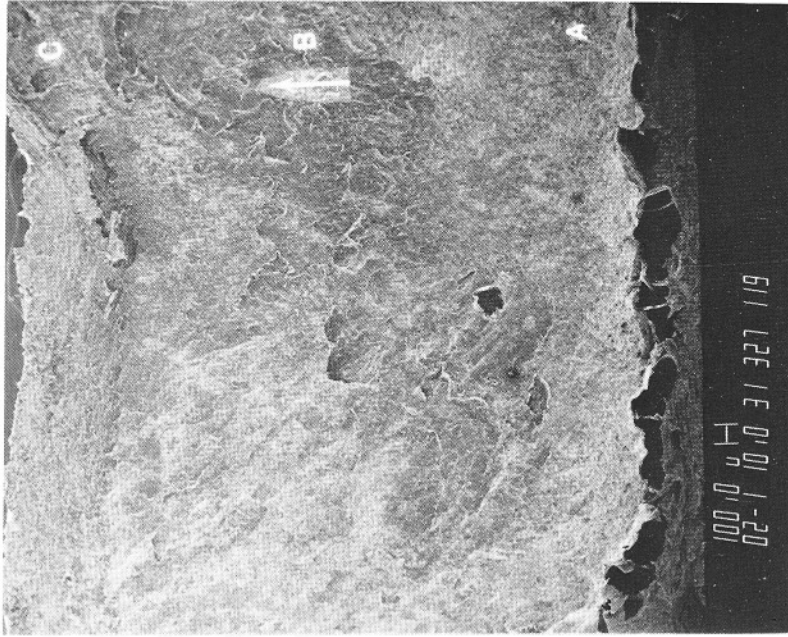


Figure 8.16 Fracture at top fillet weld at clip angle attachment, location 9UE (north). Initiation at A, propagation in direction B to shear lip at C. Magnification X25.

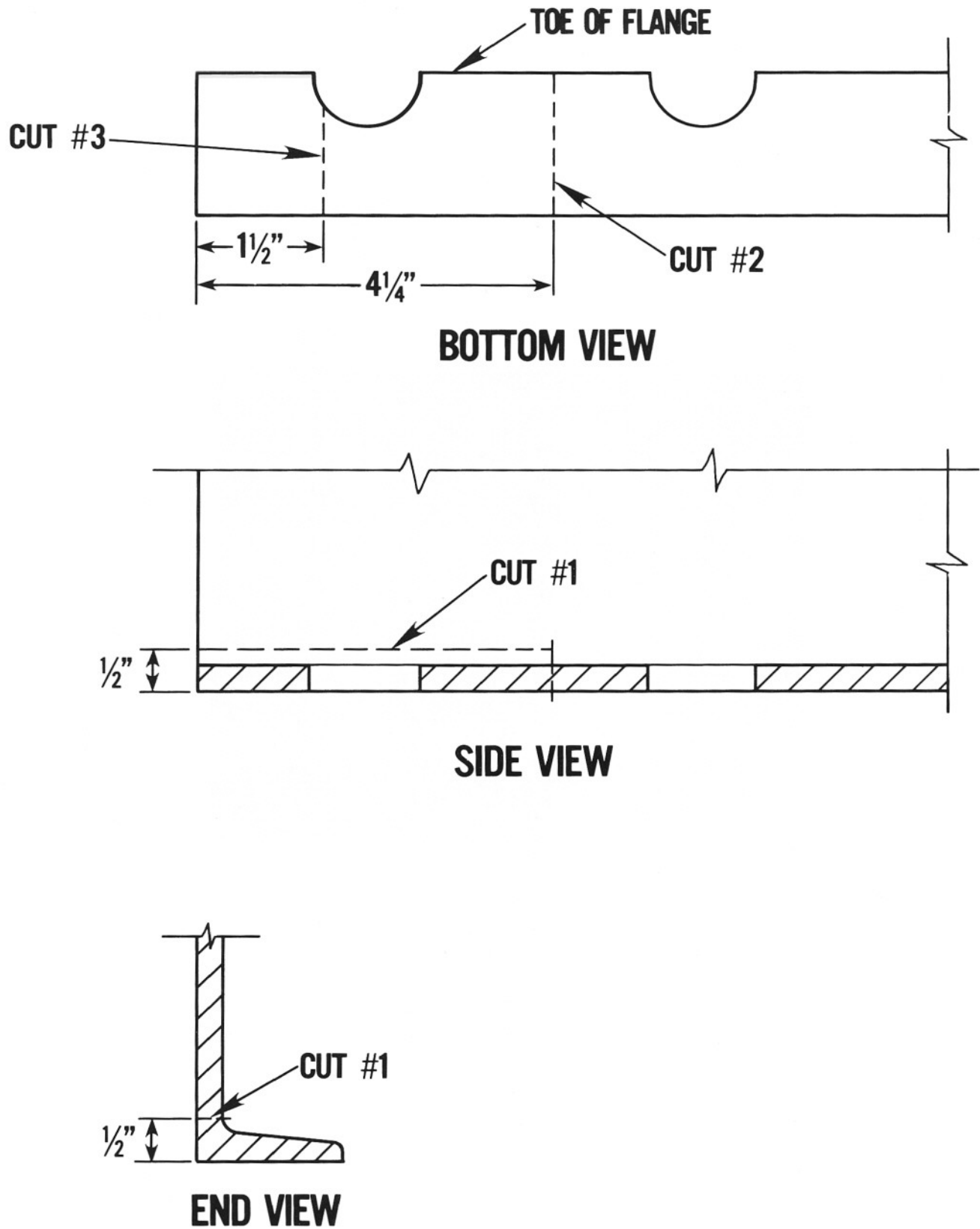
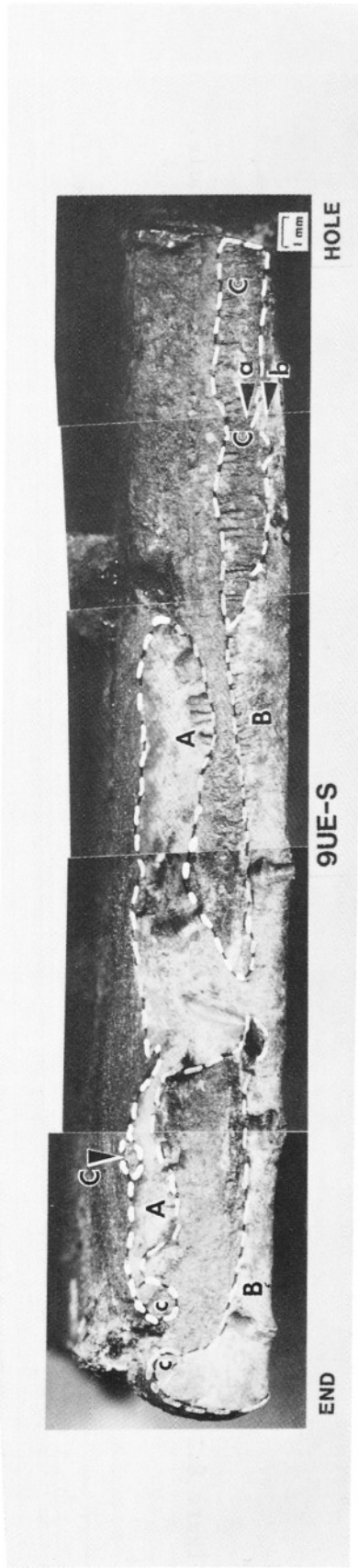
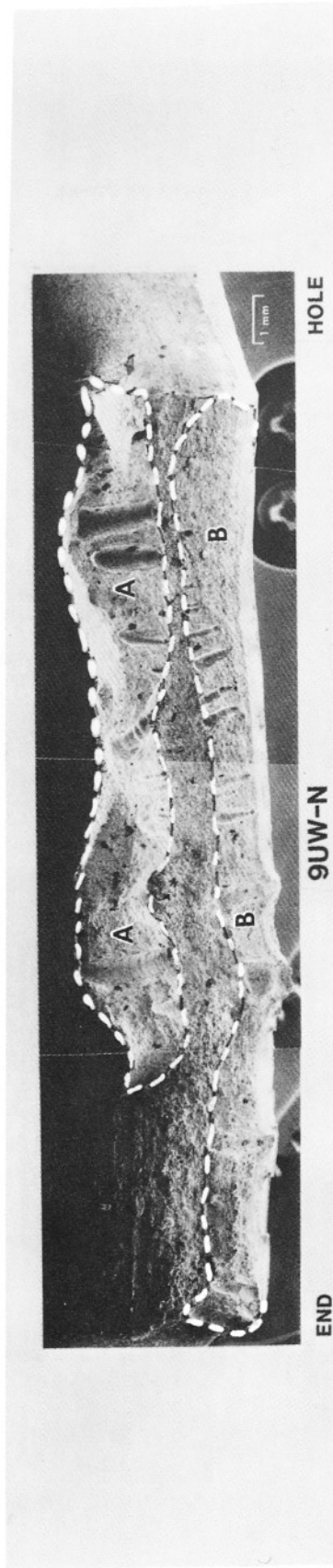


Figure 8.17 Schematic of cuts performed to remove one half of the lower fracture surfaces for fractographic analysis.



(a)



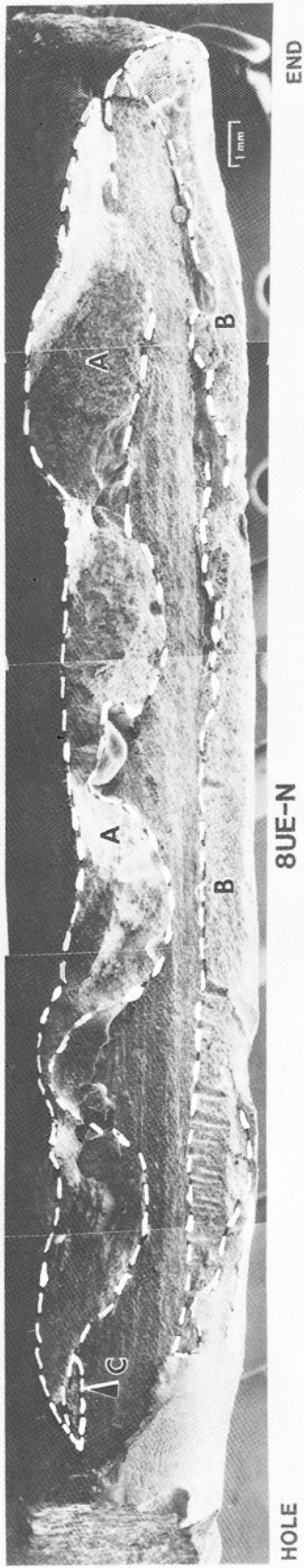
(b)

Figure 8.18 One half of box beam lower fracture surface between beam end and outer hanger rod hole.

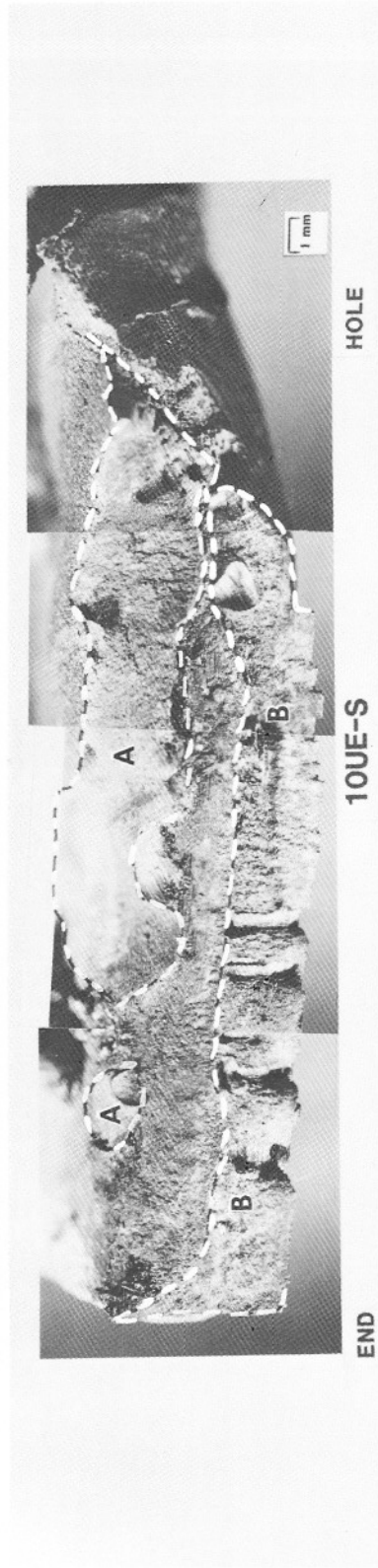
(A) fracture area of the interior tack weld, (B) exterior longitudinal weld, (C) preexisting crack regions. This designation also is applicable to figures 8.19, 8.20, and 8.21. (a) and (b) noted by arrows on 9UE, indicate locations of figures 8.22 (a) and (b), respectively.

(a) location 9UE - S (optical, magnification X4.5)

(b) location 9UW - N (SEM, magnification X6.5)



(a)

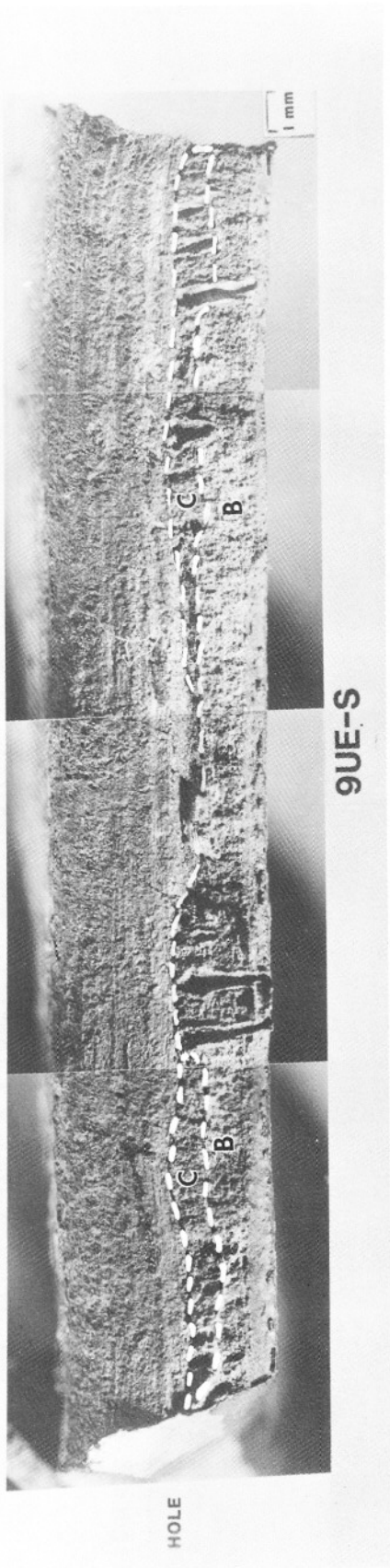


(b)

Figure 8.19 One half of box beam lower fracture surface between beam end and outer hanger rod hole.

(a) Location 8UE - N (SEM, magnification X6.5)

(b) Location 10UE - S (optical, magnification X4.5)



(a)

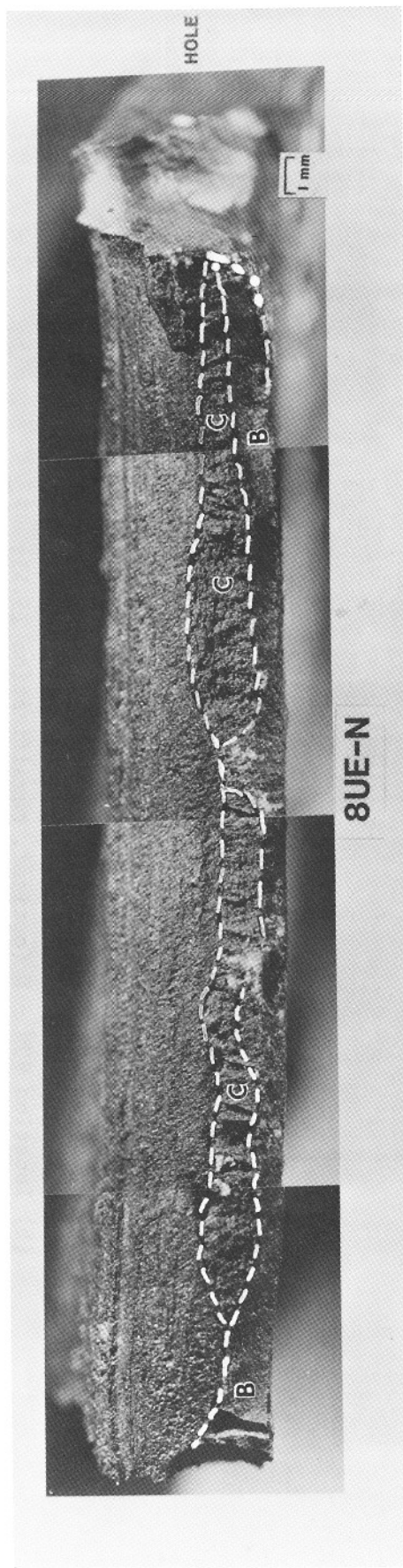


(b)

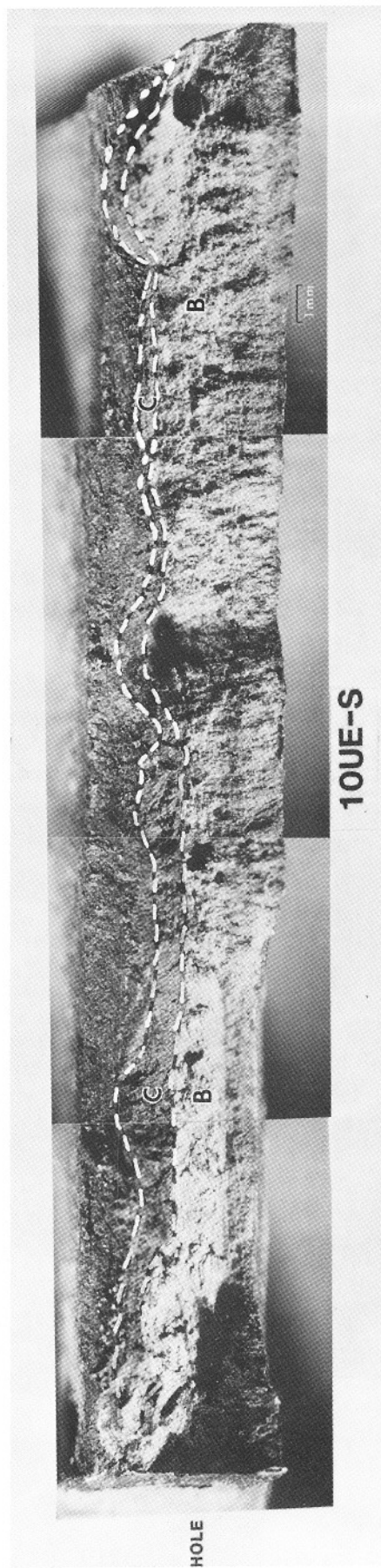
Figure 8.20 One half of box beam lower fracture surface between outer and inner hanger rod holes.

(a) location 9UE - S (optical, magnification X5.5)

(b) location 9UW - N (optical, magnification X5.5)



(a)

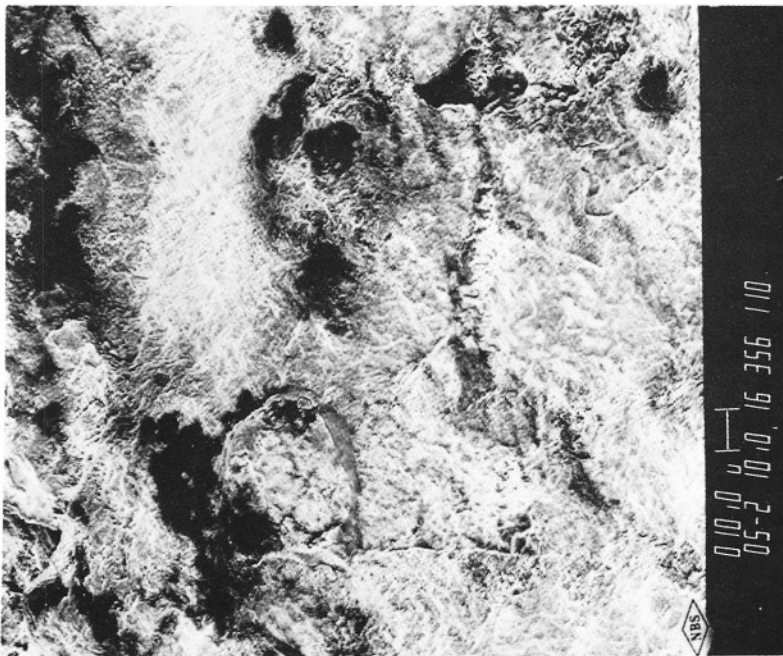


(b)

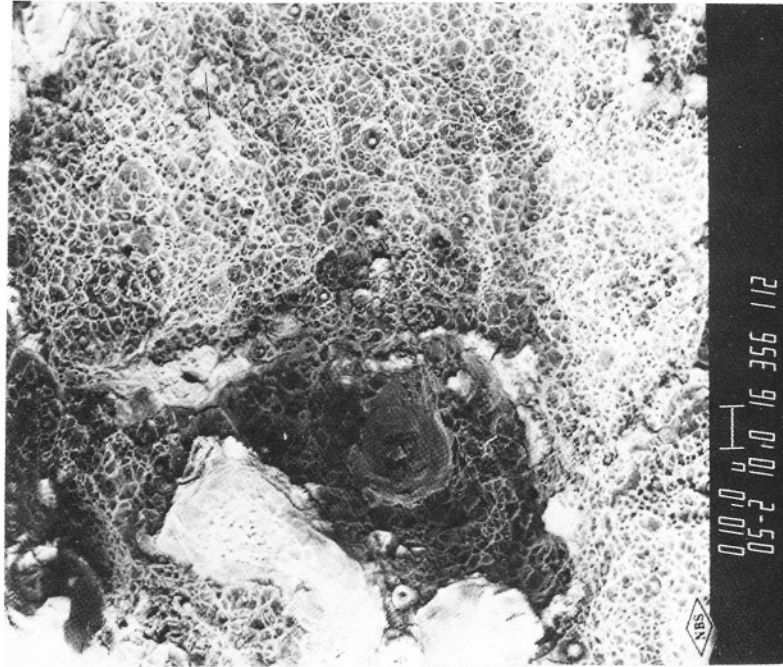
Figure 8.21 One half of box beam lower fracture surface between outer and inner hanger rod holes.

(a) location 8UE - N (optical, magnification X5.5)

(b) location 10UE - S (optical, magnification X5.5)



(a)



(b)

Figure 8.22 Fracture appearance in the preexisting crack region (a) and in the region of final crack propagation (b) at location 9UE adjacent to the outer hanger rod hole. Magnification X550.



## 9. STRUCTURAL ANALYSIS

### 9.1 INTRODUCTION

The walkway design loads and the loads believed to have been acting on the walkways at the time of collapse are discussed in this chapter. Also discussed are the adequacy of structural components and connections, walkway deflections and the significance of dynamic loads.

Section 9.2 addresses dead loads, design live loads and the upper-bound live loads associated with walkway occupancy at the time of collapse.

Section 9.3 presents the results of analyses carried out on walkway components and connections to establish their compliance with the project specifications as set out in reference 2.1. Forces believed to have been acting on the box beam-hanger rod connections at the time of collapse are addressed in section 9.4. Section 9.5 describes the procedure used to determine walkway deflections at the hanger rod locations due to dead load. Section 9.6 considers the matter of dynamic excitation of the walkways and the significance of dynamic effects when compared with the static loads discussed in section 9.2. Findings reported in this chapter are summarized in section 9.7.

### 9.2 LOADS

In this section the walkway design loads and the loads believed to have been acting on the walkway system at the time of collapse are discussed. While the loads at the time of collapse will never be known exactly, it is possible to place reasonable bounds on their intensity and distribution. For purposes of structural analysis and comparisons with code-specified design loads, it is convenient to differentiate between dead load and live load. Each of these load categories is discussed separately in the following subsections.

#### 9.2.1 Dead Load

The dead load includes the weight of all structural and architectural components and materials that are permanently fastened to or supported by the walkways. Normally the dead loads can be determined with sufficient accuracy simply

by preparing a list of quantities of materials from "as built" drawings and then calculating total weights from nominal unit weights. As has been discussed in section 5.3.6, the observed variability in the thickness of the concrete deck and topping material, the limited number of representative thickness measurements that could be made, and uncertainty with regard to unit weights prompted the weighing of selected walkway spans.

The approach used to obtain dead load estimates was to take the total weights of the damaged spans as listed in table 5.9 and deduct the estimated weights of all walkway materials, including all debris on the decks, but excluding the concrete deck with topping, shear studs and welded wire fabric. Weights of the damaged concrete decks so calculated were then corrected for loss of concrete and topping material during the collapse or during the rescue operation. The total weight of each span prior to collapse was then estimated by adding on the weights of all materials other than the deck that went into the "as built" configuration. Details of these calculations are presented in section A9.2.1 of the appendix. It should be pointed out that any errors in estimating weights of other materials attached to the damaged spans are reflected in the estimated concrete deck weights.

Results of these calculations are presented as estimated weights of undamaged spans in table 9.1. Allowing for the second to fourth floor hanger rods, the upper walkway spans average some 550 lbs (249 kg) more than the lower spans. This is consistent with the observation that more topping material was used to level the upper decks. With regard to errors in the estimated span weights, it is to be expected that the gypsum board could be a major contributor. Even though selected gypsum board assemblies were weighed, it is likely that the estimated weights are in error by as much as  $\pm 5$  percent. This is also the case for other walkway components and architectural features such as the hand-rail assembly, footlights and carpeting. Weights of structural shapes could be expected to vary from their nominal weights by  $\pm 2.5$  percent. Based on this, errors in the estimated span weights of the order of  $\pm 300$  lbs (136 kg) are to be expected.

To provide an independent check on the above calculations, the estimated concrete deck weights from table 9.1 are compared with calculated deck weights based on a nominal deck thickness of 3 1/4 in (83 mm) and an air-dry unit weight of 113.5 pcf (1,820 kg/m<sup>3</sup>) for the concrete as was determined in section 7.6. An allowance of 200 lbs (91 kg) per span has been made to account for the weight of shear studs and welded wire fabric. For a valid comparison, it is necessary to deduct the weight of the topping material from the estimated deck weight as is indicated in table 9.2. This adjustment is based on the topping thicknesses listed in table 5.12 and on an air-dry unit weight of 116.8 pcf (1,870 kg/m<sup>3</sup>) for the topping material.

It is seen from table 9.2 that the estimated deck weights (excluding span L8-9) average 500 lbs (227 kg) more than the calculated weights. In the case of span U8-9, this difference is 1,130 lbs (513 kg). If the average thickness of the concrete cores (table 7.17) is substituted for the nominal deck thickness, the calculated deck weights increase by approximately 150 lbs (68 kg), resulting in an average difference between estimated and calculated deck weights of

350 lbs (159 kg). In view of the uncertainties involved in assessing the weights of the damaged spans, the topping thickness, and the unit weight of the topping material, this difference is not considered to be excessive. Based on the average estimated deck weight of 39.0 psf (190 kg/m<sup>2</sup>) for seven spans, the deck weight and total in-place weight of span L8-9 have been back-calculated as indicated in tables 9.1 and 9.2. From table 9.1, the average estimated in-place weight of a walkway span is 17,750 lbs (8,050 kg).

In design calculations, the precise unit weights would not be known. If a nominal unit weight of 110 pcf (1,760 kg/m<sup>3</sup>) is assumed for lightweight concrete and if no allowance is made for the weight of the topping material, the calculated weight of the concrete deck with shear studs and welded wire fabric averages 8,400 lbs (3,810 kg) per span. Assuming that the weight of all other materials that make up a walkway span are as listed in table 9.1, the nominal dead load due to each upper walkway span would be about 16,500 lbs (73 kN), and about 200 lbs (890 N) less for the lower walkway spans, as will be described in further detail in section 9.3.1. Thus the actual span weights would, on average, exceed the nominal span weight by approximately 1,300 lbs (590 kg), or about 8 percent.

In section 2.7 it was noted that a modification of the walkways, involving the addition of gypsum board to meet fire endurance requirements, was agreed to on April 4, 1978. It was also noted in section 2.4 that structural drawings S303 through S305 were issued March 30, 1978. Although these same drawings were issued for review on May 26 and June 30, 1978, it is not clear what, if any, changes were made to the walkway structural details because of the addition of gypsum board. Failure to account for this component of the dead load could be significant as can be seen in table 9.3 which lists the principal contributions to the dead load for a typical walkway interior span.

#### 9.2.2 Live Loads

Live loads are those loads produced by the use and occupancy of the structure. They include loads produced during maintenance and during the life of the structure by movable objects and by people. The project design criteria listed on structural drawing S601 imply a walkway design live load of 100 psf (4.79 kPa). Section 2306 of the Uniform Building Code [2.3] allows for the reduction of unit live loads based on the extent of floor area supported by a structural member. However, it specifically excludes live load reductions in the case of places of public assembly or where the design live loads are in excess of 100 psf. The atrium and adjoining balconies in the hotel tower section and function block are clearly places of public assembly. The walkways are located within and connect places of public assembly and, therefore, it would be inappropriate to apply a live load reduction factor.

In section 4.4 an assessment was made of the second floor walkway occupancy based on the analysis of selected videotape frames. It was concluded that approximately 40 people occupied this walkway shortly before the collapse. In addition, it was concluded that 63 people, distributed as indicated in table 4.1, represented a credible upper bound for the combined second and fourth floor walkway occupancy at the time of collapse. To translate this occupancy

into an equivalent distributed live load, it is necessary to make certain assumptions regarding body weight and centroidal position. Data presented in reference 9.1 and summarized in reference 9.2 suggests a body weight of 159 lbs (72 kg) for an average adult. Reference 9.3 presents data on centroidal locations (also summarized in reference 9.2) which suggest that for people standing along the walkway railing, the distance from railing to body center of gravity is approximately 16 in (406 mm). Given the box beam dimensions of figure 3.10, it follows that approximately 80 percent of the live load distributed along the east railing as described above is carried by the east line of walkway hanger rods and end supports. Live loads due to people standing near the center of the walkway were assumed to be distributed equally between the east and west line of walkway hanger rods and end supports.

Using the average body weight and centroidal location indicated above, the upper-bound walkway occupancy described in table 4.1 is translated into east and west live load components acting in the plane of the fourth floor to ceiling hanger rods. These loads, which in the following analysis are assumed to be uniformly distributed over the length of a given span, are listed as total span live loads in table 9.4.

### 9.3 ANALYSIS OF WALKWAY STRUCTURAL COMPONENTS

#### 9.3.1 General

As a part of this investigation, the walkway structural components and their connections were checked for compliance with the project specifications [2.1]. Specifically, this involved the checking of structural details and stresses against the geometric limitations and working stress provisions of the AISC Specification for the Design, Fabrication and Erection of Structural Steel for Buildings [2.4] using the nominal dead load and specified design live load discussed in section 9.2. In this analysis the walkway system was assumed to be statically determinate, i.e., all stringer to box beam connections and the shear connections at column line 7 were considered to be pinned. The nominal dead loads are based on a unit weight of 110 pcf (1,760 kg/m<sup>3</sup>) for concrete, a deck thickness of 3 1/4 in (83 mm) and the estimated weight of all other materials for each span as listed in table 9.1. The area over which the 100 psf (4.79 kPa) live load acts is based on the clear width of walkway (inside face to inside face of railing glass) which is 8.25 ft (2.51 m) for the second and fourth floor walkways. These loads are listed in table 9.5. Under the combined action of nominal dead load and design live load, the maximum load acting on a fourth floor box beam-hanger rod connection would be 40.7 kips (181 kN). The maximum load on a second floor box beam-hanger rod connection would be 20.3 kips (90 kN). From this analysis of the walkway system, it was concluded that the box beam-hanger rod connections and the fourth floor to ceiling hanger rods do not satisfy the requirements of the AISC Specification.

#### 9.3.2 Box Beam-Hanger Rod Connections

The box beam-hanger rod connection detail used in the walkway construction is not among the connection details suggested in the AISC Manual of Steel Construction [9.4]. Without a properly validated analytical model or supporting

test data, there can be no reasonable certainty as to the load capacity of such a connection.

The hanger rods apply concentrated loads to the flanges of the box beam. It is well recognized that concentrated loads may cause a problem in steel structures unless their effects are taken into account properly in design. Section 1.10 of the AISC Specification addresses this point. Section 1.10.5 indicates that bearing stiffeners shall be provided, where required, at points of concentrated load. Section 1.10.10 limits the compressive stress at the web toe of fillets resulting from concentrated loads not supported by bearing stiffeners to  $0.75 F_y$ ; otherwise, bearing stiffeners shall be provided. It is common practice to limit this compressive stress by providing a bearing plate for the concentrated load. The purpose of these provisions is to distribute the effects of concentrated load over a larger area of the structural member and, by doing so, prevent instability or local plastification of the web. It is implicit in these provisions that the loads are applied in the plane of the web. These provisions do not anticipate intentional and significant eccentricities of applied load, as in the case of the box beam-hanger rod connections.

The absence of any stiffeners or bearing plates in the box beam-hanger rod connections indicates that the effects of concentrated load were not given proper attention. By depending solely on the channel flanges to transfer load from the hanger rod to the webs, there can be no assurance that the webs are stable or that the web stresses are not critical. It is therefore concluded that this connection detail does not satisfy the intent of the AISC Specification with regard to the proportioning of such connections.

### 9.3.3 Hanger Rods

With regard to hanger rod stresses, section 1.5.2 of the AISC Specification allows a tensile stress equal to  $0.60 F_y$  applied to a tensile stress area equal to

$$0.7854 D - \frac{0.9743}{n}^2$$

where  $D$  is the major thread diameter and  $n$  is the number of threads per inch. For the 1 1/4 in (32 mm) diameter rods used in the walkway construction,  $F_y = 36$  ksi (250 MPa) and the allowable load per hanger rod is 21.3 kips (95 kN). The combined nominal dead loads and design live loads of table 9.5 call for a design capacity of 20.3 kips (90 kN) for the second to fourth floor hanger rods and 40.7 kips (181 kN) for the fourth floor to ceiling hanger rods. Under dead load alone, the fourth floor to ceiling hanger rods are loaded to approximately 75 percent of allowable design load. The required design capacity for the third floor walkway hanger rods would be approximately 23.1 kips (103 kN).

### 9.3.4 Summary of Analysis

To summarize the analysis of walkway components under the action of nominal dead load plus specified design live load, it is concluded that without a

properly validated analytical model or supporting test data, there can be no reasonable certainty as to the load capacity of the box beam-hanger rod connection used in the walkway construction. It is further concluded that the connection detail does not satisfy the intent of the AISC provisions for the proportioning of such connections.

With regard to hanger rods, it is concluded that the second to fourth floor hanger rods complied with the the AISC provisions for allowable stresses, but the fourth floor to ceiling hanger rods and the third floor walkway hanger rods did not.

#### 9.4 FORCES ACTING ON THE HANGER RODS AT TIME OF COLLAPSE

A two-dimensional finite element representation of the walkway system was used to obtain estimates of forces acting on the hanger rods at the time of collapse. At the box beams it was assumed that the length of channel flanges acting in longitudinal walkway bending induced by the stringers was equal to 30 times the average flange thickness. Both top and bottom box beam flanges were assumed to be effective. This is consistent with the idealization used in the dynamic analysis to be discussed in section 9.6.1. For the distribution of loads applied after placement of the concrete deck, composite action was assumed. The transformed section for one stringer was based on an effective width of concrete deck equal to the sum of the stringer flange width and six times the total depth of the deck [9.4]. The walkways were assumed to be pin-connected at column line 7 and the hanger rod stiffnesses were modified to account for the load/deformation characteristics of the box beam-hanger rod connections as described in chapter 6. The computer code used in the analysis is an in-house version of GIFTS [9.5].

Dead loads due to the span weights listed in table 9.1 were applied in three stages. The first stage loading included the hanger rods, structural steel and formed steel deck. Loads were distributed to the hanger rods with the assumption that the connections at the ends of each stringer were pinned. The second stage loading consisted of the concrete deck weights without topping material as listed in table 9.2. In this case the box beam flanges were considered to be acting in longitudinal walkway bending as previously described. The final stage included the topping material and all other walkway components with the stringers and deck assumed to be acting as a composite.

The two-dimensional finite element model of the walkway system was also used to distribute the upper-bound live loads of table 9.4 to the hanger rods and walkway end supports. Implicit in this approach is the assumption that the east and west halves of the walkway system are uncoupled and compatibility between east- and west-side vertical deflections can be ignored. In view of the small load differential between east and west sides as indicated in table 9.4, this is not considered to be a serious limitation. The resultant forces acting on the walkway hanger rods and end supports due to combined dead load and upper-bound live load are listed in table 9.6. It is seen from table 9.6 that the estimated maximum load acting on a fourth floor to ceiling hanger rod is 21.4 kips (95 kN)

at location 8UE. The estimated maximum load acting on a second to fourth floor hanger rod is 11.5 kips (51 kN) at location 8LE.

## 9.5 WALKWAY DEFLECTIONS

Walkway dead load deflections at the hanger rod positions are listed in table 9.7 according to the composition of span weight listed in table 9.3. Although little information is available regarding the walkway construction sequence, it is reasonable to assume that the walkways were brought into final vertical alignment after placement of the formed steel deck. Subsequent placement of the concrete and topping material would have caused an initial vertical displacement of approximately 0.33 in (8.4 mm) at location 9L. Addition of the handrail assembly would have increased this to 0.41 in (10.5 mm) and the addition of gypsum board and various finish materials would have resulted in a total vertical displacement of approximately 0.5 in (13 mm) at location 9L. As has been noted in section 3.4, the handrail assembly was adjusted to compensate for midspan deflections, and it is reasonable to assume that a similar procedure was followed during installation of the gypsum board. Thus the cumulative displacements due to dead load would be apparent only at the hanger rod locations. Given the length of the walkways, it is doubtful that these displacements, if detected, would have been cause for concern.

## 9.6 EFFECTS OF DYNAMIC EXCITATION

Thus far in this chapter the emphasis has been on statically applied loads and their effect on various components of the walkway system. As has been noted in chapter 4, there was at least one report of people dancing on the walkways at the time of collapse. It is the purpose of this section to examine the dynamic characteristics of the walkways, the manner in which activities such as dancing could have excited the walkway system, and the significance of the resulting forces when compared with the static load effects discussed earlier in this chapter.

### 9.6.1 Dynamic Characteristics of the Walkways

Preliminary to investigating the role of dynamic excitation in the collapse, the walkway system, consisting of the second and fourth floor walkways, was modeled analytically to determine the undamped natural frequencies. This work, which involved the development of a three-dimensional discrete element analytical model, is reported in reference 9.6.

Procedures used in the analysis were verified by modeling the third floor walkway first. Results were then compared with field measurements reported in reference 2.5. Essential features of the idealized third floor walkway are as follows:

- Walkway end supports: All supports are constrained in the vertical direction. No rotational constraints are imposed. North-south translation is constrained at location 7ME. East-west translation is constrained at locations 7ME and 11ME.

- Longitudinal beams: Assumed to be of continuous composite construction (W16 x 26 stringer and portion of concrete deck). Longitudinal continuity is provided at each box beam by a short flexural element consisting of portions of the deck and of the top and bottom flanges of the box beam.
- Deck: Portions of composite concrete deck act with longitudinal beams in resisting vertical and horizontal flexure. Deck also provides horizontal shearing resistance and, for this purpose, is idealized as an equivalent truss web of crossed diagonals.
- Masses: Masses are lumped at the nodes which correspond to the locations of the stringer to box beam and stringer to cross beam connections. Assumed weight per span is 19,000 lbs (8,620 kg). Live load is assumed to be zero.

Calculated and measured dynamic characteristics of the third floor walkway are compared in table 9.8. For those modes that could be clearly identified in the measured acceleration spectra of reference 2.3 the agreement is exceptionally good.

With this confirmation of the analytical technique, the next step was to model the second and fourth floor walkways as a combined system using essentially the same idealization outlined above. In the resulting model there were 610 static and 120 dynamic degrees of freedom. Two cases were considered: (1) dead load equal to 17,500 lbs (7,940 kg) per span and (2) dead load plus a superimposed live load of 20 psf (958 Pa). Results of these analyses for the first 10 modes and the second horizontal mode (mode no. 17) are listed in table 9.9. Note that the first two modes are essentially identical and correspond to horizontal excitation of the second and fourth floor walkways, respectively.

Three other frequencies associated with the walkway system are of interest in assessing dynamic effects:

- In addition to those constraints as described for the third floor walkway end supports, constraints on north-south and east-west translations at locations 7UW and 7LW.
  - Dead load only, first horizontal mode.  $f = 4.98$  Hz
  - Dead load plus superimposed live load of 20 psf (960 Pa), first horizontal mode.  $f = 4.43$  Hz
- Simply supported walkway stringer with corresponding dead load, vertical mode.  $f = 8.24$  Hz
- Vertical vibration of hanger rod and masses due to dead load on associated second and fourth floor influence areas (2 degrees of freedom).  $f = 8.11$  Hz

### 9.6.2 Sources of Dynamic Excitation

In assessing the significance of dynamic excitation, the walkway system is considered to be represented adequately by a single degree of freedom, viscously damped system. The magnification factor, or ratio of the dynamic deflection to the zero frequency deflection, is determined for the frequency of harmonic excitation using the most critical walkway natural frequency. The ratio of the induced force to the applied force is taken to be equal to the magnification factor.

Given the range of frequencies of the walkway system, both steady state harmonic oscillations and transient vibrations need to be addressed. Considering first the case of harmonic oscillations, the lowest natural frequency of the walkway system in the vertical mode is 6.6 Hz for the case of a 20 psf (958 Pa) live load. The corresponding frequency for the upper-bound live load, assumed to be uniformly distributed over the two walkways, is approximately 7.1 Hz. Estimates of the damping ratio, obtained from time histories of the third floor walkway vertical mode accelerations presented in reference 2.5, ranged from 0.012 to 0.028. Considering the fact that these time histories were obtained at very low levels of response, it is reasonable to select a damping ratio of at least 0.02 for this analysis.

Although no reference to actual measurements of dynamic excitation associated with dancing could be found in the literature, reference 9.7 presents response spectra for floor systems excited by a person treading at a fixed point. For lack of a better model, this motion will be taken as an acceptable approximation of vertical motions due to dancing. A recording of the music being played at the time of the collapse was analyzed and the tempo corresponds to a treading frequency of about 1.1 Hz. For a natural frequency of 7.1 Hz and a damping ratio of 0.02, the magnification factor from reference 9.7 is 0.6. Taking the dynamic component of the treading load to be equal to body weight as suggested by reference 9.7, the corresponding effective dynamic force is 0.6 times 159, or 95 lbs (422 N) per person. The force imposed on a hanger rod would depend upon the mode shape of the walkway system and body location, but it can be conservatively taken to be divided equally between a hanger rod pair, or 95 lbs (422 N) per hanger rod for each couple dancing.

While the effects of horizontal vibrations on hanger rod forces would be expected to be negligible, they are examined here for completeness. It is shown in reference 9.6 that the walkways essentially respond as uncoupled structures. From table 9.9, the lowest natural frequency for the horizontal mode is 2.87 Hz for the case of a 20 psf (958 Pa) live load. The corresponding frequency for the estimated fourth floor walkway dead load and upper-bound live load is approximately 3.2 Hz. Taking the frequency of the horizontal excitation to be one-half that of the vertical excitation, or 0.55 Hz, the corresponding magnification factor is 1.03. When the north-south and east-west translations at location 7UW are constrained (pinned connections at column line 7), the natural frequency is approximately 4.9 Hz and the magnification factor is 1.01. Assuming the higher harmonics of the horizontal component of forces applied by dancing to be negligible, the walkway would be expected to respond in a quasi-static manner. Reference 9.8 presents data that suggest a horizontal component

of contact force equal to 32 percent of body weight for the case of right angle turns while walking. Using this to approximate the horizontal component of force due to dancing, the corresponding applied force would be approximately 100 lbs (445 N) for each couple dancing. Unlike the vertical forces, the horizontal forces would tend to be randomly directed and would not be directly additive.

Based upon this brief analysis, it does not appear that dancing involving a reasonable number of walkway occupants would give rise to steady state oscillations that would warrant a more detailed analysis.

Transient vibrations arise from impulse loads such as heel drop (sudden release from tiptoe position, landing on heels). These forces are of short duration (less than 0.060 sec) and their magnitude is strongly influenced by the hardness of the contact surface. Reference 9.7 presents response spectra for heel drop loading on floor systems and suggests a contact force equal to 3.75 times the static contact force. The largest magnification factors occur at natural frequencies of approximately 16 Hz. In section 9.6.1 the vertical mode frequencies for a simply supported walkway stringer and a hanger rod with tributary masses are listed as 8.24 and 8.11 Hz, respectively. Taking a heel drop directly adjacent to a hanger rod as the worst case, the corresponding magnification factor from reference 9.7 is approximately 1.05. With body position taken to be along the railing as described in section 9.2.2, the increase in hanger rod loading due to heel drop would be approximately  $0.8[(1.05)(3.75)(159) - 159] = 375$  lbs (1.7 kN). Because of their short duration time, simultaneous heel drops by two or more people would be difficult to achieve.

Considering the fact that the fourth floor box beam-hanger rod connections would respond inelastically at a load level equal to dead load plus upper-bound live load and the fact that the walkway surface was covered with a commercial grade carpet and underlying pad, the actual increase in hanger rod load would be less than 375 lbs. With only a modest attenuation of -3dB, the increment of hanger rod load due to heel drop would be reduced to approximately  $0.71 \times 375 = 265$  lbs (1.2 kN) or about 1 percent of the average hanger rod load at the fourth floor level under dead load plus upper-bound live load (see table 9.6). This is within the range of uncertainty for estimates of span weights as pointed out in section 9.2.1.

## 9.7 SUMMARY

Based on load data, relevant codes and standards, and analytical studies, the following conclusions regarding the walkway system were drawn:

1. The average estimated in-place weight of a walkway span is 17,750 lbs (8,050 kg).
2. Actual span weights would, on average, exceed the nominal span weights by approximately 1,300 lbs (590 kg) or about 8 percent.

3. Under the combined action of nominal dead load and design live load, the maximum load acting on a fourth floor box beam-hanger rod connection would be 40.7 kips (181 kN). The maximum load on a second floor box beam-hanger rod connection would be 20.3 kips (90 kN).
4. The box beam-hanger rod connection detail used in the walkway construction does not satisfy the intent of the AISC provisions for the proportioning of such connections.
5. The fourth floor to ceiling hanger rods and the third floor walkway hanger rods do not comply with the AISC provisions for allowable stresses.
6. The maximum load believed to have been acting on a fourth floor to ceiling hanger rod at the time of collapse is approximately 21.4 kips (95 kN) at location 8UE. For the second to fourth floor hanger rods, this load is approximately 11.5 kips (51 kN) at location 8LE.
7. The maximum walkway deflection due to dead load was approximately 0.5 in (13 mm).
8. Dynamic loads induced by walking or dancing on the walkways would not have been significant in comparison to the static loads.

Table 9.1 Summary of Span Weights

Span Number	Weight in Damaged Condition (lbs)			Estimated Weights of Undamaged Spans (lbs)		
	Measured Span Weight	Calculated Weights of Materials Other Than Deck	Concrete Deck <sup>(a)</sup>	Concrete Deck <sup>(a)</sup>	All Other Materials	Total Weight of Span
U7-8	15,760	6,130	9,630	9,630	8,090	17,720
U8-9	15,950	6,240	9,710	10,140	8,200	18,340
U9-10	14,600	4,850	9,750	9,950	8,210	18,160
U10-11	14,000	4,530	9,470	10,150	8,120	18,270
L7-8	15,130	5,630	9,500	9,500	7,960	17,460
L8-9	Span weight not measured			10,050 <sup>(b)</sup>	7,940	17,990
L9-10	14,160	4,800	9,360	9,380	7,950	17,330
L10-11	13,170	4,570	8,600	8,700	7,990	16,690

Note: (a) Includes topping material, shear studs and welded wire fabric.

(b) Deck weight based on average unit deck weight of all other spans as indicated in table 9.2.

1 lb = 0.4536 kg

Table 9.2 Comparison of Concrete Deck Weights Based on Measured Span Weights and on Measured Unit Weights

Span Number	Weight (lbs)			
	Estimated Weight of Deck <sup>(a)</sup> (see table 9.1)	Weight of Topping Material ( $\gamma = 116.8$ pcf)	Weight of Deck Without Topping <sup>(a)</sup>	Calculated Deck Weight <sup>(a)</sup> ( $\gamma = 113.5$ pcf)
U7-8	9,630	360	9,270	8,640
U8-9	10,140	450	9,690	8,560
U9-10	9,950	860	9,090	8,560
U10-11	10,150	1,080	9,070	8,650
L7-8	9,500	390	9,110	8,640
L8-9	10,050	990	9,060 <sup>(b)</sup>	8,560
L9-10	9,380	450	8,930	8,560
L10-11	8,700	90	8,610	8,650

Note: (a) Includes shear studs and welded wire fabric.

(b) Based on average unit deck weight of 39.0 psf for seven other spans.

1 lb = 0.4536 kg

1 pcf = 16.02 kg/m<sup>3</sup>

Table 9.3 Composition of Span Weight for Typical Walkway Interior Span

Walkway Component	Weight (lbs)	Percent of Total
Walkway deck <sup>(a)</sup>	9,880	55.0
Handrail assembly	2,450	13.6
Structural steel	2,370	13.2
Gypsum board	2,310	12.9
Other <sup>(b)</sup>	950	5.3
Total	17,960	100.0

Notes: (a) Includes topping material, shear studs and welded wire fabric.

(b) Includes formed metal deck, footlights, carpet, sprinkler pipes and aluminum slats.

1 lb = 0.4536 kg

Table 9.4 Upper-Bound Live Loads for Second and Fourth Floor Walkway Spans

Span Number	Resultant Live Load Acting in Plane of Hanger Rods	
	East Side (lbs)	West Side (lbs)
U7-8	382	95
U8-9	254	64
U9-10	127	32
U10-11	127	32
L7-8	2,162	1,018
L8-9	2,003	859
L9-10	1,590	636
L10-11	509	127

1000 lbs = 4.448 kN

Table 9.5 Span Loadings Based on Nominal Dead Load and Design Live Load

Span Number	Nominal Dead Load (lbs)	Design Live Load (lbs)	Total Design Load (lbs)
U7-8	16,500	24,400	40,900
U8-9	16,500	24,100	40,600
U9-10	16,500	24,100	40,600
U10-11	16,500	24,400	40,900
L7-8	16,300	24,400	40,700
L8-9	16,200	24,100	40,300
L9-10	16,300	24,100	40,400
L10-11	16,400	24,400	40,800

1000 lbs = 4.448 kN

Table 9.6 Forces Acting on Walkway Hanger Rods and End Supports  
Due to Combined Dead Load and Upper-Bound Live Load

Location	Dead Load Component (lbs)	Upper-Bound Live Load Component (lbs)	Total (lbs)
7UE	3,800	200	4,000
7UW	3,800	60	3,860
8UE	18,900	2,490	21,390
8UW	18,900	1,060	19,960
9UE	18,210	2,080	20,290
9UW	18,210	830	19,040
10UE	18,600	1,190	19,790
10UW	18,600	420	19,020
11UE	3,930	60	3,990
11UW	3,930	20	3,950
7LE	3,850	950	4,800
7LW	3,850	450	4,300
8LE	9,270	2,200	11,470
8LW	9,270	1,000	10,270
9LE	9,040	1,860	10,900
9LW	9,040	770	9,810
10LE	8,860	1,060	9,920
10LW	8,860	380	9,240
11LE	3,690	180	3,870
11LW	3,690	40	3,730

1000 lbs = 4.448 kN

Table 9.7 Walkway Vertical Displacements Due to Dead Load

Dead Load Component	Vertical Displacements (inches)			
	Location			
	8U&10U	9U	8L&10L	9L
Concrete deck and topping	.22	.23	.32	.33
Handrail assembly	.06	.06	.08	.08
Gypsum board	.05	.05	.08	.08
Other items	.01	.01	.02	.02

1 in = 25.4 mm

Table 9.8 Calculated and Measured Characteristics of the Third Floor Walkway

Mode No.	Calculated			Measured	
	Classification*	Period (Sec.)	Frequency (Hz)	Classification*	Frequency (Hz)
1	Hor.	.266	3.76	Hor.	3-3/4
2	Vert.	.127	7.88	Vert.	7
3	Tors.	.127	7.88		
4	Vert.	.122	8.20	Vert.	8-1/4
5	Tors.	.118	8.46		
6	Vert.	.112	8.91	Vert.	10
7	Vert.	.106	9.46		
8	Tors.	.103	9.70		
9	Tors.	.094	10.65		
10	Hor.	.068	14.64	Hor.	12

\* Predominant motion.

Table 9.9 Calculated Characteristics of the Second and Fourth Floor Walkways

Mode No.	Classification*	No Live Load		20 psf Live Load	
		Period (Sec.)	Frequency (Hz)	Period (Sec.)	Frequency (Hz)
1	Hor.	.310	3.23	.349	2.87
2	Hor.	.310	3.23	.349	2.87
3	Vert.	.135	7.42	.152	6.60
4	Vert.	.134	7.44	.151	6.62
5	Vert.	.129	7.76	.145	6.90
6	Tors.	.125	7.98	.141	7.10
7	Tors.	.124	8.03	.141	7.14
8	Tors.	.123	8.14	.138	7.23
9	Vert/Tors	.122	8.21	.137	7.30
10	Tors.	.122	8.21	.137	7.30
17	Hor.	.079	12.65	.089	11.25

\* Predominant motion.

## 10. INTERPRETATION OF TESTS, ANALYSES AND OBSERVATIONS

### 10.1 INTRODUCTION

This chapter evaluates the results of structural tests and the analysis of the walkway system for the purpose of determining the most probable cause of the collapse. The probable sequence of collapse, effect of change in hanger rod arrangement, and quality of materials and workmanship are also addressed.

Section 10.2 makes a direct comparison of estimated fourth floor box beam-hanger rod connection capacities with loads believed to have been acting on the connections at the time of collapse.

Section 10.3 compares the mean ultimate capacities of the box beam-hanger rod connections with the ultimate capacity that would be expected of a connection designed in accordance with the AISC Specification.

Section 10.4 combines observations of damage described in chapter 5 of this report to establish the probable sequence of the collapse.

Section 10.5 addresses the significance of the change from a continuous hanger rod to interrupted rods in the second and fourth floor walkway construction. Quality of materials and workmanship is discussed in section 10.6. The findings and conclusions of this chapter are summarized in section 10.7.

### 10.2 COMPARISON OF LOADS AND BOX BEAM-HANGER ROD CONNECTION CAPACITIES

A layout of the 6 fourth floor box beam-hanger rod connections is shown in figure 10.1. Two bar diagrams, one for load capacity of the connection and one for imposed load, are shown adjacent to each hanger rod. The bar diagram on the left side of the figure will be discussed in section 10.3.

Location 8UE is described in detail to illustrate the meaning of the diagrams. The bar diagram to the left of the hanger rod denotes load capacity of the connection. The range from 16.3 to 20.2 kips (73 to 90 kN) is the 95 percent confidence interval estimate for the ultimate capacity of this particular box beam-hanger rod connection based on tests conducted on NBS fabricated specimens

as reported in section 6.13. The estimated mean ultimate capacity of 18.2 kips (81 kN) is also shown. The connection at location 8UE was required to support forces imposed by combined dead and live load actions. These forces are shown in the bar diagram to the right of the hanger rod. Of the 6 fourth floor box beam-hanger rod connections, the connection at location 8UE was the most heavily loaded. The estimated dead load action at location 8UE is 18.9 kips (84 kN) and the contribution of the upper-bound live load at the time of collapse is 2.5 kips (11 kN), resulting in a total load of 21.4 kips (95 kN) as addressed in section 9.4 and as listed in table 9.6. Under the action of nominal dead load plus code-specified live load, this load would have been 40.7 kips (181 kN). Thus the maximum load acting on a fourth floor box beam-hanger rod connection at the time of collapse was 53 percent of what was required for design under the Kansas City Building Code.

Figure 10.1 presents similar information for the other fourth floor box beam-hanger rod connections. This figure shows that, with the exception of locations 8UE and 10UW, the estimated mean ultimate capacity of each fourth floor box beam-hanger rod connection either equals or slightly exceeds the estimated dead load effect. However, the estimated mean ultimate capacity is exceeded by the sum of the estimated dead load and upper-bound live load in every case.

As noted in section 6.12.2, the data base for connections tested using box beam specimens, nuts and washers removed from the walkway debris consists of only three points. When compared with the NBS box beam test series, all three points are within or near the 95 percent confidence band, but there is a tendency toward the upper limit of the band. The MC8 x 8.5 shapes used in the walkway box beams are slightly heavier than those used to fabricate the NBS specimens (see table 6.6). Of particular significance is the larger average web thickness (0.190 vs 0.184 in (4.83 vs 4.67 mm)) which would increase the bending resistance of the webs. It is also possible that the actual live load on the walkways at the time of collapse was less than the upper-bound live load used to arrive at the estimated hanger rod loads shown in figure 10.1. Recall from chapter 4 that approximately 40 people were observed on the second floor walkway shortly before the collapse and that 63 people are considered to be a credible upper bound on combined second and fourth floor walkway occupancy.

Regardless of these qualifications on estimated loads and ultimate capacities, it is clear that each of the 6 fourth floor box beam-hanger rod connections had a high probability of failure; each connection was a candidate for initiation of walkway collapse. Failure of any one of the connections would have been accompanied by a redistribution or transfer of load to other hanger rods. With no apparent significant reserve capacity to accommodate this redistribution, progressive failure of the remaining connections was assured. Thus, failure of any one connection would have led to complete collapse of the walkway system.

### 10.3 ULTIMATE CAPACITY BASED ON CODE REQUIREMENTS

It is important to point out that the load capacities described in figure 10.1 are ultimate values. As noted in section 9.3.3, the design load (estimated nominal dead load plus code-specified design live load) for a fourth floor to

ceiling hanger rod is 40.7 kips (181 kN). This is the load that should be used in a working stress approach to design in which the nominal strengths of materials are reduced by an appropriate factor of safety.

Because of the safety factor, the resulting connection would be expected to have an ultimate load capacity substantially higher than the working stress value of 40.7 kips (181 kN). Using a factor of safety of 1.67, which is the lowest value that would govern any part of the design of the box beam-hanger rod connections under the applicable provisions of the AISC Specification, it would be expected that the ultimate load capacity of the resulting connection would be at least 1.67 times 40.7, or 68 kips (302 kN). Thus any given box beam-hanger rod connection in the fourth floor walkway should have been able to support an ultimate load of at least 68 kips (302 kN) instead of the average ultimate capacity of 18.6 kips (83 kN) estimated for the 6 fourth floor walkway connections. Since the AISC Specification is the basis for the steel design provisions of the Kansas City Building Code, this same ultimate load capacity would be expected of a connection designed under the Kansas City Building Code. The hanger rod load to be applied in working stress design under the Kansas City Building Code and the expected ultimate load capacity are shown in the bar diagram on the left in figure 10.1.

#### 10.4 PROBABLE SEQUENCE OF COLLAPSE

While the collapse could have initiated at any of the connections, the physical evidence described in chapter 5 points to 9UE as the initiating point. To summarize that evidence, the observed mirror symmetry of distortions about box beam 9U is a compelling argument for initiation of collapse at column line 9. As has been discussed in sections 5.2.5 and 5.3.2, observations made in the atrium and on the debris at the warehouse strongly suggest that the west side box beam-hanger rod connections of each of the three fourth floor box beams failed after the corresponding east side connection.

The sequence of collapse is believed to have been loss of support at location 9UE with loads being transferred to locations 8UE, 9UW, and 10UE. It is not entirely certain which of these three connections failed next, but it is clear that all three box beams rotated downward about the west line of hanger rods. With the failure of connection 9UW, spans U8-9 and U9-10 would have rotated downward about box beams 8U and 10U, respectively, and in the process, would have pulled span U10-11 off of its bearing seats at column line 11. The nature of the clip-angle weld failures on box beam 9U suggests that spans U8-9 and U9-10 separated during their downward rotation. At that same time the fourth floor walkway would have experienced severe negative bending at column lines 8 and 10. However, the evidence suggests that the clip-angle welds at these locations did not fail until after the box beam-hanger rod connections at locations 8UW and 10UW had failed (see section 5.3.4). In both cases the clip-angle fillet welds fractured from bottom to top, indicating positive bending moments in the walkway at column lines 8 and 10. In the case of box beam 8U it is likely that positive moment was induced by the north end of span U8-9 striking the second floor walkway while span U7-8 was rotating downward about the shear connections at column line 7. The behavior of the second floor walkway

during the collapse is much less clear, but it is believed to have generally followed the progression of failure in the fourth floor walkway.

#### 10.5 EFFECT OF CHANGE IN HANGER ROD ARRANGEMENT

As has been noted in chapters 3 and 5, the hanger rod detail actually used in the construction of the second and fourth floor walkways is a departure from the detail shown on the contract drawings (Dwgs. A412 and A508). In the original arrangement each hanger rod was to be continuous from the second floor walkway to the hanger rod bracket attached to the atrium roof framing. The design load to be transferred to each hanger rod at the second floor walkway would have been one-half the sum of the dead load and the resultant live load for a single span, or approximately 20.3 kips (90 kN) (see table 9.5). An essentially identical load would have been transferred to each hanger rod at the fourth floor walkway. Thus the design load acting on the upper portion of a continuous hanger rod would have been twice that acting on the lower portion, but the required ultimate capacity of the box beam-hanger rod connections would have been the same for both walkways (20.3 kips).

As has been described in chapter 3, the hanger rod configuration actually used consisted of two hanger rods: the fourth floor to ceiling hanger rod segment as originally detailed and the second to fourth floor segment offset 4 in (102 mm) inward along the axis of the box beam (see figure 10.2). The washer and nut arrangement called for in the original connection detail as shown on Dwg. S405.1 was retained in the actual construction. With this modification the design load to be transferred by each second floor box beam-hanger rod connection was unchanged, as were the loads in the upper and lower hanger rod segments. However, the load to be transferred from the fourth floor box beam to the upper hanger rod under this arrangement was essentially doubled, thus compounding an already critical condition. The design load for the fourth floor box beam-hanger rod connection would be 40.7 kips (181 kN) for this configuration.

Had this change in hanger rod detail not been made, the ultimate capacity of the box beam-hanger rod connection would still have been far short of that expected of a connection designed in accordance with the AISC Specification. In terms of ultimate load capacity of the connection, the minimum value should have been 1.67 times 20.3 or 33.9 kips (151 kN). Based on test results reported in chapter 6, the mean ultimate capacity of a single-rod connection is approximately 20.5 kips (91 kN), depending on the weld area. Thus the ultimate capacity actually available using the original connection detail would have been approximately 60 percent of that expected of a connection designed in accordance with the AISC Specification. Note that, because of the greater dead load and design live load, the third floor walkway connection would have had approximately 53 percent of the expected ultimate capacity. Had the change in hanger rod arrangement not been made, the third floor walkway would have been the most critical of the three.

#### 10.6 QUALITY OF MATERIALS AND WORKMANSHIP

With the possible exception of the box beam longitudinal welds, there is no evidence to indicate that either quality of materials or quality of workmanship

played any significant role in initiating the collapse. As noted in chapter 7, tensile properties and chemical compositions of the walkway box beams and hanger rods were found to comply with the requirements of ASTM Standard A36 for structural steel which was specified. Microstructure and hardness of the box beam welds and the box beam and hanger rod materials were normal. Compressive strength of the lightweight concrete used in the walkway decks exceeded the requirement of the project design criteria.

Although misalignment of the embedded plates at column line 7 required a retrofit of the stringer bearing pads on the north span of the fourth floor walkway, direct measurements and observed scratch marks indicate that the walkways were properly aligned with the bearing seats prior to collapse. There was sufficient room to install a nut and washer on the lower end of each fourth floor to ceiling hanger rod, and there is clear evidence that all hanger rod washers were installed.

In general, the structural welding exhibited good workmanship. Although certain deficiencies were observed in the field welding of the clip angles to the embedded plates at column line 7, these connections experienced large rotational distortions prior to failure of the fillet welds, thus indicating good weld performance. Dimensions of fillet welds were, with few exceptions, in agreement with what was called for on the shop drawings.

The welding symbol and field observations relevant to the box beam longitudinal welds have been discussed in sections 3.3 and 5.3.3, respectively. As noted in section 3.3, the welding symbol used on the shop drawings is interpreted to require a prequalified partial joint penetration groove weld. However, the geometry of the mating surfaces as discussed in section 5.3.3 and as illustrated in figure 10.3 does not satisfy the dimensional tolerances for a prequalified partial joint penetration groove weld as stated in section 2.10 of AWS D1.1-79; the root face is less than 3 mm (Item 2.10.2.4), and the required minimum root opening was not provided.

For the case of an MC8 x 8.5 shape, flange thickness at the toe is approximately 3/16 in (5 mm). According to AWS D1.1-79 (table 2.10.3), the corresponding minimum effective throat for partial joint penetration groove welds is 3 mm. As noted in section 7.4.1 of this report, joint penetration averaged 2.2 mm at interior sections of the fourth floor walkway box beams. Data obtained from fracture surfaces at the ends of the box beams indicate average joint penetrations of from 1.5 to 2.4 mm in the region between the outer hanger rod hole and the beam end. Because of reductions in area at fracture, the latter represent minimum values of joint penetration.

To evaluate the significance of the weld actually provided, the effect on ultimate capacity of the box beam-hanger rod connections must be examined. For an effective throat of 3 mm and a weld length of 1 3/8 in (35 mm), the corresponding weld area is 105 mm<sup>2</sup>. From the plot of estimated peak upper rod load vs index weld area on figure 6.38, the expected ultimate capacity is approximately 17.3 kips (77 kN). With the contribution of the interior tack weld, estimates for the mean ultimate capacities of the actual fourth floor box beam-hanger rod connections range from 18.2 to 19.3 kips (81 to 86 kN).

Based on observations of the fracture surfaces and on the relationship between connection load capacity and index weld area, it is concluded that the actual connection load capacities were probably higher than the capacity that would be expected for a partial joint penetration groove weld having an effective throat of 3 mm and acting alone. It is therefore concluded that quality of workmanship did not play any significant role in initiating the collapse.

#### 10.7 SUMMARY

The following are the major points resulting from the structural tests, analysis, and observations of damage.

1. The maximum load acting on a fourth floor box beam-hanger rod connection at the time of collapse was 53 percent of what was required for design under the Kansas City Building Code.
2. With the exception of locations 8UE and 10UW, the estimated mean ultimate capacity of each fourth floor box beam-hanger rod connection either equals or slightly exceeds the estimated dead load effect. However, the estimated ultimate capacity is exceeded by the sum of the estimated dead load and upper-bound live load in every case.
3. Each of the 6 fourth floor box beam-hanger rod connections had a high probability of failure; each connection was a candidate for initiation of walkway collapse.
4. Failure of any one of the fourth floor box beam-hanger rod connections would have been accompanied by a redistribution or transfer of load to other hangers. With no apparent significant reserve capacity to accommodate this redistribution, progressive failure of the remaining connections was assured. Thus, failure of any one connection would have led to complete collapse of the walkway system.
5. The design of a fourth floor box beam-hanger rod connection under the AISC Specification would be expected to result in a connection with an ultimate capacity of at least 68 kips (302 kN). The average ultimate capacity of the 6 fourth floor walkway connections is estimated to have been 18.6 kips (83 kN).
6. Observed distortions of the fourth floor to ceiling hanger rods and the fourth floor walkway box beams strongly support the initiation of the collapse at box beam-hanger rod connection 9UE.
7. The change in hanger rod arrangement from a continuous rod to interrupted rods essentially doubled the load to be transferred by the fourth floor box beam-hanger rod connections.
8. For the continuous hanger rod arrangement, the design load to be transferred to each hanger rod at the second and fourth floor levels would have been approximately 20.3 kips (90 kN).

9. For the continuous hanger rod arrangement, a box beam-hanger rod connection designed in accordance with the AISC Specification would be expected to provide an ultimate capacity of at least 33.9 kips (151 kN).
10. Had the change in hanger rod arrangement not been made, the third floor walkway would have been the most critical of the three, the ultimate capacity of the connections being approximately 53 percent of that which would be expected of a connection designed in accordance with the AISC Specification.
11. Average joint penetration for the box beam longitudinal welds was less than that required by AWS D1.1-79 for a prequalified partial joint penetration groove weld. However, it is concluded that due to the presence of tack welds the actual ultimate capacities of the box beam-hanger rod connections probably were higher than would be expected for a partial joint penetration groove weld with the prescribed minimum effective throat acting alone.
12. There is no evidence to indicate that either quality of workmanship or materials played any significant role in initiating the collapse.

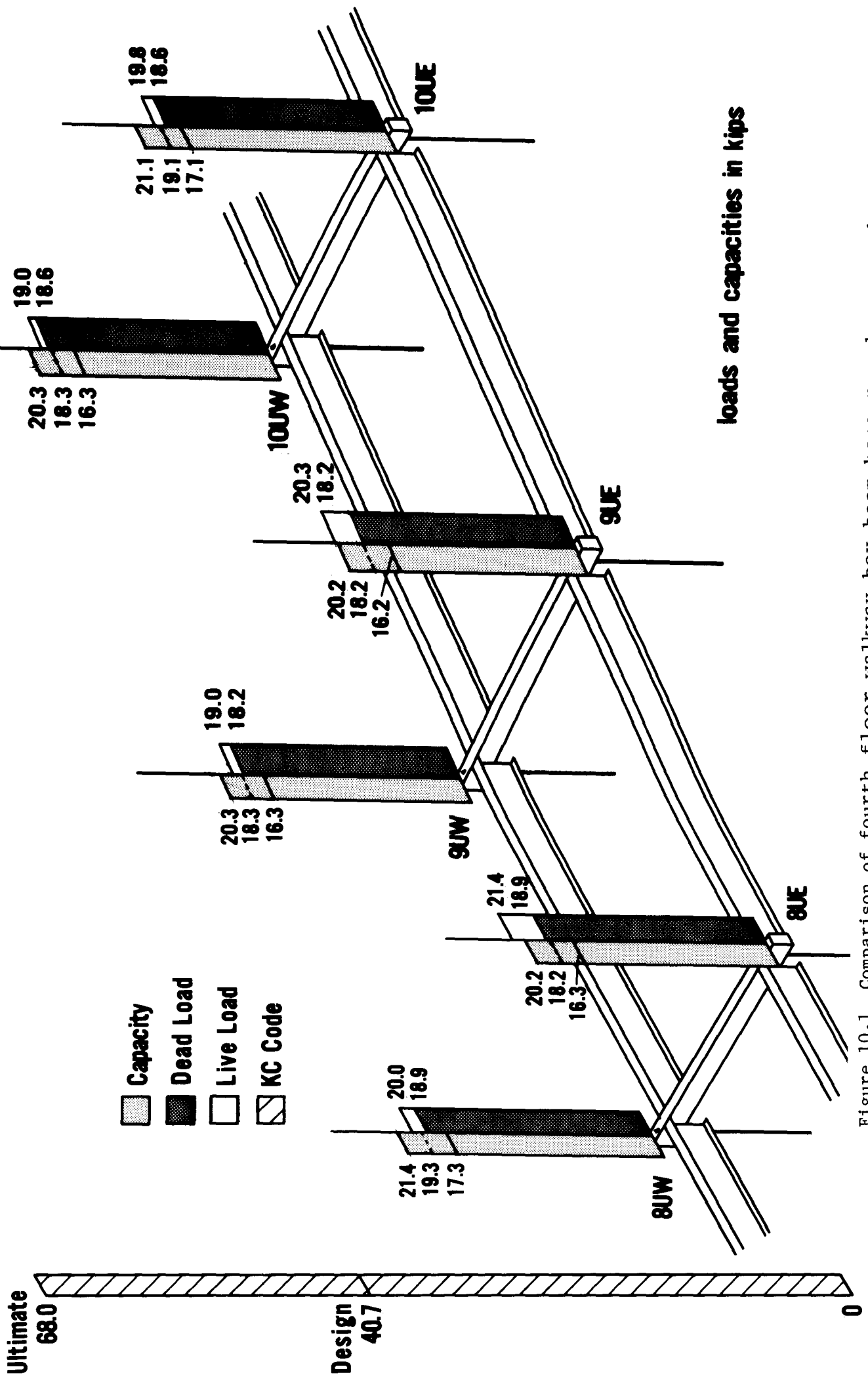
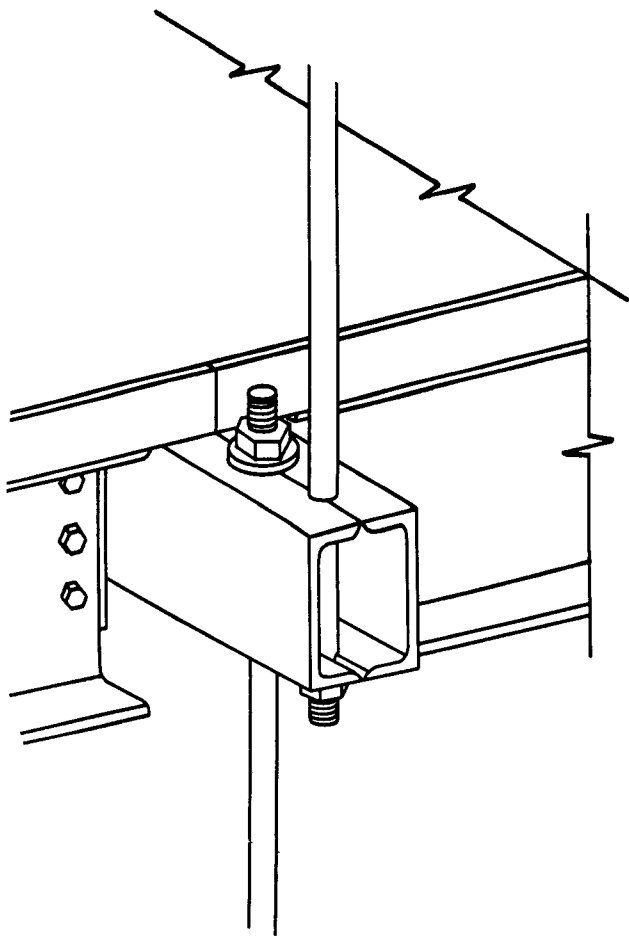
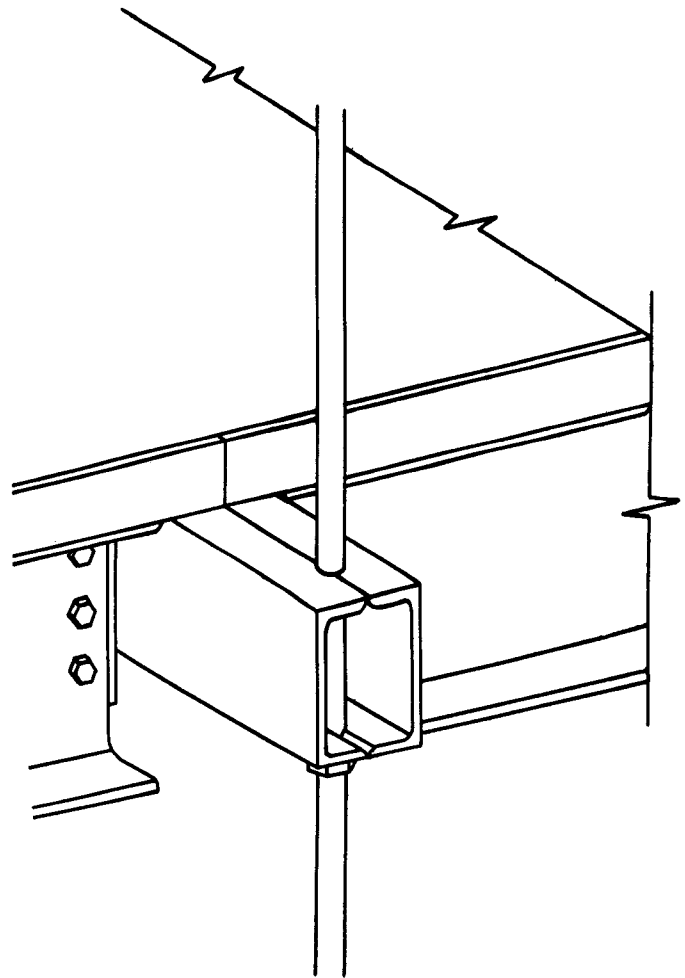


Figure 10.1 Comparison of fourth floor walkway box beam-hanger rod connection capacities with loads believed to have been acting at time of collapse.



As Built



Original Detail

Figure 10.2 Comparison of interrupted and continuous hanger rod details.

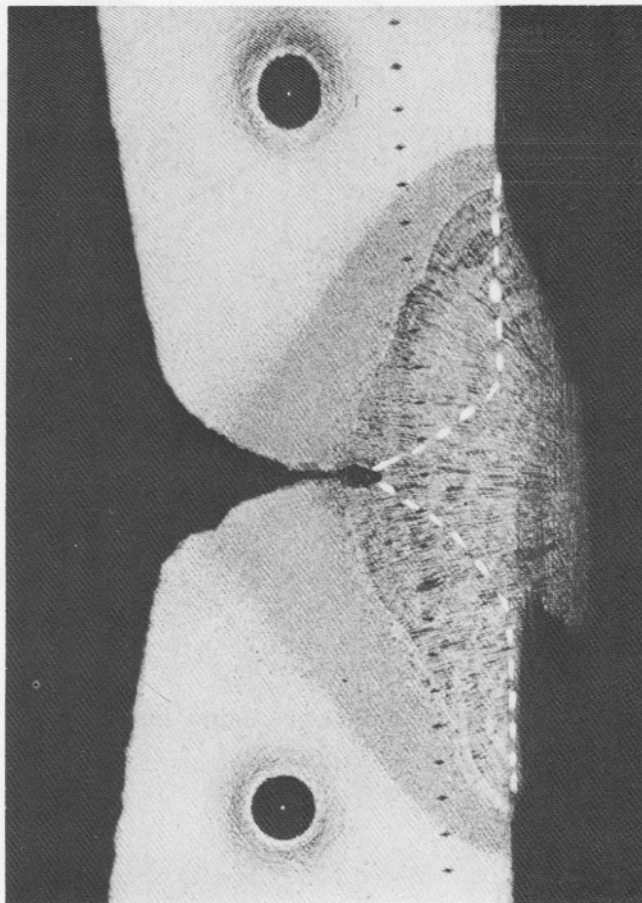


Figure 10.3 Cross section through weld region of walkway box beam 8L showing the exterior longitudinal weld joint at the bottom flange. Dotted lines indicate approximate original geometry of the flange toes. X8 1/2

## 11. SUMMARY AND CONCLUSIONS

Following the collapse of two suspended walkways within the atrium area of the Kansas City Hyatt Regency Hotel in Kansas City, Mo., Mayor Richard L. Berkley formally requested the National Bureau of Standards (NBS) to independently ascertain the most probable cause of the collapse. In response to this request, NBS carried out an extensive field investigation to reconstruct events preceding the collapse and to establish the condition of the walkways at the time of collapse. This included review of documents related to the design and construction of the walkways and measurements and inspections of the debris remaining after the collapse. NBS also conducted comprehensive laboratory studies of materials and mockups representative of the walkway construction and laboratory studies of specimens removed from the debris. These studies were supported by structural analyses of the walkways under the loading condition believed to have existed at the time of collapse. Conclusions drawn from this investigation are summarized in the following statements:

1. *Collapse of the walkways occurred under the action of loads that were substantially less than the design loads specified by the Kansas City Building Code.*
  - (a) It is concluded that a total of 63 people represents a credible upper-bound combined occupancy of the second and fourth floor walkways at the time of collapse.
  - (b) Based upon measured weights of damaged walkway spans, the dead load prior to collapse averaged 17.8 kips (79 kN) per walkway span. This is approximately 8 percent higher than the nominal dead load that would be estimated on the basis of the contract drawings.
  - (c) Dynamic loads induced by walking or dancing on the walkways would not have been significant in comparison to the static loads.

- (d) The maximum load (estimated dead load plus upper-bound live load) believed to have been acting on a fourth floor box beam-hanger rod connection at the time of collapse is 21.4 kips (95 kN). Under the action of nominal dead load plus code-specified live load, this load would have been 40.7 kips (181 kN). Thus the maximum load acting on a connection at the time of collapse was 53 percent of what was required for design under the Kansas City Building Code.
2. *The ultimate capacity of box beam-hanger rod connections can be predicted on the basis of laboratory test results.*
  - (a) Extensive structural tests show that ultimate capacity varies linearly with an index weld area.
  - (b) Welding process has little effect on ultimate capacity.
  - (c) Mean ultimate capacities of the fourth floor box beam-hanger rod connections were estimated on the basis of the NBS test series and these capacities ranged from 18.2 kips (81 kN) to 19.3 kips (86 kN) with an average value of 18.6 kips (83 kN).
3. *Under the action of the loads estimated to have been present on the walkways at the time of collapse, all fourth floor box beam-hanger rod connections were candidates for initiation of walkway collapse.*
  - (a) With the exception of locations 8UE and 10UW, the estimated ultimate capacity of each connection either equals or slightly exceeds the estimated dead load effect. However, the estimated ultimate capacity is exceeded by the sum of the estimated dead load and upper-bound live load in every case.
  - (b) Because of the small reserve load capacity of the connections and because of load redistribution that would have accompanied initial failure, progressive failure of the walkway system was assured.
4. *Observed distortions of structural components strongly suggest that failure of the walkway system initiated in the box beam-hanger rod connection at location 9UE (east end of middle box beam in fourth floor walkway).*
  - (a) The lower ends of the west side hanger rods were bent to the west, while those along the east side showed no such distortion, indicating that the box beam-hanger rod connections along the east side of the fourth floor walkway failed first.
  - (b) Mirror symmetry of distortions about the longitudinal axis of the middle box beam in the fourth floor walkway, coupled with the hanger rod distortions, indicate initiation of failure at location 9UE.
5. *As constructed, the box beam-hanger rod connections, the fourth floor to ceiling hanger rods, and the third floor walkway hanger rods did not satisfy the design provisions of the Kansas City Building Code.*

- (a) The AISC Specification for the Design, Fabrication and Erection of Structural Steel for Buildings forms the basis for the steel design provisions of the Kansas City Building Code.
  - (b) The box beam-hanger rod connection detail used in the walkway construction does not satisfy the intent of the AISC provisions for the proportioning of such connections.
  - (c) The design of a fourth floor box beam-hanger rod connection under the AISC Specification would be expected to result in a connection with an ultimate capacity of at least 68 kips (302 kN). The average ultimate capacity of the six fourth floor walkway connections as constructed is estimated to have been 18.6 kips (83 kN).
  - (d) The fourth floor to ceiling hanger rods and the third floor walkway hanger rods do not comply with the AISC provisions for allowable stresses.
6. *The change in hanger rod arrangement from a continuous rod to interrupted rods essentially doubled the load to be transferred by the fourth floor box beam-hanger rod connections.*
- (a) For the continuous hanger rod arrangement, the design load to be transferred to each hanger rod at the second and fourth floor levels would have been approximately 20.3 kips (90 kN).
  - (b) For the interrupted hanger rod arrangement, the design load to be transferred by a fourth floor box beam-hanger rod connection would have been 40.7 kips (181 kN) (see item 1(d)).
7. *The box beam-hanger rod connection would not have satisfied the Kansas City Building Code under the original hanger rod detail (continuous rod).*
- (a) See items 5(a) and 5(b).
  - (b) Under the original hanger rod arrangement (continuous rod), a box beam-hanger rod connection designed in accordance with the AISC Specification would be expected to provide an ultimate capacity of at least 33.9 kips (151 kN).
  - (c) Based on NBS structural tests, the mean ultimate capacity of a single-rod connection as detailed on the contract drawings is estimated to be 20.5 kips (91 kN).
  - (d) Had the change in hanger rod arrangement not been made, the third floor walkway would have been the most critical of the three, the ultimate capacity of the connections being approximately 53 percent of that which would be expected of a connection designed in accordance with the AISC Specification.

8. *Under the original hanger rod arrangement (continuous rod) the box beam-hanger rod connections as shown on the contract drawings would have had the capacity to resist the loads estimated to have been acting at the time of collapse.*
  - (a) The maximum load (estimated dead load plus upper-bound live load) believed to have been acting on a second floor box beam-hanger rod connection at the time of collapse is 11.5 kips (51 kN).
  - (b) The ultimate capacity of a single-rod connection is estimated to be 20.5 kips (91 kN) (see item 7(c)).
  
9. *Neither the quality of workmanship nor the materials used in the walkway system played a significant role in initiating the collapse.*
  - (a) Tensile properties and chemical compositions of the walkway box beam channels and hanger rod materials satisfy the requirements of ASTM Standard A36 for structural steel.
  - (b) Microstructure and hardness of the walkway box beam channels, box beam longitudinal welds, and hanger rod materials were normal.
  - (c) Average joint penetration for the box beam longitudinal welds was less than that required by AWS D1.1-79 for a prequalified partial joint penetration groove weld. However, it is concluded that due to the presence of tack welds the actual ultimate capacities of the box beam-hanger rod connections probably were higher than would be expected for a partial joint penetration groove weld with the prescribed minimum effective throat acting alone.
  - (d) Evidence indicates that hanger rod washers at locations 8UE and 9UE, missing after the collapse, had been installed.

## 12. REFERENCES

- 2.1 "Specifications, Hyatt Regency, Kansas City," PBNMML, Kansas City, MO, August 1978.
- 2.2 "Kansas City Building Code," Kansas City, MO, June 1, 1977.
- 2.3 "Uniform Building Code," 1976 Edition, International Conference of Building Officials, Whittier, CA, 1976.
- 2.4 "Specification for the Design, Fabrication and Erection of Structural Steel for Buildings," American Institute of Steel Construction, New York, NY, February 1969.
- 2.5 "Summary of Data from Vibration Testing of the Third Level Skybridge in the Kansas City Hyatt Regency Hotel," Wiss, Janney, Elstner and Associates Confidential Report WTE No. 81553 (with supplement of data), September 28, 1981, Northbrook, IL.
- 3.1 "Structural Welding Code-Steel," Third Edition, AWS D1.1-79, American Welding Society, Miami, FL, 1978.
- 5.1 "Miscellaneous Locations, Hyatt Regency Hotel, Kansas City, Jackson County, Missouri," The Tuttle-Ayers-Woodward Co., Project No. 220587, August 5, 1981, Kansas City, Missouri.
- 5.2 "Symbols for Welding and Nondestructive Testing," AWS A2.4-79, American Welding Society, Miami, FL, 1979.
- 6.1 "Welding Terms and Definitions," AWS A3.0-80, American Welding Society, Miami, FL, 1980.
- 6.2 Lipson, C. and Sheth, W. J., Statistical Design and Analysis of Engineering Experiments, McGraw Hill, New York, 1973.
- 7.1 Annual Book of ASTM Standards, Parts 4, 6, 10 and 14, American Society for Testing and Materials, Philadelphia, PA, 1981.
- 9.1 Diffrient, N., Tilley, A. and Bardagjy, J., Humanscale 1/2/3, MIT Press, Massachusetts Institute of Technology, Cambridge, MA, 1974.
- 9.2 Fattal, S. G., Cattaneo, L. E., Turner, G. E. and Robinson, S. N., "Personnel Guardrails for the Prevention of Occupational Accidents," NBSIR 76-1132, National Bureau of Standards, Washington, D.C., July 1976.
- 9.3 Swearingen, J. J., "Determination of Centers of Gravity of Man," Report 62-14, Aviation Medical Service, Federal Aviation Service, Oklahoma City, OK, August 1962.
- 9.4 Manual of Steel Construction, Seventh Edition, American Institute of Steel Construction, New York, NY, 1970.

- 9.5 Kamel, H. A. and McCabe, N. W., "Graphics-Oriented Interactive Finite Element Time-Sharing System," Version 5.0 User's Manual, University of Arizona, Tucson, AZ, May 1979.
- 9.6 McGuire, W., "Dynamic Response Characteristics of the Kansas City Hyatt Regency Hotel Skybridges," Consultant's Report to the National Bureau of Standards, December 3, 1981, Ithaca, NY.
- 9.7 Becker, R., "Simplified Investigation of Floors Under Foot Traffic," Journal of the Structural Division, ASCE, Vol. 106, No. ST11, Proc. Paper 15804, Nov. 1980, pp. 2221-2234.
- 9.8 Harper, F. C., Warlow, W. J. and Clarke, B. L., "The Forces Applied to the Floor by the Foot in Walking," National Building Studies Research Paper 32, Department of Scientific and Industrial Research, Building Research Station, London, 1961.

## APPENDIX

Presented here are additional graphic, tabular, and photographic data, referenced in the main body of this report. These data are keyed to the report's sections by use of the section number preceded by an "A" (for Appendix), e. g. A6.10.

Sections A6.10 and A6.11

Thirty-two load-deflection curve graphs,  
30 for short box beam specimens (A6.10),  
and two for full-length specimens (A6.11),  
follow.

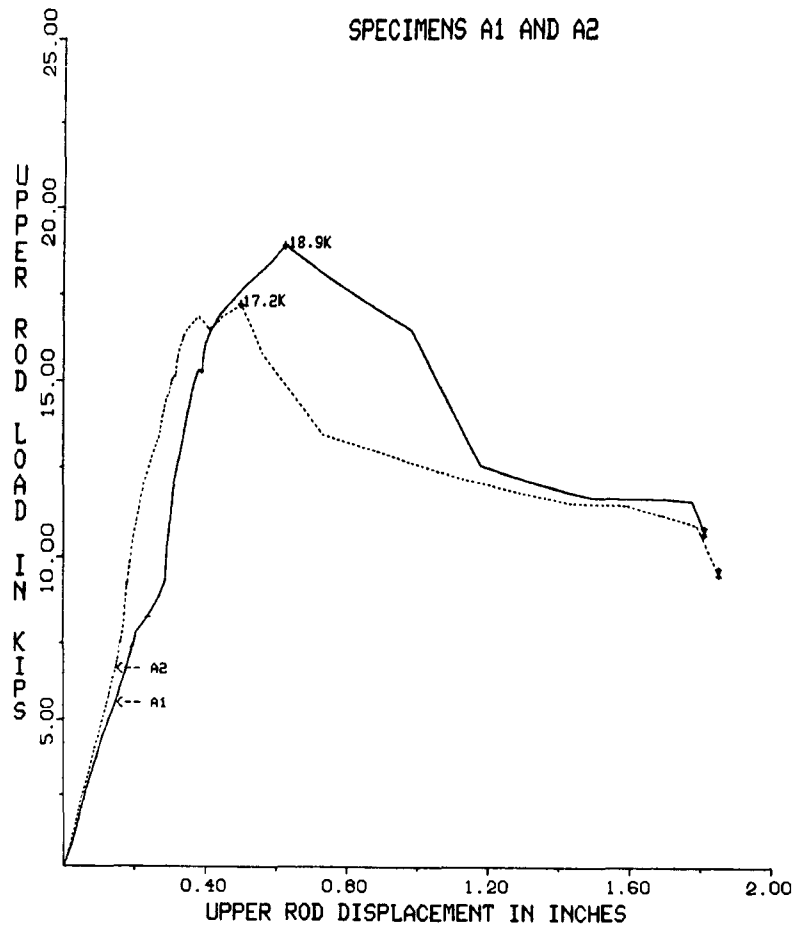


Figure A6.10-1 In-plane load vs displacement curves for specimens A1 and A2.

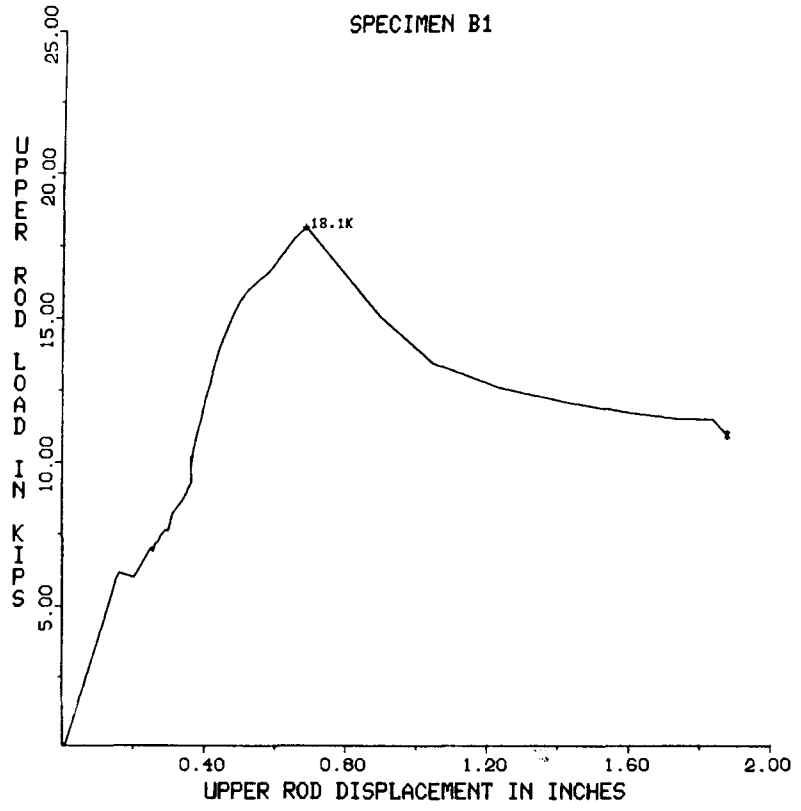


Figure A6.10-2 In-plane load vs displacement curve for specimens B1.

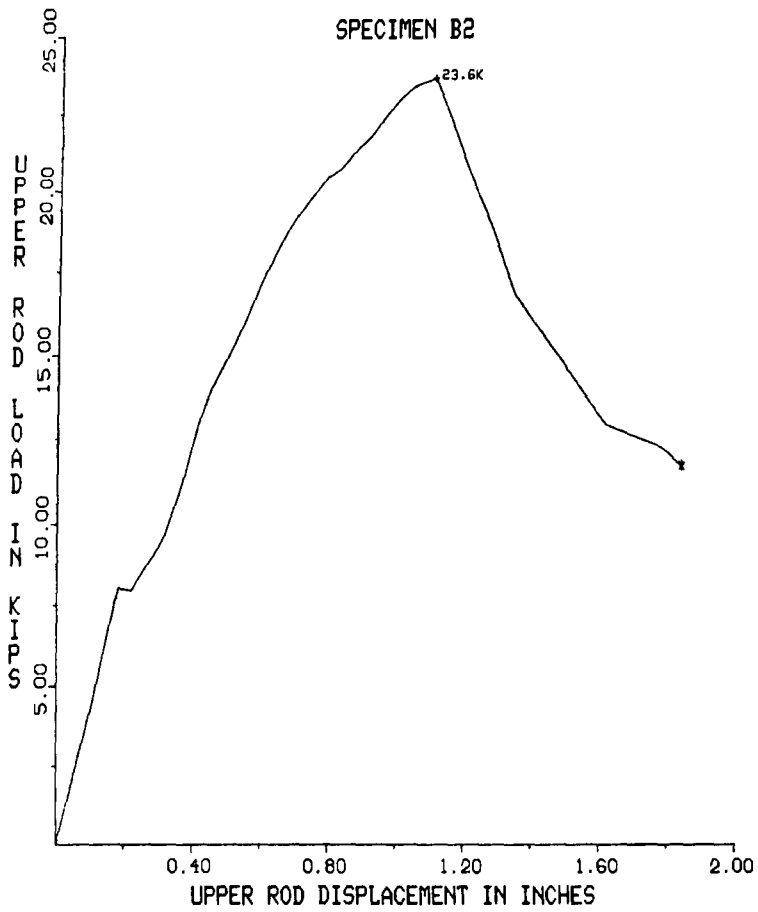


Figure A6.10-3 In-plane load vs displacement curve for specimens B2.

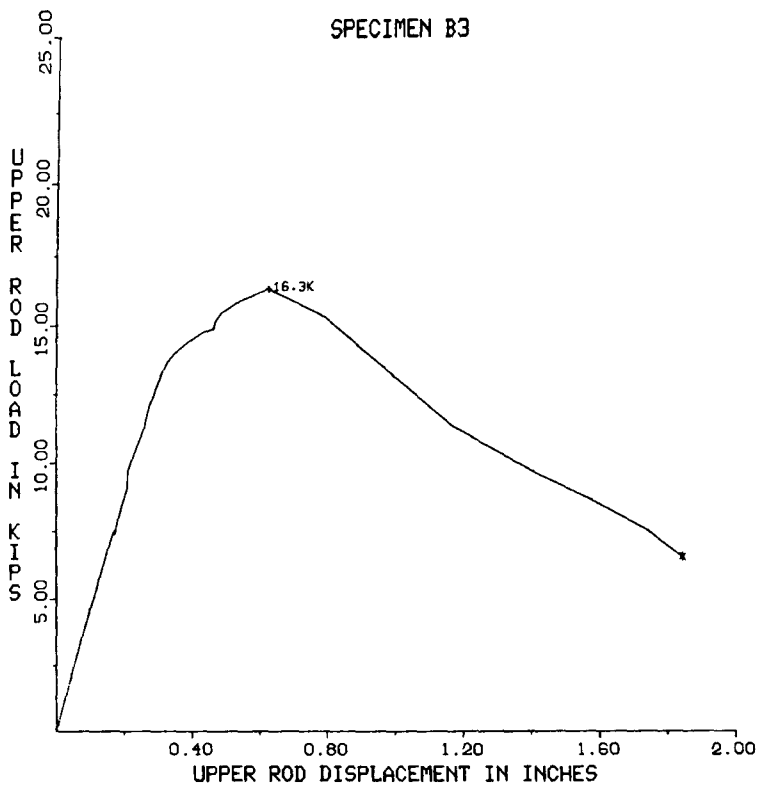


Figure A6.10-4 In-plane load vs displacement curve for specimens B3.

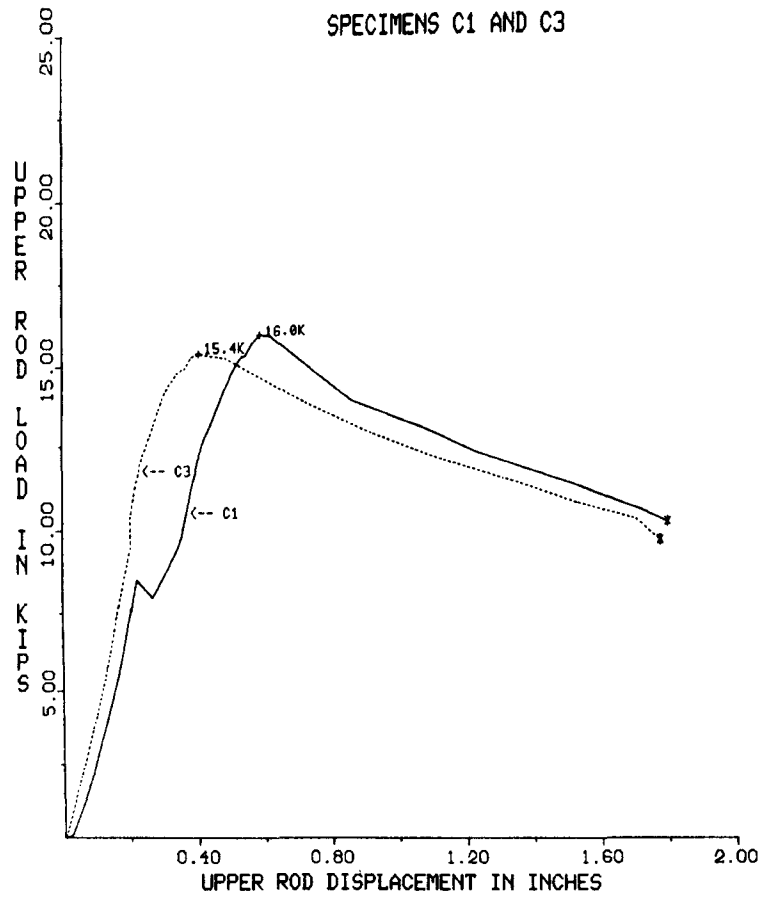


Figure A6.10-5 In-plane load vs displacement curves for specimens C1 and C3.

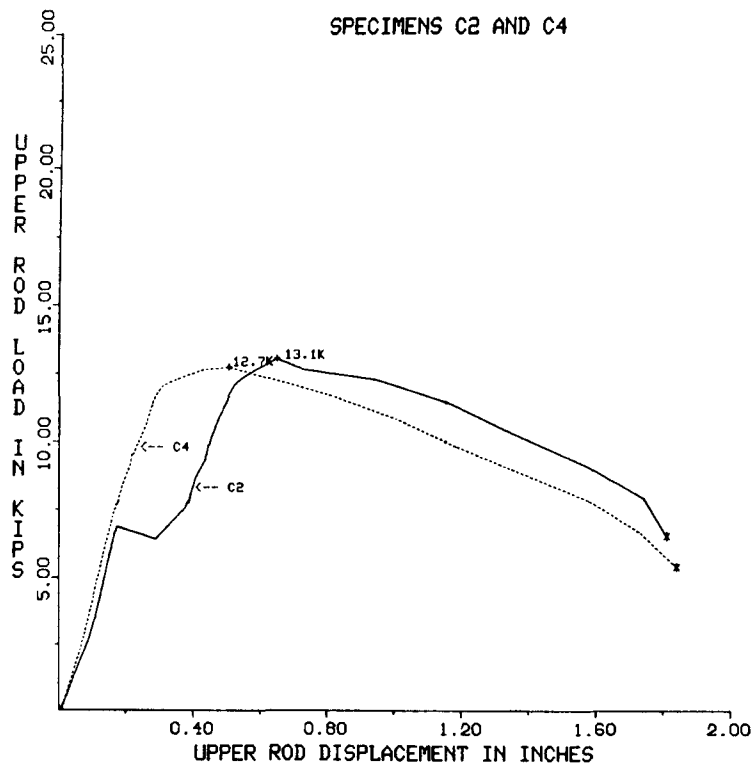


Figure A6.10-6 In-plane load vs displacement curves for specimens C2 and C4.

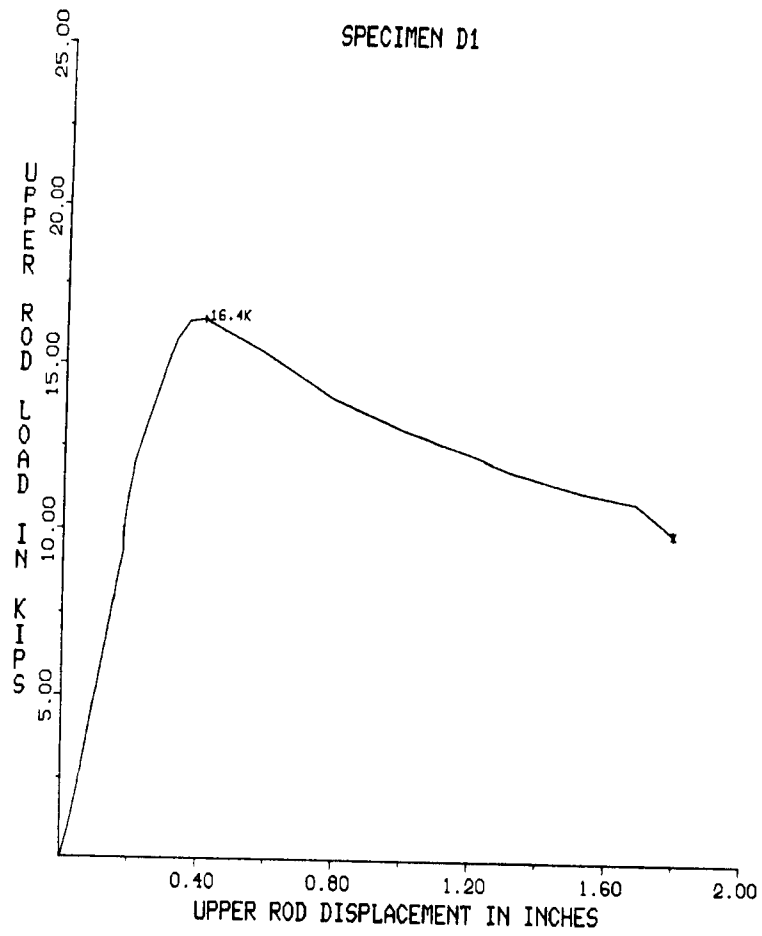


Figure A6.10-7 In-plane load vs displacement curve for specimens D1.

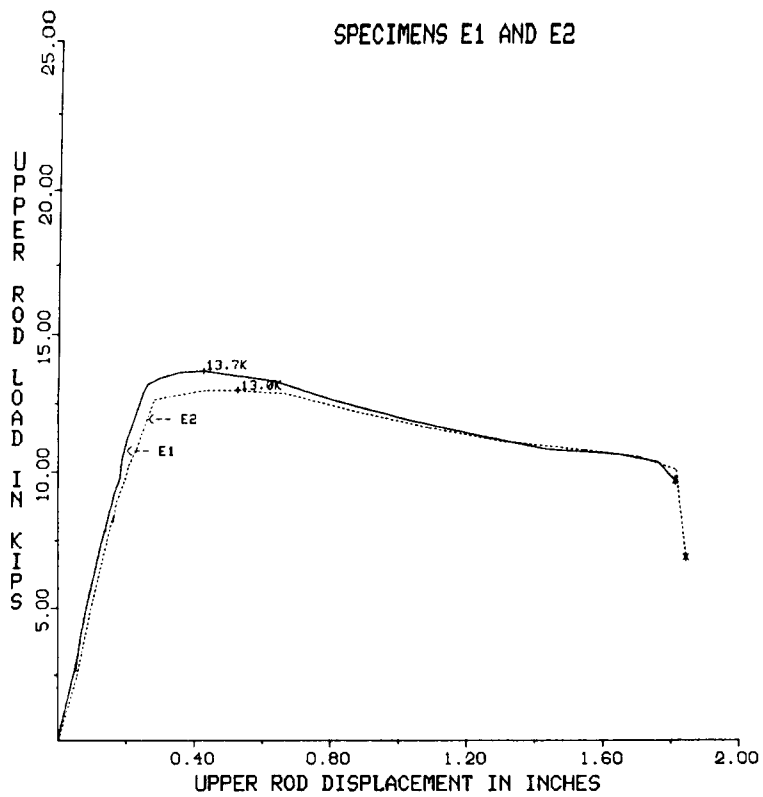


Figure A6.10-8 In-plane load vs displacement curves for specimens E1 and E2.

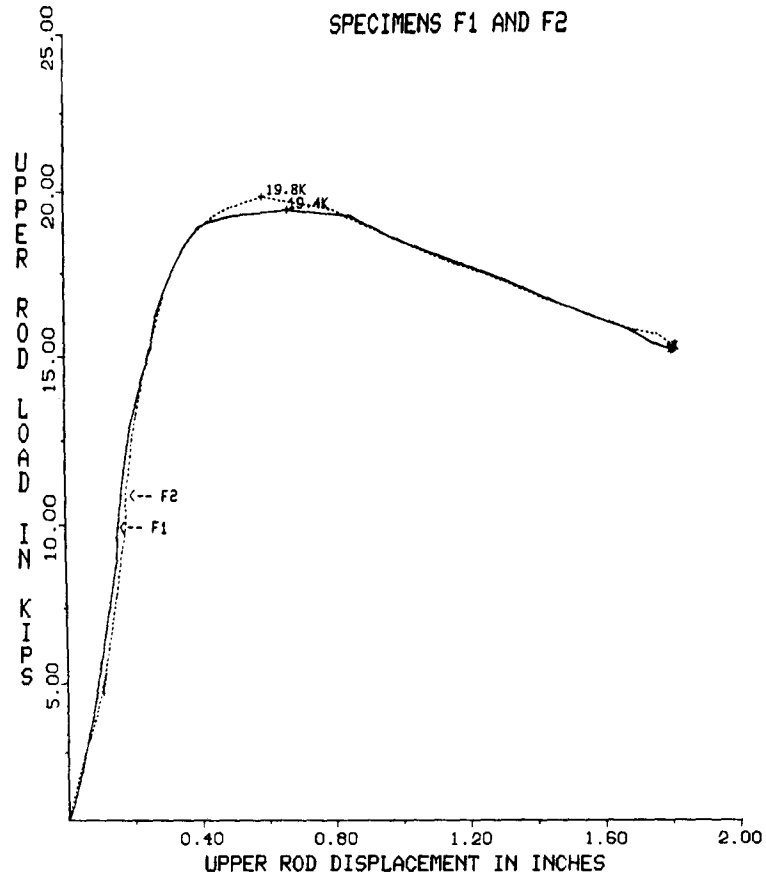


Figure A6.10-9 In-plane load vs displacement curves for specimens F1 and F2.

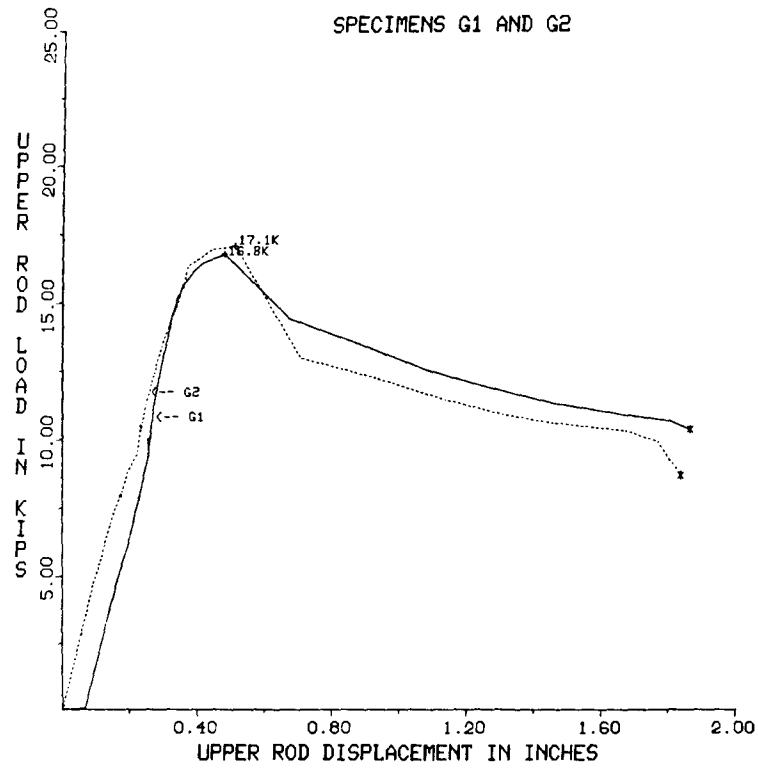


Figure A6.10-10 In-plane load vs displacement curves for specimens G1 and G2.

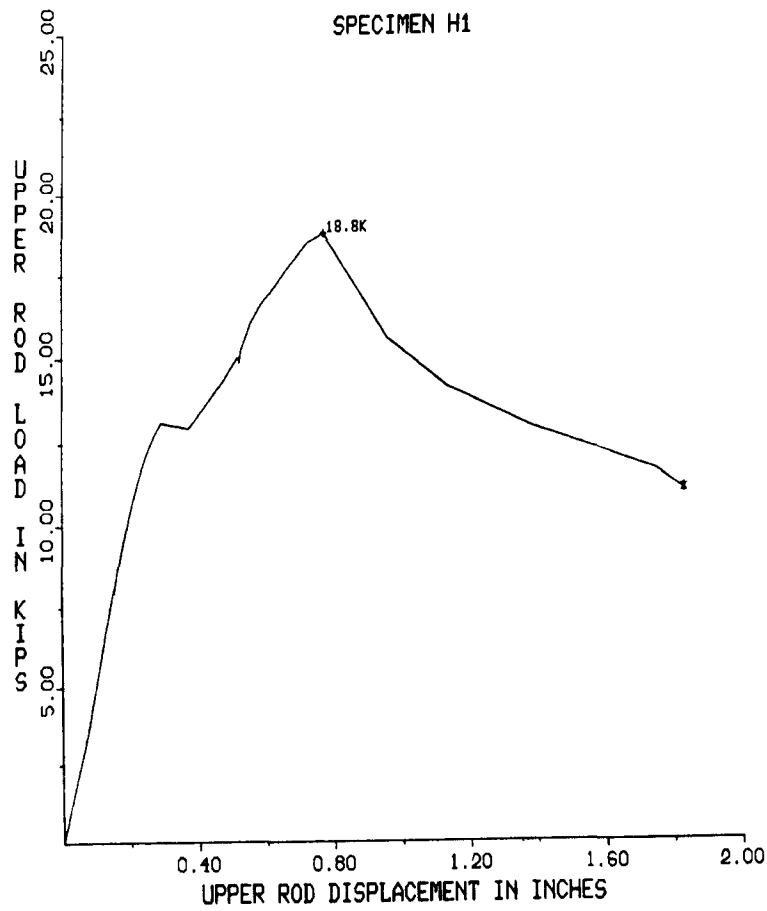


Figure A6.10-11 In-plane load vs displacement curve for specimens H1.

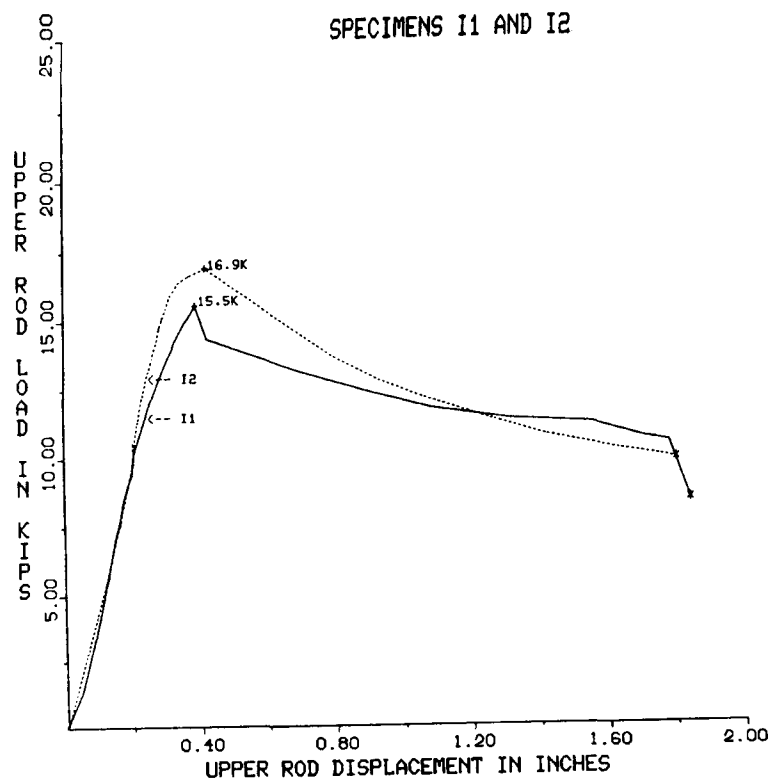


Figure A6.10-12 In-plane load vs displacement curves for specimens I1 and I2.

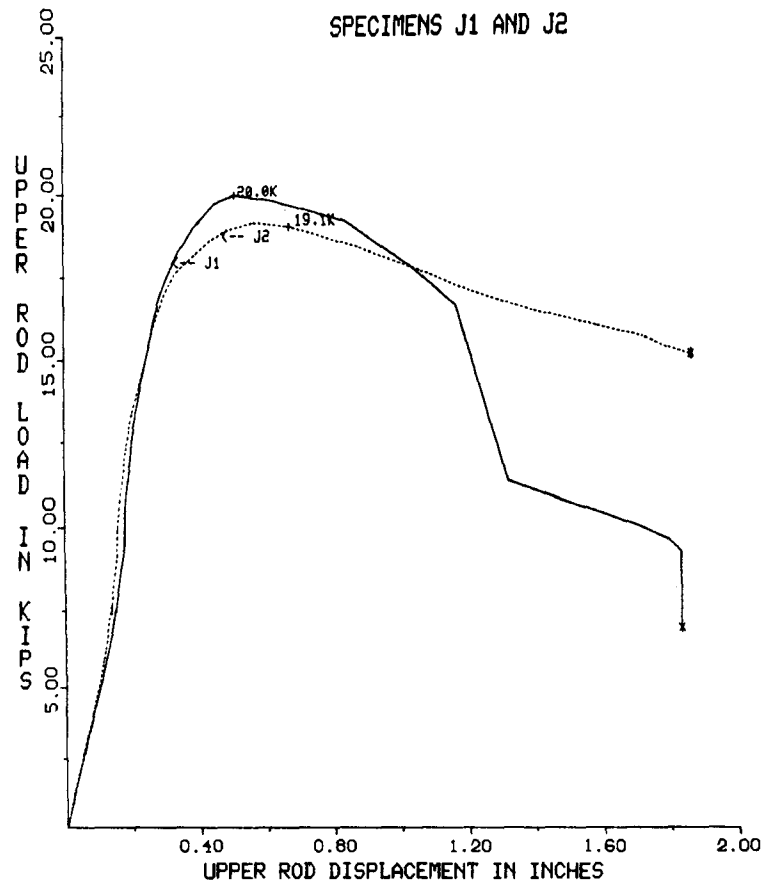


Figure A6.10-13 In-plane load vs displacement curves for specimens J1 and J2.

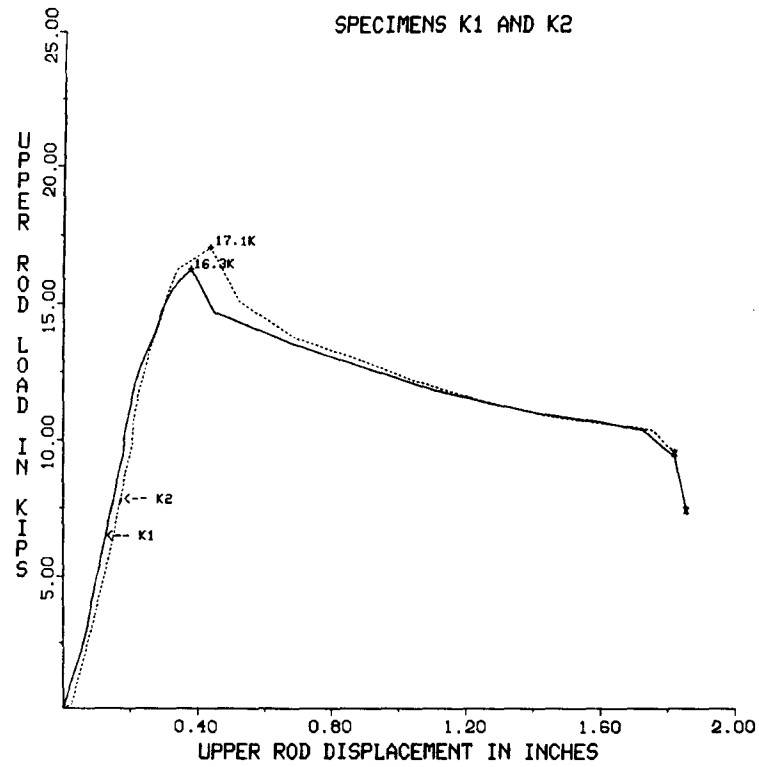


Figure A6.10-14 In-plane load vs displacement curves for specimens K1 and K2.

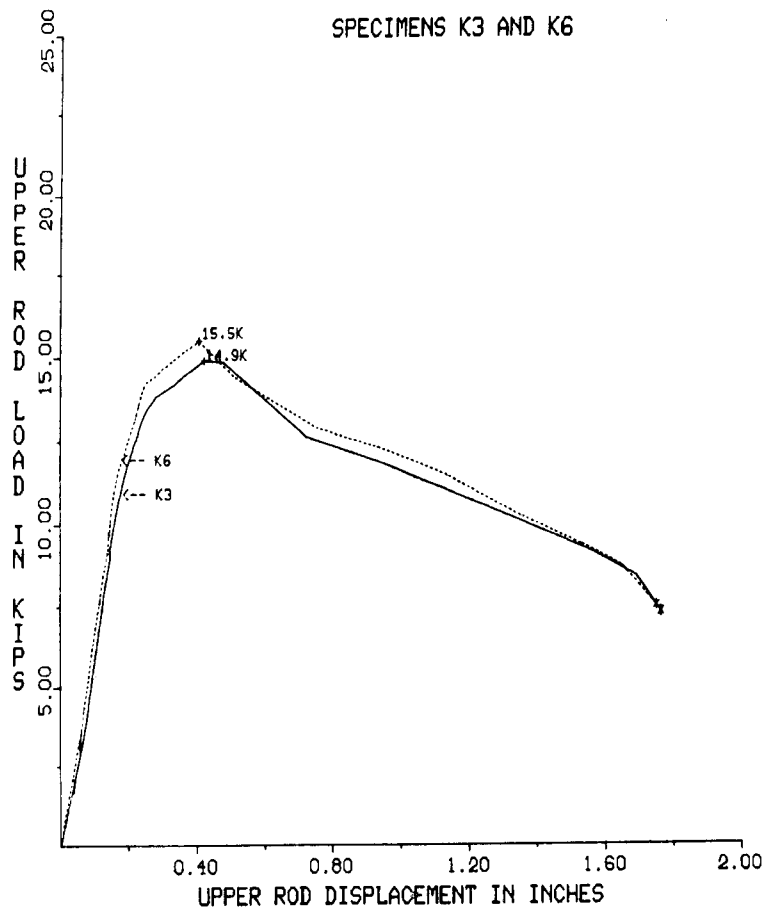


Figure A6.10-15 In-plane load vs displacement curves for specimens K3 and K6.

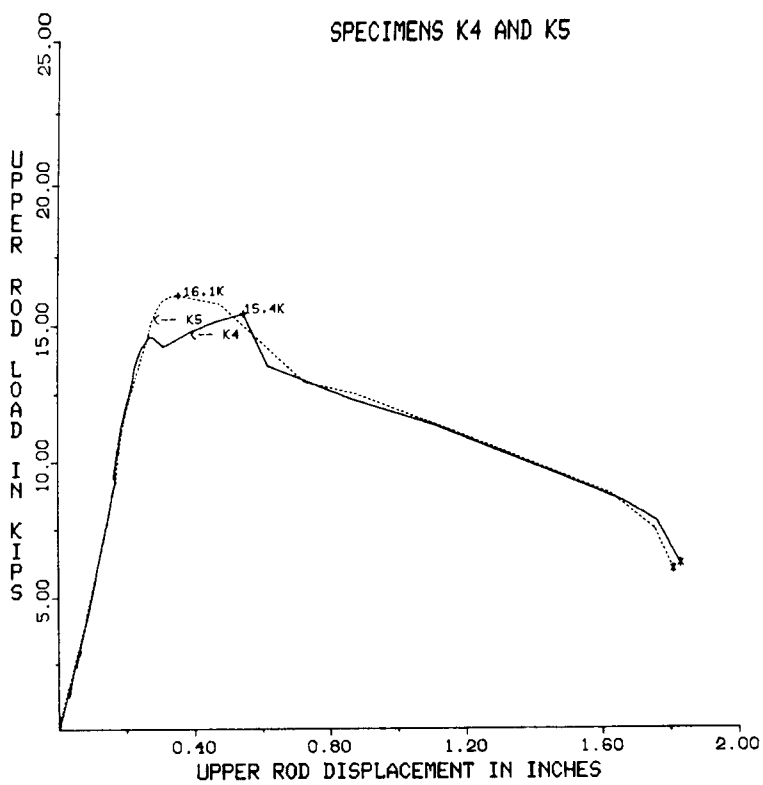


Figure A6.10-16 In-plane load vs displacement curves for specimens K4 and K5.

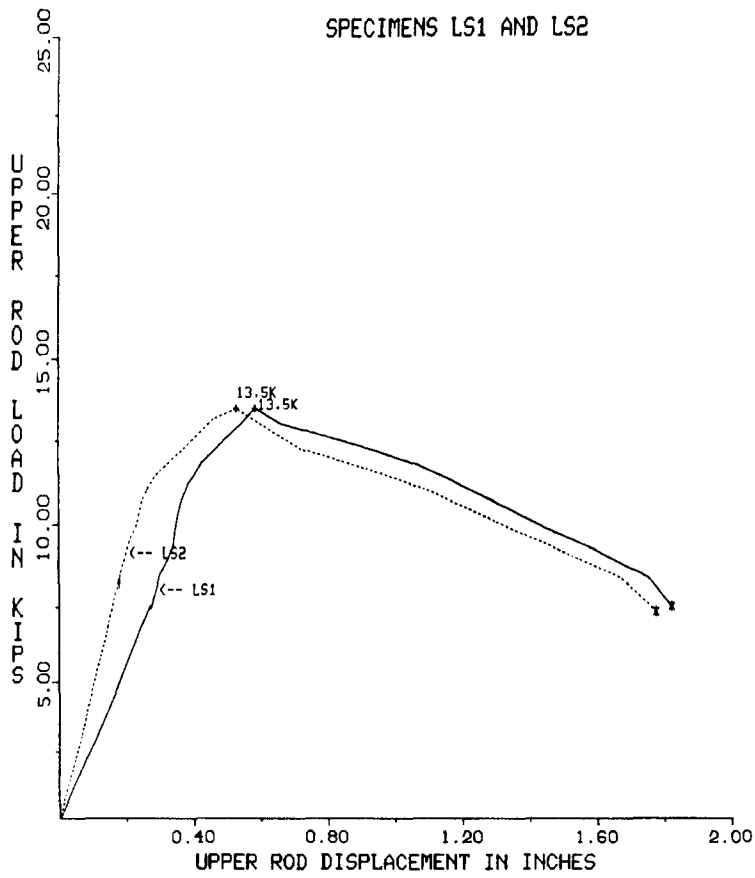


Figure A6.10-17 In-plane load vs displacement curves for specimens LS1 and LS2.

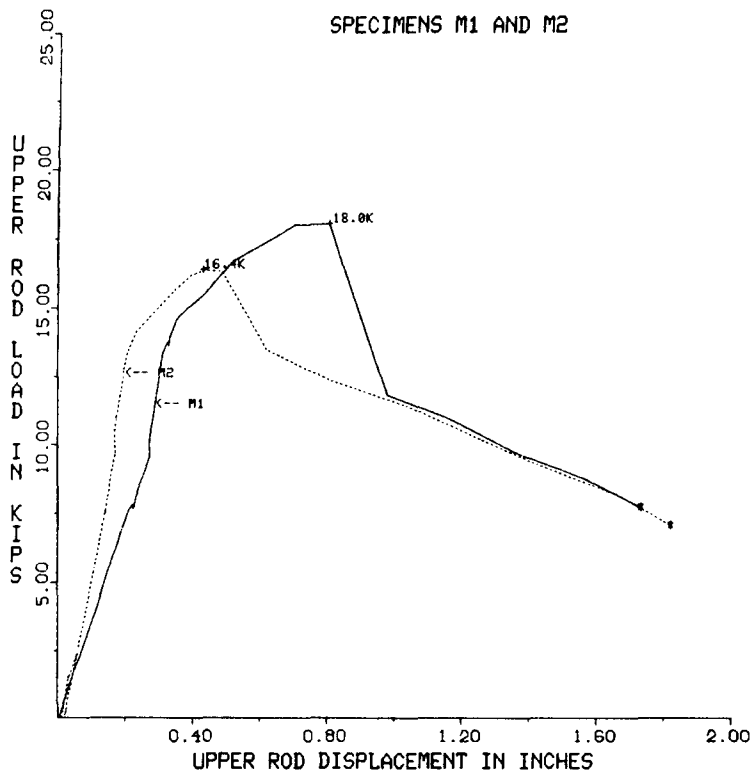


Figure A6.10-18 In-plane load vs displacement curves for specimens M1 and M2.

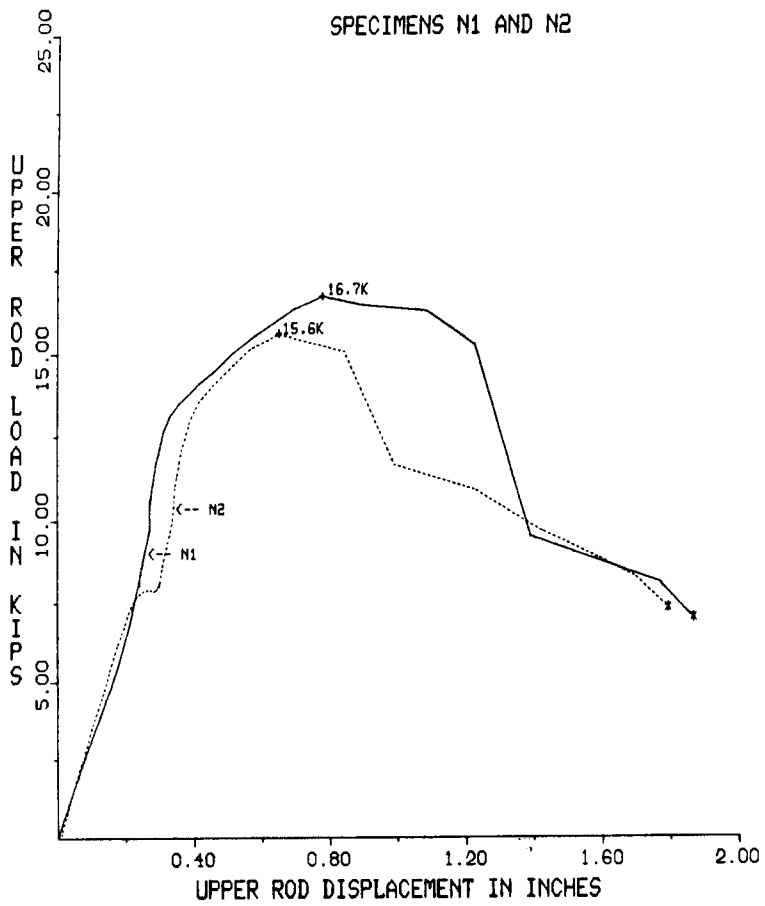


Figure A6.10-19 In-plane load vs displacement curves for specimens N1 and N2.

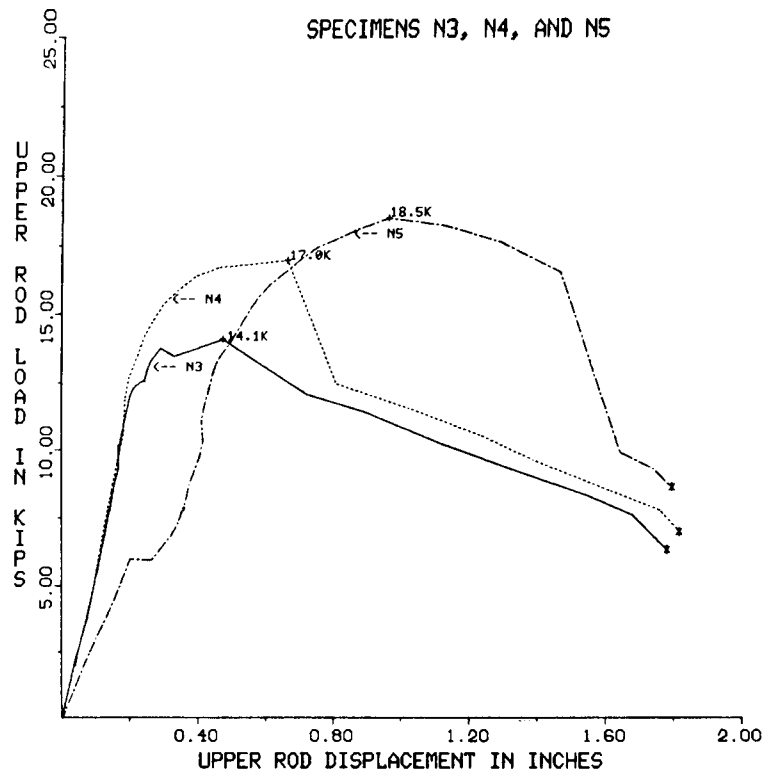


Figure A6.10-20 In-plane load vs displacement curves for specimens N3, N4, and N5.

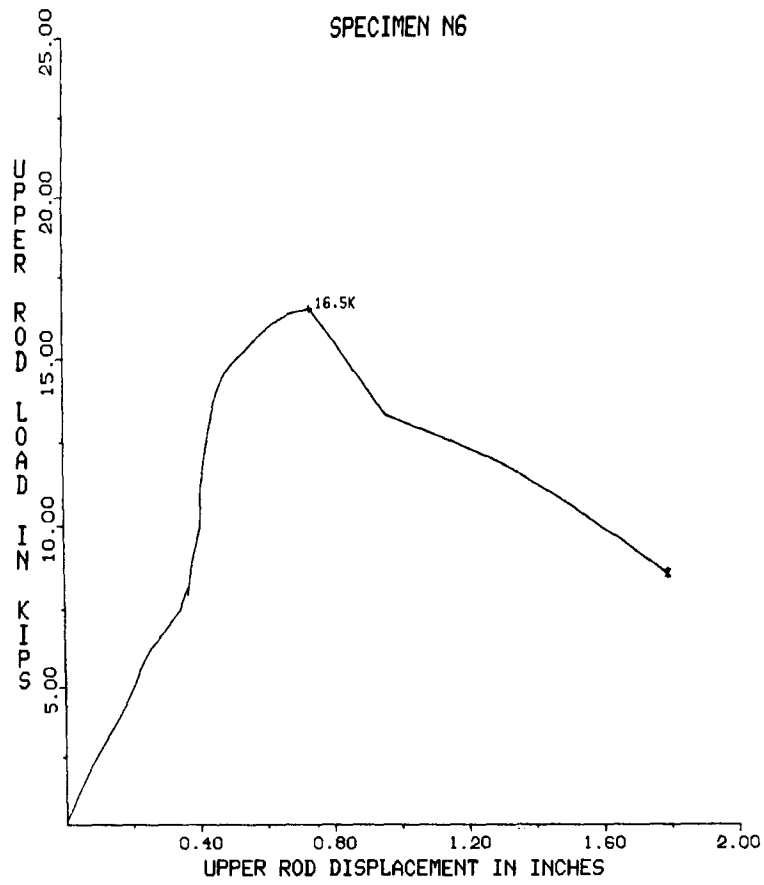


Figure A6.10-21 In-plane load vs displacement curve for specimens N6.

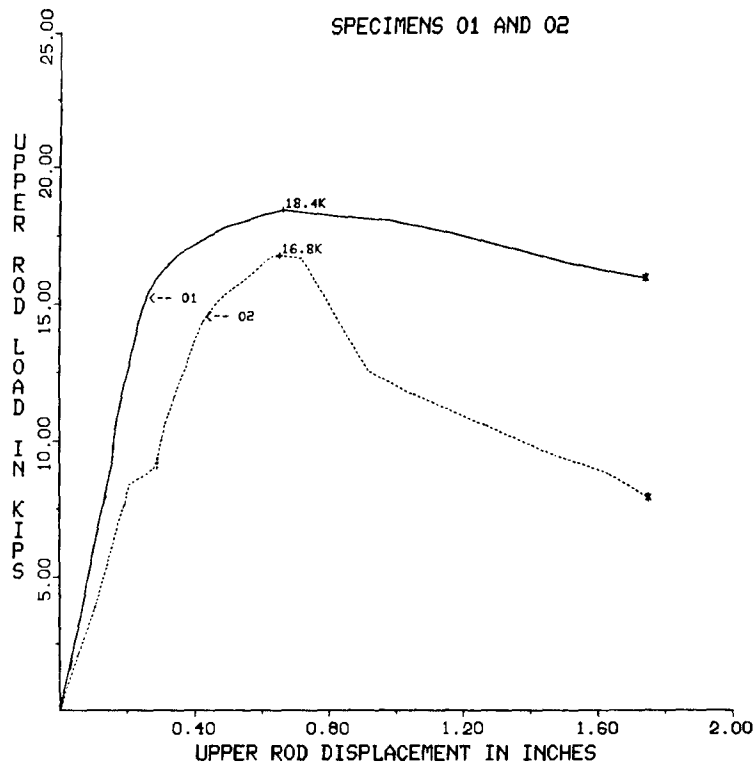


Figure A6.10-22 In-plane load vs displacement curves for specimens 01 and 02.

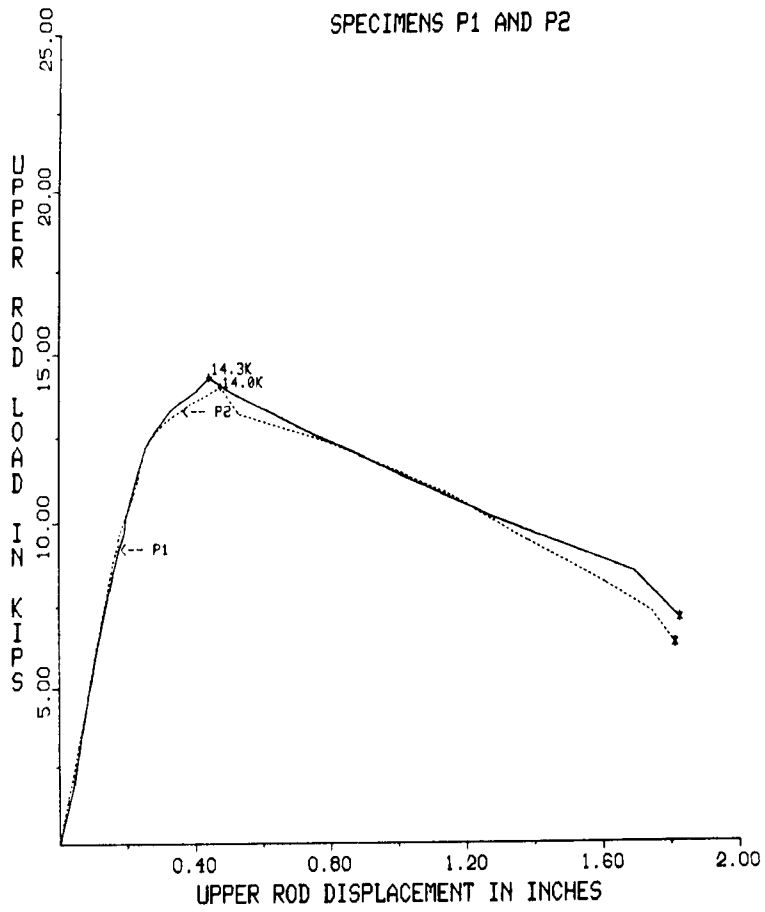


Figure A6.10-23 In-plane load vs displacement curves for specimens P1 and P2.

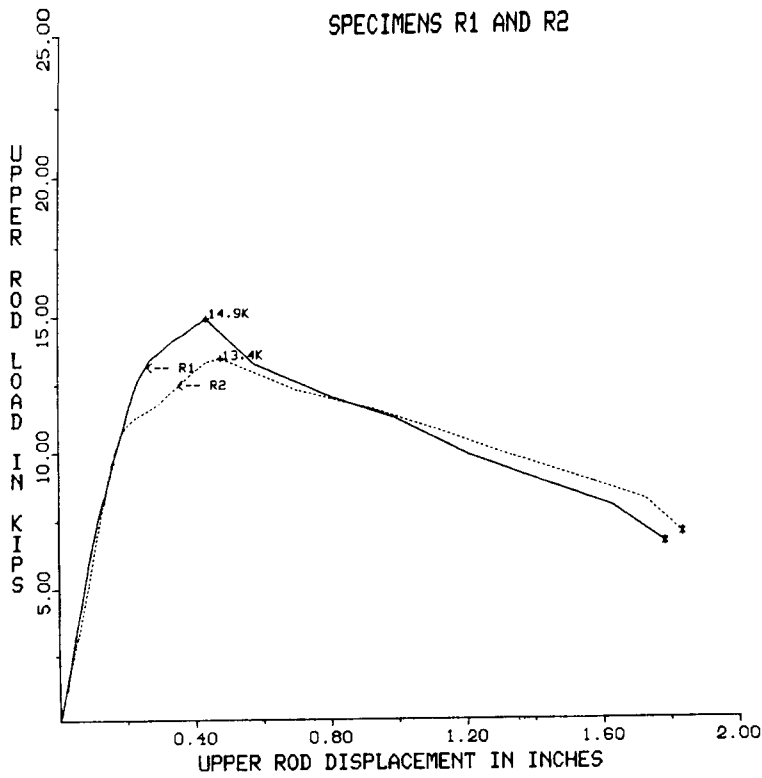


Figure A6.10-24 In-plane load vs displacement curves for specimens R1 and R2.

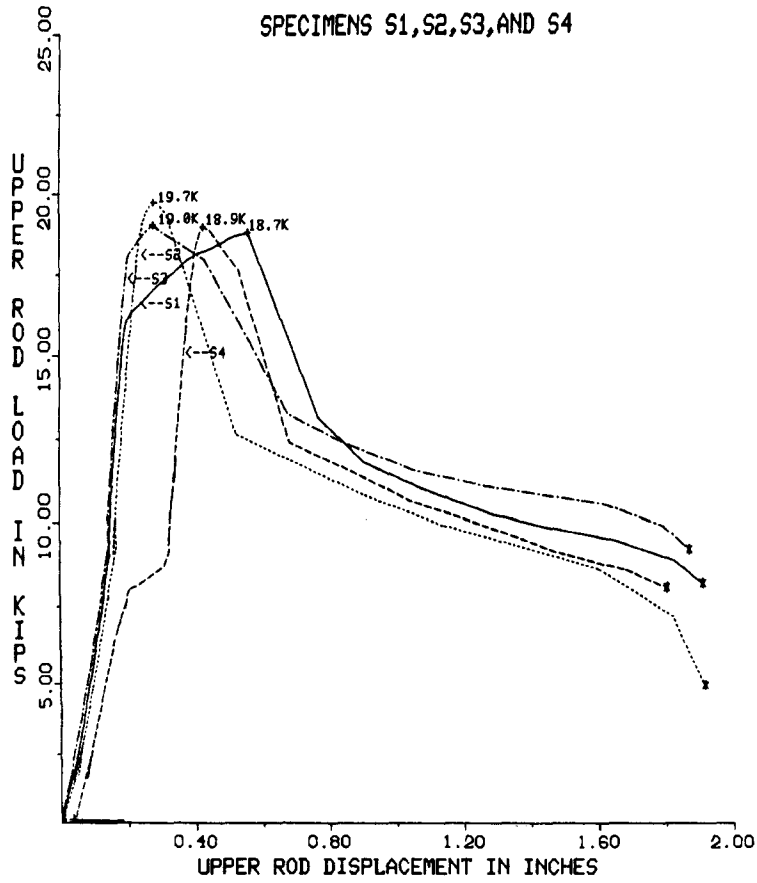


Figure A6.10-25 In-plane load vs displacement curves for specimens S1, S2, S3, and S4.

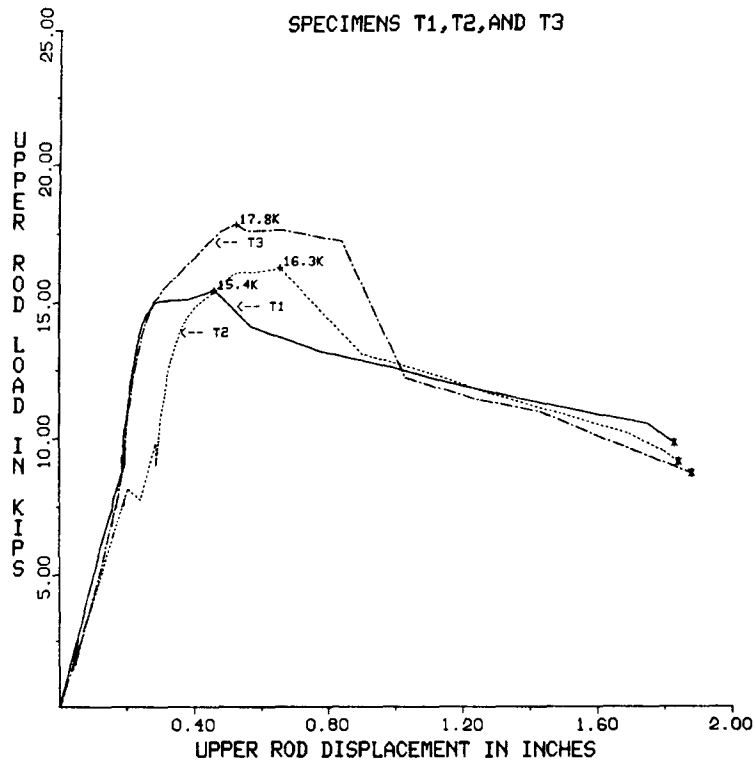


Figure A6.10-26 In-plane load vs displacement curves for specimens T1, T2, and T3.

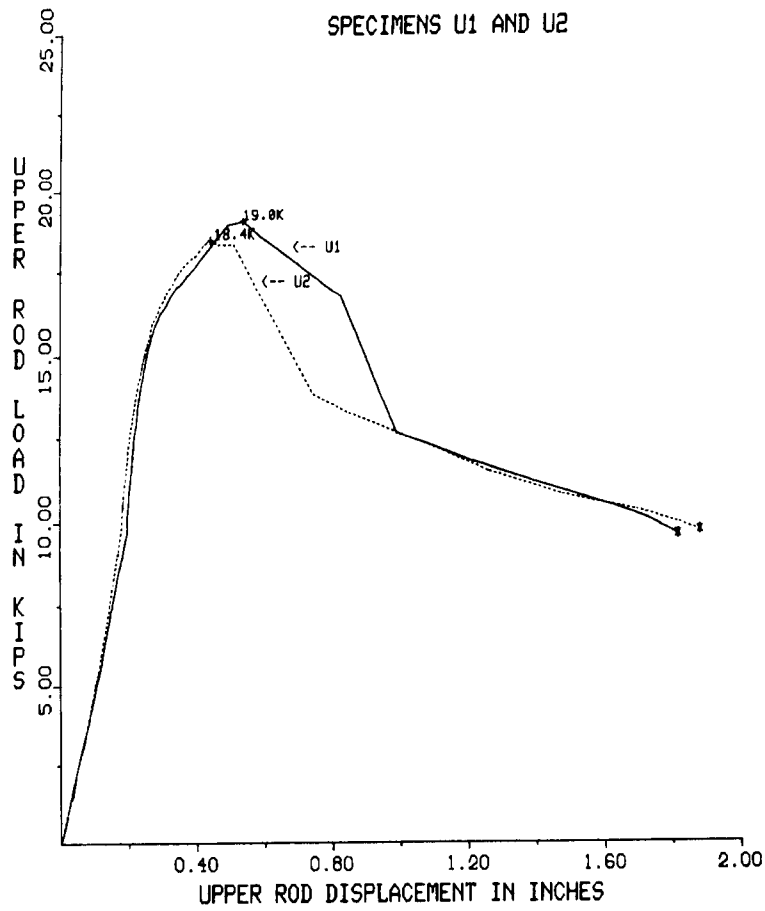


Figure A6.10-27 In-plane load vs displacement curves for specimens U1 and U2.

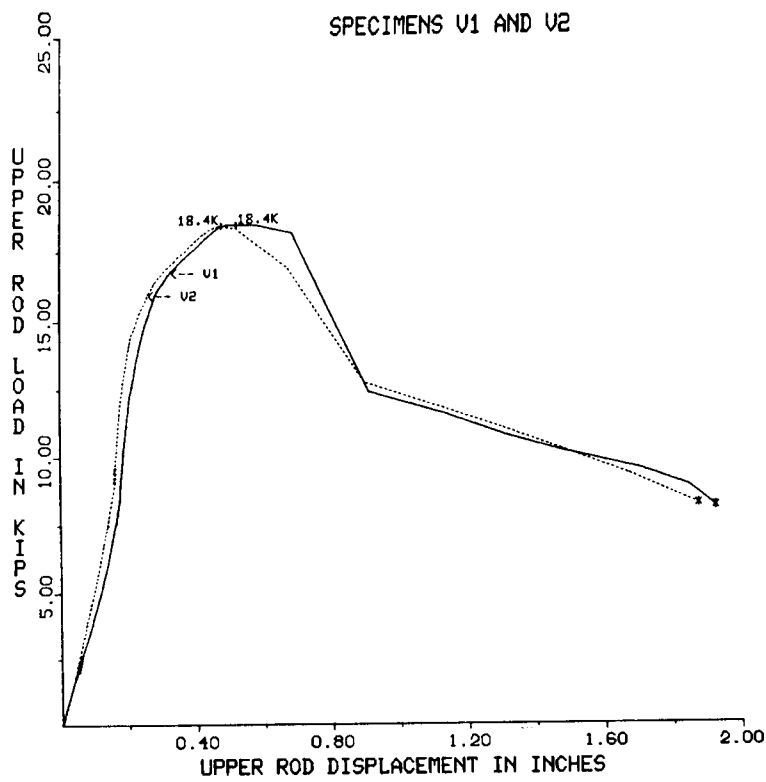


Figure A6.10-28 In-plane load vs displacement curves for specimens V1 and V2.

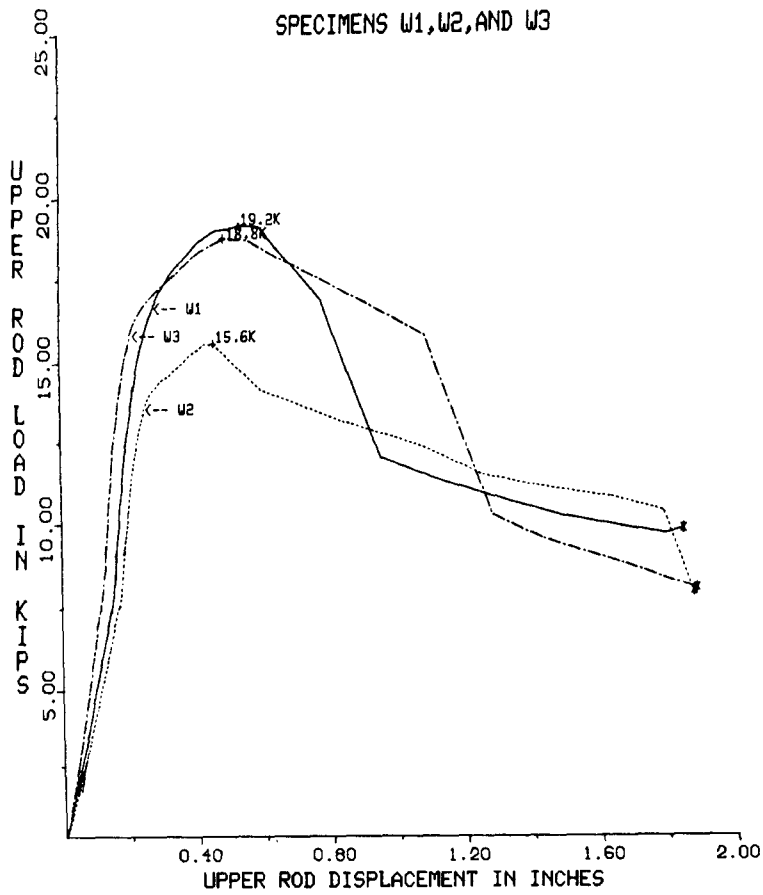


Figure A6.10-29 In-plane load vs displacement curves for specimens W1, W2, and W3.

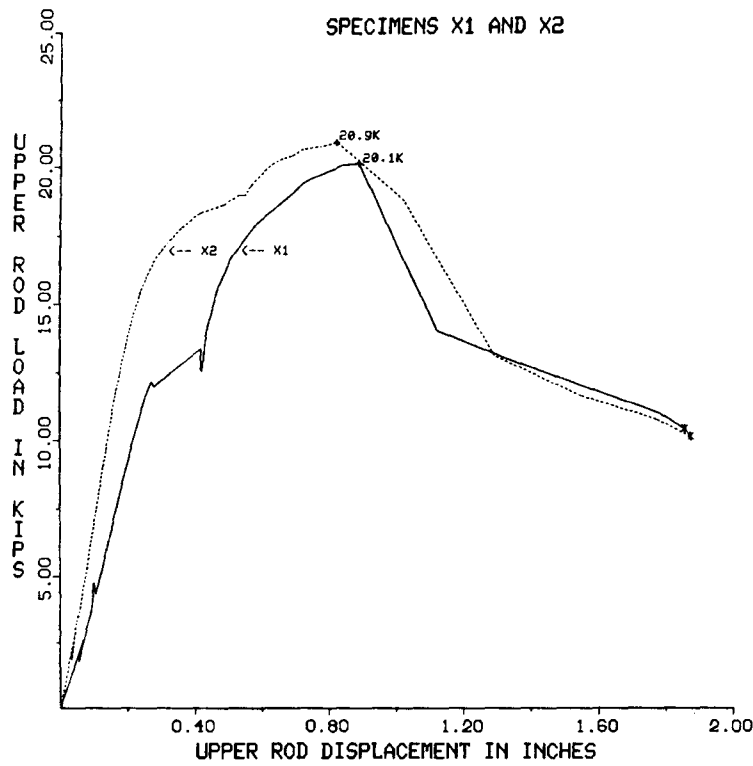


Figure A6.10-30 In-plane load vs displacement curves for specimens X1 and X2.

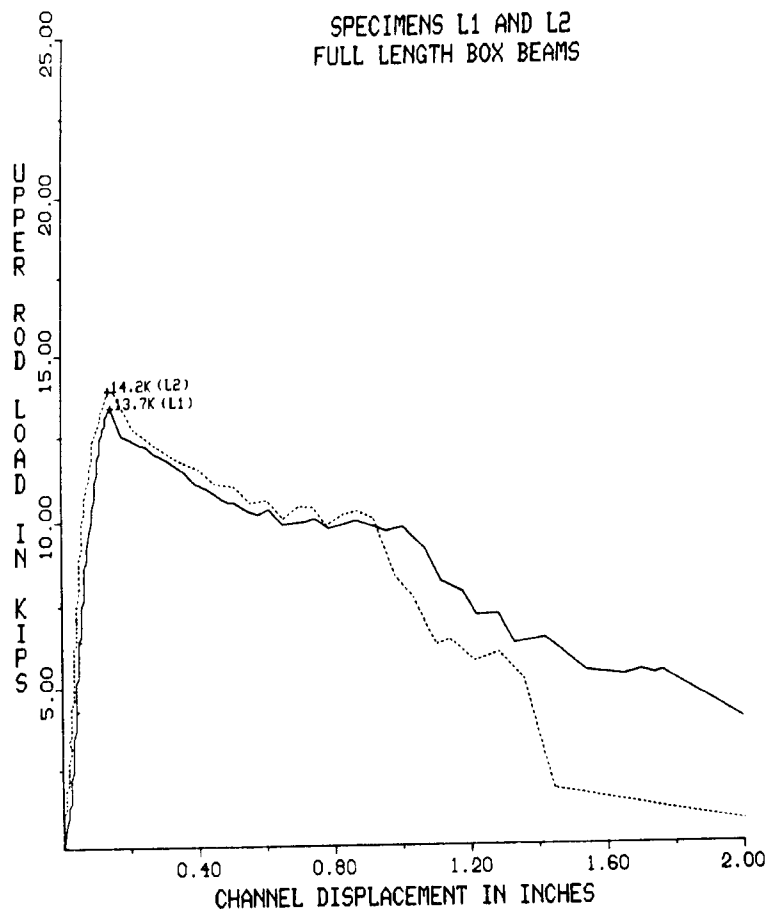


Figure A6.11-1 In-plane load vs deflection curves for specimens L1 and L2.

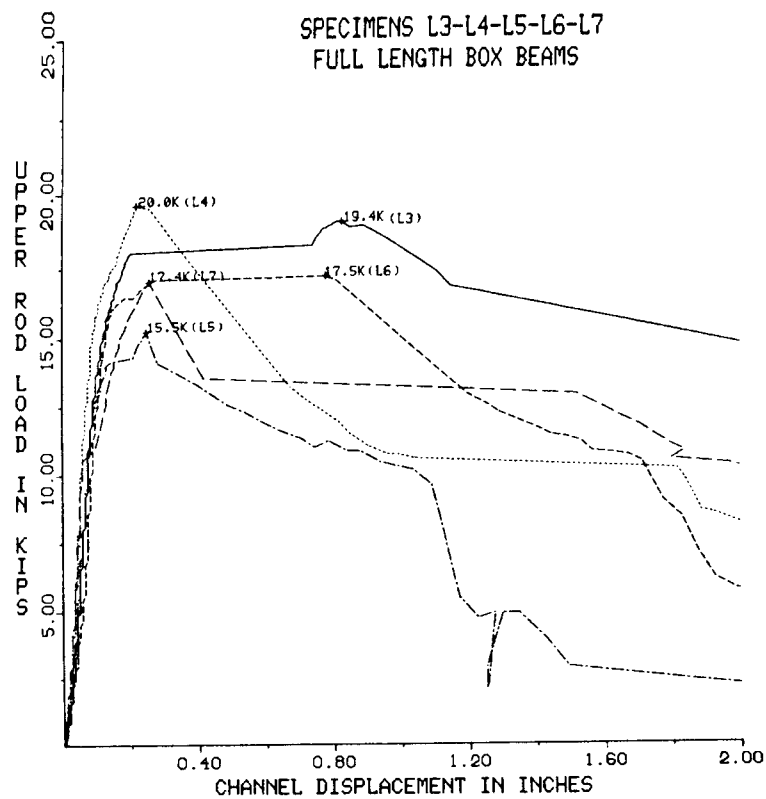


Figure A6.11-2 In-plane load vs deflection curves for specimens L3, L4, L5, L6, and L7

Sections A7.2 through A7.5

The photographs, tables, and graphs that follow provide additional data on the physical and chemical properties of walkway materials.

## A7. NBS MATERIALS TESTING PROGRAM

### A7.2 INITIAL INSPECTION

#### A7.2.2 Radiography

Radiographs of portions of box beam 9M used in the analysis described in section 7 of the report are produced in figure A7.2.2-1.

### A7.3 MECHANICAL PROPERTIES OF STRUCTURAL STEEL AND WELDMENTS

#### A7.3.1 NBS Channel Specimens

Load-strain plots for tensile tests performed on NBS channel specimens are given in figures A7.3.1-1 to A7.3.1-3.

#### A7.3.2 Walkway Box Beams

Locations from which base metal tensile specimens were removed from box beams 9U, 8L and 9M are illustrated in figures A7.3.2-1 through A7.3.2-3. Load-strain plots for the tensile tests performed on walkway box beam specimens appear in figures A7.3.2-4 through A7.3.2-9.

#### A7.3.3 Walkway Hanger Rods

Locations from which tensile specimens were removed from hanger rods NBS 5A and 5B are illustrated in figure A7.3.3-1. Load-strain plots for the walkway hanger rod tests appear in figure A7.3.3-2.

#### A7.3.4 Walkway Box Beam Longitudinal Welds

Locations from which tensile specimens were removed from box beams 9U, 8L and 9M are illustrated in figures A7.3.2-1 through A7.3.2-3.

### A7.4 METALLOGRAPHY AND HARDNESS MEASUREMENTS

#### A7.4.1 Box Beam Weldments

A "U" shaped transverse section through NBS weldment IC was examined for microstructure and hardness. Weldment IC was welded by the GMAW process using a mild steel electrode. The section examined, shown at low magnification in figure A7.4.1-1, included the welded flange region and part of the web region of each box beam channel. The section was metallographically polished and chemically etched to reveal the microstructure. The region of this section containing the weld is shown at higher magnification in figure A7.4.1-2. In this figure, the light region in the center represents weld metal; the darker regions on either side of the weld are the heat affected zones associated with the weld. The light regions at both sides of the figure, adjacent to the heat affected zones, are flange base metal.

Knoop microhardness measurements at a load of 500 grams force (HK<sub>500</sub>) were made across the weld metal, across one of the heat affected zones, and into the base material on this same transverse section through NBS weldment IC. The indentations produced by the microhardness tests appear as a line of small, dark, elongated marks in figure A7.4.1-2. Approximately equivalent Rockwell B (HRB) hardness values, converted in accordance with ASTM E140-79 (Standard Hardness Conversion Tables for Metals) [7.1], are reported along with the HK<sub>500</sub> values.

A representative region of the weld metal appears in figure A7.4.1-3. The microstructure consists primarily of bainite. Microhardness values based on 17 measurements average 205 HK<sub>500</sub> (90.9 HRB) and range from 195 to 228 HK<sub>500</sub> (88.5 to 95.5 HRB).

The transition region between the weld metal and the heat affected zone is shown in figure A7.4.1-4. Nothing unusual was observed at the transition. The microstructure within the heat affected zone is shown in figure A7.4.1-5. The microstructure consists of ferrite, primarily as a network in prior austenite grain boundaries, bainite, partially spheroidized carbides, and tempered martensite. Average hardness of the heat affected zone based on five measurements is 202 HK<sub>500</sub> (90.2 HRB) with a range of 196 to 206 HK<sub>500</sub> (89 to 91 HRB). Figure A7.4.1-6 shows the transition from the heat affected zone to the base material of the box beam. Hardness in this region averages 173 HK<sub>500</sub> (83 HRB) and the hardness range is 167 to 177 HK<sub>500</sub> (81 to 84 HRB).

A region representative of the base material away from the heat affected zone is shown in figure A7.4.1-7. The microstructure is relatively fine grained and consists primarily of ferrite (light) and pearlite (dark) in a normalized condition. Within the base material, the average hardness is 152 HK<sub>500</sub> (75.4 HRB) and the range is 139 to 161 HK<sub>500</sub> (70 to 70.9 HRB).

Two transverse sections similar to that described in the previous section on the NBS weldment were examined from each of the two box beam segments (9U and 8L) and the full length box beam (9M) obtained from the walkway debris. The locations of these sections in the box beams are indicated in figures A7.3.2-1 through A7.3.2-3. Each "U" shaped transverse section included the bottom of the beam (channel flanges and weld region) and parts of the web region of each box beam channel. To facilitate handling during metallographic preparation, parts of the channel web regions were removed from each section. The metallographic examination was concentrated in the remaining shorter "U" shaped sections, but hardness measurements were made both in the shortened sections and in the pieces that had been removed. The sections were polished metallographically and chemically etched to reveal microstructure. Knoop microhardness measurements at a load of 500 grams force (HK<sub>500</sub>) were taken in the weld, heat affected zones, and adjacent base channel material of these sections. Rockwell B (HRB) hardness measurements were taken in the flange and web regions of each channel piece. Summaries of the hardness test results appear in tables A7.4.1-1 through A7.4.1-3 for sections from box beams 9U, 8L and 9M, respectively. Approximately equivalent Rockwell B (HRB) hardness values, converted in accordance with ASTM Standard E140-79, are reported along with the HK<sub>500</sub> values.

The sections from box beam 9U (NBS 1), designated 1BM1 and 1BM2, are shown in figures A7.4.1-8 and A7.4.1-10, respectively. These two sections were separated by about 7 in (180 mm) as measured along the length of the beam. The weld regions of sections 1BM1 and 1BM2 are shown at higher magnification in figures A7.4.1-9 and A7.4.1-11, respectively. The depth of weld penetration is greater in section 1BM2 than in section 1BM1 and there is some misalignment of the channel flanges at the weld.

Representative regions of the weld metal from sections 1BM1 and 1BM2 are shown in figures A7.4.1-12 and A7.4.1-13, respectively. In both cases, the microstructure appears to consist of bainite. A number of inclusions are evident in section 1BM1. The average hardness of the weld in section 1BM1 (95 HRB) is slightly higher than in the weld of section 1BM2 (91 HRB) and the hardness range in the weld of section 1BM1 is greater.

There were some patches of hard material at the transition region from the weld material to the heat affected zone at both the north and south channels in section 1BM1. One such patch can be seen in figure A7.4.1-14. A similar region is shown at higher magnification in figure A7.4.1-15. The microstructure in this region appears to be fine-grained tempered martensite. Maximum hardness measured in these patches was 336 HK<sub>500</sub> which is approximately equivalent to a Rockwell C hardness of 33. This value compares to a hardness of 241 HK<sub>500</sub> (98 HRB) in an adjacent location of the transition region.

Hard patches were not observed in the transition region from weld to heat affected zone in section 1BM2. An area representative of this region in section 1BM2 is shown in figure A7.4.1-16.

Regions representative of the heat affected zones (HAZ) of sections 1BM1 and 1BM2 are shown in figures A7.4.1-17 and A7.4.1-18, respectively. In both cases, the microstructure appears to consist of ferrite, both as a network in prior austenite grain boundaries and as needles, bainite, partially spheroidized carbides, and tempered martensite. Hardness of the heat affected zones in section 1BM1 is somewhat greater at the south channel than at the north. At both heat affected zones, hardness decreased with distance from the weld. Hardness values in the heat affected zones of section 1BM2 were similar for both zones.

The transition regions from the heat affected zone to the base channel material appeared similar for both sections. A region representative of the transition zone in section 1BM2 is shown in figure A7.4.1-19.

Base material from both channel pieces appeared similar. A region representative of section 1BM1 is shown in figure A7.4.1-20. The microstructure consists primarily of ferrite (light) and pearlite (dark) in a normalized condition. Rockwell B hardness measurements made on both sections indicated no significant differences in hardness between the two channel pieces used to fabricate the box beam. Regions of the channel adjacent to the heat affected zones and in the web region about 0.6 to 1 in (15 to 25 mm) from the bottom of the beam were harder than elsewhere with HRB hardness averaging 81.5. The hardness of the

channel material elsewhere in the sections averaged 74.4 HRB for section 1BM1 and 74.3 HRB for section 1BM2.

The transverse sections examined from box beam 8L (NBS 2), designated 2BM1 and 2BM2, are shown in figures A7.4.1-21 and A7.4.1-23, respectively. These sections were separated by about 7 1/2 in (190 mm) as measured along the length of the beam. The regions of sections 2BM1 and 2BM2 containing the weld are shown at higher magnification in figures A7.4.1-22 and A7.4.1-24, respectively. There appears to be minor undercutting at the weld in section 2BM2 and the heat affected zone is somewhat narrower than in section 2BM1. In section 2BM1 there is a void at the base of the weldment adjacent to the gap between the channel flanges.

Regions representative of the weld metal in sections 2BM1 and 2BM2 are shown in figures A7.4.1-25 and A7.4.1-26, respectively. Overall, the microstructure in both cases appeared similar and consisted primarily of bainite. Inclusions are evident in both sections. The average hardness values for weld metal in the two sections do not differ significantly.

The transition from weld to the heat affected zone for section 2BM1 is shown in figure A7.4.1-27. There are no unusual features.

As was the case in section 1BM1 from box beam 9U, there were some hard spots at the transition from weld to the heat affected zone in section 2BM2 on the south side. The transition in section 2BM2 is shown in figure A7.4.1-28 at 200 magnifications. One of the hard regions is shown at much higher magnification (X1200) in figure A7.4.1-29. The microstructure of this region appears to be tempered martensite. The highest hardness value obtained in this region was 298 HK<sub>500</sub> which is approximately equivalent to 28 Rockwell C. Away from the hard regions, hardness averaged 247 HK<sub>500</sub> (99 HRB).

In the heat affected zones, the microstructure was similar in both sections 2BM1 and 2BM2. A representative region from section 2BM1 is shown in figure A7.4.1-30. The microstructure appears to consist of ferrite, both as a network in prior austenite grain boundaries and as needles, bainite, partially spheroidized carbides and tempered martensite. Hardness was 5 to 6 HRB points lower for the heat affected zones in section 2BM2 than in the weld metal. In section 2BM1, hardness was similar for both weld metal and the heat affected zone.

The transition regions from the heat affected zones to base channel material appeared similar for both sections. A region representative of this transition in section 2BM1 is shown in figure A7.4.1-31. A region representative of the base channel material in both sections is shown for section 2BM1 in figure A7.4.1-32. The microstructure of the channel material consists primarily of ferrite and pearlite in a normalized condition.

There were no significant differences in hardness between the two channel sections. As in the case of the section from box beam 9U, the channel material was somewhat harder adjacent to the heat affected zones and in the web about 0.6 to 1 in (15 to 25 mm) from the flange base than elsewhere.

The sections examined for microstructure and hardness from box beam 9M (NBS 3) are designated 3BM1 and 3BM2 and are shown in figures A7.4.1-33 and A7.4.1-35, respectively. These two sections were separated by about 7 1/2 in (190 mm) as measured along the length of the beam. The weld regions of sections 3BM1 and 3BM2 are shown at higher magnification in figures A7.4.1-34 and A7.4.1-36, respectively. The weld configuration differs considerably between the two sections. In section 3BM1, the heat affected zones penetrate to a point slightly greater than half the flange thickness, whereas the heat affected zones in section 3BM2 penetrate all the way through the flange.

Representative regions of the weld from sections 3BM1 and 3BM2 are shown in figures A7.4.1-37 and A7.4.1-38, respectively. In both cases, the microstructure appears to consist primarily of bainite. More inclusions are evident in section 3BM1 than in section 3BM2. The average hardness of the weld was essentially the same for both sections, being somewhat lower than that of the welds at the sections from the other two walkway box beams.

Nothing unusual was observed at the transition from the weld to the heat affected zones in either section. None of the harder regions found in the transition regions of sections 1BM1 and 2BM2 were in evidence. A region representative of these transition regions in section 3BM2 is shown in figure A7.4.1-39.

The microstructure and hardness of the heat affected zones in both section 3BM1 and 3BM2 were similar. In both cases, the microstructure consists of ferrite both as a network in prior austenite grain boundaries and as needles, bainite, partially spheroidized carbides and some tempered martensite. Hardness in the heat affected zones was similar to that of the weld. A region representative of the heat affected zone in section 3BM1 is shown in figure A7.4.1-40.

The transition from the heat affected zone to the base channel material appeared similar in both sections. A region representative of the transition zone in section 3BM2 is shown in figure A7.4.1-41.

The base material of both channel pieces of the box beam appeared similar in microstructure in both sections 3BM1 and 3BM2. In both cases, the microstructure consists of ferrite and pearlite in a normalized condition. A region representative of the channel material is shown in figure A7.4.1-42. Hardness of both channels was also similar.

In summary, the walkway and NBS box beam structural steel weldment microstructure and hardness are comparable and normal.

#### A7.4.2 Walkway Hanger Rods

Transverse and longitudinal sections from each of the walkway hanger rod segments obtained from the debris (NBS 5A and 5B) were examined metallographically. The locations of these sections in the hanger rods are shown in figure A7.3.3-1. A representative region showing the etched microstructure of the transverse section from hanger rod NBS 5A is shown in figure A7.4.2-1. The

microstructure consists of ferrite (light) and pearlite (dark) in a reasonably fine grained (ASTM grain size 9) normalized structure.

The representative microstructure of the transverse section from hanger rod NBS 5B is shown in figure A7.4.2-2. The microstructure again consists of ferrite (light) and pearlite (dark) in the normalized condition. This microstructure is coarser (ASTM grain size 7-1/2 to 8) than that of hanger rod NBS 5A, and there appears to be more pearlite present than in hanger rod NBS 5A.

Longitudinal sections through each hanger rod segment revealed the material of both to be fully normalized with equiaxed grains. Regions representative of the longitudinal microstructures are shown in figure A7.4.2-3 for rod segment NBS 5A and in figure A7.4.2-4 for rod segment NBS 5B.

Rockwell B (HRB) hardness measurements were made on each of the transverse sections examined for microstructure. Twelve measurements were made on each section. The average hardness value for the finer grained hanger rod NBS 5A material was HRB 74.5 with a range of HRB 72-76. The average hardness value for hanger rod NBS 5B material was HRB 68.5 with a range of HRB 66 to 71.5. In the section from hanger rod NBS 5B, there was a slight hardness gradient with hardness decreasing from the outside toward the center.

#### A7.4.3 Washers

Hardness measurements were made on NBS washers and on washers obtained from the walkway debris. A metallographic examination was performed on sections through a hanger rod washer obtained from the walkway debris at location 9MW and through one of the NBS hardened washers.

Rockwell C (HRC) hardness measurements were made on the surfaces of four washers obtained from the walkway debris. The results of these measurements are given in table A7.4.3-1. It is apparent from these results that the washers obtained from the walkway were hardened washers.

Rockwell C hardness measurements were made on the surface of one NBS hard washer, and Rockwell B (HRB) hardness measurements were made on the surface of one unplated regular grade washer. The results of these measurements are also given in table A7.4.3-1.

Knoop microhardness measurements at a load of 500 grams force (HK<sub>500</sub>) were made on a cross section through a washer from the walkway debris at location 9MW after it had been used in an NBS full length test on box beam 9M. During the test, the washer fractured into five pieces. A microhardness traverse was made through the thickness of the washer on the section examined. The washer thickness was approximately 0.075 in (1.80 mm). Average hardness from 16 measurements across the section was 459 HK<sub>500</sub> which is approximately equivalent to 44.3 HRC and the hardness range was 422 to 514 HK<sub>500</sub> (41.5 to 48.5 HRC). The highest values were near the center of the section and the lowest values were near the surface of the washer. The microstructure of the washer from location 9MW is shown in figure A7.4.3-1. There is a very small apparent decarburized

layer at the surface (light area at the top in the figure). Tempered martensite is the primary constituent of the microstructure.

A similar microhardness traverse on a section through one of the NBS hard washers was made. Hardness values in this section, excluding the decarburized layer at the surface, averaged 431 HK<sub>500</sub> (42.5 HRC) and ranged from 401 to 422 HK<sub>500</sub> (40 to 43.5 HRC). Measured hardness in the decarburized layer was as low as 247 HK<sub>500</sub> (99 HRB). The microstructure of the NBS hard washer is shown in figure A7.4.3-2. The decarburized layer at the surface appears light in the figure. Tempered martensite is the primary constituent in the microstructure.

#### A7.5 CHEMICAL ANALYSIS

Five specimens from the walkway box beam longitudinal welds (four exterior welds and one interior tack weld) and weld specimens from four NBS box beam replicas were analyzed for chemical composition by emission spectrometry. Also analyzed for chemical composition were two samples of hanger rod material removed from the walkway debris.

A 3/4 mm vacuum spectrometer with an adjustable waveform excitation source was used for the analysis. The instrumental analytical curves were constructed using NBS SRMs 1261, 1262, 1263, 1264 and 1265 plus other selected reference materials. All specimens were surfaced using 50 grit Al<sub>2</sub>O<sub>3</sub> sanding disks. In order to confine the analytical discharge to the weld area, a boron nitride disk with a 0.157 in (4 mm) opening was used in the excitation stand.

The specimen identification numbers and origins are listed in table A7.5-1. Actual locations of specimens within the walkway box beam and hanger rod segments are described in figures A7.3.2-1 through A7.3.2-3 and in figure A7.3.3-1. Normal laboratory routines used for SRM homogeneity testing were used in the analysis. Program outputs included averages, standard deviations and a pictorial presentation (box plots) of the individual values for those elements normally considered the most important in ferrous analysis. Each value reported in the tables of this section is an average of four exposures.

##### A7.5.1 Box Beam Longitudinal Welds

Results of the analysis of longitudinal weld specimens obtained from segments of the walkway box beams are listed in table A7.5.1-1. In table A7.5.1-2, the results obtained from the four weld specimens removed from NBS box beam replicas are presented. In each case the tables include analytical values for the base metal in the flange on either side of the longitudinal weld seam.

It is concluded that of the four NBS weld specimens analysed, specimen M2 (flux cored electrode) most closely corresponds to the weld material in the walkway box beam longitudinal welds. This is based primarily on the comparable values for manganese, silicon and titanium. While this comparison does not rule out the possibility of other types of electrodes being used in the fabrication of the walkway box beams, it is in agreement with information provided by the

fabricator's legal counsel regarding welding procedure as noted in chapter 6 of this report.

#### A7.5.2 Walkway Box Beam Interior Tack Weld

Results of the analysis of the interior tack weld specimen removed from box beam 8L (NBS 2) are listed in table A7.5.2-1. The analysis of this weld is comparable to the four walkway box beam welds discussed in section A7.5.1, and it is concluded that exterior and interior welds were made using the same type of electrode.

#### A7.5.3 Walkway Hanger Rod Specimens

The chemical analysis of two hanger rod specimens (one specimen from each of two segments designated NBS 5A and NBS 5B) is presented in table A7.5.3-1. The analysis clearly shows that the two hanger rod segments are from different heats since nine elements have significantly different concentrations. In addition, the sulfur value in specimen 5AC (NBS 5A) shows this element at or just above the limit specified for ASTM Grade A36 steel. Further analysis of this material by a gasometric method showed the sulfur value to be within specification with levels of  $0.046 \pm 0.001$  for rod 5A and  $0.033 \pm 0.001$  for rod 5B as reported in table A7.5.3-1.

Table A7.4.1-1 Hardness Test Results from Transverse Sections Through Box Beam 9U (NBS 1)

HK500 (HRB) Hardness Numbers

Region of Section	Section 1BM1			Section 1BM2		
	Number of Measurements	Average	Range	Number of Measurements	Average	Range
Weld Metal	10	227(95.2)	200-246(90-98)	13	208(91.2)	201-222(90-94)
Transition Zone Between Weld & HAZ, South Side	3	324[31.5](a)	306-336[29-33](a)			
Hard Spot	1	238(97.5)				
Away from Hard Spot						
HAZ	8	219(93.7)	200-241(90-98)	3	196(88.6)	189-204(87-90)
South	5	193(88.3)	179-201(85-90)	2	199(89.5)	198-200(89-90)
North						
Channel Adjacent to HAZ	5	174(85)	173-176(83-84)	4	172(82.5)	167-174(81-83)
South	4	183(83.7)	173-191(83-88)	5	178(84.4)	171-186(82-86)
North						
Direct HRB Measurements						
Flange adjacent to HAZ and web about 0.6 to 1 in from base of flange	5	81	80-83	4	82.1	81.5-83
Elsewhere in flange and web						
South	22	74.5	72-77.5	21	75.1	73-79.5
North	21	74.3	72-76	21	73.4	70.5-77

(a) Values in brackets are HRC hardness numbers

1 in = 25.4 mm

Table A7.4.1-2 Hardness Test Results from Transverse Sections Through Box Beam 8L (NBS 2)

HK500 (HRB) Hardness Numbers

Region of Section	Section 2BML			Section 2BM2		
	Number of Measurements	Average	Range	Number of Measurements	Average	Range
Weld Metal	12	210(91.8)	199-230(89.5-96)	8	223(94.3)	211-234(92-96.5)
Transition Zone Between Weld & HAZ, South Side						
Hard Spot				1	298[28](a)	
Away from Hard Spot				2	247(99)	241-253(98-100)
HAZ						
South	2	209(91.8)	205-213(91-92.5)	3	208(89)	196-227(89-95)
North	4	196(88.8)	177-212(84-92)	2	194(88.5)	187-201(87-90)
Channel Adjacent to HAZ						
South	5	178(84.4)	173-188(83-87)	5	171(82)	161-191(79-88)
North	5	167(81.1)	156-180(77.5-85)	4	166(80.5)	158-180(78-85)
Direct HRB Measurements						
Flange adjacent to HAZ and web about 0.6 to 1 in from base of flange	8	81.1	79.5-82.5	5	81.9	80.5-84
Elsewhere in flange and web						
South	23	75.3	73-79	24	75.3	73.5-79
North	21	74.2	70.5-76	22	75.5	73.5-79

(a) Values in brackets are HRC hardness numbers

1 in = 25.4 mm

Table A7.4.1-3 Hardness Test Results from Transverse Sections Through Box Beam 9M (NBS 3)  
 HK500 (HRB) Hardness Numbers

Region of Section	Section 3BM1			Section 3BM2		
	Number of Measurements	Average	Range	Number of Measurements	Average	Range
Weld Metal	21	188(87)	162-210(79-92)	17	190(87.2)	153-203(76-90.5)
HAZ North	7	191(87.6)	174-201(83-90)			
HAZ South				12	186(86.5)	171-201(82-90)
Channel Adjacent to HAZ, North	4	173(82.6)	162-180(79-85)			
Channel Adjacent to HAZ, South				6	170(81.9)	159-173(78-83)
Direct HRB Measurements Flange adjacent to HAZ and web about 0.6 to 1 in from base of flange	5	79.6	78-82	3	80.7	79-82
Elsewhere in flange and web	22	74.4	73-77.5	22	73.3	70-76

1 in = 25.4 mm

Table A7.4.4-1 Results of Washer Hardness Tests

<u>Washer Identification</u>	<u>Number of Measurements</u>	<u>Hardness</u>			
		<u>HRC</u>		<u>HRB</u>	
		<u>Average</u>	<u>Range</u>	<u>Average</u>	<u>Range</u>
8UE Top	8	40.2	39.0-41.0		
8LW Top	8	43.0	40.0-45.0		
9ME Top	8	37.5	34.5-40.5		
9MW Top	8	44.0	42.5-45.0		
NBS Hardened	5	39.6	38.5-41.9		
NBS Regular Grade	5			60.7	58.9-61.3

Table A7.5-1 Origin of Specimens Analyzed for Chemical Composition

<u>Specimen Identification</u>	<u>Origin</u>
1BX4	Bottom flange of walkway box beam 9U (NBS 1)
2BX1	Bottom flange of walkway box beam 8L (NBS 2)
3BX1	Bottom flange of walkway box beam 9M (NBS 3)
2TFX4	Top flange of walkway box beam 9M (NBS 3)
B2	NBS box beam replica B2. E7018 electrode
C3	NBS box beam replica C3. E7014 electrode
M2	NBS box beam replica M2. Flux cored electrode
N6	NBS box beam replica N6. Mild steel electrode
2C	Interior tack weld, bottom flange, walkway box beam 8L (NBS 2)
5AC	Fourth floor to ceiling walkway hanger rod 8E (NBS 5A)
5AB	Second to fourth floor walkway hanger rod (NBS 5B)

Table A7.5.1-1 Chemical Analysis of Walkway Box Beam Longitudinal Welds  
Analytical Values--Percent by Weight

Element	Specimen Identification Number										
	1BX4		2BX1		3BX1		2TFX4				
	base	weld	base	base	base	weld	base	base	weld	base	
Carbon	.181 .187	.121 .123	.185 .184	.185 .183	.117 .118	.183 .186	.169 .140	.185 .188	.180 .181	.131 .121	.188 .184
Phosphorus	.017 .017	.012 .011	.016 .017	.016 .017	.012 .012	.017 .017	.013 .011	.016 .018	.016 .017	.012 .013	.017 .017
Sulfur	.016 .016	.019 .019	.016 .016	.017 .015	.020 .019	.016 .016	.021 .019	.016 .016	.016 .015	.017 .017	.016 .016
Manganese	.672 .699	.946 .991	.726 .764	.715 .748	.992 1.028	.707 .741	1.061 1.118	.671 .710	.703 .740	1.013 1.143	.721 .749
Silicon	.181 .183	.370 .382	.191 .196	.196 .199	.413 .415	.194 .197	.480 .465	.179 .187	.191 .199	.413 .480	.197 .201
Nickel	.010 .011	.009 .010	.010 .011	.010 .011	.009 .009	.010 .011	.009 .010	.010 .011	.010 .011	.009 .009	.010 .011
Chromium	.017 .019	.020 .021	.018 .019	.018 .019	.020 .021	.017 .020	.021 .023	.018 .019	.018 .019	.021 .023	.018 .019
Vanadium	.002 .002	.005 .005	.002 .003	.002 .002	.005 .006	.002 .002	.006 .006	.002 .002	.002 .002	.005 .006	.002 .002
Titanium	.001 .001	.010 .010	.001 .001	.001 .001	.011 .011	.001 .001	.012 .012	.001 .001	.001 .001	.011 .014	.001 .001
Molybdenum	.006 .006	.005 .005	.006 .006	.006 .006	.005 .005	.006 .006	.007 .005	.006 .006	.006 .006	.005 .005	.006 .006
Copper	.012 .013	.017 .016	.012 .013	.012 .012	.015 .015	.013 .013	.013 .015	.012 .013	.011 .013	.014 .020	.013 .016
Cobalt	.006 .005	.005 .004	.006 .005	.006 .005	.005 .004	.006 .005	.007 .005	.006 .005	.005 .005	.004 .005	.006 .005
Aluminum	<.001 <.001	<.001 <.001	.001 .001	.001 <.001	<.001 <.001	.001 .001	.001 <.001	<.001 <.001	.001 .001	<.001 .001	.001 .001
Niobium	<.001 .001	.002 .003	.001 .001	.001 .001	.002 .003	<.001 .001	.001 .003	<.001 .002	<.001 .001	.002 .003	.001 .001
Zirconium	.001 .001	.002 .002	.001 .001	.001 .001	.001 .002	.001 .001	.001 .002	.001 .001	.001 .001	.001 .002	.001 .001

Table A7.5.1-2 Chemical Analysis of NBS Box Beam Longitudinal Welds  
Analytical Values--Percent by Weight

Specimen Identification Number

Element	B2		C3		M2		N6		
	base	weld	base	weld	base	weld	base	weld	
Carbon	.181	.093	.182	.119	.183	.179	.124	.181	.182
	.181	.097	.183	.117	.181	.179	.123	.178	.180
Phosphorus	.012	.011	.012	.014	.012	.012	.008	.012	.012
	.013	.009	.013	.014	.013	.013	.008	.012	.011
Sulfur	.022	.022	.023	.024	.022	.022	.021	.022	.023
	.022	.022	.023	.024	.022	.023	.021	.021	.022
Manganese	.782	.588	.784	.426	.780	.777	1.109	.782	.787
	.806	.615	.813	.443	.812	.809	1.178	.810	.806
Silicon	.208	.266	.207	.270	.207	.210	.437	.212	.212
	.210	.249	.210	.272	.210	.215	.450	.213	.213
Nickel	.010	.010	.010	.039	.010	.010	.011	.010	.011
	.011	.011	.011	.040	.011	.011	.011	.011	.011
Chromium	.040	.030	.041	.030	.040	.040	.035	.039	.041
	.041	.032	.043	.032	.042	.041	.037	.042	.041
Vanadium	.001	.007	.001	.005	.001	.001	.004	.001	.001
	.001	.007	.002	.006	.002	.001	.005	.001	.001
Titanium	.001	.005	.001	.013	.001	.001	.010	.001	.001
	.001	.005	.001	.014	.001	.001	.011	.001	.001
Molybdenum	.005	.005	.005	.005	.005	.005	.005	.005	.005
	.005	.005	.005	.005	.005	.005	.004	.005	.005
Copper	.010	.009	.010	.010	.010	.010	.013	.010	.011
	.013	.011	.012	.014	.011	.010	.014	.011	.011
Cobalt	.004	.004	.003	.006	.003	.003	.004	.003	.004
	.003	.003	.003	.006	.003	.003	.003	.003	.003
Aluminum	.006	.001	.007	.001	.006	.007	.002	.007	.007
	.006	.001	.006	.001	.006	.006	.002	.006	.008
Niobium	.001	.001	.001	.004	.001	.001	.003	.001	.001
	.001	.002	.002	.005	.002	.001	.004	.002	.002
Zirconium	.001	.001	.001	.001	.001	.001	.002	.001	.001
	.001	.001	.001	.002	.001	.001	.002	.001	.001

Table A7.5.2-1 Chemical Analysis of Walkway Box Beam Interior Tack Weld

Analytical Values--Percent by Weight

Specimen Identification Number

Element	2C		
	base	weld	base
Carbon	.184	.091	.184
	.184	.095	.181
Phosphorus	.017	.012	.016
	.018	.013	.017
Sulfur	.016	.018	.015
	.017	.018	.015
Manganese	.711	1.096	.719
	.722	1.086	.722
Silicon	.193	.452	.198
	.195	.442	.197
Nickel	.011	.010	.010
	.011	.009	.010
Chromium	.018	.023	.018
	.018	.021	.018
Vanadium	.002	.006	.002
	.002	.006	.002
Titanium	.001	.014	.001
	.001	.014	.001
Molybdenum	.005	.004	.005
	.005	.004	.005
Copper	.012	.016	.012
	.012	.016	.013
Cobalt	.005	.004	.005
	.005	.005	.005
Aluminum	.001	.001	.001
	.001	.001	.001
Niobium	.001	.003	.001
	.001	.003	.001
Zirconium	.001	.002	.001
	.001	.001	.001

Table A7.5.3-1 Chemical Analysis of Walkway Hanger Rod Specimens

Analytical Values--Percent by Weight

Specimen Identification Number

Element	5AC	5BC	5AX1*	5BX*
Carbon	.168 .168	.200 .197	.159	.200
Phosphorus	.037 .038	.010 .009		
Sulfur	.050 .052	.035 .035	.046	.033
Manganese	.510 .527	.672 .696		
Silicon	.187 .185	.038 .039		
Nickel	.094 .098	.053 .055		
Chromium	.106 .110	.115 .117		
Vanadium	.001 .001	.001 .001		
Titanium	.001 .001	.002 .002		
Molybdenum	.009 .009	.009 .009		
Copper	.330 .338	.112 .114		
Cobalt	.008 .008	.007 .007		
Aluminum	.001 .001	.003 .005		
Niobium	.001 .002	.001 .001		
Zirconium	.001 .002	.001 .001		

\* Gasometric method

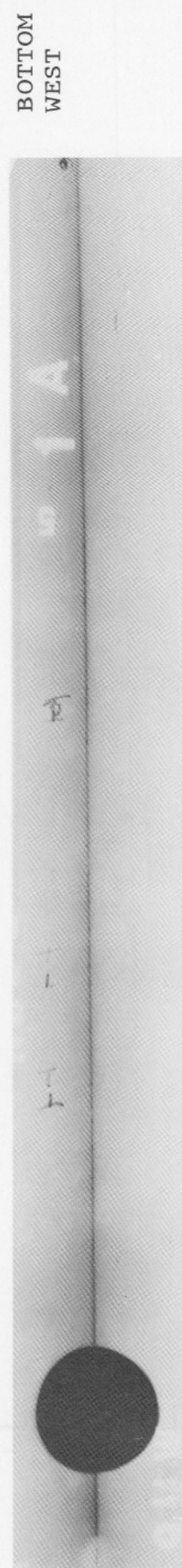
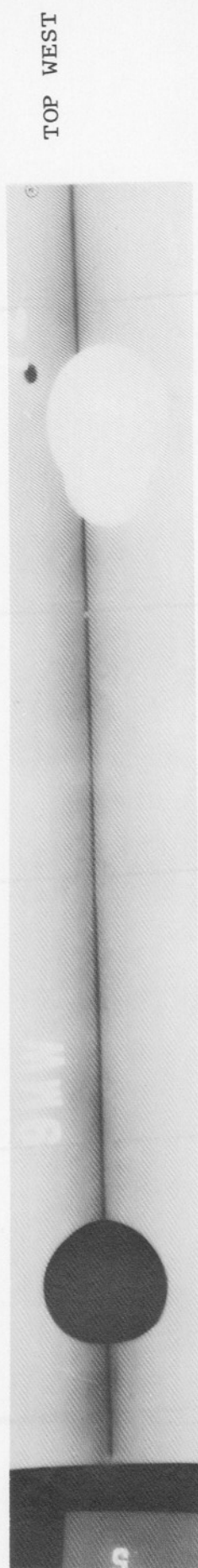
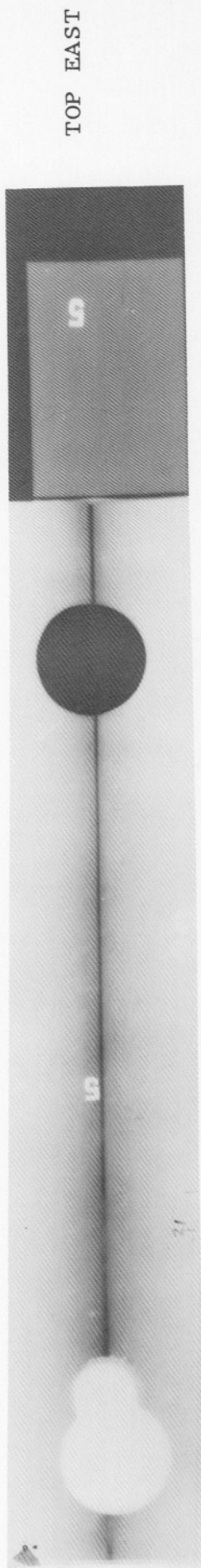


Figure A7.2.2-1 Radiographs of portions of box beam 9M used in the analysis described in section 7.2 of the report.

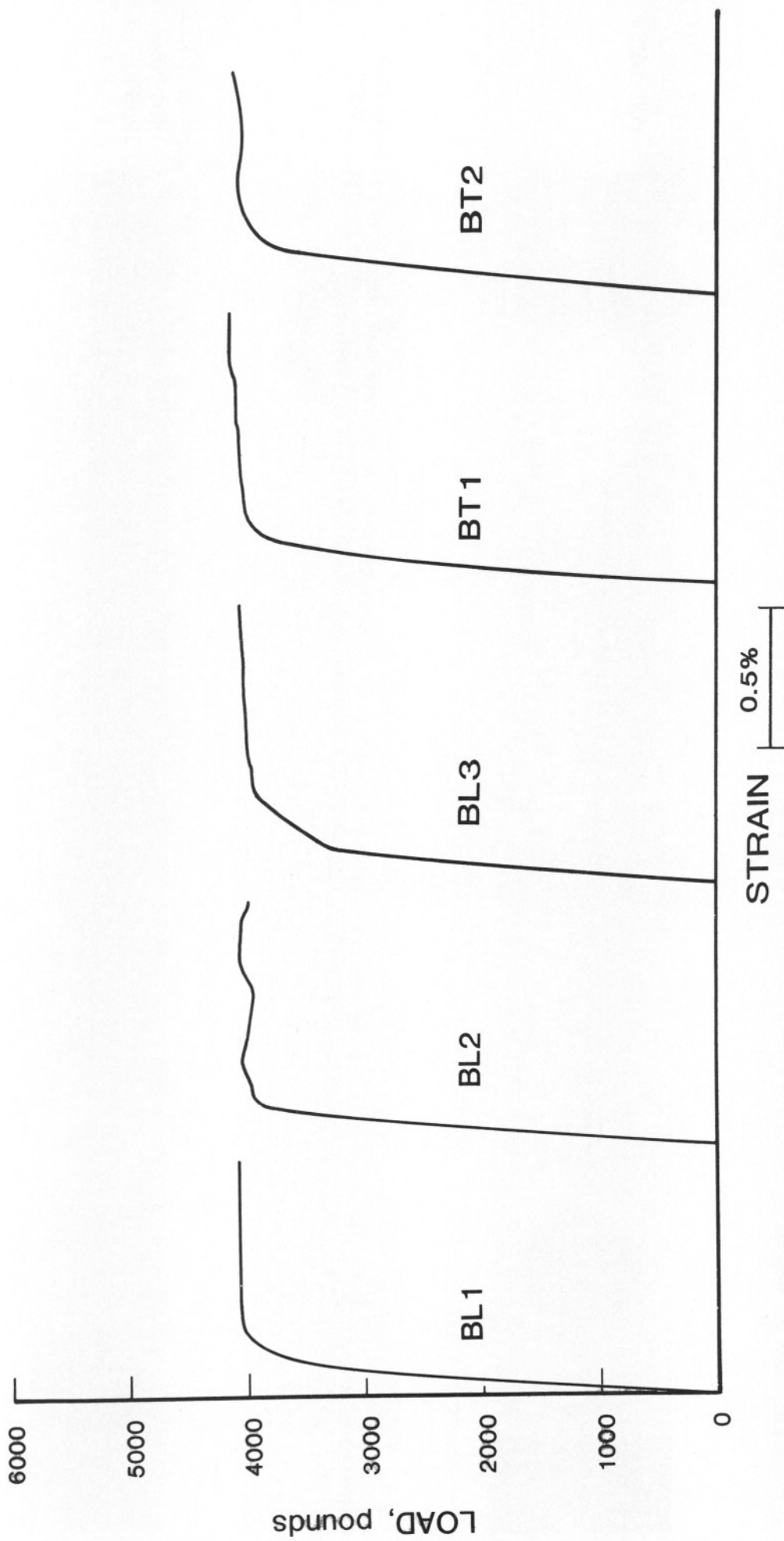


Figure A7.3.1-1 Load-strain plots for NBS channel specimens BL1, BL2, BL3, BT1, BT2.

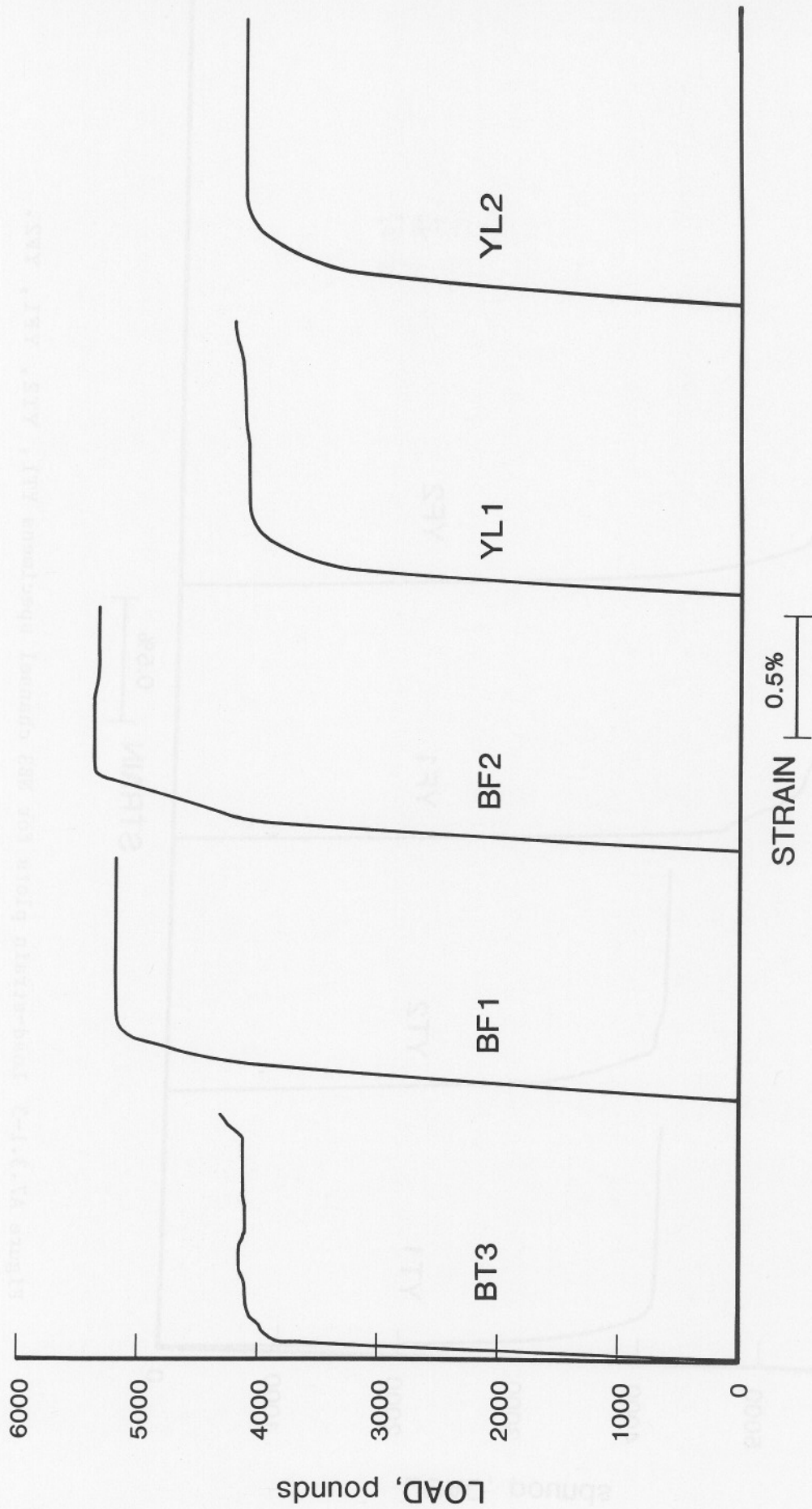


Figure A7.3.1.1-2 Load-strain plots for NBS channel specimens BT3, BF1, BF2, YL1, YL2.

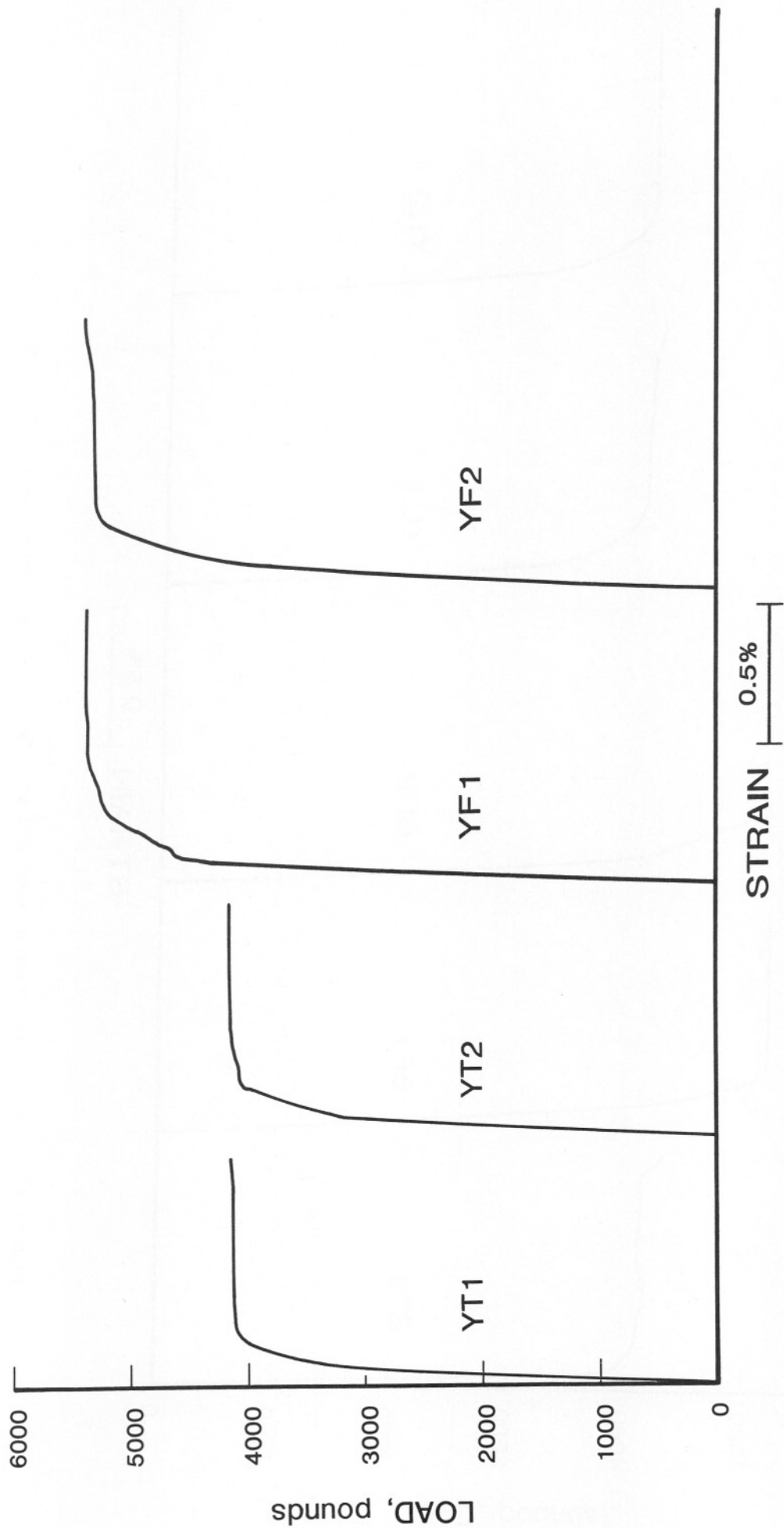
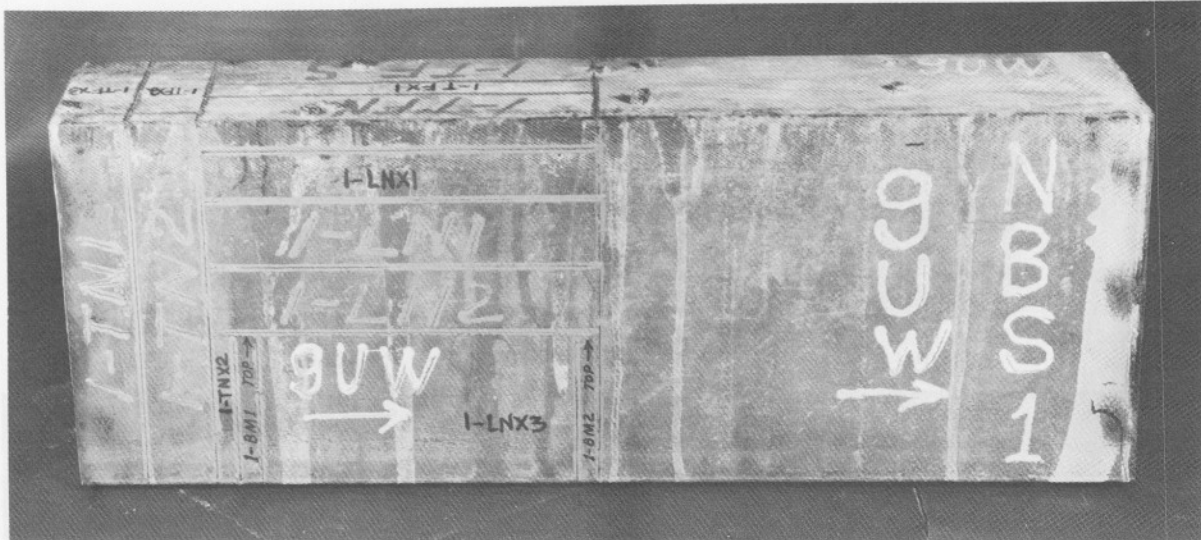


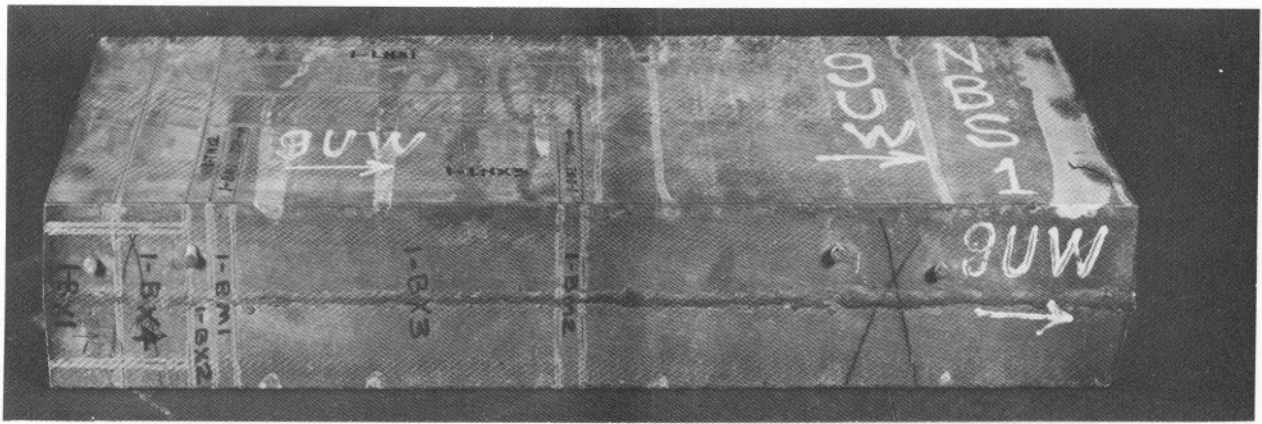
Figure A7.3.1-3 Load-strain plots for NBS channel specimens YT1, YT2, YF1, YF2.



a. North face of box beam segment 9U (NBS 1).

Figure A7.3.2-1 Location of test specimens from box beam segment 9U obtained from the walkway debris.

- a. North face:  
 Longitudinal web tensile test specimens 1-LN1, 1-LN2  
 Transverse web tensile test specimens 1-TN1, 1-TN2  
 Parts of metallographic specimens 1-BM1, 1-BM2
- b. Bottom:  
 Parts of metallographic specimens 1-BM1, 1-BM2  
 Transverse tensile test specimens across the  
 weld 1-BX3W2, 1-BX3W4  
 Chemical analysis specimen 1-BX4
- c. South face:  
 Longitudinal web tensile test specimens 1-LS1, 1-LS2  
 Transverse web tensile test specimens 1-TS1, 1-TS2  
 Parts of metallographic specimens 1-BM1, 1-BM2
- d. Top:  
 Longitudinal flange tensile test specimens 1-TFN, 1-TFS



b. Bottom of box beam segment 9U (NBS 1).

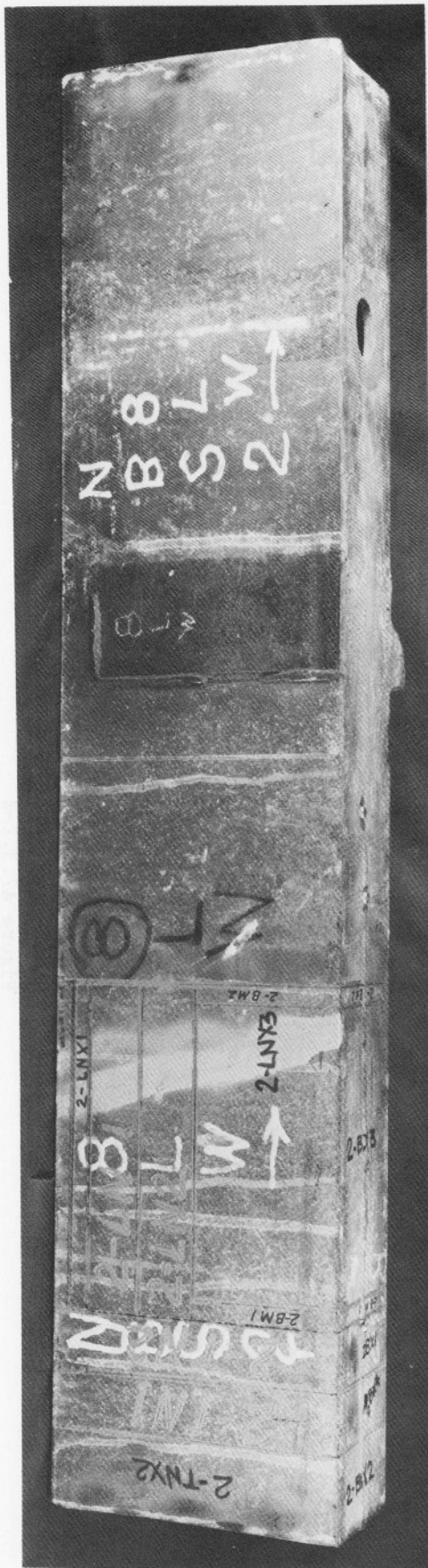


c. South face of box beam segment 9U (NBS 1).



d. Top of box beam segment 9U (NBS 1).

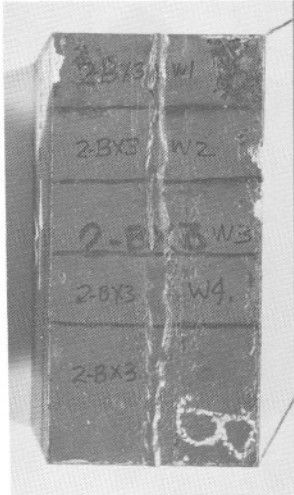
Figure A7.3.2-1



a. North face of box beam segment 8L (NBS 2).

Figure A7.3.2-2 Location of test specimens from box beam segment 8L obtained from the walkway debris.

- a. North face:  
 Longitudinal web tensile test specimens 2-LN1, 2-LN2  
 Transverse web tensile test specimens 2-TN1, 2-TN2  
 Parts of metallographic specimens 2-BM1, 2-BM2
- b. Bottom:  
 Parts of metallographic specimens 2-BM1, 2-BM2  
 Transverse tensile test specimens across the weld 2-BX3W2, 2-BX3W4  
 Chemical analysis specimen 2-BX1
- c. South face:  
 Longitudinal web tensile test specimens 2-LS1, 2-LS2  
 Transverse web tensile test specimens 2-TS1, 2-TS2  
 Parts of metallographic specimens 2-BM1, 2-BM2
- d. Top:  
 Longitudinal flange tensile test specimens 2-TFN, 2-TFS  
 Metallographic specimen 2-TFX1  
 Chemical analysis specimen 2-TFX4
- e. Bottom interior:  
 Chemical analysis specimen 2C of interior tack weld



b. Bottom of box beam segment 8L (NBS 2).



c. South face of box beam segment 8L (NBS 2).

Figure A7.3.2-2



d. Top of box beam segment 8L (NBS 2).

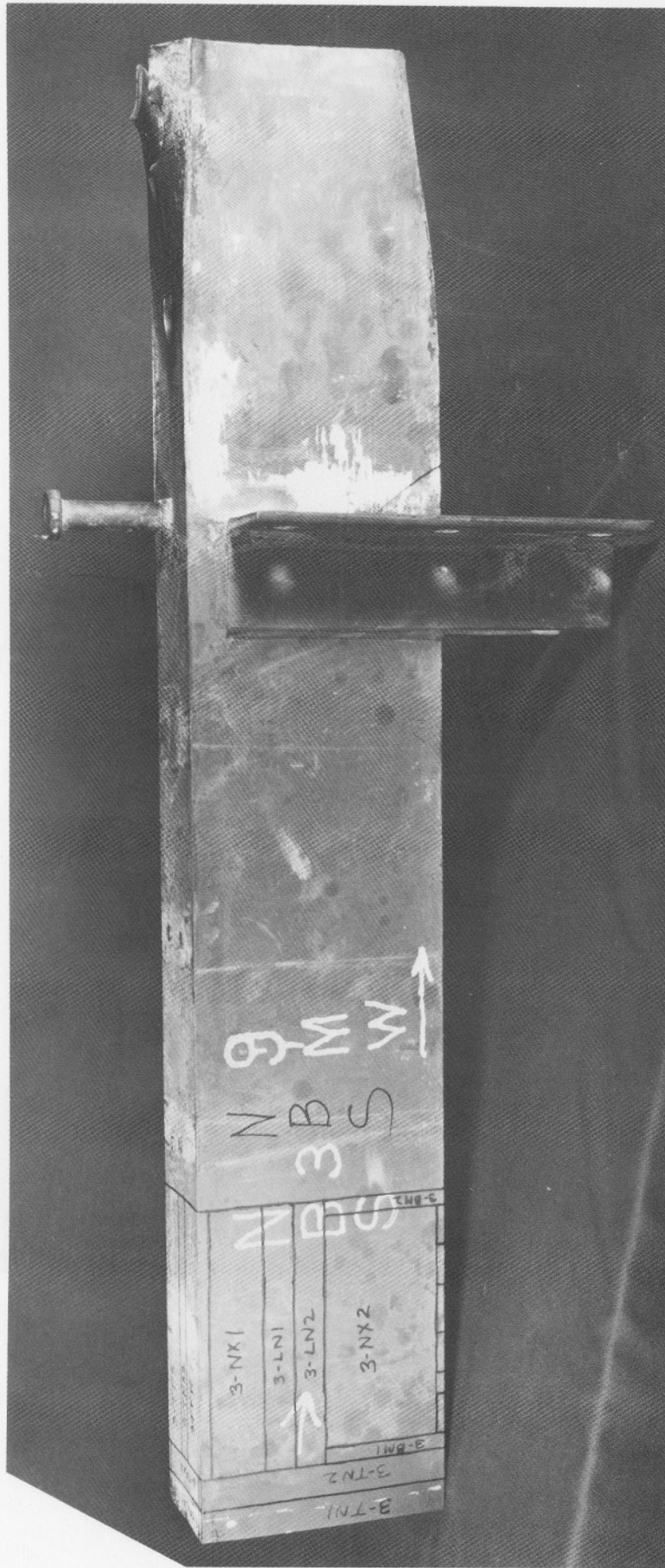


e. Bottom interior of box beam segment 8L (NBS 2).

Figure A7.3.2-2

Figure A7.3.2-3 Location of test specimens from box beam segment NBS 3-5 from box beam 9M obtained from the walkway debris.

- a. North face:
  - Longitudinal web tensile test specimens 3-LN1, 3-LN2
  - Transverse web tensile test specimens 3-TN1, 3-TN2
  - Parts of metallographic specimens 3-BM1, 3-BM2
  
- b. Bottom:
  - b.1: Parts of metallographic specimens 3-BM1, 3-BM2
  - Transverse tensile test specimens across the weld 3-BW1, 3-BW4
  - Chemical analysis specimen 3-BX1
  - Fractographic analysis specimen 3-DBB-2
  
  - b.2: Fractographic analysis specimen 3-DBB-1
  
- c. South face:
  - Longitudinal web tensile test specimens 3-LS1, 3-LS2
  - Transverse web tensile test specimens 3-TS1, 3-TS2
  - Parts of metallographic specimens 3-BM1, 3-BM2
  
- d. Top:
  - Longitudinal flange tensile test specimens 3-TFN, 3-TFS

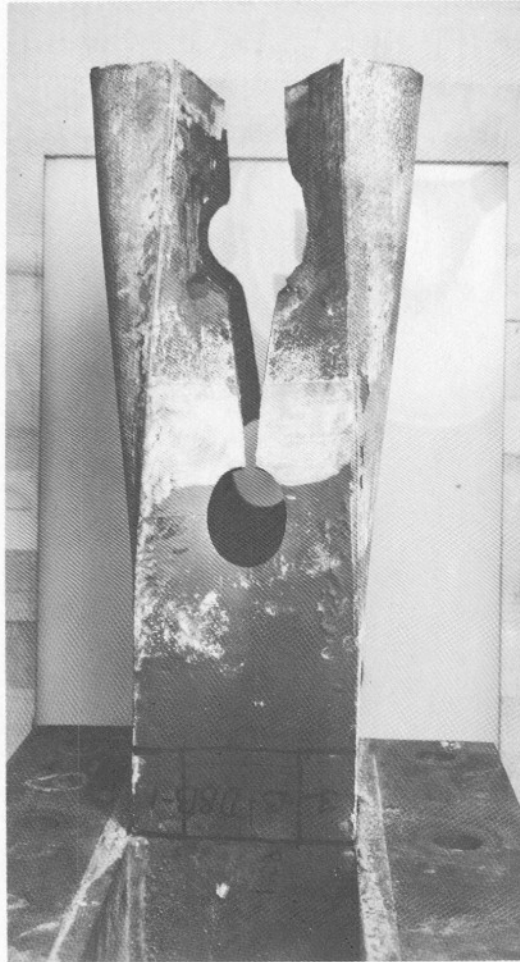


a. North face of box beam segment 9M (NBS 3-5).

Figure A7.3.2-3



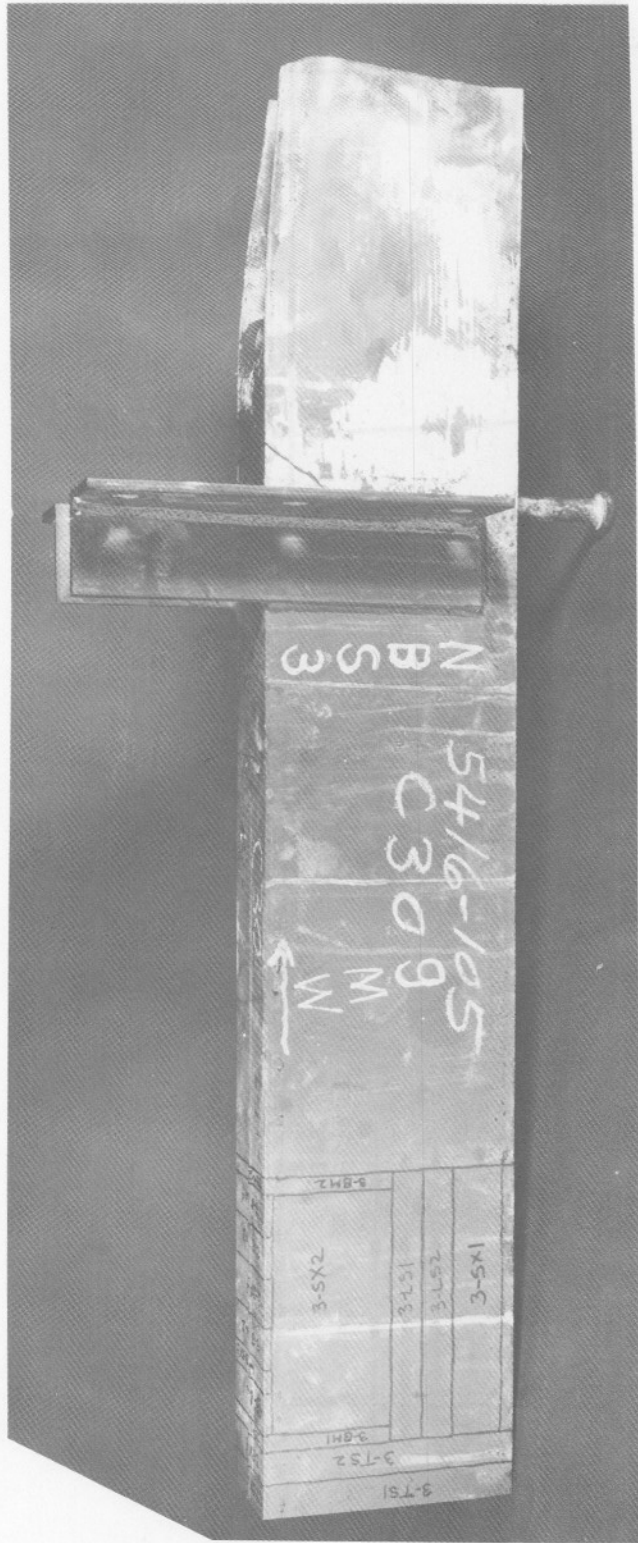
b1



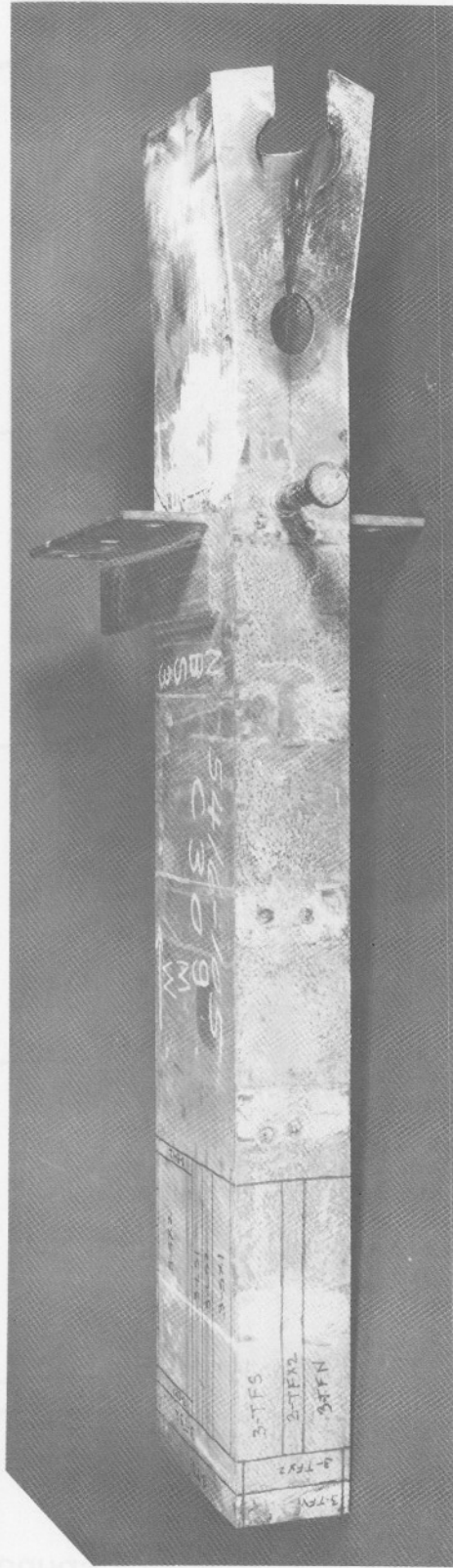
b2

b. Bottom of box beam segment 9M (NBS 3-5).

Figure A7.3.2-3



c. South face of box beam segment 9M (NBS 3-5).



d. Top of box beam segment 9M (NBS 3-5).

Figure A7.3.2-3

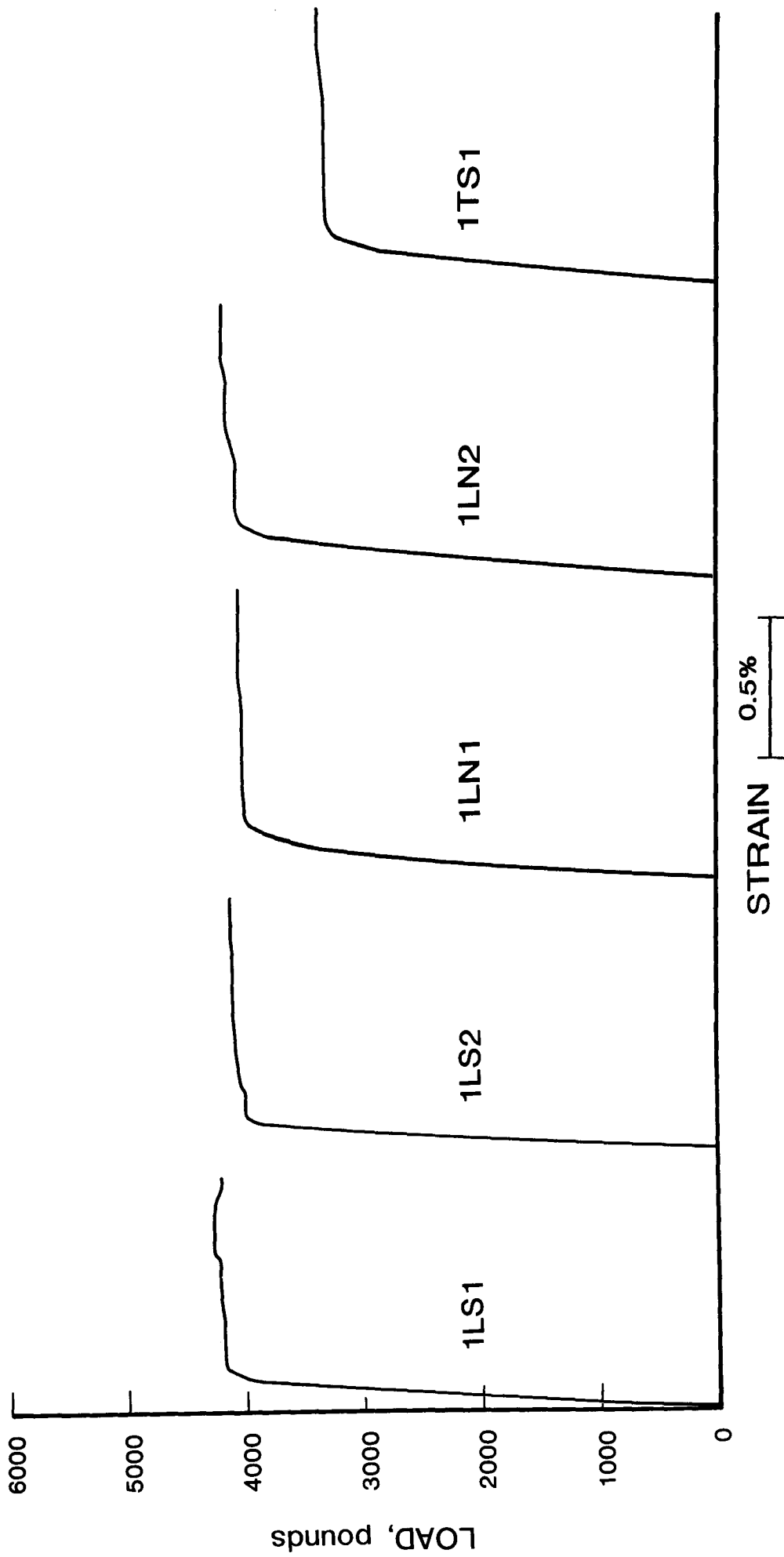


Figure A7.3.2-4 Load-strain plots for walkway box beam specimens 1-LS1, 1-LN2, 1-LN1, 1-LN2, 1-TS1.

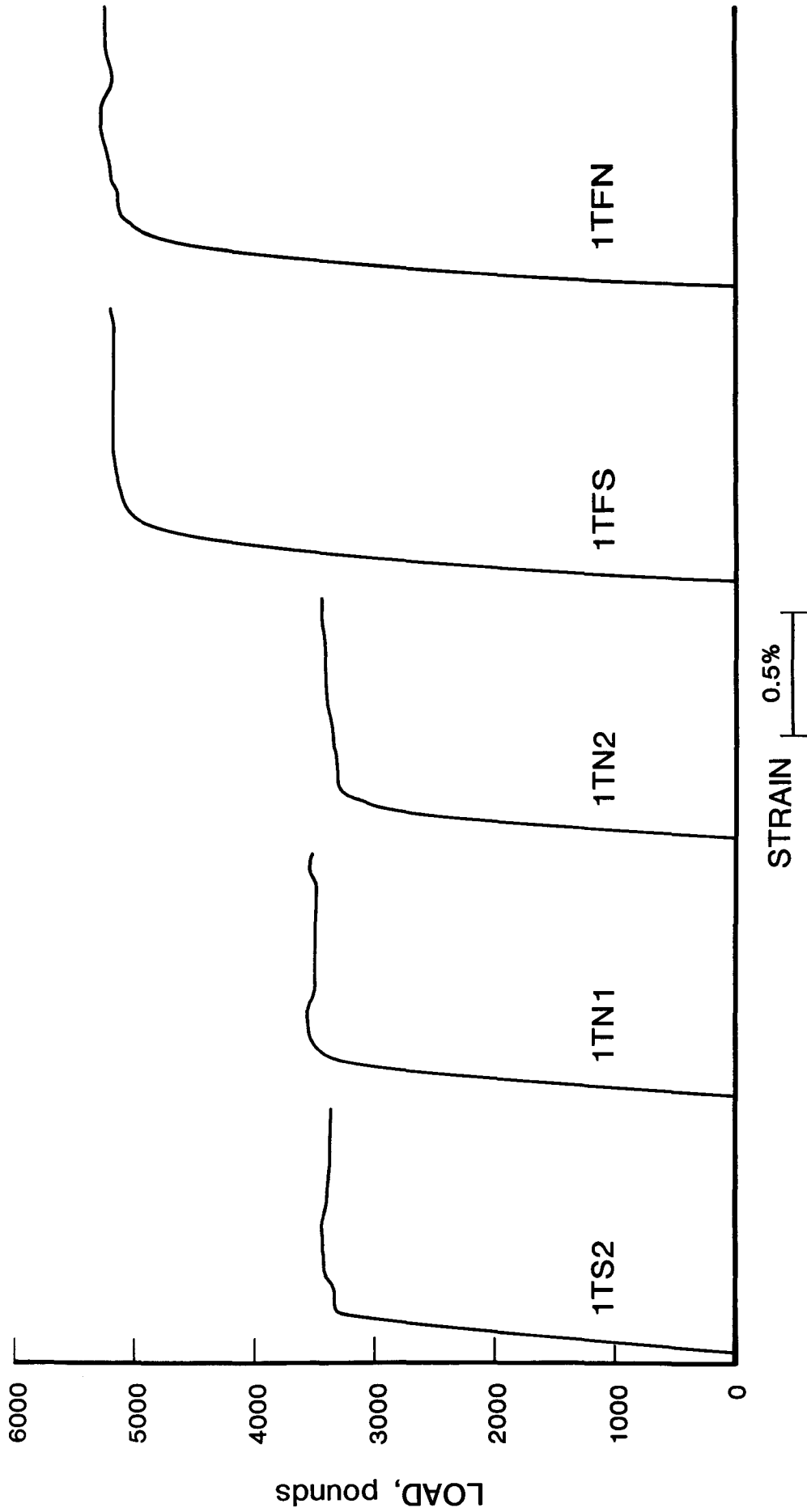


Figure A7.3.2-5 Load-strain plots for walkway box beam specimens 1-TS2, 1-TN1, 1-TN2, 1-TFS, 1-TFN.

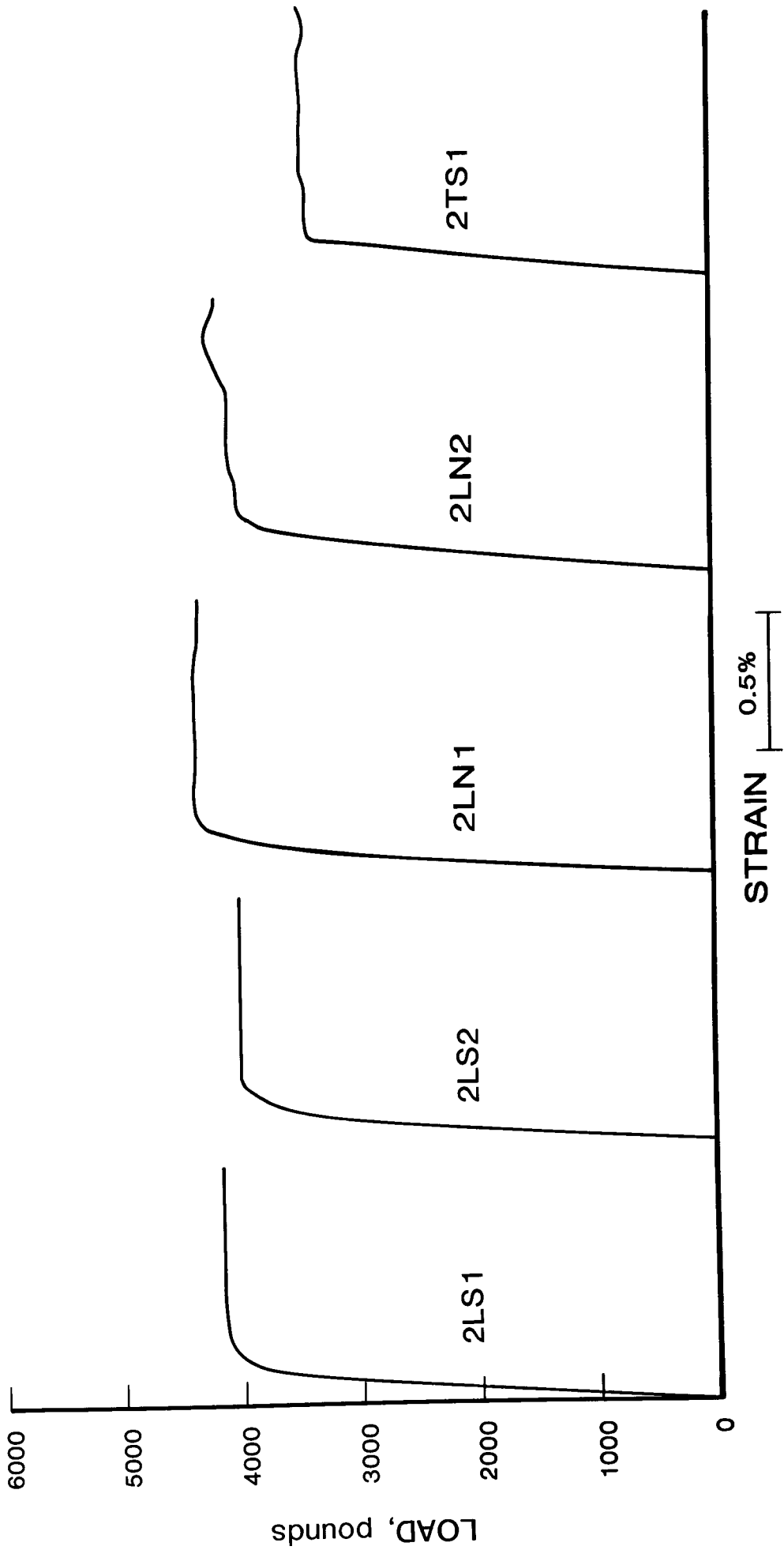


Figure A7.3.2-6 Load-strain plots for walkway box beam specimens 2-LS1, 2-LS2, 2-LN1, 2-LN2, 2-TS1.

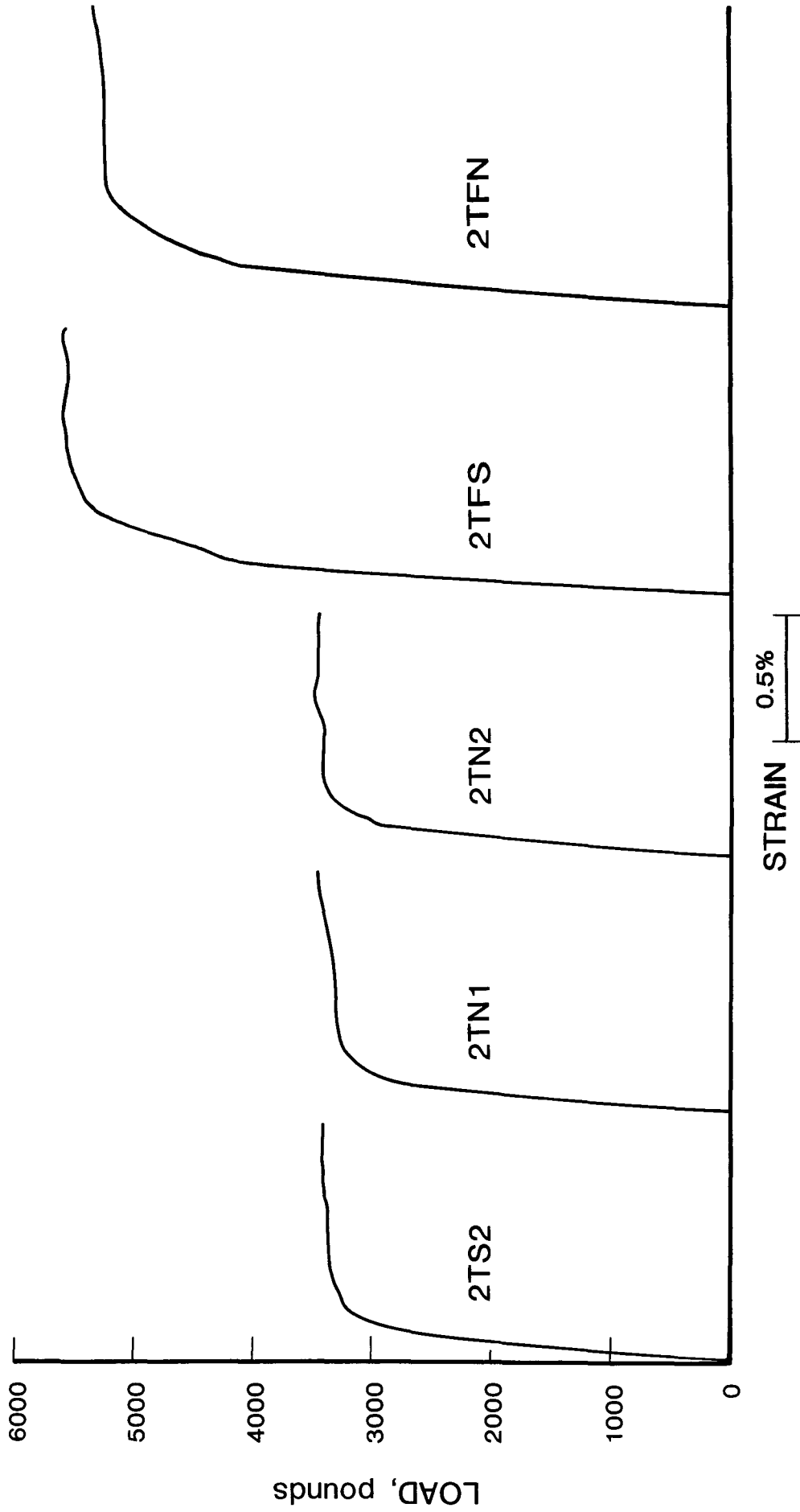


Figure A7.3.2-7 Load-strain plots for walkway box beam specimens 2-TS2, 2-TN1, 2-TN2, 2-TFS, 2-TFN.

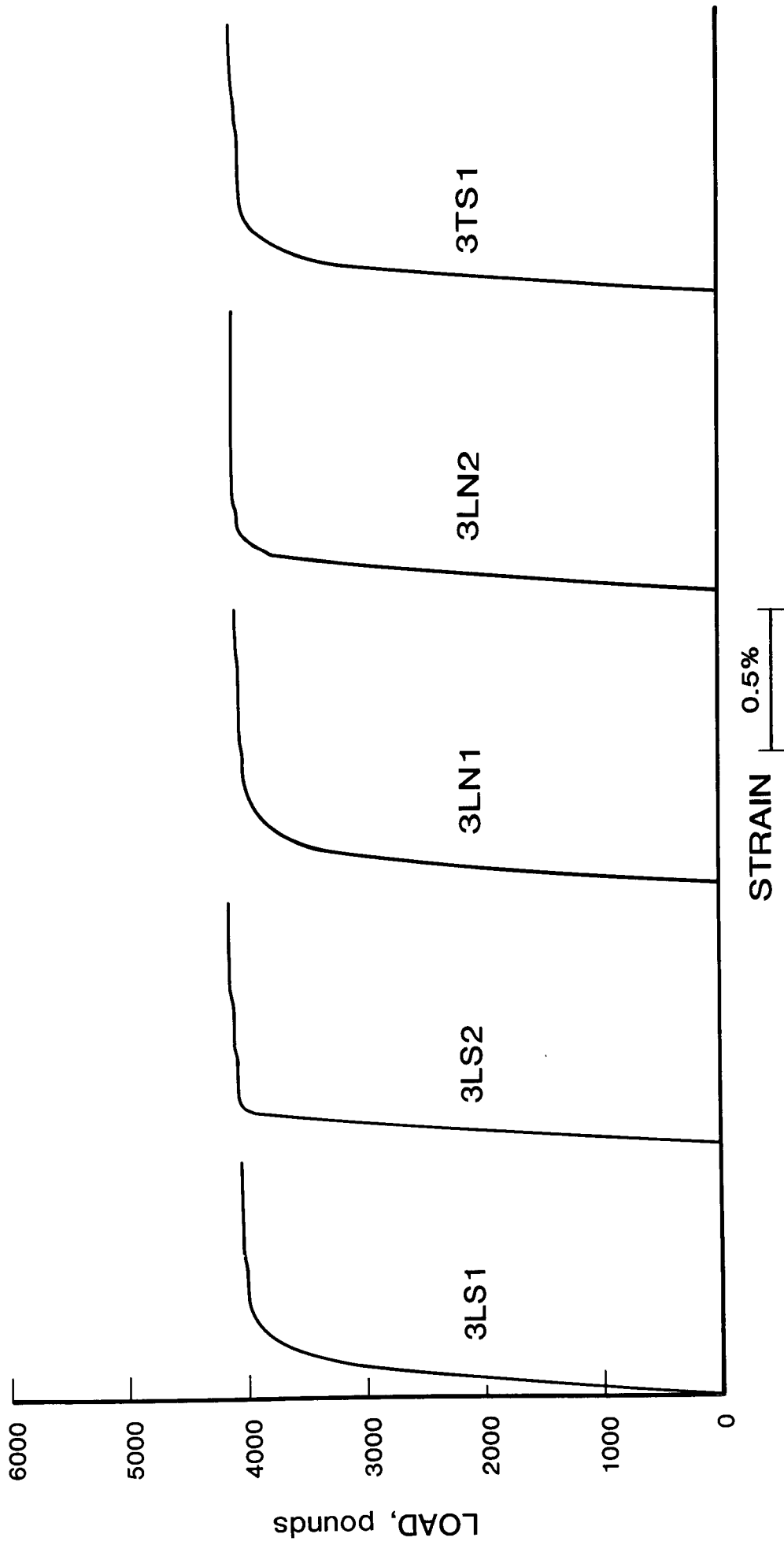


Figure A7.3.2-8 Load-strain plots for walkway box beam specimens 3-LS1, 3-LS2, 3-LN1, 3-LN2, 3-TS1.

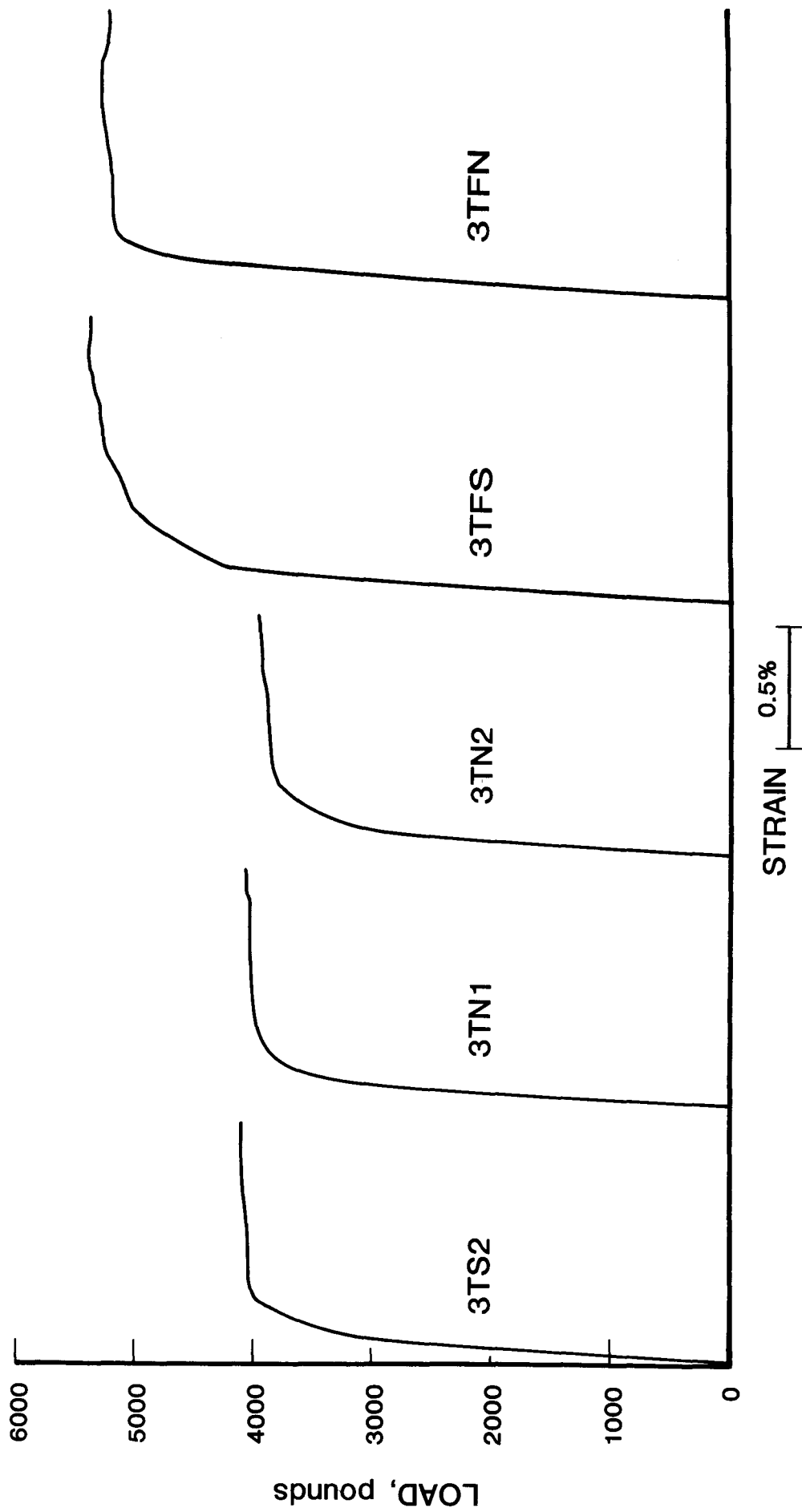


Figure A7.3.2-9 Load-strain plots for walkway box beam specimens 3-TS2, 3-TN1, 3-TN2, 3-TFS, 3-TFN.

NBS 5BM



5BC

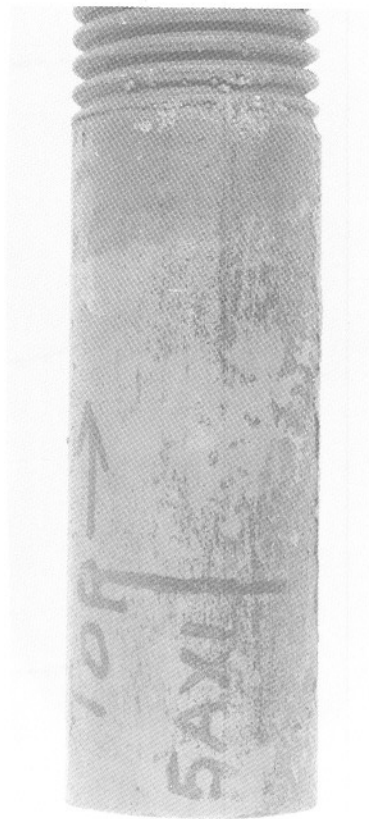


Figure A7.3.3-1. Location of test specimens from hanger rod segments NBS 5A and NBS 5B obtained from the walkway debris.

Longitudinal tensile test specimens 5AT1, 5AT2, 5BT1, 5BT2

Metallographic specimens 5AM, 5BM

Chemical analysis specimens 5AC, 5BC, 5AX1, NBS 5BX

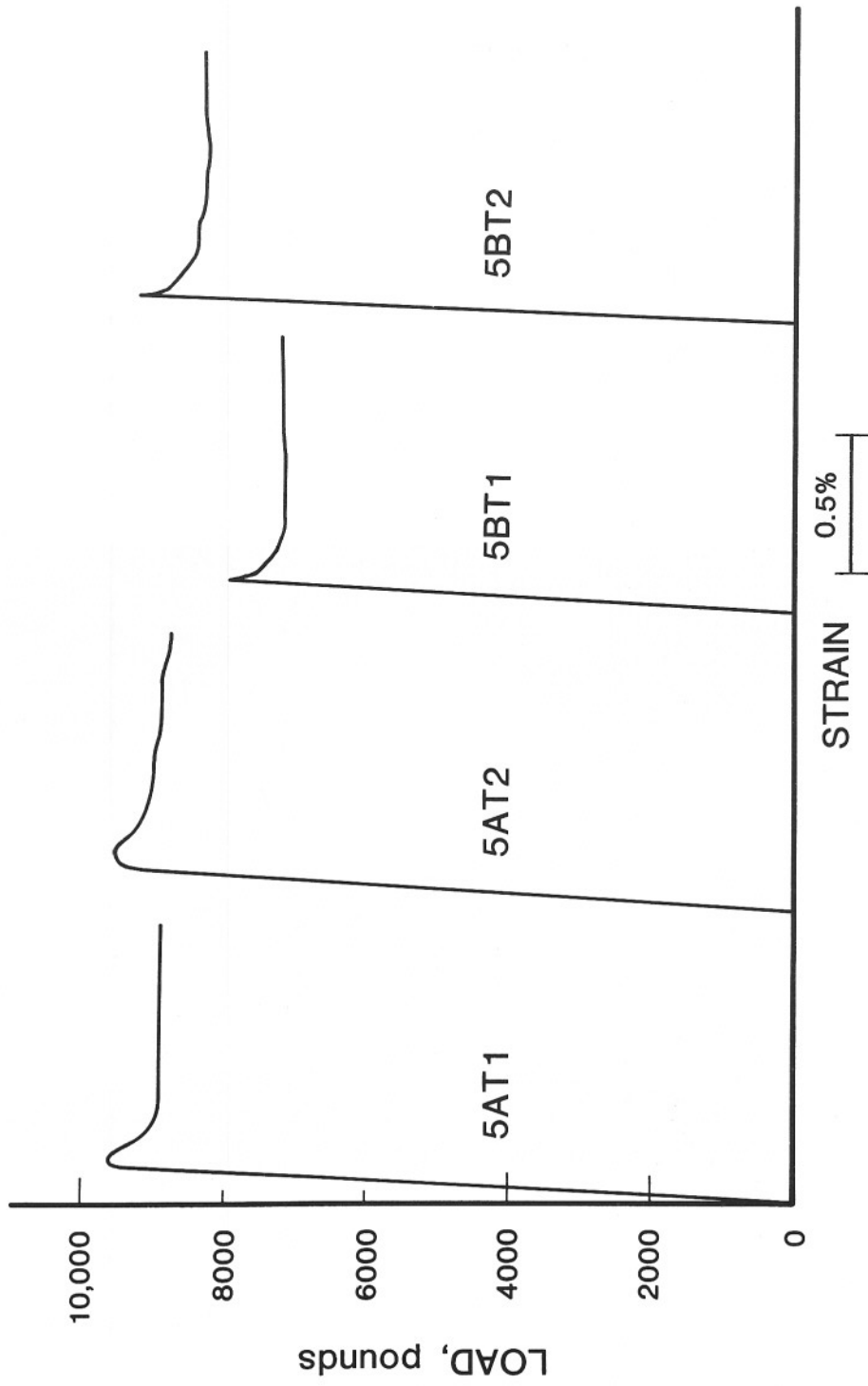


Figure A7.3.3-2 Load-strain plots for walkway hanger rod specimens 5AT1, 5AT2, 5BT1, 5BT2.

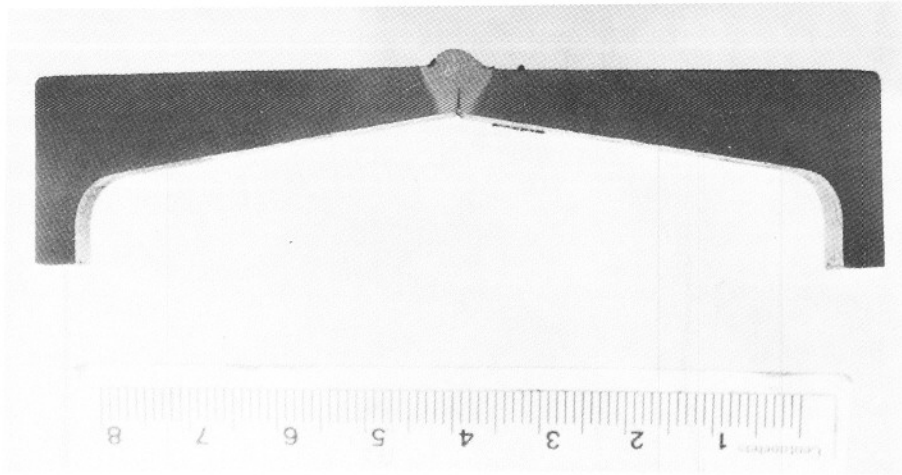


Figure A7.4.1-1 Transverse section through NBS weldment IC welded by the GMAW process using mild steel welding rod. The weld is in the center connecting flange parts of the two channel segments, Parts of the web regions of each channel are also included in the section. Etchant: two percent nital ~X1

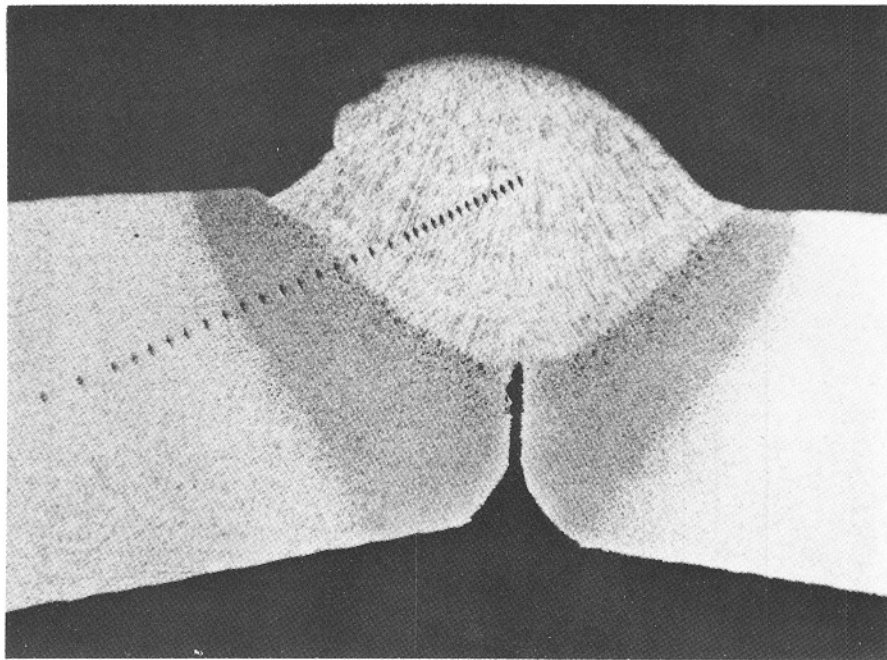


Figure A7.4.1-2. Part of the transverse section shown above, but a higher magnification. The light region in the center is weld metal. The dark regions adjacent to the weld metal are the heat affected zones. The light regions to the left and right in the photograph represent base flange regions of the channel segments. The line of small dark, elongated marks is the result of microhardness measurements. Etchant: two percent nital. X8.5



Figure A7.4.1-3 Microstructure representative of the weld metal in transverse section through NBS weldment IC. The microstructure appears to consist primarily of bainite. Etchant: two percent nital. X200

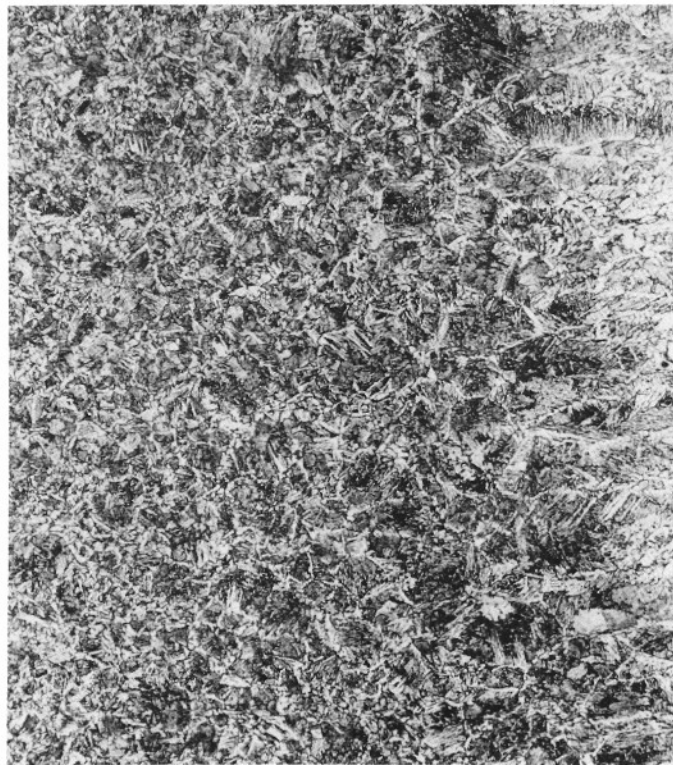


Figure A7.4.1-4 Transition region from weld metal (right) to heat affected zone (left) in transverse section through NBS weldment IC. Etchant: two percent nital. X200

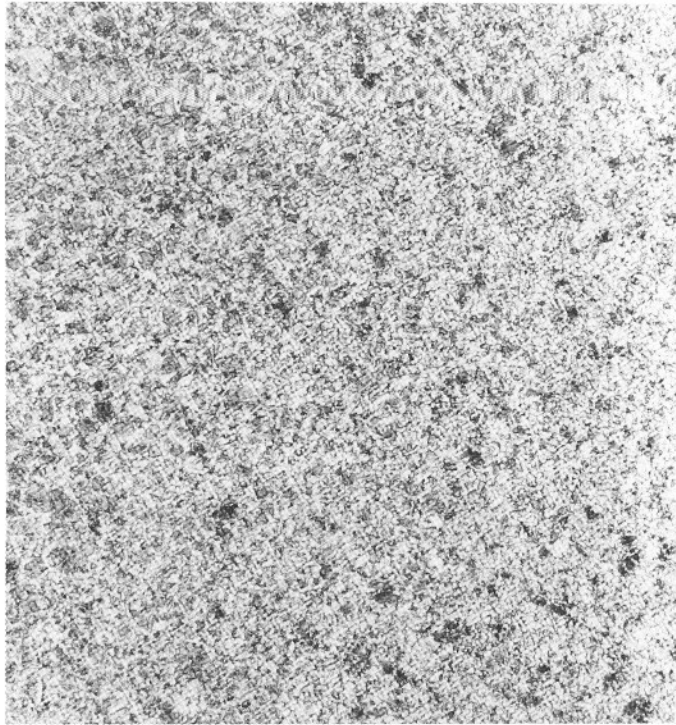


Figure A7.4.1-5 Representative microstructure of the heat affected zone in transverse section through NBS weldment IC. The microstructure consists of ferrite, primarily as a network in prior austenite grain boundaries, bainite, partially spheroidized carbides, and tempered martensite. Etchant: two percent nital. X200

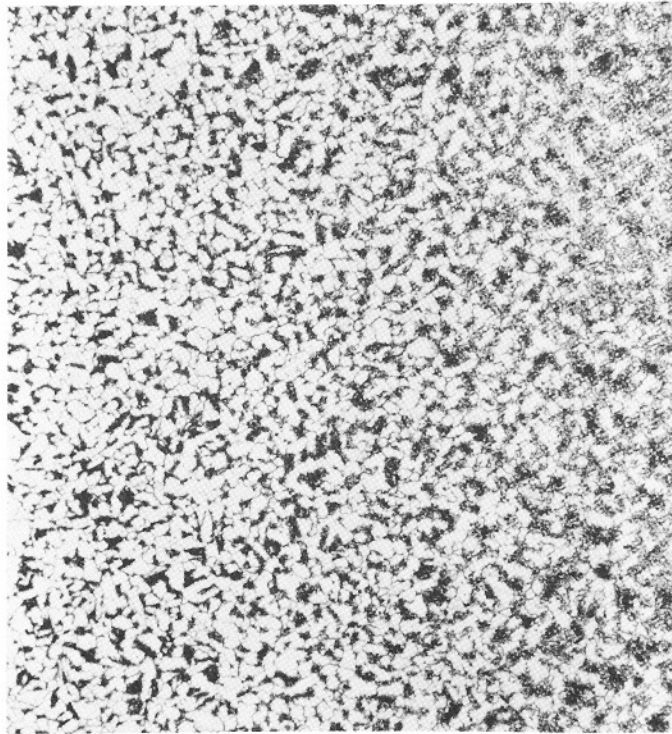


Figure A7.4.1-6 Microstructure representative of the transition region from the heat affected zone (right) to base channel material (left) in NBS weldment IC. Etchant: two percent nital. X200

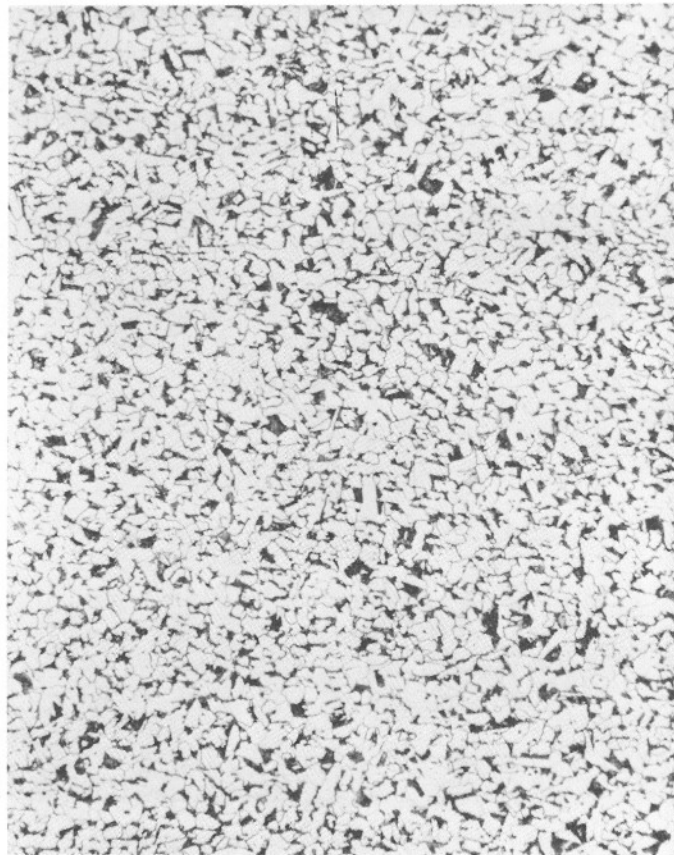


Figure A7.4.1-7 Microstructure representative of the base channel material from NBS weldment IC. The microstructure consists of relatively fine grained ferrite (light) and pearlite (dark) in a normalized condition. Etchant: two percent nital. X200

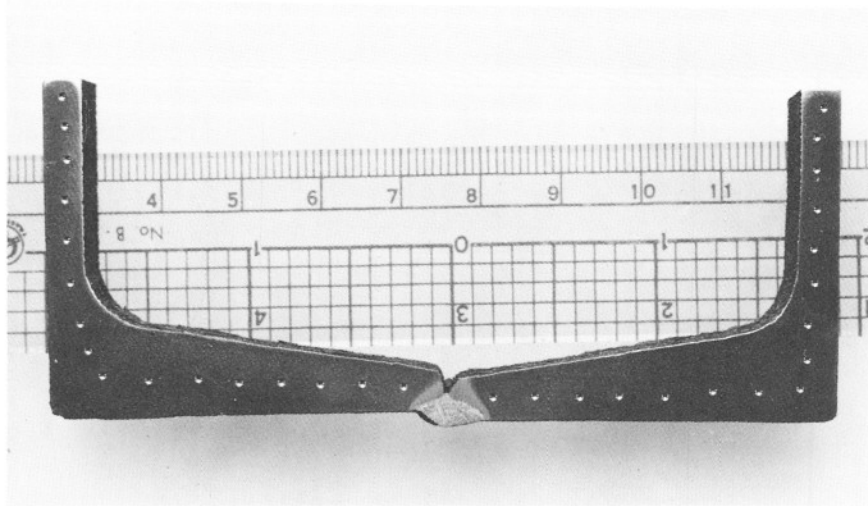


Figure A7.4.1-8 Transverse section 1B1 through the bottom of walkway box beam 9U (NBS 1). The north channel of the box beam is to the left and the south channel is to the right. The weld connecting the flanges of the two channels used to fabricate the box beam is in the center. Parts of the web regions of each channel had been removed before this photograph was taken. The indentations appearing on the surface of the section are the result of hardness measurements. Etchant: two percent nital. ~X1

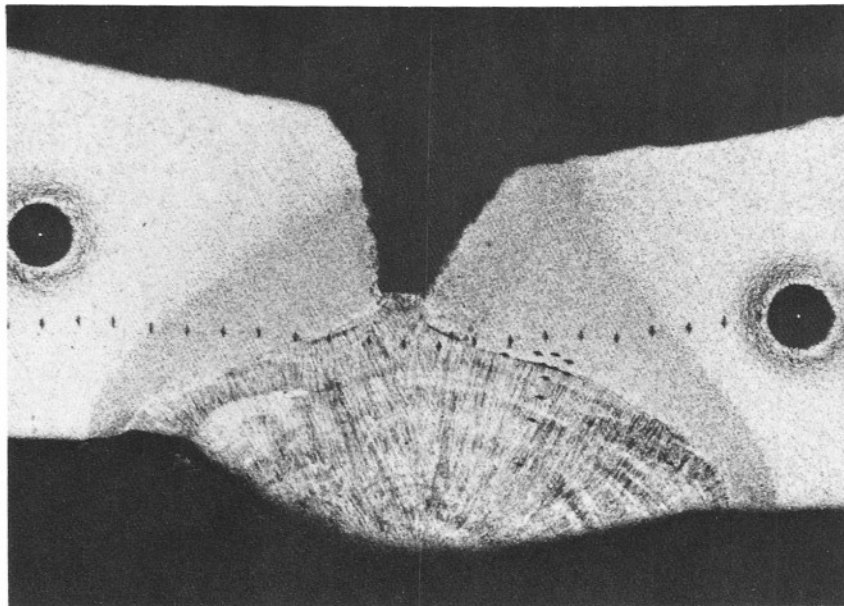


Figure A7.4.1-9 Part of the transverse section shown in figure A7.4.1-8, but at higher magnification. The region at the bottom center is weld metal. The dark gray regions on either side of the weld metal are the heat affected zones associated with the weld. The lighter regions at either side of the figure beyond the heat affected zone are base channel material. Etchant: two percent nital. X8.5

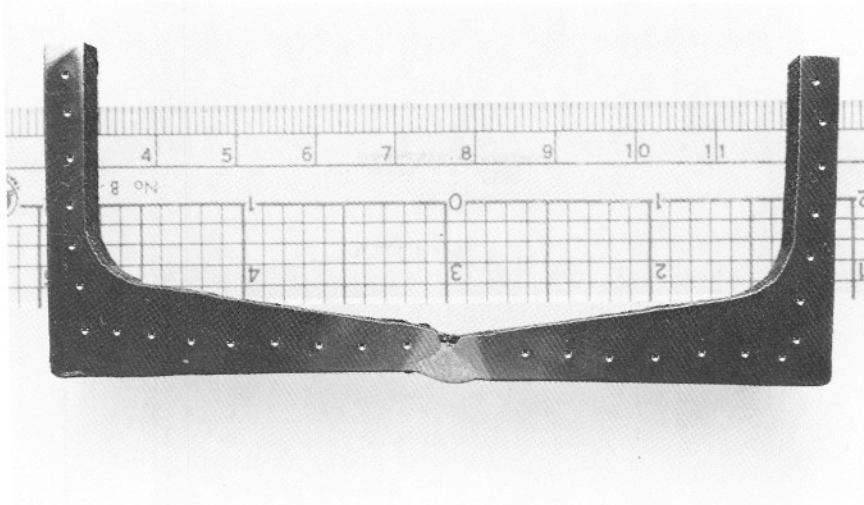


Figure A7.4.1-10 Transverse section 1BM2 through the bottom of walkway box beam 9U (NBS 1). The north channel of the box beam is to the left and the south channel is to the right. The weld connecting the flanges of the two channels used to fabricate the box beam is in the center. Parts of the web regions of each channel had been removed before this photograph was taken. The indentations appearing on the surface of the section are the result of hardness measurements. Etchant: two percent nital. ~X1

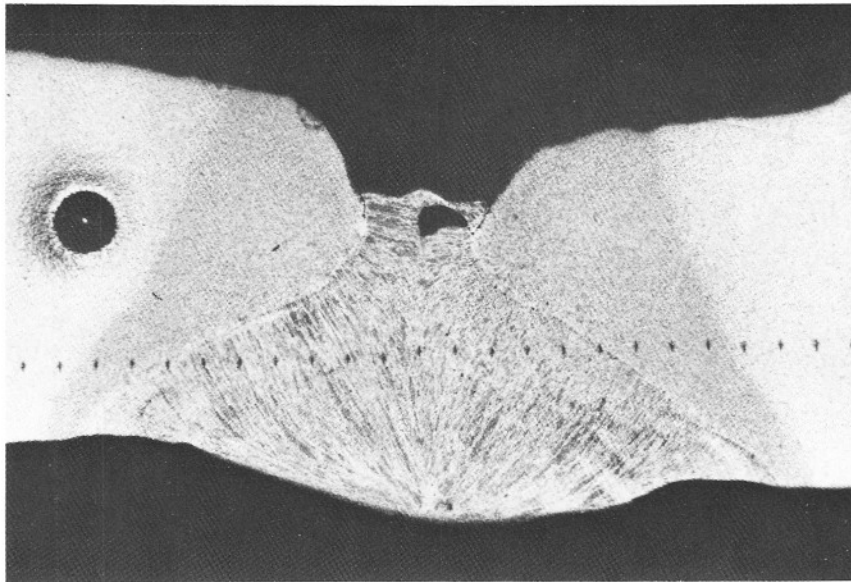


Figure A7.4.1-11 Part of the transverse section shown in figure A7.4.1-10, but at higher magnification. The region at the bottom center is weld metal. The dark gray regions on either side of the weld metal are the heat affected zones associated with the weld. The lighter regions on either side of the photomicrograph are base channel material. Etchant: two percent nital. X8.5

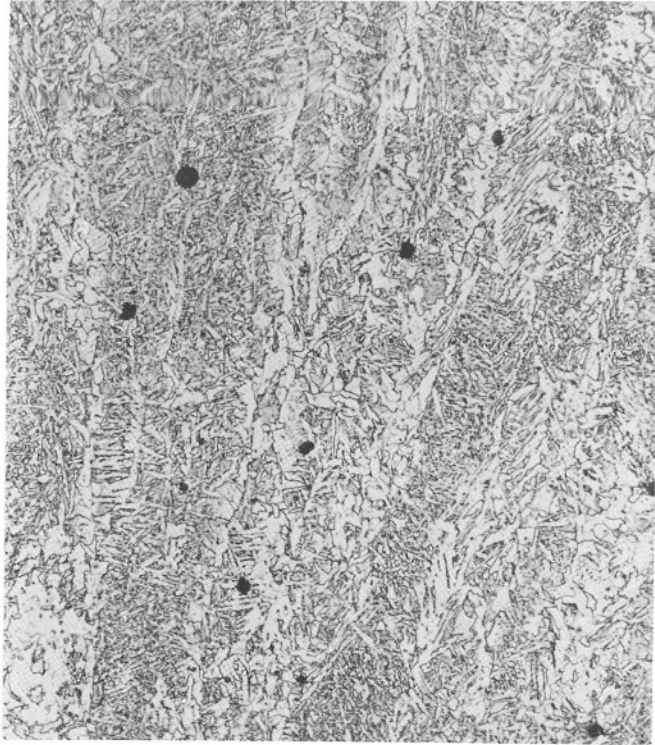


Figure A7.4.1-12 Representative microstructure of the weld metal in transverse section 1BM1 through box beam 9U (NBS 1). The microstructure consists primarily of bainite. Some inclusions are evident. Etchant: two percent nital. X200

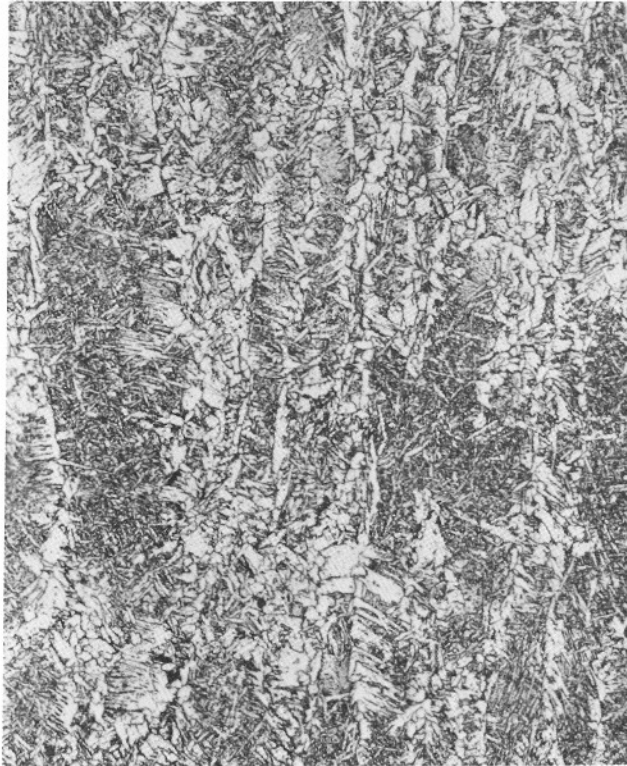


Figure A7.4.1-13 Representative microstructure of the weld metal in transverse section 1BM2 through box beam 9U (NBS 1). The microstructure consists primarily of bainite. Etchant: two percent nital. X200

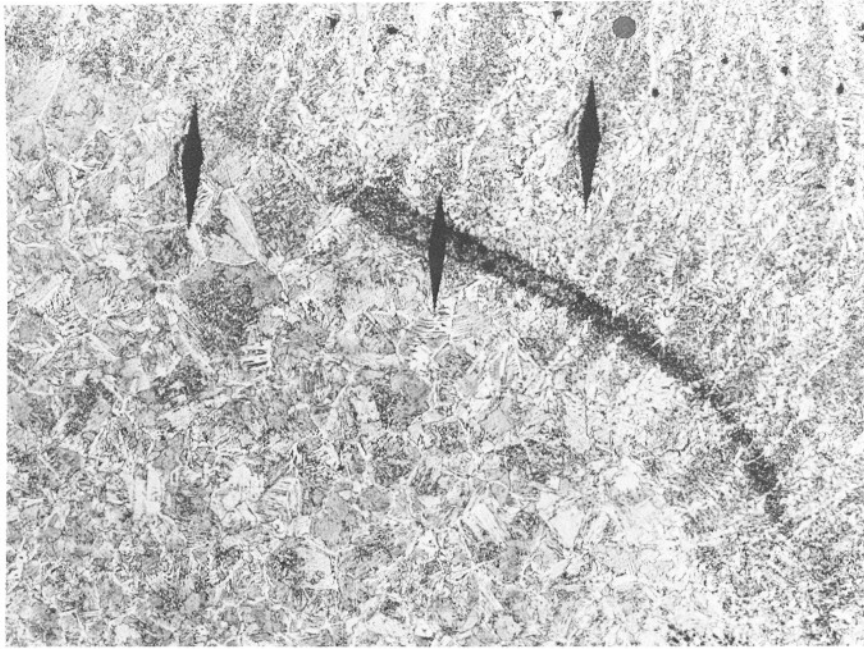


Figure A7.4.1-14 Patch of hard material (dark streak) at the transition from weld metal (top right) to the heat affected zone (bottom left) in section 1BM1. The elongated dark areas are hardness impressions. Etchant: two percent nital. X100

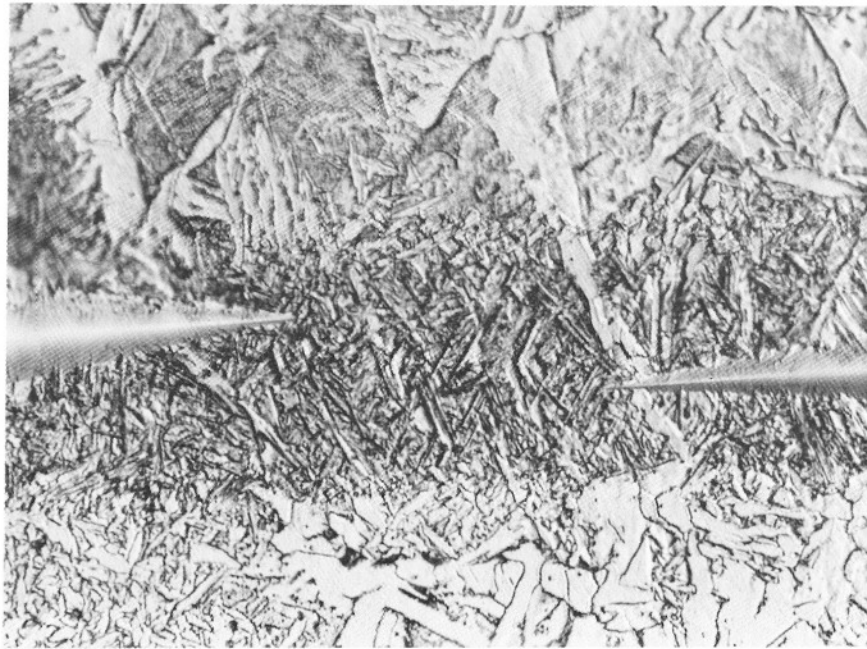


Figure A7.4.1-15 Hard area similar to that shown above, but at higher magnification. The hard area is in the center running from side to side. The microstructure appears to consist of fine grained tempered martensite. Parts of two hardness impressions can be seen at either side of the figure. Etchant: two percent nital. X800

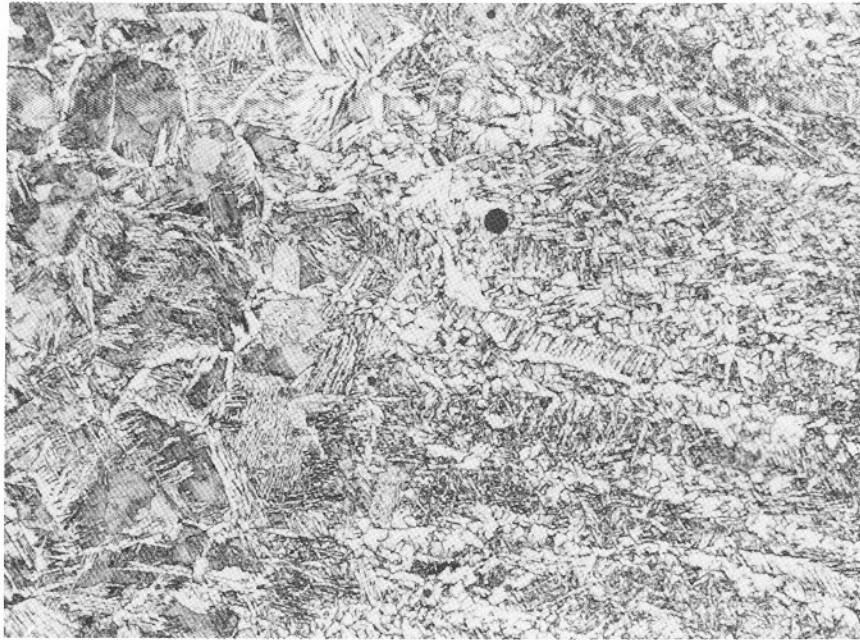


Figure 7.4.1-16 Transition zone from weld metal (right) to heat affected zone (left) in section 1BM2. Some inclusions can be seen. Etchant: two percent nital. X200



Figure A7.4.1-17 Region representative of the heat affected zone in section 1BM1. The microstructure appears to consist of ferrite, both as a network in prior austenite grains and as needles, bainite, partially spheroidized carbides, and tempered martensite. Etchant: two percent nital. X200

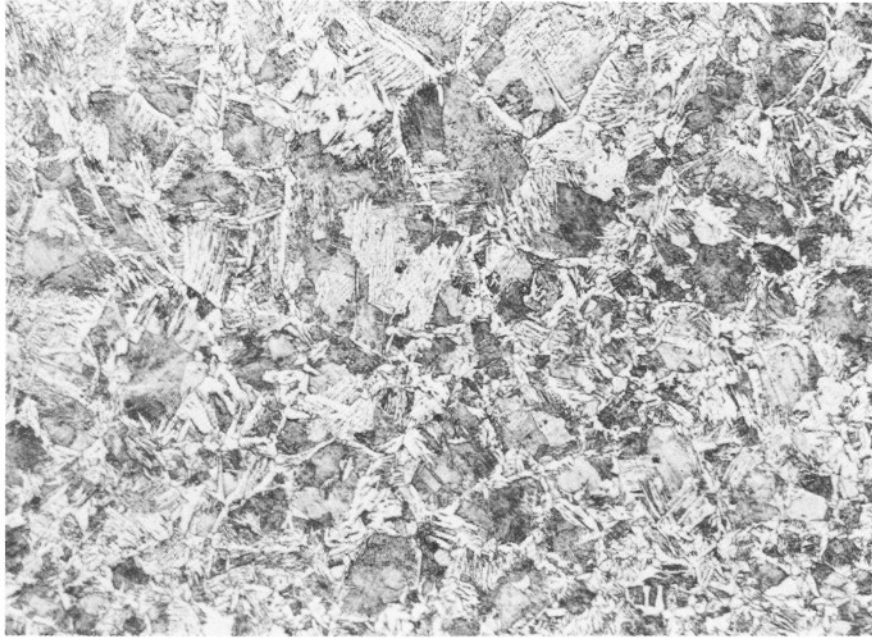


Figure 7.4.1-18 Region representative of the heat affected zone in section 1BM2. The microstructure appears to consist of ferrite, both as a network in prior austenite grains and as needles, bainite, partially spheroidized carbides, and tempered martensite. Etchant: two percent nital. X200

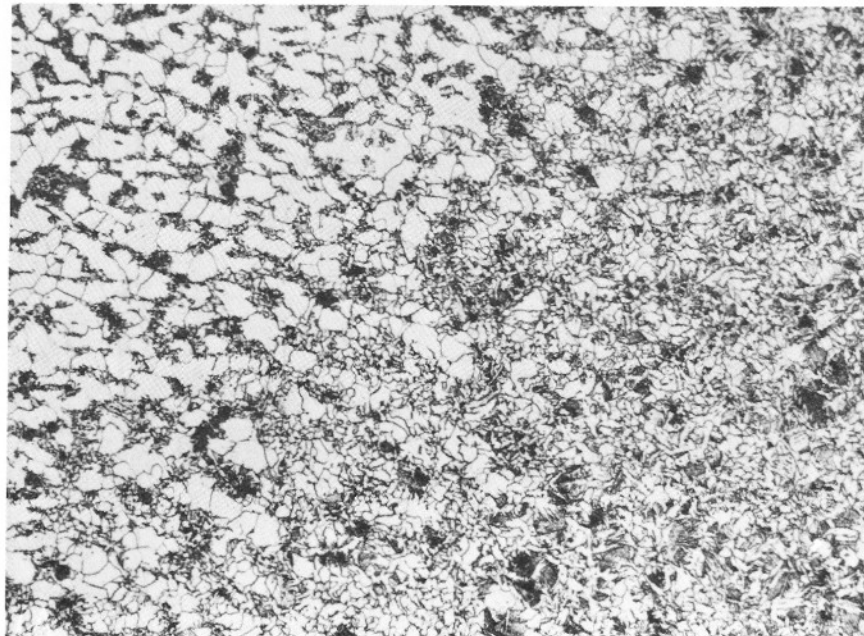


Figure A7.4.1-19 Transition from heat affected zone (right) to base channel material (left) in section 1BM2. Etchant: two percent nital. X200

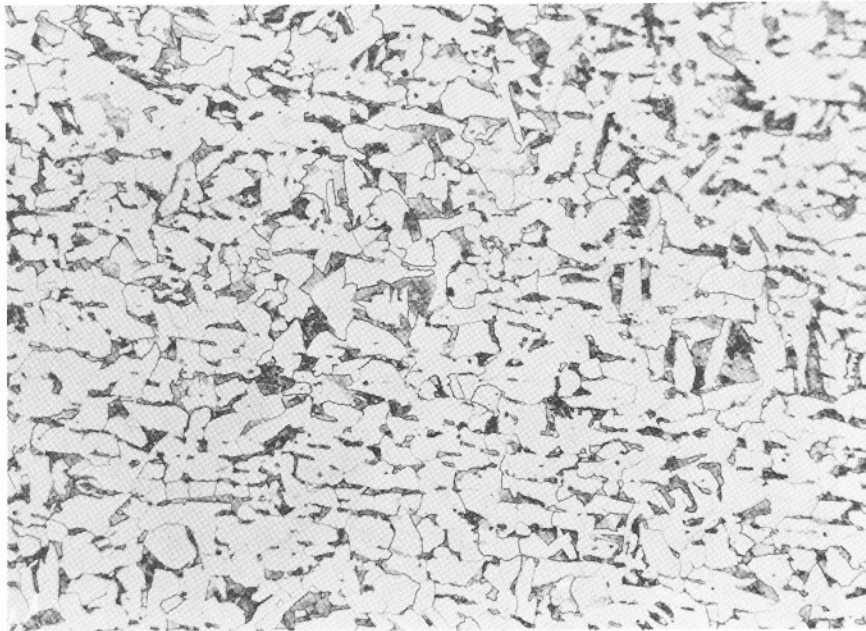


Figure A7.4.1-20 Region representative of base channel material in section 1BM1. The microstructure consists primarily of ferrite (light) and pearlite (dark) in the normalized condition. Etchant: two percent nital. X200

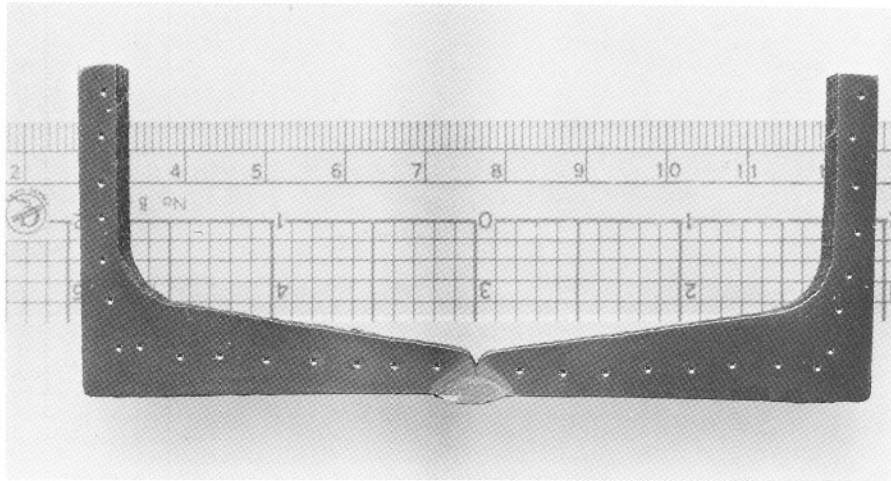


Figure A7.4.1-21 Transverse section 2BM1 through bottom of walkway box beam 8L (NBS 2). The north channel of the box beam is to the left and the south channel is to the right. The weld connecting the flanges of the two channels used to fabricate the box beam is in the center. Parts of the web regions of each channel had been removed before this photograph was taken. The indentations appearing on the surface of the section are the result of hardness measurements. Etchant: two percent nital. ~X1

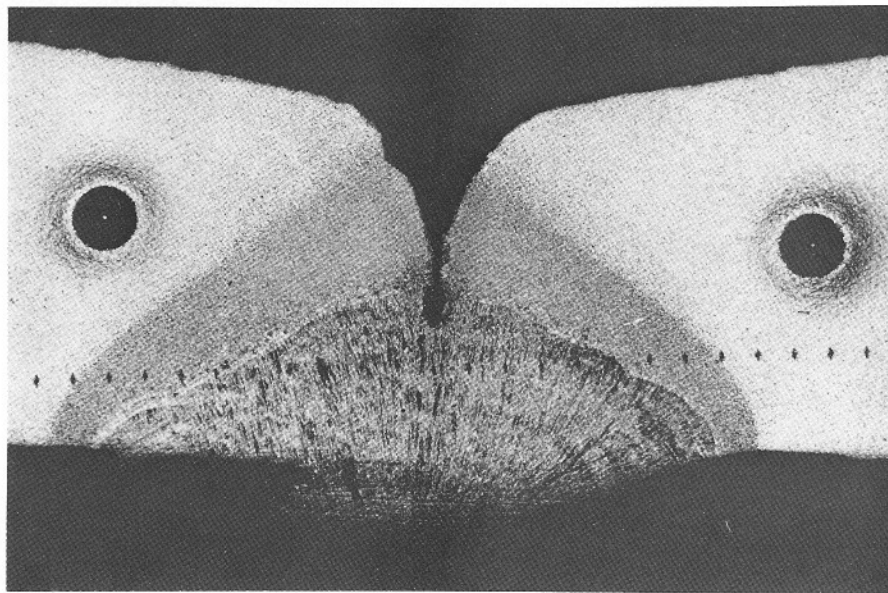


Figure A7.4.1-22 Part of the transverse section shown in figure A7.4.1-21, but at higher magnification. The region at the bottom center is weld metal. The dark gray regions on either side of the weld are the heat affected zones associated with the weld. The lighter regions on either side of the figure beyond the heat affected zones are base channel material. Etchant: two percent nital. X8.5

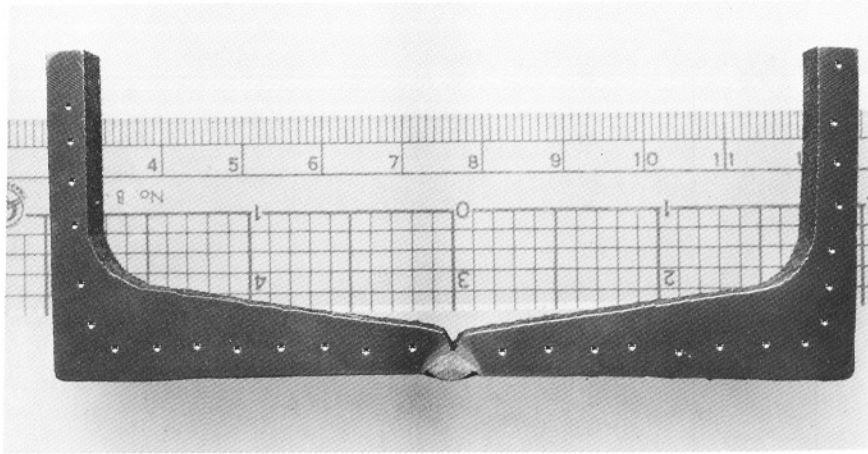


Figure A7.4.1-23 Transverse section 2BM2 through bottom of walkway box beam 8L (NBS 2). The north channel of the box beam is to the left and the south channel is to the right. The weld connecting the flanges of the two channels used to fabricate the box beam is in the center. Parts of the web regions of each channel had been removed before this photograph was taken. The indentations appearing on the surface of the section are the result of hardness measurements. Etchant: two percent nital. X1

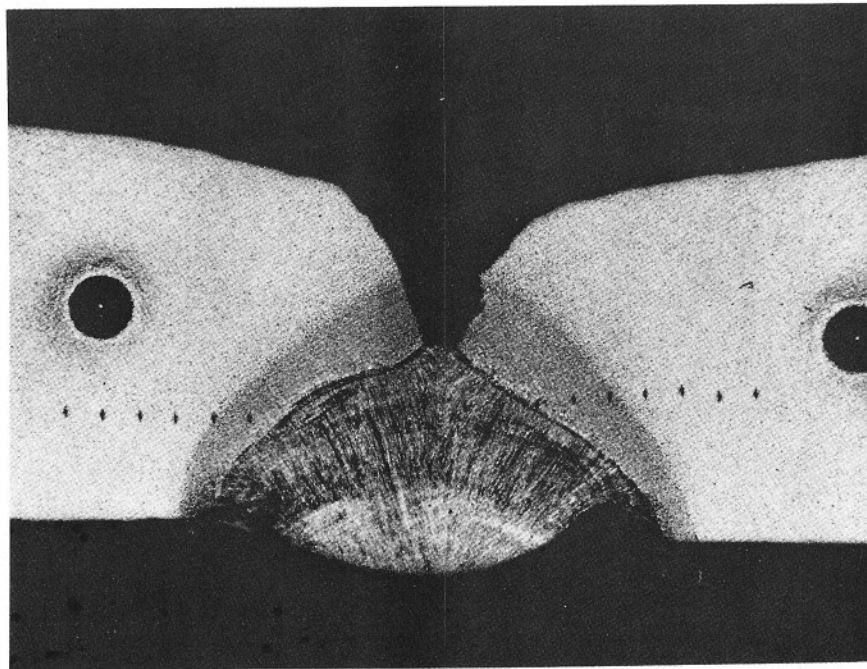


Figure A7.4.1-24 Part of the transverse section shown in figure A7.4.1-23, but at higher magnification. The region at the bottom center is weld metal. The gray regions on either side of the weld metal are the heat affected zones associated with the weld. The lighter regions on either side of the figure beyond the heat affected zones are base channel material. Etchant: two percent nital. X8.5

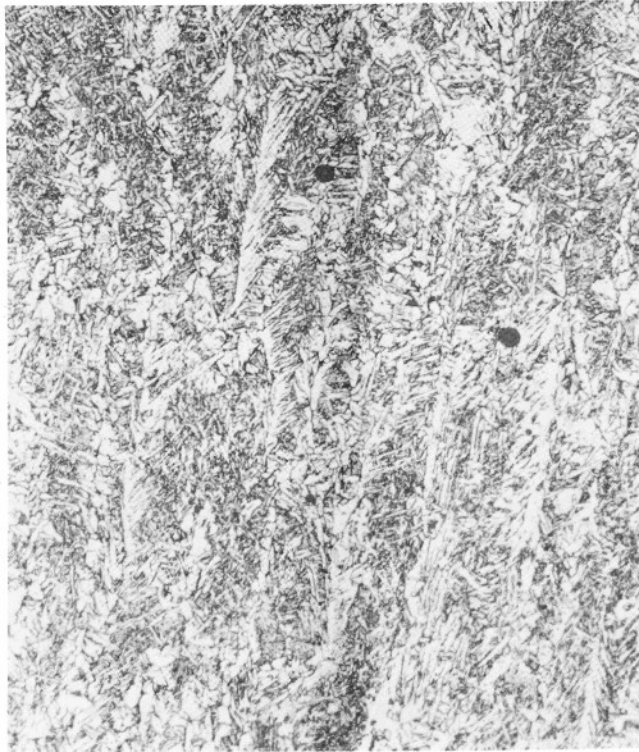


Figure A7.4.1-25 Representative microstructure of the weld metal in transverse section 2BM1 through box beam 8L (NBS 2). The microstructure appears to consist primarily of bainite. Some inclusions are evident. Etchant: two percent nital. X200

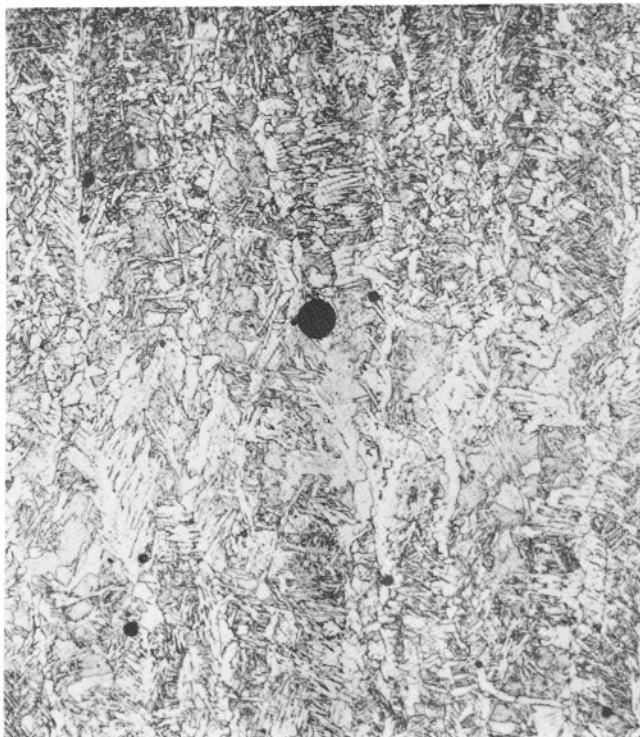


Figure A7.4.1-26 Representative microstructure of the weld metal in transverse section 2BM2 through box beam 8L (NBS 2). The microstructure appears to consist primarily of bainite. Some inclusions are evident. Etchant: two percent nital. X200

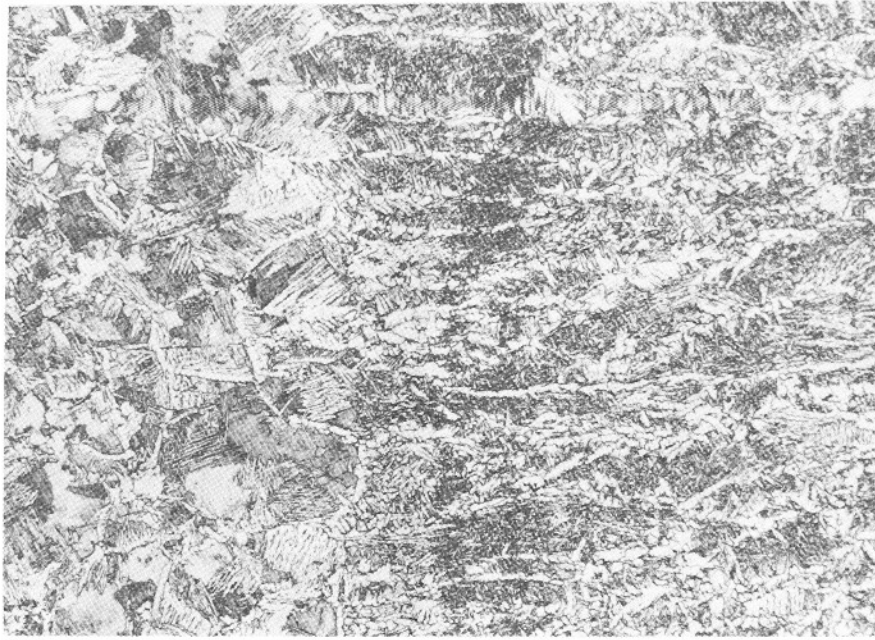


Figure A7.4.1-27 Transition zone from weld metal (right) to heat affected zone (left) in section 2BM1. Etchant: two percent nital. X200



Figure A7.4.1-28 Transition zone from weld metal (right) to heat affected zone (left) in section 2BM2. Etchant: two percent nital. X200

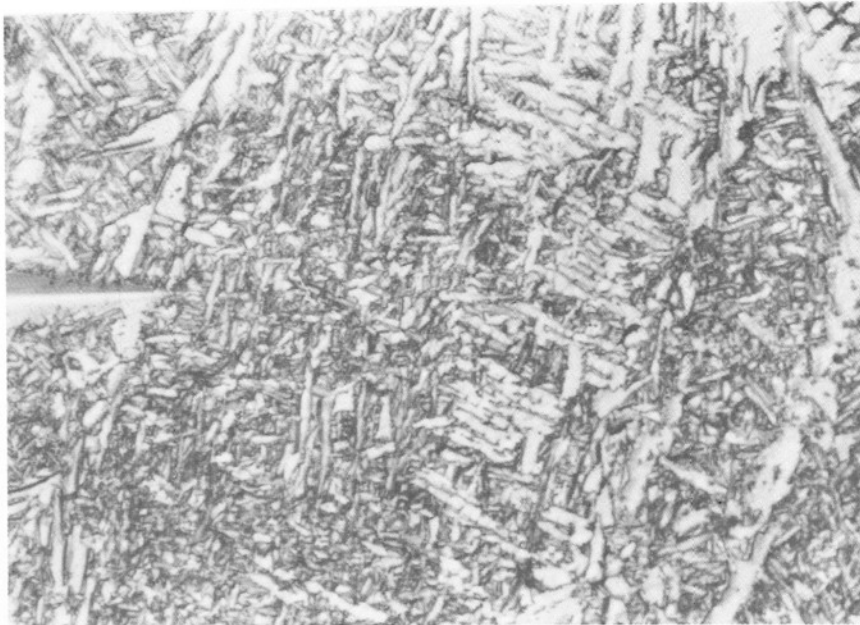


Figure A7.4.1-29 Region of the transition zone from weld metal to the heat affected zone in section 2BM2. This region is one of the hard areas. The microstructure appears to consist of tempered martensite. Part of a hardness test impression can be seen at the left center. Etchant: two percent nital. X1200

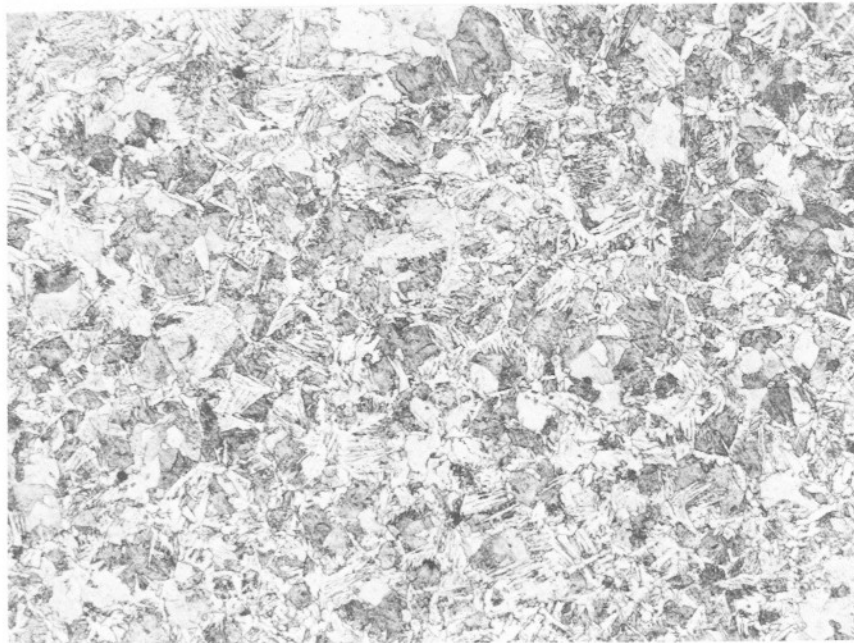


Figure A7.4.1-30 Representative microstructure of the heat affected zone in section 2BM1. The microstructure appears to consist of ferrite, both as a network in prior austenite grain boundaries and as needles, bainite, partially spheroidized carbides, and tempered martensite. Etchant: two percent nital. X200

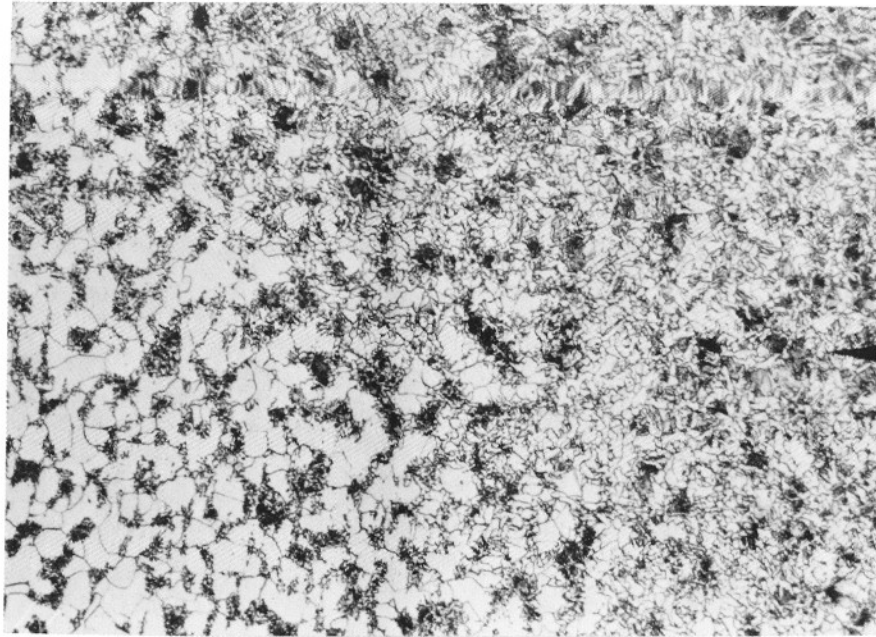


Figure A7.4.1-31 Transition region from heat affected zone (right) to base channel material (left) in section 2BM1. Etchant: two percent nital. X200

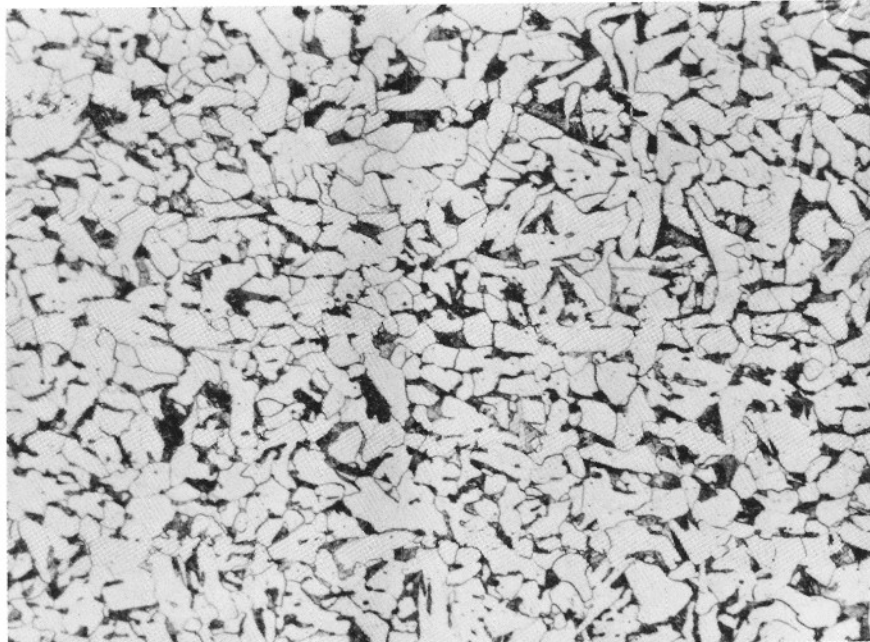


Figure A7.4.1-32 Region of section 2BM1 representative of the base channel material in both sections through box beam 8L. The microstructure consists primarily of ferrite (light) and pearlite (dark) in the normalized condition. Etchant: two percent nital. X200

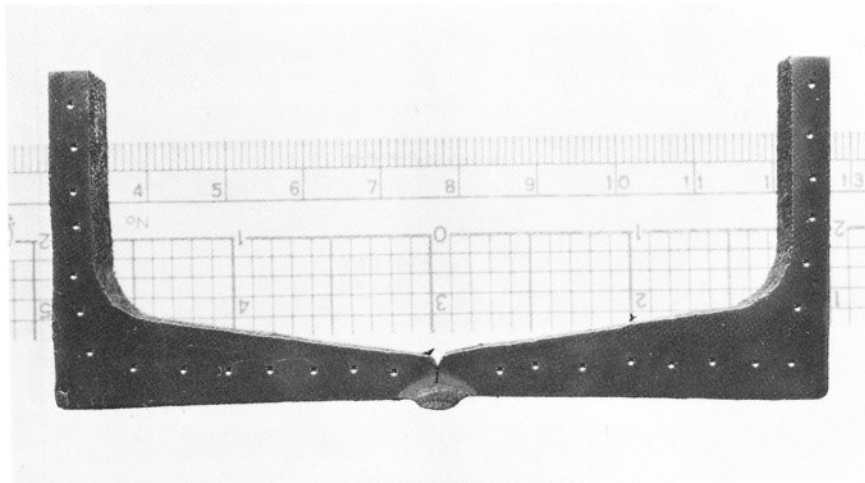


Figure A7.4.1-33 Transverse section 3BM1 through the bottom of walkway box beam 9M (NBS 3). The south channel of the box beam is to the left and the north channel is to the right. The weld connecting the flanges of the two channels used to fabricate the box beam is in the center. Parts of the web regions of each channel had been removed before this photograph was taken. The indentations appearing on the surface of the section are the result of hardness measurements. Etchant: two percent nital. ~X1

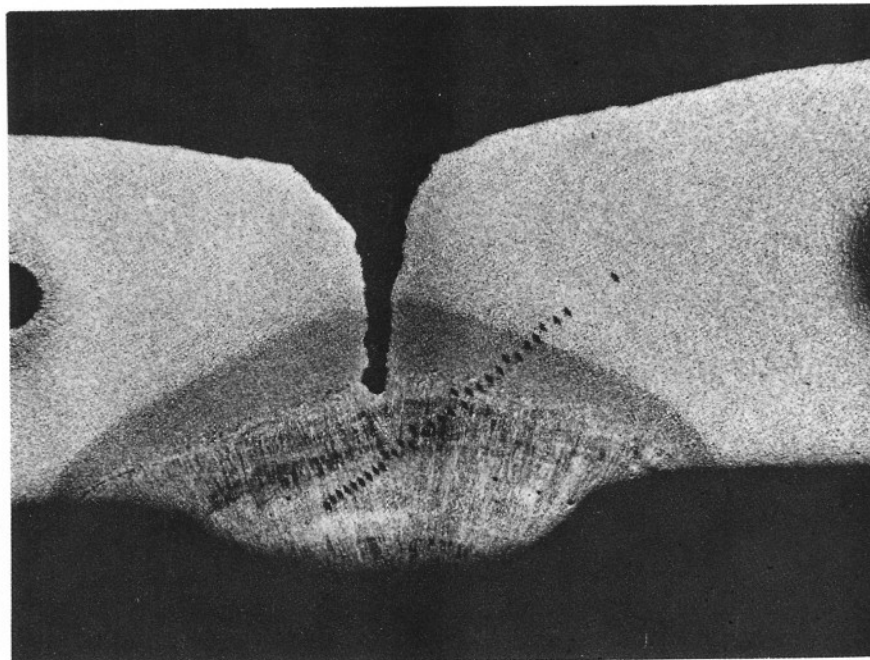


Figure A7.4.1-34 Part of the transverse section shown in figure A7.4.1-33, but at higher magnification. The region at the bottom center is weld metal. The gray regions on either side of the weld metal are the heat affected zones associated with the weld. The lighter regions at either side of the figure beyond the heat affected zone are base channel material. Etchant: two percent nital. X8.5

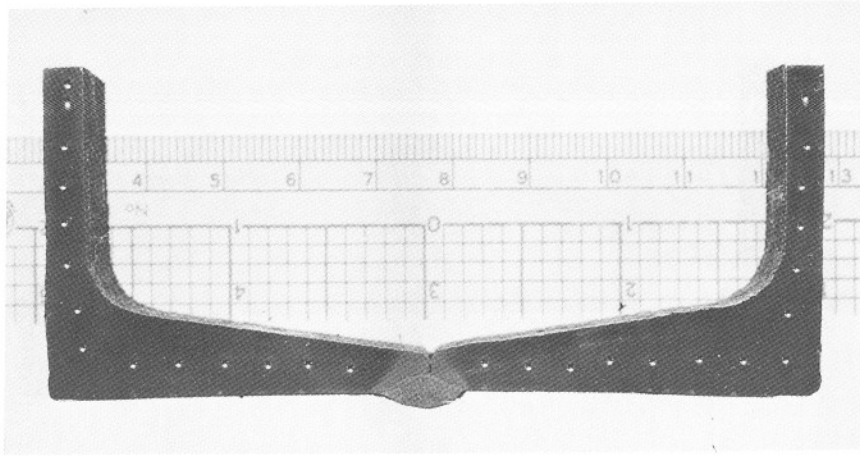


Figure A7.4.1-35 Transverse section 3BM2 through the bottom of walkway box beam 9M (NBS 3). The south channel of the box beam is to the left and the north channel is to the right. The weld connecting the flanges of the two channels used to fabricate the box beam is in the center. Parts of the web regions of each channel had been removed before this photograph was taken. The indentations appearing on the surface of the section are the result of hardness measurements. Etchant: two percent nital. ~X1

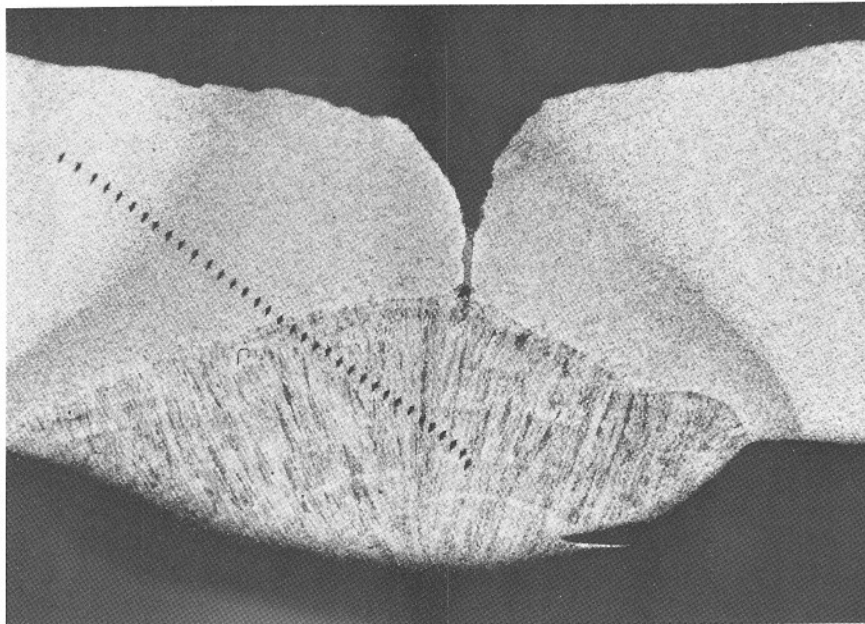


Figure A7.4.1-36 Part of the transverse section shown in figure A7.4.1-35, but at higher magnification. The region at the bottom center is weld metal. The gray regions on either side of the weld metal are the heat affected zones associated with the weld. The lighter regions at either side of the figure beyond the heat affected zones are base channel material. Etchant: two percent nital. X8.5

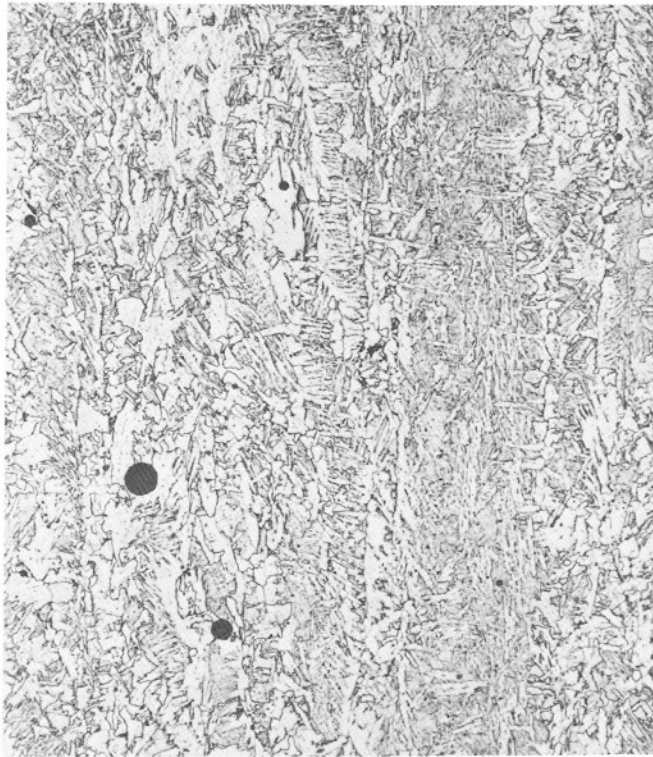


Figure A7.4.1-37 Representative microstructure of the weld metal in transverse section 3BM1 through box beam 9M (NBS 3). The microstructure consists primarily of bainite. Several inclusions are evident. Etchant: two percent nital. X200

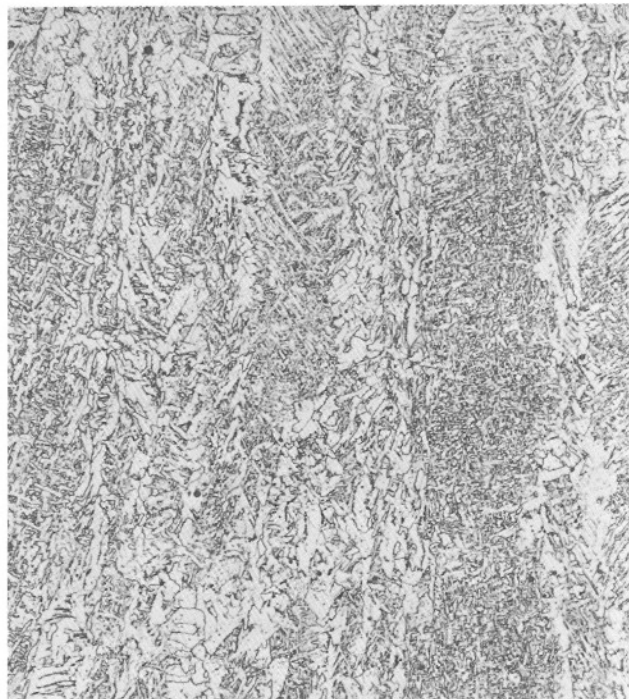


Figure A7.4.1-38 Representative microstructure of the weld metal in transverse section 3BM2 through box beam 9M (NBS 3). The microstructure consists primarily of bainite. Etchant: two percent nital. X200



Figure A7.4.1-39 Transition zone from weld metal (right) to heat affected zone (left) in section 3BM2. Some inclusions can be seen primarily in the weld metal. Etchant: two percent nital. X200



Figure A7.4.1-40 Region representative of the heat affected zone in section 3BM1. The microstructure appears to consist of ferrite both as a network in prior austenite grain boundaries and as needles, bainite, partially spheroidized carbides, and tempered martensite. Etchant: two percent nital. X200

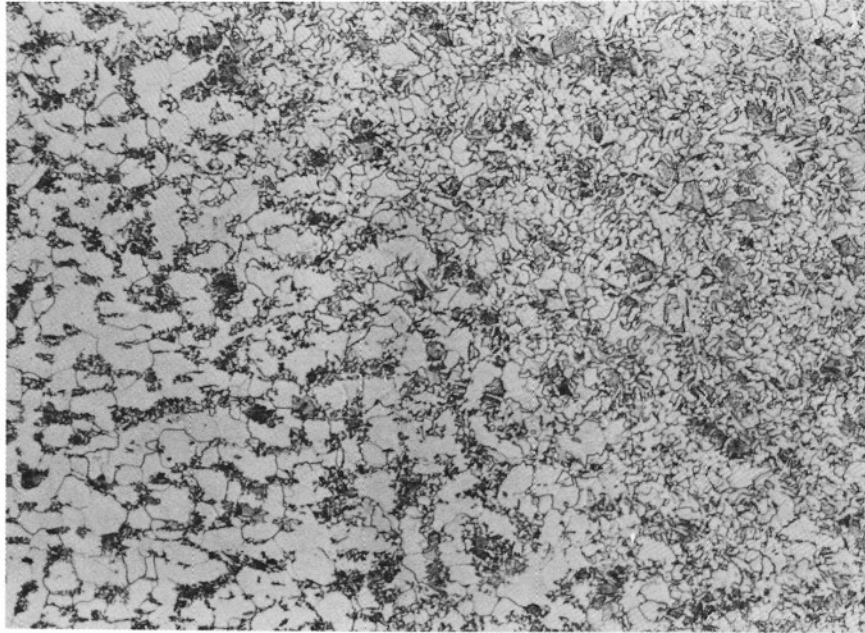


Figure A7.4.1-41 Transition zone from heat affected zone (right) to base channel material (left) in section 3BM2. Etchant: two percent nital. X200

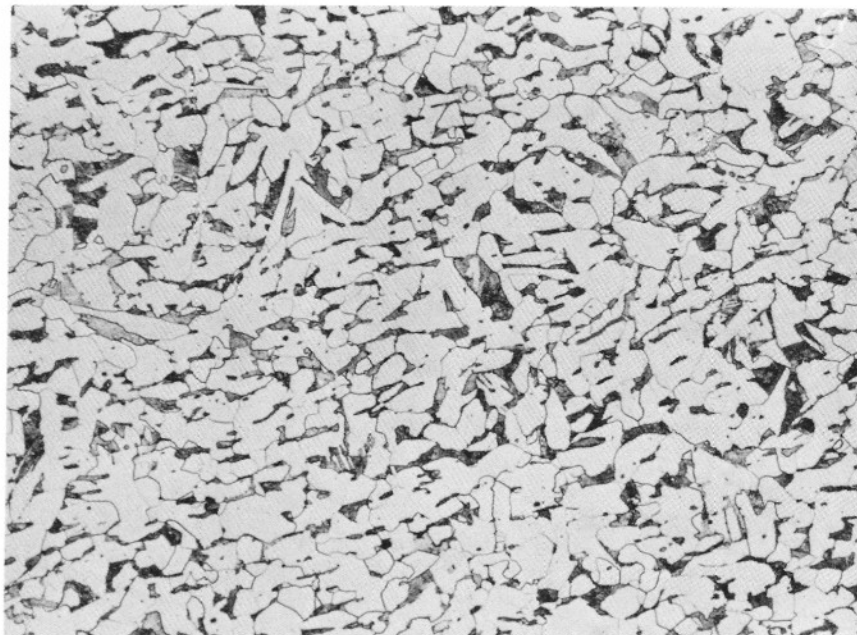


Figure A7.4.1-42 Representative region of base channel material in section 3BM1. The microstructure consists of ferrite (light) and pearlite (dark) in the normalized condition. Etchant: two percent nital. X200

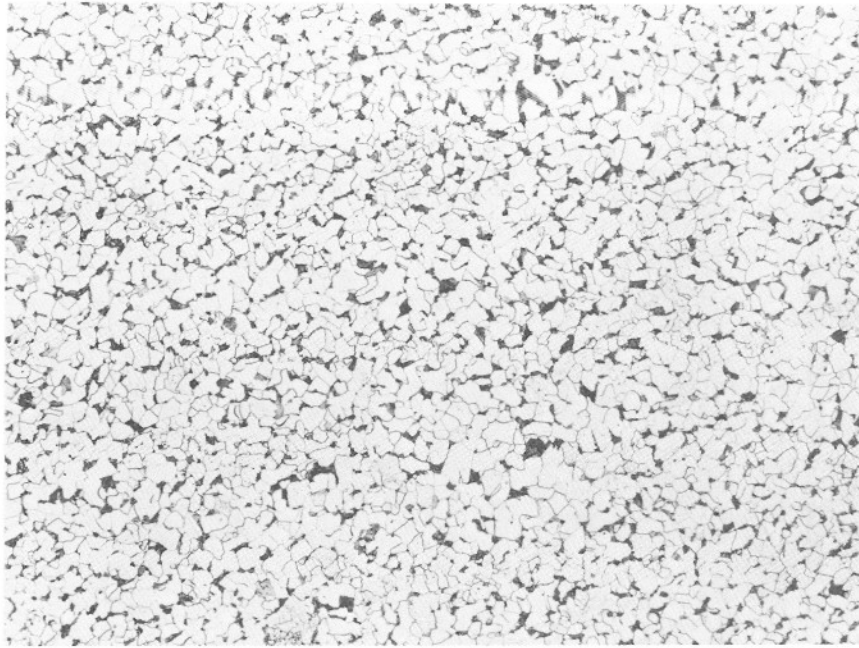


Figure A7.4.2-1 Transverse section through hanger rod NBS 5A showing the representative microstructure. The microstructure consists of relatively fine grained ferrite (light) and pearlite (dark) in a normalized condition. Etchant: two percent nital. X100

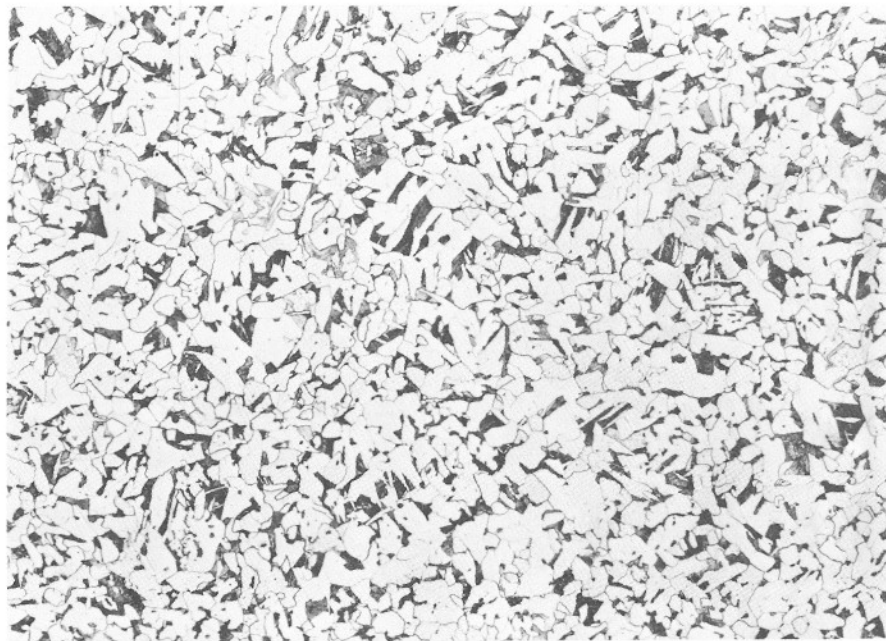


Figure A7.4.2-2 Transverse section through hanger rod NBS 5B showing the representative microstructure. The microstructure consists of ferrite (light) and pearlite (dark) in a normalized condition. Etchant: two percent nital. X100

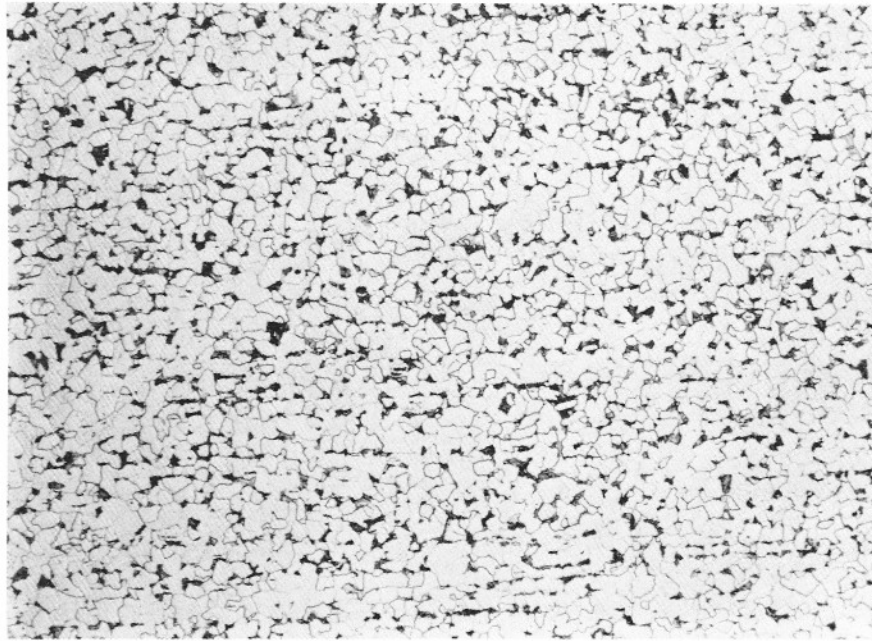


Figure A7.4.2-3 Longitudinal section through hanger rod NBS 5A showing the normalized microstructure consisting of ferrite and pearlite. Etchant: two percent nital. X100

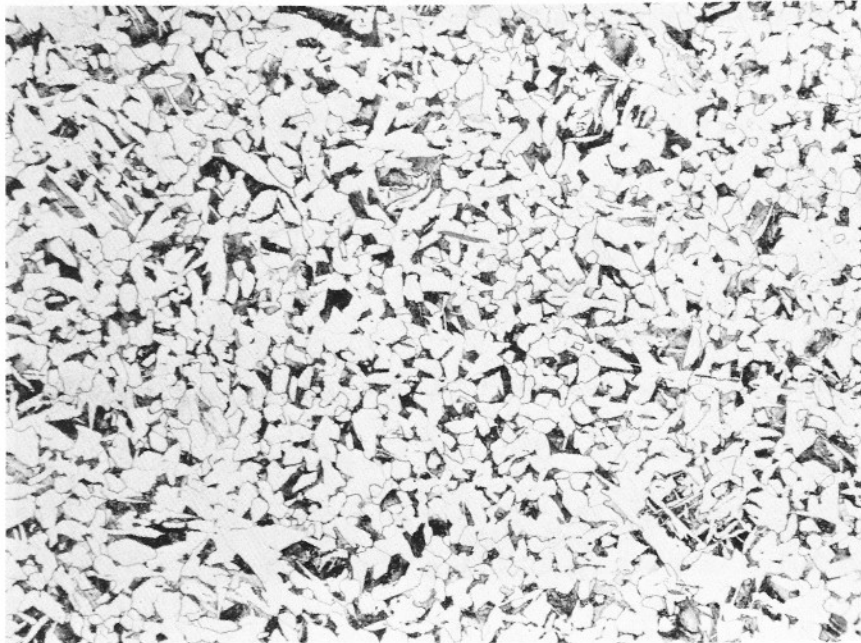


Figure A7.4.2-4 Longitudinal section through hanger rod NBS 5B showing the normalized microstructure consisting of ferrite and pearlite. Etchant: two percent nital. X100

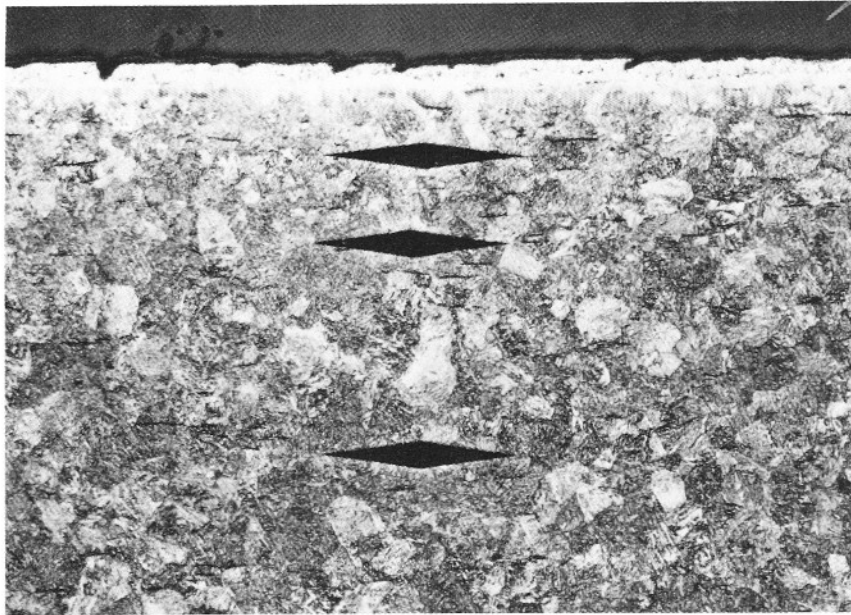


Figure A7.4.3-1 Microstructure of washer from location 9MW in the walkway debris. The thin, light layer at the surface (horizontal near the top in the figure) is the decarburized layer at the washer surface. The microstructure consists primarily of tempered martensite. Etchant: Picral. X200

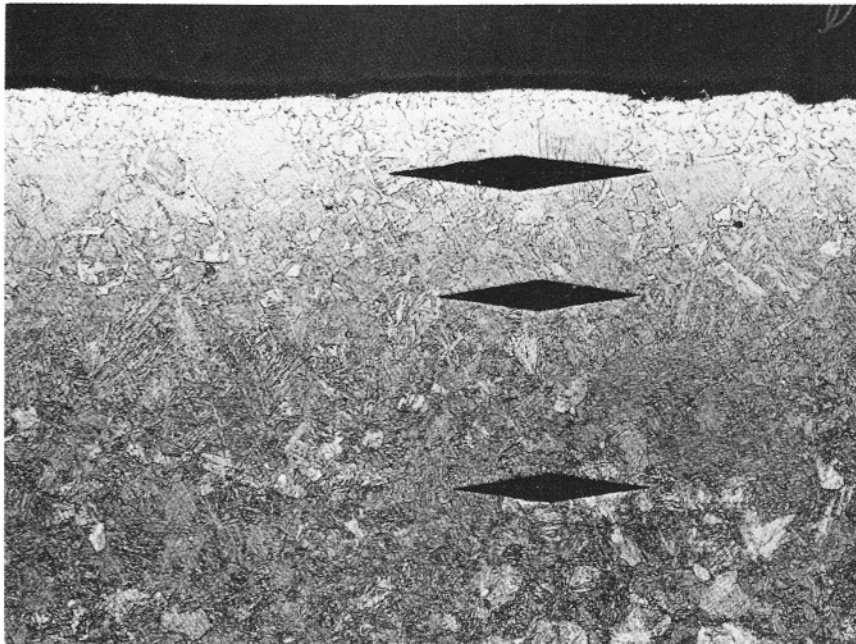


Figure A7.4.3-2 Microstructure of NBS hard washer. The light layer at the surface (horizontal near the top in the figure) is decarburized. The microstructure consists primarily of tempered martensite. Etchant: Picral. X200

## Section A7.6

The following tables and graphs offer additional data on the physical properties of walkway concrete.

Table A7.6-1 Bulk Specific Gravity of Drilled Concrete Cores

Core Number	Weight (grams)						$\frac{A}{C-D}$ (a)	$\frac{B}{C-D}$ (b)
	A	B	C	D	E	C-D		
4-02	215.4	206.2	222.8	105.1	222.7	117.7	1.83	1.75
03	238.3	227.4	245.5	114.3	245.5	131.2	1.82	1.73
04	282.3	269.4	291.3	137.5	291.3	153.8	1.84	1.75
06	299.2	286.4	310.1	147.0	310.0	163.1	1.83	1.76
08	307.8	292.7	318.1	155.9	318.1	162.2	1.90	1.80
09	287.7	273.7	297.1	140.6	297.1	156.5	1.84	1.75
11	277.5	264.9	290.9	134.7	290.7	156.2	1.78	1.70
14	268.7	256.4	280.8	127.6	281.4	153.3	1.75	1.67
15	265.5	253.6	276.5	130.3	276.4	146.2	1.82	1.73
17	323.9	308.9	336.2	157.0	336.2	179.2	1.81	1.72

Notes: A = original weight  
 B = 24 hr oven dry weight  
 C = saturated surface-dry weight  
 D = weight immersed in water  
 E = saturated surface-dry weight after immersion

(a) Bulk specific gravity, air-dry

(b) Bulk specific gravity, oven-dry

1 lb = 0.4536 kg

Table A7.6-2 Bulk Specific Gravity of Topping Material

Core Number	Weight (grams)						$\frac{A}{C-D}$ (a)	$\frac{B}{C-D}$ (b)
	A	B	C	D	E	C-D		
4-02	58.7	57.6	62.7	34.2	62.7	28.5	2.06	2.02
03	51.7	51.0	55.7	30.5	55.5	25.2	2.05	2.02
04	41.5	41.1	49.9	24.5	49.9	25.4	1.63	1.62
06	49.9	47.7	52.8	28.6	52.8	24.2	2.06	1.97
11	38.6	38.2	41.2	23.4	41.2	17.8	2.17	2.15
14	46.3	44.5	51.7	23.9	51.7	27.8	1.67	1.60
15	58.3	55.8	64.3	29.1	64.3	35.2	1.66	1.59
17	58.7	56.3	65.6	31.0	65.6	34.6	1.70	1.63

Notes: A = original weight  
 B = 24 hr oven dry weight  
 C = saturated surface-dry weight  
 D = weight immersed in water  
 E = saturated surface-dry weight after immersion

(a) Bulk specific gravity, air-dry

(b) Bulk specific gravity, oven-dry

1 lb = 0.4536 kg

Table A7.6-3 Compressive Strength of Drilled Concrete Cores

Core Number	Avg. Capped Height L (inches)	Average Diameter D (inches)	L/D	Cross-Sectional Area (in) <sup>2</sup>	Load at Failure (lbs)	Calculated Compressive Strength (psi)	CF(a)	Corrected Compressive Strength (psi)
4-01	3.829	1.984	1.930	3.09	16,950	5,485	0.993	5,447
05	3.584	1.986	1.805	3.10	15,575	5,024	0.983	4,938
07	3.635	1.980	1.836	3.08	15,975	5,187	0.985	5,109
10	3.425	1.980	1.730	3.08	16,175	5,252	0.978	5,136
12	3.608	1.986	1.817	3.10	15,075	4,863	0.984	4,785
13	3.696	1.981	1.866	3.08	13,850	4,497	0.988	4,443
16	3.150	1.982	1.590	3.08	14,500	4,708	0.967	4,553
18	3.695	1.986	1.861	3.10	17,325	5,589	0.988	5,522
19	3.722	1.985	1.875	3.09	16,525	5,348	0.989	5,289

Note: (a) Strength correction factor. See ANSI/ASTM C42-77, Standard Method of Obtaining and Testing Drilled Cores and Sawed Beams of Concrete.

1 in = 25.4 mm

1 lb = 4.448 N

1000 psi = 6.9 MPa

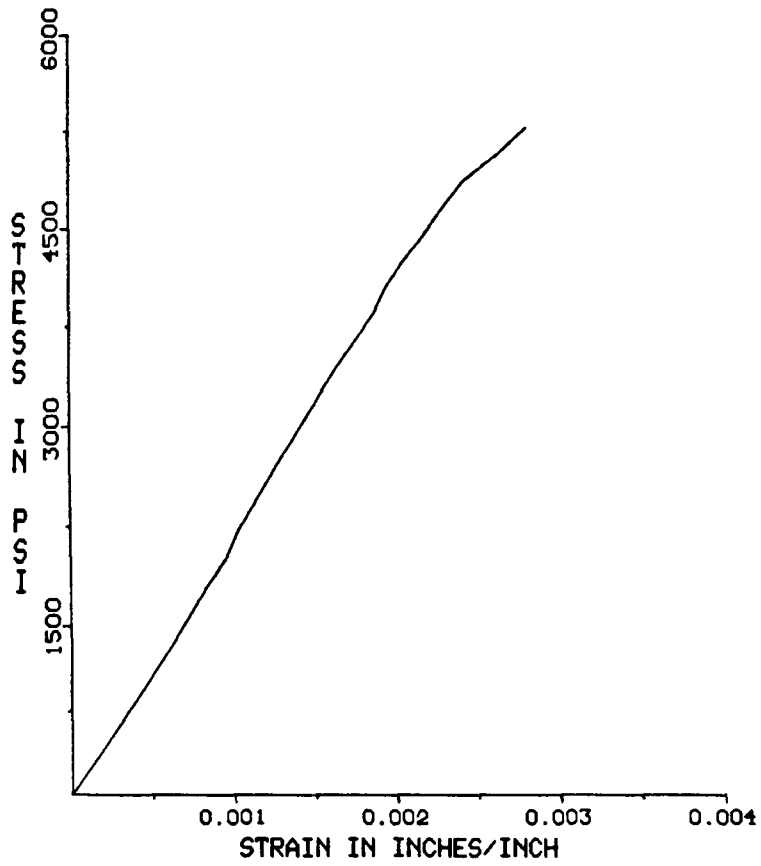


Figure A7.6-1. Stress-strain plot for concrete core 4-01.

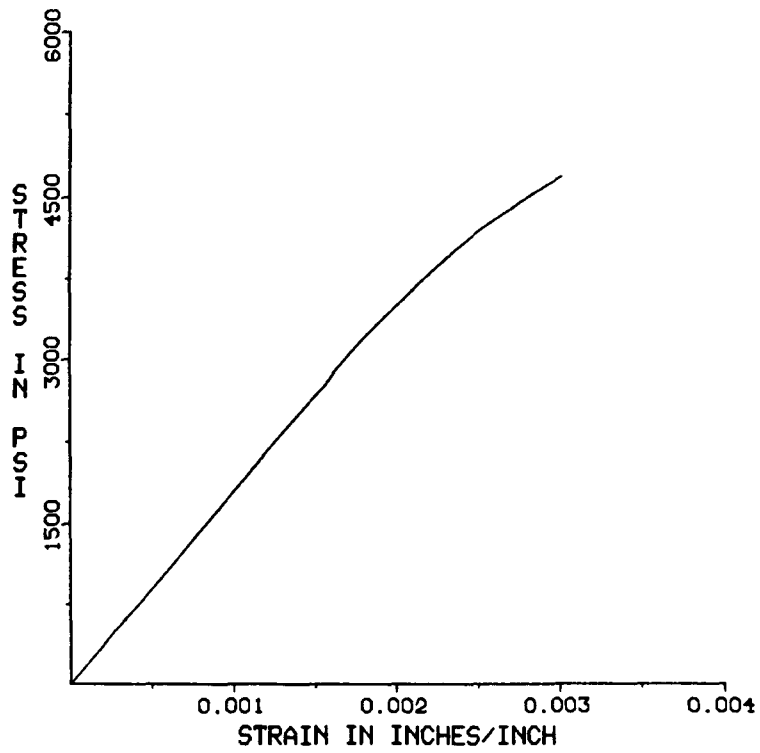


Figure A7.6-2. Stress-strain plot for concrete core 4-05.

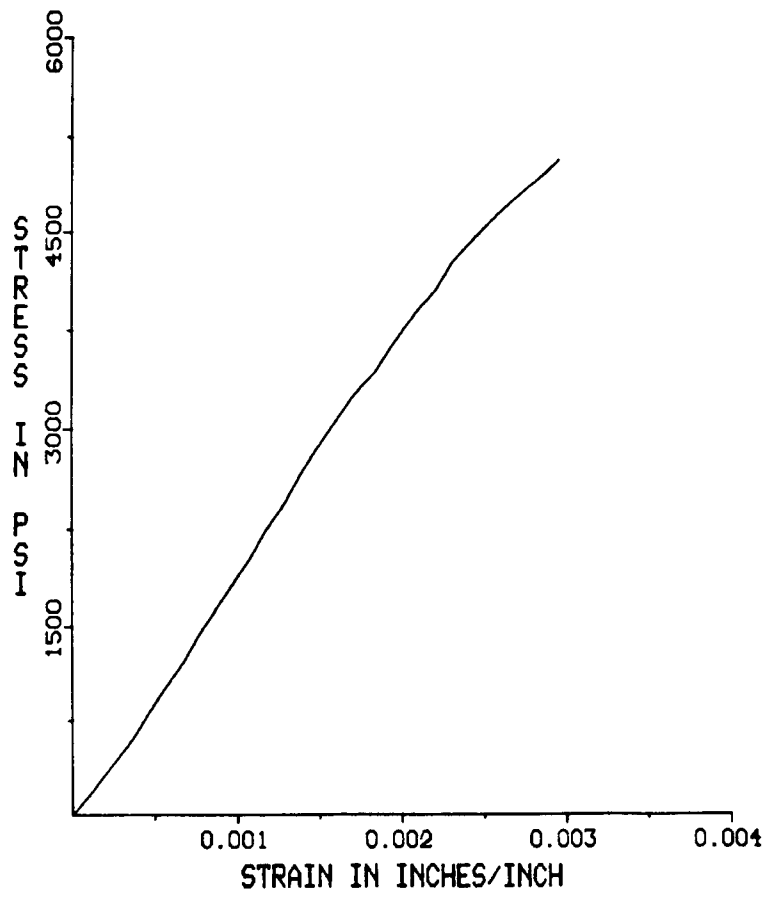


Figure A7.6-3. Stress-strain plot for concrete core 4-07.

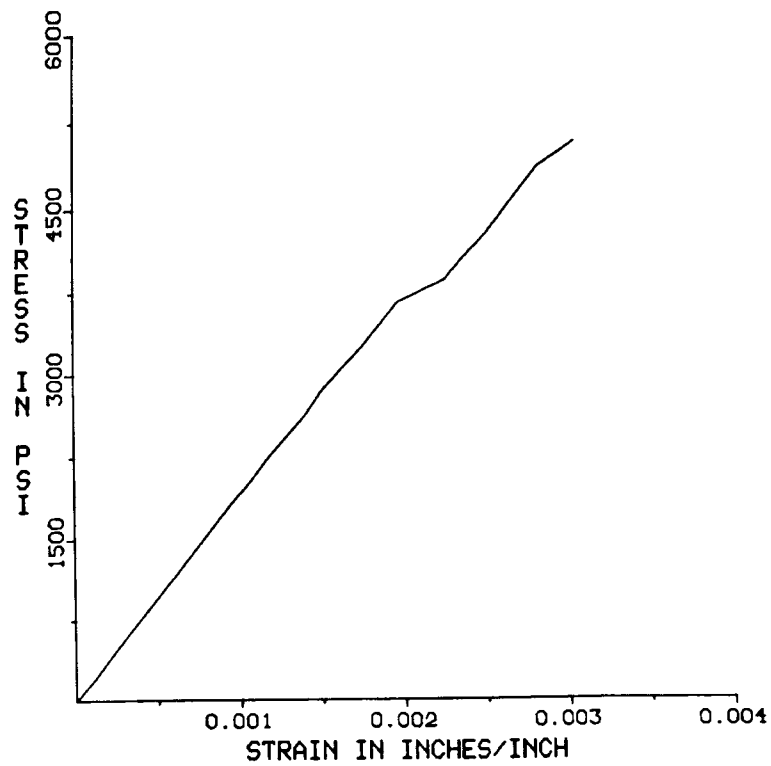


Figure A7.6-4. Stress-strain plot for concrete core 4-10.

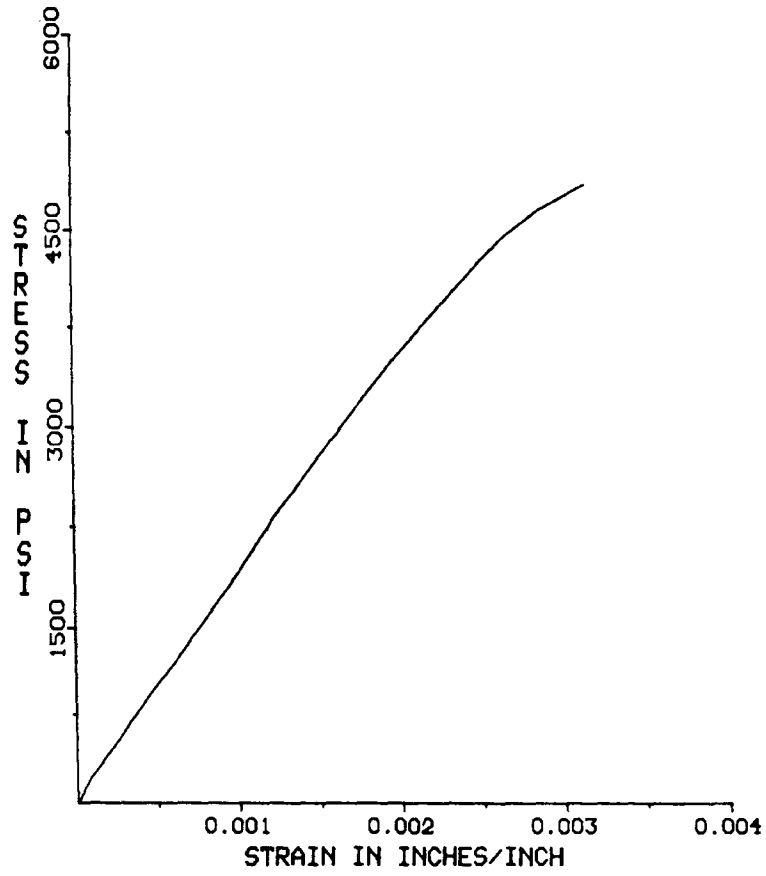


Figure A7.6-5. Stress-strain plot for concrete core 4-12.

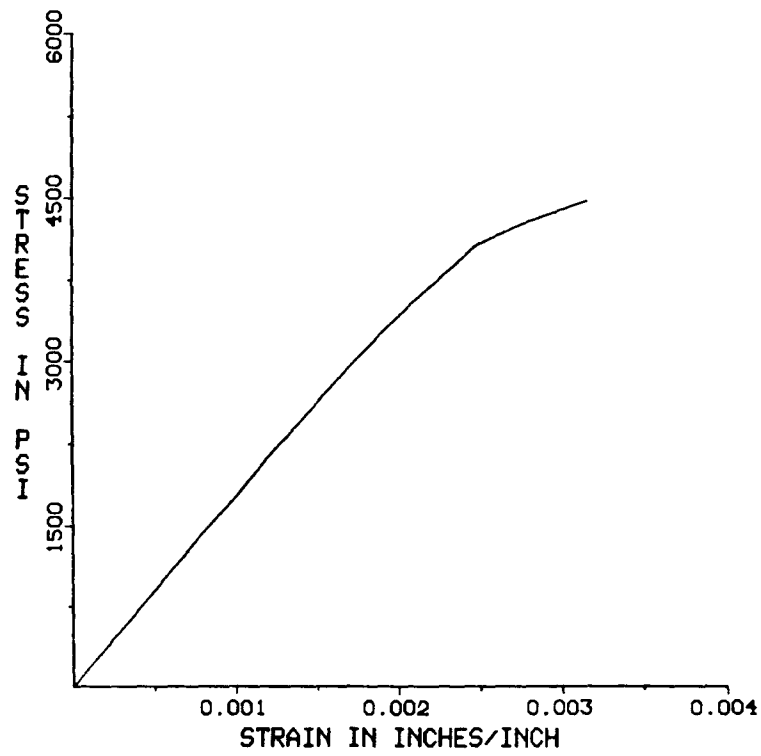


Figure A7.6-6. Stress-strain plot for concrete core 4-13.

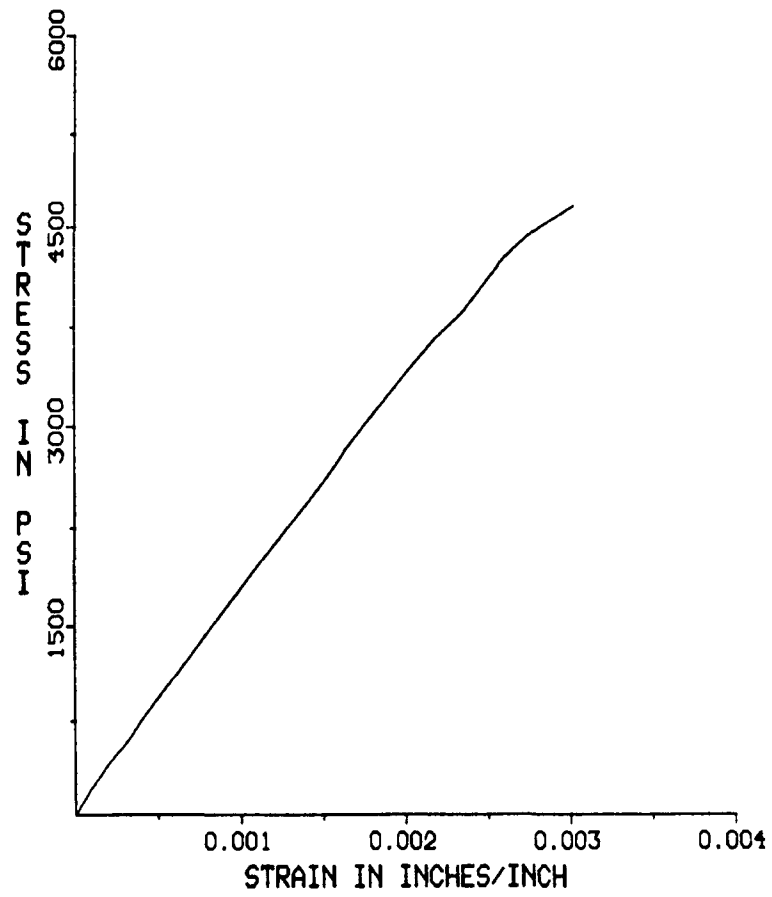


Figure A7.6-7. Stress-strain plot for concrete core 4-16.

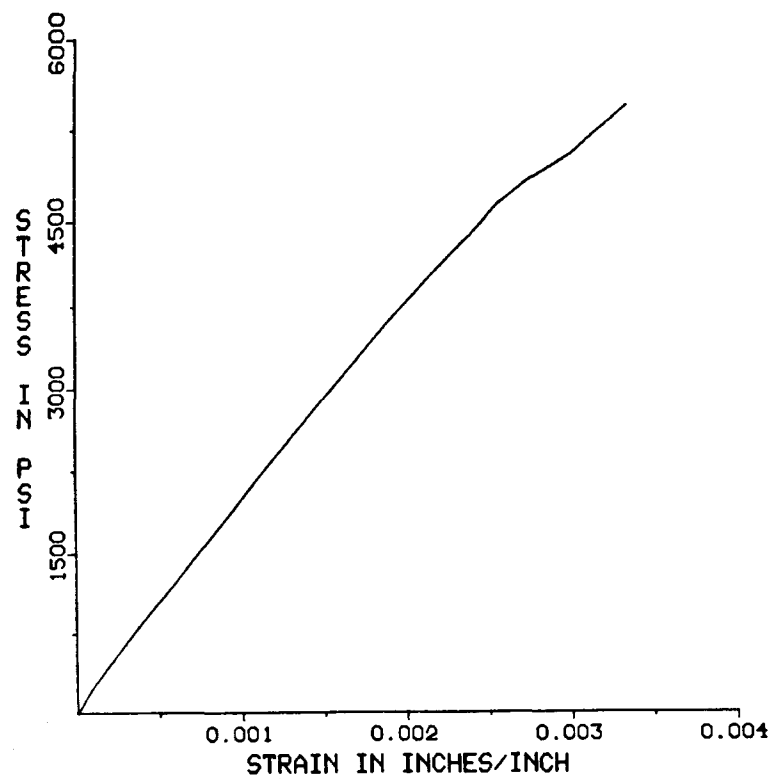


Figure A7.6-8. Stress-strain plot for concrete core 4-18.

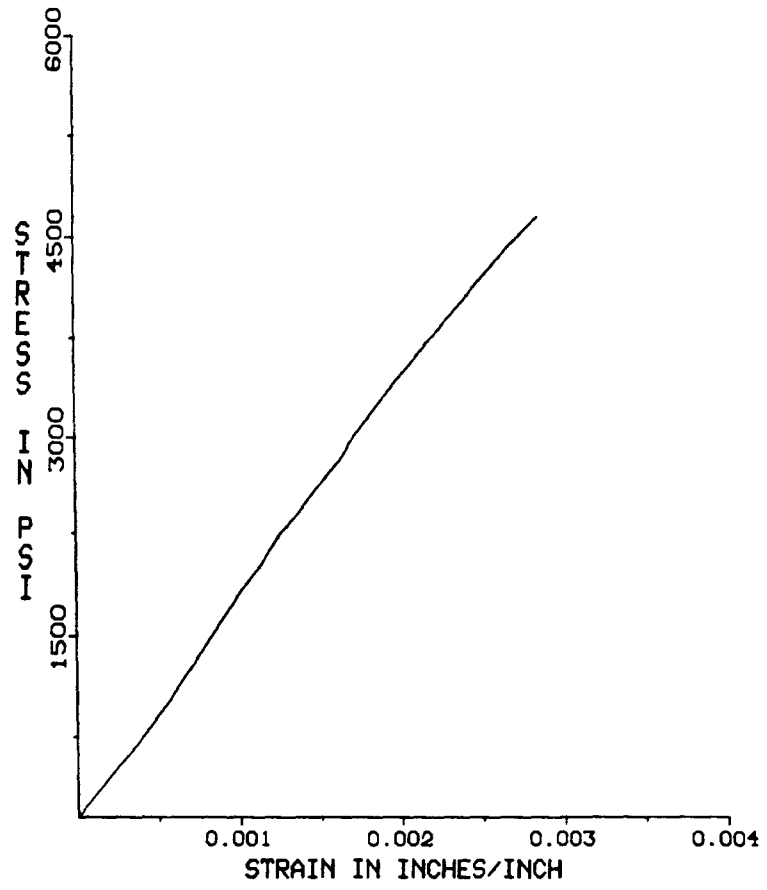


Figure A7.6-9. Stress-strain plot for concrete core 4-19.

Section A9.2

Additional data on the weights of walkway materials and spans are provided by the following tables.

Table A9.2.1-1 Unit Weights of Walkway Materials

Item	Unit Weight
Structural Steel	Per AISC Manual of Steel Construction
1 1/2" x 20 Ga. Formed Steel Deck	2.20 lbs/ft <sup>2</sup>
5/8" Type "X" Gyp. Bd. & Framing	
(a) 5/8" Gyp. Bd.	2.56 lbs/ft <sup>2</sup>
(b) 24 Ga. Steel Studs	0.39 lbs/ft
(c) 24 Ga. Steel Runners	0.31 lbs/ft
Wood Handrail & Brass Extrusion	5.30 lbs/ft
Top Glass Grip	1.78 lbs/ft
1/2" Tempered Plate Glass	6.54 lbs/ft <sup>2</sup>
Bottom Glass Grip	5.19 lbs/ft
Steel Support Angle (4 x 3 x 3/8)	8.50 lbs/ft
Footlights	2.26 lbs each
Footlight Base Plate & Cap	1.33 lbs/ft
Carpet	0.60 lbs/ft <sup>2</sup>
Padding	0.25 lbs/ft <sup>2</sup>
Sprinkler Pipes and Fittings	Per AISC Manual of Steel Construction
Aluminum Slats	70.4 lbs/span

Table A9.2.1-2 Weight Analysis of Damaged Walkway Spans

Item	Weight/Span (lbs)							
	U7-8	U8-9	U9-10	U10-11	L7-8	L8-9	L9-10	L10-11
Cross Beams & Stringers	2191.7	2057.1	2057.1	2174.5	2191.7		2057.1	2174.5
Box Beams	--	343.8	184.6	--	--		184.6	--
Clip Angles	12.7	--	--	12.7	12.7		--	12.7
1 1/4" $\phi$ Hanger Rods	--	110.0	--	--	--		--	--
1 1/2" x 20 Ga. Formed Steel Deck	498.9	493.4	493.4	498.9	498.9		493.4	498.9
Gyp. Bd. Attached to Span	1369.2	976.5	968.6	836.8	985.9		932.7	850.1
24 Ga. Steel Framing for Gyp. Bd.	67.6	67.6	67.6	67.6	67.6		67.6	67.6
Gyp. Bd. Scattered on Deck	--	52.0	39.0	41.6	26.0		7.8	--
Handrail Assembly	79.5	297.4	106.2	--	63.6		155.0	--
Top Glass Grip	102.5	--	--	--	52.1		--	--
1/2" Tempered Plate Glass Panels	416.5	520.6	--	--	208.2		--	--
Broken Plate Glass Panels	52.1	156.2	--	13.1	52.1		--	--
Bottom Glass Grip & Support Angle	795.8	790.0	790.0	800.4	795.8		790.0	800.4
Footlights & Baseplate	95.9	89.3	45.8	24.4	69.0		26.7	33.0
Carpet & Padding	187.3	187.3	--	--	187.3		--	--
Sprinkler Pipes	--	--	97.1	64.4	43.7		86.9	58.0
Miscellaneous Metal Work	--	100.0	--	--	100.0		--	--
Miscellaneous Debris	100.0	--	--	--	--		--	20.0
Timber Cribbing	156.2	--	--	--	--		--	59.4
Embedded Steel Plate	--	--	--	--	10.2		--	--
Broken Granite Panels	--	--	--	--	262.5		--	--
<b>Total</b>	<b>6125.9</b>	<b>6241.2</b>	<b>4849.4</b>	<b>4534.4</b>	<b>5627.3</b>		<b>4801.8</b>	<b>4574.6</b>

Span L8-9 not weighed

Table A9.2.1-3 Weights of Undamaged Walkway Span  
Excluding Concrete Deck and Topping

Component Description	Weight/Span (lbs)			
	U7-8 L7-8	U8-9 L8-9	U9-10 L9-10	U10-11 L10-11
W16 x 26 Stringers & 1/4 x 6 Bent Plate	1847.0	1798.6	1798.6	1829.8
W8 x 10 Cross Beams & Clip Angles	344.7	258.5	258.5	344.7
MC8 x 8.5 Box Beams & Clp Angles	92.3	184.6	184.6	92.3
1 1/4" $\phi$ Hanger Rods (Fourth Floor)	130.5	261.0	261.0	130.5
(Second Floor)	--	--	--	--
1 1/2" x 20 Ga. Formed Steel Deck	498.9	493.4	493.4	498.9
5/8" Type "X" Gyp. Bd. & Framing	2309.4	2309.4	2309.4	2309.4
Handrail Assy & Top Glass Grip	408.3	408.3	408.3	408.3
1/2" Tempered Plate Glass	1249.4	1249.4	1249.4	1249.4
Bottom Glass Grip & Support Angle	795.8	790.0	790.0	800.4
Footlights & Baseplate	104.8	104.8	104.8	104.8
Carpet & Padding	187.3	187.3	187.3	187.3
Sprinkler Pipes	51.1	88.2	97.1	91.8
Aluminum Slats	70.4	70.4	70.4	70.4
Total for Fourth Floor Spans	8089.9	8203.9	8212.8	8118.0
Total for Second Floor Spans	7959.4	7942.9	7951.8	7987.5



# Investigation of the Kansas City Hyatt Regency Walkways Collapse

## ABSTRACT - (continued)

Two factors contributed to the collapse: inadequacy of the original design for the box beam-hanger rod connection which was identical for all three walkways, and a change in hanger rod arrangement during construction that essentially doubled the load on the box beam-hanger rod connections at the fourth floor walkway. As originally approved for construction, the contract drawings called for a set of continuous hanger rods which would attach to the roof framing and pass through the fourth floor box beams and on through the second floor box beams. As actually constructed, two sets of hanger rods were used, one set extending from the fourth floor box beams to the roof framing and another set from the second floor box beams to the fourth floor box beams.

Based on measured weights of damaged walkway spans and on a videotape showing occupancy of the second floor walkway just before the collapse, it is concluded that the maximum load on a fourth floor box beam-hanger rod connection at the time of collapse was only 31 percent of the ultimate capacity expected of a connection designed under the Kansas City Building Code. It is also concluded that had the original hanger rod arrangement not been changed, the connection capacity would have been approximately 60 percent of that expected under the Kansas City Building Code. With this change in hanger rod arrangement, the ultimate capacity of the walkways was so significantly reduced that, from the day of construction, they had only minimal capacity to resist their own weight and had virtually no capacity to resist additional loads imposed by people.

Supplementary material is contained in an appendix to this report and published as NBSIR 82-2465A.

U.S. DEPT. OF COMM. <b>BIBLIOGRAPHIC DATA SHEET</b> <i>(See instructions)</i>	<b>1. PUBLICATION OR REPORT NO.</b>  BSS-143	<b>2. Performing Organ. Report No.</b>	<b>3. Publication Date</b>  May 1982
<b>4. TITLE AND SUBTITLE</b> Investigation of the Kansas City Hyatt Regency Walkways Collapse			
<b>5. AUTHOR(S)</b> R. D. Marshall, E. O. Pfrang, E. V. Leyendecker, K. A. Woodward, R. P. Reed, M. B. Kasen, and T. R. Shives			
<b>6. PERFORMING ORGANIZATION</b> <i>(If joint or other than NBS, see instructions)</i>  <b>NATIONAL BUREAU OF STANDARDS          DEPARTMENT OF COMMERCE          WASHINGTON, D.C. 20234</b>		<b>7. Contract/Grant No.</b>	<b>8. Type of Report &amp; Period Covered</b>  Final
<b>9. SPONSORING ORGANIZATION NAME AND COMPLETE ADDRESS</b> <i>(Street, City, State, ZIP)</i>  Same as Item 6.			
<b>10. SUPPLEMENTARY NOTES</b>  Library of Congress Catalog Card Number: 81-600538  <input type="checkbox"/> Document describes a computer program; SF-185, FIPS Software Summary, is attached.			
<b>11. ABSTRACT</b> <i>(A 200-word or less factual summary of most significant information. If document includes a significant bibliography or literature survey, mention it here)</i>  An investigation into the collapse of two suspended walkways within the atrium area of the Hyatt Regency Hotel in Kansas City, Mo., is presented in this report. The investigation included on-site inspections, laboratory tests and analytical studies.  Three suspended walkways spanned the atrium at the second, third, and fourth floor levels. The second floor walkway was suspended from the fourth floor walkway which was directly above it. In turn, this fourth floor walkway was suspended from the atrium roof framing by a set of six hanger rods. The third floor walkway was offset from the other two and was independently suspended from the roof framing by another set of hanger rods. In the collapse, the second and fourth floor walkways fell to the atrium floor with the fourth floor walkway coming to rest on top of the lower walkway.  Based on the results of this investigation, it is concluded that the most probable cause of failure was insufficient load capacity of the box beam-hanger rod connections. Observed distortions of structural components strongly suggest that the failure of the walkway system initiated in the box beam-hanger rod connection on the east end of the fourth floor walkway's middle box beam.  (continued, next page)			
<b>12. KEY WORDS</b> <i>(Six to twelve entries; alphabetical order; capitalize only proper names; and separate key words by semicolons)</i> building; collapse; connection; construction; failure; steel; walkway.			
<b>13. AVAILABILITY</b>  <input checked="" type="checkbox"/> Unlimited <input type="checkbox"/> For Official Distribution. Do Not Release to NTIS <input checked="" type="checkbox"/> Order From Superintendent of Documents, U.S. Government Printing Office, Washington, D.C. 20402.  <input type="checkbox"/> Order From National Technical Information Service (NTIS), Springfield, VA. 22161		<b>14. NO. OF PRINTED PAGES</b>  360	<b>15. Price</b>



# NBS TECHNICAL PUBLICATIONS

## PERIODICALS

**JOURNAL OF RESEARCH**—The Journal of Research of the National Bureau of Standards reports NBS research and development in those disciplines of the physical and engineering sciences in which the Bureau is active. These include physics, chemistry, engineering, mathematics, and computer sciences. Papers cover a broad range of subjects, with major emphasis on measurement methodology and the basic technology underlying standardization. Also included from time to time are survey articles on topics closely related to the Bureau's technical and scientific programs. As a special service to subscribers each issue contains complete citations to all recent Bureau publications in both NBS and non-NBS media. Issued six times a year. Annual subscription: domestic \$18; foreign \$22.50. Single copy, \$4.25 domestic; \$5.35 foreign.

## NONPERIODICALS

**Monographs**—Major contributions to the technical literature on various subjects related to the Bureau's scientific and technical activities.

**Handbooks**—Recommended codes of engineering and industrial practice (including safety codes) developed in cooperation with interested industries, professional organizations, and regulatory bodies.

**Special Publications**—Include proceedings of conferences sponsored by NBS, NBS annual reports, and other special publications appropriate to this grouping such as wall charts, pocket cards, and bibliographies.

**Applied Mathematics Series**—Mathematical tables, manuals, and studies of special interest to physicists, engineers, chemists, biologists, mathematicians, computer programmers, and others engaged in scientific and technical work.

**National Standard Reference Data Series**—Provides quantitative data on the physical and chemical properties of materials, compiled from the world's literature and critically evaluated. Developed under a worldwide program coordinated by NBS under the authority of the National Standard Data Act (Public Law 90-396).

NOTE: The principal publication outlet for the foregoing data is the Journal of Physical and Chemical Reference Data (JPCRD) published quarterly for NBS by the American Chemical Society (ACS) and the American Institute of Physics (AIP). Subscriptions, reprints, and supplements available from ACS, 1155 Sixteenth St., NW, Washington, DC 20056.

**Building Science Series**—Disseminates technical information developed at the Bureau on building materials, components, systems, and whole structures. The series presents research results, test methods, and performance criteria related to the structural and environmental functions and the durability and safety characteristics of building elements and systems.

**Technical Notes**—Studies or reports which are complete in themselves but restrictive in their treatment of a subject. Analogous to monographs but not so comprehensive in scope or definitive in treatment of the subject area. Often serve as a vehicle for final reports of work performed at NBS under the sponsorship of other government agencies.

**Voluntary Product Standards**—Developed under procedures published by the Department of Commerce in Part 10, Title 15, of the Code of Federal Regulations. The standards establish nationally recognized requirements for products, and provide all concerned interests with a basis for common understanding of the characteristics of the products. NBS administers this program as a supplement to the activities of the private sector standardizing organizations.

**Consumer Information Series**—Practical information, based on NBS research and experience, covering areas of interest to the consumer. Easily understandable language and illustrations provide useful background knowledge for shopping in today's technological marketplace.

*Order the above NBS publications from: Superintendent of Documents, Government Printing Office, Washington, DC 20402.*

*Order the following NBS publications—FIPS and NBSIR's—from the National Technical Information Services, Springfield, VA 22161.*

**Federal Information Processing Standards Publications (FIPS PUB)**—Publications in this series collectively constitute the Federal Information Processing Standards Register. The Register serves as the official source of information in the Federal Government regarding standards issued by NBS pursuant to the Federal Property and Administrative Services Act of 1949 as amended, Public Law 89-306 (79 Stat. 1127), and as implemented by Executive Order 11717 (38 FR 12315, dated May 11, 1973) and Part 6 of Title 15 CFR (Code of Federal Regulations).

**NBS Interagency Reports (NBSIR)**—A special series of interim or final reports on work performed by NBS for outside sponsors (both government and non-government). In general, initial distribution is handled by the sponsor; public distribution is by the National Technical Information Services, Springfield, VA 22161, in paper copy or microfiche form.

**U.S. DEPARTMENT OF COMMERCE**  
**National Bureau of Standards**  
Washington, D.C. 20234

OFFICIAL BUSINESS

Penalty for Private Use, \$300

POSTAGE AND FEES PAID  
U.S. DEPARTMENT OF COMMERCE  
COM-215



SPECIAL FOURTH-CLASS RATE  
BOOK

---